Technische Universität München

Department Chemie

Lehrstuhl II für Organische Chemie

Design and Synthesis of FVIII- and uPAR-Selective Ligands and Cross-Linked Polymers as Media for NMR-Spectroscopy

Sebastian Knör

Die vorliegende Arbeit wurde am Lehrstuhl II für Organische Chemie

der Technischen Universität München in der Zeit von Oktober 2002 bis Mai 2007

unter der Leitung von Prof. Dr. Horst Kessler angefertigt.

Meiner Frau

gewidmet

Σ'αγαπώ πολύ

*Publier dans un petit journal ne veut pas
dire petit résultat.
Ce qui compte c'est que les gens
l'essayent pour dire que ça marche!!*

*In einem kleinen Journal zu publizieren
heißt nicht, kleine Ergebnisse zu haben.
Was zählt ist, dass die Leute es
ausprobieren um zu sagen: Es geht!*

(Abdellah Benhida, Univ. Leuven)

DANKSAGUNG

Meinem Doktorvater,

Herrn Professor Dr. Horst Kessler,

danke ich besonders für die vielen interessanten Themen, die ich bearbeiten durfte. Insbesondere bedanke ich mich für die uneingeschränkte Unterstützung in jeder Hinsicht, für den großen wissenschaftlichen Freiraum, der mir gewährt wurde, sowie für die zahlreichen fruchtbaren und hilfreichen Diskussionen.

Für die ausgezeichnete Zusammenarbeit auf dem Gebiet der Faktor VIII Liganden möchte ich mich ganz herzlich bei

- Dr. Alexey Khrenov und Prof. Dr. Evgueni Saenko,
- Dr. Charlotte Hauser,
- Dr. Abdellah Benhida und Prof Dr. Jean-Marie Saint-Remy,
- Dr. Rainer Schwaab und Prof. Dr. Johannes Oldenburg sowie
- Dr. Nathalie Beaufort und PD. Dr. Viktor Magdolen

bedanken. Mit ihrer Hilfe habe ich viel über die Biologie des Faktor VIII und die Schwierigkeiten in der Behandlung der Hämophilie gelernt. Ihr großartiger Einsatz hat maßgebliche zum Erfolg des Projektes beigetragen.

Für die hervorragende Zusammenarbeit auf dem Gebieten des Tumor-Imaging und der Tumor-Therapy und bedanke ich mich bei:

- Dr. Sumito Sato, PD Dr. Viktor Magdolen und Prof. Dr. Manfred Schmitt,
- Dr. Christof Seidl und Prof. Dr. Reingard Senekowitsch-Schmidtke sowie
- Dr. Thorsten Poethko, Dr. Margret Schottelius und Prof. Dr. Hans-Jürgen Wester

Ohne Ihren unermüdlichen Eifer wäre ein Gelingen dieser Projekte nicht möglich gewesen.

Publications

Parts of this work have already been published or are in preparation:

Publications

S. Knör, A. Khrenov, B. Laufer, E. L. Saenko, C. A. E. Hauser, H. Kessler. Development of a peptidomimetic ligand for efficient isolation and purification of factor VIII *via* affinity chromatography. *Journal of Medicinal Chemistry*, submitted.

S. Knör, A. Khrenov, B. Laufer, A. Benhida, R. Schwaab, J. Oldenburg, N. Beaufort, V. Magdolen, J.-M. Saint-Remy, E. L. Saenko, C. A. E. Hauser, H. Kessler. Efficient FVIII affinity purification using a small synthetic ligand. *Journal of Thrombosis and Haemostasis*, submitted.

S. Knör, S. Sato, T. Huber, A. Morgenstern, F. Bruchertseifer, M. Schmitt, H. Kessler, R. Senekowitsch-Schmidtk, V. Magdolen, C. Seidl. Development and evaluation of peptidic ligands targeting tumour-associated urokinase plasminogen activator receptor (uPAR) for use in α-emitter therapy of disseminated ovarian cancer. *European Journal of Nuclear Medicine and Molecular Imaging*, submitted.

S. Knör, A. Modlinger, T. Poethko, M. Schottelius, H.J. Wester, H. Kessler. Synthesis of novel DOTA-derivatives for chemoselective attachment to polyfunctionalized compounds. *Chemistry — A European Journal* 2007, in press.

S. Knör, B. Laufer, H. Kessler. Efficient enantioselective synthesis of condensed and aromatic ring-substituted tyrosine derivatives. *Journal of Organic Chemistry* 2006, *71*, 5625-5630.

B. Luy, K. Kobzar, S. Knör, J. Furrer, D. Heckmann, H. Kessler. Orientational properties of stretched polystyrene gels in organic solvents and the suppression of their residual ^{1}H NMR signals. *Journal of the American Chemical Society* 2005, *127*, 6459-6465.

J. C. Freudenberger, S. Knör, K. Kobzar, D. Heckmann, T. Paululat, B. Luy. Stretched poly(vinyl acetate) gels as NMR alignment media fort he measurement of residual dipolar dipolar couplings in polar organic solvents. *Angewandte Chemie International Edition* 2005, *44*, 423-426.

Patents

S. Knör, H. Kessler, C. A. E. Hauser, A. Khrenov, E. L. Saenko. Small peptidic and peptidomimetic affinity ligands for Factor VIII and Factor VIII-like proteins. *International patent application* PCT/EP2006/011786.

H. Kessler, C. A. E. Hauser, A. Khrenov, S. Knör, E. L. Saenko. Minimized affinity ligands for Factor VIII and Factor VIII-like proteins. *European patent application* No. 04 013 852.6.

S. Knör, A. Modlinger, H.-J. Wester, H. Kessler. Novel DOTA-derivatives for chemoselective attachment to polyfunctionalized compounds. *Great Britain patent application* No. 06 245 87.2.

Abstracts

S. Knör, B. Laufer, A. Khrenov, A. Benhida, S. Grailly, J.-M. Saint-Remy, E. L. Saenko, C. A. E. Hauser and H. Kessler. Factor VIII affinity purification using small ligands. *Hämostaseologie* 2007, *1*, A 65.

H. Kessler, B. Luy, K. Kobzar, J. C. Freudenberger, S. Knör, D. Heckmann, J. Klages. RDC as a new NMR-parameter for peptides. *Biopolymers* 2005, *80*, 500.

S. Knör, D. Heckmann, L. Marinelli, E. L. Saenko, C. A. E. Hauser and H. Kessler. Linear and cyclic peptides as affinity ligands in Factor VIII purification. *Peptides 2004, Proceedings of the 28th European Peptide Symposium*, Prague, Czech Republic & *Journal of Peptide Science* 2004, *10*(S2), 272.

— Table of Contents —

— Synopsis —

Chapter 1 deals with the development of a novel peptidomimetic affinity ligand for blood coagulation factor VIII (FVIII).

FVIII is an indispensable protein for the treatment of hemophilia A. Current manufacturing processes generally employ immunoaffinity chromatography for purification. This technique, however, is expensive and suffers from the chemical and biological instability of the applied antibody ligands which are eluted along with the product and contaminate it with potentially toxic or immunogenic fragments. Recently the very large protein (~330 kDa) FVIII was successfully purified using octapeptides as affinity ligands. Nevertheless, as proven in this work, their practical use is limited due to their low resistance against proteolytic degradation.

In this work an octapeptidic FVIII ligand was systematically minimized and optimized *via* combinatorial screening and rational design to obtain the small peptidomimetic ligand (3-IAA)Eψ[CH$_2$NH]YC (Figure 1). This ligand proved to bind and purify FVIII with high efficiency and in addition, it is long-term stable and protease resistant. Hence, the new ligand offers a valuable alternative to current expensive procedures in laboratory and industry. To allow an economic access in preparative scale, a solution phase synthesis was developed (see Figure 2).
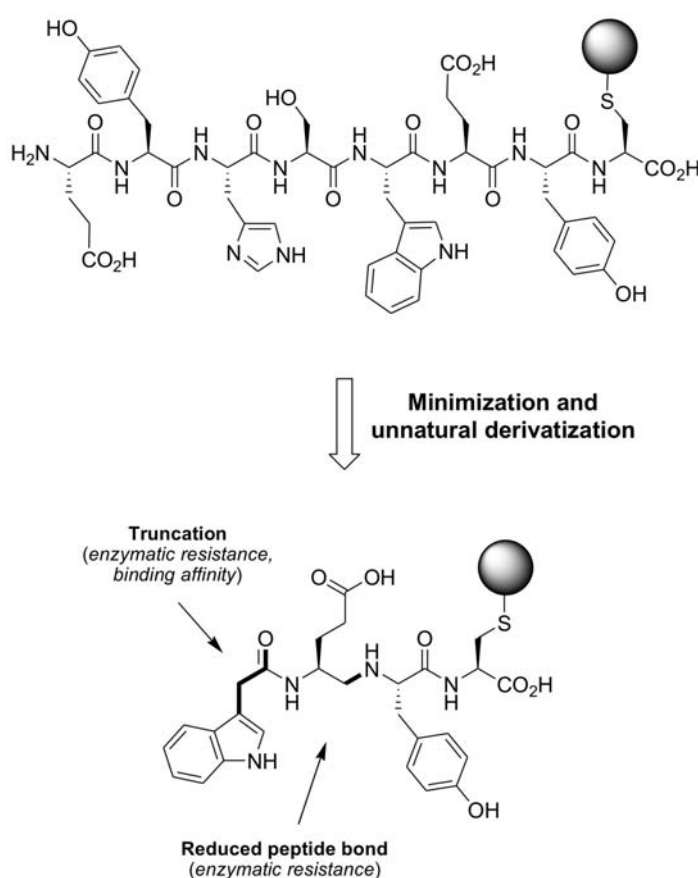
Figure 1. Development of a novel peptidomimetic affinity ligand for FVII by systematic downsizing and optimization of an octapeptidic lead compound.

The synthesis was performed in *N*- to *C*-terminal direction to introduce the sensitive cysteine residue in the last step. Starting from 3-indolylacetic acid, the amino alcohol glutamol was attached and the reduced peptide bond, which connects the glutamic acid with the tyrosine moiety, was formed *via* reductive alkylation. After coupling of the cysteine residue and final deprotection, the desired ligand was obtained as a single diastereomer in high purity without need of purification.
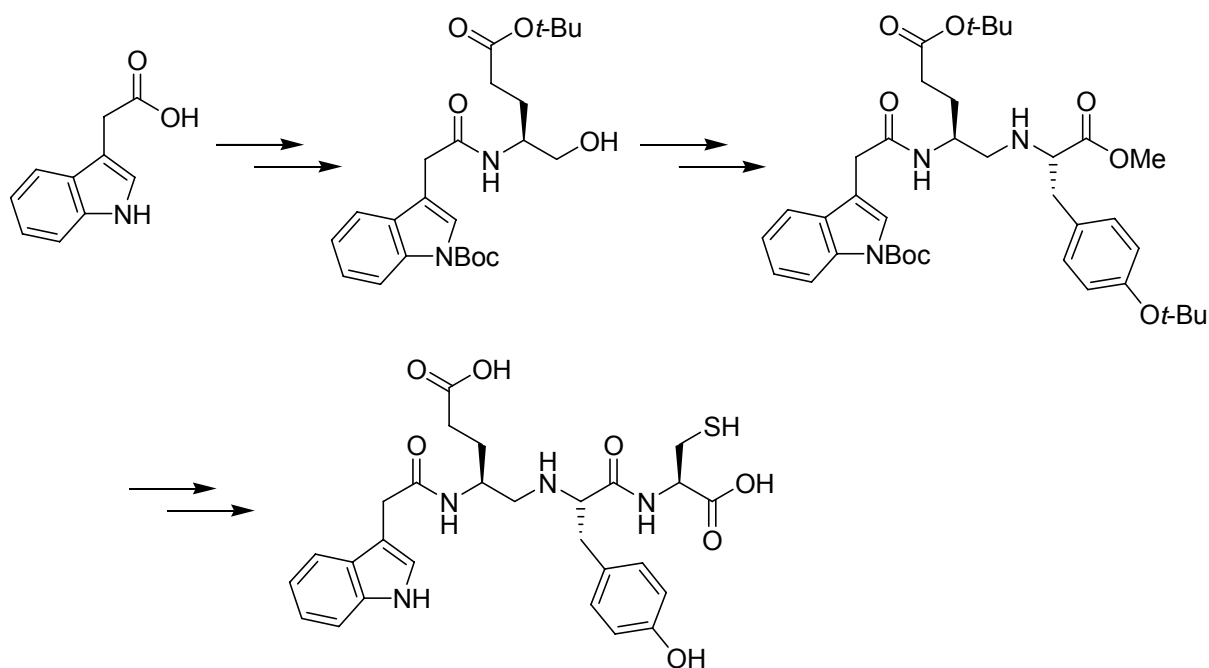
Figure 2. Solution synthesis of the novel FVIII ligand (3-IAA)Eψ[CH$_2$NH]YC.

During the studies towards (3-IAA)Eψ[CH$_2$NH]YC it was found that the phenolic hydroxyl group of the tyrosine residue is important for efficient binding to the target protein FVIII. Additionally, these studies indicated that an extended aromatic system may be preferred. Thus, an easy procedure for the synthesis of condensed and conjugated tyrosine analogues was developed for a systematic fine tuning of the tyrosine residue and structure activity relationship (SAR) studies (see Figure 3 and Figure 4).

In the approach towards extended aromatic side chain residues, the focus was on strategies allowing a rapid access of variety of compounds in few steps, avoiding complicated protecting group chemistry. L-4-Hydroxy-1-naphthylalanine was synthesized *via* an asymmetric hydrogenation of the corresponding α-enamide as a key step (Figure 3).
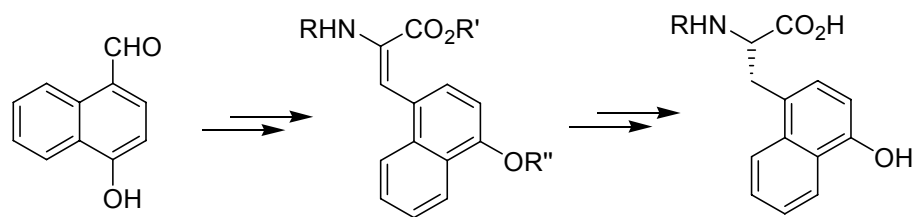
Figure 3. Asymmetric synthesis of L-4-hydroxy-1-naphthylalanine.

In an alternative approach, the α-enamide was hydrogenated unselectively and the racemic mixture was resolved using acylase I. This procedure provides a much cheaper approach in cases where both enantiomers are desired.
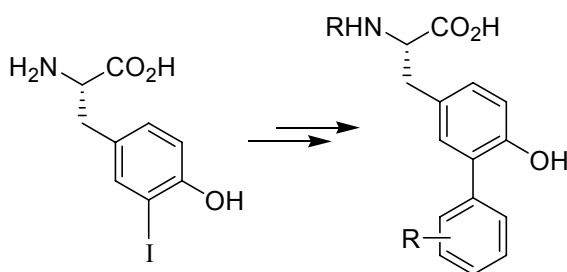
Figure 4. Synthesis of 3-aryl-substituted tyrosine derivatives.

Novel ring substituted tyrosines were synthesized by Suzuki cross couplings of appropriately protected L-3-iodo-tyrosine with a series of activated and deactivated boronic acid derivatives to achieve the enantiomerically pure target compounds in high yields (Figure 4).

Chapter 2 describes the development of new tools for nuclear medicinal applications, such as tumor imaging and radionuclide therapy.

Firstly, novel radioligands selectively targeting the urokinase-type plasminogen activator receptor (uPAR) were developed. The urokinase-type plasminogen activator (uPA) and its receptor uPAR play an important role in cancer. The system is involved at multiple stages in the formation and progression of the disease, in particular in invasion, metastasis, cell proliferation, migration and cell adhesion. Therefore, it is a promising target for cancer treatment and diagnosis. The aim of the present study was to examine whether peptidic radioligands, based on potent uPAR binding peptides, may be developed for application in α-emitter therapy of

disseminated ovarian cancer. Based on the published uPAR inhibitors AE105 and WX360, mono- and dimeric uPAR-selective ligands equipped with a DOTA chelator (1,4,7,10-tetraazacyclododecane-1,4,7,10-tetraacetic acid) for radiolabeling were developed. One compound is shown exemplary in Figure 5.

Ligand = AE105 = Asp-Cha-Phe-(D-Ser)-(D-Arg)-Tyr-Leu-Trp-Ser
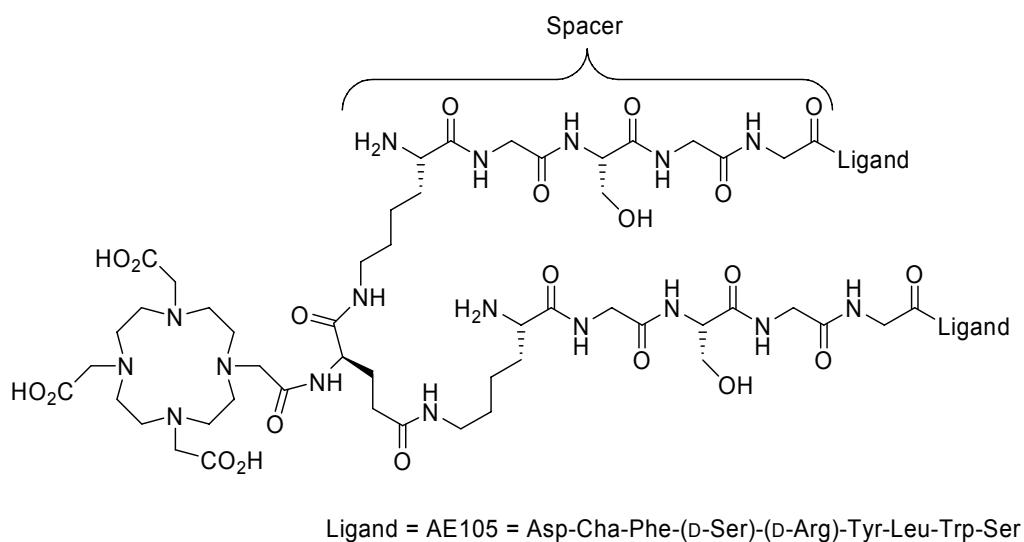
Figure 5. Structure of a new DOTA-conjugated dimeric uPAR ligand based on the AE105 peptide.

For the synthesis of the dimeric compounds, a facile procedure for *N*-terminal cross-linking of solid-phase-bound peptides was worked out, allowing the direct synthesis of the complete dimeric DOTA-conjugates with high purity (see Figure 6).
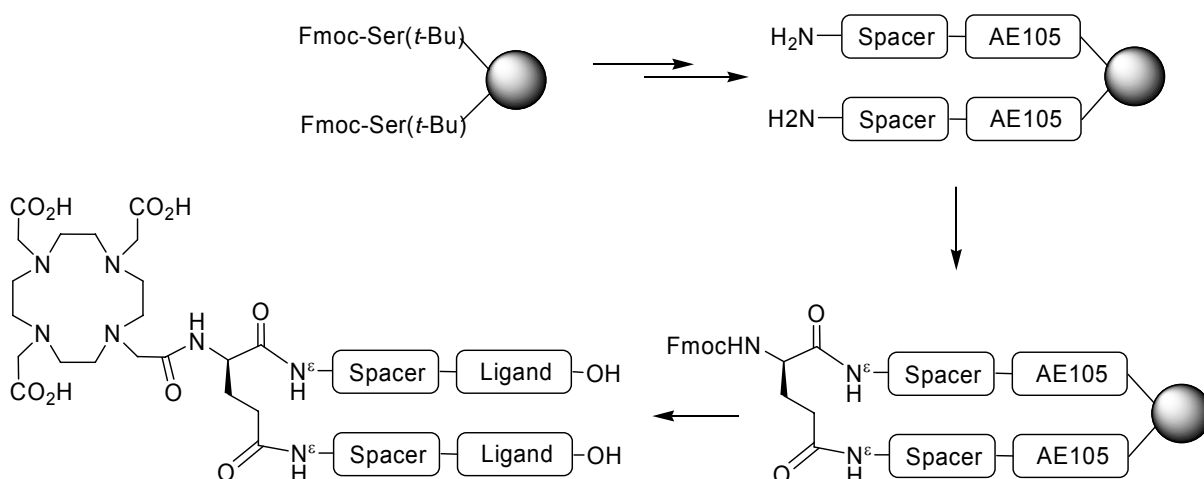
Figure 6. Solid-phase procedure for the synthesis of dimeric DOTA-conjugates.

4

In this procedure, the monomeric peptide strands including the spacer moieties were built up on solid phase by standard procedures. Thereafter, two single strands were cross-linked using glutamic acid as bivalent carbonic acid. DOTA was then attached *via* the amino terminus of the glutamic acid. The biological evaluation displayed a specific binding of the new [213]Bi-labeled ligands to OV-MZ-6 cancer cells *in vitro* as well as *in vivo*. The latter was demonstrated by specific accumulation of [213]Bi-labeled ligands in the tumor tissue of nude mice bearing intraperitoneal OV-MZ-6-derived tumors. Since kidney uptake of the ligands could be significantly reduced using gelofusine, the new radiopeptides offer promising options for therapy of disseminated ovarian cancer.

In a second project, novel derivatives of the DOTA chelator were developed. A major drawback of currently available DOTA-derivatives is that they can only be attached to amino groups of biomolecules, thus, limiting their application and possible synthetic approaches. Therefore, novel DOTA derivatives allowing chemoselective conjugation with unprotected biomolecules *via* click reactions were developed.
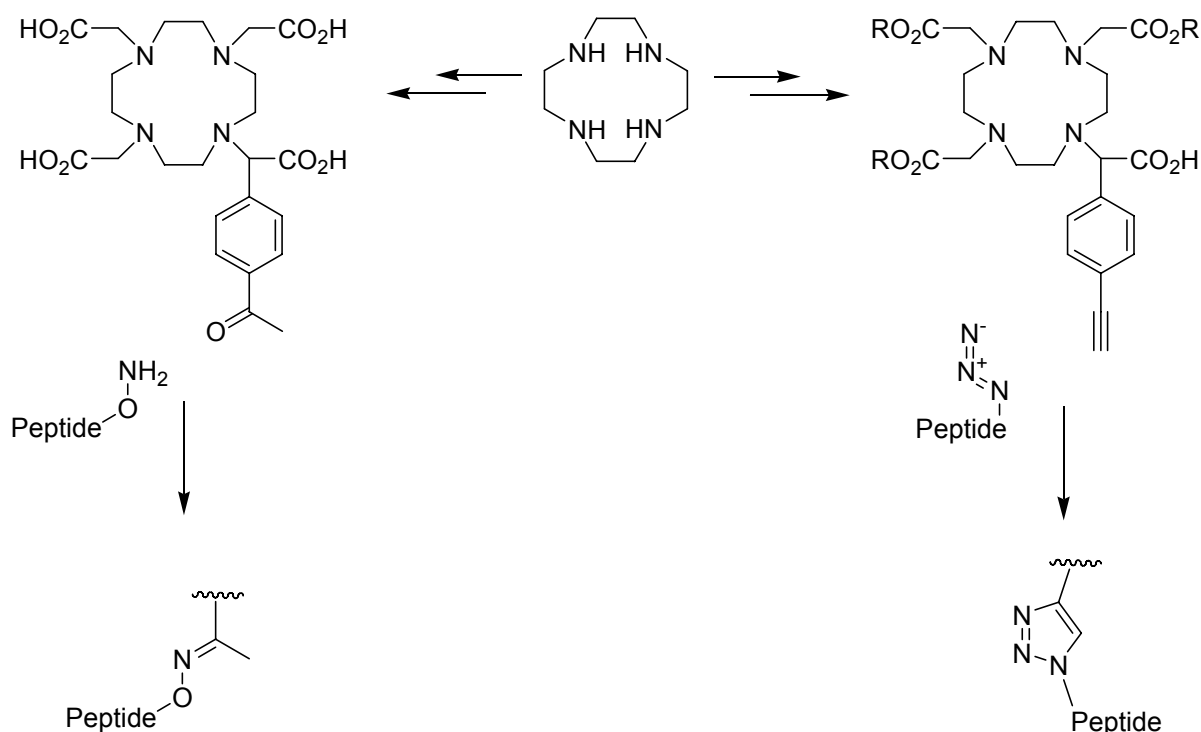
Figure 7. Novel DOTA derivatives for chemoselective attachment *via* click reaction.

For the synthesis, 1,4,7,10-tetraazacyclododecane (cyclen) was alkylated with one equivalent of para-functionalized alkyl 2-bromophenyl-acetate and three equivalents of *tert*-butyl 2-bromoacetate (Figure 7). The resulting compounds having an additional carbonyl or alkyne functionality can be chemoselectively ligated with appropriately functionalized unprotected biomolecules *via* oxime ligation and copper(I)-catalyzed azide-alkyne cycloaddition (Figure 7). This was demonstrated by the attachment to derivatives of the somatostatin analog Tyr[3]-octreotate. Initial biodistribution studies in mice with the radiometalated compound demonstrated the general applicability of the new chelators.

Chapter III deals with the preparation of cross-linked polymer sticks as alignment media for measurement of residual dipolar couplings (RDCs) in high resolution NMR (Figure 8).
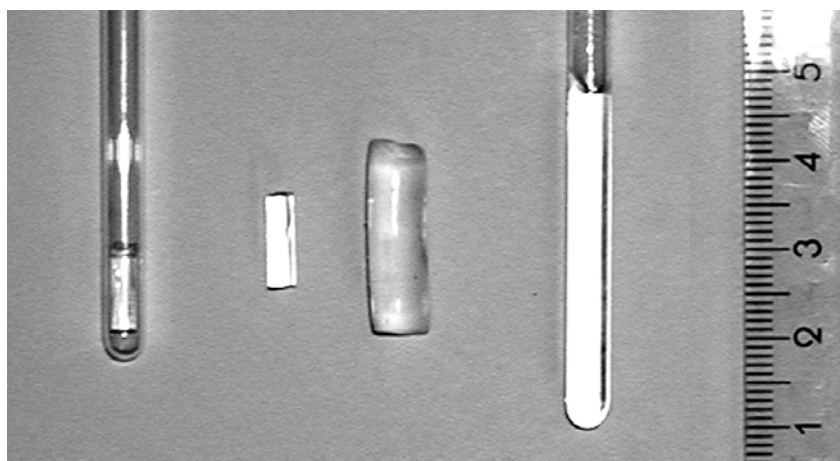
Figure 8. Photograph of the cross-linked PS stick in different states of swelling. From left to right: unswollen polymer stick in standard 5 mm NMR-tube, polymer stick directly after polymerization, free polymer stick completely swollen, polymer stick swollen in the NMR-tube.

RDCs have revolutionized the NMR-based structure determination of large biomolecules. Their measurement in high resolution NMR requires the partial alignment of the molecules in the sample. A number of standard methods like phospholipid bicelles, filamentous phage, or other liquid crystalline phases exist for biological molecules in aqueous solution.

To make the method also applicable to unpolar molecules, a series of cross-linked polymer sticks was developed allowing swelling and stretching in a variety of

organic solvents of different polarity (see Figure 8 and Table 1). Three variables were adopted to optimize the polymers with regard to the NMR application in different solvents: the amounts of radical starter, cross-linker and the diameter of the polymer sticks.

Table 1. Cross-linked polymers for measurement of RDCs.

Material	Cross linking agent	Applicable solvents
cross-linked PS[a]	divinylbenzene	dichloromethane (DCM), chloroform, tetrahydrofuran (THF), benzene, and dioxane
cross-linked PS-d$_8$[a]	divinylbenzene	dichloromethane (DCM), chloroform, tetrahydrofuran (THF), benzene, and dioxane
cross-linked PVA[b]	adipic acid divinylester	dichloromethane (DCM), chloroform, tetrahydrofuran (THF), benzene, dioxane, ethylacetate (EtOAc), acetone, acetonitrile (ACN), methanol (MeOH), dimethyl sulfoxide (DMSO)
cross-linked PMMA[c]	ethylenglycol dimethacrylate	dichloromethane (DCM), chloroform, tetrahydrofuran (THF), benzene, and dioxane

[a] PS: polystyrene; [b] PVA: poly(vinyl acetate); [c] PMMA: poly(methyl methacrylate)

In addition to these achiral polymers, different cross-linked polymers bearing chiral side chain functionalities were prepared. Using chiral polymers, it is possible to distinguish enantiomers and to determine their absolute configuration and/or the enantiomeric excess. This has recently been shown for stretched gelatin as alignment medium. The use of swollen gelatin, however, is limited to compounds dissolvable in aqueous solvents. The development of chiral polymers swellable in organic solvents would allow such measurements also for more unpolar compounds.

Thus, based on chiral acrylates a series of cross-linked polymers was prepared by copolymerization (a) of the pure chiral monomer with ethylenglycol dimethacrylate as cross-linking agent (Type A) and (b) of a dilution of the chiral monomer in methylacrylate, again adding ethylenglycol dimethacrylate as cross-linking agent (Type B). The general structures are shown in Figure 9. The application of these polymers in RDC measurement by NMR is currently under investigation.

Type **A**

Type **B**

R* =
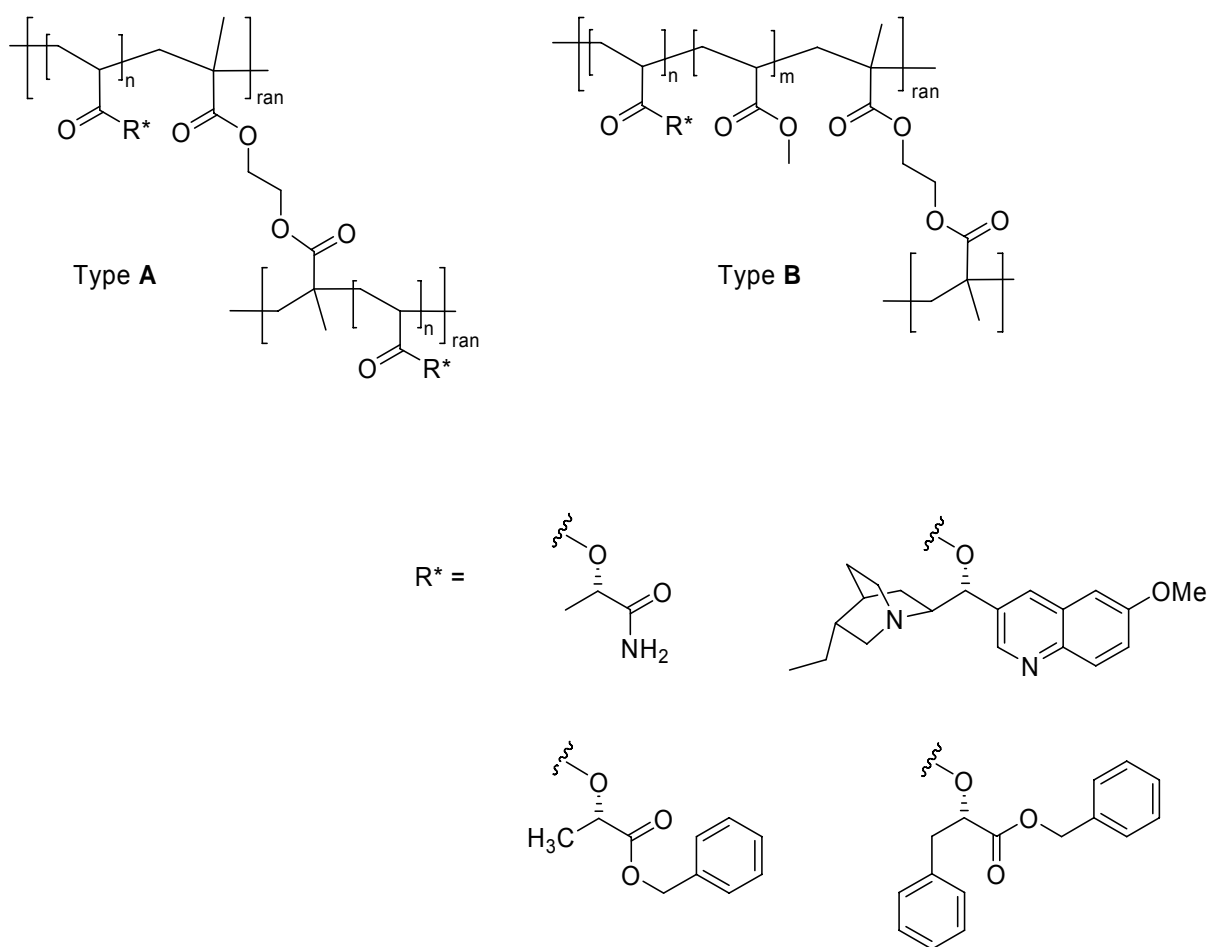
Figure 9. General structures of cross-linked polymers bearing chiral side chain moieties (R*) prepared in this work; ran: random.

<div align="center">

— Chapter 1 —

1 Development of Small Molecule Ligands for Affinity Purification of Factor VIII

</div>

1.1 Background

The ability of the body to control the flow of blood after vascular injury is indispensable for survival. The process of blood clotting and subsequent dissolution of the clot, following repair of the injured tissue, is termed hemostasis.[1]

Hemostasis consists of four major events that occur in a certain order after the loss of vascular integrity:[1]

(1) The initial phase of the process is vascular constriction to limit the flow of blood to the injured area.

(2) Then, primary hemostasis occurs, wherein platelets become activated by thrombin and aggregate at the site of injury, forming a loose hemostatic plug within seconds after injury. Platelets clump by binding to collagen that becomes exposed following the rupture of the endothelial lining of vessels.

(3) To insure stability of the initially loose platelet plug, a fibrin mesh forms and entraps the plug (secondary hemostasis or coagulation). The coagulation pathway involves a complex cascade of coagulation factors, ultimately resulting in the transformation of fibrinogen into polymerized fibrin, forming the clot. This process takes several minutes.

(4) The attracted clot stimulates the growth of fibroblasts and smooth muscle cells within the vessel wall and initiates the repair process. Finally the clot is dissolved in order to allow normal blood flow (fibrinolysis).

1.1.1   Blood coagulation and fibrinolysis

The coagulation is a complex proteolytic cascade which has been proposed for the first time by Davie *et al.* in 1964.[2,3] Each enzyme involved is present in the plasma as a zymogen (inactive form), which is activated by proteolytic cleavage to release the active factor from the precursor molecule. The coagulation cascade functions as a series of positive and negative feedback loops which control the activation process. The ultimate goal is to produce thrombin (factor IIa, FIIa), which then converts soluble fibrinogen into fibrin, which forms the clot.[2,4-6]

The whole cascade can be divided into three pathways: the intrinsic and extrinsic pathway, which are initiated by different processes, and which both converge on the common pathway to finally lead to clot formation (Figure 10). The intrinsic pathway is initiated by abnormal vessel wall in the absence of tissue injury, whereas the extrinsic pathway is initiated as a result of tissue injury. Both pathways are complex and involve numerous different proteins termed clotting factors.[1,3-5] An overview over the clotting factors and other proteins involved in coagulation as well as their functions can be found in the appendix (Supplementary Data 1 and 2 on pages 243-244).

1.1.1.1   The intrinsic pathway

The intrinsic pathway (also termed contact activation pathway) is activated when blood comes into contact with sub-endothelial connective tissues or with negatively charged surfaces that are exposed as a result of tissue damage. Quantitatively it is the more important of the two pathways, but fibrinogen activation proceeds significantly slower than *via* the extrinsic pathway. The pathway involves the clotting factors VIII (FVIII), IX (FIX), X (FX), XI (FXI), and XII (FXII). Also required are the proteins prekallikrein (PK) and high-molecular-weight kininogen (HMWK), as well as calcium ions (Ca^{2+}) and phospholipids (PL) secreted from platelets.[2,4-6]

The intrinsic pathway is initiated by binding of PK, HMWK, FXI and FXII to a sub-endothelial surface exposed by an injury.[2,4-6] The assemblage results in conversion of prekallikrein to kallikrein, which in turn activates FXII to FXIIa ("a" signifies active) (Figure 10). Factor XIIa is then able to hydrolyze more prekallikrein to kallikrein, establishing a reciprocal activation cascade. There is also evidence that the FXII can autoactivate, which makes the pathway self-amplifying.[7-9] FXIIa in turn activates FXI to FXIa, which, in the presence of Ca^{2+}, then activates FIX to FIXa (Figure 10). Factor IX is a proenzyme that contains vitamin K-dependent γ-carboxy-glutamate (*gla*) residues, whose serine protease activity is activated following Ca^{2+} binding to these *gla* residues. Several of the serine proteases of the cascade (thrombin, FVII, FIX, and FX) are *gla*-containing proenzymes.
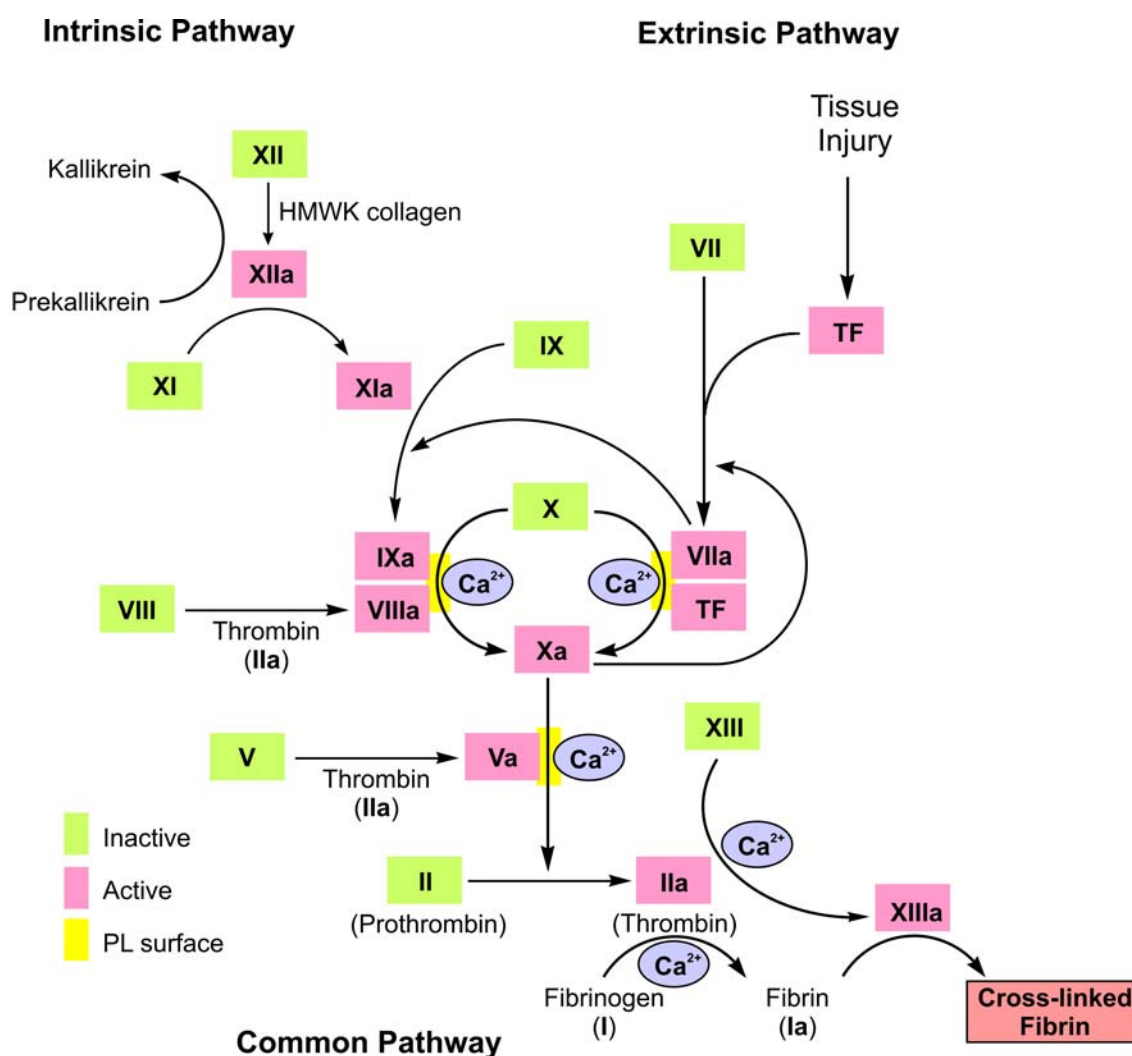
Figure 10. Simplified illustration of the clotting cascade. PL: Phospholipid; HMWK: high molecular weight kininogen.

The intrinsic pathway ultimately activates FX, a process which can also be triggered by the extrinsic pathway (Figure 10).[2,4-6] The activation of FXa requires assembly of the intrinsic tenase (also termed Xase) complex (FVIIIa/FIXa/FX) on the surface of activated platelets which activates FX to FXa in presence of Ca^{2+}. The role of FVIIIa in this process is to act as a receptor for FIXa and FX and as a cofactor of FIXa and FX.[10-12] The activation of FVIII to FVIIIa occurs in the presence of minute quantities of thrombin. As the concentration of thrombin increases, FVIIIa is ultimately cleaved by thrombin and inactivated. FVIIIa activity is furthermore controlled by activated protein C (APC) which is an important cofactor inhibitor.[13] It degrades FVIIIa (and also FVa) and is activated by thrombin in presence of thrombomodulin (a protein on the surface of endothelial cells) and requires its coenzyme protein S (PS) to function. The dual action of thrombin (FVIII activation and deactivation) ensures a limited extent of the tenase complex formation.[11]

1.1.1.2   The extrinsic pathway

The extrinsic pathway (also termed the tissue factor pathway) is an alternative route for the activation of the clotting cascade.[2,4-6] It provides a very rapid response to tissue injury, generating activated factor X almost instantly, compared with the minutes, required for the intrinsic pathway to activate factor X. The main function of the extrinsic pathway is to augment the activity of the intrinsic pathway.[14]

There are two components unique to the extrinsic pathway, tissue factor (TF) and factor VII (FVII). Tissue factor is present in most human cells bound to the cell membrane and is released at the site of injury. Once activated, circulating FVIIa binds rapidly to TF which serves as a cofactor in the FVIIa-catalyzed activation of FX to generate small amounts of FXa (Figure 11a).[15] The TF/FVIIa/FX complex is termed the extrinsic tenase complex. Factor VIIa, a *gla* residue containing serine protease, cleaves FX to FXa in a manner identical to FIXa in the intrinsic pathway. Factor Xa is the major activator of zymogen FVII (FVII is also activated by FIXa, FVIIa/TF, and thrombin),[16-22] establishing a reciprocal activation cascade by catalysis of the formation of more FVIIa and activation of thrombin, which begins activating the cofactors V and VIII (Figure 11a; compare also Figure 10).[23]
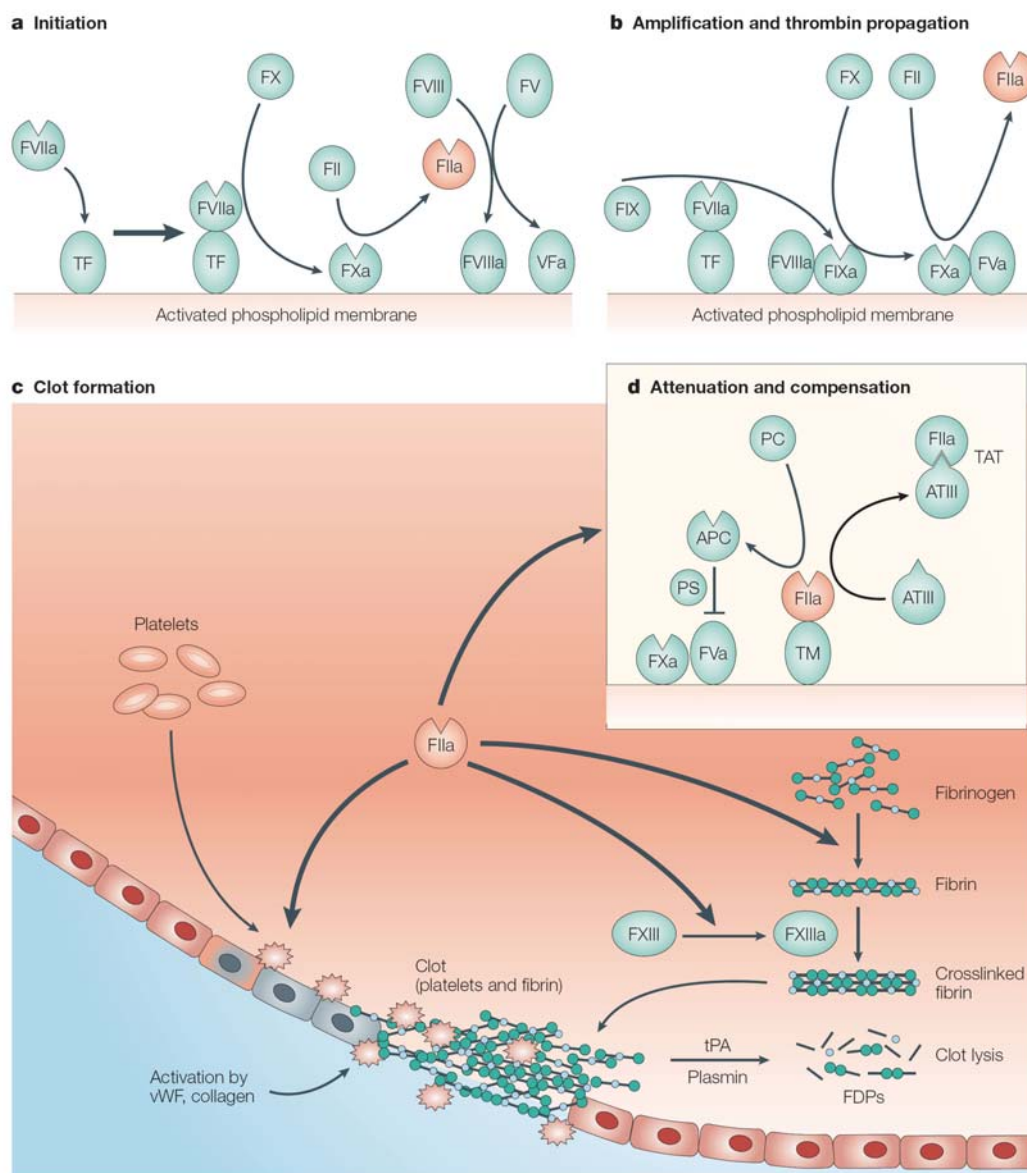
Figure 11. The key enzymatic and cellular events leading to clot formation. From Bishop *et al*.,[6] reprinted by permission from Macmillan Publishers Ltd: *Nature Reviews Drug Discovery* 2004, *3*(8), 684-694, Copyright © 2004. The primary event initiating the coagulation pathway (a) occurs when activated factor VIIa (FVIIa) binds to tissue factor, which is present on extravascular tissue and activated endothelium (inflamed). This complex activates traces of FX and thrombin (FIIa). Thrombin, in turn, activates small amounts of cofactors FV and FVIII. The procoagulant signal is then rapidly amplified (b) *via* assembly of a series of enzymatic coagulation factor complexes (see Figure 10) that culminate in a burst of thrombin generation. Thrombin then directly propagates clot formation by cleaving fibrinogen to fibrin (the fibrous substance comprising the growing thrombus) and also activates FXIII, which stabilizes the clot by cross-linking fibrin fibres and several other proteins, including inhibitors of plasmin (c). Because the coagulation cascade results in an explosive release of thrombin, mechanisms exist (d) that attenuate and compensate thrombin generation through negative feedback. Attenuation occurs through inactivation of FVa by protein S (PS) and activated protein C (APC) generated by the thrombomodulin–thrombin complex. Excess thrombin is compensated by direct inhibition by antithrombin III (ATIII) *via* formation of the thrombin–anti-thrombin III (TAT) complex.[6]

The ability of FXa to activate FVII creates a link between the intrinsic and extrinsic pathways (see Figure 10). An additional link between the two pathways exists through the ability of TF and FVIIa to activate FIX (Figure 10).[24] These initial catalytic events provide the elements for the formation of two essential procoagulant complexes, which sequentially amplify the procoagulant stimulus: FVIIIa/FIXa, which activates FX, and FXa/FVa, which activates prothrombin to thrombin which directly propagates clot formation (Figure 11b).[24,25]

A major mechanism for the inhibition of the extrinsic pathway occurs at the activation of FX by TF/FVIIa. The protein, lipoprotein-associated coagulation inhibitor (LACI) specifically binds to this complex.[26] LACI is also referred to as extrinsic pathway inhibitor (EPI) or tissue factor pathway inhibitor (TFPI) and was formerly named anticonvertin.[2,4-6] The intrinsic and extrinsic systems converge at factor X to a single common pathway which is responsible for the production of thrombin.[1]

1.1.1.3   The common pathway and clot formation

a) Activation of thrombin and control of thrombin activity:

FXa activates prothrombin (factor II, FII) to thrombin (Figure 11b). Thrombin, in turn, converts fibrinogen to fibrin (Figure 11c). The activation of thrombin occurs on the surface of activated platelets and requires the formation of a prothrombinase complex. This complex is composed of the platelet phospholipids, Ca^{2+}, FVa, FXa, and prothrombin (Figure 11b). FVa functions as cofactor of FXa in the prothrombinase complex, similar to the role of FVIII in the intrinsic tenase complex formation. Like FVIII activation, FV is activated to FVa by means of minute amounts of thrombin and is inactivated by increased levels of thrombin. FV activity is controlled by APC which degrades FVa in presence of cofactor PS (Figure 11d).[13]

In addition to its role in activation of fibrin clot formation, thrombin plays an important regulatory role in coagulation. Thrombin associates with thrombomodulin present on endothelial cell surfaces forming a complex that efficiently converts PC to APC.[13] The APC/PS complex, in turn, degrades FVa as well as FVIIIa, thereby limiting the activity of these two factors in the coagulation cascade and thus thrombin formation. Hence, thrombin is a major regulator of its own production and of the coagulation cascade.[5,11,15] The activation of thrombin is

furthermore regulated by four specific thrombin inhibitors: Antithrombin III (ATIII) is the most important as it can also inhibit the activities of factors IXa, Xa, XIa and XIIa.[5,11,15] The activity of ATIII is potentiated in the presence of heparin. This effect of heparin is the basis for its clinical use as an anticoagulant. Furthermore, thrombin activity is inhibited by α_2-macroglobulin, heparin cofactor II and α_1-anti-trypsin.[5,11,15]

b) Clot formation:

Fibrinogen (factor I, FI) consists of three pairs of polypeptides ($[A\alpha][B\beta][\gamma])_2$.[27,28] The A and B portions of the Aα and Bβ chains comprise the fibrinopeptides, A and B. The fibrinopeptide regions of fibrinogen are highly negatively charged by several glutamate and aspartate residues, which improves the solubility of fibrinogen in plasma.[27,28] Exposure of fibrinogen to thrombin results in rapid proteolysis of fibrinogen and the release of fibrinopeptide A. The loss of the small peptide A is not sufficient to render the resulting fibrin molecule insoluble, a process that is required for clot formation, but it tends to form complexes with adjacent fibrin and fibrinogen molecules. Then, fibrinopeptide B is cleaved by thrombin, and the fibrin monomers formed by this second proteolytic cleavage polymerize spontaneously to form an insoluble gel (Figure 11c). The polymerized fibrin, held together by non-covalent and electrostatic forces, is stabilized by the transamidating enzyme factor XIIIa, produced by the action of thrombin on factor XIII (Figure 11c).[27,28] These insoluble fibrin aggregates together with aggregated platelets, blocks the damaged blood vessel and prevents further bleeding.[6]

1.1.1.4   Temporal and spatial control of clot formation

As described, the coagulation cascade itself is highly regulated by several positive and negative feedback loops and inhibitors to ensure blood coagulation in case of injury and to prevent undesired blood coagulation (*e.g.* thrombosis). Beside the temporal control, coagulation is also localized to the site of injury. Recently, this phenomenon was explained by introduction of the conception of spatial heterogeneity into the basic scheme of the coagulation cascade.[13] This conception (as described below) tries to determine the roles of the different pathways of the cascade at different temporal and spatial stages of clotting:

Figure 12. Schematic representation of the reaction-diffusion model of coagulation. Reprinted from M. A. Penteleev *et al*. *Biophysical Journal* 2006, *90*, 1489-1500.[13]

Blood coagulation near the activator (*e.g.* TF exposure on TF-expressing cells) is determined by the FXa production from extrinsic tenase complex located on TF-expressing cells (Figure 12 left). Upon diffusion into the blood flow, FXa is rapidly inhibited and thus does not diffuse at long distances.[13] Far from the activator (propagation), FXa is formed by intrinsic tenase complex. The limiting component of intrinsic Xase, FIXa, is still produced by extrinsic tenase, because FIXa is inhibited slowly and can diffuse efficiently (Figure 12). During further clot elongation, additional FIXa production by the FXIa-mediated long-range feedback becomes essential (intrinsic pathway).[13] Finally, clot formation is terminated because of the action of thrombomodulin. In a potent negative feedback, the thrombin-thrombomodulin complex produces APC, which cleaves FVa and FVIIIa and stops thrombin formation.[13]

1.1.1.5   Fibrinolysis

Once hemostasis is restored and the tissue is repaired, the clot or thrombus must be removed from the injured tissue. This is achieved by the fibrinolytic pathway (Figure 13).[1,6,14,29,30] The end product of this pathway is the enzyme, plasmin. Plasmin is formed by activation of the proenzyme plasminogen by either plasma or tissue activators, uPA (urokinase type plasminogen activator) and tPA (tissue plasminogen activator) respectively.[29] The level of tissue activator in the plasma is normally low, but can be increased by exercise and stress. Plasminogen activation is regulated by natural inhibitors, in particular plasminogen activator inhibitor 1 (PAI-1) and 2 (PAI-2) (Figure 13).[29,30]
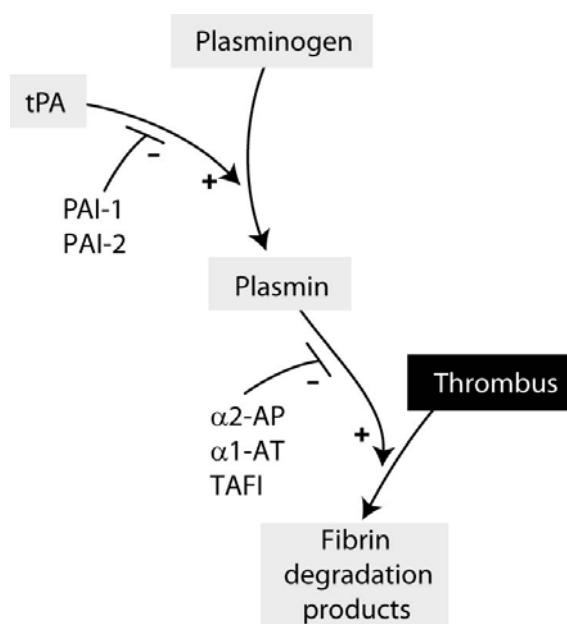
Figure 13. Schematic representation of the fibrinolysis pathway.

Triggering of fibrinolysis occurs when the plasminogen activator, plasminogen, and fibrin are all in close proximity. Both plasminogen and its activator readily bind to fibrin as the clot forms.[29] This close association prevents inhibition of plasmin activity by its inhibitors allowing the proceeding of fibrinolysis. Plasmin inhibitors which can control plasmin activity include: α_1-antitrypsin (α_1-AT), α_2-antiplasmin (α_2-AP), thrombin-activatable fibrinolysis inhibitor (TAFI), C1 inhibitor and ATIII.[29-34] Plasmin attacks fibrin at at least 50 different sites, reducing its size and thus its

hemostatic activity. Many fragments are formed during this process, and some retain the capacity to polymerize. This may prevent the clot being removed before the tissue is repaired.[29]

1.1.2 Hemophilia

1.1.2.1 Bleeding disorders: A general overview

It is evident that any defect in the highly controlled cascade can lead to severe disorders, *i.e.* to thrombosis or hemophilia. Table 2 summarizes and classifies the most important bleeding disorders with respect to the kind of dysfunction, severity and prevalence.

Table 2. Incidence of coagulation deficiencies.[6]

Conditions associated with bleeding	Examples	Incidence	Severity
Congenital coagulation factor deficiencies	Factor VIII (Hemophilia A)	1/5,000	Moderate to severe
	Factor IX (Hemophilia B)	1/25,000	Moderate to severe
	Von Willebrand disease	~1/1,000	Mild to severe
Rare coagulation factor deficiencies	Fibrinogen	$1/10^6$	None to severe
	Prothrombin	Very rare	Mild to moderate
	Factor V	$1/10^6$	Moderate
	Factor VII	$2/10^6$	Mild to severe
	Factor X	$2/10^6$	Mild to severe
	Factor XI	Rare	Mild to moderate
	Factor XIII	$>1/10^6$	Moderate to severe
	α_2-Antiplasmin inhibitor	UK	Mild to moderate
	α_1-Antitrypsin inhibitor	Very rare	Can be severe

The most common bleeding disorder is the von Willebrand disease, which results from a dysfunction or a lack of von Willebrand factor (vWF). vWF is an important protein for blood coagulation as it binds to both, the subendothelium and platelets and mediates platelet adhesion. Furthermore, vWF binds to circulating FVIII and stabilizes it against proteolytic inactivation. However, most cases of von Wille-

brand's disease are mild; hemarthroses and muscle bleedings occur only in the most severe type 3 which is uncommon.[6,10]

Hemophilia A results form a lack or dysfunction of FVIII and is one of the most common and most severe bleeding disorders (Table 2). Incidence and treatment of hemophilia A will be presented in more detail in the following chapter.

Hemophilia B results from deficiencies in factor IX. The prevalence of hemophilia B is approximately one-tenth that of hemophilia A (Table 2). All patients with hemophilia B have prolonged coagulation time and decreased factor IX clotting activity. Like hemophilia A, there are severe, moderate and mild forms of hemophilia B and reflect the factor IX activity in plasma.[6,10] All other bleeding disorders are rare (see Table 2)[6,10] and shall not be discussed in detail herein.

1.1.2.2 Hemophilia A – The Royal disease

Hemophilia A, also called the Royal disease, is one of the most common and severe bleeding disorders (Table 2).[35] The name Royal disease arose from the prevalence of the disease in the royal families of England, Spain, Germany and Russia, as a result of Queen Victoria of England (1819-1901) being a carrier. The marriage of Queen Victoria and Prince Albert marked the beginning of hemophilia in the British royal line. Queen Victoria had nine children and as English royal family members married into royalty of other countries, the disease eventually infected most of the royal houses of Europe.[35]

Hemophilia A is the result of an X-linked inherited deficiency of FVIII function leading either to reduced FVIII levels or to a dysfunction of FVIII. Due to the X-linked inheritance, hemophilia A affects mostly males as illustrated in (Figure 14):[10,36,37] Supposing a hemophilic father and a healthy mother, all sons will be healthy, but all daughters will be carrier. In turn, supposing a mother, which is carrier, and a healthy father, one of two sons will be bleeder and one of two daughters will be carrier.
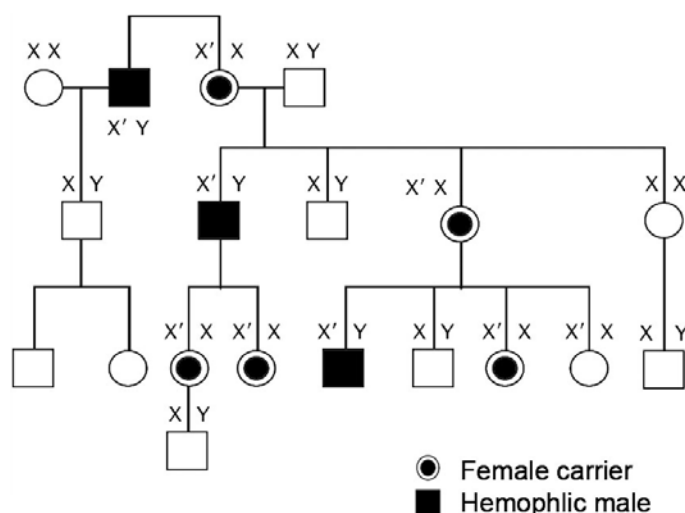
Figure 14. Inheritance of hemophilia A.

Hemophilia A arises from a variety of mutations. Around 150 different point mutations have been characterized in the factor VIII gene in hemophilia A.[10,35,38,39] The incidence of hemophilia A is approximately one in 5000 males, and does not vary appreciably between populations.[10,35] With respect to the FVIII blood level, the disease is classified as mild (5-40% of normal), moderate (1-5% of normal) and severe (<1% of normal) (see also Table 3).

Table 3. Classification of hemophilia A.[10]

Factor level	Classification	Clinical picture
0.05-0.40 IU/mL (5-40% of normal)	Mild	Spontaneous bleeding does not occur; bleeding after surgery, dental extraction, and accident
0.01-0.05 IU/mL (1-5% of normal)	Moderate	Bleeding into joints and muscles after minor injuries; excessive bleeding after surgery and dental extraction
<0.01 IU/mL (<1% of normal)	Severe	Spontaneous joint and muscle bleeding; bleeding after injuries, accidents, and surgery

The severe form of the disease is characterized by spontaneous bleedings, as well as uncontrollable bleedings in case of trauma or surgery. Other clinical hallmarks are acute recurrent painful hemarthroses, which can progress to chronic arthropa-thy characterized by progressive destruction of the cartilage and the adjacent bone, muscle hematomas, intracerebral hemorrhages and hematuria.[38]

1.1.2.3 Treatment of hemophilia A

The current treatment for hemophilia A is the infusion of FVIII (replacement therapy), either purified from human blood plasma (plasma-derived FVIII; pdFVIII) or expressed in recombinant cells (recombinant FVIII; rFVIII),[6,40-42] which normalizes the clotting process and stops or prevents bleeding. Hemophilia A is also an attractive target for gene-therapy, which is rapidly developing but nevertheless stands at its beginnings.[10,35,38,43-53]

Hence, the survival and well-being of people with hemophilia depends on the supply of safe therapeutic products.[54] In the past, numerous hemophilia patients have been infected with HIV-1 or hepatitis C virus *via* injections of contaminated plasma-derived FVIII preparations.[35,40,55] While the safety of pdFVIII products has been continuously improved during the last decades,[40,56,57] the isolation of the factor VIII gene in 1984 opened new opportunities for treatment.[58-60] The preparation of novel recombinant FVIII (rFVIII) molecules significantly improved supply and product safety.[42,61-64] Nevertheless, rFVIII is a biotechnologically derived product produced by cell culture and carries a risk of transmitting infectious agents.[65] Approximately 25% of the first-generation rFVIII concentrates were positive for transfusion-transmitted viruses from contaminated human serum albumin, which is added as stabilizer.[66] In contrast, the second-generation rFVIII products like Kogenate® FS (Bayer) and ReFacto® (Wyeth-Ayerst Pharmacia and Upjohn) the first licensed B domain deleted rFVIII (BDD-rFVIII) molecule (the FVIII structure will be discussed in detail in the following chapter),[67] do not have added albumin and instead use sucrose or other non-human derived material as a stabilizer.[42] This advancement significantly improved the product safety, so the therapeutic use of recombinant FVIII has been significantly increased in the past years.[68]

However, as long as human albumin is added to the cell culture media and monoclonal antibodies (mAbs) are used as ligands in affinity purification there is still a risk of transfusing pathogens. Especially transmissible spongiform encephalopathies and new variants of Creutzfeldt-Jakob disease as well as previously unknown pathogens, including new murine viruses, may contaminate today's rFVIII products.[65,69] Hence, all efforts should be made to eliminate all human or animal proteins from the manufacturing process of recombinant products.[70] Consequently

there is a great demand for novel procedures avoiding such components in order to develop the next generation of recombinant FVIII products.

Besides product safety, financial aspects are major factors in the development of new FVIII products. While 88% of the safer but more expensive rFVIII is consumed in Europe and North America, the majority of the world's population with hemophilia is reliant on blood products or does not receive any treatment at all due to economic reasons.[40,41,54,55,71] Novel techniques reducing production costs can help to improve the FVIII supply and make treatment accessible for a broader range of the population.

1.1.3   FVIII structure and mechanism of cofactor action

FVIII is a large secretory glycoprotein containing 2351 amino acids. The first 19 amino acids serve as a signal peptide for translocation of the protein to the endoplasmatic reticulum and later for the export out of the cell.[60] Without the signal peptide the FVIII molecule has a molecular weight of ~330 kDa (2332 amino acids) with a multi-domain structure A1-a1-A2-a2-B-a3-A3-C1-C2 (see Figure 15).[12,59,60,72,73] The A and C domains (A1 ($FVIII_{1-329}$), A2 ($FVIII_{380-711}$), A3 ($FVIII_{1649-2019}$), C1 ($FVIII_{2020-2172}$), C2 ($FVIII_{2173-2332}$)) provide 30-40% homology with the A and C domains of the structurally related proteins ceruloplasmin and factor V, whereas the B domain and the acidic regions a1, a2 and a3 with a high density of negatively charged amino acids Asp and Glu are distinctive for FVIII.[72,74,75] The large B domain is not important for the FVIII procoagulant activity[76] but recent studies demonstrated its role in protecting the activated form of FVIII from proteolytic inactivation.[77]

Prior to its secretion into plasma, FVIII is processed intracellularly to a series of noncovalently associated, Cu^{2+}-linked heterodimers by cleavage at the B-A3 junction (Figure 15).[12,78,79] The cleavage generates the heavy chain (HC) consisting of the A1, A2 and B domains and the light chain (LC) composed of the A3, C1 and C2 domains.[12,35] The resulting protein varies in size due to additional cleavages within the B domain, giving molecules of different length. Thus, preparations of plasma-derived human FVIII (pdFVIII) contain a heterogeneous mixture of differently sized FVIII molecules.[72,80]
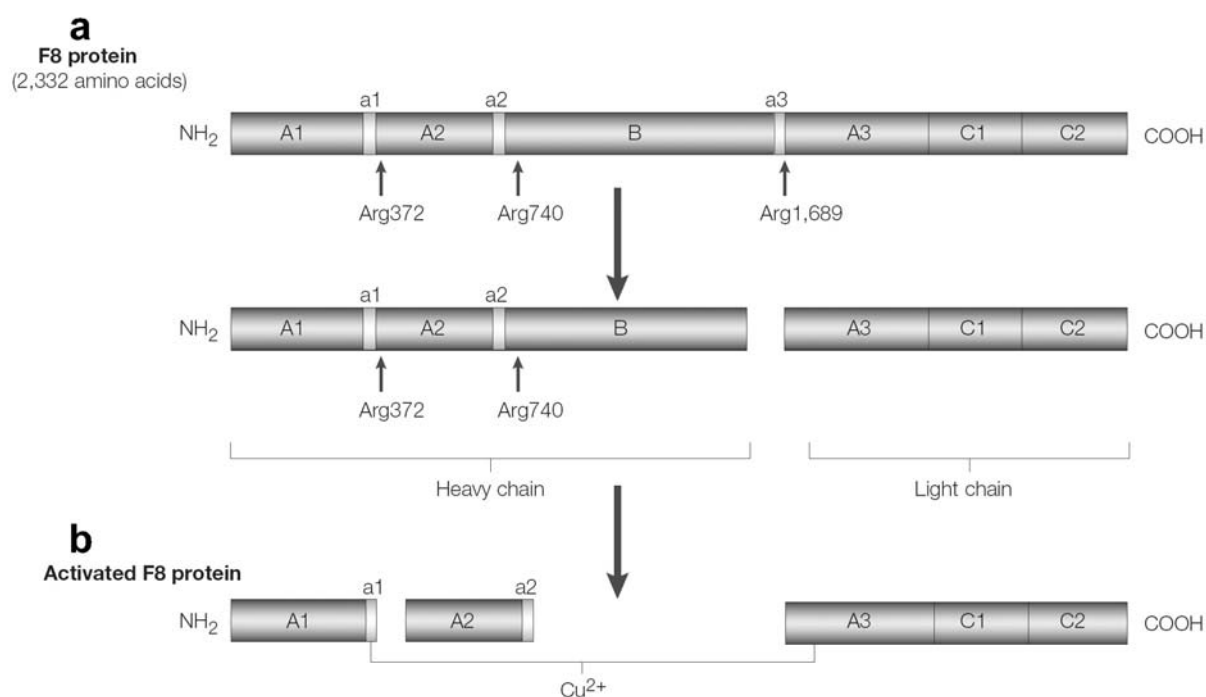
Figure 15. Processing and activation of the encoded factor VIII protein. From Graw *et al.*,[35] adapted by permission from Macmillan Publishers Ltd: *Nature Reviews Genetics* 2005, *6*(6), 488-501, Copyright © 2005. (a,b) The FVIII mRNA is translated into a precursor protein of 2,351 amino acids, which is processed to the final product (shown in a, upper panel) that lacks only 19 amino acids from its *N*-terminal leader sequence. Further processing by thrombin leads to the activation of FVIII. First, cleavage at Arg[1689] (at the B–A3 junction) generates a variably-sized (90–210 kDa) heavy chain, consisting of domains A1 and A2 and heterogeneous fragments of the partially proteolysed B domain; during the process, a 40-amino-acid acidic peptide (a3) is released from the *C*-terminal product to form a 73-kDa light chain that consists of domains A3–C1–C2 (a, lower panel). Further cleavage by thrombin (b) removes most of the B domain and cleaves the protein between the A1 and A2 domains: cleavage at Arg[372] (between the A1 and A2 domains) and at Arg[740] (between the A2 and B domains) generates the 54-kDa A1 and the 44-kDa A2 domains (b). The activated protein is held in a complex with Cu^{2+}.[35]

As a cofactor FVIII interacts during coagulation with a variety of other proteins. After secretion into the plasma FVIII binds von Willebrand Factor (vWF) with high affinity in an inactive form through its a3 and C2 domains (K_d about 0.4 nM)[81-83] as well as the C1 domain (Figure 16).[84] vWF stabilizes FVIII and protects it against proteolysis.[85,86] Association with vWF increases half life of FVIII in plasma from 2-3 hours to 12-14 hours.[81,87] At the site of coagulation, FVIII is activated by thrombin and FXa.[88] Both proteases cleave the FVIII molecule at Arg[372] (A1a1/A2 junction) and Arg[740] (A2a2/B junction) within the HC and at Arg[1689] (B/a3A3 junction) within the LC, producing the A1a1, A2a2 and a3A3-C1-C2 fragments that compose the

heterotrimeric-activated FVIII (see Figure 15 and Figure 16). The cleavage at Arg[1689] results in removal of a3 and release of vWF.[83] This cleavage is important for maximal cofactor activity of FVIIIa.[89] The heterotrimeric FVIIIa binds to negatively charged phospholipids (PLs) *via* the C2 domain[90-93] (Figure 16 and Figure 17) and to factor IXa *via* the A2 and A3 domains[94-99] to form the intrinsic tenase complex with FXa by binding *via* the C2 domain (Figure 16).[100]
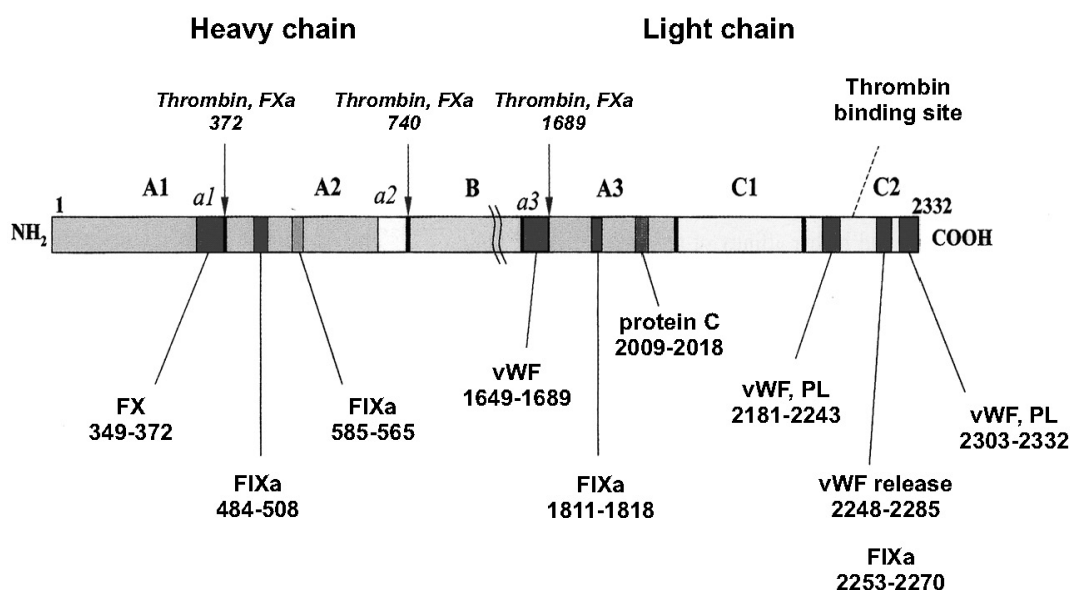
Figure 16. Major functional binding sites and epitopes of natural ligands on the factor VIII molecule (cleavage sites are indicated in italics). PL: phospholipid. Modified from Klinge *et al.*.[38]

The exact structure of FVIII and the tenase complex is so far unknown. However, it is clear that the high affinity interaction of FVIIIa and FIXa (K_d ~15 nM) is mainly provided by residues $FVIII_{1811-1818}$ within the A3 domain of the LC of FVIII and the epidermal growth factor (EGF)-1 like domain of FIXa (Figure 17). The A2 domain is also involved in FIXa interaction via two regions ($FVIII_{558-565}$ and $FVIII_{484-508}$). These binding sites only become exposed after the cleavage at Arg[372] by thrombin of FXa. Although the affinity of the isolated A2 subunit for FIXa is rather low (K_d ~300 nM), this interaction defines the cofactor activity of FVIIIa because the A2 domain amplifies the enzymatic activity of FIXa by modulating its active site.
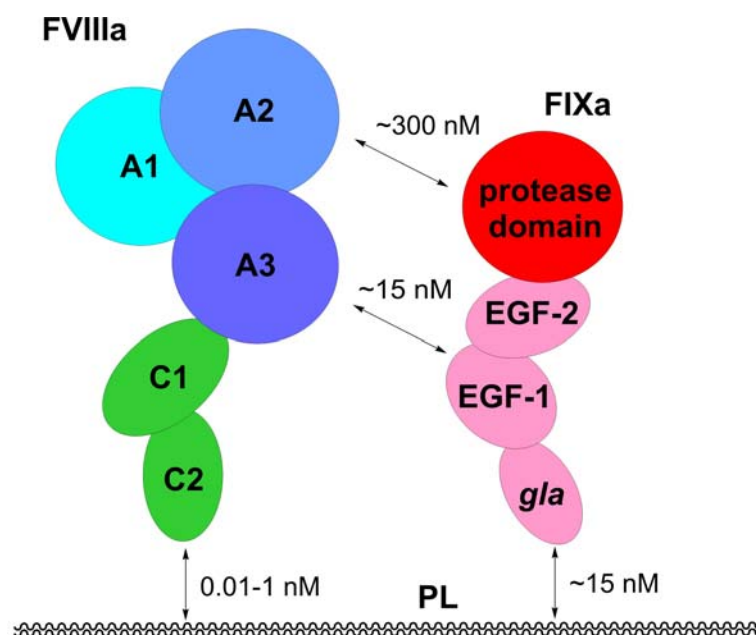
Figure 17. Schematic illustration of the hypothetic FVIIIa/FIXa complex configuration. PL: phospholipid membrane; EGF: epidermal growth factor like domain; *gla*: γ-carboxyglutamate residue.

In a first attempt to further elucidate the structure of FVIII, a homology model for the A domains of FVIIIa, based on the crystal structure of human plasma copper-binding protein ceruloplasmin (hCp),[101] which shares approximately 34% sequence identity with the A domains of FVIII, has been reported by Pemberton *et al.*.[102] This study let suggest that the FVIIIa A domains are most likely arranged in a triangular manner like in hCp, a view also supported by an engineered FVIII A2-A3 disulfide-bond.[103] This first structural model is in agreement with numerous biochemical data including naturally occurring mutations at the A1–A2 and A1–A3 interfaces.[104] The recent X-ray structure of inactivated bovine FVa (biFVa) further supports the notion that hCp is the appropriate template to model the A domains of FVa or FVIIIa.[105] A crystal structure of the membrane-binding C2 domain and models of the C1 domain have been reported. The different FVIIIa domains were fitted into a low-resolution three-dimensional density map, obtained by electron microscopy (EM), to give an overall picture of the molecule anchored into a membrane surface.[106] These data indicated that only some loops of the C2 domain were directly interacting with the phospholipids. However, the role of the C1 domain with regard to membrane binding is under debate.[107-109] Based on these data and on the crystal structure of FXIa,[110] several models for FVIIIa/FIXa complex have

been reported so far,[79,108,111,112] but the exact structure and the arrangement of FVIIIa domains remain unclear.[108]

1.1.4   FVIII production and purification

The purification of FVIII remains a challenging task. It involves a complex sequence of different purification techniques such as affinity chromatography,[113] ion-exchange chromatography and virus inactivation.[67,114-120] Today, all recombinant FVIII preparations and many plasma-derived FVIII products are purified *via* immunoaffinity chromatography employing monoclonal antibodies (mAbs) as ligands.[42,121,122] Nevertheless, the use of protein ligands in affinity chromatography is not only very expensive but also limited by several other factors.[123-126] Antibodies are known to be eluted along with the product contaminating or inactivating it or even evoking immune responses.[114,118,126] As biologically derived products, they show lot-to-lot variation and they may be contaminated with *e.g.* host DNA, viruses or prions which can be transfused to the product.[125] Their low stability shortens the column life and they suffer from low binding capacities, limited life cycles and low scale-up potential.[123,125,126] Moreover, because of the very strong binding of antibody ligands to FVIII, harsh conditions are required for elution of the protein which can harm both the target protein and the ligand.[127]

Synthetic ligands like peptides had so far only limited use in affinity separation. However, the introduction of combinatorial libraries has expanded the repertoire of peptide-based affinity ligands.[128] Two independent groups recently reported the development of oligo- and polypeptides as affinity ligands for factor VIII. Kelley *et al.*[129,130] described the isolation of a 27 amino acid sequence using phage display techniques. The cyclic polypeptide is currently used in the manufacturing of ReFacto AF (Wyeth), a third-generation product, currently in clinical trial.[119] Another promising result was reported by the group of Jungbauer.[131,132] They found a series of octapeptides with high affinity towards FVIII, derived from a combinatorial library using spot technology on cellulose sheets. The immobilized ligands could be used to purify FVIII from diluted plasma.

Nevertheless, the application of oligo- and polypeptides is associated with several problems restricting their use, above all their high susceptibility towards enzymatic degradation.[123,126] This significantly limits their application as raw materials such as serum or cell culture extracts contain proteases. A degradation of the ligands, covalently bound to the column medium, may rapidly lead to inefficiency and reduced selectivity and consequently shorten the life of the expensive affinity column. Furthermore, peptides, although cheaper than antibodies, are still quite cost-intensive and not trivial to produce in large scale, as they are typically synthesized on solid phase and purified by HPLC.

Even so, peptidic ligands are promising lead structures for the development of small unnatural molecules. Such compounds have the potential to reduce production costs and to improve the safety of current and future FVIII products. The present study describes the systematic downsizing of an octapeptidic FVIII ligand into a small peptidomimetic ligand. This novel ligand is protease-resistant and binds FVIII with high affinity. Using this ligand, FVIII of high purity was isolated from a complex mixture containing contaminant proteins in vast excess. Moreover, a stereoselective straightforward solution synthesis was developed allowing cost-effective production of the ligand in preparative scale.

1.1.5　General synthetic aspects: Solid-phase peptide synthesis

Modern solid-phase peptide synthesis (SPPS) is a powerful tool for lead structure optimization as it offers the opportunity to synthesize large libraries of compounds in a short time.[133-137]

Peptide chemistry and synthesis have gone through dramatic changes since T. Curtius[138] and E. Fischer[139] have synthesized the first simple peptide derivatives. The interest in preparing these chains of amino acids linked by amide bonds stemmed from the observation made by F. Hofmeister[140] and E. Fischer,[141] that proteins are polymers consisting of amino acids. Although methods for the coupling of two amino acids were available, it was due to failures in the development of applicable protecting groups that substantially delayed further progress in peptide chemistry.[139,142] A first breakthrough occurred in 1932 when M. Bergmann introduced the benzyloxycarbonyl (Boc) protecting-group.[143] A further milestone was

marked by R. B. Merrifield in 1963 with the development of the automated peptide synthesis on solid support, a copolymer of styrene cross-linked with 1-2% divinyl-benzene.[133,134]

The SPPS technique substantially facilitates the practical peptide synthesis procedure, because the anchoring of the *C*-terminal amino acid to the insoluble support allows the use of an excess of amino acids and coupling reagents, which enables almost quantitative yields for the coupling steps of small peptides. Furthermore, after reaction, coupling reagents and by-products can be removed by simple filtration.

Scheme 1. *General procedure for solid-phase peptide synthesis (SPPS) following Fmoc-strategy.*
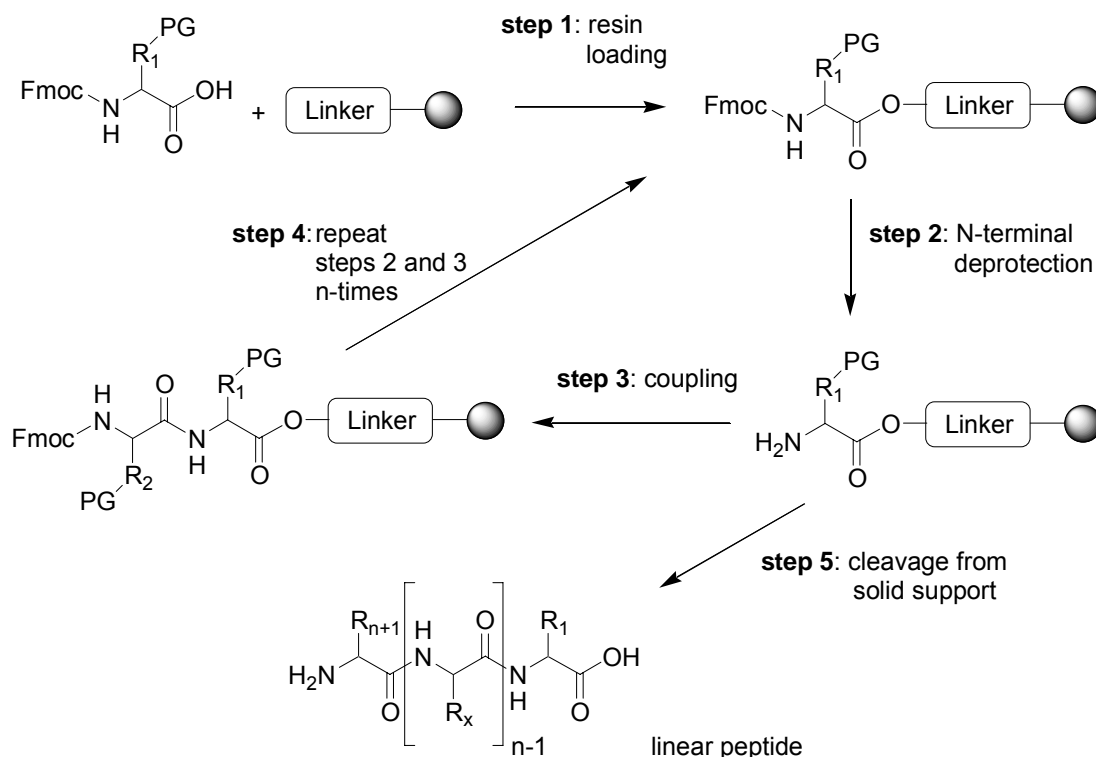
The synthesis of peptides longer than two amino acids requires the utilization of orthogonal temporary and permanent protecting groups.[144] Among others,[145,146] the Boc-strategy[133,134] and the later developed 9-fluorenylmethoxycarbonyl (Fmoc)/*t*-Bu-strategy[135,137,147] are most prominent today. The Fmoc/*t*Bu-strategy, which has proved to be especially practicable in combination with SPPS (Scheme

1), was used for the synthesis of all peptidic ligands described in the following chapters.

In modern Fmoc SPPS, the *C*-terminal properties of a peptide can easily be determined by the choice of the appropriate linker. The linkers employed for the synthesis of peptidic ligands in this work are summarized in Figure 18: The trityl chloride linker[148] (1) was used for the synthesis of peptide carboxylic acids and the Sieber amide linker[149] (2) was used for the synthesis of peptide amides. Besides other coupling methods such as the azide process,[138] acid chlorides,[136] acid fluorides,[150] mixed- and symmetrical anhydrides,[151] or nitrophenyl- and penta-fluorophenyl active esters,[146,152] the use of *in situ* activated amino acids became very popular, also because this method is very compatible with automated synthesis.
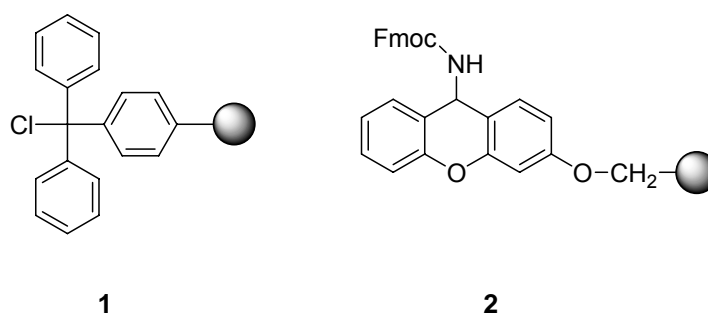
Figure 18. Linkers employed for the synthesis peptidic ligands: 1 trityl chloride linker. 2 Sieber amide linker.

Originally, carbodiimides such as dicyclohexylcarbodiimide (DCC) (Figure 19, A) have been used for activation,[153] however due to low solubility of the formed dicyclohexylurea and because amino acids were especially prone to racemization,[154] it has been mostly displaced by other coupling reagents such as *O*-(7-azabenzotriazol-1-yl)-*N*,*N*,*N'*,*N'*-tetramethyluronium hexafluorophosphate (HATU) or *O*-(benzotriazol-1-yl)-*N*,*N*,*N'*,*N'*-tetramethyluronium tetrafluoroborate (TBTU) (Figure 19, A).[155-162] Racemization could be further reduced by addition of additives (*e.g.* 1-hydroxybenzotriazol (HOBt) or 1-hydroxy-7-azabenzotriazole (HOAt); Figure 19, B),[154,163-166] and the use of sterically hindered and weak bases such as 2,4,6-collidine (Figure 19, C).[167,168]
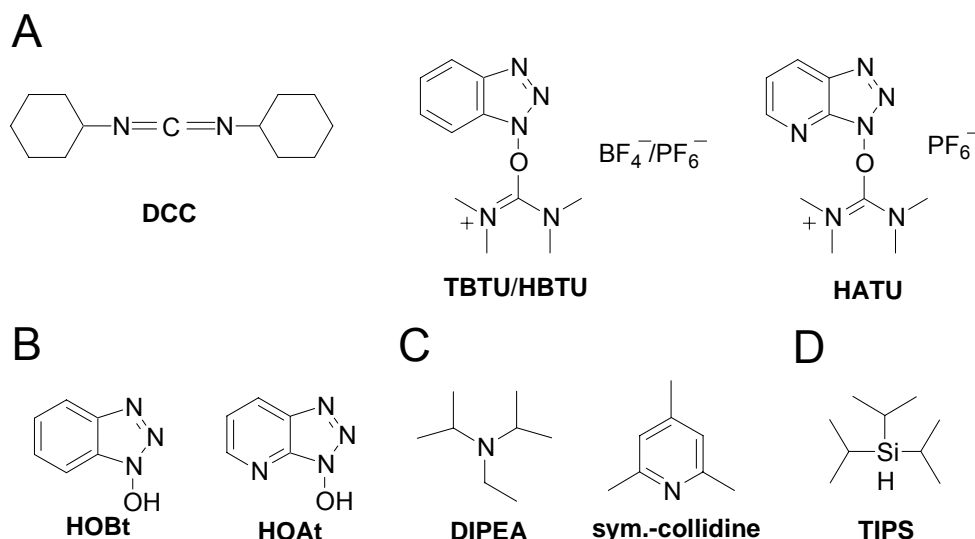
Figure 19. Coupling reagents (A), coupling additives (B), sterically hindered bases (C) and scavengers (D) that were used for peptide synthesis (with the exception of DCC and HBTU).

In Fmoc/*t*-Bu SPPS, deprotection of the temporary protecting group Fmoc is carried out with 20% piperidine in *N*-methylpyrrolidinone (NMP) (v/v).[135] For the final cleavage of the peptide from solid support and simultaneous deprotection of the permanent protecting groups a mixture of trifluoroacetic acid (TFA) and suitable scavengers is used. For this work, the use of side chain protecting groups was limited to triphenylmethyl- (Trt) at Cys, Gln, Asn and His, *tert*-butyloxycarbonyl- (Boc) at Trp and Lys, *tert*-butyl (*t*-Bu) at Ser, Thr, Tyr, Glu and Asp and 2,2,4,6,7-pentamethyldihydrobenzofuran-5-sulfonyl- (Pbf) at Arg. Triisopropylsilane (TIPS) has proved to be especially suitable as scavenger because it irreversibly hydrates carbocations and is easy to remove.[329,330]

1.2 Systematic lead optimization and minimization: From an octa-peptide to an unnatural dipeptide

In advance: The biochemical experiments within this project were mainly performed by Dr. A. Khrenov in the laboratories of Prof. E. L. Saenko (University of Maryland; Baltimore/USA). Further studies were performed by Dr. A. Benhida, Dr. S. Grailly in the laboratories of Prof. J.-M. Saint-Remy (University of Leuven, Leuven/Belgium), by Dr. R. Schwaab in the laboratories of Prof. J. Oldenburg (University of Bonn, Bonn/Germany), by Dr. N. Beaufort in the laboratories of PD Dr. V. Magdolen as well as by B. Laufer from our group. The quantitative binding data of all compounds are summarized in the Supplementary Data 4, page 246ff.

1.2.1 Preliminary studies. Development of the binding assay and selection of the lead structure

For measurement of the FVIII binding ability of the ligands, a microbead assay based on Jungbauer's procedures[131,132] was developed in which the binding of ^{125}I-labeled pdFVIII to the immobilized ligands is measured. The affinity resin Toyopearl AF-Epoxy-650M (Tosoh Bioscience, Stuttgart, Germany) was chosen as solid support giving best binding results and enabling a chemoselective immobilization of the peptides via a cysteine residue.

Kinetic studies of the immobilization reaction gave that the maximal loading density is reached after two days of incubation, independent of the peptide sequence and the amounts of peptide used (see Supplementary Data 3, page 244). This time frame is also required for the hydrolysis of unoccupied epoxy groups. After scanning various octapeptides from Jungbauer's libraries[131,132] the ligand EYHSWEYC (3) was selected as the most promising lead candidate binding ~50% of the applied FVIII at a loading density of 10.3 µmol per mL resin. The applied FVIII concentration of about 0.7 nM let suggest a subnanomolar affinity for FVIII. Beside its high affinity to pdFVIII, the peptide proved to bind B domain-deleted (BDD)-

rFVIII as well as full-length rFVIII (FL-rFVIII) with similar affinity (see Table 7 below). This was an important feature with respect to the goal of developing a ligand with general applicability. The introduction of an additional spacer molecule (*e.g.* 6-amino hexanoic acid, Aha) did not influence the binding ability (see ligand 4 in Figure 21 below), indicating that the peptide does not bind into a deep binding pocket rather than to the surface of factor VIII.[169]

Therefore, it was decided to stay with the micro-beads binding assay and the studies were performed with the immobilized ligands, since the binding of the ligand to FVIII might be significantly affected by the solid support itself or by the presentation of the ligand on the resin surface. As a consequence, the measured effects were the combined results of both, the modified sequence itself and influences coming along with changes of *e.g.* the loading densities and/or an altered presentation of the ligands on the resin surface. This made the systematic combinatorial design more complex but gave directly the practical binding results of the affinity material, ready to use.

1.2.2   Optimization of the lead octapeptide EYHSWEYC (3)

To gain basic information about the importance of each amino acid in the sequence to binding, an Ala- and a D-amino acid scan were carried out for ligand 3. In the Ala-scan the amino acids were subsequently replaced by alanine, thereby deleting the side chain moiety of the entire amino acid but conserving the chiral information. This experiment (see dark grey bars in Figure 20 for relative binding data) indicated a *C*-terminal core binding sequence which was already proposed by Pflegerl *et al.* before.[132]

Especially the amino acids Trp^5, Glu^6 and Tyr^7 were found to be highly important for efficient pdFVIII binding, as the corresponding substitutions to alanine led to a great decrease of the FVIII binding affinity. In addition the amino acid Tyr^2 proved to be of importance, while the Ala-substitution of Glu^1 did not greatly alter the affinity toward FVIII and the side chain residues of His^3 and Ser^4 even seemed to be unfavorabe for efficient binding. As expected, the peptide with Cys^8 replaced by Ala practically did not immobilize to the resin resulting in FVIII binding similar to

that of uncoated control resin and proving the high selectivity of the immobilization *via* the cysteine sulfur.[169]

In the D-amino acid scan no significant change in binding affinity was observed for any of the ligands (see light grey bars in Figure 20). These minor effects of structural modifications were surprising and might be due to the high flexibility of the linear peptide which enables easy structural adjustment to fit into the FVIII binding site.
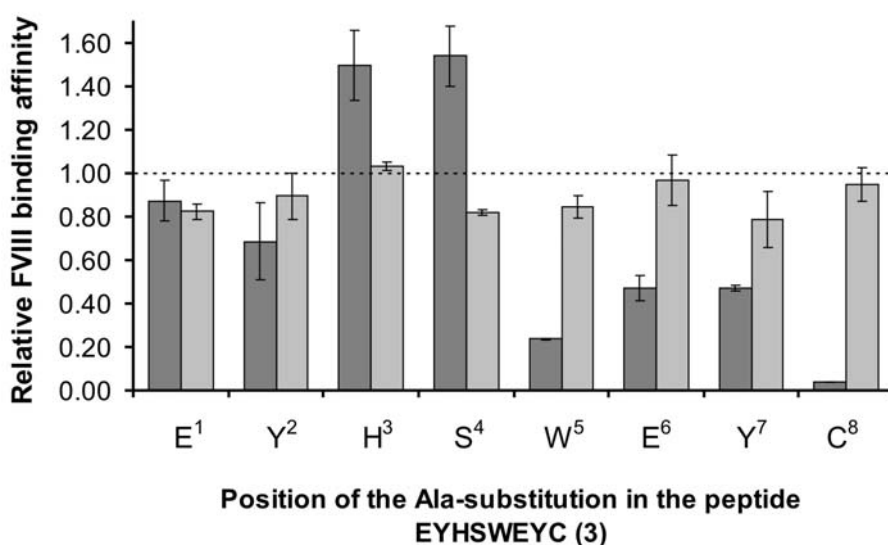
Figure 20. Influence of Ala- and D-amino acid substitutions in peptide 3 (EYHSWEYC) on the pdFVIII binding affinity. Dark grey bars denote Ala replacements, light grey bars denote D-amino acid replacements. Compound numbers: AYHSWEYC (6); EAHSWEYC (7); EYASWEYC (8); EYHAWEYC (9); EYHSAEYC (10); EYHSWAYC (11); EYHSWEAC (12); EYHSWEYA (13) eYHSWEYC (14); EyHSWEYC (15); EYhSWEYC (16); EYHsWEYC (17); EYHSwEYC (18); EYHSWeYC (19); EYHSWEyC (20); EYHSWEYc (21); lower case letters denote D-amino acids.[169]

Although alanine replacement and D-scanning experiments were useful for identifying important side chains and structural restrictions, they provided little information about the nature of the interactions. Therefore, the effects of single amino acid substitutions with natural and unnatural amino acids providing an isofunctional or isosteric frame, comparable spatial space requirement or contrasting properties were explored. Binding of FVIII to selected derivatives is presented in Figure 21.

As mentioned above, the substitution of Glu[1] by Ala resulted in a slight decrease of FVIII binding. Similar results were also found for the substitutions by Gln and

Asp, whereas a replacement with the sterically demanding Val residue resulted in a great decrease of binding ability. Furthermore it was proven by *N*-terminal acetylation (ligand 5 in Figure 21) that the *N*-terminal charge as well is not important for efficient binding, as a corresponding mutant showed equal binding properties. Altogether these results were promising in terms of a desired minimization of the peptide sequence.[169]
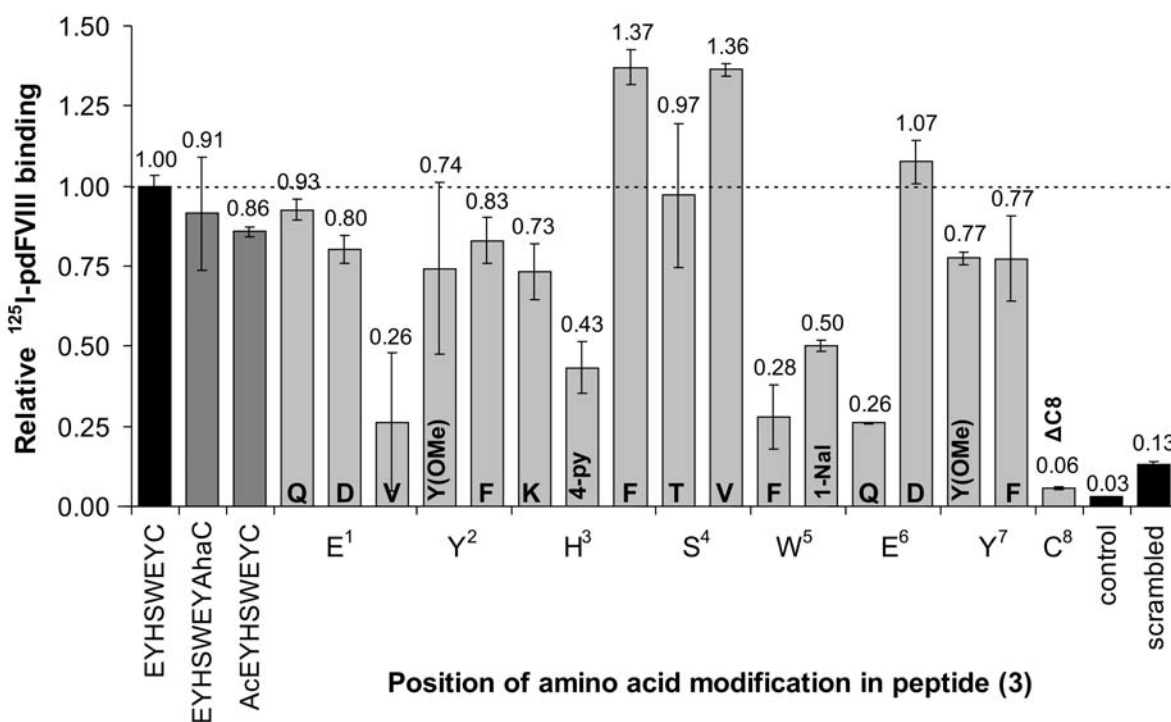
Figure 21. Examples for modifications in the sequence of peptide 3 (EYHSEWYC; reference set as 1.00) and their influence on the FVIII binding affinity. Aha: 6-aminohexanoic acid; 4-py: 4-pyridylalanine; 1-Nal: 1-naphthylalanine; ΔC8: EYHSWEY; control: uncoated resin;.Compound numbers: EYHSWEY(Aha)C (4), AcEYHSWEYC (5), QYHSWEYC (22), DYHSWEYC (23), VYHSWEYC (24), EY(OMe)HSWEYC (25), EFHSWEYC (26), EYKSWEYC (27), EY(4-py)SWEYC (28), EYFSWEYC (29), EYHEWEYC (30), EYHVWEYC (31), EYHSFEYC (32), EYHS(1-Nal)EYC (33), EYHSWQYC (34), EYHSWDYC (35), EYHSWEY(OMe)C (36), EYHSWEFC (37),EYHSWEY (38), scrambled peptide: ECYYEHWS (39).[169]

Tyr[2], in contrast, was found to be quite important for FVIII binding. To determine the nature of its interactions, Tyr[2] was replaced by phenylalanine and *O*-methylated tyrosine. Both derivatives were found to result in a similar loss of FVIII binding ability (~20%). This indicates that Tyr[2] acts as a hydrogen bond donor *via* its hydroxyl group.

Following the results of the Ala-scan, the positions His[3] and Ser[4] should allow further optimization since both side chain residues seemed to be unfavorable for efficient FVIII binding. In case of the histidine residue, this was probably due to the positive charge of the side chain residue, as the substitution by other basic amino acids like 4-pyridylalanine (4-py) and lysine resulted in a further decrease of the binding affinity. In contrast, replacing His[3] by phenylalanine improves the ability to bind FVIII by almost 40% (see Figure 21).[169]

For the Ser[4] residue the reduced binding affinity of 3 to the corresponding Ala-mutant refers to the polar hydroxyl side chain functionality as the more hydrophobic derivatives, especially the Ala and the Val mutant, led to increased binding properties. Modifications in the *C*-terminal part of the molecule proved that this moiety is critical for efficient FVIII binding. All of the mutants at Trp[5] showed at least 50% reduction in FVIII binding ability. Tyr[7], like Tyr[2], could not be replaced by phenylalanine and *O*-methylated tyrosine without loss of binding affinity indicating an important hydrogen bridge to this residue. Glu[6] could only be replaced by aspartic acid. The negative charge of the carboxylic group was found to be essential as shown by the reduced binding affinity of the corresponding glutamine mutant (see Figure 21).[169]

Consequently, numerous other substitutions and combinations of amino acid replacements, which gave positive results before, were screened, but no significant improvements of the FVIII binding ability and no additive effects could be gained. A selection of prepared ligands is summarized in the Supplementary Data 5 (page 248). It should be emphasized, that most data presented in there do only allow a rough estimation of the ligands binding properties, as the ligand loading has not been determined for all compounds). Consequently, the attempts to optimize the octapeptidic sequence were stopped and the further work was focused on the systematic minimization of the ligand length.

1.2.3 First approach in minimizing EYHSWEYC (3): Development of hexapeptidic FVIII ligands

The *N*-terminal glutamine, as expected, could be deleted without losing binding ability (see Figure 22 for relative and Table 4 for absolute binding data). In the resulting heptapeptide 40, however, the substitution of His^3 by phenylalanine (ligand 41), which resulted in a promising gain of the FVIII binding ability in 3 (see Figure 21), had no effect on FVIII binding.

Additional truncation of the peptide by removing the important Tyr^2 residue (hexapeptide 42) accordingly resulted in a noticeable (>30%) loss of binding affinity. Hence, to further reduce ligand 40 while conserving the Tyr^2 residue, the *C*-terminal cysteine linker was placed in the position of the unimportant His^3 residue to obtain the hexapeptide YCSWEY (43). This ligand proved to have a high affinity towards FVIII, binding 62% of the applied protein at a loading density of 17.0 µmol per mL.[169]
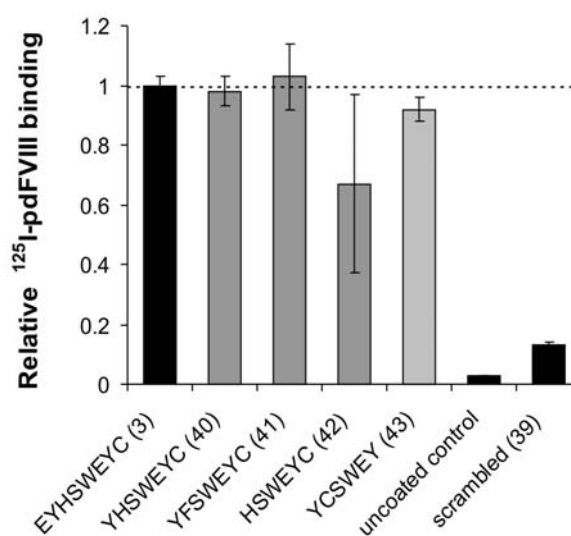
Figure 22. Downsizing of the octapeptidic ligand 3 (reference set as 1.00) to the hexapeptidic ligand YCSWEY (43); control: uncoated resin.[169]

To optimize 43, various substituents were introduced: single amino acid replacements showed that Glu^6 can be substituted by Asp (ligand 44) without effecting the binding affinity while the substitution of Trp^5 by the more hydrophobic 1-naphthyl alanine (1-Nal) residue (ligand 45) led to a great loss of FVIII binding ability (Figure 23) indicating again the critical role of this residue. Substitutions of Ser^4 indicated the preference of a more hydrophobic residue in this position as described above. Ala (ligand 46), Thr (ligand 47) as well as Val (ligand 48) residues gave remarkable improvements of binding affinity with the best results for 48 binding the applied FVIII almost completely. Surprisingly, the corresponding substitutions of Ser^4 in

combination with an Asp residue at position 5 (ligand 49-51) exhibited lower binding affinity.[169]

Table 4. Absolute FVIII binding data for different ligands: minimization of octapeptide 3.[169]

Sequence	no.	Ligand loading (μmol/mL)	^{125}I-pdFVIII binding (%)[a]
EYHSWEYC	3	10.3 ± 0.4	50.2 ± 1.6
YHSWEYC	40	14.0 ± 0.7	61.3 ± 3.2
YFSWEYC	41	15.2 ± 1.1	66.8 ± 7.2
HSWEYC	42	12.7 ± 0.6	39.8 ± 16.8
YCSWEY	43	17.0 ± 0.5	62.0 ± 2.4
control[b]	-	–	01.6 ± 0.1
scrambled[c]	39	10.3 ± 0.1	06.5 ± 0.5

[a] % of total applied material; [b] uncoated resin;
[c] scrambled sequence: ECYYEHWS (39)

Achieving highly potent FVIII ligands, an effort was made to improve the resistance against proteolytic degradation by the synthesis of the corresponding fully retro-inverso derivatives, which generally provide an enhanced enzymatic stability due to their all-D sequence.[170-174] If the hydrogen bonding and the secondary structure is mirrored, the original side chain orientation remains conserved but the N- and the C-termini and the direction of the peptide bonds are inversed.[175] It was assumed that neither the peptide bonds nor the termini are involved in target interactions.
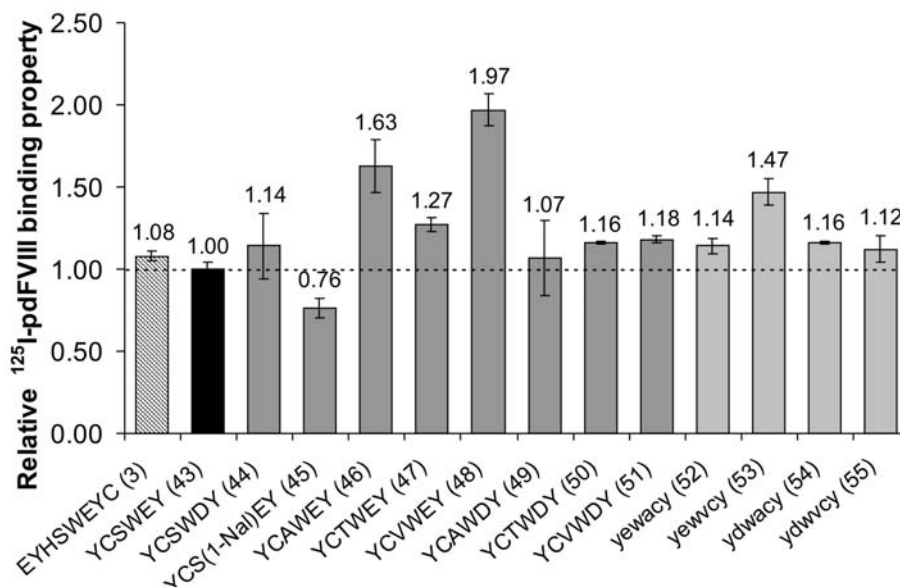
Figure 23. Normalized ^{125}I-pdFVIII binding of mutants of ligand 43 (black bar); dark grey bars represent all-L derivatives, light grey bars represent fully retro-inverso ligands (1-Nal: 1-naphthylalanine; lower case letters denote D-amino acid residues).[169]

Indeed, the retro-inverso peptides 52-55 worked fine and showed only a slightly reduced binding affinity (see Figure 23 for relative and Table 5 for quantitative binding data), thus providing highly potent factor VIII ligands with improved enzymatic stability as shown below.

However, with regard to the ultimate goal to develop a novel method for FVIII purification which is a real improvement in terms of cost efficiency this kind of compound was not completely satisfying. The goal was to create a novel kind of ligand which is easy to synthesize in large scale in solution thereby avoiding expensive techniques like solid phase synthesis and HPLC purification to reduce production costs. This is practically not possible for the hexapeptidic ligands. In addition, the unnatural D-amino acid building blocks used for the synthesis of the fully retro-inverso derivatives make this kind of ligand rather expensive.

Table 5. Optimization of ligand 43: loading density and absolute FVIII binding data for various mutants of ligand 43.[169]

Sequence	no.	Ligand loading (µmol/mL)	^{125}I-pdFVIII binding (%)[a]
YCSWEY	43	17.0 ± 0.5	62.0 ± 0.4
YCSWDY	44	16.7 ± 1.0	69.8 ± 12.2
YCS(1-Nal)EY	45	12.7 ± 0.6	35.3 ± 3.0
YCAWEY	46	12.2 ± 0.6	72.1 ± 7.2
YCTWEY	47	14.9 ± 0.7	70.7 ± 2.4
YCVWEY	48	12.9 ± 0.6	94.1 ± 4.7
YCAWDY	49	19.3 ± 1.0	72.0 ± 15.5
YCTWDY	50	17.6 ± 0.0	73.6 ± 0.7
YCVWDY	51	16.5 ± 0.8	72.0 ± 1.2
yewacy	52	12.8 ± 0.6	53.6 ± 2.5
yewvcy	53	14.1 ± 0.7	77.0 ± 4.2
ydwacy	54	18.0 ± 0.9	75.1 ± 0.6
ydwvcy	55	18.5 ± 0.9	73.4 ± 5.6
control[b]		–	1.6 ± 0.1
scrambled[c]	39	10.3 ± 0.1	6.5 ± 0.5

[a] FVIII binding is given as percentage of total bindable material; [b] uncoated resin; [c] scrambled sequence: ECYYEHWS; 1-Nal is 1-naphthylalanine.

1.2.4 Second approach in minimizing EYHSWEYC (3): Development of the small molecule FVIII affinity ligand (3-IAA)Eψ[CH$_2$NH]YC (69)

The next goal was the reduction of the initial octapeptide EYHSWEYC (3) down to its *C*-terminal core binding sequence WEYC (57, Figure 24). As mentioned above, Glu^1 could be deleted without reducing the FVIII affinity but the truncation of the Glu^1-Tyr^2 fragment resulted in a 30% loss. However, the larger fragments Glu^1-Tyr^2-His^3 as well as Glu^1-Tyr^2-His^3-Ser^4 could be deleted without additional loss of FVIII binding (peptides 56 and 57, respectively). Considering the great simplification of the sequence in 57 the 30% reduced affinity seemed acceptable to proceed with optimizing this new lead structure.[169]
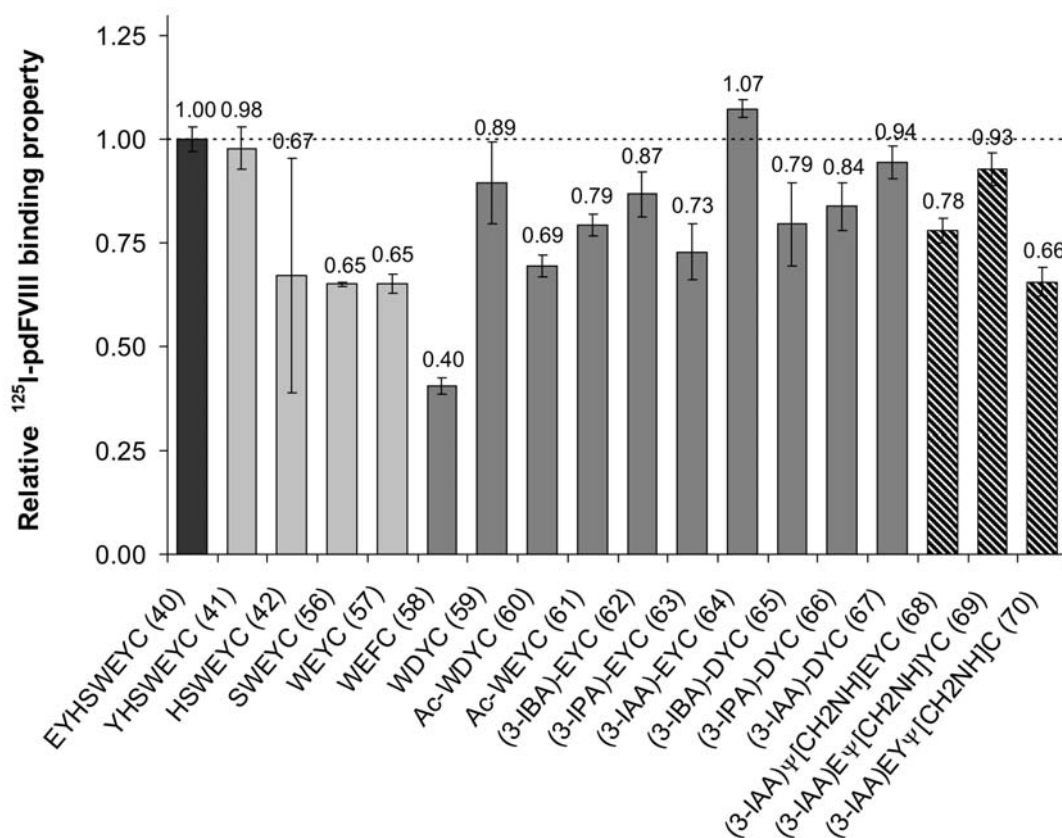
Figure 24. Relative binding data of minimized mutants of ligand 3. Stepwise minimization of 3 (black bar) to its core binding motive WEYC (57) (light grey bars), side chain optimization of 57 (dark grey bars) and backbone modification of 64 (dashed bars).[169]

39

Scanning the minimized lead sequence Trp[5]-Glu[6]-Tyr[7]-Cys[8], it was found that Tyr[7] can not be substituted by Phe but Glu[6] can be substituted by Asp confirming the results described above. Therefore, the work was continued with both alternative residues in position 6, Glu and Asp. In order to optimize the critical Trp[5] residue, the *N*-terminal amino function was initially acetylated. This modification did not significantly alter the binding affinity of the corresponding tetrapeptides 60 and 61 (see Figure 24) indicating that the amino terminus might not be necessary for efficient binding.[169]

Consequently, Trp[5] was substituted by 3-indolylpropionic acid (3-IPA), which corresponds to a truncation of the amino function of tryptophan. This modification led to a slight increase of the affinity towards FVIII in both sequences, (3-IPA)EYC (63) and (3-IPA)DYC (66). Thus, the length of the side chain was varied to optimize the position of the indole residue by substituting 3-IPA by 3-indolylacetic acid (3-IAA) and 3-indolylbutyric acid (3-IBA). This experiment indicated a tendency of better binding properties with shorter side chain for the Asp containing derivative but a significant improvement could not be achieved (compare ligands 65-67 in Figure 24). In contrast, for the corresponding derivatives with a glutamic acid in position 6 (ligands 62-64) the substitution of 3-indolylpropionic acid by 3-indolyl-acetic acid (ligand 64) led to a 50% increase of the affinity towards FVIII, binding 77% of the applied ^{125}I-pdFVIII at a ligand loading of 23 µmol/mL (Table 6).[169]

68	X = CH$_2$,	Y = CO,	Z = CO
69	X = CO,	Y = CH$_2$,	Z = CO
70	X = CO,	Y = CO,	Z = CH$_2$
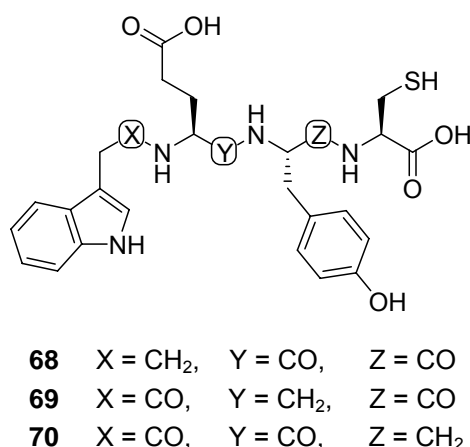
Figure 25. Structures of the small molecule factor VIII ligands 68-70 with modified peptide bonds.

After successful minimization, the goal was now to optimize the resistance of the ligand against proteolytic degradation. Hence, all peptide bonds in 64 were subsequently substituted by a reduced peptide bond (CH_2-NH) producing ligands 68-70 (Figure 25). These unnatural peptides were synthesized on solid phase[133,134] using Fmoc/t-Bu-strategy[135,150,176] on TCP resin[148] and HOBt/TBTU[156,165] as coupling reagents. The CH_2-NH bonds were introduced *via* a reductive alkylation following a procedure of Krchnak *et al.*.[177] Exploring the binding properties of the unnatural ligands, it was found that the substitutions of the *N*-terminal peptide bond connecting 3-IAA and Glu[6] (compound 68) or of the *C*-terminal peptide bond connecting Tyr[7] and Cys[8] (compound 70), both led to a significant loss of affinity, indicating that these peptide bonds are involved in FVIII interactions.[169]

Table 6. Absolute binding data of selected small molecule FVIII ligands.[169]

Sequence	no.	Ligand loading (μmol/mL)	^{125}I-pdFVIII binding (%)[a]
WEYC	57	22.7 ± 0.5	46.4 ± 1.7
WDYC	59	20.5 ± 1.0	62.8 ± 6.9
(3-IAA)EYC	64	23.4 ± 1.2	76.7 ± 1.6
(3-IAA)DYC	67	24.3 ± 0.7	67.7 ± 2.8
(3-IAA)ψ[CH_2NH]EYC	68	18.4 ± 0.9	53.7 ± 1.9
(3-IAA)Eψ[CH_2NH]YC	69	20.8 ± 1.0	65.3 ± 3.0
(3-IAA)EYψ[CH_2NH]C	70	16.0 ± 0.8	43.4 ± 2.3

[a] FVIII binding is given as percentage of total bindable material.

In contrast, the modification of the central peptide bond connecting Glu[6] and Tyr[7] (compound 69; Figure 25) had little effect on the FVIII binding (see Figure 24 and Table 6). As the Glu-Tyr bond might be cleaved by matrix metalloproteinase-3 (MMP-3), this substitution may significantly contribute to an enhanced resistance against enzymatic degradation.[178] Due to its high affinity and the expected very high enzymatic stability, the peptidomimetic ligand 69 was chosen as the most promising lead structure for further evaluation.

1.3   Solution synthesis of (3-IAA)Eψ[CH₂NH]YC (69)

Altogether, the peptidomimetic **69** fulfilled all requirements for a FVIII affinity ligand and was found to be the most promising candidate for further evaluation. Hence, a solution phase synthesis was developed for **69** to allow a cost efficient production in preparative scale for further experiments.[169]

Scheme 2. *Synthesis of the* N-*substituted glutamol* **76**. *[a]*
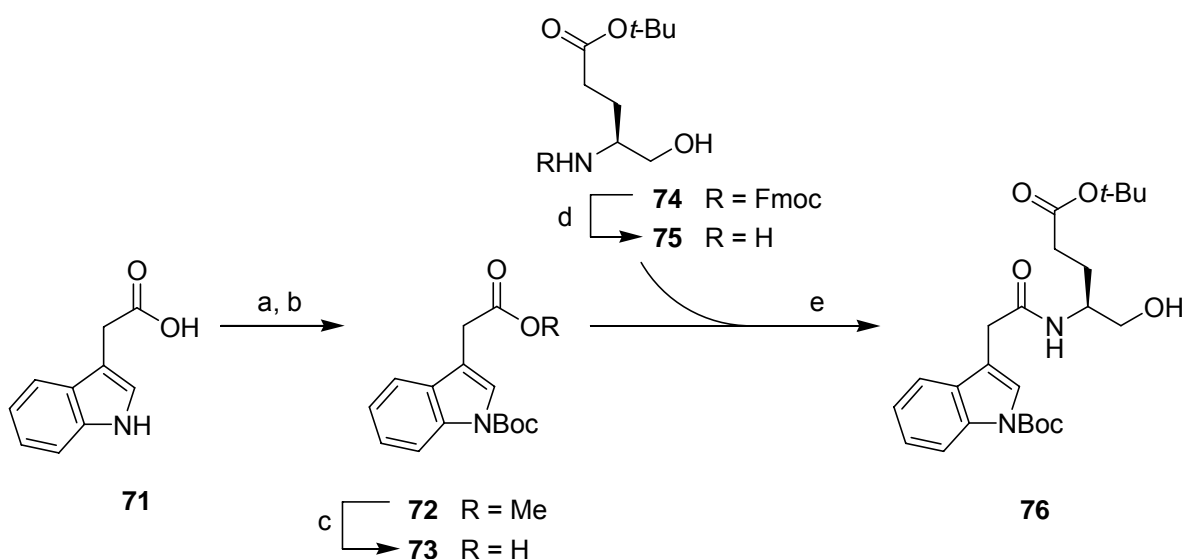
[a] Reagents and conditions: (a) SOCl₂, MeOH, 18 h, 98%; (b) Boc₂O, DMAP, acetonitrile, 4 h, 86% (two steps); (c) LiOH, THF, MeOH, H₂O, 18 h, 83%; (d) piperidine, DMF, 1h; (e) HOBt, TBTU, DIPEA, 0°C → rt, 4h, 95% (two steps).[169]

The synthesis of peptides from the *C*-terminus to the *N*-terminus is the most common strategy.[179] However, the inverse direction seemed more favorable in this special case: In peptide synthesis the cysteine side chain is most commonly protected with a trityl (Trt) group as this group is easily removable under acidic conditions.[180] In case of a *C* to *N* synthesis, Cys would be introduced in the first step. Since the Cys side chain protection group is acid sensitive, this might implicate side reactions in a multi-step synthesis that includes several washing and chromatography columns. In addition the cysteine amino acid itself is very prone to

racemize.[181] The main disadvantage of the *N* to *C* direction is the risk of racemization by oxazolone formation.[182,183] However, this requires a *C*-activated *N*-acyl-amino acid, an arrangement which is not present in the *N* to *C* procedure for the synthesis of 69 as described below.[169]

Accordingly, the synthesis was started from 3-indolylacetic acid (71). The indole nitrogen of 71 was protected with a Boc group in a three-step reaction sequence according to literature procedures (Scheme 2): 71 was transformed into its methyl ester by treating with $SOCl_2$ in MeOH and the indole nitrogen subsequently protected with a Boc group by reacting with *tert*-butyl dicarbonate and 4-dimethyl aminopyridine (DMAP)[184] in acetonitrile to achieve 72.[185-187] Saponification then produced the desired indolylacetic acid 73 with 70% overall yield. The conversion to 76 was achieved by coupling 73 to the side chain protected glutamol 75 using HOBt and TBTU as coupling reagents. 75 was readily available from commercial Fmoc-Glutamol(O*t*-Bu) (74) by treating with piperidine and could be used without further purification. For the coupling to 73 a protection of the free hydroxyl functionality in 75 was not necessary and the reaction proceeded cleanly to give the *N*-substituted glutamol 76 in 95% yield.[169]

The reduced peptide bond linking the glutamic acid- and tyrosine residue in the target compound 69 was formed by a reductive alkylation of the corresponding aldehyde 77 and commercial Tyr(*t*-Bu)OMe (Scheme 3). Unfortunately, the first experiments for the synthesis of the secondary amine 78 led to an inseparable 8:2 mixture of diastereomeric isomers due to racemization of the highly sensitive aminoaldehyde 77. It was found that this was due to the basic reaction conditions during the aldehyde formation by Swern oxidation[188,189] using the relatively strong base *N,N*-diisopropylethylamine (DIPEA).[190,191] Also the further transformation to the imine by treating with Tyr(O*t*-Bu)OMe*HCl was performed in presence of DIPEA and $MgSO_4$.[192] Racemization was completely overcome by the use of Dess-Martin periodinane oxidation[193-195] instead of Swern oxidation and preformation of the imine *in-situ* in absence of base, rapidly followed by addition of the reducing agent. This procedure gave the desired secondary amine 78 in 75% yield over two steps. The methyl ester in 78 was cleaved by saponification and the resulting free acid was coupled to Cys(Trt)O*t*-Bu*HCl[196] in the presence of HOBt/TBTU and the mild base 2,4,6-collidine to yield 79 (83% yield, two steps). Under these conditions,

no side reaction by the free secondary amine in 78 were observed due to its significantly lower reactivity compared to the primary amine in Cys(Trt)O*t*-Bu*HCl. Although the cysteine *tert*-butyl ester we used is not commercially available it was favored over the commercial methyl ester as it is readily synthesizable[196] and it allows a one-step deprotection of 79 to obtain the desired free peptidomimetic 69 under acidic conditions.[169]

Scheme 3. *Synthesis of the peptidomimetic 69.*[a]
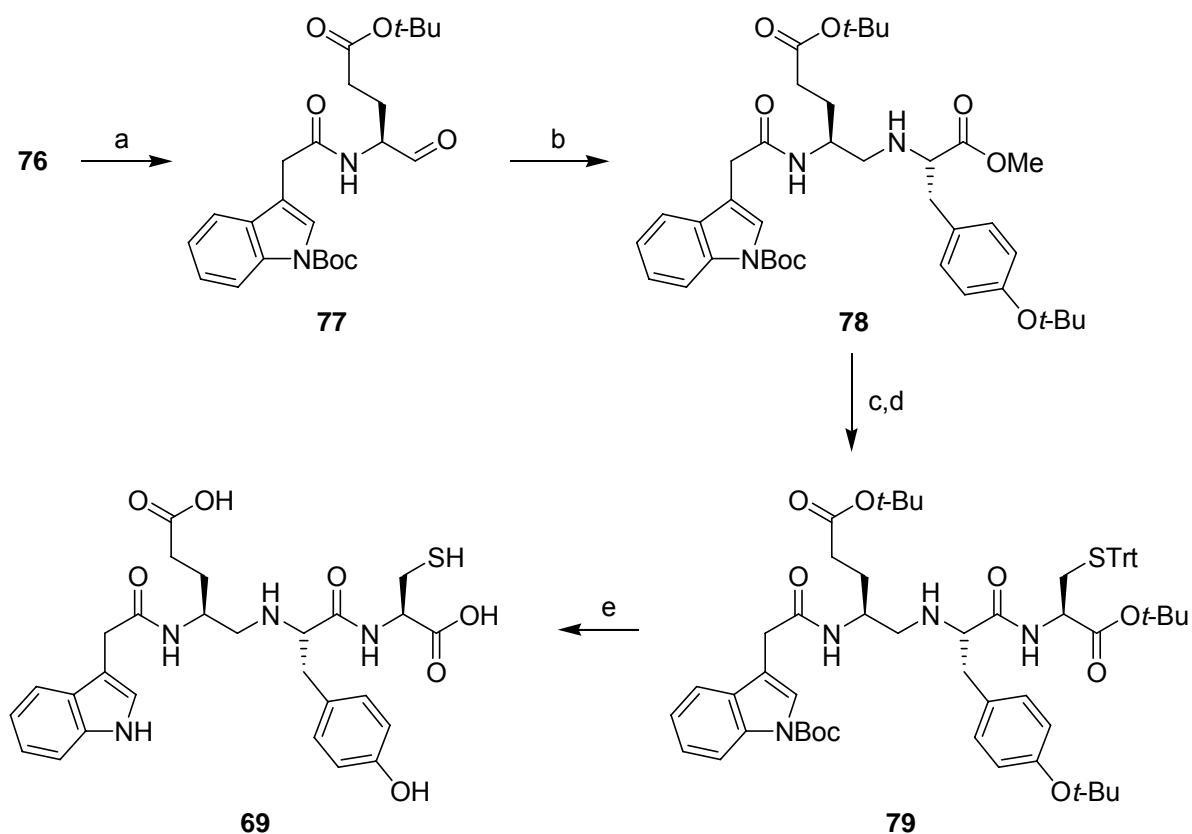
[a] Reagents and conditions: (a) Dess-Martin periodinane, DCM, 6 h; (b) 1) Tyr(*t*-Bu)OMe*HCl, MgSO$_4$, DCM, 30 min; 2) NaB(OAc)$_3$H, 18 h, 75% (two steps); (c) LiOH, THF, dioxane, H$_2$O, 1.5 h; (d) Cys(Trt)O*t*-Bu*HCl, HOBt, TBTU, 2,4,6-collidine, 10°C → rt, 18 h, 83% (two steps); (e) TIPS, H$_2$O, TFA 0% → 95%, 8 h, 98%.[169]

The final deprotection and purification is the critical step in terms of an economic production of 69. Therefore, the focus was on an optimization of the deprotection reaction in order to reduce byproduct formation to avoid a purification of the final product. The key to minimize side product formation was to avoid a sudden high concentration of *tert*-butyl cations which occurs if 79 is directly treated with the cleavage mixture TFA/TIPS/H$_2$O 95:2.5:2.5 (v/v/v).[197] Thus, the

problem was solved by suspending 79 in a vigorously stirred mixture of the scavengers water and TIPS (1:1) and slowly adding the TFA over a period of 8 hours to a final concentration of 95%. By this procedure the byproduct formation (typically 15% as determined by HPLC) was significantly reduced to obtain the final peptidomimetic 69 in 98% yield (purity >95%) after precipitation in ether/pentane. To prove the diastereomeric purity, all possible diastereomers of 69 were synthesized and analyzed by HPLC. Coinjection with 69 gave baseline separation for all diastereomers.[169]

1.4   Evaluation of biological and biochemical ligand characteristics

1.4.1   Verification of the enzymatic stability

The resistance against enzymatic degradation was determined by treating the ligands with fresh human serum (single donor). The amounts of intact ligand were determined by quantitative HPLC and HPLC-MS analysis. For this study the octapeptide 3 (EYHSWEYC) as well as the fully retro-inverso peptide 55 (ydwycy), the tetrapeptide 57 (WEYC) and the peptidomimetic 69 ((3-IAA)Eψ[CH$_2$NH]YC) were chosen.

As shown in Figure 26, the octapeptide 3 was completely degraded after three hours of incubation with serum proving its limited applicability as affinity ligand. Despite the reduced size, the tetrapeptide 57 also turned out to be very unstable in human serum.[169,198]
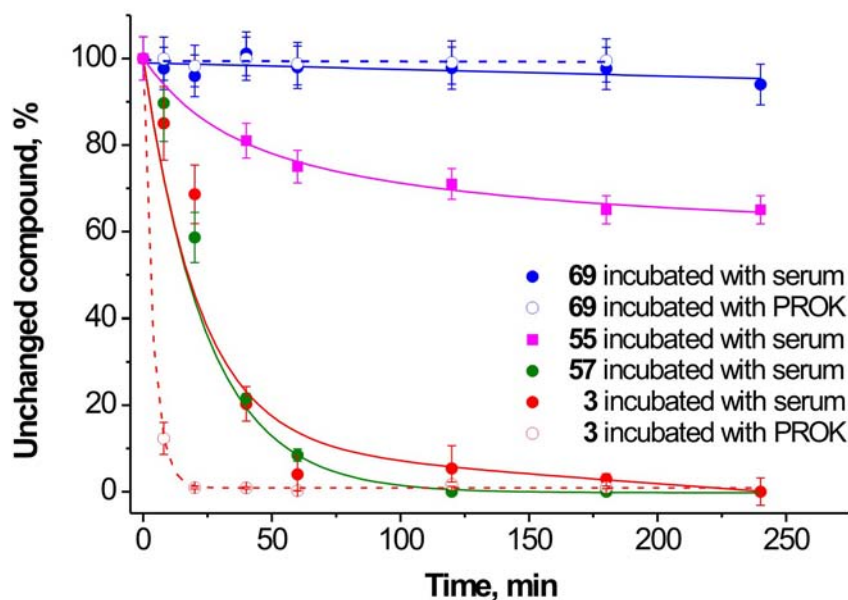
Figure 26. Determination of the stability of octapeptide EYHSWEYC (3), fully retro-inverso peptide ydwycy (55), tetrapeptide WEYC (57) and the minimized peptido-mimetic 69 against enzymatic degradation by treating with fresh human serum (single donor). PROK: Proteinase K.[169,198]

The fully retro-inverso peptide 55, as assumed, showed a significantly enhanced resistance against enzymatic degradation. Nevertheless, a slow decomposition was observed to obtain a final content of 40% unchanged ligand after three hours of treatment. This result was confirmed in an independent experiment incubating ligand 69 and 3 with Proteinase K (PROK),[199] a non-specific protease that cleaves peptide bonds at the carboxylic sides of aliphatic, aromatic or hydrophobic amino acids. As a result of exposure to a higher protease concentration compared to human serum, an even much faster degradation of ligand 3 was observed, whereas ligand 69 again proved to be unaffected by the enzyme (Figure 26).[169,198]

1.4.2 Evaluation of FVIII binding characteristics of ligand coated resins

1.4.2.1 Influence of the ligand loading on FVIII binding

The ability to capture proteins with an affinity resin greatly depends on ligand properties as well as on its concentration on the resin.[200] To determine the effects of the latter, resins with different ligand loadings were prepared for the two best small ligands, (3-IAA)EYC (64) and (3-IAA)Eψ[CH$_2$NH]YC (69), and the high binding hexapeptides 43 (YCSWEY) and 50 (YCTWDY) to measure their ability to capture FVIII (Figure 27). The initial octapeptide EYHSWEYC (3) as well as the tetrapeptide WEYC (57) served as references.[169,198]
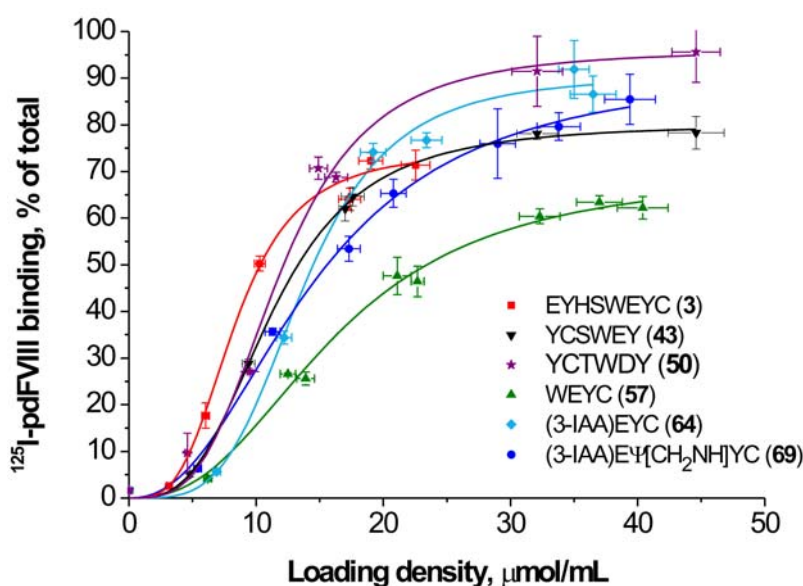
Figure 27. Effect of the ligand loading on the capture of ^{125}I-pdFVIII.[169,198]

As expected, an increase of ligand density resulted in an increase of FVIII adsorption. However, there is a minimum concentration of about 5 to 10 μmol ligand per mL resin (depending on the nature of the ligand) which is crucial for efficient binding and saturation was observed at high loading densities. The data points for each compound could be fitted by a Hill function confirming this observation. Another limit was found for the maximal reachable ligand density. Here, a significant difference between the lead octapeptide 3 and the minimized ligands 43, 50, 57, 64 and 69 was observed. While a loading density of 25 μmol/mL could not be exceeded for 3, even if applying a vast excess of ligand, the minimized compounds readily immobilized up to 40 μmol/mL. At these high loading densities, the small peptidomimetics 64 and 69 bound almost 90% and the hexapeptide 50 95% of the applied FVIII, in contrast to 3, where a maximum of 70% binding could not be exceeded.[169,198]

1.4.2.2 Binding of recombinant FVIII molecules

The different factor VIII molecules (pdFVIII, FL-rFVIII and BDD-rFVIII) vary in their structure and glycosylation.[201,202] Thus, a binding site, independent from glycosylation and outside the B domain, was a basic requirement to fulfill the goal of a broad applicability of the ligands for purification of all kinds of FVIII products.

Table 7. Binding data for recombinant factor VIII molecules.[169]

Sequence	no.	Ligand loading (μmol/mL)	^{125}I-FL-rFVIII binding (%)[a]	^{125}I-BDD-rFVIII binding (%)[a]
EYHSWEYC	3	8.8 ± 0.4	40.8 ± 0.8	35.0 ± 7.2
YCTWEY	47	16.3 ± 0.8	57.8 ± 3.7	62.9 ± 8.6
(3-IAA)EYC	64	19.2 ± 1.0	54.9 ± 6.3	49.6 ± 1.7
(3-IAA)Eψ[CH$_2$NH]YC	69	17.3 ± 0.9	53.3 ± 2.3	40.6 ± 2.3

[a] *FVIII binding is given as percentage of total bindable material.*

As mentioned above, the lead compound 3 was found to bind to such a site as it binds to various FVIII molecules with similar affinity. Minimized derivatives were also checked for their binding to these FVIII molecules and their high affinity to

FL-rFVIII as well as to BDD-rFVIII was confirmed. A selection of results is presented in Table 7.

1.4.2.3   Localization of the binding site in FVIII

To localize the binding site in FVIII of the new ligands, an epitope mapping was performed. In this experiment, the binding of the following FVIII fragments and domains to immobilized ligands was tested: HC (A1a1A2a2; FVIII$_{1-758}$), A1a1 (FVIII$_{1-398}$), a1A2a2 (FVIII$_{318-758}$), B domain, LC (FVIII$_{1637-2332}$), a3A3C1 (FVIII$_{1637-2173}$), C2 (FVIII$_{2170-2332}$).

Table 8. Mapping of recombinant FVIII epitopes. The strength of binding of ligand-coated resins to different recombinant FVIII epitopes is valuated as: (++) very strong binding; (+) significant binding; (−) no or minimal binding.[198]

Ligand	no.	HC	A1a1	a1A2a2	B	LC	a3A3C1	C2
ydwacy	54	−	−	−	−	+	−	++
(3-IAA)EYC	64	−	−	−	−	+	+	++
(3-IAA)Eψ[CH$_2$NH]YC	69	−	−	−	−	+	+	−
YCAWEY	46	+	−	+	−	+	−	−
YCTWEY	47	+	+	−	−	+	−	−
YCVWEY	48	+	−	−	−	+	−	+
ECYYEHWS	39	−	−	−	−	−	−	−

The obtained results were somewhat surprising. As shown in Table 8, the studies indicated a strong binding to the light chain of FVIII for the fully retro-inverso peptide 54 as well as the small ligands 64 and 69. Moreover, among all FVIII fragments tested, only the a3A3C1 polypeptide showed a distinct binding to ligand 69-coated resin, whereas ligand 64-coated resin strongly bound the C2 domain, and to a lesser extent the a3A3C1 polypeptide.

In contrast, the all-L hexapeptides 46, 47 and 48 were found to bind to both, the LC and the HC, however, distinct binding to shorter fragments and domains was mainly found within the HC. The scrambled peptide 39 was used as a negative

control. It did not show binding to any of the FVIII fragments, hence verifying the accuracy of the experiment.

These astonishing results may be explained by the high homology between the A domains among each other and the C domains among each other, which might result in multiple similar binding sites on FVIII. On the other hand, looking at the proposed model of FVIII (Figure 17, page 25), one could also suppose an inter-domain binding site which is differently addressed by the ligands. However, these statements are very speculative and additional experiments (*e.g.* mapping with shorter FVIII epitopes to localize the binding site more exactly) will have to be performed to explain the obtained results.

1.4.2.4 Evaluation of the strength of the FVIII-ligand interaction

To evaluate the strength of the FVIII binding to the ligand-coated resins, beads with bound ^{125}I-pdFVIII were incubated with fresh buffer solution and the release of FVIII into the buffer was measured. For this experiment, the peptidomimetic 69, as well as the tetrapeptide 57 and the octapeptide 3 were chosen.
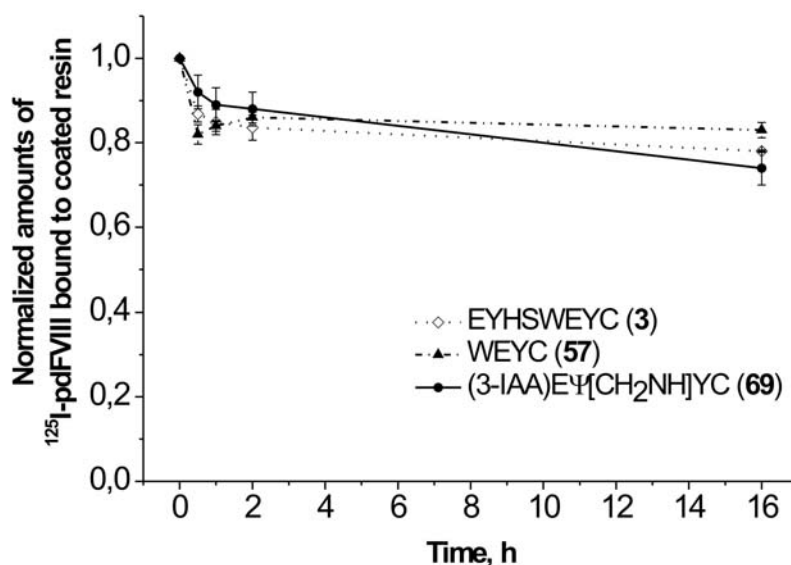
Figure 28. Spontaneous dissociation of bound ^{125}I-pdFVIII from coated resin. Ligand-coated resins with bound FVIII were incubated with fresh buffer solution for variable periods of time. The graph shows the normalized amounts of ^{125}I-pdFVIII bound to the resin as a function of the time.[198]

Figure 28 shows that only minor amounts of FVIII (~10-20%) were released within 16 h of incubation from the coated resins. The main release was observed within the first two hours which may be due to not optimally bound material or to the formation of an equilibrium between bound and free FVIII. These experiments show a high-affinity binding of FVIII to the small ligands and a very low off-rate. This is an important property for the coated resins, as it provides the opportunity to extensively wash the resin during affinity purification and thus to elute contaminating proteins without loss of FVIII.[198]

1.4.3   Purification of pdFVIII using peptidomimetic (69)-coated resin

To demonstrate the potential of peptidomimetic 69 as ligand for FVIII affinity purification, sample purification from cell-conditioned fetal bovine serum (FBS)-containing Dulbecco's Modified Eagle Medium (DMEM) was performed (Figure 30). Affinity purification *via* ligand 69-coated resin was achieved using two buffers varying only in their NaCl content. This is an indication that the interaction between FVIII and the evaluated peptides has predominantly ionic character, as observed for various antibodies before.[203,204] 0.1 M NaCl was used for FVIII adsorption and elution was done under very mild conditions applying 0.6 M NaCl at pH 6.8 to give sharp elution peaks (Figure 29 and Figure 30; left-hand panels). The pH of the buffers was furthermore adjusted to 6.8 as the slightly acidic condition were found to give a better elution threshold, and as FVIII is generally more stable under these conditions. More detailed information about purification conditions are presented in the Supplementary Data 6.

As a positive control, binding and elution of pure pdFVIII was carry out, resulting in high FVIII column retention (~90%). Analysis of the flow-through and wash fractions by SDS-PAGE followed by silver staining (Figure 29 middle panel) and Western blotting (Figure 29 right-hand panel) revealed only traces of FVIII in those fractions (lanes 3, 8; Figure 29). In the FVIII-rich eluate, the heterogeneous 230-90 kDa heavy chain bands and the ~80 kDa light chain doublet bands were visually distinguished. In addition, traces of proteolytic bands (~73 kDa, ~50 kDa, ~43 kDa) were found, from which the ~50 kDa band (A1 domain) was strongly reactive against mAb C5 in the blot.[198]
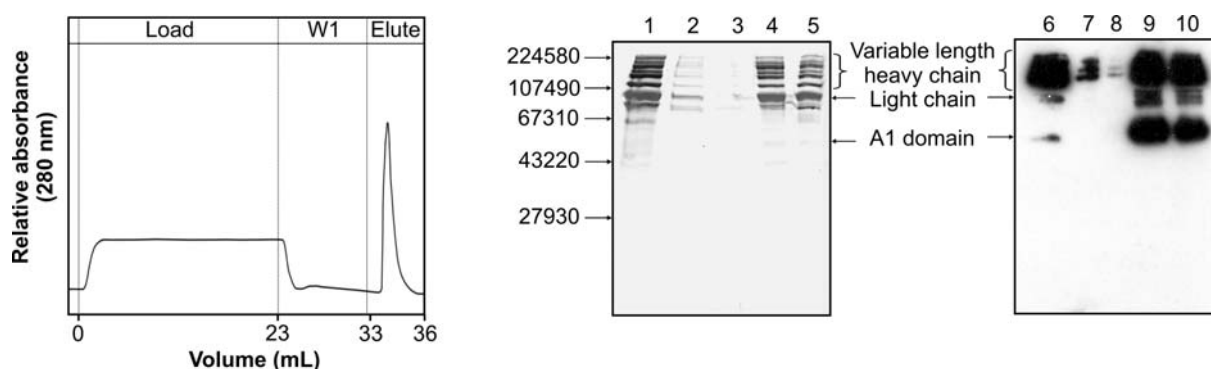
Figure 29. Adsorption and elution of pure pdFVIII. 0.5 mg of pdFVIII were applied to 1 mL of resin. Samples from different purification fractions (see profile in left-hand panel) were analyzed by 10% SDS-PAGE followed by silver staining (middle panel) or Western blotting (right-hand panel) using mAbs C5 and 413 against FVIII. Lanes 1, 6: pure FVIII; Lanes 2, 7: source solution with pure FVIII for the column; Lanes 3, 8: flow-through fraction; Lanes 4, 5, 9, 10: elution fraction with 0.8 M NaCl.[198]

To test the ligand 69-coated resin in a typical application, a purification of pdFVIII from cell-conditioned FBS-containing DMEM, which was spiked with prepurified pdFVIII, was performed. Again, a very satisfying retention (89%) was achieved and the vast majority of contaminant proteins were eluted with the flow-through containing only traces of FVIII (Figure 30: lanes 3, 8).
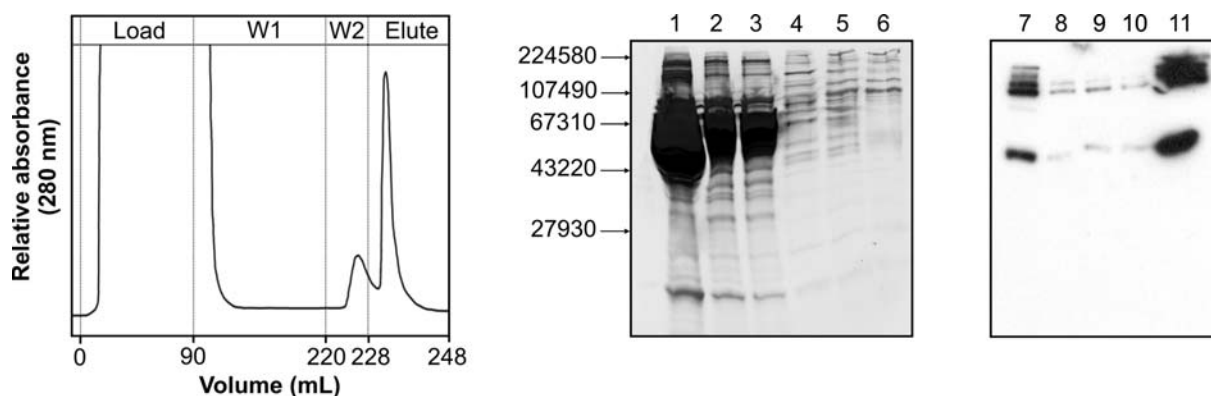
Figure 30. Purification of pdFVIII diluted in cell-conditioned FBS-containing DMEM. 0.5 mg of pdFVIII were applied to 1 mL of resin. Samples from different purification fractions (see profile in left-hand panels) were analyzed by 10% SDS-PAGE followed by silver staining (middle panel) or Western blotting (right-hand panel) using mAbs C5 and 413 against FVIII. Lane 1: media; Lanes 2, 7: media with FVIII for column; Lanes 3, 8: flow-through fraction (W1); Lanes 4, 5, 9, 10: wash fractions (W2) with 0.2 M NaCl; Lanes 6, 11: elution fraction with 0.6 M NaCl.[198]

The purification was further optimized by additional washing with buffer containing 0.2 M NaCl (wash W2 in the elution profile in Figure 30). Thereby additional contaminating proteins were eluted without losing FVIII (Figure 30: lanes 4, 5 and 9, 10). Altogether, contaminant proteins, presented in vast excess to FVIII in source solutions were successfully removed to achieve a 63-fold FVIII concentration using peptidomimetic 69-coated resin. Functional activity of eluted FVIII samples was confirmed by a one-stage clotting assay.[198]

In an additional experiment, the affinity purifications were repeated under equal conditions using tetrapeptide 57-coated resin. Also for this ligand very satisfying results were obtained (the purification date are summarized in the Supplementary Data 8, page 252). However, in line with the reduced FVIII binding ability of the ligand (see Figure 27), the performance of 57-coated resin was not as good as 69-coated resin. A 13-fold concentration of FVIII was achieved using ligand 57 (*vs.* 63-fold applying ligand 69) for the purification of FVIII from FBS-containing DMEM.

1.4.4 Ligand stability, toxicity and biological properties

As described in chapter 1.1.4, the instability and elution of antibody ligands during immunoaffinity chromatography is a major complication. To explore the stability of the peptidomimetic 69-coated resin, a sample was incubated in the elution buffer for 18 h and the supernatant was analyzed by ESI-MS and HPLC–ESI-MS with a cut off limit of 14 nM mL^{-1} as determined for ligand 69. As expected, no release of material, *i.e.* the ligand or fragments of it, was observed, hence proving the high stability of the material.

Nevertheless, for additional validation of the ligand's biological properties, its influence on the FVIII procoagulant activity was investigated and cytotoxicity studies were performed.

The activity of isolated pdFVIII in presence of increasing amounts of free ligands 47, 54, 64, and 69 was measured using a chromogenic assay. This experiment proved that there is no inhibitory effect of the ligands on FVIII function up to a vast (~10^8 fold) excess of the ligands (Figure 31). The same results were obtained for scrambled peptide 39 which was used as control. The results were independently

confirmed in a one-stage clotting assay using normal plasma as FVIII source (data not shown).[198]
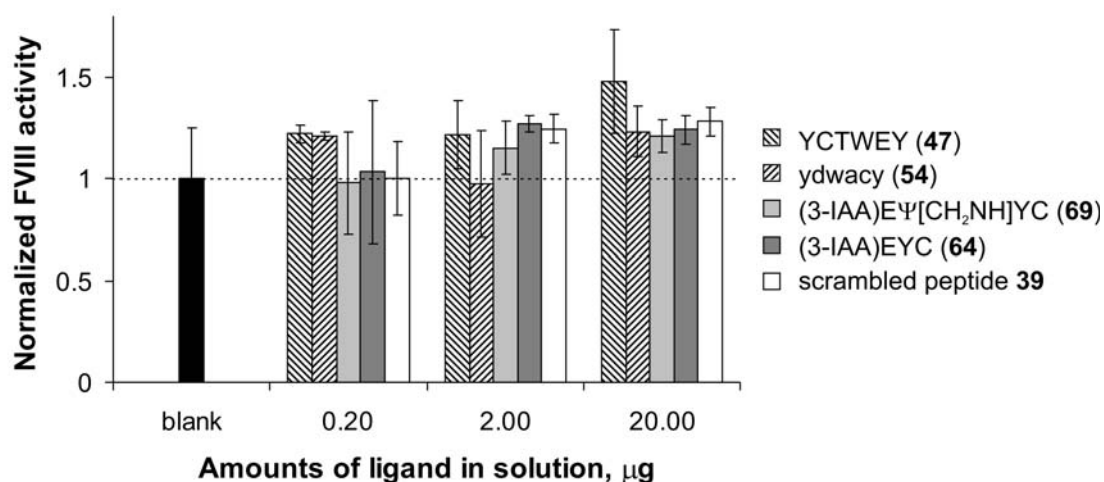
Figure 31. Effect of dissolved ligands on the procoagulant activity of pdFVIII. FVIII was exposed to variable amounts of ligands 47, 54, 64, 69 or scrambled peptide 39 (control) prior to determination of FVIIII activity by chromogenic assay. Values are normalized to those measured for a control sample without added ligand.[198]

Finally, the potential cytotoxicity of peptidomimetic 69 towards human cells was investigated. For this, human OV-MZ-6 cells[205] were exposed to varying concentrations of ligand 69, to control scrambled peptide 39, or to medium only.
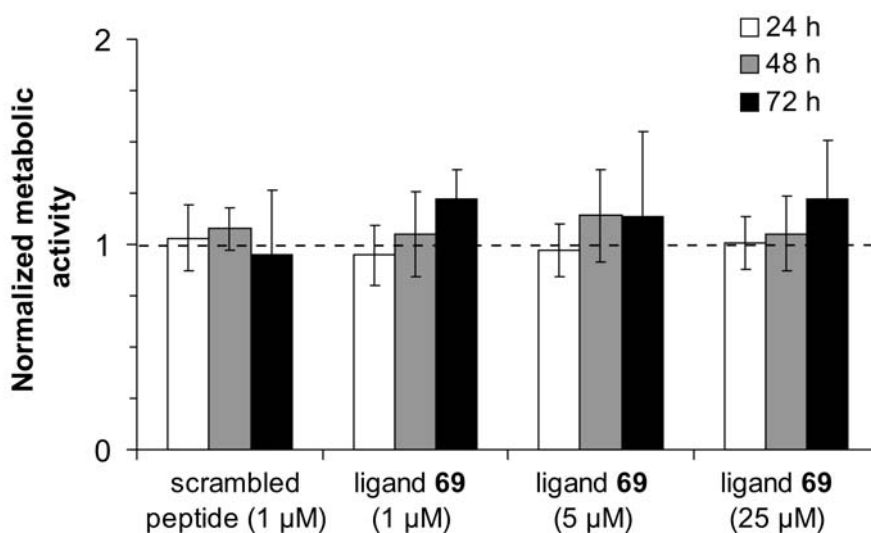
Figure 32. Cytotoxicity assay. Human OV-MZ-6 cells were exposed to 1 to 25 µM of ligand 69, 25 µM of scrambled peptide 39, or medium only for 24, 48 or 72 h. The cell viability was evaluated by measuring the metabolic activity of the cells (MTT assay).[206] Values are normalized to those observed for cells exposed to medium only.[198]

As depicted in Figure 4B, analysis of the cell viability at 24, 48 and 72 h, *via* measurement of the metabolic activity of the cells revealed no cytotoxicity of the ligands, although using concentrations up to 25 μM. In a complementary approach applying identical experimental conditions, cell proliferation by direct cell counting was analyzed and again no indication for any cytotoxicity of ligand 69 (data not shown) was found.[198]

1.5   Cyclic factor VIII ligands

The synthesis of cyclic peptides is a common procedure for the determination of the bioactive conformation and for the generation of lead structures.[207] By cyclization of the peptide backbone, the flexibility of the molecule is drastically decreased which can lead to increased binding affinity. Moreover, the selectivity and the stability against proteolytic degradation can be significantly improved.[208,209] For the study on cyclic FVIII ligands, the two linear hexapeptides FSWEYC (40% FVIII binding; see Supplementary Data 5, page 248ff) and YCSWEY (62% FVIII binding; see Table 4, page 37) were chosen as starting points.

Table 9. ^{125}I-pdFVIII binding ability of cyclic ligands relative to their respective linear precursors. (++) significantly increased FVIII binding; (+) slightly increased FVIII binding; (±) similar FVIII binding; (-) slightly decreased FVIII binding; (--) significantly decreased FVIII binding.[a]

Ligand	no.	Relative FVIII binding	Ligand	no.	Relative FVIII binding
FSWEYC	80	40%	YCSWEY	43	62%
c(FSWEYC)	81	-	c(YCSWEY)	93	--
c(FSWEYc)	82	++	c(YcSWEY)	94	-
c(FSWEyC)	83	±	c(YCSWEY)	95	--
c(FSWEyc)	84	±	c(YcSWEY)	96	-
c(FSWeYC)	85	--	c(YCSWEY)	97	--
c(FSWeYc)	86	--	c(YcSWEY)	98	--
c(FSwEYC)	87	+	c(YCSWEY)	99	-
c(FSwEYc)	88	--	c(YcSWEY)	100	-
c(FsWEYC)	89	++	c(YCSWEY)	101	-
c(FsWEYc)	90	+	c(YcSWEY)	102	--
c(fSWEYC)	91	+	c(YCSWEY)	103	-
c(fSWEYc)	92	±	c(YcSWEY)	104	--

[a] *Lower case letters denote D-amino acid residues.*

Initially, a D-scan was performed to selected appropriate candidates for further sequence optimization. This was done for both stereochemical configurations of the cysteine linker (L- and D-cysteine), as the configuration of the linker might significantly affect the presentation of the ligand on the resin surface. Table 9 summarizes the determined FVIII binding abilities of the diverse cyclic peptide mutants relative to their respective linear precursor molecule.

As shown in Table 9, all cyclic derivatives of ligand 43 bound worse than the linear precursor molecule. In contrast, the two ligands c(FSWEYc) (82) and c(FsWEAC) (89) were found to exhibit a significantly improved FVIII binding ability with respect to the linear precursor 80. The detailed binding data and methods for the synthesis of the cyclic peptides are presented in Supplementary Data 7 (page 252). The work on the two ligands is continued in the PhD thesis of D. Heckmann.[210]

1.6   Discussion and conclusion

By systematic optimization of the FVIII ligand EYHSWEYC (3) two groups of affinity ligands, hexapeptidic and small peptidomimetic ligands, each showing specific advantages, were developed. Their choice for application in FVIII affinity purification processes will depend on process characteristics and/or the objective. The best hexapeptides proved to have a superior FVIII binding profile than the small peptidomimetics, while suffering from lower enzymatic stability and higher production costs comparing with the small peptidomimetics. However, in specific applications, in particular if extremely high FVIII binding properties are needed, these peptide ligands will be the material of choice.

The small peptidomimetic 69 is by far the smallest ligand known to date for the separation of such a large protein as FVIII. Toyopearl AF-Epoxy-650M resin was found to be the support material of choice giving the best FVIII binding results in initial studies. Moreover, ligand 69 can be chemoselectively attached to this resin *via* a cysteine residue acting as linkage. The potential of ligand 69-coated resin was shown in two examples: adsorption and elution of pre-purified FVIII and a successful purification from cell-conditioned FBS-containing media spiked with FVIII. Both examples demonstrated the high efficiency of ligand 69-coated resin: Using a mild buffer for FVIII elution, sharp elution peaks and a high FVIII retention of 90% were achieved. SDS-PAGE and Western blot analysis confirmed that the source and the eluted FVIII display the same protein bands and repartition of the material among protein bands (Figure 29 and Figure 30).

The unnatural structures introduced in ligand 69 not only improved the FVIII affinity but also significantly enhanced its resistance against enzymatic degradation. This was shown by treatment with fresh human serum and Proteinase K (Figure 26). Moreover, the ligand 69-coated resin offers a promising overall stability: After a long incubation period of 18 hours in elution buffer at a high concentration of immobilized ligand (1 mL coated resin was suspended in 1 mL of buffer), no release of material was detected by ESI-MS analysis. In an ongoing study (data not shown), the ligand 69-coated resin preserved its properties over several

months, even if treated with a wide pH range and alcohols for sterilization, conditions under which protein ligands would be severely altered.

The chemical origin is another important feature of the peptidomimetic ligand 69. Ligand synthesis by established solid-phase procedures or by the solution procedure described herein is straightforward and considerably cheaper than the biotechnological production of antibodies. Furthermore, it offers opportunities for easy modification of the ligand's structure. This can be used *e.g.* for further optimizations in terms of stability, or to improve the loading capability or the elution conditions, which is practically not possible for antibodies. As the synthesis is performed without use of any materials of human or animal origin, this ligand does also not carry a risk of transmitting pathogens. Moreover, the ligand shows no cytotoxicity (Figure 32) and it does not affect the procoagulant activity of FVIII (Figure 31).

Hence, it was shown that the novel small-molecule FVIII ligand 69 is a valuable alternative to antibody-based techniques for FVIII purification in laboratory and industrial production. It has the potential to reduce production costs and to improve the safety of current and future FVIIII products.

1.7 Asymmetric synthesis of condensed and aromatic ring-substituted tyrosine derivatives

1.7.1 Background

1.7.1.1 Intention

As described above, the phenolic hydroxyl group of the tyrosine residues (Tyr^2 and Tyr^7) is important for ligand binding affinity as the corresponding phenylalanine derivatives bound significantly worse (see Figure 21). In addition, the preference of larger aromatic systems in the position of Tyr^2 and Tyr^7 was found in several examples (see Supplementary Data 5, page 248). Thus, the substitution of tyrosine by analogues bearing both, an expanded aromatic system as well as the phenolic hydroxyl group, would be interesting in terms of optimizing the binding properties.

1.7.1.2 Non-proteinogenic amino acids in drug development

Non-proteinogenic amino acids play an important role in drug development. While proteinogenic amino acids provide limited variation in size and shape, the introduction of unusual substituents allows a systematic study of structure-activity relationships (SAR). Consequently, non-proteinogenic amino acids have been found to significantly improve the biological properties of numerous biologically active peptides and peptido-mimetics, *e.g.* by limiting conformational flexibility, enhancing enzymatic stability, improving pharmaco-dynamics or bioavailability.[211-213] Especially modified aromatic amino acids are important structural features in various pharmaceuticals which are currently under development or have already been introduced into the market. Among the latter are, for example, the broad-spectrum antibiotics Ampicillin® and Amoxicillin® which contain a D-phenylglycine and D-4-hydroxyphenylglycine moiety, respectively, and Nafarelin® a luteinising hormone releasing hormone (LHRH) analogue for treatment of endometrioses comprising a D-2-naphthylalanine residue.[214]

60

It is evident that such unnatural aromatic amino acids are indispensable tools in pharmaceutical research. Thus, there is a great demand in methods allowing the synthesis of a variety of derivatives in a short time. In the past few years several groups have reported strategies for the synthesis of aromatic substituted phenylalanines,[215-220] tryptophans[218,219] and naphthylalanines.[215,218,219] Although of general interest, procedures for the synthesis of corresponding tyrosine derivatives have not been reported in the literature, yet.

In contrast to phenylalanine, tyrosine provides an additional hydroxyl group in the side chain which can be crucial for the activity or selectivity of biologically active compounds, *e.g.* by acting as a hydrogen bond donor or acceptor as shown for the FVIII ligands above. To enable systematic studies of structure-activity relationships going along with the tyrosine residue, an efficient access to a wide range of substituted tyrosine analogues is required.

1.7.1.3   General strategy and target structures

In the approach towards tyrosine analogues with extended aromatic side chain residues, the focus was on strategies that allow an easy and short access to a variety of compounds in few steps while avoiding complicated protecting group chemistry.
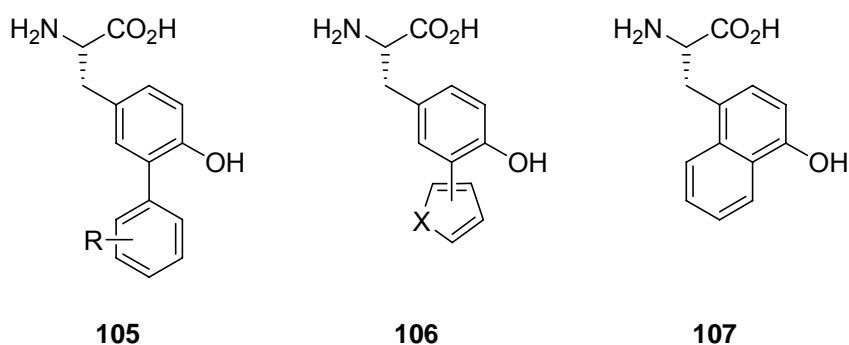
Figure 33. Structures of condensed and aromatic ring-substituted tyrosine derivatives.[214]

The following section describes the development of a general three-step procedure for the synthesis of enantiomerically pure 3-aryl-substituted L-tyrosine analogues of the types 105 and 106 *via* a Suzuki-type cross coupling reaction

(Figure 33). To extend the aromatic residue, a second approach was used in which the condensed 2-naphthylalanine analogue of tyrosine 107 was synthesized *via* an asymmetric hydrogenation of the corresponding α-enamide as key step. In an alterative approach the α-enamide was hydrogenated unselectively and the racemic mixture was resolved using acylase I.[221] This procedure provides a much cheaper approach in cases where both enantiomers are desired. The procedures were worked out for publication in collaboration with B. Laufer.[214]

1.7.2 Synthesis of 3-aryl-substituted tyrosine derivatives

The synthesis of 3-aryl-substituted L-tyrosine derivatives started with commer-cially available L-3-iodo-tyrosine (108). The amino function was protected with Boc to ensure stability under Suzuki coupling conditions (Scheme 4).

Scheme 4. *Synthesis of 3-aryl-substituted tyrosine derivatives.*[a]
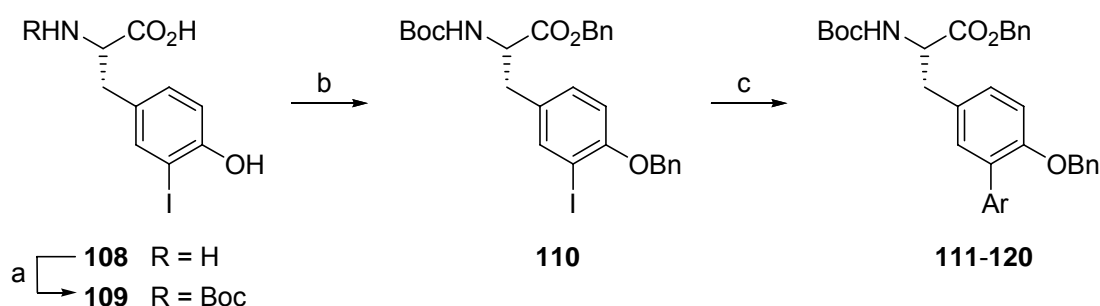
[a] Reagents and conditions: (a) Boc_2O, dioxan/H_2O, 0°C, 18 h, 96%; (b) BnBr, Na_2CO_3, acetone, rf, 5 h, 93%; (c) Ar-B(OH)$_2$, Na_2CO_3, Pd(OAc)$_2$, P(*o*-tolyl)$_3$, DME/H_2O, 80°C, 4-6 h, 39-99%.[214]

As expected, attempts to use compounds 108 or 109 directly for Suzuki couplings failed, probably due to complexation of palladium by the neighboring free phenolic hydroxyl group after insertion into the carbon-iodine bond. This made a side chain protection necessary. For standard peptide coupling purposes, both in solution or solid phase, a protection of the phenolic side chain is generally not crucial. Thus, the phenolic side chain and the carboxylic acid were protected in one step as a benzyl ether and benzyl ester, respectively. This procedure avoids an additional protection and deprotection step as both groups can be removed simultaneously by hydrogenation, but offers the opportunity of a selective saponification of the

benzyl ester when a side chain protection is needed. The benzyl protection was performed under mild conditions using sodium carbonate as base to give the fully protected amino acid 110 in 93% yield and without loss of enantiomeric purity as shown below.[214]

Table 10. Suzuki cross coupling of 110 with arylboronic acids.[214]

Compound	Ar-B(OH)$_2$	Yield (%)[a]
111		95
112		93
113		79
114		70
115		80
116		39
117		94
118		92
119		99
120		45
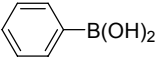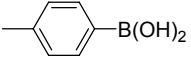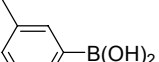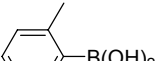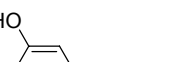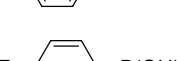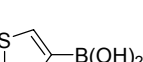
[a] *Yields refer to isolated pure products.*

For Suzuki cross couplings, PdOAc$_2$/P(*o*-tolyl)$_3$ was used as catalyst and sodium carbonate as base, a system which has proven to give good results in similar systems.[215-219] Thus, in collaboration with B. Laufer, a series of 3-aryl-substituted tyrosine derivatives were synthesized in moderate to high yields using a variety of activated and deactivated phenylboronic acids as well as heteroaromatic boronic

acids (Table 10). The formation of the dimeric homo coupling product was generally less than 2% as measured by HPLC-MS, except for the 3-chloro-phenylboronic acid where higher amounts of this side product were formed.[214]

To demonstrate the further procedure and to verify the optical purity of the products, samples of 111 and 114 were deprotected to apply them in solid-phase peptide synthesis. The benzyl ester in both compounds could be cleaved chemoselectively using lithium hydroxide to give the free acids 121 and 122 in 86% and 83% yield (Scheme 5). Alternatively, simultaneous cleavage of both benzyl groups can be achieved by hydrogenation with palladium on charcoal, yielding 123 and 124 in 95% and 87%, respectively.[214]

Scheme 5. *Regioselective deprotection of 3-aryl-substituted tyrosine derivatives.*[a]

R = phenyl	121	R = phenyl	111	R = phenyl	123
R = o-tolyl	122	R = o-tolyl	114	R = o-tolyl	124
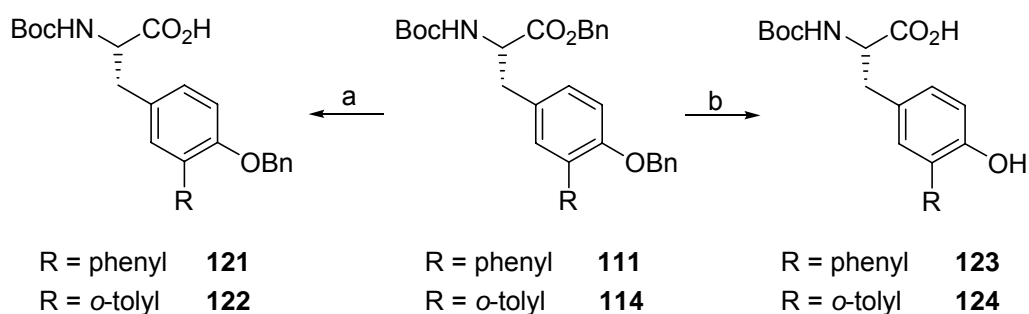
[a] Reagents and conditions: (a) LiOH, THF/H$_2$O, 0°C → rt, 18 h, 111: 86%, 114: 83%.; (b) H$_2$, Pd/C, MeOH/AcN(Me)$_2$, 6 h, 123: 95%, 124: 87%.[214]

The latter compounds were coupled to the amino free resin-bound L-valine using 1.8 equivalents of the amino acid 123 and 124, respectively, TBTU and HOBt in NMP for 30 min. After cleavage from the resin and deprotection, the resulting dipeptides H-*m*-(phenyl)Tyr-Val-OH (125) and H-*m*-(o-tolyl)Tyr-Val-OH (126) were isolated in high purity (Scheme 6). A formation of side products due to the free phenolic side chain was not observed.[214]

Scheme 6. *Solid-phase peptide synthesis applying side chain unprotected tyrosine analogues.*[a]
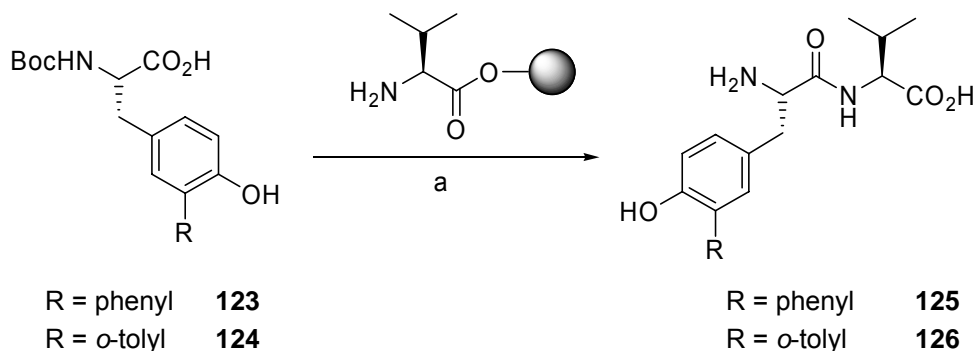
R = phenyl **123**
R = o-tolyl **124**

R = phenyl **125**
R = o-tolyl **126**

[a] Reagents and conditions: (a) *i*) TBTU, HOBt, NMP, rt, 30 min; *ii*) TFA/DCM/H$_2$O (50:40:10, v/v), rt, 1 h, >98% purity.[214]

The corresponding diastereomeric dipeptides H-*m*-(phenyl)Tyr-D-Val-OH (**127**) and H-*m*-(*o*-tolyl)Tyr-D-Val-OH (**128**) were synthesized in an analogous way by coupling to D-valine (Scheme 7).

Scheme 7. *Solid-phase peptide synthesis applying side chain unprotected tyrosine analogues.*[a]
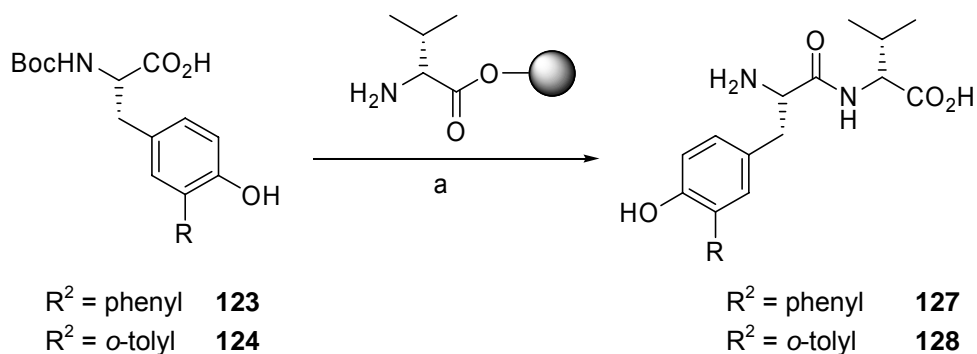
R^2 = phenyl **123**
R^2 = o-tolyl **124**

R^2 = phenyl **127**
R^2 = o-tolyl **128**

[a] Reagents and conditions: (a) *i*) TBTU, HOBt, NMP, rt, 30 min; *ii*) TFA/DCM/H$_2$O (50:40:10, v/v), rt, 1 h, >98% purity.[214]

NMR and HPLC analyses of 125-128 (Supplementary Data 9, page 254) showed the formation of only one single isomer, proving that no reasonable racemization of the 3-aryl-substituted tyrosine derivatives occurred during the synthesis.[214]

1.7.3 Synthesis of 4-hydroxy-1-naphthylalanines

A synthesis of 4-hydroxy-1-naphthylalanine has already been reported by Vela *et al.*.[222] By their procedure, 4-hydroxynaphthalene-1-carbaldehyde (129) was condensed with hippuric acid to form the (Z)-oxazolone 130, which was subsequently opened using ethanolate. Hydrogenation and cleavage of the protection groups by refluxing in 6N hydrochloric acid in dioxane then gave the desired 4-hydroxy-1-naphthylalanine (132).

Scheme 8. *Racemic synthesis of 4-hydroxy-1-naphthylalanine by Vela et al.*[222]
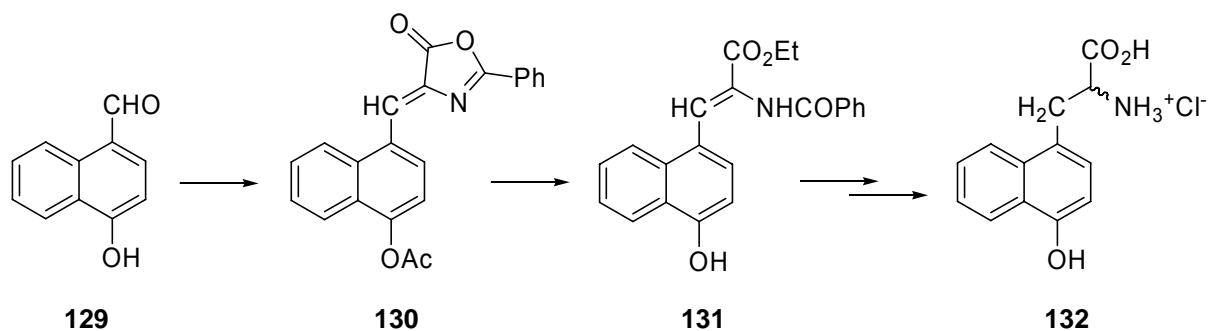
Obviously, their procedure requires harsh conditions and it is not stereoselective. Therefore, a more efficient access was worked out to achieve the compound in high enantiomeric purity, applying protection groups which can be cleaved under mild conditions.

1.7.3.1 Enantioselective synthesis *via* catalytic asymmetric hydrogenation

The synthesis was also started from commercially available 4-hydroxy-naphthalene-1-carbaldehyde (129) whose hydroxy group was protected as a *tert*-butyldimethylsilyl (TBS) ether in 88% yield (133) (see Scheme 9). In initial experiments, a benzyl protection group was used instead, however, the final cleavage by catalytic hydrogenation led to a partial hydrogenation of the naphthalene residue. This was circumvented by the use of the TBS group. The Horner-Emmons olefination of aldehyde 133 with Schmidt's Boc-α-phosphonoglycine trimethyl ester[223,224] gave the

dehydroamino acid 134 with the *Z*-configuration as the major product[*] (*Z/E* = 93/7)[†] in 91% yield. The TBS group in this system was found to be quite acid-labile. For that reason, triethylamine had to be added to the eluent for column chromatography to avoid decomposition.[214]

Scheme 9. *Enantioselective synthesis of (S)-Boc-4-hydroxynaphthyl alanine (**136**) by asymmetric hydrogenation.[a]*
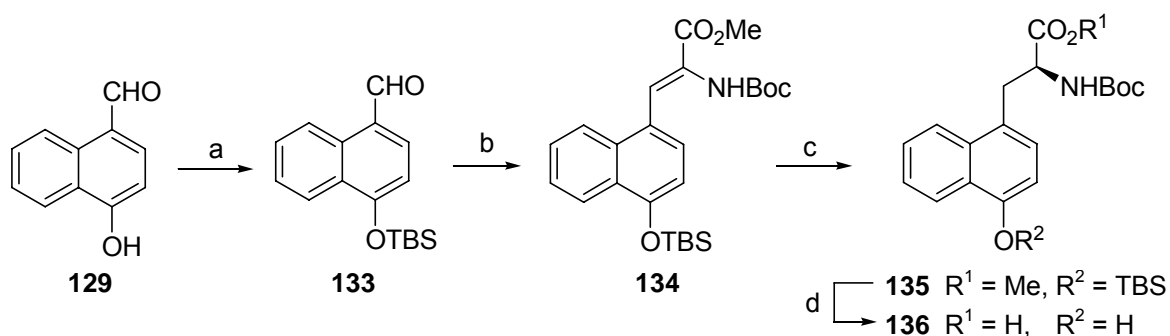
[a] Reagents and conditions: (a) TBS-Cl, imidazole, THF, 0°C → rt, 18 h, 88%; (b) Boc-α-phosphono-glycine trimethyl ester, DBU, THF, 0°C → rt, 18 h, 91%; (c) H$_2$, [(*S,S*)-Et-DuPHOS-Rh(I)] OTf, DCM, 40 bar, 6 h, 95%; (d) *i*) TBAF, THF, 0°C, 15 min; *ii*) LiOH, THF/H$_2$O, rt, 3 h, 89% (two steps).[214]

For the asymmetric hydrogenation of **134**, Burk's 1,2-bis((2*S*,5*S*)-2,5-diethyl-phospholano)-benzene(cyclooctadiene) rhodium(I) trifluoromethane sulfonate ([(*S,S*)-Et-DuPHOS-Rh(I)] OTf) was chosen, which generally gives high yields (>95%) and high enantiomeric excess (97%ee) when applied to hydrogenation of dehydro-amino acids.[216,217,225-228] Moreover, using this type of catalyst both diastereomers, *Z* and *E* respectively, are hydrogenated to give the same enantiomer in similar enantiomeric purity.[216,217,226] Thus, a preceding separation of the two isomers is not essential.[214]

In the first attempts, however, working in MeOH[215-219] as solvent, no conversion even at high pressures (1-50 bar) was observed. Therefore, various solvents were scanned and the highest conversion rates were found when using dichloromethane (DCM) or tetrahydrofuran (THF) (see Table 11). Surprisingly, in both solvents, working at 1 bar pressure, a complete conversion could not be reached even at prolonged reaction times and/or by addition of fresh catalyst. Separation and

---

[*] The *Z* configuration was assigned by NOESY.
[†] The *Z/E* ratio was determined by analytic reversed-phase (RP) HPLC.

analysis of the unreacted starting material gave pure *E*-isomer of the dehydroamino acid 134, indicating a much slower reaction rate for this isomer. For complete conversion of the obtained *Z/E*-mixture of 134 the pressure had to be raised to 40 bar using DCM as solvent. The pure *Z*-isomer, which could be isolated in 75% yield from 133, proved to react to completion at 1 bar pressure.

Table 11. Asymmetric hydrogenation of dehydroamino acid 134.[214]

(*Z/E*)-ratio of 13	Solvent	Pressure (bar)	Time (h)	Conversion (%)	Yield (%)[a]
93/7	MeOH	1	24	0	–
93/7	MeOH	50	24	0	–
93/7	Benzene	1	24	<10	–[b]
93/7	THF	1	24	93	–[b]
93/7	DCM	1	24	93	91
99/1	DCM	1	24	99	–[b]
93/7	DCM	40	4	100	95

[a] Yields refer to isolated pure products; [b] yield not determined.

Working under 40 bar hydrogen pressure in DCM, the (*S,S*)-catalyst gave the amino acid derivative 135 with an absolute (*S*)-configuration based on the selectivity of the (*S,S*)-Et-DuPHOS ligand[216,217,226] in 95% yield. The enantiomeric purity was determined after subsequent cleavage of the TBS group and the methyl ester (Scheme 9).

Scheme 10. *Solid-phase peptide synthesis applying side chain unprotected (S)-4-hydroxynaphthyl alanine 136.[a]*
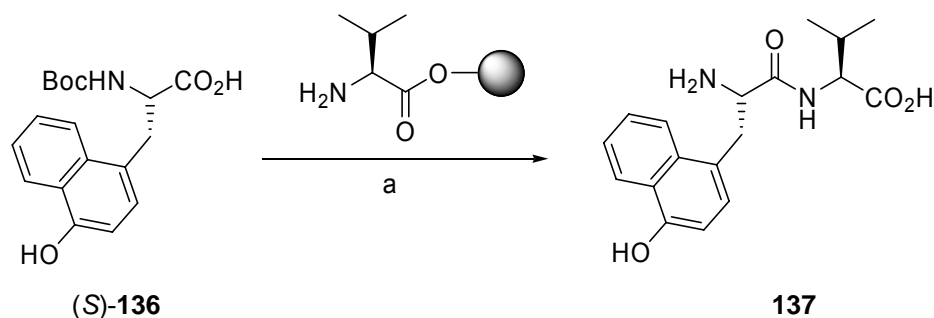
(*S*)-**136**   **137**

[a] Reagents and conditions: (a) i) TBTU, HOBt, NMP, rt, 30 min; ii) TFA/DCM/H₂O (50:40:10, v/v/v), rt, 1 h, >98% purity.[214]

The resulting free acid (*S*)-136 was coupled to amino free resin-bound L-valine as described above. Cleavage from the resin and deprotection yielded the dipeptide H-(4-hydroxy)Nal-Val-OH (137) (Scheme 10).

As a reference for verification of the enantiomeric purity of (*S*)-135 and (*S*)-136, the diastereomeric mixture H-(D/L)-(4-hydroxy)Nal-Val-OH (138) was synthesized (Scheme 11): Unselective hydrogenation of 134 with palladium on charcoal (Pd/C) formed racemic 135 which was subsequently deprotected as described above and coupled to resin-bound L-valine to yield 138.

Scheme 11. *Synthesis of H-(D/L)-(4-hydroxy)Nal-Val-OH (138).*[a]
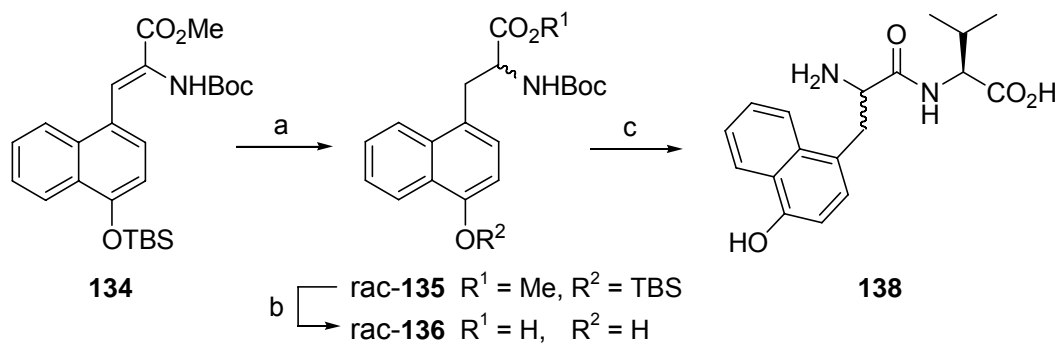
[a] Reagents and conditions: (a) H_2, Pd/C, MeOH, 1 h, 95%; (b) *i*) TBAF, THF, 0°C, 15 min; *ii*) LiOH, THF/H_2O, rt, 3 h, 89% (two steps); (c) *i*) L-Val-TCP, TBTU, HOBt, NMP, rt, 30 min; *ii*) TFA/DCM/H_2O (50:40:10, v/v), rt, 1 h, >98% purity.[214]

The enantiomeric purity of (*S*)-135 and (*S*)-136 was assigned to be greater than 95% by HPLC and NMR analysis (see Supplementary Data 10 on page 257).The catalyst proved to work highly efficient (a catalyst to substrate ratio of 1/500 was used) and the (*S*)-136 could be obtained in a high overall yield of 76% over three steps.[214] ^{1}H-NMR analysis of several *N*-Boc-protected compounds, *e.g.* 135 and 136, showed two groups of proton signals which referred to the existence of two rotamers as reported by Kessler *et al.*[229] more than three decades ago. As usual, for *N*-acetyl protected or unprotected compounds the existence of rotamers has not been observed.

1.7.3.2 Alternative procedure *via* unspecific hydrogenation and enzymatic resolution

Although the procedure described above was shown to be quite efficient, the high costs for the catalyst limit the scope of this procedure, especially if both enantiomers, the L- and the D-form, are needed. Therefore, a second approach was developed offering a concurrent synthesis of both enantiomers. Here the aldehyde 133 was condensed in an analogous way as described above with Cbz-α-phosphono-glycine trimethyl ester to give the (*Z*)-dehydroamino acid 139[*] (*Z*/*E*>95/5)[†] in 87% yield (Scheme 12). Again, triethylamine had to be added to the eluent for column chromatography to avoid decomposition.[214]

Scheme 12. *Synthesis of H-(D/L)-(4-hydroxy)Nal-Val-OH (138).*[a]
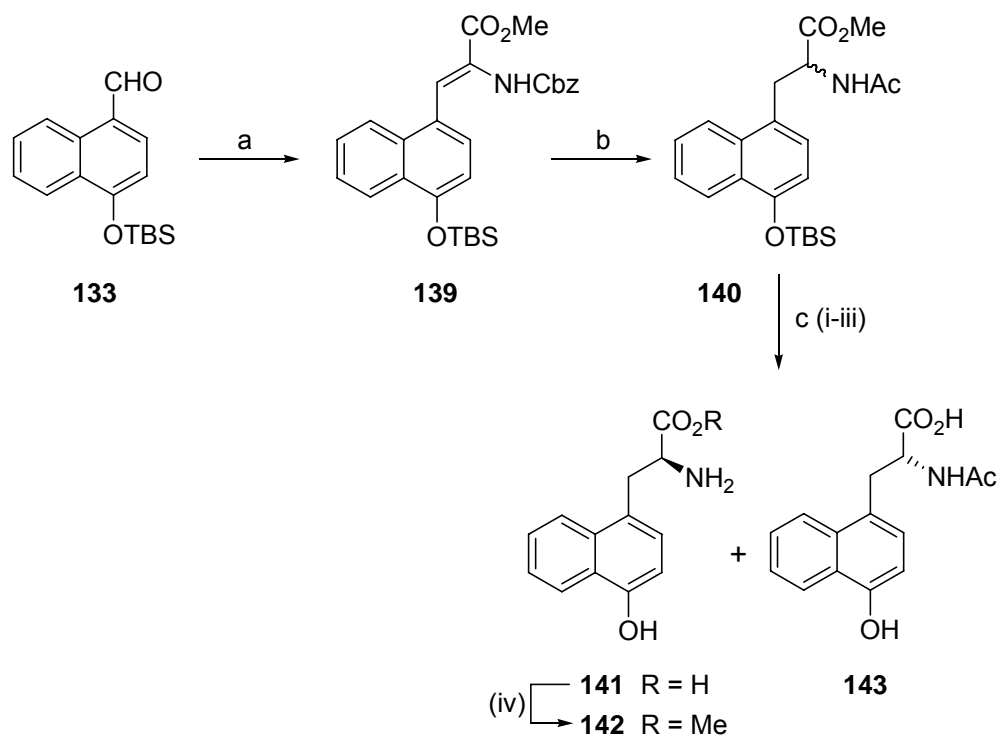
[a] Reagents and conditions: (a) (CH$_3$O)$_2$P(O)CH(NHCbz)CO$_2$CH$_3$, DBU, THF, 0°C → rt, 18 h, 87%; (b) *i*) H$_2$, Pd/C, MeOH, 1 bar, 2 h; *ii*) Ac$_2$O, NEt$_3$, DCM, rt, 18 h, 76% (two steps); (c) *i*) TBAF, THF, 0°C, 15 min; *ii*) LiOH, THF/H$_2$O, rt, 3 h; *iii*) acylase I, H$_2$O (pH 7-8), 3 h, 40°C, 143: 46% (three steps); (iv) SOCl$_2$, MeOH, rt, 18h, 142: 41% (four steps).[214]

---

[*] The *Z* configuration was assigned by NOESY.
[†] The *Z*/*E* ratio was determined by HPLC.

In contrast to the previous procedure, the hydrogenation was carried out using palladium on charcoal as catalyst leading to a simultaneous hydrogenation of the double bond and cleavage of the Cbz protection group. The reaction was monitored by TLC and mass spectroscopy and quenched after complete conversion to the saturated free amine (4 h). Prolonged reaction times (18 h) led to partial hydrogenation of the naphthalene residue. The resulting racemic mixture was directly acetylated by treating with acetic acid anhydride in presence of triethylamine to yield 140 in 76% yield over two steps.[214]

Subjecting the fully protected compound 140 to enzymatic resolution led to an unseparatable product mixture due to a partial loss of the TBS group and partial cleavage of the methyl ester. Thus, both protecting groups were removed prior to the resolution improving the solubility in aqueous conditions. To avoid additional separation steps, a one-pot procedure was developed: the TBS ether and the methyl ester were subsequently cleaved and the racemic mixture was resolved using acylase I to give the L-isomer 141 as free amine, while the D-isomer 143 remained in the *N*-acetylated form which was easily separated by extraction in high purity (93% by HPLC analysis).[221] As the isolation of the free L-amino acid 141 by crystallization failed, it was converted to the corresponding methyl ester 142 and also isolated by extraction (90% purity by HPLC analysis). Further purification by column chromatography gave the pure enantiomer 142[221] and 143 (96%ee)* in high yields (41% over four steps and 46% over three steps, respectively).[214]

1.7.3.3   Discussion and outlook

The sequences described above provide a variety of tyrosine analogues stereoselectively in high yields. A convenient route was developed for the synthesis of aromatic ring-substituted tyrosine derivatives *via* a Suzuki cross coupling reaction, thereby introducing a variety of substituted and unsubstituted aromatic as well as heteroaromatic residues in high yield. Even heavily deactivated boronic acids could be coupled in moderate yields. To provide a structural alternative, methods for the asymmetric synthesis of the ring-condensed tyrosine analogue 4-hydroxy-naphthyl-alanine were developed. For the synthesis, two alternative methologies were

---

* The enantiomeric purity of 143 was determined by chiral HPLC analyses after conversion to the corresponding methyl ester.

explored to offer the most economical access if only one or both enantiomers are desired. In case of the latter, the unselective hydrogenation of the corresponding dehydroamino acid and enzymatic resolution of the racemic mixture is the most cost efficient procedure, as acylase I is cheap and both enantiomers are obtained simultaneously. In contrast, if only one single enantiomer is required the racemic synthesis is associated with 50% loss of substance due to the undesired second enantiomer. The asymmetric hydrogenation of the dehydroamino acid provides a high-yielding access to a single enantiomer. Although the catalyst is quite expensive, its great efficiency and the high yields make this procedure the most economic in case only one enantiomer is desired. The procedure now provides the opportunity to systematically scan above-mentioned FVIII ligands to study the impact of the modified tyrosine analogues.

— Chapter 2 —

2 Radioligands for Tumor Imaging and Tumor-Specific Radionuclide Therapy

2.1 Background

2.1.1 Development and spread of cancer

Cell division or cell proliferation is a physiological process that occurs in almost all tissues and under many circumstances. Normally this process is highly controlled and the balance between proliferation and programmed cell death (apoptosis) is tightly regulated to ensure the integrity of organs and tissues.

The uncontrolled and often rapid proliferation of cells can lead to an initially benign tumor but it may carry a risk of turning malignant (cancer). Benign tumors do not spread to other parts of the body or invade other tissues, and they are rarely a threat to life unless they extrinsically compress vital structures. Malignant tumors can
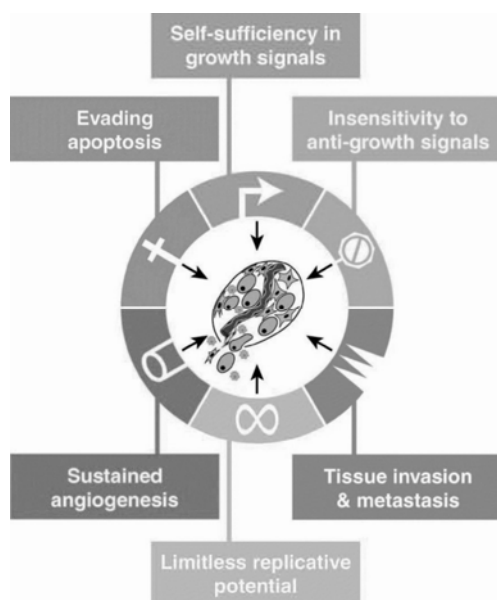
Figure 34. Essential alterations for malignant cell growth.[*]

---

[*] Reprinted from D. Hanahan, and R. A. Weinberg *Cell* 2000, *100*(1), 57-70; Elsevier, Copyright (2000), with permission from Elsevier.

73

invade other organs, spread to distant locations (metastasize) and become life-threatening. Six alterations are believed to be essential for malignant growth:[230,231] self-sufficiency in growth signals, insensitivity to growth-inhibitory (antigrowth) signals, evasion of apoptosis, limitless replicative potential, sustained angiogenesis, and tissue invasion and metastasis (Figure 34). Changes in adhesion are prominent during the metastatic journey.
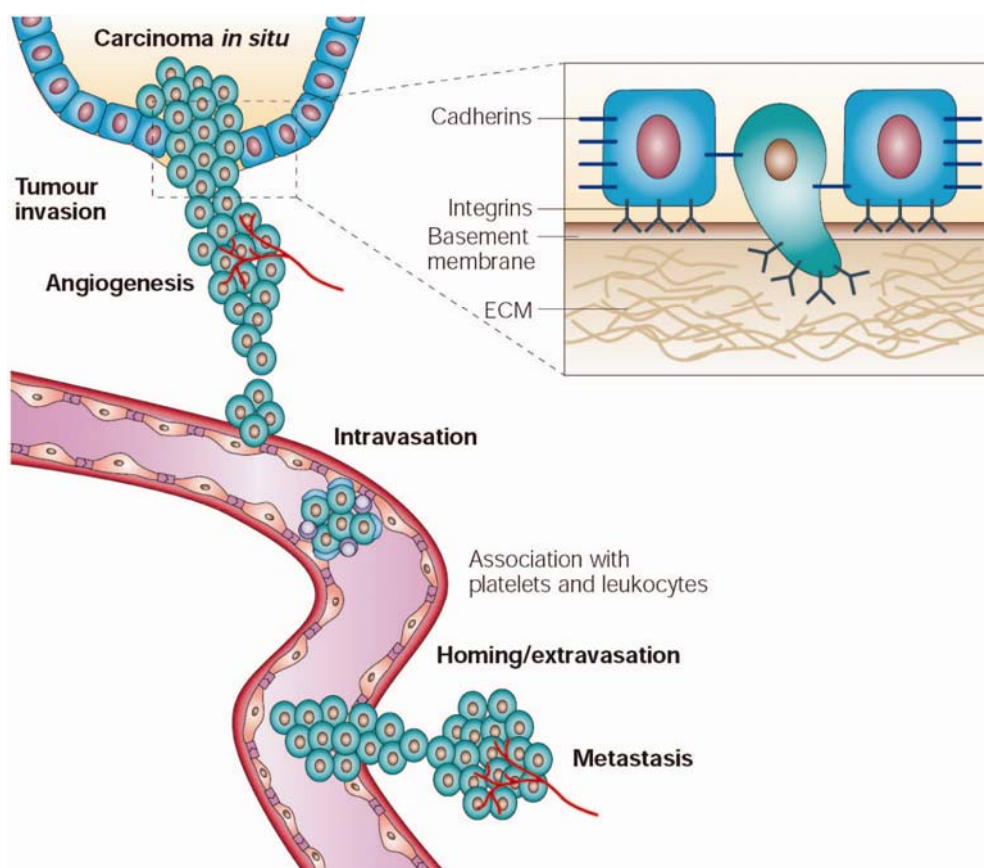
Figure 35. The metastatic cascade by Guo *et al.*,[232] reprinted by permission from Macmillan Publishers Ltd: *Nature Reviews Molecular Cell Biology* 2004, *5*, 816-826, Copyright © 2004.

For the formation of metastasis, cancer cells have to detach from neighboring cells by losing E-cadherin-dependent intercellular adhesion.[232,233] Subsequently, they degrade the basement membrane and the extracellular matrix (ECM) to traverse the interstitial stroma (Figure 35).[232] After passing through the endothelial basement membrane of blood vessels or penetrating into lymphatic vessels which lack a continuous basement membrane and tight junctions (intravasation), the tumor cells reach the circulatory system. In the blood stream, tumor cells often

form emboli by adhering to platelets and leukocytes which stops the microcirculation of target organs. The tumor cells then again traverse the basement membrane of the blood vessel (extravasation) to form a metastasis (Figure 35).[232] Hence, traversing the basement membranes and the ECM is basic requirement for the formation of metastasis.

The basement membrane consists of an membrane called basal lamina, and an underlying network of reticular collagen fibrils (Figure 36). In addition to collagen, this supportive matrix contains intrinsic macromolecular components such as laminin and other glycoproteins, including sulfated proteoglycans.[234,235]
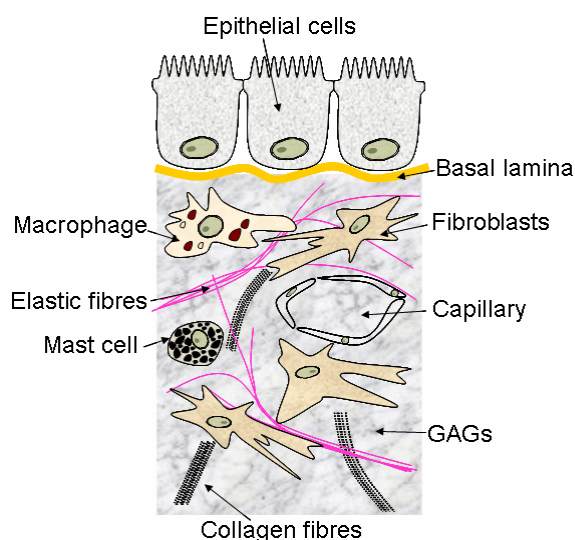
Figure 36. Composition of the extracellular matrix with basement membrane and stroma by S. Cook.[236] GAGs: glycosaminoglycans.

The main macromolecular components of the ECM are various proteins like collagen, fibrin and elastin as well as glycoproteins (*e.g.* fibronectins) and proteoglycans (proteins with glycosaminoglycans (GAGs) attached covalently) (Figure 36). Collagen is the most abundant protein in the human body. Further components are proteins such as laminins and nidogens and minerals such as hydroxylapatite, or fluids such as blood plasma or serum with secreted free flowing antigens. The numerous hygroscopic macromolecules form a gel matrix in which the cells of the stroma such as fibroblasts, endothelial cells lymphocytes or microphages are embedded (Figure 36). Cells are bound to the ECM *via* receptors from the integrin superfamily to adhesive proteins like laminin or fibronectin.[237-

[239] In addition the ECM sequesters a wide range of cellular growth factors, and acts as a local depot for them. Changes in physiological conditions can trigger protease activities that cause local release of such depots. This allows the rapid and local activation of cellular functions, without *de novo* synthesis.[236]

2.1.2 Proteolysis in tumor growth and metastasis

The proteolytic degradation of the basement membrane ECM is fundamental for invasive processes and cell migration.[240] In normal physiological growth and modification processes, proteases capable to degrade the ECM are highly regulated *e.g.* in embryogenesis, morphogenesis or wound healing.[241] Malign tumors, in contrast, show an increased secretion of such proteases in form of pro-enzymes or zymogens, which are further activated by auto-proteolysis leading to an accumulation in the ECM-cell interface.[242,243] Based on the catalytic center, these proteases are classified in four groups (Table 12). Although there are a large number of proteins which are capable to degrade components of the ECM, it seems that in particular the matrix metalloproteinases (MMPs)[244-246]and the serine proteinases of the plasmin activator system are responsible for this process.[247-249]

Table 12. Proteases capable to degrade the extracellular matrix.[250]

Protease family	Active center	Example
Serine protease	Serine	Plasmin,[251] uPA[a],[252] tPA[b],[234] matripase[253]
Matrix metalloproteinase (MMP)[244,252,254]	Zinc	Collagenases (MMP-1, MMP-8, MMP-13), metalloelastase (MMP-12), stromelysines (MMP-3, MMP-10),[255] gelatinase (MMP-2)
Cysteine protease[256]	Cysteine	Cathepsin B,[252,257] H und L
Aspartic protease	Aspartic acid	Cathepsin D[258]

a uPA: urokinase type plasminogen activator; b tPA: tissue plasminogen activator.

2.1.3 The uPA/uPAR pathway and pericellular proteolysis

The uPA/uPAR system (Figure 37) is a tumor cell surface-associated system consisting of the serine proteases urokinase-type plasminogen activator (uPA) and plasmin, the membrane-bound uPA receptor (uPAR; CD87) and the uPA inhibitors plasminogen-activator inhibitor type 1 and 2 (PAI-1 and PAI-2) which belong to the superfamily of the serpins (serine protease inhibitors).
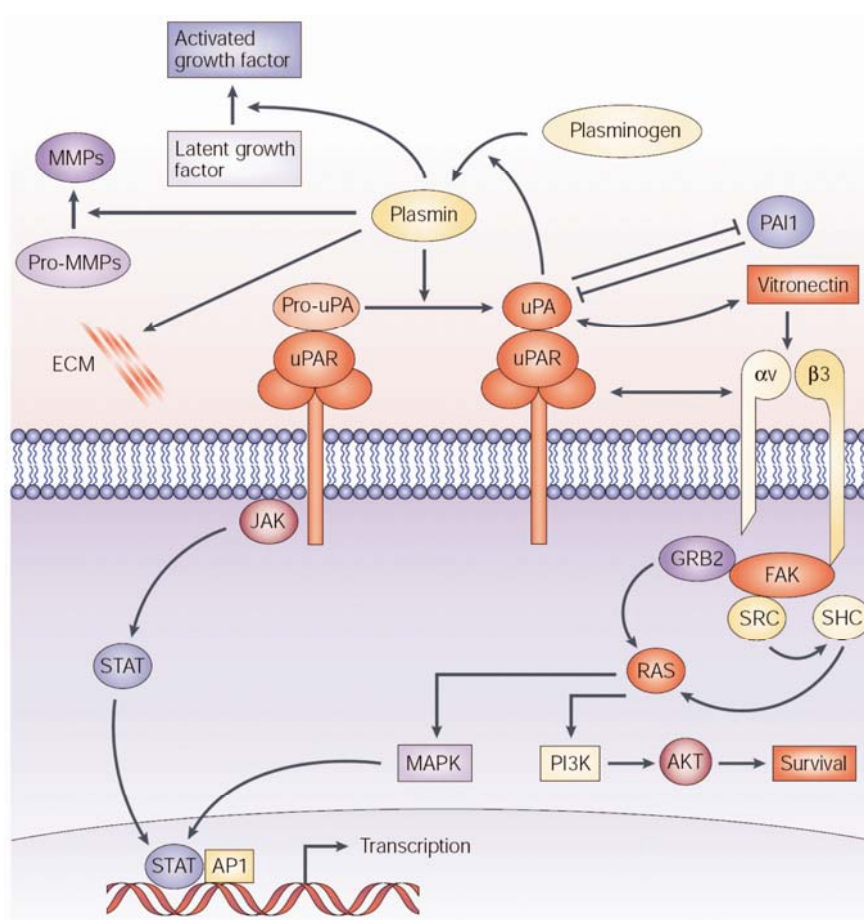
Figure 37. The uPA-uPAR pathway by J. Rao,[252] reprinted by permission from Macmillan Publishers Ltd: *Nature Reviews Cancer* 2003, *3*(7), 489-501, Copyright © 2003. Schematic representation of urokinase-type plasminogen activator receptor (uPAR)-mediated cellular events on the cell surface. Binding of pro-uPA to uPAR provides the cell surface with potential plasmin-dependent proteolytic activity that determines matrix degradation. Also shown is the involvement of integrins in several signalling pathways. ECM, extracellular matrix; FAK, focal adhesion kinase; GRB2, growth factor receptor-bound protein 2; JAK, Janus kinase; MAPK, mitogen-activated protein kinase; PAI1, plasminogen activator inhibitor 1; PI3K, phosphatidylinositol 3-kinase; STAT, signal transducer and activator of transcription.

uPA bound to its receptor efficiently converts inactive plasminogen into active plasmin (Figure 37), whose key role in fibrinolysis has already been described above. The serine protease degrades various components of the extracellular matrix such as fibrin, fibronectin and laminin.[259] Furthermore, plasmin activates the pro-enzyme form of uPA, pro-uPA, and other proteases, *e.g.* the matrix metalloproteinases MMP-3, -9, -12, and -13 (as described below) or elastase, thereby supporting tumor cell invasion and metastasis (Figure 38).[259] In contrast to most other proteases, plasmin can bind to the cell surface which protects it against its natural inhibitors, amongst others α_2-antiplasmin.[260] This focuses the proteolytic activity on the cell surface[260-262] and potentizes the proteolytic activity due to its ability to activate receptor-bound pro-uPA.[263]
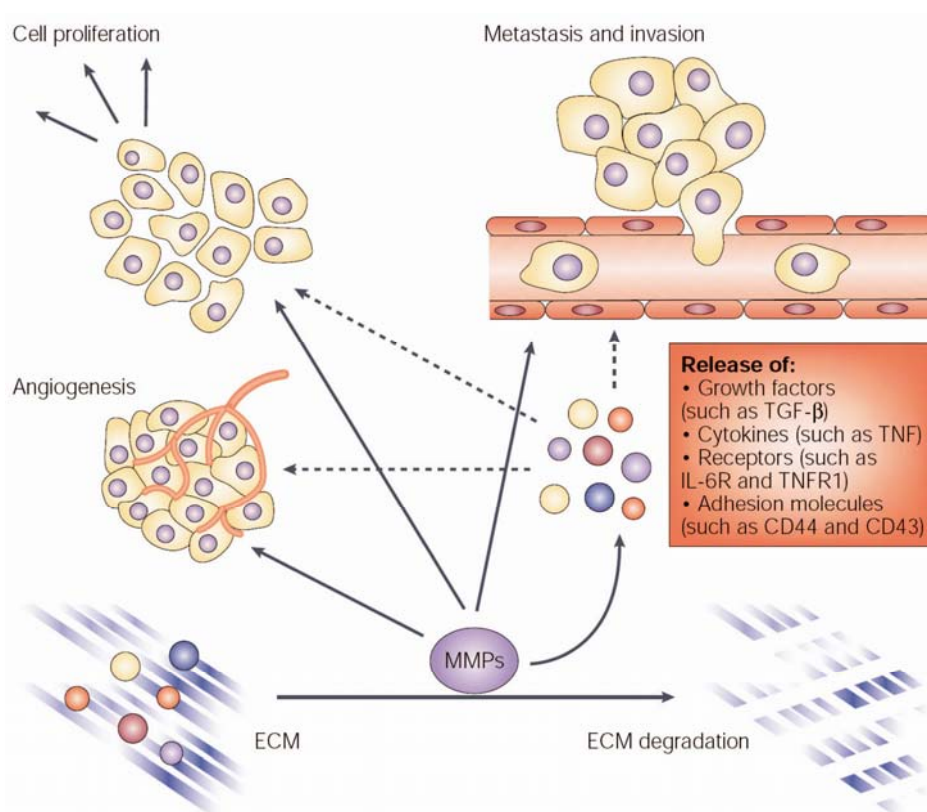
Figure 38. Effects of MMPs on the growth of cancer cells.[252] Reprinted by permission from Macmillan Publishers Ltd: *Nature Reviews Cancer* 2003, *3*(7), 489-501, Copyright © 2003.

The uPA/uPAR interaction is controlled by its natural inhibitors, in particular PAI-1 and PAI-2, which efficiently inhibit the free as well as the receptor-bound

form of uPA (Figure 37).[264,265] The stable ternary complexes (uPA/uPAR/PAI-1 and uPA/uPAR/PAI-2) are subsequently internalized[266-268] in a process that requires the α_2-macroglobulin receptor/low-density lipoprotein (LDL) receptor-related protein (LRP) (α_2MR/LRP).[269-273] New investigations show that tumor cells possess a mechanism to recycle the internalized uPAR back to the cell surface from the cytoplasm which may help to maintain invasive potential.[271,274-277]

The activation of MMPs plays a fundamental role in cancer progression (Figure 38). MMPs not only directly degrade structural components of the ECM, in particular laminin-5, hence regulating invasion and migration, but they also promote the growth of cancer cells by interacting with a variety of ECM molecules, cleaving insulin-like growth factors and shedding transmembrane precursors of growth factors, including transforming growth factor-α (TGF-α) (Figure 38).[252] In addition, MMPs interact with integrins and promote angiogenesis by increasing the bioavailability of pro-angiogenic growth factors.[252]

2.1.4   Molecular structure of uPA

The urokinase-type plasminogen activator is expressed by numerous malign and normal cells in form of the inactive 52 kDa single-chain pro-enzyme pro-uPA comprising 12 disulfide bridges.[278,279] The domain structure is shown in Figure 39. The *N*-terminal growth factor-like domain (GFD) (uPA$_{1-44}$) is part of the amino-terminal fragment (ATF; uPA$_{1-135}$) and comprises the uPA receptor binding site.[280] Although significant sequence homologies to the epidermal growth factor (EGF) and the TGF-α have been found,[281,282] the binding of uPAR is selective for GFD.[235] uPA$_{45-135}$ is called the kringle domain. It is a highly conserved structure motive which is found in a number of proteins involved in hemostasis or fibrinolysis.[283] In contrast to the kringle domain of tPA and plasminogen, the kringle domain of uPA does not exhibit affinity to fibrin but binds to heparin.[284] The *C*-terminal region uPA$_{136-411}$ comprises the enzymatically active region of the serine protease with the catalytic triad, residues His^{204}, Asp^{255} und Ser^{356}.[285] X-ray structures of the *C*-terminal domain in complex with different inhibitors have been solved by Sperl *et al.* and Spraggon *et al.*.[286,287]
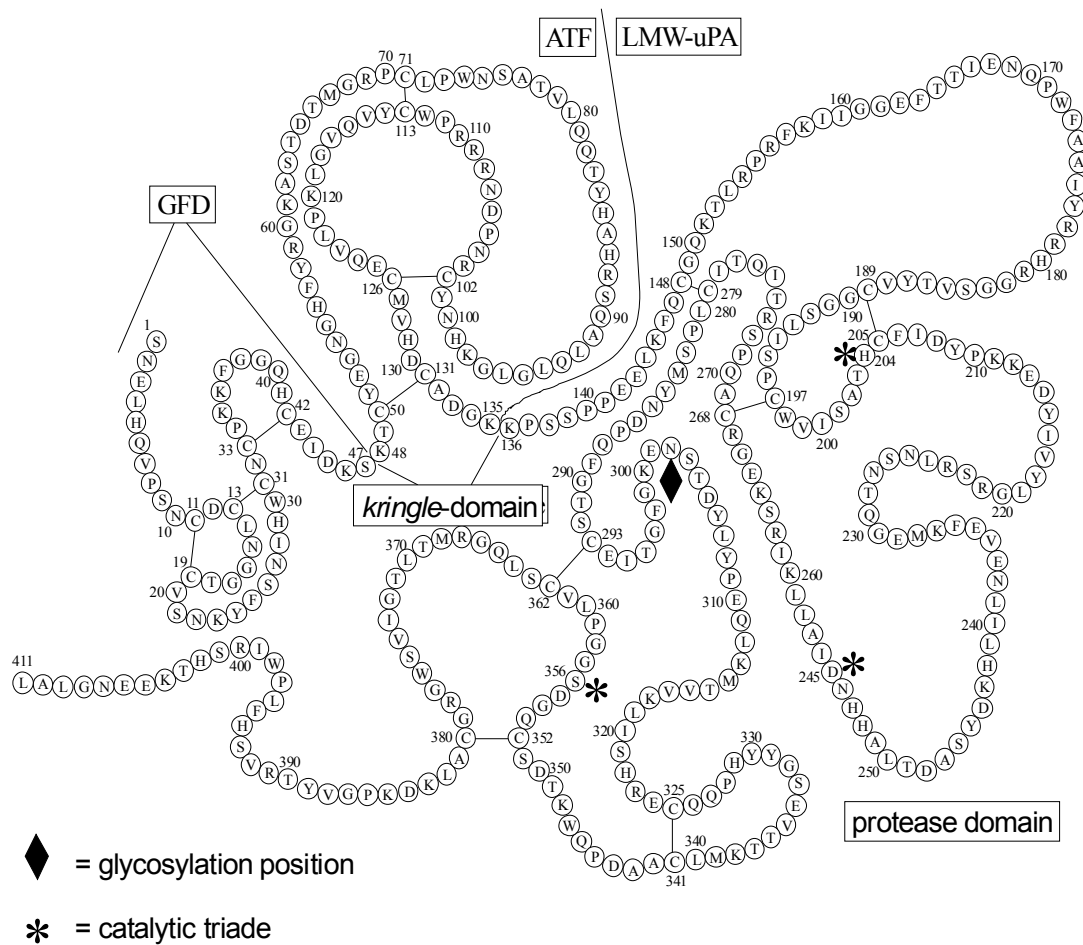
Figure 39. Primary structure of pro-uPA (modified from N. Schmiedeberg).[288]

Inactive pro-uPA is activated by proteolytic cleavage of the Lys[158] und Ile[159] junction to form the active high molecular weight (HMW)-uPA, which's two-chains (A uPA$_{1-158}$ and B uPA$_{159-411}$) are connected *via* a disulfide bridge between Cys[148] and Cys[279]. The induced structural changes lead to the exposure of the active center. The proteolytic activation can be induced by plasmin, callicrein, cathepsin B/L, thrombin and the nerve growth factor NGF-γ leading to a positive feedback.[289-292] Further cleavage between Lys[135] and Lys[136] forms two biologically active fragments ATF (uPA$_{1-135}$) and low molecular weight (LMW)-uPA (uPA$_{136-411}$) which bind to uPAR and exhibit proteolytic activity.[293]

2.1.5 Molecular structure of uPAR

The urokinase receptor uPAR (CD87) was found on numerous malign and non-malign cells[294-297] and was characterized by Ploug *et al.* (Figure 40).[298] Active uPA, pro-uPA, ATF and GFD all bind with high affinity to the receptor (IC_{50} = 1-20 nM depending of the domain and the test system).[299-302]
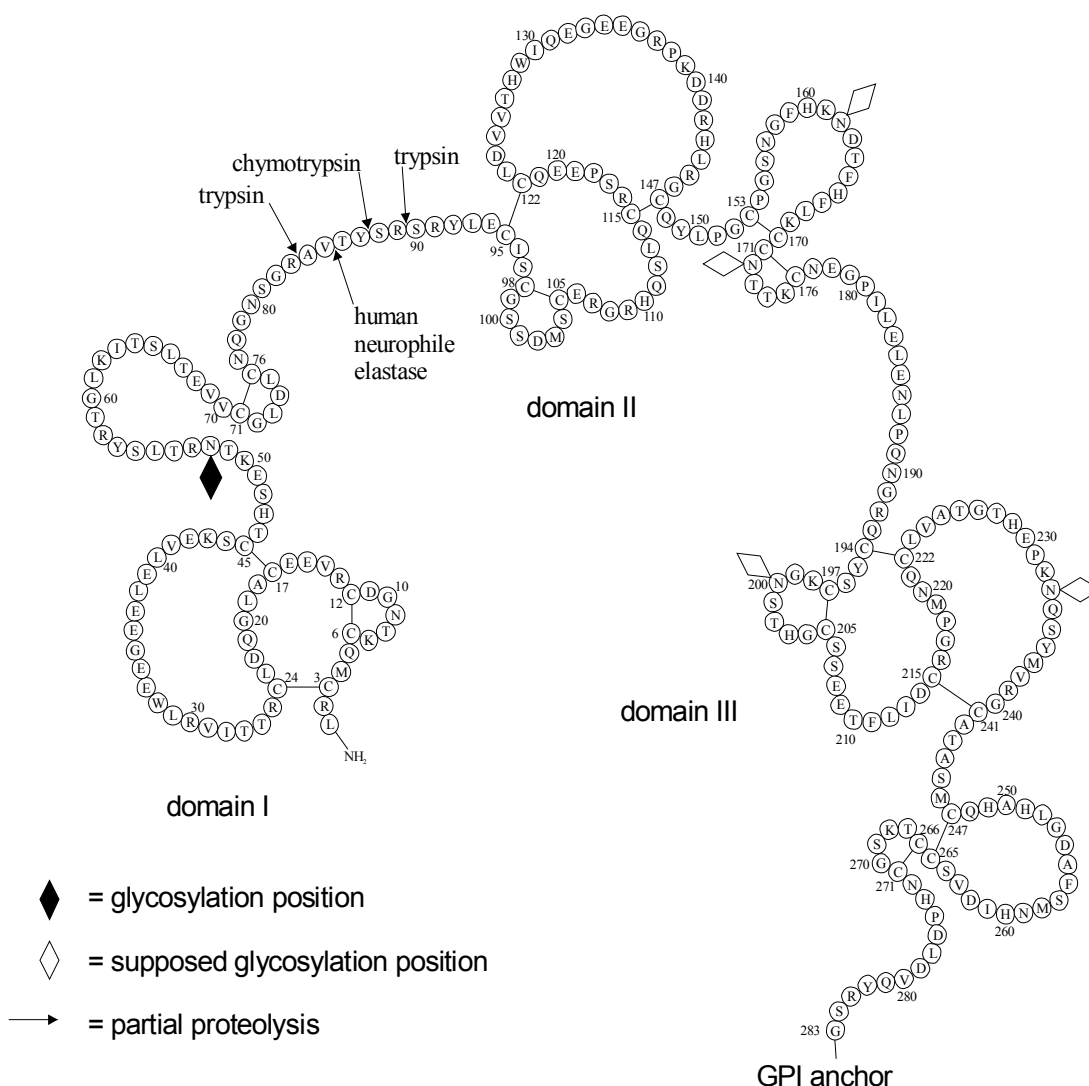
Figure 40. Primary structure of the urokinase-type activator receptor uPAR (modified from N. Schmiedeberg).[288] GPI: glycosylphosphatidylinositol.

It is a 335 amino acids long polypeptide comprising the following features: (a) an *N*-terminal signal sequence of 21 amino acids, (b) two highly homologous cysteine-rich domains of 188 amino acids, and (c) a highly hydrophobic *C*-terminal sequence

of 15 to 20 amino acids.[303] During posttranslational processing, the signal sequence and the hydrophobic region are cleaved subsequently in the endoplasmatic reticulum and the newly formed *C*-terminus binds to a glycosyl-phosphatidylinositol (GPI) anchor (described below), thereby forming the active receptor as shown in Figure 40.[298,304] The receptor glycosylation (~30%), which is important for its intracellular transport, its folding and its affinity to uPA,[305] varies depending of the expressing cell line to give a final molecular weight of 45-55 kDa,[306] but the exact glycosylation is still unknown.[306-308] Recently, two groups independently solved the crystal structure of uPAR: Huai *et al.*[309] presented the structure of soluble uPAR (suPAR) in complex with ATF and ATN615, the fragment antigen binding (Fab) fragment of an antibody against suPAR (see next chapter) whereas Llinas *et al.*[310] crystallized uPAR in complex with its inhibitor AE147.
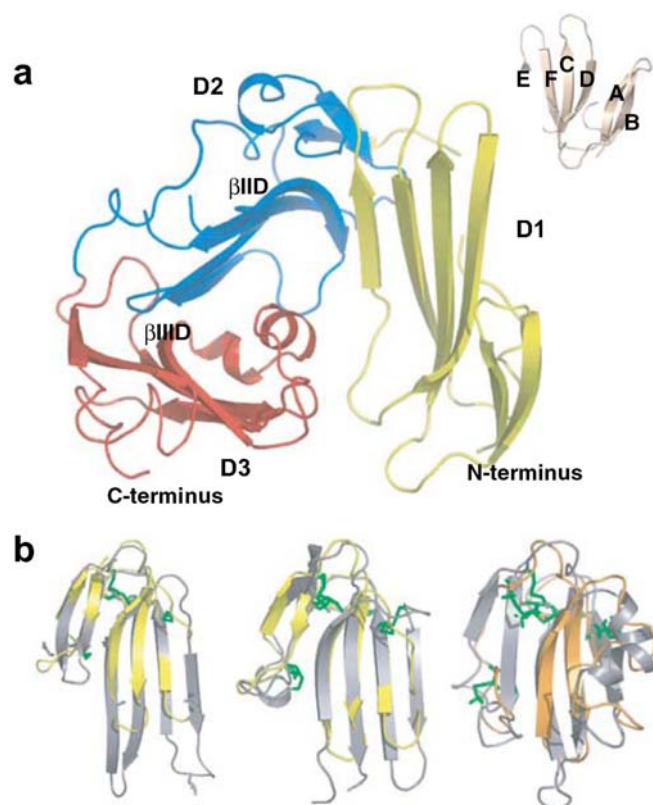
Figure 41. The structure of human uPAR from Llinas *et al.*, reprinted by permission from Macmillan Publishers Ltd: *The EMBO Journal* 2005, 24(9), 1655-1663, Copyright © 2005. (a) The overall modular structure of uPAR as a ribbon diagram. The individual uPAR domains are assembled in a right-handed orientation and are colored yellow (D1), blue (D2) and red (D3). The bended β-strands in D2 and D3, βIID and βIIID respectively are indicated separately.[310] (b) From left to right, superimpositions of bucandin (yellow) on uPAR DI and DII (grey) and of CD59 (orange) on uPAR DIII (grey). Disulfide bonds are colored green in the superimpositions.[310]

The crystal structure determined by Llinas *et al.*[310] (presented in Figure 41 without and in Figure 52 (page 102) as complex with its inhibitor AE147) revealed the proposed domain structure of uPAR. The receptor comprises three domains (D1, D2 and D3), each of which adopts a typical three-finger fold with three adjacent loops (Figure 41a). In general, this fold possesses four disulfide bonds: three at the base of the loops and a fourth that locks the *C*-terminal loop. This property is replicated in D2 and D3, but not in D1, which lacks the third consensus cysteine (compare Figure 40).[310]

The determined domain structure displays similarity with the Ly-6 superfamily,[311,312] comprising, for example, bucandin, a snake venom α-neurotoxin,[313,314] and the glycolipid-anchored membrane proteins CD59, a mammalian protein that inhibits complement activation,[315,316] E48[317] and Ly-6.[318] As illustrated in Figure 41b, the overall folding topology of D1 and D2 resembles that of bucandin, whereas D3 is reminiscent of CD59. The secondary structure of uPAR is thus dominated by three consecutive β-sheets. D1 and D2 provide six β-strands each, whereas D3 donates only five β-strands.[310]
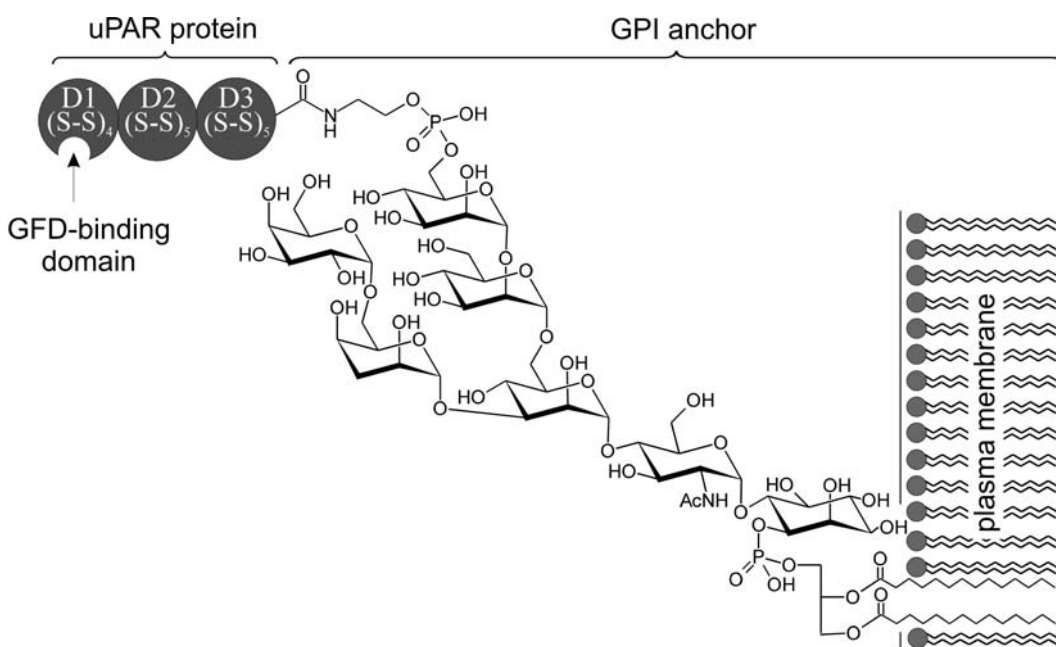
Figure 42. Molecular structure of the glycosylphosphatidylinositol (GPI) anchor with bound uPAR (modified from M. Bürgle).[319]

The GPI-anchor[273] (Figure 42) is preferably attached to uPAR *via* Gly^{283}, but also *via* Ala^{284} or Ser^{282}. It consists of a core sequence, which contains ethanolamine, a

variable sequence of diverse mannoses, *N*-acetyl glucosamine, phosphatidylinositol and diacetyl glycerol (Figure 42), and lacks transmembrane and cytosolic components and therefore intrinsic signal transduction potential. uPAR cleavage from its anchor by phosphatidylinositol-specific phospholipase C or D (PI-PLC and PI-PLD, respectively) forms soluble uPAR (suPAR)[320,321] which also binds to uPA and which can be detected in the body fluids of cancer patients.

2.1.6   New insights into the uPA-uPAR interaction

The X-ray structure of suPAR in complex with ATF and ATN615 obtained by Huai *et al*. (Figure 44)[309] recently demonstrated more explicit data about the uPA-uPAR interaction.

2.1.6.1   The amino-terminal fragment ATF

Looking at the structure of ATF (Figure 43), the authors have shown that ATF is constrained in the ternary complex, with tow adjacent domains tightly packed and forming hydrophobic interactions with each other.[309] This is in contrast to previous results obtained from NMR studies where the GFD and kringle domains of unbound ATF were found to exhibit a high degree of structural independence involving little or no interdomain interaction.[280]

2.1.6.2   The structure of soluble uPAR

The X-ray structure furthermore revealed that the D1 and the D3 domains of suPAR are connected with each other.[309] Key residues for this interaction are His^{47}, Glu^{49}, Lys^{50}, Arg^{53}, Leu^{252}, Asp^{254}, Asn^{259}, and His^{260} which maintain the D1D3 domain interface in the suPAR-ATF structure by three hydrogen bonds, His^{47}-Asn^{259}, Lys$^{50\text{-}}$Asp^{254}, and Arg^{53}-Asp^{254} between the two domains. Together, the three domains of suPAR form a concave shape (Figure 45a) with a cone-shaped cavity at the center. The ATF inserts into the cavity of uPAR, but does not occupy it completely (Figure 45).[309]
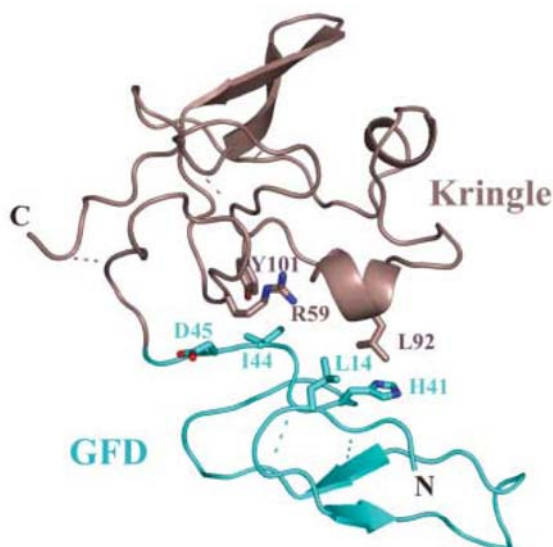
Figure 43. Ribbon structure of ATF in the suPAR-ATF-ATN615 complex. From Q. Huai *et al*. *Science* 2006, *311*(5761), 656-659.[309] Reprinted with permission from AAAS. The GFD domain is shown in cyan and the kringle domain in dark salmon. The residues Leu[14], His[41], Ile[44,] Asp[45], Arg[59], Leu[92], and Tyr[101] involved in domain interactions are shown as sticks. W-loop (residues 23 to 29) connects two β–strands (residues 18-22 and 30-32) in the GFD domain. The kringle domain contains two strands (residues 112-117 and 120-125) and two short α helices (78-81 and 91-94).[309]

2.1.6.3   The ATF-suPAR interaction

Results from biochemical studies about the uPA-uPAR interaction available so far indicated a major role of the D1 domain of uPAR in uPA binding.[296] Point mutations by alanine in the D1 domain, in particular, Arg[53], Leu[55], Tyr[57] und Leu[66], but also in the region uPA$_{2\text{-}10}$ led to a significant loss of the binding activity.[322] Also Tyr[57] was found to be important.[323] Other studies also showed a contribution of Arg[53], Leu[66] and His[251] (D3),[324] of His[249], Asp[254] und Phe[256][325] as well as of the D2 domain.[326] According to the crystal structure, the suPAR-ATF interface can be divided into three contact regions:[309]

First, one stretch of residues in the GFD domain of uPA (Ser[21], Asn[22], Lys[23], and Tyr[24]), buried deep in the suPAR cavity, contacts mainly the D2 domain of suPAR (Figure 45b). This region has both hydrogen bonds and polar interactions between uPA and its receptor. In consistence with the biochemical studies, it was found that Tyr[24] of ATF forms hydrogen bonds with Arg[53], Asp[254] of suPAR and a polar interaction with Asp[254].[309]
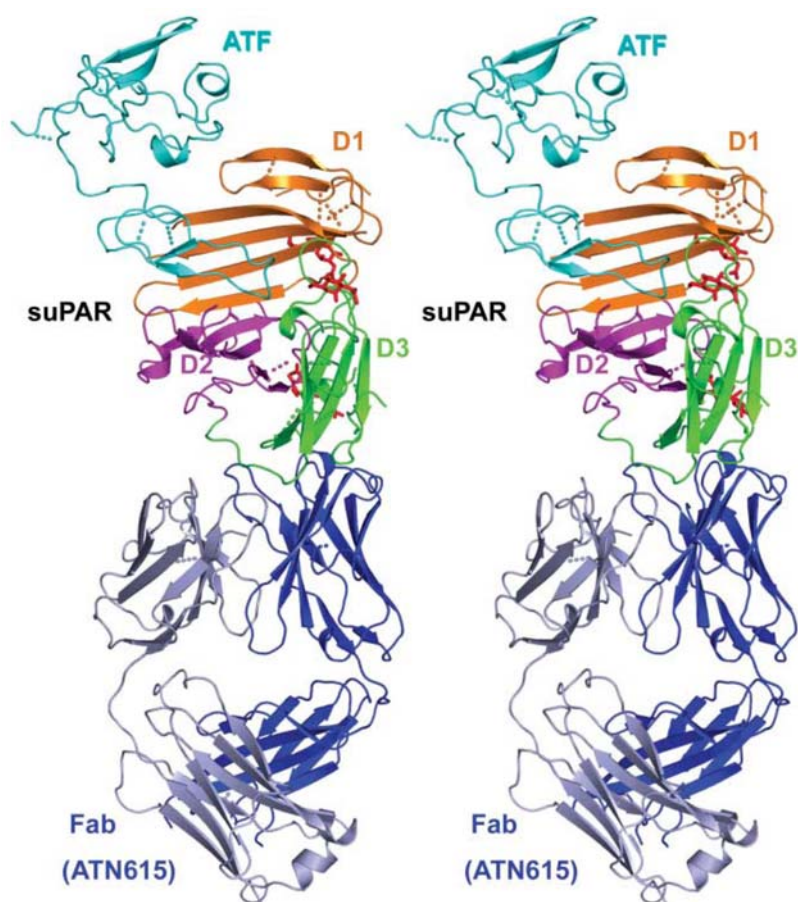
Figure 44. Stereo view of the X-ray structure of the suPAR-ATF-ATN615 complex. From Q. Huai *et al.* *Science* 2006, *311*(5761), 656-659.[309] Reprinted with permission from AAAS. Ribbon diagram showing the D1 domain of suPAR (orange), the D2 domain (magenta) and the D3 domain (green). The ATF is shown in cyan, light chain of the antibody ATN615 in light blue and the heavy chain in dark blue. Carbohydrates in suPAR are shown as red sticks. Disulfide bonds are shown in dashed lines colored as is the backbone to which they are attached.[309]

The hydrophobic patch at the inner surface, near the opening of the suPAR cavity, forms the second region of the suPAR-ATF interface.[309] It is formed mainly by the residues in the D1 domain (Val^{29}, Leu^{31}, Leu^{40}, Leu^{55} and Leu^{66}) which interact with Phe^{25}, Ile^{28} and Trp^{30} of ATF (Figure 45b) thereby forming significant hydrophobic interactions.[309]

The third region, located at the edge of the cavity, contacts the D1 domain of suPAR and residues of ATF, *e.g.* the kringle domain forming a hydrogen bond and van der Waals contacts (Figure 45a).[309]
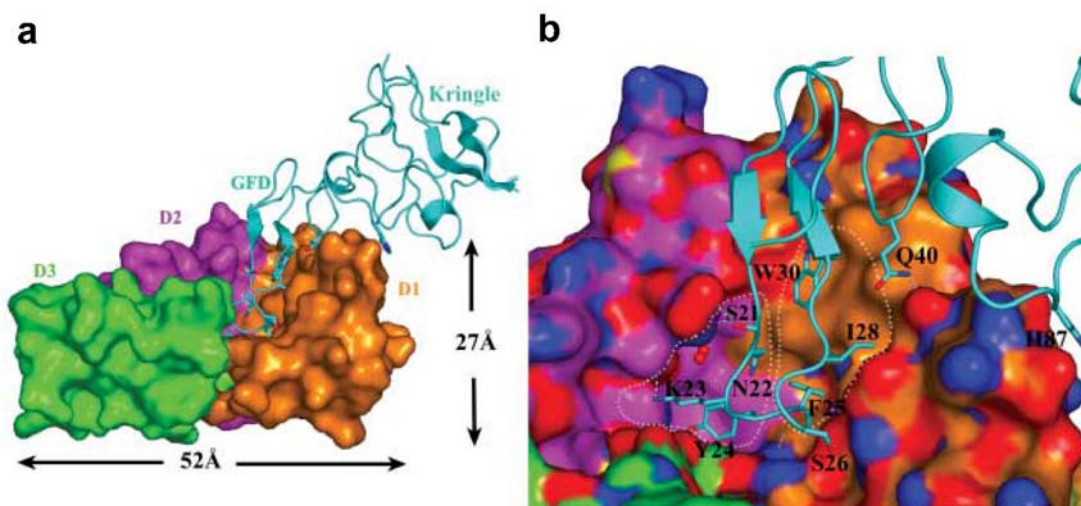
Figure 45. The suPAR-ATF binding surface. From Q. Huai *et al*. *Science* 2006, *311*(5761), 656-659.[309] Reprinted with permission from AAAS. The carbon atoms of the D1 domain of uPAR are shown in orange, the D2 in magenta and the D3 in orange. The ATF is shown in a ribbon diagram in cyan. (a) Molecular surface representation of the overall suPAR-ATF binding. The three uPAR domains form a conical cavity with a wide opening (25 Å) and large depth (14 Å) that are involved in the ATF binding. (b) Surface representation of the uPAR-ATF binding. The circled areas are regions 1 and 2 (from left to right) of uPAR-ATF interface. Oxygen atoms are shown in red, nitrogen atoms in blue and sulfur in yellow. Water molecules involved in uPAR-ATF binding are shown as red spheres. Hydrogen bonds are shown as dashed lines (light blue).[309]

Taken together, it is confirmed that the D1 and D2 domains of uPAR play a critical role in the uPA-uPAR interaction. In addition, also contributions of the D3 domain were described which contacts ATF through van der Waals interactions.[309] Hence, all three uPAR domains and both uPA domains are crucial for the high-affinity binding between uPA and uPAR.

2.1.7   uPAR mediated signal transduction

uPAR, although lacking a signal-transducing cytoplasmic tail, furthermore orchestrates the initiation of several intracellular signal-transduction pathways by interaction, for example, with caveolin[327-329] and G-protein-coupled receptors (GPCRs)[330] as well as with vitronectin and members of the integrin adhesion-receptor superfamily[331] (Figure 46).[330,332] As a result, uPAR activates intracellular signaling molecules such as tyrosine- and serine protein kinases (such as EGF receptor, lymphocyte protein tyrosine kinase (Lck), hematopoietic cell kinase (Hck), Src,

focal adhesion kinase (FAK) and extracellular-signal-regulated kinase (ERK)/mitogen-activated protein kinase (MAPK)) (see also Figure 37).[244,333]

2.1.8   Signaling *via* integrins and vitronectin

Integrins are transmembrane proteins which are involved *e.g.* in cell-cell and cell-matrix adhesion, the regulation of inflammatory processes and tumor progression (*e.g.* neoangiogenesis).[232,334] To participate in adhesion, an activation of the integrins by binding of a ligand or a cellular signal is necessary. So far, uPAR has been proven to interact with a number of other integrins, such as $\alpha 4\beta 1$, $\alpha v\beta 3$, $\alpha 6\beta 1$, $\alpha 9\beta 1$, $\alpha v\beta 5$, $\alpha 3\beta 1$, $\alpha v\beta 5$, $\alpha 5\beta 1$ and $\alpha 5\beta 1$.[334-345]
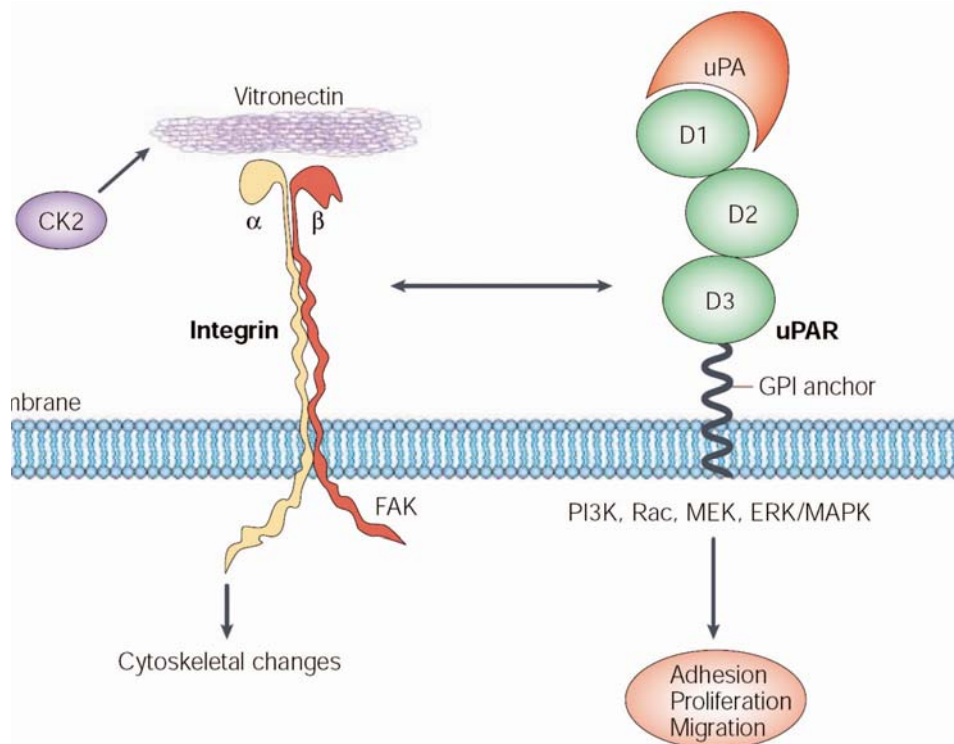
Figure 46. Scheme depicting the role of a uPAR–integrin complex as a signalling receptor. Reprinted by permission from Macmillan Publishers Ltd: *Nature Reviews Molecular Cell Biology* 2002, *3*(12), 932-943, Copyright © 2002. Protein kinase casein kinase-2 (CK2) phosphorylates vitronectin and regulates uPA-dependent cell adhesion to vitronectin. uPAR lacks a cytosolic domain but transmits intracellular signals through its association with transmembrane integrins. The intracellular signaling components are positioned in the order in which the cascade is presumed to proceed, but the pathways remain speculative. ERK, extracellular-signal-regulated kinase; FAK, focal adhesion kinase; MAPK, mitogenactivated protein kinase; MEK, MAPK and ERK kinase; PI3K, phosphatidylinositol 3-kinase.[332]

These interactions initiate signal-transduction pathways such as mitogen-activated protein kinase (MEK)–ERK[344,346,347] (important for adhesion and migration) (Figure 46) and JAK-STAT[348-350] (Janus kinase–signal transducer and activator of transcription; responsible for transcription and DNA-STAT binding) pathways (Figure 37) that involve cytoskeletal components and cytosolic and transmembrane kinases.[252,332,350]

uPAR binding to the ECM protein vitronectin, which is a ligand of integrin $\alpha v \beta 3$, is mediated by uPA (Figure 46). uPA controls the receptor oligomerization[351] which is an important determinant for the high-affinity binding to vitronectin.[351,352] In addition, the protein kinase casein kinase-2 (CK2) phosphorylates vitronectin and regulates uPA-dependent cell adhesion to vitronectin.[332] The uPAR binding site on vitronectin was found to be located in the somatomedin B domain,[353-355] the exact binding domain of uPAR, however, is unknown so far.[355-358] uPAR binding to vitronectin is competed by PAI-1 which also binds to the somatomedin B domain.[353-355,359]

2.1.9 Signaling *via* G protein-coupled receptors

The migration in a specific direction is an important feature of cancer cells. Migration is mediated by cell surface receptors that 'sense' the presence of a gradient of chemoattractants, such as chemokines.[332] Recently, uPAR was proven to interact and activate the G protein-coupled chemotactic formyl peptide receptor-like 1 (FPRL1), also known as lipoxin A4 receptor (LXA4R).[330,360] To induce cytoskeletal changes and intracellular signal transduction, the motif Ser-Arg-Ser-Arg-Tyr (uPAR$_{88-92}$) which is located between the D1 and the D2 domain has to be unmasked. This can be achieved by uPA binding to uPAR or by cleavage of the domain 1 of uPAR to release the fragment D2D3 (Figure 47) which directly binds to FPRL1.[332,361-363] It was found, that this binding can be inhibited by FPRL1 ligands.[330]
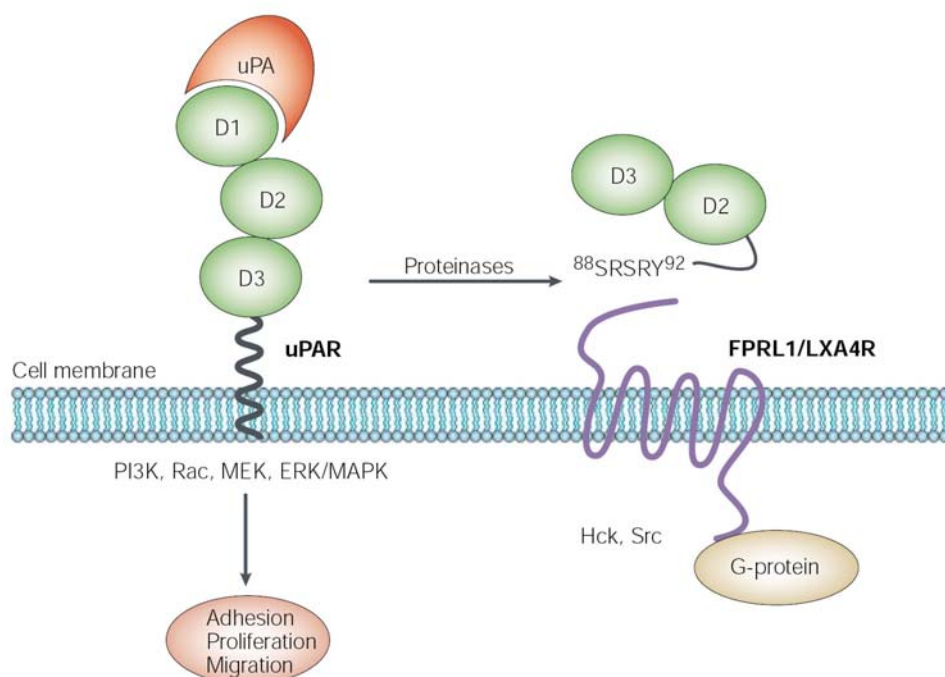
Figure 47. Scheme depicting the role of a uPAR–GPCR complex as a signaling receptor. Reprinted by permission from Macmillan Publishers Ltd: *Nature Reviews Molecular Cell Biology* 2002, *3*(12), 932-943, Copyright © 2002. Binding of the D2D3 fragment of soluble urokinase (suPAR) to the G-protein-coupled receptor formyl peptide receptor-like 1 (FPRL1) transmits chemotactic signals. The intracellular signaling components are indicated, but the pathways remain speculative. ERK, extracellular-signal-regulated kinase; Hck, haematopoietic cell kinase; MAPK, mitogenactivated protein kinase; MEK, MAPK and ERK kinase; PI3K, phosphatidylinositol 3-kinase.[332]

2.1.10 Tumor-associated prognostic factors of the uPA/uPAR system: clinical significance of uPA, uPAR, PAI-1 and PAI-2

After the discovery of a casual connection of plasminogen activation and cancer in the 1960s,[364,365] Åstedt *et al*. were the first to report the overexpression of uPA in ovarian carcinoma.[366,367] As early as in the 1980s, an increased concentration of uPA in tumor tissue was linked with high metastatic potential of tumors and poor prognosis for the patients.[368] The natural inhibitor PAI-1, however, proved to be correlated with poor prognosis as well. This is in contrast to the assumption that PAI-1 as uPA inhibitor should suppress plasminogen activation and metastasis and is explained by the diverse biological properties[369] of PAI-1 which is not only inhibitor of uPA but also is involved in cell adhesion, proliferation and migration as well as in signal transduction and apoptosis.[249,368,370-379] Today, the prognostic impact of

uPA and PAI-1 is validated at high level of evidence,[248,368,380-382] and also uPAR has been linked with poor prognosis in numerous studies.[383] In contrast to PAI-1, increased PAI-2 levels have been linked with low metastatic potential of tumors and good prognosis for the patients.[368,384-386]

2.1.11 The uPA/uPAR system as potential target in cancer therapy

As presented above, a large body of evidence obtained from both *in vitro* and *in vivo* experiments as well as from clinical studies shows that the uPA-system, especially the protease uPA, its major inhibitor PAI-1 and its cellular receptor uPAR, plays an important role in a variety of malignant tumors.[259,374,387,388] uPAR not only is focusing pericellular proteolysis to the tumor cell, but through direct or indirect interactions with extracellular matrix proteins or transmembrane receptors such as the integrins and the EGF receptor, it modulates cell migration, cell-cell and cell-matrix interactions and signaling pathways. Altogether, the system is involved at multiple stages in the formation and progression of the disease,[389] in particular in invasion and metastasis,[252,332] cell proliferation,[390,391] migration[392] and cell adhesion.[252] As overexpression of uPAR (as well as uPA and PAI-1) in tumor tissue is strongly correlated with poor prognosis for patients afflicted with different types of cancer, it represents an attractive target for cancer therapy.[393]

Hence, numerous efforts have been made to inhibit the catalytic activity of uPA or to inhibit uPAR function by biologic and synthetic ligands.[388,393] A selection of synthetic inhibitors is presented in chapter 2.2.1.1.. Goal of the present study was now to examine whether peptidic radioligands, based on potent uPAR binding peptides, may be developed for application in receptor-based radionuclide therapy.

2.1.12 Visualization and treatment of tumors by radiopharmaceuticals

2.1.12.1 Tumor imaging and radionuclide therapy

Antibodies, peptides or non-peptidic compounds which are capable to selectively bind to antigens or receptors overexpressed on tumor cells, are promising candidates for tumor imaging or antigen- or receptor-based radiotherapy.[394-397] Over the past years, great progresses have been made in tumor imaging and several new methods have been developed: for example, the magnetic resonance imaging (MRI),[398,399] fluorescence-mediated molecular tomography (FMT),[400] doppler sonography and szintigraphy methods.[401]

The szintigraphy methods SPECT (single photon emission computed tomography) and PET (positron emission tomography)[402] use molecular antibodies (mAbs) or small organic compounds like sugars, amino acids, peptides or peptidomimetics as ligands which are labeled with a radionuclide. The resulting tracers interact *in vivo* with their target structures and allow a non-invasive visualization and even a quantification of the distribution of targeted processes. This offers *e.g.* the opportunity to quantify specific targets prior to a therapy and predict its success. Moreover, the dosage of the chemotherapeutic can be adjusted and optimized and the success of the therapy can be observed by decreasing target binding. Recently also hybrid techniques like SPECT-computed tomography (CT) or PET-CT found application, which enable the simultaneous detection of a biochemical signal (PET/SPECT) and morphology (CT).[403] The radionuclide used is dependent on the desired application (diagnosis, therapy) and the method (*e.g.* PET, SPECT). Table 13 summarizes important radionuclides for various applications.

Widely used radionuclides in PET scanning are for example ^{11}C, ^{18}F or ^{68}Ga,[404] whereas ^{18}F turned out to have several advantages over the others:[405]

- Its relatively long half-life permits enough time for the synthesis of the tracer and for PET and allows kinetic studies.

- In non-fluorine-containing metabolic substrates, the introduction of a fluorine atom (F for H, F for OH) does not cause significant sterical changes.

- The ^{18}F positron energy is the lowest of the first row positron emitters and for this reason imaging can be done at the highest resolution.

Table 13. Selection of important radionuclides in tumor imaging.

Isotope	t(½)	Type of radiation	Application
^{11}C	20 min	β$^+$	PET
^{15}O	2 min	β$^+$	PET
^{18}F	110 min	β$^+$	PET
^{68}Ga	68 min	β$^+$ (88%)	PET
^{124}I	4.2 d	β$^+$ (23%)	PET
^{123}I	13 h	γ	SPECT
^{99m}Tc	6 h	γ	SPECT
^{111}In	2.8 d	γ, Auger	SPECT

A powerful and widely used tracer for PET is the glucose analogon ^{18}F-2-fluorode-oxyglucose (FDG). The high tumor uptake as exogenic substrate of the glucose transporter and of the hexokinase in tumor cells enables a visualization (tumor localization) and quantification (tumor staging and grading) of the enhanced glucoseutilisation in tumors *via* PET.[406,407] Nevertheless, there is no "best" radionuclide for PET application, as the nuclear characteristics of the radionuclide have to correlate with the physiologic target structure and tracer kinetic. Hence, nuclides with a relatively long half-life like ^{124}I or ^{86}Y (t$_{1/2}$ = 15 h) are used, for example, for labeling of mAbs providing a longer biodistribution.[408]

Typical γ-emitter used in SPECT are ^{123}I, ^{99m}Tc and ^{111}In. Ligands labeled with ^{99m}Tc or ^{111}In are used for peptide receptor imaging for receptor systems like the somatostatin (sst) receptor 2,[409] the glucagon like peptide-1 (GLP-1) receptor,[410] cholecystokinin receptors[411] and neurokinin 1 receptor NK.[412]

Beside their use in tumor imaging, radiopharmaceuticals become more and more important in tumor therapy as alternative to the conventional chemotherapy or in adjuvant therapies.

2.1.12.2 Receptor-based radionuclide therapy

A major goal is to destroy tumor cells directly by nuclear radiation. For use in targeted tumor therapy, radionuclides are frequently coupled to antibodies specifically recognizing cell surface antigens that are overexpressed or exclusively expressed on tumor cells to selectively target the tumor cells.[394,395] Table 14 gives an overview over commonly used radionuclides in therapy.

Table 14. Selection of important radionuclides in tumor therapy.

Isotope	t(½)	Type of radiation
^{131}I	8.0 d	γ, β^-
^{177}Lu	6.7 d	β^-
^{188}Re	17 h	γ, β^-
^{213}Bi	46 min	α
^{90}Y	2.7 d	β^-

Several radiolabeled mAbs have already been approved by the Food and Drug Administration (FDA) for radioimmune therapy of cancers or are in clinical trials:[413] for example, the labeled anti-CD20 antibody ^{131}I-Tositumomab (Bexxar; GlaxoSmithKline) or ^{90}Y-Ibritumomab tiuxetan (Zevalin; Biogen Idec) for the treatment of non-Hodgkin's lymphomas (NHL). Nevertheless, the treatment with antibodies is limited. One major limitation of using mAbs to target cancer is that the antibody molecule is relatively large. This makes it difficult for the molecule to get into the interior of a large tumor where the blood supply is inadequate. Another major problem is the nonspecific uptake of the antibody molecules into the reticuloendothelial system such as the liver, spleen and bone marrow. The dose-limiting toxicities of radiolabeled antibody are liver and bone marrow toxicities. A general problem is, furthermore, the immunogenicity of anti-mouse antibodies making repeated treatments difficult.[414] A promising alternative to mAbs as ligands are peptides, peptidomimetics or steroids which will be described more detailed below.[415-417]

Beside antibodies, radiolabeled peptides targeting receptors overexpressed in numerous human cancers have proven to be promising candidates for use in radiotherapy as well.[396,418,419] Moreover, peptides are often superior to monoclonal antibody carrier systems due to small molecular weight, outstanding permeability and facile synthesis, while preserving high affinity receptor binding. In addition,

handling of peptides is convenient since they usually do not cause an antigenic response.[420]

Several peptides are currently under evaluation or have already been administered in clinical studies.[396] Medullary thyroid cancer shows *e.g.* high expression of cholecystokinin B (CCK-B) receptors that are specifically targeted by radiolabeled minigastrin analogs.[421] In several of the more prevalent cancers, including breast and small cell lung cancer, the gastrin releasing peptide (GRP) receptor is abundantly expressed. Therefore, ^{177}Lu-labeled GRP analogs are presently developed for GRP receptor-mediated radiation therapy.[422] Targeting of the GLP-1 receptor, displaying high expression in human insulinomas and gastrinomas, by radiolabeled GLP-1 analogs may also provide an attractive new therapeutic option.[423] Finally, tumor tissue from patients suffering from neuroendocrine gastroenteropancreatic (GEP) tumors is, in principle, characterized by overexpression of somatostatin receptors. Accordingly, treatment of patients with the receptor ligands DOTA-Tyr^3-octreotide (DOTATOC) as well as DOTA-Tyr^3-octreotate (DOTATATE) labeled with the β-emitters ^{90}Y or ^{177}Lu has turned out to be very encouraging in terms of tumor regression.[424-428] In a recent study, DOTATOC labeled with the α-emitter ^{213}Bi was reported to significantly reduce growth of pancreatic tumors in a preclinical animal model.[420]

In contrast to β-emitters, α-emitting radionuclides, such as ^{213}Bi, emit high linear energy transfer (LET), low range particles manifested by a high relative biological effectiveness. Consequently, a great fraction of the total α-emission energy is deposited into the targeted cancer cell and only a few nuclear hits are required to irreversibly damage the cell.[429-431] Thus, targeted therapy with α-particle emitting nuclides is thought to be particularly efficient in case of tumor cell dissemination into the peritoneal cavity.[432-434] Radioimmunotherapy using high LET α-emitters coupled to antibodies that specifically target surface antigens on tumor tissue has turned out to be a promising concept in treating ovarian cancer.[394,429] Based on its high energy (8.4 MeV), short range in tissue (80 μm) and short half life ($t_{1/2}$ = 46 min), the α-emitter ^{213}Bi is especially suited to eliminate micrometastases or circulating cancer cells while sparing normal tissue. Furthermore, ^{213}Bi found application in treatment of human cancer cells with overexpression of the somatostatin

receptor, which were efficiently eliminated both *in vitro* and *in vivo* using [213]Bi-DOTATOC.[420,435]

In the following, some of the most convenient methods for the preparation of radiopharmaceuticals will be presented as examples. In principle, radionuclides can be covalently attached to the carrier molecule or they can be complexed by a chelator which is covalently attached to the carrier molecule.[436]

2.1.12.3 Radiolabeling by covalent attachment of the radionuclide

Iodine-labeling can be achieved by a electrophilic aromatic substitution in *ortho*-position to a phenolic hydroxyl group, *e.g.* using chloramines-T[437] or Iodogen[®] (Figure 48).[438] These reagents lead to a oxidation of iodides to iodine which then reacts with the activated aromatic residue.

144   **145**
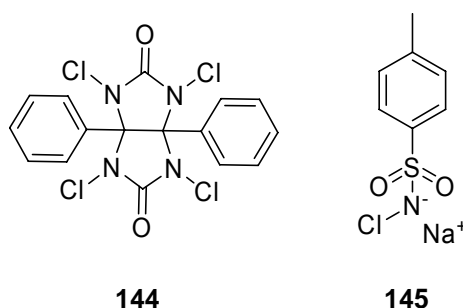
Figure 48. Structures of Iodogen[®] (144) and chloramine-T (145).

Monoiodotyrosine, however, is enzymatically deiodogenated *in vivo*. Therefore, procedures were developed to introduce iodine also in aromatic residues lacking a hydroxyl group. Successful approaches are reported *via* ipso-substitution of precursors like silyl[439] or stannyl[440] derivatives.[441,442] In a recent approach, a direct iodination of non-activated phenylalanine incorporated into peptides or proteins was reported using bis(pyridine)iodonium (I) tetrafluoroborate in presence of TFA. This widens iodine labeling opportunities to molecules lacking a tyrosine residue.

[11]C for PET analysis is often introduced *via* methylation of *e.g.* alcohols[443,444] or amines[445] using [^{11}C]-iodomethane or *via* nucleophilic substitution by [^{11}C]-cyanide.[446] [18]F can be introduced by nucleophilic substitution of activated alcohols using K[18]F/Kryptofix[447] or *via* electrophilic aromatic substitution using ^{18}F-acetyl

hypofluoride[448]. Furthermore, ^{18}F-labelled prosthetic groups like 2-[^{18}F]-fluoro-propionic acid or 4-[^{18}F]fluorobenzoic acid or the corresponding precursors are used in acetylation reactions.[449,450] Recently, a facile method enabling ^{18}F-labeling in a rapid manner *via* oxime ligation was developed in a co-project of our group with the laboratory of Prof. Wester (Klinikum rechts der Isar, München). *p*-[^{18}F]-fluoro-benzaldehyde was prepared by a nucleophilic aromatic substitution which is then reacted with an aminooxy-functionalized peptide (Scheme 13).[451]

Scheme 13. *[18]F-labeling procedure by Poethko et al.[451]*

146   **147**   **148**
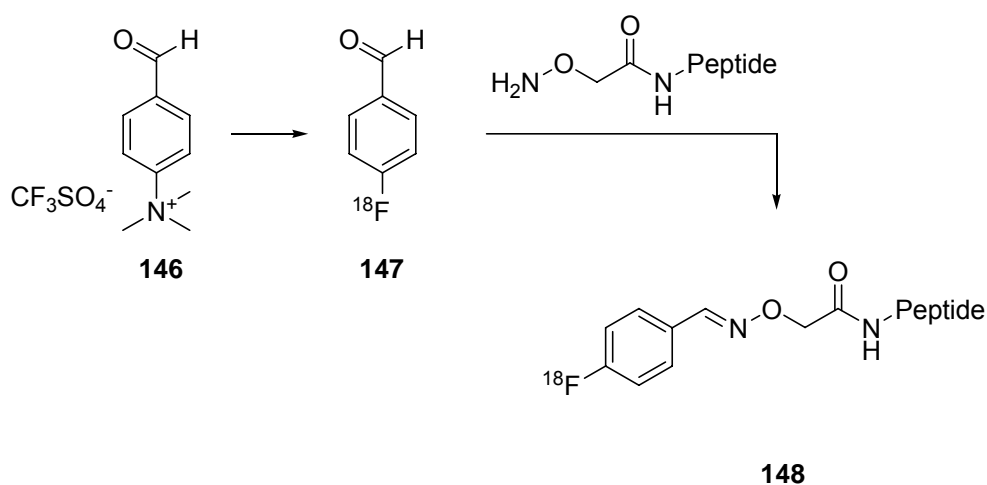
2.1.12.4 Non-covalent radiolabeling using chelators

For non-covalent binding of radionuclides, bifunctional chelating agents (BFCAs) are used to connect radioactive markers and a targeting molecule. This procedure provides the opportunity to introduce various different radionuclides into the target compound to adopt the nuclear characteristics with respect to the application (imaging or therapy), the physiologic target structure or the carriers biodistribution. An ideal chelator should complex the radionuclide efficiently and quickly under mild conditions and it should form stable complexes *in vivo*.

Commonly used BFCAs are poly(aminocarbonic acid) derivatives are, for example, diethylene triamine pentaacetic acid (DTPA) (149), 1,4,7,10-tetraazacyclodecane-1,4,7,10-tetracetic acid (DOTA) (150) or 1,4,7-triazacyclononane-1,4,7-triyltri-acetic acid (NOTA) (151) (Figure 49). These ligands are suitable for complexation

of divalent and trivalent metals by an up to eightfold coordination *via N/O*-donors, whereas the cyclic ligands were found to be superior in terms of complex stability.[452] DOTA complexes are even stable under strong acidic conditions (pH <2).[453,454] Hence, radiopharmaceuticals containing the DOTA ligand as metal chelator have found widespread use in therapy and diagnostic imaging.[394,418]

149   **150**   **151**
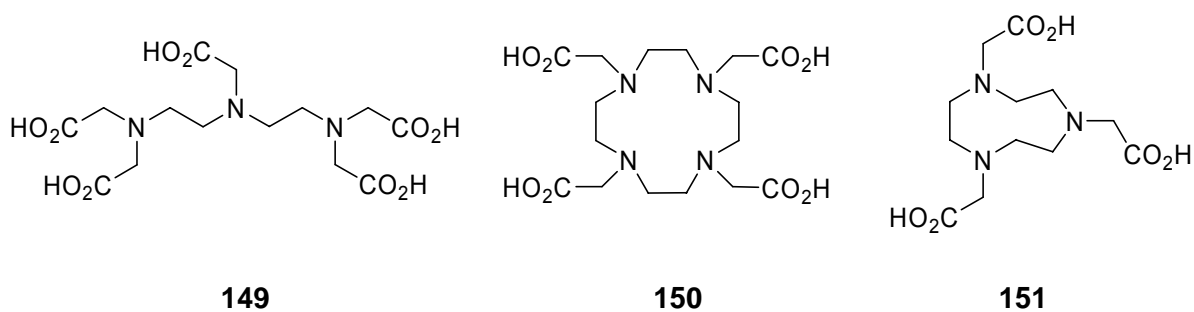
Figure 49. Structures of the BFCAs diethylene triamine pentaacetic acid (DTPA) (149), 1,4,7,10-tetraazacyclodecane-1,4,7,10-tetracetic acid (DOTA) (150) or 1,4,7-triazacyclononane-1,4,7-triacetic acid (NOTA) (151).

2.2   Development of uPAR-selective radioligands

2.2.1   Background

Peritoneal spread of tumor cells in ovarian cancer implies poor prognosis owing to the lack of efficient standard therapies and chemo-resistance. Surgery combined with chemotherapy can cause a survival benefit, nevertheless the median survival of patients suffering from peritoneal carcinomatosis is only three to six months.[455] Hence, while ovarian cancer accounts for only 4% of all cancers in women,[456] it displays the highest rate of mortality of all gynecologic malignancies. Since intraperitoneal spread is the most common characteristic of ovarian cancer, in more than 75% of all cases the disease has already disseminated beyond the ovary at the time of diagnosis. Accordingly, the major cause of treatment failure is incomplete debunking of cancer cells from the peritoneal cavity. Following relapse due to chemo-resistance, there is currently no further therapeutic option available.[457] Therefore, targeting and efficient elimination of single remaining tumor cells or small tumor cell clusters could considerably improve prognosis.

2.2.1.1   Synthetic peptides targeting uPAR

As described above, the urokinase-type plasminogen activator (uPA) system is overexpressed in numerous malignant human cancers. Hence, it represents a promising target for anti-cancer therapy.[388,393,458-460] ^{213}Bi-PAI-2 conjugates, indirectly targeting tumor cell-associated uPAR, have been successfully applied in preclinical studies for the control of pancreatic, prostate and ovarian cancer.[461-464] Synthetic peptides directly binding to uPAR may offer another approach for uPAR-targeted ^{213}Bi-therapy. In fact, by different approaches, potent uPAR binding peptides have recently been identified, among them the competitive uPA inhibitors WX360 (*cyclo*[21,29][D-Cys^{21}Cys^{29}]-uPA$_{21-30}$)[465] and AE105 (Asp–Cha–Phe–(D-Ser)–(D-Arg)–Tyr–Leu–Trp–Ser).[466]

WX360 is derived from the uPAR-binding site of uPA, which has been optimized by alanine and D-amino acid scanning procedures as well as by disulfide bridging of the two essential cysteines within the identified peptide lead structure (Figure 50).[465,467,468]

Figure 50. Development of the uPAR antagonist (cyclo[21,29][D-Cys^{21}Cys^{29}]-uPA$_{21-30}$) (155; WX360) from the aminoterminal fragment (ATF) of uPAR.

Starting point for the development of WX360 in our group was the discovery of the peptide [Ala^{19}]uPA$_{12-32}$ by Appella *et al.*[469] which was found to inhibit the uPA-uPAR interaction. The epitope was derived from the GFD domain of uPA which is responsible for the binding to uPAR.[302,322] *N-* and *C-*terminal truncation of [Ala^{19}]uPA$_{12-32}$ by M. Koppitz led to the development of the inhibitor uPA$_{16-32}$ (IC$_{50}$ = 4 µM). Ala-scan analysis gave that especially the amino acids Cys^{19}, Tyr^{24}, Phe^{25}, Ile^{28}, Trp^{30} und Cys^{31} are important for uPAR binding.[470] Further modifications by M. Bürgle led to the cyclic peptide *cyclo*[19,31]-uPA$_{19-31}$ (152) with an IC$_{50}$ value of 300 nM.[319,468] Substitution of Cys^{19} by D-Cys^{19} (*cyclo*[19,31][D-Cys^{19}]-uPA$_{19-31}$ (153)) significantly enhanced the uPAR affinity (IC$_{50}$ = 40 nM).

After an additional Ala-scan of *cyclo*[19,31]-uPA$_{19-31}$ (152), the non-essential residues Val^{20}, Ser^{21} und His^{29} were deleted leading to *cyclo*[21,29][Cys^{21},Cys^{29}]-uPA$_{21-30}$ (154) with an IC$_{50}$ value of 910 nM.[319] N. Schmiedeberg found that the substitution of the *N*-terminal Cys^{21} by D-Cys^{21} leads to a dramatic improvement of the ligands affinity towards the uPA receptor (*cyclo*[21,29][D-Cys^{21},Cys^{29}]-uPA$_{21-30}$

(155/WX360); IC$_{50}$ = 40 nM) (Figure 50 and Figure 51). This was in line with the observation for peptides 152 and 153 described above.[465]

Human uPAR	⦃Ser-Asn-Lys-Tyr-Phe-Ser-Asn-Ile-His-Trp-Cys-Asn-⦄
WX360	H-Cys-Asn-Lys-Tyr-Phe-Ser-Asn-Ile-Cys-Trp-OH
Clone 20	H-Ala-Glu-Pro-Met-Pro-His-Ser-Leu-Phe-Ser-Asn-Tyr-Leu-Trp-Tyr-Thr-OH
AE68	H-Ser-Leu-Asn-Phe-Ser-Gln-Tyr-Leu-Trp-Ser-OH
AE105	H-Asp-Cha-Phe-Ser-Arg-Tyr-Leu-Trp-Ser-OH
AE147	H-Lys-Ser-Asp-Cha-Phe-Ser-Lys-Tyr-Leu-Trp-Ser-Ser-Lys-OH

Figure 51. Comparison of the sequences of human uPAR, WX360, Clone 20, AE68, AE105 and AE147. Cha: cyclohexyl alanine; D-Amino acid residues are underlined.

Peptide AE105, displaying comparable uPAR binding, has been developed *via* a combination of phage-display technology, affinity maturation by combinatorial chemistry and affinity measurements by surface plasmon resonance spectroscopy (Figure 51): After isolation of the "clone 20" peptide (AEPMPHSLNFSQYLWYT) in the laboratory of Rosenberg,[471,472] Ploug *et al*. were able to shorten the sequence to yield the decapeptide AE68 (SLNFSQYLWS) displaying a similar binding affinity.[473,474] Using the one-bead-one-compound method,[475] a series of derivatives was generated leading to the discovery of the AE105 peptide with improved uPAR affinity compared to AE68 (Figure 51). Another derivative very recently found application as affinity ligands for the purification of uPAR.[476]

The interaction of uPA with uPAR is in general species selective,[301] however, little cross-reactivity to murine and monkey uPAR has been shown.[466,477] In contrast, AE105 does only bind to human uPAR.[466,478] This led to the assumption that the binding mode of AE105 is somewhat different to that of ATF or WX360. Recently, this assumption was confirmed by a crystal structure: Llinas *et al*. were able to crystallize the uPA receptor in complex with the antagonist AE147, a variant of AE105 which provides improved solubility (Figure 52).[310] They found that the ligand binds in a helical conformation and with a large external surface (Figure 52b,c) - in contrast to the receptor binding loop of ATF (Figure 52d),[280,309,479] which is mimicked by WX360.[465]
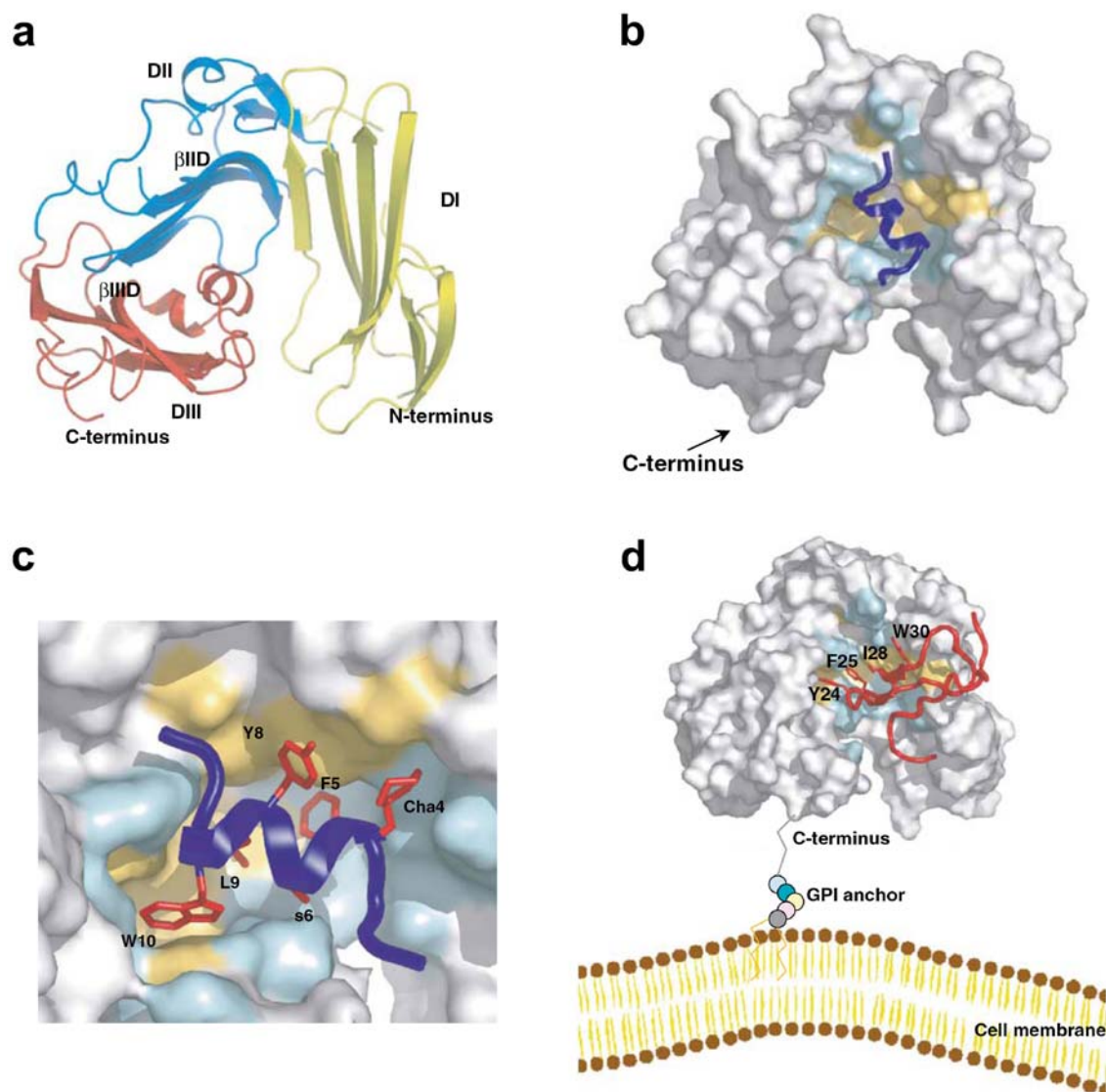
Figure 52. The structure of human uPAR from Llinas *et al.*,[310] reprinted by permission from Macmillan Publishers Ltd: *The EMBO Journal* 2005, *24*(9), 1655-1663, Copyright © 2005. (a) The overall modular structure of uPAR as a ribbon diagram. The individual uPAR domains are assembled in a right-handed orientation and are colored yellow (DI), blue (DII) and red (DIII). The bended β-strands in DII and DIII are indicated separately.[310] (b) Molecular surface representation of the uPAR–peptide complex. The surface of uPAR is shown in grey, whereas the bound antagonist peptide (AE147) is shown as a ribbon diagram in dark blue. Receptor residues interacting with AE147 are coloured orange (hydrophobic) or cyan (polar) and the asparagine-linked glycosylation sites coloured light green. (c) Enlarged uPAR binding cavity of AE147 (illustrated by a combined ribbon and stick representation in dark blue). The indole side chain of W10 engages the deep and prominent hydrophobic hole of the central cavity of uPAR and the side chain of L9 is located proximate to its entrance. (d) Model for the structure of the human GFD–uPAR complex. The uPAR molecule is shown as a molecular surface representation. The receptor-binding module of uPA is shown in red as a ribbon diagram with the side chains of Y^{24}, F^{25}, I^{28} and W^{30}, which are highlighted by sticks. Note that W^{10} and L^9 of AE147 exhibit a spatial superimposition with Y^{24} and F^{25} in uPA. A schematic representation of the glycolipid (GPI) anchor is shown to connect the *C*-terminus of uPAR to a model of the cell membrane.[310]

Although direct comparison of uPAR/ATF and uPAR/AE147 complexes confirms a spatial overlap between the GFD and AE147 in the binding cavity of uPAR, pronounced differences exist in the positioning of the individual side-chains and in their interactions with the receptor.[480] The residues W^{10} and L^9 of AE147, for example, exhibit a spatial superimposition with Y^{24} and F^{25} of ATF (compare Figure 52b and d).[310] These differences could be responsible for observed species selectivity of the inhibitory peptides towards human uPAR.

2.2.1.2   Overall aim and target structures

The aim of the present study was to examine whether peptidic radioligands, based on potent uPAR binding peptides (*i.e.* the 10-mer peptide cyclo[21,29]-[D-Cys^{21}Cys^{29}]-uPA$_{21\text{-}30}$ (WX360)[465] and the 9-mer peptide AE105[466]), may be developed for application in α-emitter therapy of disseminated ovarian cancer. For this, the chelator DOTA, which stably chelates ^{213}Bi, was coupled to the uPAR-binding peptides *via* different types of spacers. For the synthesis of *N*-terminally cross-linked dimeric ligands, a straight-forward procedure was worked out allowing the synthesis of the complete DOTA-conjugate with high purity on solid phase. The synthetic work in this project was performed in collaboration with T. Huber in our group.

2.2.2 Development and evaluation of mono- and dimeric uPAR selective DOTA-peptide conjugates

2.2.2.1 Preparation and evaluation of monomeric DOTA conjugates

For analysis of the uPAR binding capacity of DOTA-conjugated peptide ligands, a competitive flow cytofluorometric receptor binding assay[466-468] was performed in the laboratory of Prof. M. Schmitt and PD Dr. V. Magdolen (Klinikum rechts der Isar, München) using fluorescein isothiocyanate (FITC)-labeled uPA as ligand and human monocytoid U937 cells as the cellular source of uPAR.

Table 15. Binding of monomeric and dimeric DOTA-conjugated ligands to uPAR.[481]

| Label | Ligand structure | | | | IC_{50} [nM][b] |
	DOTA	Spacer[a]	Peptide	monomer/dimer	
WX360	–	–	WX360	monomer	35
156	+	K(K*-Aha-S-Aha)[c]	WX360	monomer	390
157	+	K(Aha*-Ado-Aha)	WX360	monomer	831
AE105	–	–	AE105	monomer	20[d]
158	+	G*-D	AE105	monomer	1124
159	+	G*	AE105	monomer	427
160	+	Aha*-G	AE105	monomer	369
161	+	G*-Aha-G	AE105	monomer	345
162	+	Aha*	AE105	monomer	298
163	+	K*-G-S-G-G[c]	AE105	monomer	34
164	+	K(Aha*)-S-Aha	AE105	monomer	60
165	+	Aha*-Ado-Aha	AE105	monomer	126
166	+	K**-G-S-G-G	AE105	dimer	18
167	+	K(Aha**)-S-Aha	AE105	dimer	73
168	+	Aha**-Ado-Aha	AE105	dimer	1355

[a] Asterisks (*) denotes the amino acid the DOTA residue is attached to in monomeric ligands. Double asterisks (**) indicate the site of cross-linkage and DOTA conjugation in dimeric ligands: DOTA is attached to the N^{α} of a D-Glu which carboxyl groups crosslink two Spacer-AE105 moieties via the N^{ε} of the marked amino acid; Aha is 6-aminohexanoic acid; Ado is 8-amino-3,6-dioxaoctanoic acid. [b] The uPAR-binding capacities of ligands were tested by flow cytofluorometry: PMA-stimulated human U937 cells were coincubated with FITC-pro-uPA and varying amounts of the ligands and cell-associated fluorescence determined; ATF (IC_{50} = 1 nM)[302] was used as internal standard. [c] The DOTA residue is attached to N^{ε} of K*. [d] Result taken from the literature.[466]

ATF was used as an internal standard in the binding assay (IC_{50} = 1 nM[302]) (Table 15). Initially, the uPAR binding peptides were modified by conjugation with the chelator DOTA (for efficient binding of the α-emitter ^{213}Bi), which is relatively large in size and highly charged. As this modification was supposed to significantly alter the binding properties of AE105 and WX360, introduction and optimization of different spacer sequences between the DOTA moiety and the receptor binding ligand were performed by variation of their length and nature in order to maintain the peptide's original binding properties. Previous studies by M. Sukopp in our group[482] have shown that *N*-terminal elongation of WX360 is possible if performed *via* the side chain of an *N*-terminally attached lysine, thereby maintaining the essential *N*-terminal positive charge of WX360. Still, attachment of DOTA *via* this residue resulted in a significant (>10 fold) loss of binding affinity even after having introduced additional spacer molecules.

R* = AE105 = Asp-Cha-Phe-(D-Ser)-(D-Arg)-Tyr-Leu-Trp-Ser
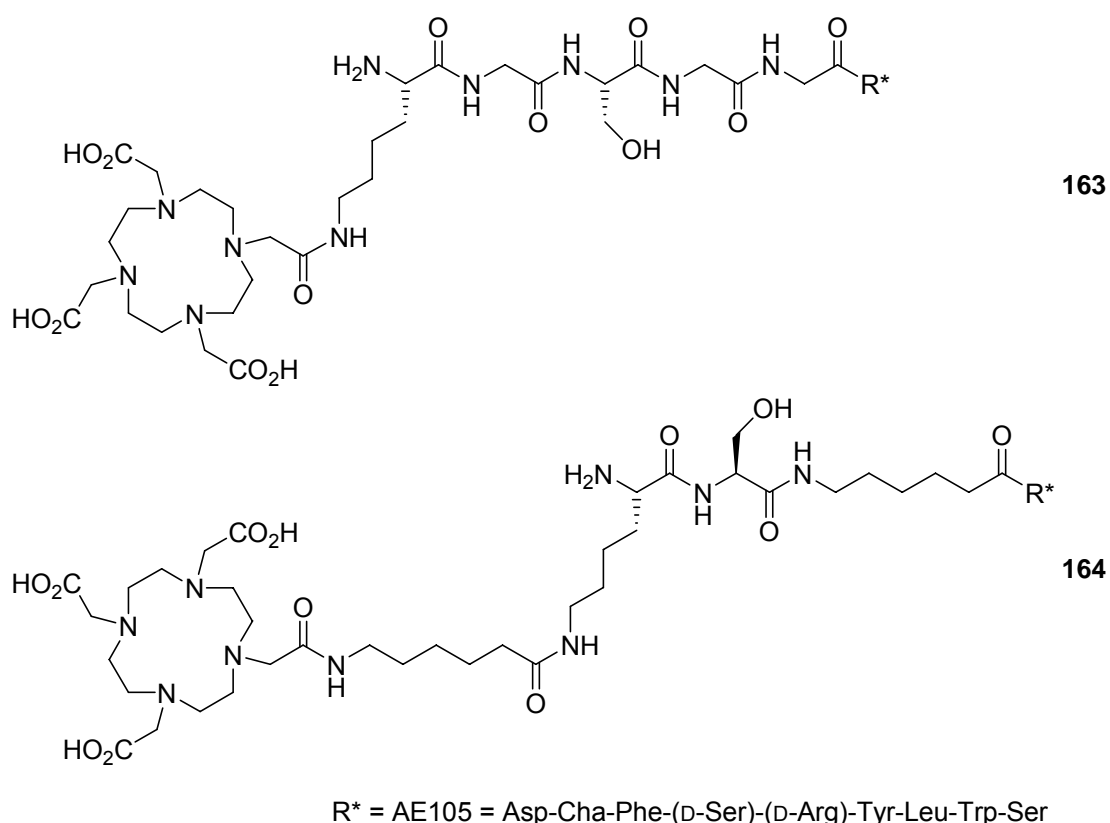
Figure 53. Structures of the AE105-derived monomeric DOTA-conjugated uPAR ligands 163 and 164.

In contrast to that, after optimization of the spacer sequence monomeric AE105-based DOTA-conjugates preserved their high affinity towards uPAR. Compared to unsubstituted AE105 (IC_{50} = 20 nM[466]), the AE105-DOTA conjugate **159** equipped with a single glycine residue as spacer, showed an approximately 20-fold reduction of the binding affinity (IC_{50} = 427 nM), whereas the binding capacity of the ligand **163** (see Figure 53) with the five amino acid spacer Lys-Gly-Ser-Gly-Gly[466] was only slightly reduced (IC_{50} = 34 nM). Using spacers containing the more hydrophobic aminohexanoic acid (Aha) building block (**160, 164**), peptide binding was found to be less effective compared to **163** (Table 15).[481]

2.2.2.2   Preparation and evaluation of dimeric DOTA conjugates

Since multimeric ligands often show superior binding affinities compared to monomeric ligands[483-486], the monomeric ligands **163, 164** (structures shown in Figure 53) and **165** were dimerized by cross linking *via* the spacer moiety. For this, a novel straightforward procedure was developed:

The AE105 sequence was built up on solid phase and the different spacer moieties were attached. Then, the deprotected N^ε-termini of two resin-bound monomers were cross-linked *via* side chain unprotected Fmoc-D-Glu as bivalent carbonic acid (Scheme 14). The amino group of glutamic acid was finally used to attach the DOTA chelator by coupling of DOTA-tris (*tert*-butyl ester).[487] The coupling of DOTA-tris(*tert*-butyl) ester (**169**)[487] to the solid-phase bound mono- and dimeric ligands using the standard coupling reagents HOBt and TBTU proceeded smoothly and in case of the dimeric ligands not to completion. Therefore, HOAt and HATU[166] were used as significantly stronger reagents leading to a complete conversion within 1 h. Cleavage and deprotection resulted in crude dimers **166, 167** (structures shown in Figure 54, page 108) and **168** with already high purity (~60-80% by HPLC) and good overall yields after HPLC purification (~25%).[481]

The strategy for the synthesis arose from experiences in directed intramolecular reactions of solid phase-bound peptides. The realization of selective intramolecular reactions (*e.g.* cyclisation) on solid-phase is often limited by concurring intermolecular reactions. In the attempt to synthesize *N*-terminally cross-linked peptide dimers, this normally undesired effect was switched into a highly selective intermolecular reaction between the single strands. The key event in the cross linking

reaction was to apply the bifunctional acid Fmoc-D-Glu in a very low concentration to allow a smooth reaction of both acid functionalities with one peptide strand each. Cross-linking was carried out by four couplings applying 0.15 equiv of Fmoc-D-Glu and 0.3 equiv of coupling reagents in each step. This procedure produced DOTA-conjugated AE105-derived dimers with high purity. Figure 55 (page 109) shows exemplary the HPLC spectrum of crude dimer 166 as obtained directly after cleavage from the solid support proving the high efficiency of the procedure.

Scheme 14. *Illustration of the solid-phase cross-linking procedure for the synthesis of the dimeric N-terminally cross-linked uPAR ligands 166, 167 and 168.*[a]
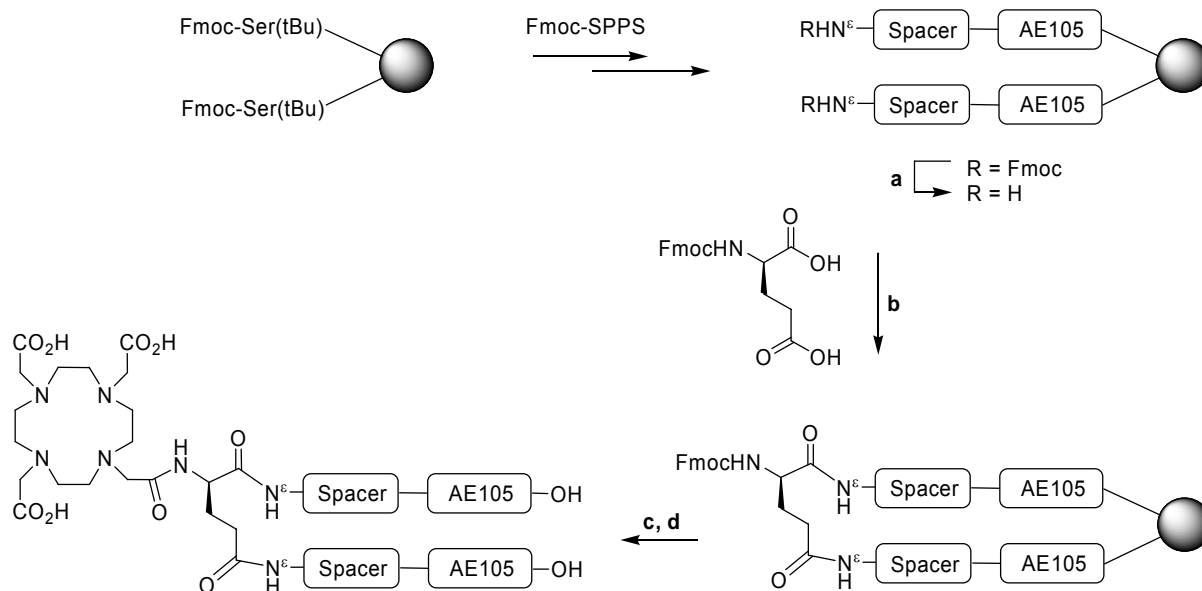
[a] The sequence of the uPAR-selective ligand AE105 (Asp-Cha-Phe-(D-Ser)-(D-Arg)-Tyr-Leu-Trp-Ser) was built up on solid-phase according to standard protocols for Fmoc-strategy and the corresponding spacers (ligand 166: K*-G-S-G-G; ligand 167: K(Aha*)-S-Aha; ligand 168: Aha*-Ado-Aha; asterisks (*) denote the amino acid to which the DOTA residue is linked) were attached by the same procedure. The solid-phase bound single strands were then cross-linked *via* Fmoc-D-Glu and the DOTA residue was attached to the *N*-terminus. *Reagents and conditions:* (a) 20% piperidine in NMP (3×10 min); (b) HOAt, HATU, 2,4,6-collidine (4×8 h); (c) 20% piperidine in NMP (3×10 min); (d) DOTA-tris(*tert*-butyl) ester (169),[487] HOAt, HATU, 2,4,6-collidine (2×8 h).[481]

166

167

R* = AE105 = Asp-Cha-Phe-(D-Ser)-(D-Arg)-Tyr-Leu-Trp-Ser
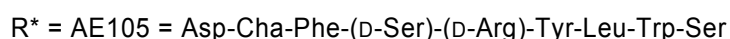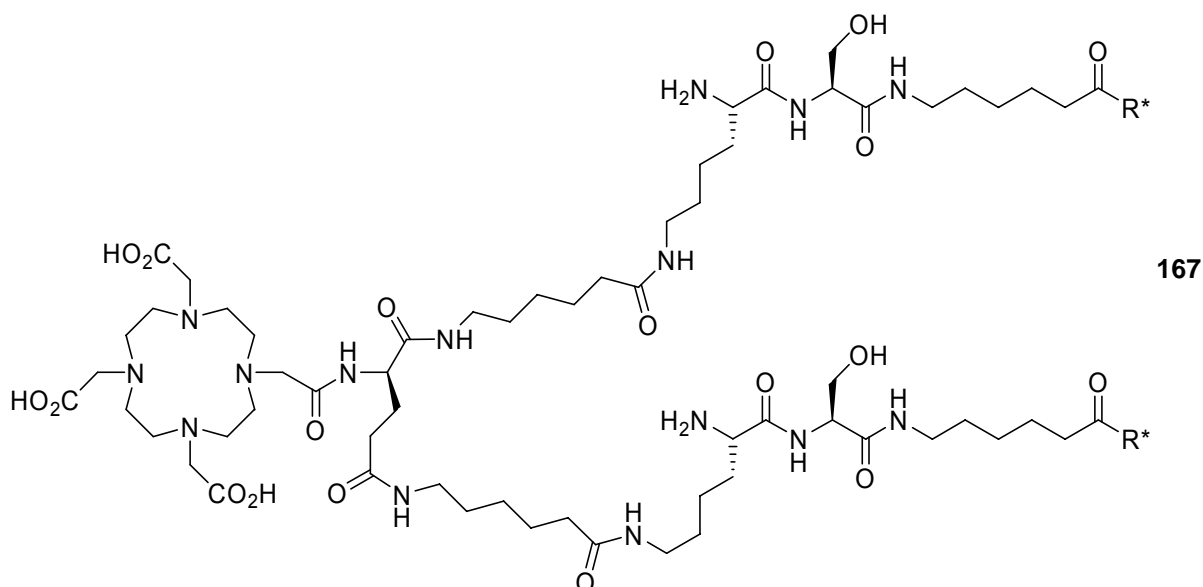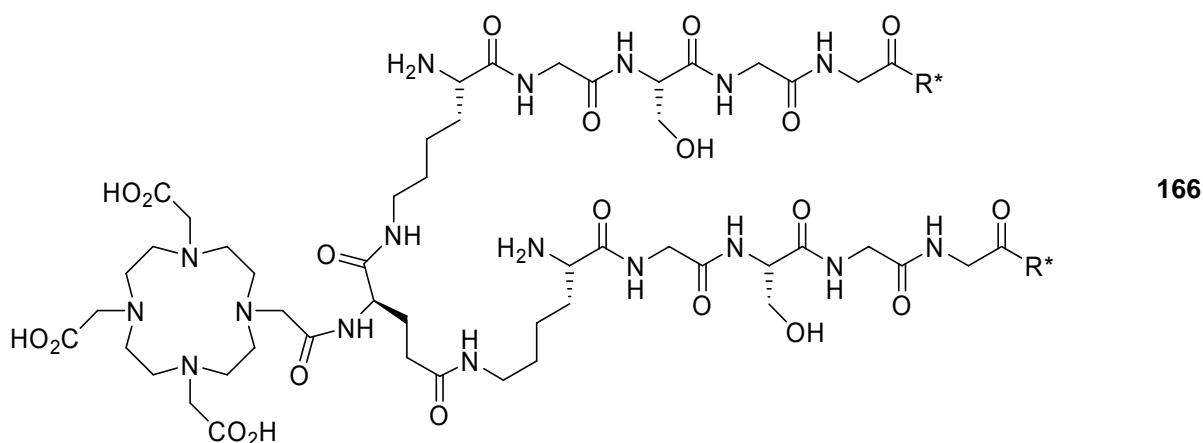
Figure 54. Structures of the AE105-derived dimeric DOTA-conjugated uPAR ligands 166 and 167.[481]

The biological evaluation of the DOTA-conjugated dimeric compounds again suggested a negative effect of the hydrophobic Aha moiety in the spacers of 167 and 168 and of the 8-amino-3,6-dioxaoctanoic acid (Ado) group in the spacer of 168 on receptor binding: despite the twofold concentration of the receptor binding group in the dimers 167 and 168, the compounds surprisingly bound even worse than the respective monomers (Table 15). In contrast, dimeric 166 showed a twofold better binding than monomeric 163 (IC_{50} = 18 nM vs. 34 nM) which is in line with the doubled ligand concentration. Importantly, coupling of stable [209]Bi to 163 and 166

via DOTA caused an only 1.4 fold reduction of binding affinities (data not shown).[481]
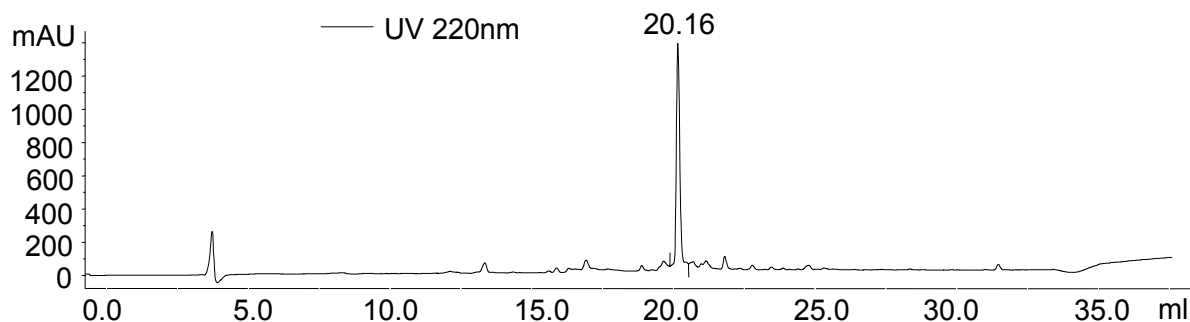
Figure 55. HPLC analysis of crude dimer **166** obtained *via N*-terminal cross-linking on solid-support. The application of the bifunctional acid Fmoc-D-Glu in a very low concentration produced crude DOTA-conjugated AE105-derived dimers with already high purity.

2.2.3 *In vitro* and *in vivo* evaluation of ^{213}Bi-labeled ligands

The preparation and evaluation of ^{213}Bi-labeled ligands was performed by C. Seidl (group of Prof. R. Senekowitsch-Schmidtke, Klinikum rechts der Isar München) and S. Sato (group of PD Dr. V. Magdolen).

2.2.3.1 Binding of ^{213}Bi-labeled ligands to uPAR expressing cells

For further analysis, the two monomeric ligands **163** and **164** (Figure 53) as well as the corresponding dimeric derivatives **166** and **167** (Figure 54), which displayed the highest affinity for uPAR (Table 15), were chosen. The incubation of 20 μM of each ligand with 7.4 MBq – 51.8 MBq ^{213}Bi resulted in an average ^{213}Bi-labeling of 84.5% (ranging from 64% to 96%) within 10 min of incubation at 60°C. A prolonged incubation further increased the degree of ^{213}Bi-labeling. Hence, as the binding experiments were performed approximately 40 min after start of the labeling reaction, it is supposed that more than 90% of ^{213}Bi were bound to the respective peptides at the time of application. The achieved specific activities varied from

0.12 MBq/μg to 2.4 MBq/μg. This corresponds to a ^{213}Bi-labeling of approximately 1/280,000 to 1/26,000 peptide molecules.[481]

U937 cells were used for the initial characterization of binding of radiolabeled peptides to cells. Subsequently, the cells were treated with acid, to remove uPA bound to uPAR on the cell surface and ^{213}Bi-labeled peptide (20 nM, 10 – 54 kBq) was added to 3×10^6 cells. The binding characteristics were evaluated by quantifying ^{213}Bi-activities in cell sediments and supernatants after 30 min incubation on ice. It turned out, that the binding of ^{213}Bi-labeled dimeric peptides 166 and 167 to the uPAR-expressing cells was distinctly better than that of the monomeric peptides 163 and 164 (Figure 56 and Supplementary Data 12 on page 260). To estimate the specificity of the ligands, the U937 cells were pre-incubated with both pro-uPA 12 μg and the soluble form of uPAR (suPAR) (1.6 – 4.8 μg), each leading to a significant reduction of the binding of the monomeric as well as the dimeric ligands (Figure 56 and Supplementary Data 12 on page 260). Since suPAR competes with membrane-anchored uPAR and also high levels of pro-uPA block the uPAR binding site of the peptides, these results demonstrate that ^{213}Bi-labled peptides bind specifically to uPAR expressed by U937 cells.[481]

The U937 cells used for this initial study, are well-suited for analysis of the binding characteristics of uPAR-directed peptides[488] but do not correspond to the potential target cells in treatment of disseminated ovarian cancer. Therefore, the ability of monomeric (163, 164) and dimeric ligands (166, 167) to bind also to OV-MZ-6 ovarian cancer cells was explored. These cells produce and secrete different members of the plasminogen activation system including uPAR, uPA and PAI-1.[488] Considering that OV-MZ-6 cells intrinsically produce and secrete the uPAR ligand (pro-)uPA, the cells were not acid-treated in this experiment to test the ligands under more realistic conditions.[481]

As shown in Figure 56b, [^{213}Bi]166 distinctly binds to OV-MZ-6 cells (19.3±3.3%) and binding was almost completely blocked in the presence of suPAR (3.2 μg) (3.0±0.5%). Both binding of [^{213}Bi]167 to OV-MZ-6 cells (16.5±2.0%) and blockage of binding with suPAR (3.7±0.1%) were somewhat reduced compared to [^{213}Bi]166.[481]
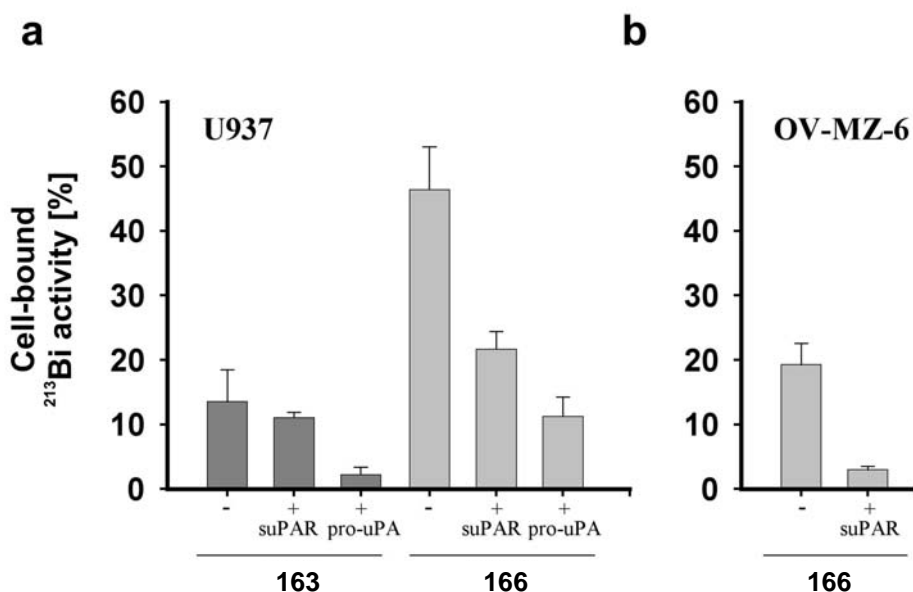
Figure 56. Binding characteristics of ^{213}Bi-labeled peptides to human cells. (a) PMA-stimulated, acid-treated U937 cells were incubated with AE105-derived ^{213}Bi-labeled peptides 163 and 166 either without or following pre-incubation with pro-uPA or soluble uPAR for 30 min on ice. (b) Binding of ^{213}Bi-labeled peptide 166 to non-acid-treated human OV-MZ-6 ovarian cancer cells in the absence and presence of soluble uPAR. Binding to the cellular pellet is expressed as percentage of total ^{213}Bi activity. Bars indicate standard deviation.[481]

2.2.3.2 Evaluation of the cytotoxic potential of ^{213}Bi-labeled and non-labeled ligands

To test whether non-labeled AE105-derived peptides display cytotoxicity, OV-MZ-6 cells were cultured for 72 h in the presence of either 163, 166 (100 nM each), or phosphate-buffered saline (PBS) (control). No significant differences in the growth pattern were detected between peptides (163, 166) versus control as well as monomeric 163 versus dimeric 166 (Figure 57a). In contrast, peptides labeled with the α-emitter ^{213}Bi should possess a high cytotoxic potential. Cytotoxicity of [^{213}Bi]166 was evaluated by a colony forming assay 7 days after administration of the radiopeptide. The results clearly show a correlation between decreasing sur-vival rate of OV-MZ-6 cells and increasing [^{213}Bi]166 activity (Figure 57b). At 18.5 kBq/mL of [^{213}Bi]166, 69.0% of seeded cells could still form colonies. 37 kBq/mL reduced cell viability to 23.5% and almost all of the cells were killed at 185 kBq/mL

of [^{213}Bi]166 (1.9% survival). At 370 kBq/mL of [^{213}Bi]166, no cell growth was observed.[481]
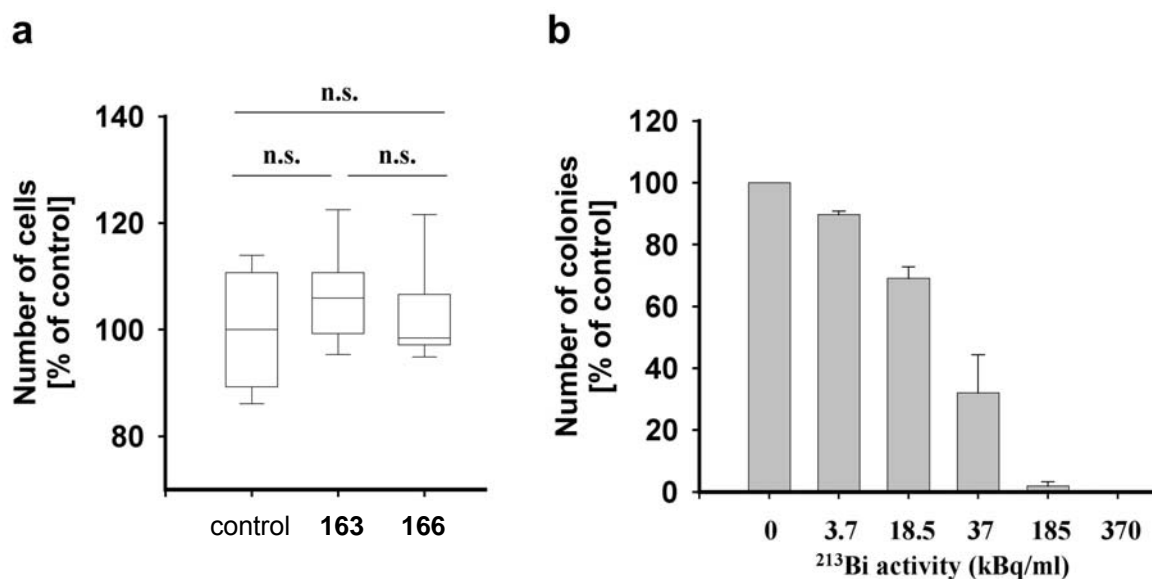
Figure 57. Cytotoxicity assays. (a) OV-MZ-6 ovarian cancer cells were cultured for 72 h in the presence of either non-labeled 163, 166 (100 nM each), or PBS (control). The box plot indicates the 25th and 75th percentiles, the vertical bars mark the 10th and 90th percentiles, respectively. The mean value is indicated in the box. n.s., not significant. (b) OV-MZ-6 cells (200 cells/well) were seeded in octaplicate into 24 well-plates and incubated with increasing activity concentrations of [^{213}Bi]166 (0, 3.7, 18.5, 37, 185 and 370 kBq/mL) 24 h later. Cytotoxicity was evaluated by counting the number of colonies formed by OV-MZ-6 cells 7 days after treatment compared to controls. Bars indicate standard deviation.[481]

2.2.3.3 Tumor accumulation and organ distribution of [^{213}Bi]166

For evaluation of tumor accumulation of [^{213}Bi]166, the radiopeptide (3.7 MBq) was injected intraperitoneally (i.p.) into tumor bearing nude mice 28 d after inoculation of OV-MZ-6 ovarian cancer cells. Biodistribution of [^{213}Bi]166 was investigated 20, 45 and 90 min after injection: As shown in Figure 58, tumor uptake of [^{213}Bi]166 reached its maximum already 20 min after injection (9%±0.9% of injected dose (ID)/g tissue).[481]

Uptake decreased to 4.8% (±1.5%) at 45 min and to 2.2% (±0.4%) at 90 min after injection. Nevertheless, [^{213}Bi]166 uptake by tumor tissue was higher than in all organs throughout the observation period, except for pancreas and kidney (Figure 58). The kidney showed increasing accumulation of [^{213}Bi]166 from approximately

18.9% (±3.6%) of ID/g tissue after 20 min to approximately 31.9% (±8.8%) of ID/g tissue after 90 min, while in all other organs ^{213}Bi-activity decreased over time (Figure 58).[481]
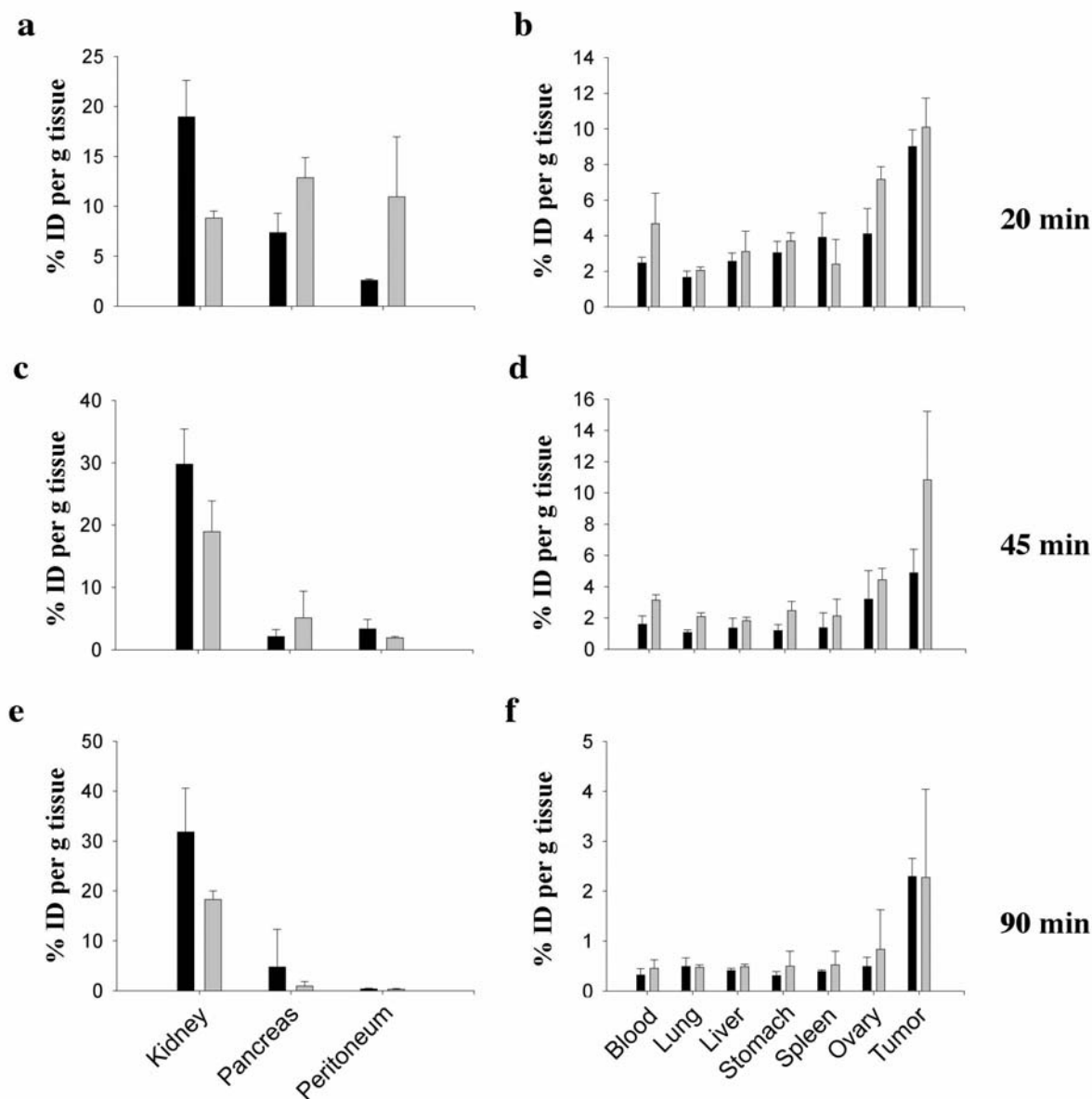
Figure 58. Biodistribution of [^{213}Bi]166 in nude mice bearing intraperitoneal ovarian tumors. Nude mice carrying OV-MZ-6-derived tumors were analyzed at 20 min (a, b), 45 min (c, d) and 90 min (e, f) after injection of the radiopeptide in the absence (black bars) or presence (grey bars) of the plasma expander gelofusine. High-uptake organs (a, c, e) and low-uptake organs (b, d, f) as deduced from uptake values 20 min after injection. Tumor uptake of [^{213}Bi]166 proved to be superior over organ uptake throughout the observation period except for pancreas and kidney. Intravenous injection of gelofusine 5 min before i.p. injection of [^{213}Bi]166 reduced kidney accumulation roughly by half (grey bars) compared to the animals which had not received gelofusine (black bars).[481]

Half of the animals were injected intravenal (i.v.) with the plasma expander gelofusine[489,490] 5 min before i.p. injection of [^{213}Bi]166 to reduce kidney uptake of [^{213}Bi]166. Gelofusine caused a mean reduction of [^{213}Bi]166 kidney uptake to 55.8% (±11%) of the uptake without gelofusine: to 46.6% (±3.6%) at 20 min, to 63.5% (±16.5%) at 45 min and to 57.3% (±5.3%) at 90 min. In contrast, [^{213}Bi]166 uptake in almost all of the other organs and in tumor tissue was slightly elevated in the presence of gelofusine.[481]

In tumor-free mice, kidney uptake of [^{213}Bi]166 was 1.4 fold higher than in mice presenting tumor, indicating that [^{213}Bi]166 efficiently binds to tumor tissue. Gelofusine reduced kidney uptake of [^{213}Bi]166 by half also in tumor free mice (data not shown).

2.2.3.4 Discussion of the therapeutic potential

The goal of the present study was to test whether peptidic radioligands, based on potent uPAR binding peptides (*i.e.* the 10-mer peptide cyclo[21,29][D-Cys^{21}Cys^{29}]-uPA$_{21\text{-}30}$ (WX360)[465] and the 9-mer peptide AE105[466]), may be developed for application in α–emitter therapy of disseminated ovarian cancer overexpressing the uPA receptor. For this, the uPAR binding peptides were modified by conjugation with the chelator DOTA (for efficient binding of the α-emitter ^{213}Bi). It turned out that the WX360 ligand is not suitable for this purpose, as the modification with DOTA led to a great decrease of the uPAR affinity even after introduction of spacer sequences. In contrast, after optimization of the spacer moiety, the DOTA chelator could by attached to the AE105 peptide thereby only minimally affecting the binding affinity.

Evaluation of the AE105-based ligands demonstrated that the newly developed monomeric and dimeric peptides, labeled with the α-emitter ^{213}Bi, specifically recognized uPAR on the surface of both the human monocytoid U937 cells and OV-MZ-6 ovarian cancer cells. While the extent of binding of peptides to U937 cells clearly improved with removal of receptor-bound uPA *via* acid wash, OV-MZ-6 cells showed excellent binding of dimeric ^{213}Bi-peptides irrespective of this pre-treatment. This strongly suggests that OV-MZ-6 ovarian cancer cells, not only expressing uPAR but also its ligand uPA and other members of the plasminogen activation system,[488]

present a considerable number of cell surface-associated uPARs that are not occupied by uPA and therefore can be targeted by appropriate peptide conjugates. Excellent binding of dimeric [^{213}Bi]166 to OV-MZ-6 cells was also confirmed *in vivo* following intraperitoneal injection into nude mice bearing intraperitoneal tumor nodules. Tumor binding was approximately 9-10%, 5-10% and 2.5% of injected dose/g (ID/g) of tissue at 20, 45 and 90 min after administration of [^{213}Bi]166, respectively. In contrast, tumor binding of ^{213}Bi-DOTATOC, targeting the somatostatin receptor, was reported to be only 0.75% ID/g tissue 1 h after injection.[420] Also, tumor binding of ^{111}In-minigastrin targeting the CCK-B receptor was described to be comparatively low, amounting to 2% ID/g tissue at 10 min and 0.45% ID/g tissue at 1 h after injection of the radiopeptide.[421] ^{177}Lu-AMBA targeting GRP receptor with high affinity was reported to show approximately 5% ID/g tissue tumor binding 1 h after administration, which is comparable to the presented results.

Although peptides have distinct advantages compared to monoclonal antibodies as carriers for radionuclides,[491] potential kidney toxicity of radiopeptides might impair their efficacy in targeted radiotherapy of tumors. The kidney is a major site in the catabolism of peptides. Due to their small size, radiopeptides can traverse the glomerular basement membrane of the kidney leading to kidney damage.[492] Therefore, efforts are made in order to reduce kidney uptake of low-molecular-weight radiopeptides. Promising results in terms of prevention of renal damage following administration of radiopeptides have been obtained previously *via* co-infusion of polyglutamic acids[421] or the basic amino acids arginine and lysine.[493,494] Nevertheless, co-infusion of amino acids also involves a number of drawbacks. Since large volumes of the amino acid solutions have to be administered, generally, hyperkalemia arises, which may lead to cardiac arrhythmia.[492] Therefore, novel compounds for reduction of renal uptake of radiopeptides are currently being explored. Among them are the aldosterone receptor antagonist spironolactone,[495] probenecid[496] and the plasma expander gelofusine.[489] For instance, it was demonstrated that infusion of gelofusine significantly reduced renal uptake of radiolabeled octreotide by 45% without any side effects.[489] In line with that, it was demonstrated that gelofusine injection also significantly reduced kidney uptake of [^{213}Bi]166, approximately by half.

The extent of radiation induced kidney damage following therapy with low molecular weight radiopeptides also has turned out to be dependent on the physical properties of the applied radionuclide. Administration of DOTATOC labeled with short-lived, short-ranged ^{213}Bi caused only minimal to mild nephrotoxicity compared to moderate to severe nephrotoxicity following DOTATOC therapy with the longer-lived, longer-ranged β-emitter ^{90}Y.[420]

In summary, the synthetic DOTA-modified, ^{213}Bi-labeled peptide **166**, which efficiently targets uPAR expressing tumor cells *in vitro* and *in vivo*, is a very promising new candidate for peptide receptor radiotherapy. The project is continued in the thesis of T. Huber.

2.3 Development of "clickable" DOTA derivatives for chemo-selective attachment to polyfunctionalized compounds

2.3.1 Background

2.3.1.1 Previous strategies for the synthesis of DOTA-conjugated biomolecules and their limitations

DOTA-peptides are generally synthesized either in solution[497] or on solid support attaching the DOTA residue to a free amine of the resin bound peptide.[487,498-501] For this, unprotected[500] or more conveniently, protected DOTA derivatives are used to overcome side reactions by polyactivation of the four carboxylic groups of DOTA. Therefore, a number of DOTA-derivatives were developed allowing selective formation of monoconjugates. For example, the triprotected and commercially available DOTA-tris(*tert*-butyl) ester (169),[487] which has been used for the synthesis of DOTA-conjugate uPAR ligands above and the corresponding benzyl protected analog DOTA-tris(benzyl) ester (170).[499]
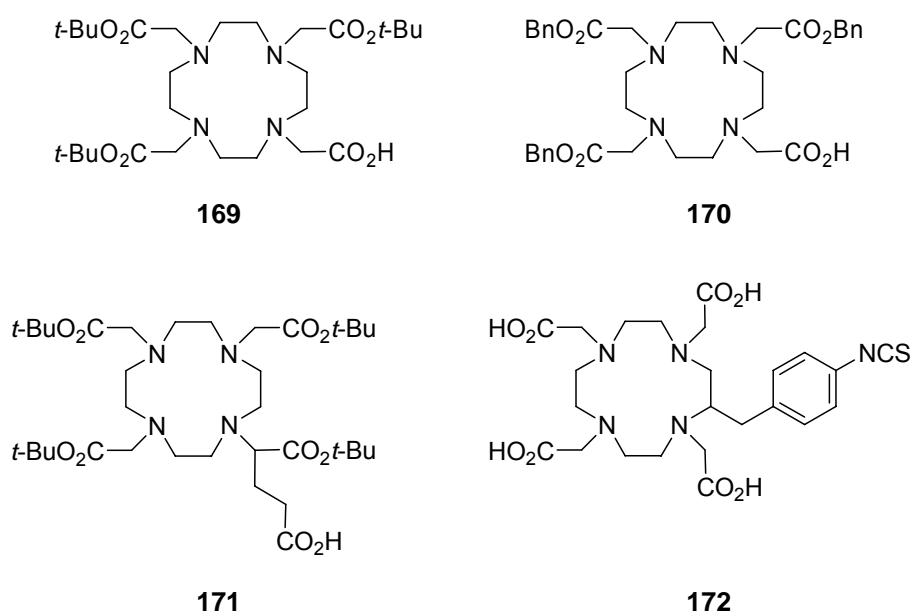
Figure 59. Structures of DOTA derivatives previously described in the literature.

Further derivatives are DOTAGA(*t*Bu)$_4$ (171), offering an additional unprotected carboxylic group,[498] and the isothiocyanate-functionalized *p*-NCS-Bz-DOTA (172).[501] Furthermore, derivatized amino acids containing a DOTA moiety were used[502] or DOTA was synthesized stepwise on a resin bound peptide.[503,504]

The main limitation of all these methods is the introduction of the DOTA residue into the bioconjugate *via* an electrophilic reaction. This procedure tolerates no other *N*- or *S*-nucleophilic groups for a selective reaction which greatly limits the application of above derivatives. Chemoselective approaches allowing a site-selective functionalization of unprotected polyfunctionalized compounds remained in demand. Such a method would be a powerful tool for the synthesis of DOTA-linked radiopharmaceuticals enabling new synthetic strategies and the synthesis of complex structures. For example, Thumshirn *et al.* recently developed multimeric aminooxy-functionalized RGD-derivatives[505] which were ^{18}F-labeled *via* oxime ligation using 4-[^{18}F]fluorobenzaldehyde.[506] A carbonyl functionalized DOTA derivative would allow a selective conjugation with DOTA and subsequent labeling with various radiometals. Very recently, Lin and coworkers have demonstrated a site-specific protein modification through Cu(I)-catalyzed 1,2,3-triazole formation.[507] Applying this methodology and using an alkyne functionalized DOTA derivative would enable site specific DOTA labeling of proteins. In a recent publication, J. Hovinen reported the synthesis of an aminooxy-functionalized chelate by derivatization of the tris *tert*-butyl ester of DOTA which was conjugated with naltrexone and 2-deoxy-D-ribose.[508] However, the reported procedure requires expensive starting material and the applicability to polyfunctionalized compounds like peptides remains unclear.

2.3.1.2 Motivation and target structures

Considering above mentioned limitations, the idea was to design novel DOTA-derivatives enabling the chemoselective attachment in presence of a wide range of functional groups. Thereby, the focus was on structures readily accessible in few synthetic steps from cheap commercial materials to make the method convenient and even a general alternative to the widely used but quite expensive DOTA-tris-(*tert*-butyl) ester. Furthermore, the accessibility of the correspondingly polyfunctionalized compounds was an important aspect in the consideration.

Click reactions,[509] in particular the oxime ligation[510,511] as well as the Cu(I)-catalyzed azide-alkyne cycloaddition,[512,513] are well-studied and powerful reactions for chemoselective couplings which fulfill all requirements for this purpose. The oxime ligation denotes the highly selective reaction between an aminooxy component and aldehydes or methylketones[514] under formation of an oxime bond, which is known to be stable both *in vitro* and *in vivo*.[515] The reaction was shown to tolerate every free amino acid side chain except an *N*-terminal cysteine and found widespread use, *e.g.* in the synthesis of template assembled synthetic proteins,[516,517] radioactive labeled peptide conjugates,[515,518] cyclic peptides[519] and protein analogs.[520,521] The Cu(I)-catalyzed azide-alkyne cycloaddition is a catalyzed variant of the chemoselective Huisgen 1,3-dipolar cycloaddition[522-525] of an azide and an alkyne for the formation of a triazole which has found application in various developments in medicinal chemistry.[526-531] Thus, to provide users with different methodologies for the synthesis of DOTA-conjugates, the focus was on appropriate DOTA-derivatives for both types of reaction described above.

The following chapters describe the synthesis of 2-[1-(1,4,7,10-tetraazacyclodecane)-4,7,10-tris(*tert*-butylacetate)]-(4-acetylphenyl) acetic acid *tert*-butyl ester (173) and 2-[1-(1,4,7,10-tetraazacyclodecane)-4,7,10-tris(*tert*-butylace-tate)]-(4-acetylphenyl) acetic acid (174) as carbonyl components for oxime ligations with aminooxy-functionalized compounds and 2-[1-(1,4,7,10-tetraaza-cyclodecane)-4,7,10-tris(*tert*-butylacetate)]acetic acid methyl ester (175) as alkynyl component for Cu(I)-catalyzed azide-alkyne cycloaddition with azide functionalized compounds (Figure 60).[532] 174, bearing one free acid functionality and the orthogonally protected alkynyl derivative 175 were designed to enable a selective further transformation as described below. Initial steps of the synthesis have been worked out by A. Modlinger.[533] In a proof-of-principal experiment, the applicability of the novel derivatives was proven by reacting both types of DOTA derivatives with appropriately functionalized Tyr[3]-octreotate, a somatostatin analog which is a well known targeting molecule for tumor diagnostics and endoradiotherapeutic purposes.[428,534-538] Tyr[3]-octreotate was chosen as a highly functionalized model compound providing a broad range of functionalities. In addition, one of the radioligands was labeled with ^{68}Ga and an initial biodistribution study in AR42J tumor bearing nude mice was performed proving the applicability of the modified linkage.
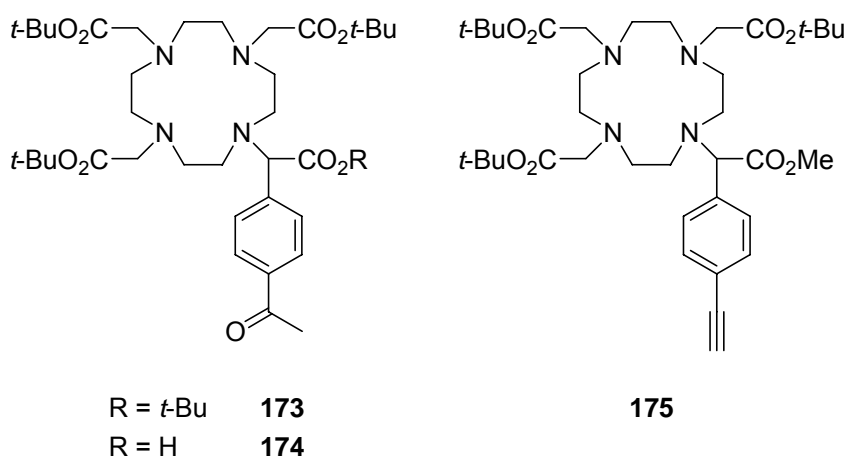
Figure 60. Structures of novel 4-acetylphenyl-DOTA derivatives 173 and 174 and ethynylphenyl-DOTA derivative 175.[532]

2.3.2 Synthesis of the keto-functionalized DOTA derivatives (173) and (174)

Planning the synthetic strategy, it was decided to attach the carbonyl functionality to the DOTA moiety. The aminooxy group can be readily implemented in peptides as an aminooxy-functionalized building block (*e.g.* (Boc-aminooxy)-acetic acid, Boc-*O*-(Fmoc-amino)-serine (Boc-Ams(Fmoc)-OH) and 3-(Boc-aminooxy-acetamido)-2-Fmoc-amino-propionic acid (Fmoc-Dpr(Boc-Aoa)-OH)). As carbonyl functionality, a methylketone was preferred over an aldehyde due to its significant higher stability. This procedure avoids additional protection and deprotection steps, which would have been essential when working with n aldehyde and makes the final compound storable for longer periods.

Furthermore, the idea was to widen the scope of potential applications of the new DOTA derivatives. While in the past the main focus was on derivatives allowing selective formation of monoconjugates, the development of novel DOTA derivatives offering two different functionalities which can be converted selectively, would open new opportunities, *e.g.* the selective synthesis of homo- and heterooligomers[484] or the attachment of additional groups like sugars, which has been shown to result in improved pharmacokinetics.[539] Therefore, two different pro-

tecting group strategies were developed: (a) an orthogonal protection with one base labile protecting group, which enables the selective deprotection and derivatization of one carboxylic group and (b) a complete protection with acid labile groups offering a one step deprotection where only a monoconjugation is desired. The synthesis started with 4-acetylphenylboronic acid (176) which was reacted with methyl and *tert*-butyl 2-bromoacetate, respectively, in a Suzuki-type cross coupling reaction (see Scheme 15).

Scheme 15. *Synthesis of the keto-functionalized DOTA derivatives **173** and **174**.*[a]

176	
177 R = Me	**179** R = Me
178 R = *t*-Bu	**180** R = *t*-Bu
183 R = Me	**181** R = Me
173 R = *t*-Bu	**182** R = *t*-Bu
174 R = H	
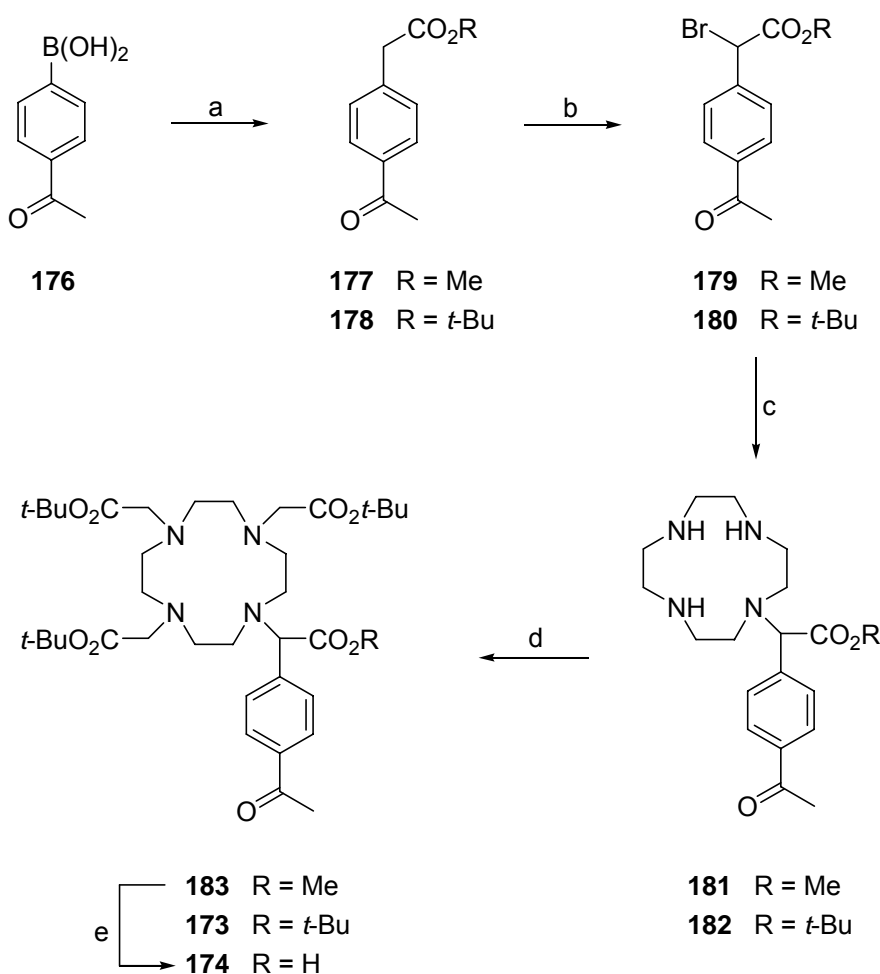
[a] Reagents and conditions: (a) BrCH$_2$CO$_2$R, Pd(OAc)$_2$/P(*o*-Tol)$_3$, K$_2$CO$_3$, THF/H$_2$O, rt, 18 h; 177: 66%, 178: 76%; (b) NBS, Br$_2$, *hv*, CCl$_4$, 60°C, 1 h; 179: 89%, 180: 88%; (c) 1,4,7,10-tetraazacyclodecane, K$_2$CO$_3$, DMF, rt, 10 h; 181: 62%, 182: 75%; (d) BrCH$_2$CO$_2$*t*-Bu, K$_2$CO$_3$, DMF, rt, 4 h; 183: 83%, 173: 72%; (e) LiOH, THF/H$_2$O, rt, 18 h; 38% (66% related to recovered 183).[532]

The resulting 2-(4-acetylphenyl) substituted acetates 177 and 178 were obtained in good yields.[540] The α-bromination under radical conditions using *N*-bromosuc-

cinimide (NBS) in presence of catalytic amounts of bromine and initiation by illumination gave the α-bromo esters 179 and 180 in high yields (89% and 88%). The latter compounds were slowly added to a solution of cyclen in DMF in the presence of K_2CO_3 to afford the corresponding monoalkylated cyclen-adducts 181 and 182 in 62% and 75% yield. Subsequent peralkylation with *tert*-butyl 2-bromoacetate then gave the tetraesters 183 and 173 (83% and 72% yield).[532]

Surprisingly, during saponification of the methyl ester 183 using LiOH partial deprotection of the *tert*-butyl ester was observed. However, as this side-reaction proceeds slower than the primary reaction, the desired free acid 174 could be obtained in good yield if the reaction was stopped at about 50% conversion to prevent the further cleavage of the product. In this manner 174 was obtained in 38% yield (66% based on recovered 183) after purification by HPLC. Attempts to saponify using LiI[541,542] lead to inseparable mixtures of several products and when using carbonate no saponification occurred.

2.3.3   Synthesis of alkynyl-substituted DOTA derivative (175)

To design the appropriate DOTA derivative for attachment to peptides *via* Cu(I)-catalyzed azide-alkyne cycloaddition,[509] it was decided to introduce the alkyne functionality to the DOTA derivative, as azido functionalized peptides are readily accessible, *e.g.* by introduction of azido acids[543-545] or by diazo-transfer on solid phase.[546] After the positive experiences in the synthesis of the carbonyl-substituted derivative, 2-bromo-2-phenylacetic acid was again chosen as the core residue for the implementation of the alkyne, providing an analogous synthetic route as described above.

The synthesis was started from commercially available 4-iodophenylacetic acid (184). The free acid was protected as methyl ester (185) by treating with thionyl chloride in methanol in almost quantitative yield (93%) and high purity (see Scheme 16). Subsequently, 185 was coupled with trimethylsilyl (TMS) acetylene in a Sonogashira reaction using Pd(PPh3)4/CuI as a catalyst affording the 4-alkynyl-phenylacetate 186 in 93% yield.[547,548]

Scheme 16. *Synthesis of alkyne-functionalized DOTA derivatives.*[a]
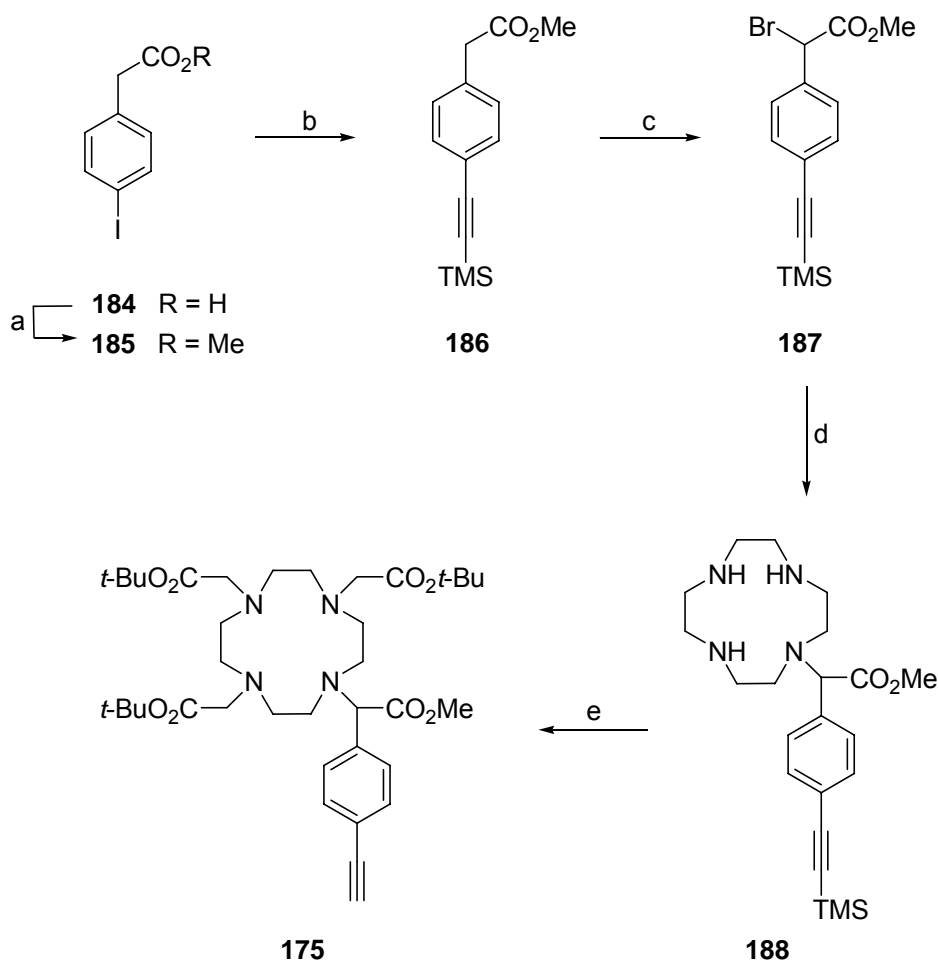
[a] Reagents and conditions: (a) SOCl$_2$, MeOH, 0°C → rt, 1 h; 93%; (b) HC≡C–TMS, Pd(PPh$_3$)$_4$/CuI, NEt$_3$, CH$_3$CN, 0°C → rt, 3 h; 93%; (c) 1) LDA, THF, -78°C, 1 h; 2) NBS, THF, -78°C → rt, 18 h; 47% (92% related to recovered **186**); (d) 1,4,7,10-tetraazacyclodecane, K$_2$CO$_3$, DMF, rt, 10 h; 73%; (e) 1) BrCH$_2$CO$_2$t-Bu, K$_2$CO$_3$, DMF, rt, 4 h; 2) TBAF, THF, rt, 15 min; 85%.[532]

However, the α-bromination of **186** with NBS failed with both, Br$_2$/*hv* and 2,2'-azobisisobutyronitrile (AIBN) as initiators. This is most likely due to side reactions caused by the presence of a triple bond. This problem was circumvent by introducing the bromide in an electrophilic manner. For this purpose, the ester **186** was transformed into the boron enolate in an analogous manner as described by Evans *et al.*,[549] treating subsequently with lithium diisopropyl amide (LDA) and Bu$_2$BOTf. After addition of *N*-bromosuccinimide as electrophilic brominating reagent, the α-bromo ester **187** was isolated in rather poor yield. In an attempt to further optimize the reaction, it was found that the conversion proceeds cleanly if

123

the lithium enolate of 186, obtained by deprotonation with LDA, was directly reacted with NBS. In this manner, 187 could be obtained in 47% yield together with unreacted 186 which was recovered in 49% yield. This result is explained by the much higher acidity of the α-bromo ester 187 compared to 186 leading to a rapid deprotonation of the formed product with one equivalent of the lithium enolate of 186 during the reaction. The yield could not be increased by optimizing the reaction conditions, *e.g.* by adding the enolate to a great excess of NBS. However, based on recovered starting material 186, which could be readily separated by flash chromatography, the yield was almost quantitative.[532]

The monoalkylation of cyclen with the α-bromo ester 187 was performed in an analogous way as described above to yield 188. After peralkylation with *tert*-butyl 2-bromoacetate and cleavage of the TMS group using tetrabutylammonium fluoride (TBAF), the tetraester 175 was obtained in 85% yield over two steps.[532]

As described in the synthesis of 174 it was also tried to selectively saponify the methyl ester of 175. Surprisingly, in presence of one equivalent of LiOH, cleavage of a *tert*-butyl ester of 175 proceeded even faster and the corresponding compound with one of the *tert*-butyl and the methyl ester cleaved was found as the major product. The desired product among regioisomers without one *tert*-butyl group could only be detected in minor amounts.

2.3.4   Application of DOTA derivatives (173) and (175): Chemoselective conjugation with unprotected biomolecules *via* click reactions

With these novel functionalized chelators in hand, chemoselective attachment to *N*-terminally aminooxy and azide functionalized Tyr³-octreotates 190 and 196 was scrutinized.

2.3.4.1   Conjugation of DOTA-keto derivative (173) and Tyr³-octreotate (190) *via* oxime ligation

In initial experiments, the *tert*-butyl protected DOTA ketone 173 was directly used for the oxime ligation. However, the oxime bond of the resulting conjugate

was unstable under the strong acidic conditions required for deprotection of the *tert*-butyl groups.

Scheme 17. *Chemoselective oxime ligation reaction of DOTA derivative **173** and aminooxy functionalized Tyr³-octreotate **190**.*[a]

190

a ⌐ **173** R = *t*-Bu
  └→ **189** R = H

b

191
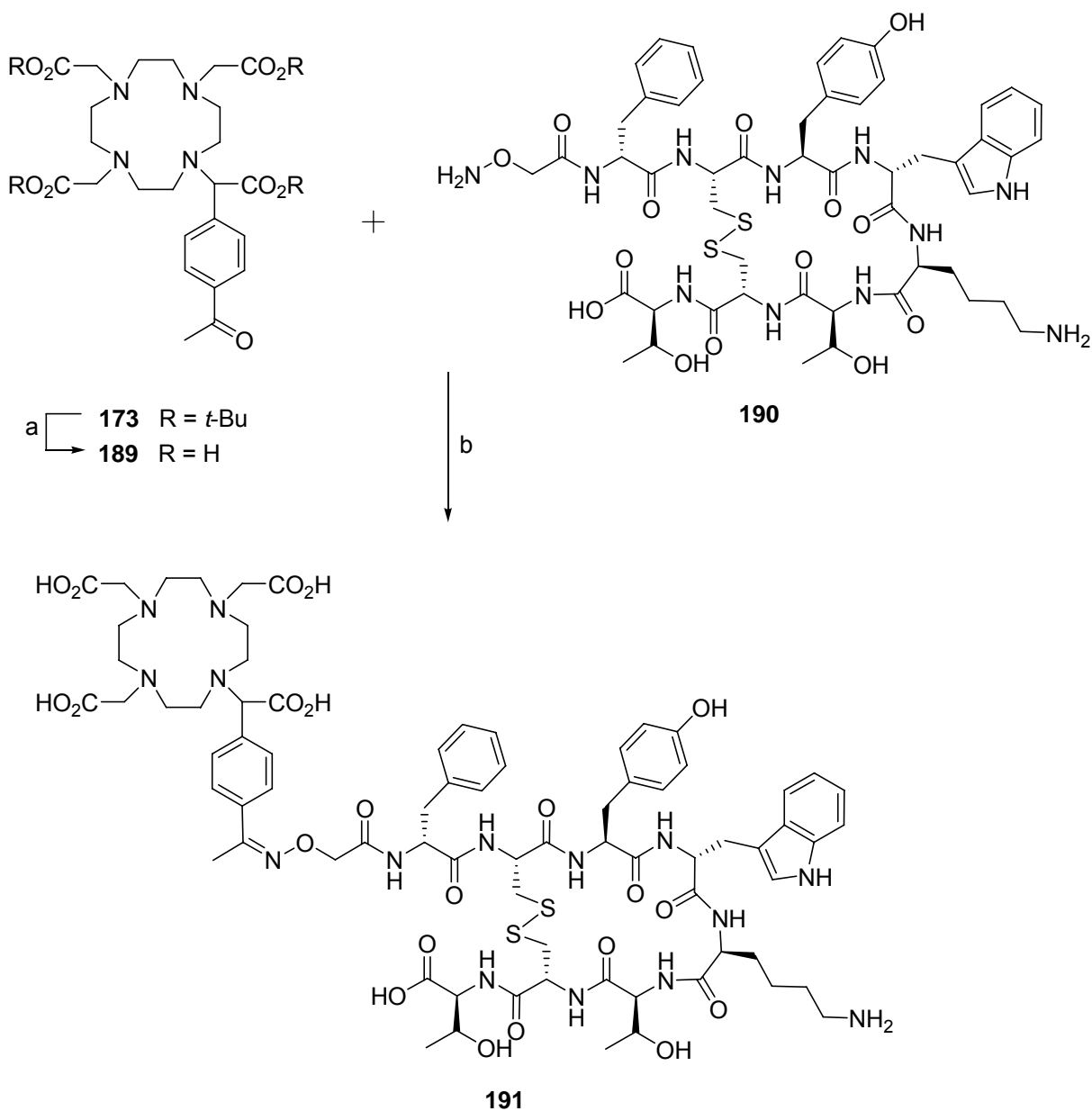
[a] Reagents and conditions: (a) 10N HCl/dioxane (1:1, v/v), rt, 18 h; (b) CH₃CN/H₂O (1:1, v/v; HPLC grade) pH 4 (TFA, HPLC grade), rt, 18 h; 73% (two steps).[532]

Therefore, the procedure was switched and 173 was protected *in situ* prior to the ligation. A quantitative cleavage was realized treating with 10N aqueous HCl in

dioxane (50/50, v/v) (Scheme 17). Alternative methods applying formic acid,[550] 50% TFA/H$_2$O or a mixture of trifluoroacetic acid (TFA), triisopropyl silane (TIPS) and water (95/2.5/2.5, v/v/v)[197] - a standard deprotection mixture used in Fmoc peptide chemistry - failed. The latter procedure in addition let to a reduction of the keto group to the alcohol. The obtained free chelator **189** reacted cleanly with equimolar amounts of aminooxy-functionalized Tyr^3-octreotate **190*** in an acetonitrile/water mixture at pH 4 (TFA) to give the desired conjugate **191** with high purity, as proven by HPLC analysis (Figure 61).[532]

It should be stressed that any reaction where free aminooxy functionalities occur, demands high solvent purities (HPLC grade) in order to prevent side reactions with carbonyl functionalized impurities. The final product was further purified by preparative HPLC to give **191** in 73% yield and 97% purity.
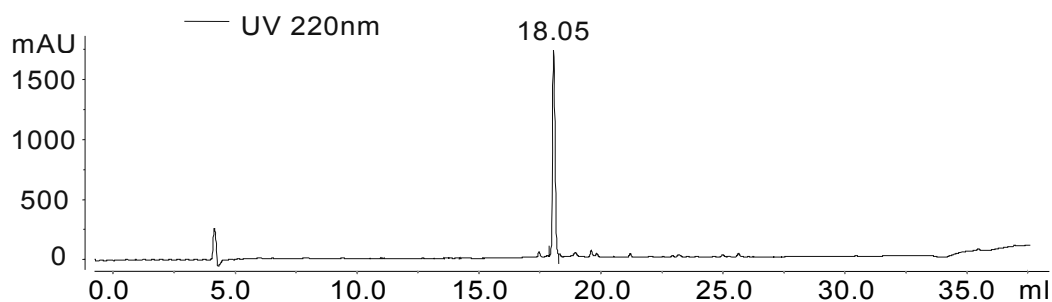
Figure 61. HPLC spectrum of crude DOTA conjugate **191** obtained by oxime ligation.[532]

2.3.4.2 Conjugation of DOTA-keto derivative (175) and Tyr^3-octreotate (196) *via* Cu(I)-catalyzed azide-alkyne cycloaddition

With respect to the azide functionalization of Tyr^3-octreotate, a simple *N*-terminal elongation with 3-(3-azidopropylcarbamoyl) propanoic acid **194** on solid support was performed. Since in several biological active peptides it is of great importance to use a spacer between the DOTA chelator and the targeting moiety and based on earlier experiences in our group, **194** was the linker of choice. The two-step synthesis of **194** starting from 1-bromo-3-aminopropane (**192**) is cheap,

---

* **190** was synthesized following a standard peptide coupling protocol (see Experimental Procedures)

high yielding, easy to scale up and does not require any chromatography (Scheme 18): 1-bromo-3-aminopropane was converted to the corresponding azide 193 by treating with sodium azide in water to obtain 193 as an equimolar mixture with diethyl ether in 84% yield. The crude mixture was directly reacted with succinic anhydride in presence of trimethyl amine to yield 194 (71% yield).[532]

Scheme 18. *Synthesis of 3-(3-azidopropylcarbamoyl)propanoic acid (194).*[a]
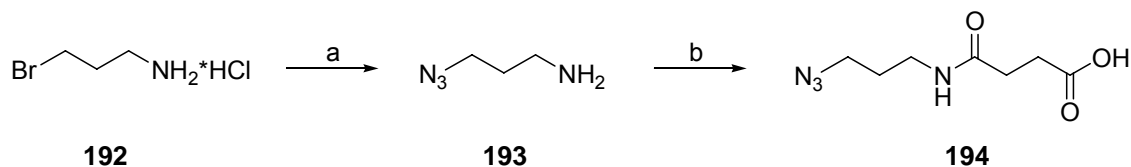
[a] Reagents and conditions: (a) NaN$_3$, H$_2$O, 80°C, 24 h; 84%; (b) succinic anhydride, NEt$_3$, acetone, rt, 15 h; 71%.[532]

194 was attached to Tyr^3-octreotate following a standard peptide coupling protocol (see Experimental Procedures) to obtain the azido functionalized Tyr^3-octreotate 196.
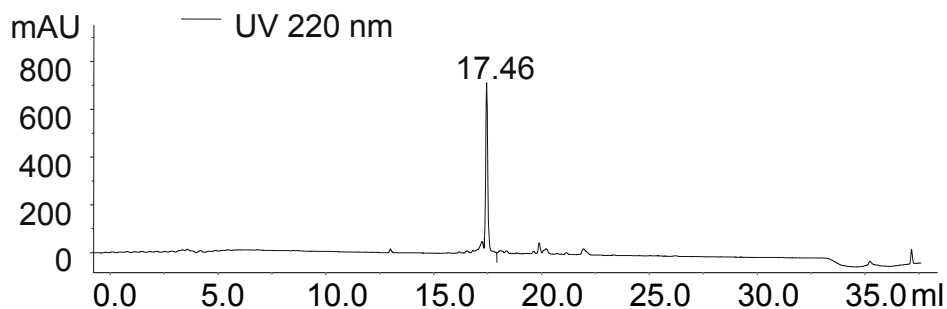
Figure 62. HPLC spectrum of crude DOTA conjugate 197 obtained after Cu(I)-catalyzed azide-alkyne cycloaddition and subsequent deprotection (Scheme 19, step 2).[532]

For the Cu(I)-catalyzed azide-alkyne cycloaddition, a one-pot procedure was worked out: Prior to the cycloaddition, the methyl ester 175 was saponified *in situ* using lithium hydroxide in THF/water. As described above, this resulted in a partial cleavage of *tert*-butyl groups as well, which, however, had no impact on the further procedure. The resulting mixture was further reacted with the azido functionalized Tyr^3-octreotate 196 using Cu/CuSO$_4$ as catalyst system (Scheme 19).

After evaporation, the crude mixture was directly deprotected by adding TFA/TIPS/H$_2$O (95/2.5/2.5, v/v/v)[197] to afford the crude product 197 with high purity, as shown by HPLC analysis (Figure 62).[532]

Scheme 19. *Chemoselective Cu(I)-catalyzed azide-alkyne cycloaddition of DOTA derivative 175 and azido functionalized Tyr³-octreotate 196.*
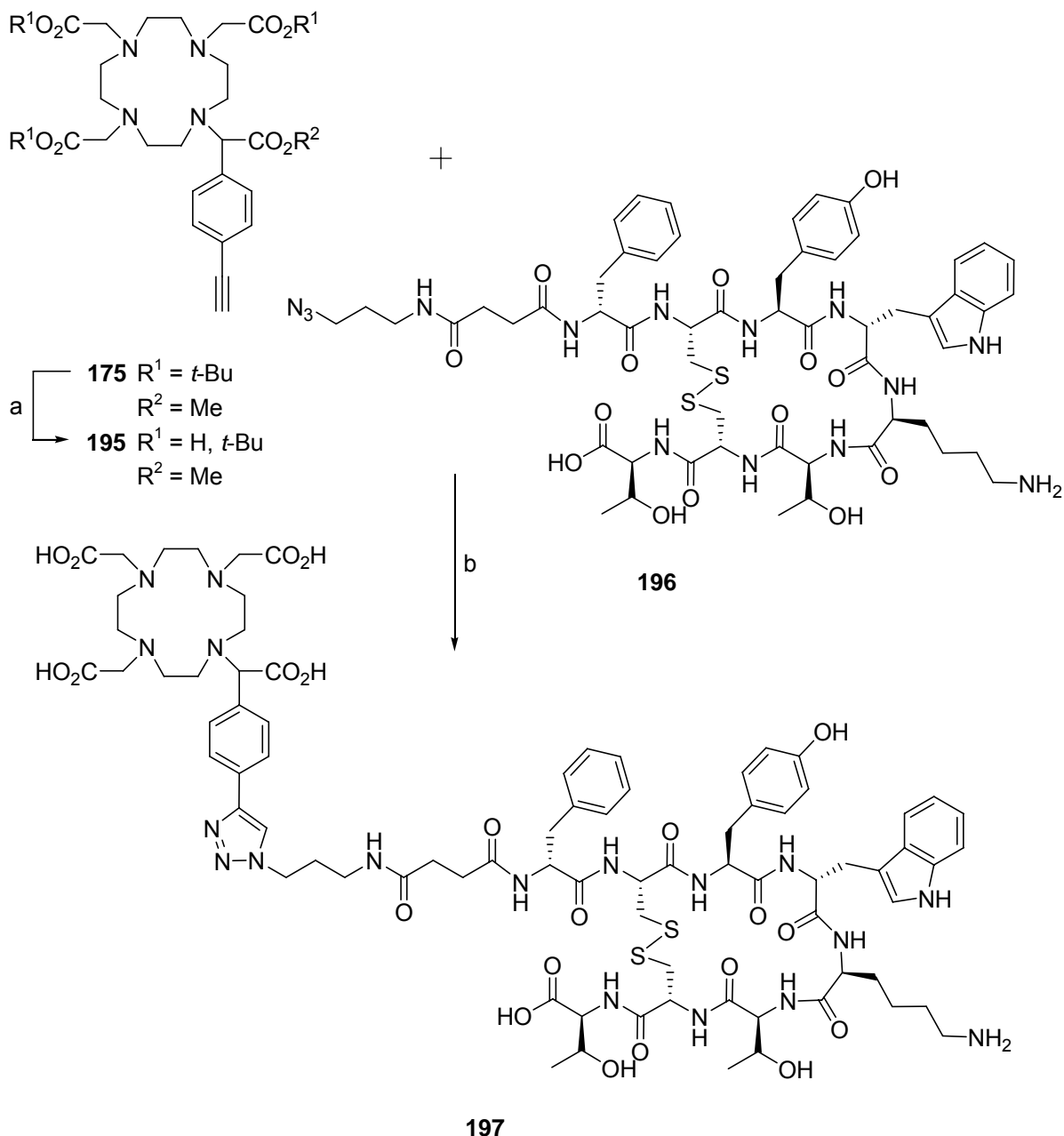
[a] Reagents and conditions: (a) LiOH, THF/H$_2$O, rt, 18 h; (b) 1) Cu/CuSO$_4$, THF/H$_2$O, rt, 18 h; 2) TFA/TIPS/H$_2$O (95:5:5, v/v), rt, 2 h; 3) Na$_2$S, THF/H$_2$O, rt; 4) DMSO, NH$_3$, CH$_3$CN/H$_2$O, rt, 24 h; 37% (five steps).[532]

ESI mass spectroscopy showed that 197 was obtained as a copper complex. Thus, the copper ions were removed from the solution and from the chelator by precipitation with sodium sulfide to give the pure free conjugate. During the four-step procedure, no side reactions with functional groups were observed, except of a reductive opening of the intramolecular disulfide bond in the last step which was easily reformed in quantitative yield by treating with DMSO in acetonitrile/water for 24h. After HPLC purification, 197 was obtained in 37% yield and 97% purity from 196 (five-steps).[532]

In order to check the procedure, the reaction was repeated with the azido functionalized, but non-cysteine containing sample 3-(3-azidopropylcarbamoyl)-propanoyl-Tyr-Glu-Trp-Lys (198). As expected, the reaction sequence proceeded without side reactions. Deprotection of the *tert*-butyl esters gave crude 199 (Figure 63) with high purity (see Supplementary Data 11, page 259). After HPLC purification the corresponding conjugate 199 was obtained in 51% yield.
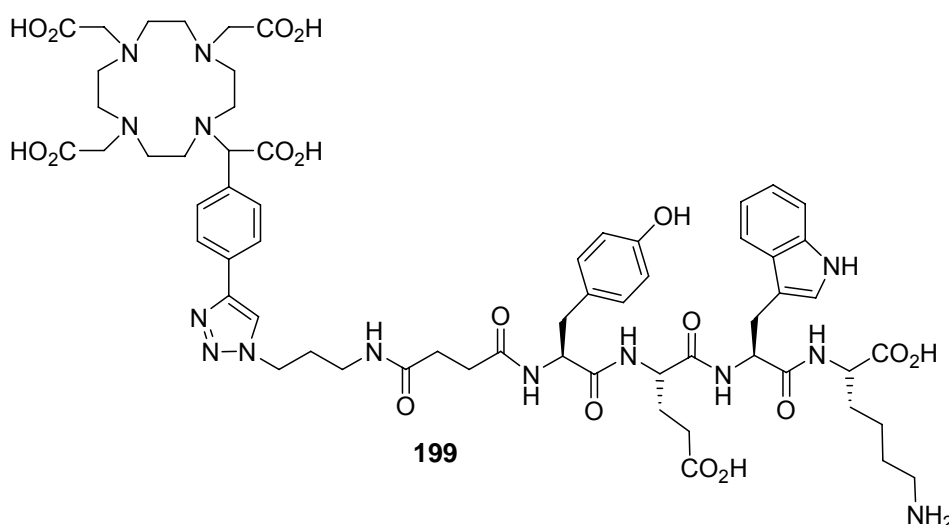
Figure 63. Structure of DOTA conjugate 199.

2.3.4.3 Biodistribution of ^{68}Ga-labeled DOTA conjugate 191

The biodistribution studies were performed by T. Poethko and M. Schottelius at the laboratory of Prof. H.-J. Wester (Klinikum rechts der Isar, München). The DOTA-Tyr[3]-octreotate conjugate 191 was chosen for biodistribution studies to verify the applicability of the new DOTA-derivatives. [68]Ga labeling was performed

using a ^{68}Ge/^{68}Ga-generator to give [^{68}Ga]191 with specific activity of 570 Ci/mmol at the time point of injection into mice. [^{68}Ga]191 was obtained in 55.7% radiochemical yield and 91.4% radiochemical purity. The biodistribution data for [^{68}Ga]191 in AR42J tumor bearing nude mice 30 and 60 min *post*-injection (*p.i.*) are displayed in Figure 64. At both time points, blood concentration of the radioligand was comparably high (2.4±0.4 and 1.7±0.2 %iD/g at 30 and 60 min *p.i.*).[532]
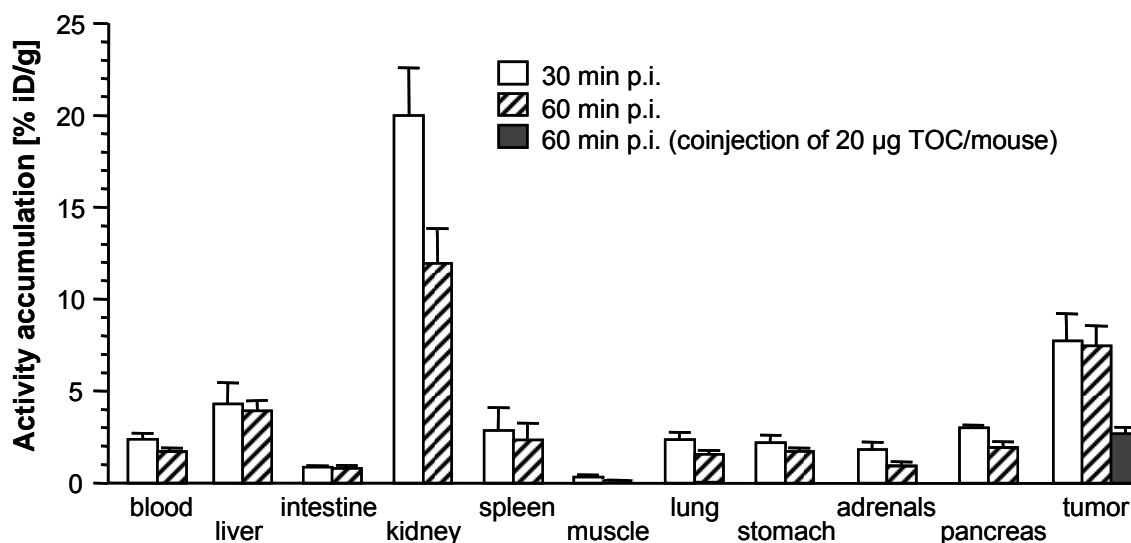
Figure 64. Biodistribution of [^{68}Ga]191 in AR42J tumor bearing nude mice 30 and 60 min *p.i.* (n = 5; for the competition study n = 3). Data are given in % injected dose per gram tissue (%iD/g) and are means ± SD.[532]

While kidney accumulation rapidly decreased within the observation period (20.0±2.4 to 11.9±1.9 %iD/g), indicating renal clearance of [^{68}Ga]191, the tracer accumulation in the other excretion organs, *i.e.* liver and intestine, decreased only slowly over time, probably due to nonspecific accumulation that is not associated with excretion.[532]

In the somatostatin (sst)-expressing tissues, a strong divergence between the tumor and the other sst-positive organs was observed. While tracer accumulation in pancreas, adrenals and stomach significantly decreased between 30 and 60 min *p.i.*, tumor accumulation remained almost constant within this period (7.7±1.5 and 7.5±1.3 %iD/g at 30 and 60 min *p.i.*). This and the overall decrease in non-specific tracer accumulation in the other organs lead to increasing tumor/organ ratios between 30 and 60 min *p.i.* (see Figure 65). That the tumor accumulation is mainly

receptor mediated was demonstrated in a competition study (60 min *p.i.*) by coinjection of an excess of unlabeled competitor (20 μg Tyr^3-octreotate/mouse). Under these conditions, tumor accumulation was reduced 2.7±0.4 % iD/g.[532]
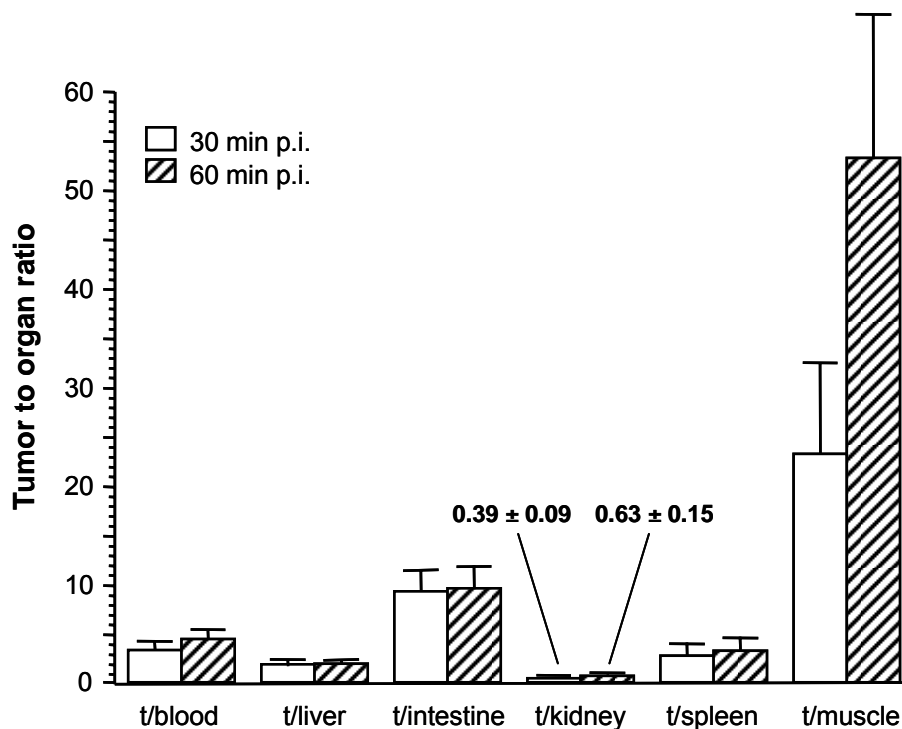
Figure 65. Tumor to non-tumor ratios found for [^{68}Ga]191 in AR42J tumor bearing nude mice 30 and 60 min *p.i.* (n = 5). Data are means ± SD.[532]

2.3.4.4 Discussion and outlook

DOTA and its derivatives emerged as an important class of chelators for imaging technologies in medicine due to their ability to form very stable complexes with a variety of di- and trivalent metal ions. For the convenient synthesis of chelator conjugated targeting biomolecules, different suitable prochelators bearing orthogonally protected carboxy-groups have been described. However, so far there is only one report published in the literature on the synthesis of prochelators enabling connections other than through amine or carboxyl functionalities within the targeting molecule.[508] The approach described above resulted in the development of novel DOTA derivatives which allow chemoselective attachment *via* oxime ligation or Cu(I)-catalyzed azide-alkyne cycloaddition.

For the synthesis of the new compounds, a monoalkylation of cyclen had to be accomplished to obtain 181, 182 and 188. In the literature, there are several examples of similar monoalkylations where high yields of monoalkylated product were achieved by applying cyclen in great excess (*e.g.* 2 equiv[487] or 5 equiv[499]) and where the yields are calculated based on the amount of alkylating agents. As a result of cyclen being the most expensive reagent in the sequence, almost equimolar amounts of the alkylating agent were used in the synthesis to obtain satisfying yields of approximately 70% for the three compounds. Although the crude product could be directly further alkylated, purification of this intermediate was carried out *via* flash chromatography at this stage, as it was easier to separate the monoalkylated product from higher alkylated products and unreacted cyclen, rather than separation after peralkylation, where the resulting compounds only differ in the nature of the alkyl substituent. It should also be noted that in general separation of cyclen derivatives on silica is sometimes quite laborious due to diffuse bands and that purification by preparative RP-HPLC is a good alternative. The syntheses of the α-bromo esters 179, 180 and 187 were straightforward and the products were obtained in good yields.

For the Cu(I)-catalyzed azide-alkyne cycloaddition[509,512,526-531] 1.2 equivalents of copper sulfate together with an excess of copper metal were used, which leads to *in situ* generation of the catalytically active Cu(I) species. Although there are reports[551] where only 1 mol% of Cu(II) salts are used, an excess had to be used, given the fact that one equivalent of the Cu(II) is immediately complexed with the DOTA residue. However, in the literature there is a plethora of different procedures[551] and for this purposes, optimization of the catalyst loading was not essential as dissolved copper ions could be precipitated and filtered off by addition of sodium sulfide. Using Tyr³-octreotate as a model compound, the conjugation by Cu(I)-catalyzed azide-alkyne cycloaddition was shown to be applicable with a broad range of functionalities. As the only side reaction, an opening of disulfide bridge was found. However, this causes no problem, as the reduced DOTA conjugate is smoothly recyclized in quantitative yield. Nevertheless, this side reaction should be kept in mind when planning to synthesize a disulfide bridged conjugate. Of course, it can be avoided if the linear precursor peptide is used for conjugation and the disulfide bridge is formed afterwards. Hence, the alkyne derivatized chelator offers

a promising alternative for attachment of BFCAs in a highly chemoselective manner as demonstrated by reaction with model peptides **197** and **199**. It is worth mentioning that Prasuhn *et al*. concurrently reports an alternative approach for DOTA conjugation *via* azide-alkyne cycloaddition.[552]

The oxime ligation of the new methyl ketone functionalized chelator **189** with unprotected *N*-terminally aminooxy-functionalized Tyr³-octreotate proceeded smoothly and without byproducts, thereby adding another example of the chemoselective condensation of a methyl ketone and a hydroxylamine. In comparison to the recently presented aminooxy-functionalized DOTA-derivatives,[508] the inverse approach presented here allows the introduction of the chelator at any position in a peptide sequence, since various appropriate aminooxy functionalized building blocks for SPPS are commercially available (*e.g.* (Boc-aminooxy)-acetic acid, Boc-Ams(Fmoc)-OH and Fmoc-Dpr(Boc-Aoa)-OH).

As a first proof of principle, the ⁶⁸Ga-labeled derivative of the oxime linked DOTA conjugate **191** was used in an *in vivo* experiment. AR42J tumor bearing nude mice were treated with 20 µg [⁶⁸Ga]**191** per mouse and investigated for tumor accumulation at 30 and 60 min *p.i.*. The results exhibit good contrast and high accumulation in the tumor (see Figure 64).

2.3.4.5   Conclusion

The novel alkyne and keto-functionalized DOTA derivatives described above allow a facile and chemoselective conjugation with polyfunctionalized compounds. With regard to the synthesis of the new modified chelators, economical straightforward procedures were developed avoiding complicated protection group chemistry considering the final application of the BFCA. This allows easy access to labeled compounds in few synthetic steps. Both the alkyne as well as the methylketone-functionalized DOTA derivatives proved to react selectively in the corresponding conjugation with *N*-terminally modified Tyr³-octreotate. Furthermore, the pharmacokinetics of [⁶⁸Ga]**191** in AR42J tumor bearing nude mice demonstrate the suitability of the chemoselective BFC-conjugation approach for the synthesis of new radiometallated peptide ligands for diagnostic and therapeutic *in vivo* applications.

— Chapter 3 —

3 Development and Optimization of Novel Cross-Linked Polymers as Media for Measurement of Residual Dipolar Couplings

3.1 Background

3.1.1 Alignment media for measurement of residual dipolar couplings – introduction and motivation

Magnetically active nuclei are magnetic dipols and hence interact in molecules through space. These dipolar couplings contain important structural information about the distance between two atoms and the angle between this pair of atoms and a static magnetic field. In solid state NMR, where molecules are highly oriented, such couplings are in the order of several kHz and cause immense numbers of splittings. In solution, in contrast, the Brownian motion averages out all dipolar couplings, resulting in the narrow line width of high resolution NMR-spectroscopy but also in a significant loss in potential structural information. Therefore, an intermediate state between solid and liquid is desirable in which the narrow line width is maintained and anisotropic interactions are measurable, but significantly reduced in size compared to solid state NMR. This can be achieved by a so-called alignment medium in which the molecules are just partially aligned but show almost free rotation. In such media the huge dipolar couplings observed in solid-

state are reduced to only a few Hz and therefore called residual dipolar couplings (RDCs).[553-559] This has already advanced to a standard technique in high resolution NMR of biomacromolecules and numerous aqueous alignment media have been described, such as lipid bicelles,[558,560] stretched polyacrylamide gels,[561-564] filamentous phage[565] and other liquid crystalline phases[566,567] are available. However, quite recently this technique started to find application in the field of small molecule NMR.[568-580]

A limiting step for the application of RDCs to small molecules is still the availability of alignment media for organic solvents. Liquid crystalline phases such as poly-γ-benzyl-L-glutamate (PBLG)[573,574,581-584] are known to align organic molecules in CDCl$_3$ and similar apolar organic solvents. Liquid crystals, however, have the disadvantage that for the phase transition a minimum concentration is needed and therefore a minimum anisotropy is induced in the sample. The development of specially designed crystalline phases with lower minimum alignment, as shown in the case of 4-n-pentyl-4'-cyanobiphenyl (PCBP)[585] and poly-γ-ethyl-L-glutamate (PELG),[572] improves the applicability of such systems.

A second approach for partial alignment is strain induced alignment in a gel (SAG) as shown by the pioneering work of DeLoche and Samulski[586] and many follow up applications in polymer NMR spectroscopy.[587-589] This technique is not limited by a minimum anisotropy and it was extensively used to study the properties of polymer gels by means of high resolution deuterium NMR.[590] Nevertheless, gel alignment was only lately used to induce RDCs in molecules dissolved in the gel.[561,562] SAG allows the unrestricted scaling of alignment over a wide range and can be used for aqueous as well as organic solvents, depending on the polymer used.[563,579,580,591,592] As a first example in organic solvents, RDC measurements in stretched cross-linked polystyrene (PS) gels swollen in CDCl$_3$ were reported by B. Luy from our group as a promising alignment method.[579]

After the proof of principle, the aim of this study was to optimize the procedure to control the alignment and to widen the scope of applicable solvents by development of novel polymeric media. The focus here was on materials available by radical polymerization. A polymerization technique was worked out allowing the production of long sticks which can be cut into peaces suitable for the NMR application and whose diameter can be easily controlled.[593] Moreover, the amounts of

cross-linking agent and radical starter were varied to adopt the swelling properties of the polymers. As PS-sticks are mainly swellable in relatively unpolar organic solvents like $CHCl_3$ or benzene, a major goal was to find suitable polymers for polar organic solvent like CH_3CN, MeOH or DMSO. This was successfully achieved with cross-linked poly(vinyl acetate) (PVA).[594]

3.1.2 The dipolar interaction

A simplistic picture for the dipolar interaction is described by Luy *et al.*:[595] Spins can be illustrated as magnets with an inherent rotation at the Larmor frequency. Although spins are not oriented directly along the static magnetic field B_0, the averaging over time of the fast rotating magnets yields a resulting magnetic moment parallel or antiparallel to B_0 (Figure 66a, b).
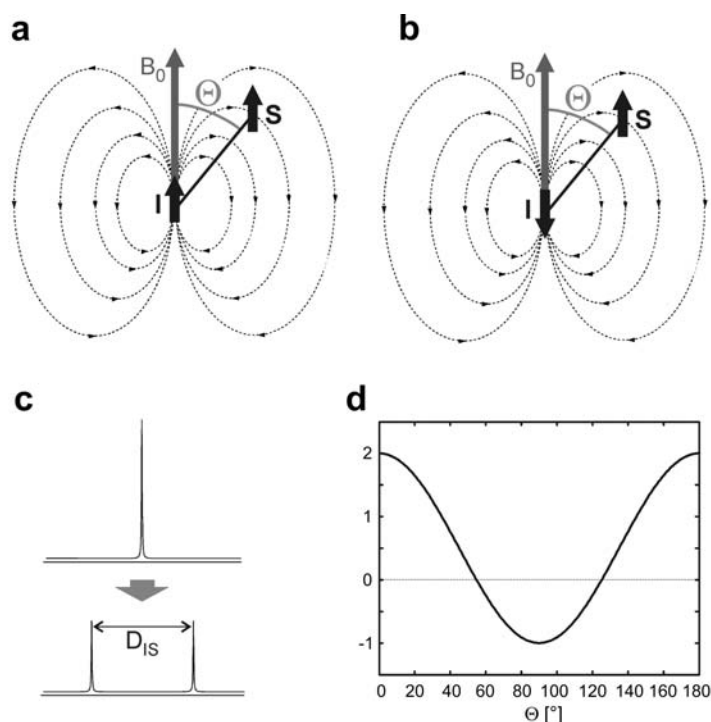
Figure 66. Illustration of the dipolar interaction. (a, b) The magnetic field induced by spin I adds up to the static magnetic field B_0 and leads to a shift of the resonance frequency of the close-by spin S. Since spins parallel and antiparallel to the magnetic field are almost equally distributed, this leads to a splitting with the dipolar coupling D_{IS} (c). The $(3 \cos^2 \Theta - 1)$ angular dependence is shown in (d).[595]

The magnetic moment of a spin results in the same magnetic field as a classical magnet with the typical r^{-3} dependence of the magnetic field strength with respect to the distance. In addition to the distance, there is an angular dependence scaling the dipolar interaction. With respect to the angle θ relative to the axis of the magnetic moment, the magnetic field strength varies with $3 \cos^2 \theta - 1$. Since the magnetic moment of the spin is oriented along the static magnetic field B_0, the angle θ is identical to the angle Θ with respect to B_0. A second spin close in space feels the magnetic field contribution of the magnetic moment of the first spin and therefore resonates at a slightly different frequency as compared to an isolated spin. Since spins parallel and antiparallel to B_0 are about equally populated, the field contributions of neighboring spins lead to a split signal with the distance in Hz between the doublet components being the so-called dipolar coupling (Figure 66c). Size and sign of coupling depends (a) on the distance between the two coupling nuclei, (b) on the angle between their interaction vectors and (c) on the field and therefore gives valuable structural information.

3.1.3   Structural characteristics and physical properties of polymers

The term polymer is used to describe large molecules of high relative molecular mass consisting of repeating structural units (monomers) connected by covalent chemical bonds. The term homopolymer denotes polymers derived from one species of monomer, whereas a polymer derived from more than one species of monomers is called a copolymer.[596] Since a copolymer consists of at least two types of monomers, they can be classified based on how these units are arranged along the chain (see Figure 67).
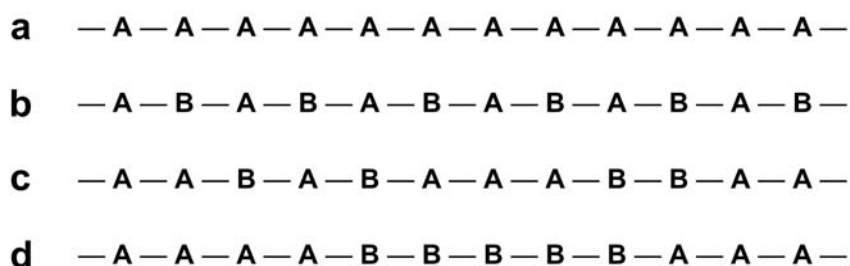
Figure 67. Illustration of the arrangement of monomers in (a) a homopolymer or (b) an alternating, (c) a random or (d) a block copolymer.

Most common are alternating copolymers with regular alternating A and B units, random copolymers with random sequences of monomer A and B and block copolymers with well separated blocks of A and B segments.[597,598] The type of copolymer formed can be estimated having regard to the monomer reactivity ratio of a specific mixture of A and B, as described in detail in chapter 3.1.5.3.
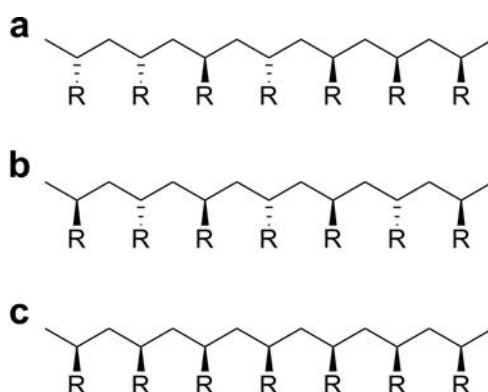
Figure 68. Illustration of (a) an atactic, (b) a syndiotactic and (c) an isotactic macromolecular chain.

The orderliness of the succession of configurational repeating units in the chain of a macromolecule gives the tacticity of a polymer.[596] It can be distinguished between an atactic, syndiotactic and isotactic polymer chain (Figure 68).[597,598]

As an additional structural feature, the polymer chains can be linear, branched or cross-linked (Figure 69) depending on the polymerization process and on the monomers used.
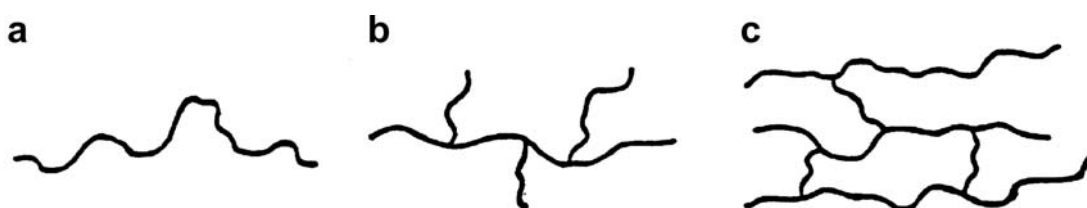
Figure 69. Schematic illustration of (a) linear, (b) branched and (c) cross-linked macromolecular units.

Together, these constitutional and configurational properties strongly affect the conformation and physical properties of the polymer and therefore its possible application. As a result, polymers are typically classified according to physical

behavior into three main groups: thermoplastics, thermosetting polymers (thermosets) and elastomers.

Thermoplastics are plastic or deformable materials which consist of linear or branched macromolecular chains. The chains are associated through van der Waals forces (*e.g.* polyethylene or polypropylene), dipole-dipole interactions and hydrogen bonding (nylon) or stacking of aromatic rings (polystyrene). Therefore, such materials normally melt to a liquid when heated and dissolve readily in appropriate solvents (*e.g.* toluene for polystyrene).[597,598]

Thermosetting polymers are heavily cross-linked materials and therefore generally stronger than thermoplastic materials due the 3-D network of bonds. Thermosets, once formed and cured, can never be remelted and remolded again and are insoluble.[597,598]

Elastomers are slightly cross-linked thermoplastics or thermosets that can be stretched and then return to its original shape without permanent deformation. This is due to the loose network in which the macromolecular chains are hold together by single cross-linkages: If a stress is applied, the polymer chains are stretched out and the covalent cross-linkages ensure that the elastomer will return to its original configuration when the stress is removed (Figure 70). Without the cross-linkages the applied stress would result in a permanent deformation. Generally, such materials swell in appropriate solvents but do not dissolve.[597,598]
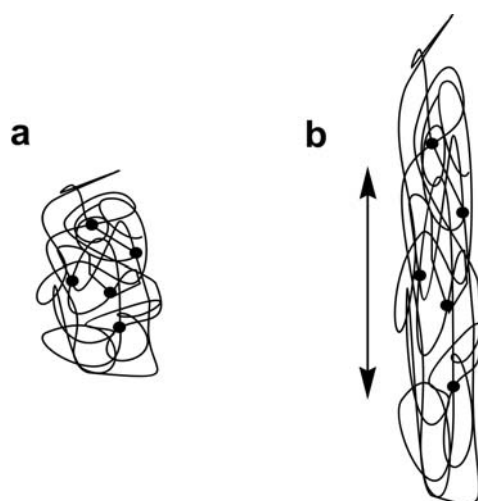
Figure 70. Schematic drawing of an elastomer. (a) Unstressed polymer; the dots denote cross-links. (b) The same polymer under stress. When the stress is removed, it will return to the (a) configuration.

As can be seen in Figure 70b, the stretching leads to an orientation of the polymer chains. This effect is used in the measurement of RDCs in stretched polymer gels, as described below.

3.1.4 Partial alignment in stretched gels: A molecular view

Polymers for use as alignment media for RDC measurement should swell readily in the desired solvent to form a gel. Thus, elastomers or moderately cross-linked and swellable thermosets are preferred. A stretching of the gel and orientation of the macromolecular chains can then easily be achieved by an external constraint, as shown by Luy *et al.*:[579] If a cylindrical PS-stick of about 1 cm length and 3 mm diameter is brought in an NMR tube with an inner diameter of ~4.2 mm together with $CDCl_3$, the polymer starts to swell and is stretched due to the constraints of the glass wall of the tube (see Figure 71c). Thereby the polymer chains become oriented along the tube.
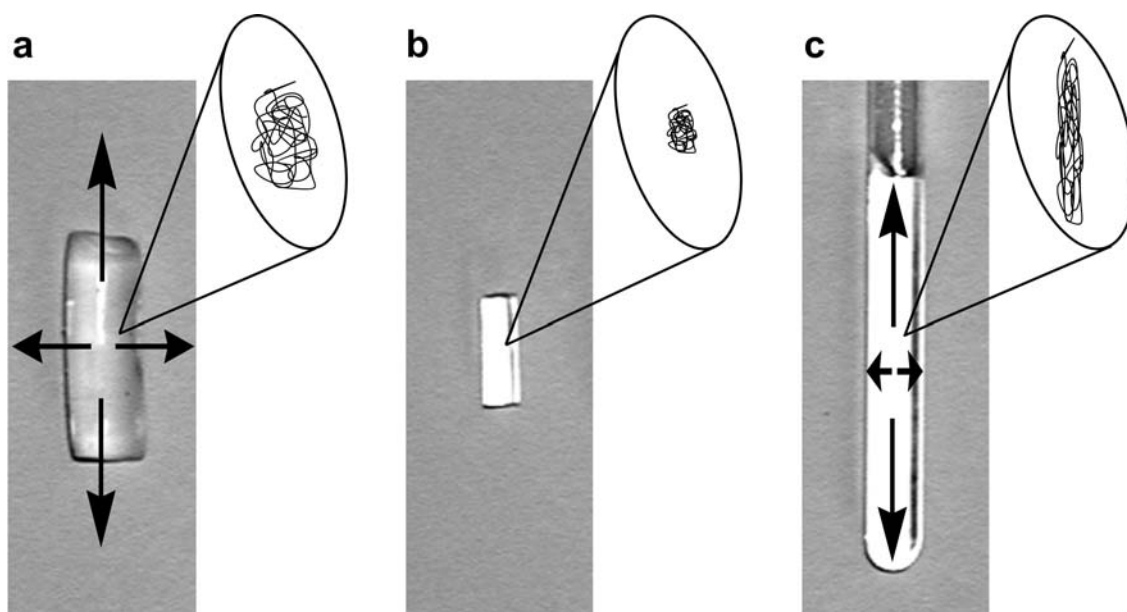
Figure 71. Photography of the cross-linked PS stick in different states of swelling. The corresponding conformation of macromolecular chains is illustrated as schematic drawing. (a) Free polymer-stick completely swollen in an isotropic state; (b) unswollen polymer stick; (c) stretched polymer stick swollen in the NMR-tube.

If a substance is dissolved in such a stretched polymer gel, the single molecules of the sample interact with the oriented macromolecular chains, as illustrated in

Figure 72, leading to a partial alignment. In contrast, if no constraint is applied during swelling, the polymer-stick swells isotropic as shown in Figure 71a and the polymer chains do not become oriented.

The partial alignment in stretched gels results in an average orientation for about 0.05 % of the time. This reduces, for example, a 46 kHz dipolar coupling between a carbon and its directly attached proton to a residual dipolar coupling of only 23 Hz, which adds or subtracts to the direct $^1J_{CH}$ coupling in the order of 130-160 Hz. A coupling of this size can accurately be measured.[553] As shown by Luy *et al.*, RDCs should be generally less than 30 Hz to avoid strong coupling and potential line broadening by long-range couplings and to avoid second order effects in NMR spectra. If RDCs are in this range, all other RDCs to carbon nuclei are small in size. The alignment properties of media are generally determined by measuring the quadrupolar splitting of a quadrupolar nucleus such as deuterium, *e.g.* in $CDCl_3$.[553,579,580,593]
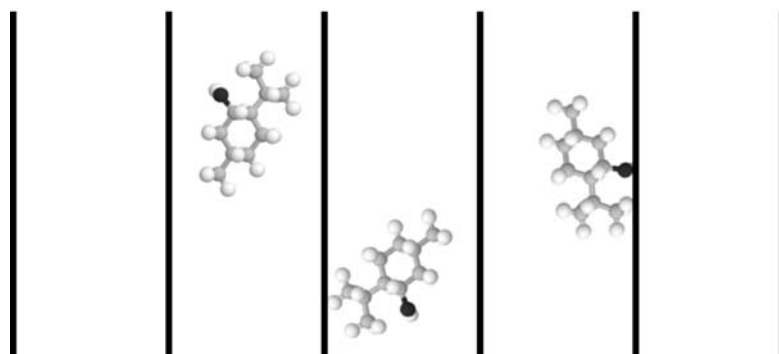
Figure 72. Schematic illustration of a compound dissolved in a stretched polymer gel.

The observed size of RDCs is influenced by numerous factors, such as the size and shape of molecules (which influences their mobility in the network of the polymer gel), the solvent (influences *e.g.* the salvation of the molecule and the swelling and therefore the degree of alignment) and characteristics of the medium. As the molecule is given and the solvent is mostly only variable in a limited range, the alignment medium should be adjustable to optimize the size of the RDCs.

Using stretched polymer gels as alignment media, the size of RDCs can be easily adjusted by varying for example the diameter of the initial dry polymer stick: A stick exactly fitting into the tube will directly abut upon the tube wall resulting in

a strong stretching during swelling. In contrast, a stick of equal composition but smaller in diameter will swell isotropic until it reaches the glass wall. As a result, the degree of orientation will be less. Hence, the degree of orientation significantly depends on the ratio of stick-diameter and the inner diameter of the NMR tube. Moreover, the polymerization conditions and the composition of the polymer itself influence the degree of alignment. It is evident, that the higher the cross-linking and therefore the cohesion of polymer chains, the less the swelling and orientation of the polymer chains will be. However, a tighter network causes also stronger interactions between the polymer chains and the embedded sample molecules which increases the degree of orientation. The polymerization conditions, in particular the reaction temperature, additionally affect the polymer's characteristics by influencing its constitution (lower reaction temperatures lead to the formation of longer polymer chains, as described below).

Beside the described facile procedure to stretch gels, there are a variety of other techniques reported in the literature, ranging from drying on a glass capillary before reswelling,[562] gel compression with a Shigemi plunger,[599] to apparatuses for squeezing a readily swollen gel into an NMR-tube[564] or stretching gelatin inside a rubber tube.[600] The focus of this work, however, was on the controlled production of sticks for alignment by swelling in NMR tubes, as this is a very simplistic and easily reproducible method requiring no additional tools such as a teflon-funnel.[564]

3.1.5   Structure and preparation of polymers

3.1.5.1   Classification of polymerization reactions

Polymerization reactions are usually classified in two main groups according to their mechanism: the step-growth polymerizations and the chain-growth polymerizations.

The step-growth polymerization occurs by consecutive reactions in which the degree of polymerization and average molecular weight of the polymer increase as the reaction proceeds.[596] As a major characteristic, in a step-growth polymerization the growth of polymer chains proceeds by reactions between molecules of all degrees of polymerization. Examples for this kind of polyreactions are polyadditions (*e.g.* polyurethanes formed from isocyanates and alcohols as bifunctional

monomers; see Figure 73a) or polycondensations, where small molecules like water are eliminated (*e.g.* polyesters formed from carbonic acids and alcohols as bifunctional monomers; see Figure 73b).[597,598]

a

$$O=C=N-R^1-N=C=O \ + \ HO-R^2\cdot OH \ \longrightarrow \ \left[\begin{matrix} O & & O \\ \| & & \| \\ C-N-R^1-N-C-O-R^2-O \\ | & | \\ H & H \end{matrix} \right]_n$$

b

$$\begin{matrix} O & & O \\ \diagdown & & \diagup \\ C-R^1-C & \\ \diagup & & \diagdown \\ HO & & OH \end{matrix} \ + \ HO-R^2\cdot OH \ \xrightarrow[-xH_2O]{} \ \left[\begin{matrix} O & O \\ \| & \| \\ C-R^1-C-O-R^2-O \end{matrix} \right]_n$$
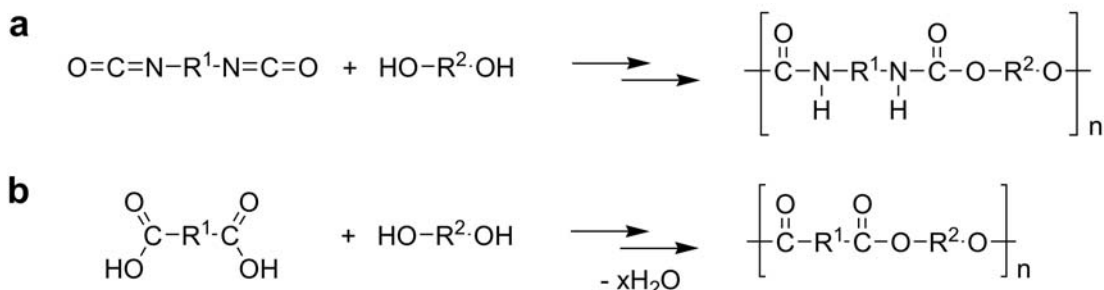
Figure 73. Examples for polymerizations following step-growth mechanism. (a) Formation of polyurethanes by polyaddition; (b) formation of polyesters by polycondensation.

A chain-growth polymerization proceeds exclusively by reactions between monomers and reactive sites on the polymer.[596] These polymers grow to high molecular weight at a very fast rate. Hence, high molecular weight polymers are formed much more quickly than in step-growth polymerizations. Examples for chain-growth polymerizations are radical polymerizations or ionic polymerizations (anionic- and cationic polymerization), according to their initiation. The radical polymerization will be described in more detail in the following chapter.[597,598]

3.1.5.2   Free radical polymerization

The free radical polymerization is one of the most common and useful reactions for preparing polymers and is mostly used to synthesize polymers from vinyl monomers. The mechanism can be divided into three stages: initiation, chain propagation and chain termination (see Figure 74).[597,598]

The whole process is typically started off with radical initiators such as dibenzoyl peroxide or AIBN which can easily be broken into free radicals. For initiation with dibenzoyl peroxide (DBP) normally temperatures of 80°C and above are required, whereas AIBN initiated polymerizations can be started at 40-60°C or by illumination. The initiator radical can than react with a monomer to start a chain. Chain propagation is the rapid reaction with another monomer and the subsequent

repetition to create the repeating chain. Termination occurs when a radical reacts in a way that prevents further propagation. The most common mechanisms are the coupling of two radicals forming a single molecule and chain disproportionation (see Figure 74). Chain disproportionation is a process where two radicals meet, but instead of coupling a proton is exchanged to give two terminated chains, one saturated and the other with a terminal double bond.

Initiation
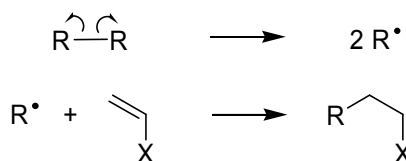
Chain propagation

Chain termination
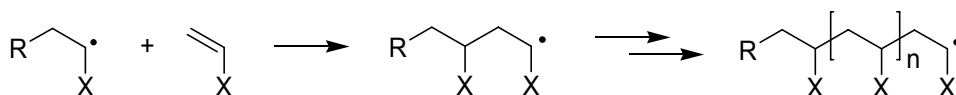
Coupling   Disproprotionation
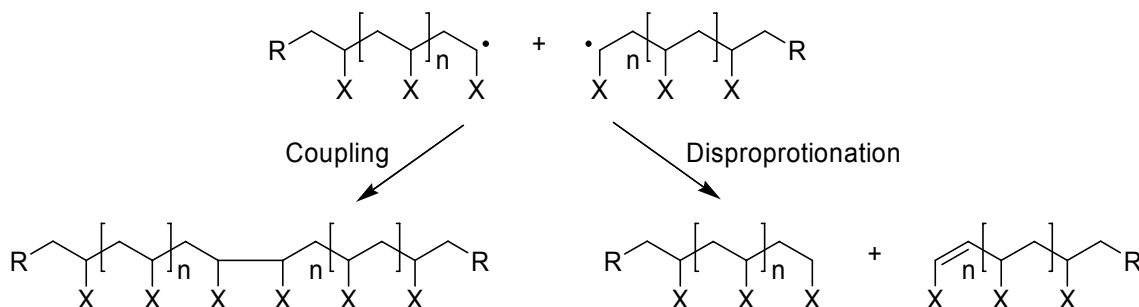
Figure 74. Main steps of the free radical polymerization.

It is evident that the number of termination reactions increases with the amounts of free radicals present: the more radicals are formed (*e.g.* by higher temperatures for initiation), the faster the chain termination will be and the shorter the average chain length and average molecular weight of the resulting polymer. Hence, the final properties of the polymer not only depend on the applied monomer but also on the reaction conditions.

3.1.5.3   The copolymer composition equation

Staudinger 1930 found that the composition of a copolymer alters during polymerization. Starting with an equimolar mixture of vinyl chloride and vinyl acetate, the ratio of chloride to acetate in the copolymer changed from 9:3 to 5:7 in the course of the reaction.[598] This shift in the composition is a result of the diverse reactivity of different types of monomer with each other which leads to a changing composition of the comonomer feed from which the copolymer is produced.

The reaction is a typical example for a copolymerization of two monomers A (vinyl chloride) and B (vinyl acetate), whereby A reacts preferably with radicals A˙ at the propagating chain ending (see below) and also B reacts preferable with radicals A˙ at the propagating chain ending. As a consequence, at the beginning of the reaction larger amounts of A are incorporated in the growing copolymer, while the source solution gets enriched in B. When a specific excess of B is reached, the introduction of B is favored as a result of lacking A. The mutual reactivity of the monomers finally defines whether a random, alternating or block polymer is formed.

In case of copolymerization of two monomers A and B, two types of propagating species are possible, one with A at the propagating end and the other with B. Assuming furthermore that the reactivity of the propagating species is dependent only on the monomer unit at the end of the chain,[597,601-603] four propagation reactions are possible:

$$
\begin{array}{ccc}
\text{\textasciitilde\textasciitilde\textasciitilde A}^\bullet + A & \xrightarrow{k_{AA}} & \text{\textasciitilde\textasciitilde\textasciitilde A}^\bullet \\
\text{\textasciitilde\textasciitilde\textasciitilde A}^\bullet + B & \xrightarrow{k_{AB}} & \text{\textasciitilde\textasciitilde\textasciitilde B}^\bullet \\
\text{\textasciitilde\textasciitilde\textasciitilde B}^\bullet + A & \xrightarrow{k_{BA}} & \text{\textasciitilde\textasciitilde\textasciitilde A}^\bullet \\
\text{\textasciitilde\textasciitilde\textasciitilde B}^\bullet + B & \xrightarrow{k_{BB}} & \text{\textasciitilde\textasciitilde\textasciitilde B}^\bullet
\end{array}
$$
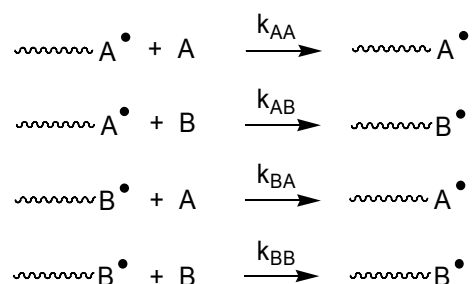
Monomers A and B can each add either to a propagating chain ending in A or to one ending in B.[597] k_{AA} is the rate constant for a propagating chain ending in A adding to monomer A, k_{AB} that for a propagating chain ending in A adding to monomer B and so on. The parameters r_A and r_B, which are defined by

$$r_A = k_{AA}/k_{AB} \quad \text{and} \quad r_B = k_{BB}/k_{BA}$$

are termed the monomer reactivity ratios. Each r is the ratio of the rate constant for a reactive propagating species adding the own type of monomer to the rate constant for its addition of the other monomer. The tendency of two monomers to copolymerize is noted by r values between zero and unity. A r_A value greater than unity means that A$^\bullet$ preferentially adds A instead of B while an r_A value less than unity means that A$^\bullet$ preferentially adds B. An r_A value of zero would mean that A is incapable of undergoing homopolymerization.[597,598] The so-called copolymerization equation or also termed the copolymer composition equation is given as:

$$d[A]/d[B] = (1+r_A[A]/[B])/(1+r_B[B]/[A]).$$

The copolymer composition, $d[A]/d[B]$, is the molar ratio of the two monomer units in the copolymer and is expressed by above equation as being related to the concentrations of the two monomers in the feed, [A] and [B] and the parameters r_A and r_B.

Different types of copolymerization behavior are observed depending on the values[604] of the monomer reactivity ratios. Copolymerizations can be classified into three types based on whether the product of the two monomer reactivity ratios $r_A r_B$ is 1, < 1 or > 1:

- $r_A r_B = 1$:

  If the product $r_A r_B$ is 1, the reaction is termed ideal copolymerization. In the special case $r_A \approx r_B \approx 1$, the two monomers show equal reactivities towards both propagating species leading to a random copolymer. If the two monomer reactivity ratios are different ($r_A > 1$ and $r_B < 1$ or $r_A < 1$ and $r_B > 1$), one of the monomers is more reactive than the other towards both propagating species. In such cases, the copolymer will contain a larger proportion of the more reactive monomer in random placement.[597,598]

- $r_A r_B < 1$:

  If $r_A r_B < 1$, in each case the reaction of the propagating species with a monomer of the other species is preferred leading to short segments of A and B. In the special case $r_A = r_B = 0$, an alternating copolymer is formed.

- $r_A r_B > 1$:

  For the case the product $r_A r_B$ is greater than 1 (thus $r_A > 1$ $r_B > 1$), the reaction of the propagating species with a monomer of the same species is preferred leading to block copolymers. In the special case that $r_A = r_B = \infty$, the two monomers do not copolymerize and only homopolymers are formed.

3.1.5.4   Methods for preparation of polymers

Polymerization techniques are classified based on the method of preparation. The most common procedures and their advantages and disadvantages are summarized in Table 16.

Table 16. Standard methods for preparation of polymers. The table summarizes the different techniques, their advantages and disadvantages.[597,598,605,606]

Method	Description	Advantages	Disadvantages
Bulk	Polymerization in the monomer itself	Low impurity level; molding possible	Thermal control difficult, limited to small scales
Solution	Mono- and polymer soluble in the solvent; polymerization with monomer in solution	Easy thermal control	Chain transfer limits molecular weight; solvent removal; high cost; drying necessary
Precipitation	Monomer soluble in the solvent; polymer precipitates during polymerization.	Easy thermal control; low impurity level; small particle size and high molecular weight possible	Chain transfer limits molecular weight; drying necessary
Suspension	Monomer and initiator are dispersed in a solvent by vigorous stirring.	Simple polymer isolation; easy thermal control; small particle size possible	Difficult control of particle size; possible contamination by suspending agent; washing and drying necessary
Emulsion	Liquid monomer is dispersed in insoluble liquid.	Good thermal control; 100% conversion, high molecular weight, high rates and small particle size possible	Removal of emulsifier, surfactants and coagulants; possible contamination; high cost; washing, drying and compacting necessary

Cross-linked polymer-sticks for RDC measurement should be of constant quality and composition to obtain reproducible results and they should be of high purity to

reduce background signals. As described above, the diameter of the sticks influences the degree of orientation of the polymer chains after swelling and therefore the size of the RDCs. Hence, it is desirable to obtain sticks of defined and controllable diameter to easily adopt the degree of alignment. Therefore, the bulk polymerization was considered as the method of choice as it provides the opportunity to control the diameter. Furthermore, no additives and solvents are necessary, hence, reducing possible contaminants and avoiding drying after polymerization.

3.2 Synthesis and evaluation of cross-linked polymers

3.2.1 Poly(styrene-co-divinylbenzene) sticks (P1)

Styrene-divinylbenzene copolymer P1 (see Scheme 20) is widely used, *e.g.* as basis for ion-exchange resins or resins for solid-phase peptide synthesis. As both monomers are quite similar in their chemical properties with respect to radical polymerization, the mixture shows an almost ideal copolymerization. The r values for styrene (200) and divinylbenzene (201) are $r_A = 0.65$ and $r_B = 1.1$ ($r_A r_B = 0.72$), meaning that there is a slight preference of divinylbenzene to be introduced into the growing chains. Initial experiments for the preparation of cross-linked PS-sticks as media for measurement of RDCs have been reported by Luy *et al.*[579] In their experiments styrene was copolymerized with technical divinylbenzene (DVB) to achieve cross linking and DBP was used as radical starter at 80-120°C.

3.2.1.1 Preparation of P1-sticks by bulk polymerization

To obtain polymer sticks of reproducible composition and properties, the procedure described above was optimized in several respects: The sticks were prepared in glass tubes, one end of which was sealed by melting. The tubes were carefully dried and the inside surface was silylated with a 1:1 mixture of chloro-trimethylsilane and dichlorodimethylsilane to ensure apolar surfaces. This was done to prevent the polymer from sticking to the glass wall which can cause fractures of the stick. Furthermore, the monomers were purified before use to remove contaminants. Hence, the monomers styrene 200 and divinylbenzene 201 were filtered through basic aluminum oxides (pH 10) and distilled under reduced pressure to remove stabilizer. Immediately before polymerization the monomers were degassed for 15 minutes by ultrasound in *vacuo* and ventilated in an argon atmosphere to remove oxygen. In addition, the radical starter dibenzoylperoxide was substituted by AIBN. This allowed a controlled polymerization at much lower temperatures (45°C). In this manner, a series of poly(styrene-co-divinylbenzene) (P1) sticks with varying the amounts of radical starter (from 0.005 to 0.5%, w/v)

and cross linking agent (from 0.05 to 5%, v/v) were prepared in diameters of 1.6 mm, 2.4 mm, 3.4 mm and 4.0 mm (Scheme 20).[593]

Scheme 20. Preparation of poly(styrene-co-divinylbenzene) (P1).[a]

	99.95%-	0.05%-		
	95.00%	5.00%		
	200	**201**		**P1**
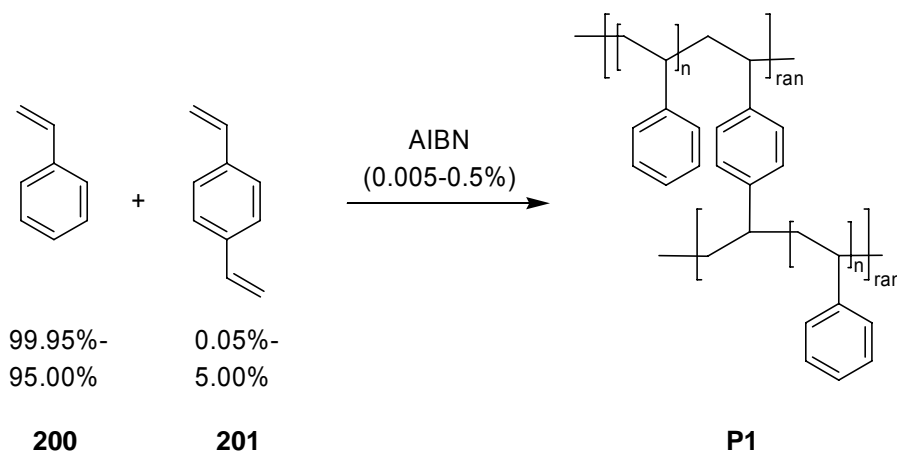
[a] Conditions: 45°C (5 d) then 60°C (2 d); ran: random.[593]

Table 17 shows a summary of prepared sticks. A clear tendency for the consistency of the formed polymers was observed. At very low concentrations of radical starter (0.05% AIBN, v/v) and cross-linking agent (0.005 and 0.01% DVB, w/v) the material did not become solid. Rising the amounts starter or cross-linker resulted first in a gummy then solid consistency. Surprisingly, at low to mediate concentrations of cross-linker (in particular from 0.2-0.75% DVB, v/v) a formation of variable amounts of bubbles was observed (see Table 17) which could not be overcome by optimizing the reaction conditions, *i.e.* polymerization temperature, reaction time or degasing. The combination of low amounts of cross-linking agent with low amounts of AIBN (0.005-0.025%, w/v) even resulted in the formation of foams. In contrast, sticks with DVB content of 1.0 % and greater were clear, transparent and very hard.

From the prepared materials, the gummy sticks, which completely dissolved in solvents and the foamy sticks, which are highly inhomogeneous, were unusable for RDC measurement. From the sticks containing bubbles, only bubble-free parts could be used. Nevertheless, the heavy formation of bubbles was found to be a special issue for the production of P1-sticks, as similar problems did not occur for any other material as described below.

Table 17. Composition and physical consistency of prepared poly(styrene-co-divinylbenzene) (P1) sticks (c.s. = clear solid).

	Amounts of AIBN (%, w/v)						
	0.005	0.01	0.025	0.05	0.075	0.10	0.50
5.0	c.s.	c.s.	c.s.	c.s.	c.s.	c.s.	c.s.
3.0	c.s.	c.s.	c.s.	c.s.	c.s.	c.s.	c.s.
2.0	c.s.	c.s.	c.s.	c.s.	c.s.	c.s.	c.s.
1.5	c.s.	c.s.	c.s.	c.s.	c.s.	c.s.	c.s.
1.0	bubbles	foamy	c.s.	c.s.	c.s.	c.s.	c.s.
0.75	foamy	c.s.	bubbles	bubbles	c.s.	bubbles	c.s.
0.5	foamy	foamy	foamy	bubbles	bubbles	bubbles	c.s.
0.2	foamy	bubbles	foamy	bubbles	bubbles	cloudy	cloudy
0.1	gummy	gummy	c.s.	cloudy	c.s.	cloudy	cloudy
0.05	liquid	liquid	gummy	c.s.	c.s.	cloudy	cloudy

Amounts of divinylbenzene (%, v/v)

3.2.1.2 Alignment properties

A point of major interest in the applicability of P1-gels is the range of solvents in which molecules can be aligned. In line with the very low solubility of non-cross-linked PS,[607] no swelling could be observed for very apolar solvents like octane and relatively polar solvents like acetone or acetonitrile. However, CHCl$_3$, DCM, THF, benzene and dioxane showed significant swelling and were used for further experiments. The NMR studies were performed by B. Luy and K. Kobzar.[593]

As it was shown previously,[579] the anisotropy induced by the gel is dependent on the amount of cross linking agent used for polymerization. To repeat the study, five samples per concentration were swollen in CDCl$_3$ and quadrupolar deuterium splittings were recorded in 5.0 mm NMR-tubes with an inner diameter of ~4.2 mm. The resulting graph is shown in Figure 75a. Anisotropies corresponding to quadru-polar deuterium splittings in the range of 0-540 Hz for P1-sticks with initial diame-

ter of 4.0 mm could be achieved, which should basically cover all needs for partial alignment.[593]

a

b
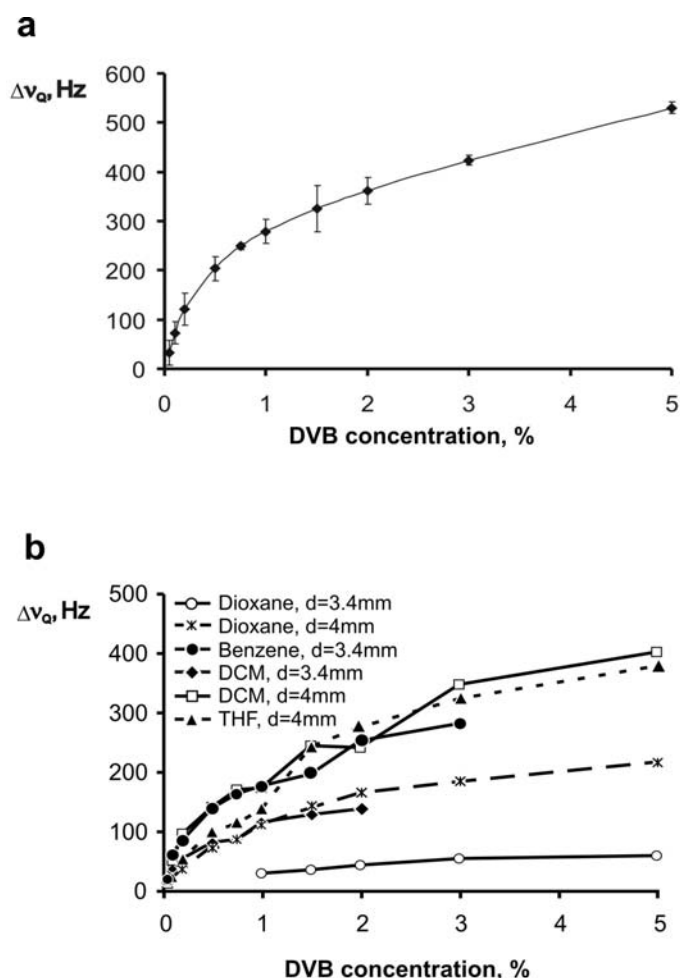
Figure 75. Deuterium quadrupolar splitting $\Delta\nu_Q$ of $CDCl_3$ as a measure of induced anisotropy with respect to amount of cross-linking agent DVB used for polymerization. (a) $\Delta\nu_Q$ of $CDCl_3$. Samples were prepared with P1-sticks of 4 mm diameters and $CHCl_3$ as solvent. (b) $\Delta\nu_Q$ of a 5-10 % of $CDCl_3$ added to the solvents used for swelling DCM, THF, dioxane and benzene. Samples were prepared with P1-sticks of 4 mm diameter for all solvents and additional 3.4 mm diameter for benzene, dioxane and DCM.[608] All samples were measured in 5.0 mm NMR tubes with an inner diameter of ~4.2 mm.[593]

The DVB- and diameter dependence of the induced anisotropy was measured by adding 5-10 % of $CDCl_3$ to the otherwise undeuterated solvents (Figure 75b). Quadrupolar deuterium splittings in the range of 0-400 Hz could be obtained for DCM and THF as solvents, showing overall similar behavior to chloroform. Benzene and dioxane both showed a relatively slow swelling with quadrupolar splittings up to 200 Hz for dioxane and up to 250 Hz in the case of benzene with only 3.4 mm

153

diameter sticks.[593] In general, the splittings observed in 3.4 mm samples were significantly smaller than those measured in the corresponding 4.0 mm samples. Sticks 1.6 mm in diameter did not induce any splitting and 2.4 mm sticks only in exceptional cases.

In contrast to previously published results, where polymerization took place at 80°C to 120°C using dibenzoyl peroxide as radical starter,[579] a dependence of the induced anisotropy on the amounts of radical starter was not confirmed. This is probably due to overall longer polymer chains produced at lower polymerization temperatures.

3.2.1.3   NMR properties

As shown in Figure 76a, a line width below 1 Hz was easily obtained for the $CHCl_3$ proton signal. A typical quadrupolar splitting of $CDCl_3$ observed in equilibrated P1-gel samples is given in Figure 76b. The main drawback of polystyrene-gels as alignment media, however, are the undesired NMR signals originating from the polymer itself.

Figure 76c shows a ^1H NMR spectrum of strychnine dissolved in P1-gel. The broad polystyrene signals in the aromatic and aliphatic region can be clearly distinguished form the sharp strychnine signals due to their significantly greater line width. This allows the measurement of coupling constants out of one-dimensional experiments and the interpretation could be further simplified using two-dimensional techniques, since the probability of signal overlap is reduced and data analysis can be accomplished in a conventional way.[593] Strychnine *e.g.* allows the measurement of a complete set of ^1H-^{13}C dipolar coupling constants from an uncoupled HSQC spectrum because only one aromatic signal partially overlaps with polystyrene, for which the reliable measurement of RDCs is still possible (Figure 76d). However, suppression of polystyrene signals would increase the overall quality of the spectra and allow the measurement of less concentrated samples.
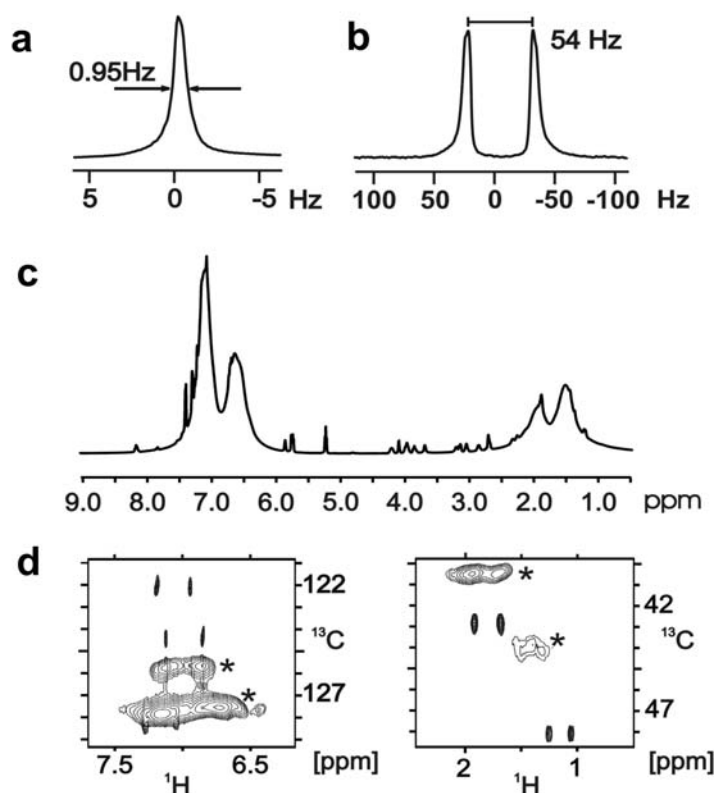
Figure 76. Achievable line width and chemical shift changes due to P1-gel. (a) Although most signals are broadened due to residual dipolar couplings, the experimentally achievable line width in a P1-gel is not significantly larger than in conventional liquid samples. (b) Typical quadrupolar splitting of $CDCl_3$ observed in equilibrated P1-gel samples. (c) 1D-spectrum of a 50 mg strychnine sample in a stretched P1-gel. The strong broad signals in the aliphatic and aromatic regions originate from P1. (d) The artefact signals do not interfere with the signals of strychnine in heteronuclear 2D-experiments. In the case of strychnine the full set of ^{1}H-^{13}C heteronuclear RDCs can be measured. 2D-contours resulting from P1-gel signals are marked with *.[593]

3.2.2 Poly(styrene-d₈-co-divinylbenzene) sticks (P2): Intention, preparation and MNR-properties

As described above, the poly(styrene-co-divinylbenzene) (P1) gel is a powerful medium for partial alignment. Nevertheless, the intensive background NMR signals of the polymer limit its applicability. First approaches to suppress the polymer signals by relaxation filter elements implemented in the NMR experiments have been reported by Luy *et al.*.[593] A more convenient method would be desirable and could be achieved by the use of a corresponding deuterized polymer.

Scheme 21. *Preparation of styrene-d$_8$-co-divinylbenzene (P2).*[a]

99.98%-99.00%	0.02%-1.00%	
202	**201**	**P2**
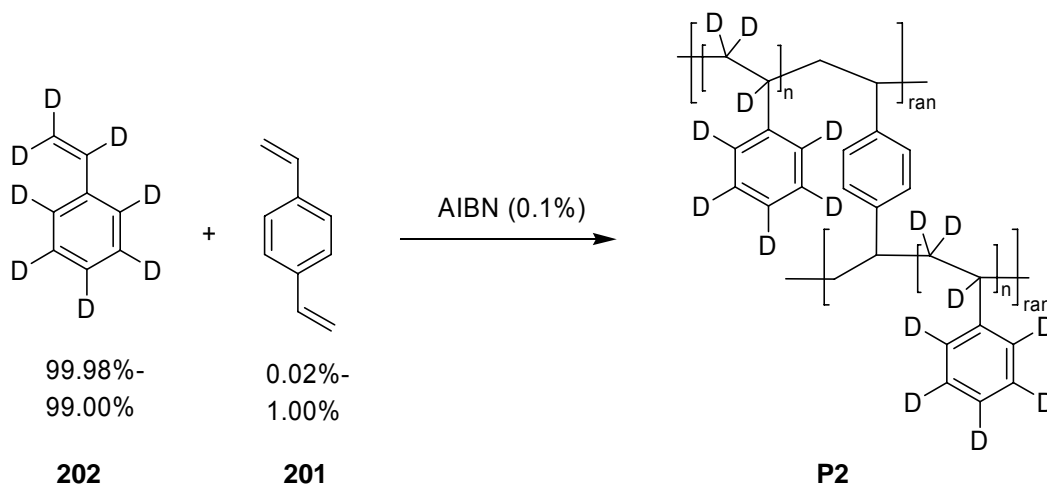
[a] Conditions: 45°C (5 d) then 60°C (2 d); ran: random.

Obviously, a major limitation of this approach could be the availability and the prize of the starting materials. Styrene-d$_8$ (202), however, is commercially available at a reasonable cost. Although deuterized divinylbenzene (201) is not available, this causes no problem as the cross-linking agent is merely added in the range of approximately one percent with respect to styrene-d$_8$ (202) which corresponds to the isotopic purity of styrene-d$_8$ (>98 atom% D).

For preparation of styrene-d$_8$-co-divinylbenzene (P2) sticks, above described procedure was optimized in one step with regard to the significantly smaller reaction scale: to reduce loss of substance during separation from stabilizers, the distillation step was substituted by a condensation allowing the purification of 5 mL of styrene-d$_8$ in approximately 90% yield. In this manner a series of sticks of 3.4 mm diameter was prepared with constant amounts of AIBN (0.1%, w/v) and variable amounts of DVB (0.2, 0.5 and 1.0%, v/v) (Scheme 21). All mixtures gave clear solids with only sporadic occurring bubbles.

Initial NMR studies performed by G. Kummerlöwe in our group showed a dramatic reduction of polymer signals in the deuterated P2 polymer (see Figure 77, lower spectra). Figure 77a shows a superposition of ^{1}H-NMR spectra of undeuterated polymer P1 (upper spectrum) and the corresponding deuterated polymer P2 (lower spectrum). NMR signals arising from the polymer are almost invisible in P2.

Moreover, ^{1}H-NMR spectra of strychnine were recorded in both polymer gels (Figure 77b). This experiment convincingly demonstrated the potential of P2 polymer in the application. Accordingly, the promising material is currently evaluated in more detail by G. Kummerlöwe.
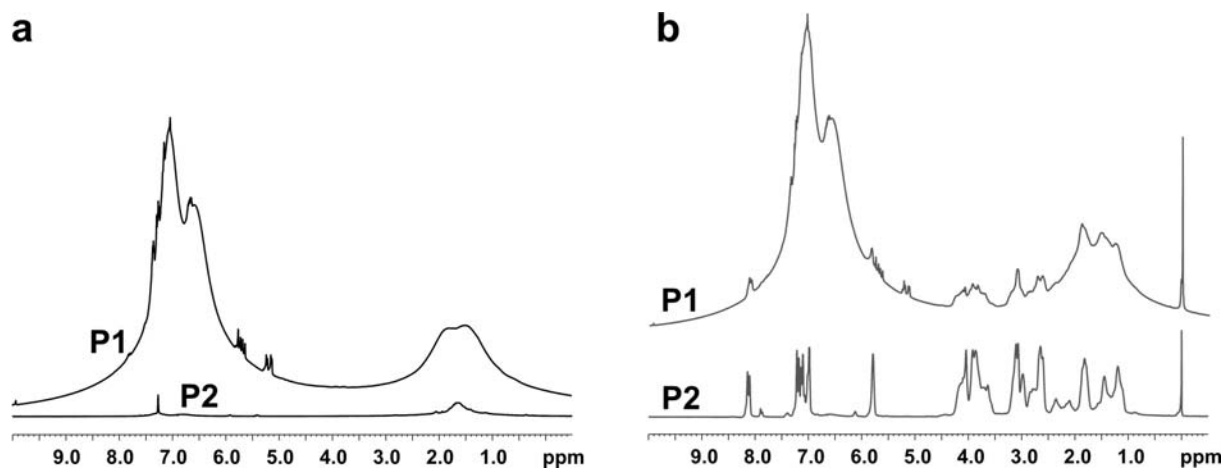
Figure 77. Superposition of ^{1}H NMR spectra of poly(styrene-co-divinylbenzene) (P1) (upper spectra) and poly(styrene-d$_8$-co-divinylbenzene) (P2) (lower spectra) recorded under equal conditions (receiver gain, number of scans, etc.). (a) 1D-spectra of pure polymers P1 and P2 swollen in CDCl$_3$. (b) 1D-spectra of 50 mg strychnine in P1 and P2 gels (solvent CDCl$_3$).

3.2.3 Poly(methyl methacrylate-co-ethylenglycol dimethacrylate) sticks (P3)

Poly(methyl methacrylate) (PMMA) is a common polymer showing solubility similar to PS.[604] Nevertheless, its application as alignment medium is quite interesting as the expected ^{1}H NMR signals of the polymer are different compared to PS which makes this material an interesting alternative in cases when substance and polymer signals overlap.

3.2.3.1 Preparation of P3-sticks by bulk polymerization

Ethylenglycol dimethacrylate (204) was chosen for cross-linking of methyl methacrylate (203) polymer chains as it provides similar structure and properties as the main monomer to give a preferred statistical incorporation into the growing poly-

mer chain. Cross-linked PMMA (P3)-sticks (Scheme 22) were prepared in a broad composition range in collaboration with D. Heckmann according to the procedure developed for cross-linked PS (P1).

In this manner methyl methacrylate (203) was copolymerized with variable amounts of ethylenglycol dimethacrylate (204) (0.05, 0.1, 0.2, 0.5, 0.75, 1.0, 1.5, 2.0, 3.0 and 5.0%, v/v) in silylated glass tubes of diameters 1.6, 2.4, 3.4 and 4.0 mm thereby varying the amounts of AIBN (0.025, 0.05, 0.075, 0.1, 0.5%, w/v). All possible combinations were prepared. In contrast to the cross-linked PS sticks, clear solids with only sporadic occurring bubbles were obtained in all cases.

Scheme 22. *Preparation of poly(methyl methacrylate-co-ethylenglycol dimetha-crylate) (P3).[a]*
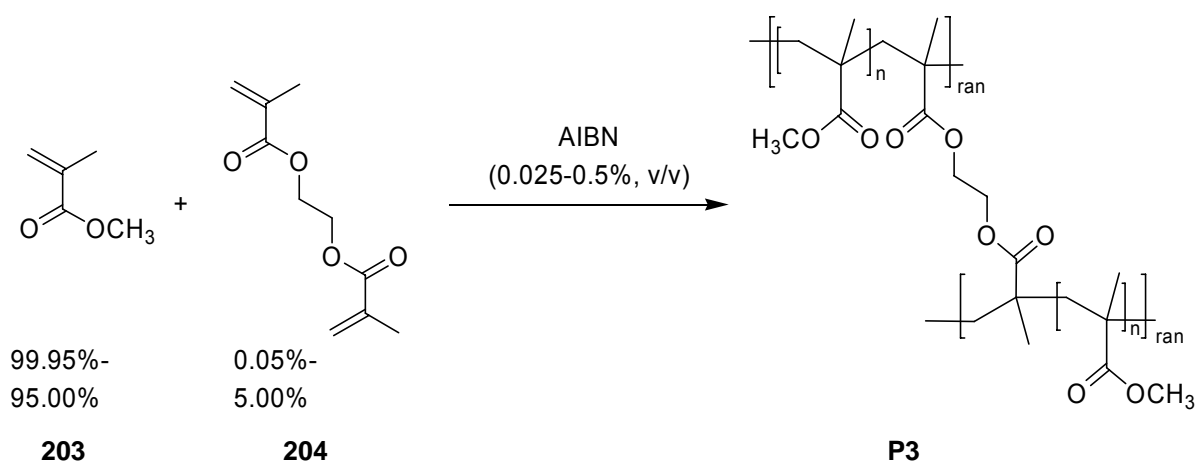
[a] Conditions: 45°C (5 d) then 60°C (2 d); ran: random.

3.2.3.2 Alignment and NMR properties

The P3-sticks are currently under acute investigation by P. Kaden in our group. Applicable solvents are DCM, $CHCl_3$, THF, benzene and dioxane. So far it was found that only sticks of 3.4 and 4.0 mm diameter show sufficient swelling to give a reasonable deuterium splitting and that swelling decreases at higher cross-linking. The absence of aromatic signals in ^{1}H NMR spectra of P3 (see Figure 78) is the main advantage over P1 as medium for partial alignment.
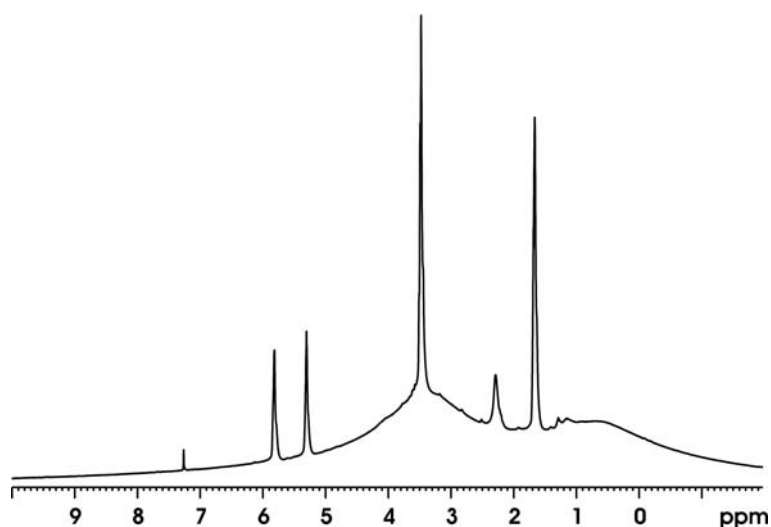
Figure 78. ^{1}H NMR spectrum of poly(methyl methacrylate-co-ethylenglycol dimethacrylate) (P3) in CDCl$_3$.

Swelling in presence of 5% (v/v) CDCl$_3$/CHCl$_3$ was performed to monitor the induced anisotropy by the deuterium quadrupolar splitting $\Delta\nu_Q$ in dependence of the amount of cross-linking agent used for polymerization. The resulting curve for the P3-gels (4.0 mm sticks were swollen in 5.0 mm NMR tubes) displays similarity to the ones observed for the P1-gels above. The induced anisotropy increases with higher cross-linking concentrations.
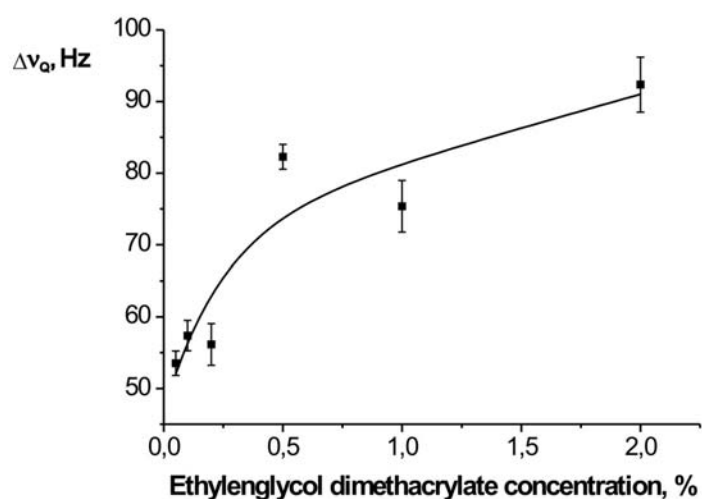
Figure 79. $\Delta\nu_Q$ of 5% (v/v) CDCl$_3$/CHCl$_3$. Samples were prepared with P3-sticks of 4 mm diameter. Samples were measured in 5.0 mm NMR tubes with an inner diameter of ~4.2 mm.

3.2.4   Poly(vinyl acetate-co-adipic acid divinylester) sticks (P4)

So far, all available media for partial alignment such as the cross-linked PS P1 and PMMA P3 described above as well as the cross-linked polydimethylsiloxane (PDMS)[580] developed by C. Freudenberger in our group are limited to relatively apolar solvents. A suitable medium for application with the important polar NMR solvents like acetone, DMSO, CH$_3$CN or MeOH would therefore be highly desirably. For this study, poly(vinyl acetate) (PVA) was chosen as promising basis as vinyl acetate is suitable for polymerization in bulk and the polymer is know to dissolve readily in the desired polar solvents.

3.2.4.1   Preparation of P4-sticks by bulk polymerization

The commercially available adipic acid divinylester (206) was chosen as cross-linking agent. Again, sticks in a broad composition range were prepared according to the procedure developed for cross-linked PS (P1) in glass tubes of 1.6, 2.4, 3.4 and 4.0 mm diameter (Scheme 23).[594]

Scheme 23. *Preparation of poly(vinyl acetate-co-adipic acid divinylester) (P4).^{a}*

99.95%-	0.05%-	
95.00%	5.00%	
205	**206**	**P4**
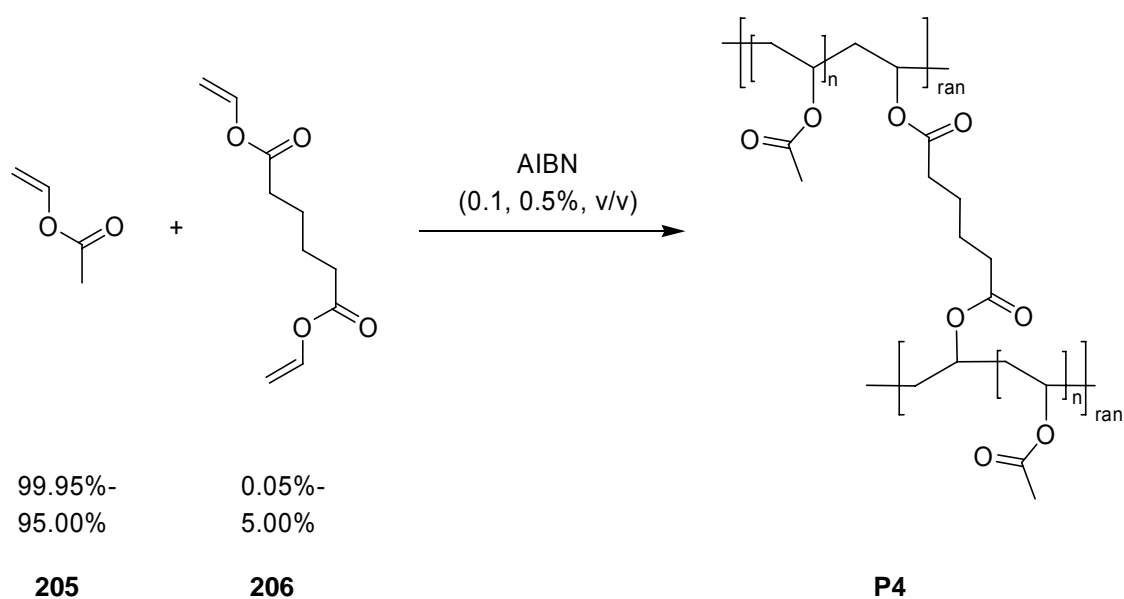
^{a} Conditions: 45°C (5 d) then 60°C (2 d).

Copolymerization of vinyl acetate (205) in presence of 0.05, 0.1, 0.2, 0.5, 0.75, 1.0, 1.5, 2.0, 3.0 and 5.0% (v/v) adipic acid divinylester (206) using 0.1 and 0.5% (w/v) of AIBN as radical starter produced clear copolymerizates P5 for all compositions. Only sporadic occurring bubbles were formed, as previously observed for cross-linked PMMA (P3).

3.2.4.2 Alignment and NMR properties

As a first test, the cross-linked PVA (P4)-sticks were put in various organic solvents and the swelling behavior was investigated. The sticks were swollen in basically all tested solvents, such as $CHCl_3$, THF, dioxane, benzene, EtOAc, acetone, CH_3CN, MeOH and DMSO. The swelling was repeated inside NMR-tubes and 5% (v/v) $CDCl_3$ was added to the non-deuterated solvents to be able to monitor any induced anisotropy by the deuterium quadrupolar splitting Δv_Q. In all cases significant splittings with sharp lines could be observed after letting the gels equilibrate for 13 days (Table 18). In addition, the dependence of the quadrupolar splitting on the amount of cross-linking agent used for polymerization was recorded for four solvents (DMSO, MeOH, THF and dioxane; Figure 80).[594]
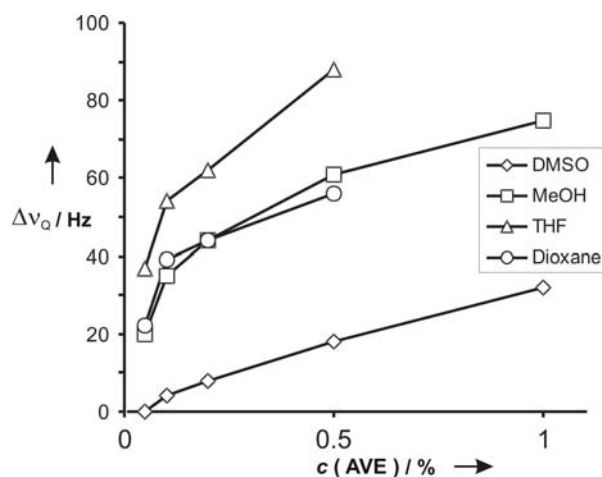
Figure 80. Dependence of the quadrupolar deuterium splitting Δv_Q of $CDCl_3$ on the amount of cross linker adipic acid divinyl ester. To obtain the splittings 5 % (v/v) of $CDCl_3$ has been added to the (P4)-sticks swollen in the otherwise non-deuterated solvents.[594]
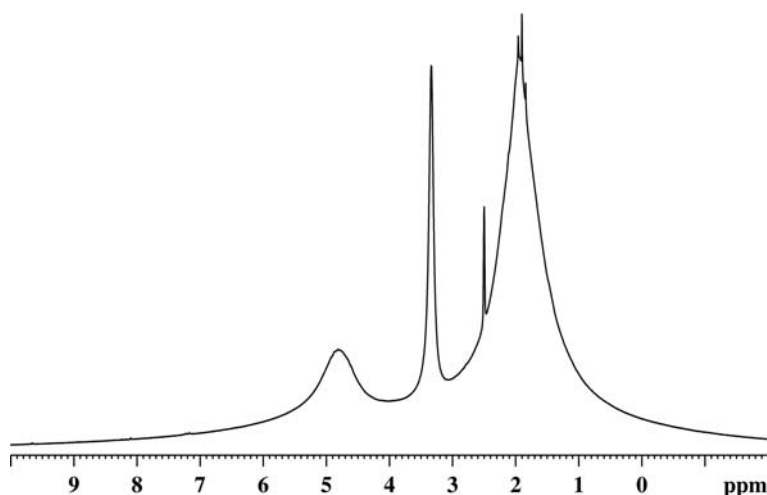
Figure 81. ^{1}H NMR spectrum of poly(vinyl acetate-co-adipic acid divinylester) (P4) in DMSO.

Table 18. Quadrupolar ^{2}H splittings $\Delta\nu_Q$ of CDCl$_3$ (5%, v/v) added to P4-sticks (0.1% (v/v) adipic acid divinylester) swollen in various non-deuterated solvents.[594]

Solvent	Diameter (mm)	$\Delta\nu_Q$ (Hz)
CH$_3$CN	3.4	36.6
	4.0	47.5
Acetone	3.4	33.8
	4.0	54.7
EtOAc	3.4	49.4
	4.0	67.7
Benzene	3.4	83.1
	4.0	—[a]
CHCl$_3$	3.4	72.8
	4.0	106.1
DMSO	4.0	10.0
MeOH	4.0	35.2
THF	4.0	54.6
Dioxane	4.0	39.5

[a] Tears during swelling.

The resulting curves for P4-gels (again, 4.0 mm sticks were swollen in 5.0 mm NMR tubes) are similar to the ones observed for the P1-gels above, corroborating the general trend that a higher cross-linking leads to stronger induced anisotropies.[580] Thus, stretched P4-gels close the gap between relatively apolar solvents like dichloromethane or chloroform and aqueous solutions. Hence, RDCs can now be measured in practically all common NMR-solvents. The ^{1}H NMR spectrum of cross-linked PVA is shown in Figure 81. An application of the new alignment method on norcamphor and the antibiotic sphaeropsidin A is already reported in the literature.[594]

3.3 Development of cross-linked polymers bearing chiral side chain moieties

3.3.1 Background

In modern organic chemistry, the determination of enantiomeric excess and verification of the enantiomeric purity of a product is a common problem. Classic procedures utilize chiral auxiliaries such as chiral derivatizing agents, lanthanide chiral-shift reagents and chiral solvating agents for discriminating enantiomers *via* NMR.[609,610] However, these methods are limited to molecules that can interact with the auxiliaries to build detectable diastereomeric compounds or adducts. Chiral orienting media, in contrast, allow a discrimination of enantiomers through the differential ordering effect of enantiomers within a chiral phase.[611,612] With this method, also saturated chiral hydrocarbons lacking polar groups[613] and prochiral elements in symmetrical molecules[614,615] have been distinguished by NMR spectroscopy.

Media, such as surfactant bilayers,[616-618] chiral liquid crystalline media,[619-623] and achiral liquid crystals with chiral cages[624] have the disadvantage to be usually difficult to prepare and to allow only limited temperature ranges. Moreover, their induced orientation is dependent on the strength of the magnetic field. Stretched-polymer gels, in contrast, are relatively easy to handle and provide field-independent orientation and the alignment strength can easily be scaled. Based on these experiences, Kobzar *et al*.[625] demonstrated the first application of a chiral polymer gel for partial alignment and successfully distinguished the two enantiomers L- and D-alanine using stretched gelatin as medium. This novel procedure combines the possibility of enantiomeric resolution with the advantages of partial alignment. Nevertheless, the procedure is limited to aqueous solvents. Hence, the goal of this work was to find suitable media for organic solvents on basis of the cross-linked polymers described above. This study was performed in collaboration with D. Heckmann.

3.3.2 Selection and preparation of chiral monomers (212)-(215)

The basic idea was to introduce chiral building blocks into the side chain of a cross-linked polymer which should then induce asymmetric interactions with chiral sample molecules. For this, vinyl monomers bearing chiral substituents were prepared from chiral alcohols which are commercially readily available *e.g.* in form of lactic acid derivatives or dihydroquinine. The reaction of alcohols 207-210 with acrylic acid chloride in presence of DIPEA and DMAP formed the corresponding chiral acrylates 212-215 in moderate yields (56-72%; not optimized) (Scheme 24).

Scheme 24. *Synthesis of chiral acrylates 212, 213, 214 and 215.*
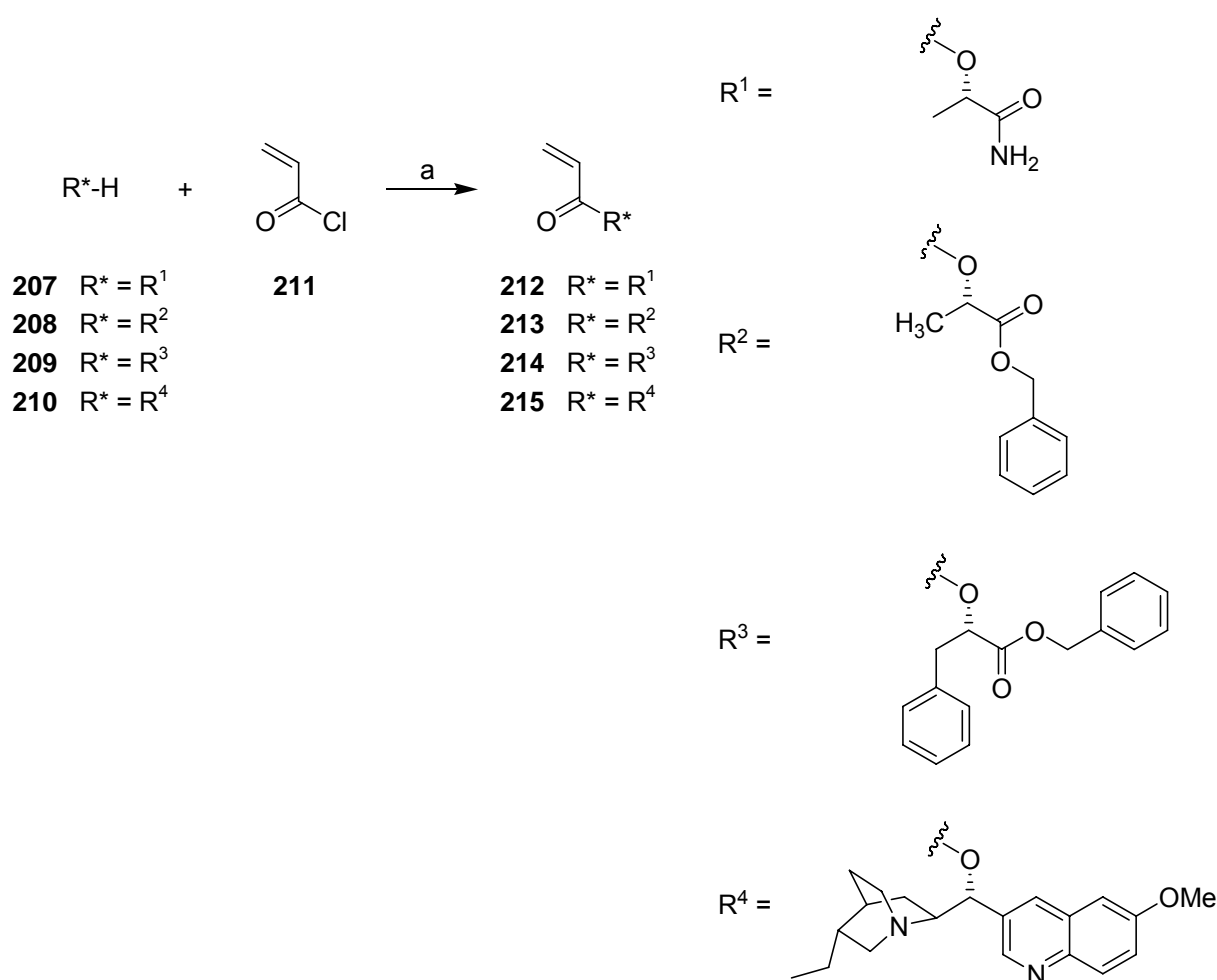
(a) Reagents and conditions: DMAP, DIPEA, 3 h, −78 °C.

3.3.3 Preparation of cross-linked polymers P5-P9

The cross-linked polymer sticks P5 and P6 from acrylates 213 and 214 respectively, were prepared by copolymerization with 0.5 and 1.0% ethylenglycol dimethacrylate (204) as cross-linking agent using 0.1% AIBN as radical starter. The polymerization was carried out in glass tubes with an inner diameter of 4.0 mm according to the procedure developed for cross-linked PS (P1). Clear solid sticks were obtained which are currently investigated in NMR for their alignment properties and their ability to discriminating enantiomers.

Scheme 25. *Preparation of cross-linked polyacrylates **P5** and **P6**.*[a]

213 R* = R^2		**P5** R* = R^2	
214 R* = R^3	**204**	**P6** R* = R^3	
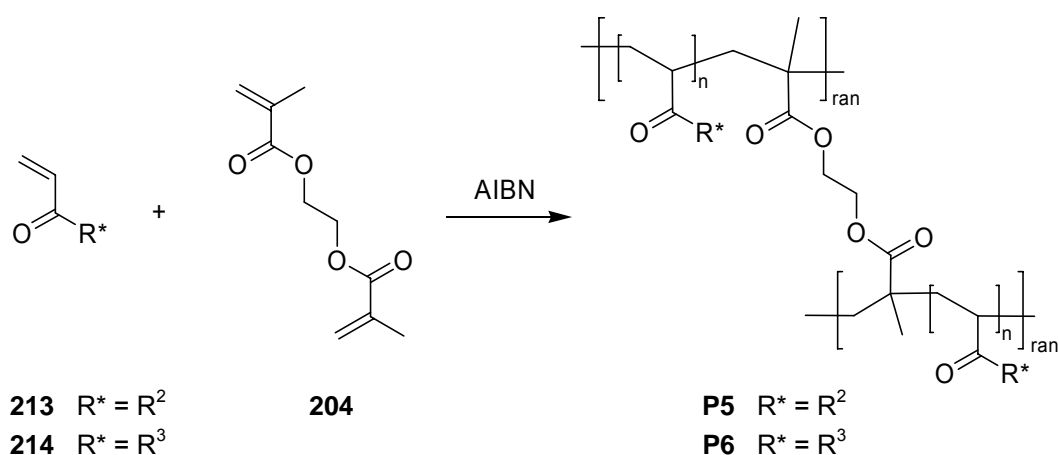
[a] R^2 and R^3 are as defined in Scheme 24; conditions: 45 °C (5 d) then 60 °C (2 d); ran: random.

In a second approach the acrylates 212, 214 and 215 were copolymerized with methyl acrylate (216) and ethylenglycol dimethacrylate (204). As shown by Green *et al.*, the copolymerization of minor amounts of a chiral "sergeant" with a non-chiral "soldier" can induce a helical preference and thus a strong chiral effect ("Sergeant-Soldier-Effect").[626,627] This would allow a significant cheaper production of chiral media.

Hence, the following sticks were prepared according to above procedure: 212 was copolymerized with 33% (v/v) methyl acrylate (216) and 1.0% (v/v) ethylenglycol dimethacrylate (204), 214 was copolymerized with 50% methyl acrylate (216) and 1.0% (v/v) ethylenglycol dimethacrylate (204) and 215 was copolymerized with

75, 81, 88, 91 and 94% (v/v) methyl acrylate (216) and 0.5% (v/v) ethylenglycol dimethacrylate (204). Again, clear solid sticks were obtained which are currently under NMR investigation.

Scheme 26. *Preparation of cross-linked polyacrylates P7, P8 and P9.*[a]

212 R* = R^1	**216**	**204**
214 R* = R^3		
215 R* = R^4		

P7 R* = R^1	
P8 R* = R^3	
P9 R* = R^4	
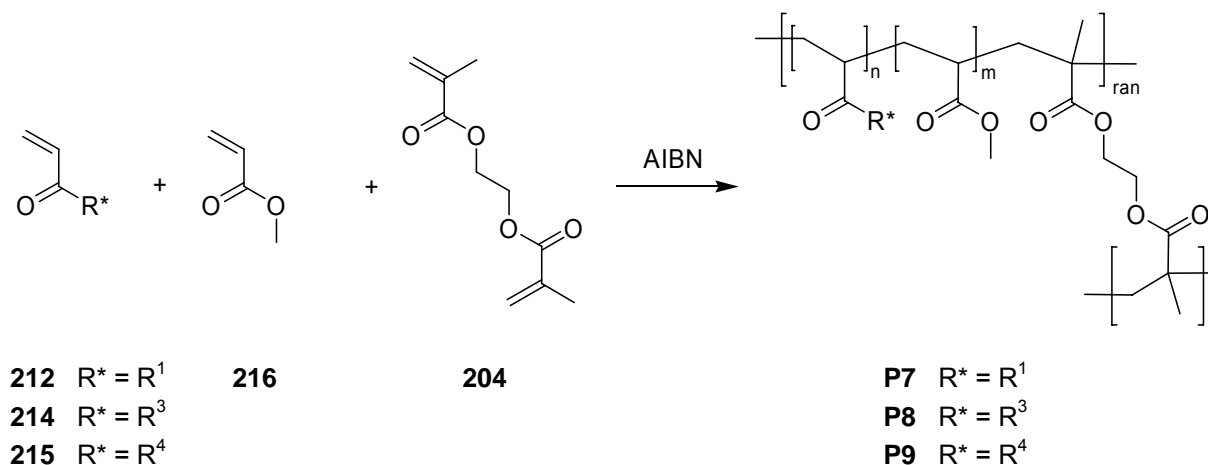
[a] R^1, R^3 and R^4 are as defined in Scheme 24; conditions: 45 °C (5 d) then 60 °C (2 d); ran: random.

3.4 Conclusion

The measurement of residual dipolar couplings is an emerging powerful technique for structure determination. So far, all methods described in the literature were limited to application in aqueous solvents. The development of novel cross-linked polymers described herein now widens the range of applicable solvents to almost all polar and unpolar solvents commonly used in NMR determination. Nevertheless, the application of RDCs for structure determination of organic molecules is just at its beginning. While in Bio-NMR the current objects are the refinement of the method and the determination of dynamics,[628,629] a lot of basic research has to be done to standardize the technique to the structure determination of organic molecules. Beside the development of new media and the optimization of existing ones, the design of suitable pulse sequences for the measurement, the *post*-processing as well as the interpretation of data to gain the molecule's structure are current

issues in this field. However, first great strides have been made, other will hopefully follow.

4 Experimental Procedures

4.1 Materials and Methods

Solvents for synthesis were either obtained 'technical grade' and distilled prior to use or purchased ('absolute' or 'for synthesis') from Fluka (Seelze, Germany), Acros Organics (Geel; Belgium) or Merck (Darmstadt, Germany). NMP (distilled) was a gift from BASF (Ludwigshafen, Germany). Solvents for column chromatography were obtained 'technical grade' and distilled prior to use except hexane, which usually was used undistilled. The HPLC-solvents acetonitrile (solvent B) and TFA were purchased 'gradient grade' from Merck, water (solvent A) was deionized and further purified using a Milli-Q system from Millipore (Molsheim, France).

Fmoc-protected amino acids were purchased from Novabiochem (Darmstadt, Germany), Advanced ChemTech (Louisville, USA) or MultiSynTech (Witten, Germany), Sieber Amide resin was purchased from Novabiochem. Tritylchloride polystyrole resin (TCP resin) was obtained from PepChem (Tübingen, Germany), HATU, TBTU and HOBt from Iris Biotech (Marktredwitz, Germany) and HOAt from GL Biochem (Shanghai, China), TFA from Solvay (Hannover, Germany). Toyopearl AF-Epoxy-650M resin was obtained from Tosoh (Stuttgart, Germany), Fmoc-Glutamol(Ot-Bu) from ChemPep Inc. (Miami, USA) and DOTA-tris (tBu ester) from Macrocyclics (Dallas, TX, USA). All other chemicals were purchased from Aldrich (Deisenhofen, Germany), Merck (Darmstadt, Germany), Lancaster (Mühlheim, Germany), Acros Organics (Geel; Belgium) or Fluka (Seelze, Germany).

Peptide Synthesis was carried out manually using PE-syringes (2 mL, 5 mL or 20 mL) from Becton-Dickinson (Fraga, Spain) or Braun (Melsungen) equipped with

4 Experimental Procedures

PE-frits from Roland Vetter Laborbedarf (Ammerbuch). To ensure optimal mixing conditions, the syringes were rotating at about 30 rpm. Loading of the resin was carried out in glassware equipped with glass frits.

The following protected amino acid building blocks were used for Fmoc-SPPS: Fmoc-Ado, Fmoc-Ala, Fmoc-Aha, Fmoc-Arg(Pbf), Fmoc-Asn(Trt), Fmoc-Asp(*t*-Bu), Fmoc-Bip, Fmoc-Bpa, Fmoc-Bta, Fmoc-Cha, Fmoc-Cys(Trt), Fmoc-Gln(Trt), Fmoc-Glu(*t*-Bu), Fmoc-Gly, Fmoc-His(Trt), Fmoc-Ile, Fmoc-Leu, Fmoc-Lys(Boc), Boc-Lys(Fmoc), Fmoc-[1]Nal, Fmoc-[2]Nal, Fmoc-Phe, Fmoc-(2,4-Cl$_2$-Phe), Fmoc-4-py, Fmoc-Ser(*t*-Bu), Fmoc-Thr(*t*-Bu), Fmoc-Trp(Boc), Fmoc-Tyr(OMe), Fmoc-Tyr(*t*-Bu), Fmoc-Val.

Air or moisture sensitive reactions were carried out in dry glassware and under argon (99.996%) atmosphere. Moisture sensitive and/or absoluted solvents were transferred in syringes under argon.

For HPLC purification, compounds were dissolved in DMSO, acetonitrile or methanol ('gradient grade') and filtered using syringe filters RC 15 or RC 25 (RC-membrane, 0.45 μm) from Sartorius (Göttingen). Purification and analytical purity determination was carried out on RP-HPLC systems from Amersham Pharmacia Bio-tech (analytical: Äkta Basic 10F with pump system P-900, detector UV-900 and Autosampler A-900; preparative: Äkta Basic 100F with pump system P-900, detector UV-900) or Beckman (System Gold with solvent module 125 and detector module 166; pump system 110B, control unit 420 and detector Knauer Uvicord) were used equipped with columns from Omnicrom YMC (analytical: ODS-A C18, 250 mm × 4.6 mm, 5 μm, flow rate: 1 mL/min; semi-preparative: ODS-A C18, 250 mm × 20 mm, 5 μm or 10 μm, flow rate: 8 mL/min; preparative: ODS-A C18, 250 mm × 30 mm, 10 μm, flow rate: 25 mL/min) or Macherey-Nagel (preparative: Nucleosil C18, 250 mm × 40 mm, 7 μm, flow rate: 25 mL/min). Compounds were eluted with linear gradients (30 min) of acetonitrile (solvent B) in water (solvent A) and 0.1 % (v/v) TFA. For analytical purity determination of the compounds after semi-preparative or preparative HPLC purification the peak integrals of the analytical

HPLC chromatogram at the detector wavelength of 220 nm or 254 nm were evaluated.

For **column chromatography** Silica Gel 60 (230-400 mesh ASTM, Korngröße 0.040-0.063 mm) from Merck (Darmstadt) was used in 50-100 fold excess to the raw material, for flash chromatography pressure of 1-1.2 bar was applied.

Thin layer chromatography (TLC) and the determination of the Rf-value was carried out using TLC aluminium sheets covered with Silica Gel 60 F254 from Merck (Darmstadt). For detection, TLC-plates were examined under UV-light (λ = 254 nm). If enhanced visualization was necessary, the plate was treated with aqueous molybdophosphoric acid/cer-(IV)-sulfate solution (6.25 g molybdophosphoric acid hydrate, 2.5 g cer-(IV)-sulfate, 15 mL sulfuric acid and 235 mL water) and heated.

Melting points were determined on a Büchi 510 melting point apparatus and are uncorrected.

Optical rotation was measured on a Perkin-Elmer 241 MC.

All ^{1}H-NMR and ^{13}C-NMR spectra were recorded on Bruker AC-250, AV-360, AV-500 and DMX500 instruments at 300 K and processed running MestRe-C software. Spectra were calibrated to their respective solvent signals (CDCl$_3$: ^{1}H 7.26 ppm, ^{13}C 77.0 ppm; MeOH-d$_4$: ^{1}H 3.31 ppm, ^{13}C 49.05 ppm; DMSO-d$_6$: ^{1}H 2.50 ppm, ^{13}C 39.43 ppm; acetone-d$_6$: ^{1}H 2.05 ppm, ^{13}C 30.83 ppm). Chemical shifts (δ) are reported in parts per million (ppm) and coupling constants (*J* values) are given in Hertz (Hz). The following abbreviations were used to explain the multiplicities: s, singulet; d, doublet; t, triplet; q, quartet; dd, doublet of doublets; dt, doublet of triplets; m, multiplet; br, broad.

Electrospray ionisation (ESI)-mass spectra were recorded on a Finnigan LCQ mass spectrometer in combination with a Hewlett Packard 1100 HPLC-system equipped with a ODS-A C18 (125 mm × 2 mm, 3 μm, flow rate: 0.2 mL/min) column from Omnicrom YMC. Compounds were eluted with linear gradients (15 min) of water (solvent A) and acetonitrile (solvent B) in 0.1% (v/v) formic acid. **High-resolution mass spectra (HRMS-EI)** were recorded on a Finnigan MAT 8200.

Lyophilization was carried out using an Alpha 2-4 lyophilizer from Christ (Osterode).

4.2   General procedures

General procedure I. Attachment of *N*-Fmoc-amino acids to TCP resin

After swelling in dry DCM (10 mL) for 20 min, the TCP resin (theoretical loading 0.96 mmol/g, 1.00 g, 0.96 mmol, 1.0 equiv) was treated with a solution of Fmoc-protected amino acids (1.2 mmol, 1.2 equiv) in dry DCM (8 mL) and DIPEA (490 μL, 2.9 mmol, 3.0 equiv) at room temperature (rt) for 2 h. MeOH (1 mL) and DIPEA (0.2 mL) were added to cap unreacted sites on the resin and the reaction mixture was shaken for 15 min. The resin was washed with NMP (3×10 mL), DCM (5×10 mL) and NMP (3×10 mL) and dried under *vacuo* to give resin bound *N*-Fmoc-amino acids.

General procedure II. Fmoc deprotection

The Fmoc-protected resin was treated with 10 ml of 20% piperidine in NMP (3×10 min) and washed with NMP (5×10 ml).

General procedure III. Coupling with TBTU/HOBt

Fmoc-amino acid (2.0 equiv), TBTU (2.0 equiv), HOBt (2.0 equiv) were dissolved in NMP to achieve a 0.2 mM solution of the single components. Then, DIPEA (5.6 equiv) was added and the solution given to the resin. The reaction mixture was shaken at rt for 60 min and washed with NMP (5×10 mL).

General procedure IV. Coupling with HATU/HOAt

Fmoc-amino acid (2.0 equiv), HATU (2.0 equiv), HOAt (2.0 equiv) were dissolved in NMP to give a 0.2 mM solution of the single components. Then, 2,4,6-collidine (15 equiv) was added and the solution given to the resin. The reaction mixture was shaken at rt for 60 min and washed with NMP (5×10 ml).

General procedure V. Capping

The resin was treated with 10 ml of a solution of acetic anhydride and DIPEA in NMP (7/2/91, v/v/v; 15 min) and washed with NMP (5×10 mL).

General procedure VI. *N*-Terminal dimerization on solid phase

Fmoc-D-glutamic acid (0.17 equiv), HATU (0.33 equiv), HOAt (0.33 equiv) and 2,4,6-collidine (10 equiv) were dissolved in NMP to give a 0.04 mM solution of the amino acid, which was added to the resin. The reaction mixture was shaken at rt for 8 h. The resin was removed by filtration and the procedure repeated three times. Finally, the resin was washed with NMP (5×10 mL).

General procedure VII. Cleavage and deprotection with trifluoroacetic acid

The resin was washed with DCM (3×10 mL) and treated with $TFA/H_2O/triisopropyl$-silane (95:2.5:2.5, v/v/v; 20 mL) for 3×10 min. After removal of the resin by filtration, the filtrates were combined and stirred for another 90 min. The solvent was concentrated under reduced pressure to precipitate the peptide with diethyl ether.

General procedure VIII: Disulfide cyclization of the linear peptide using H_2O_2.

The linear peptide was dissolved in high dilution (c = 1 mM) in water and the pH was adjusted to 7-8 by addition of concentrated aqueous $NaHCO_3$. Then, 30% aqueous H_2O_2 (3 equiv) was added drop wise under vigorous stirring. The reaction was stopped after 30 min and the solvent removed by lyophilization.

General procedure IX: Disulfide cyclization of the linear peptide using DMSO.

The linear peptide was dissolved in high dilution (c = 1 mM) in water and the pH was adjusted to 7-8 by addition of concentrated aqueous $NaHCO_3$. Then, DMSO (2%, v/v) was added under vigorous stirring. After complete conversion (usually 2-4 d; ESI-MS or HPLC control) the reaction was stopped and the solvent removed by lyophilization.

General procedure X: Cleavage of side-chain-protected peptides from TCP-resin.

The resin was swollen in DCM and then treated with a solution of DCM, acetic acid and TFE (6 / 3 / 1, v/v/v). After shaking for 1 h, the procedure was repeated and finally the resin washed once with the cleavage solution. The collected solutions were diluted with toluene and concentrated *in vacuo*. The dilution with toluene and evaporation was repeated twice (no smell of acetic acid). The peptide was obtained as acetate.

General procedure XI: Backbone cyclization of linear peptides.[630]

The linear, side-chain protected peptide was diluted with DMF to 10^{-3} - 10^{-4} M. After addition of DPPA (3 equiv) and $NaHCO_3$ (5 equiv), the mixture was stirred until all starting material was consumed (HPLC / LC-MS monitoring), usually 12 h. The solution was concentrated under reduced pressure and the cyclic peptide precipitated by addition of water. In case of an improper precipitation, water was substituted with brine. The peptide was spun down in a centrifuge, washed twice with water and dried under vacuum.

General procedure XII: Synthesis of *N*-Fmoc-amino aldehydes.

N-Fmoc-amino aldehydes were synthesized from the corresponding *N*-Fmoc-amino alcohols using Dess-Martin periodinane[194,195] as described.[193]

General procedure XIII: Reductive alkylation on solid phase.

The reaction was carried out following a slightly modified procedure of Krchnak *et al.*[177] The resin was washed with trimethyl orthoformate (3×10 mL) and the *N*-Fmoc-amino aldehyde (5.0 equiv) was added as a 0.1 M solution in trimethyl orthoformate. The mixture was shaken for 18 h, after which the solution was ejected and a 0.1M suspension of sodium triacetoxyborohydride (5.0 equiv) in dry DCM was added. The mixture was shaken for 16 h and the resin was washed with NMP (5×10 mL).

174

4.3   Synthesis of peptidic and peptidomimetic FVIII ligands

4.3.1   Solid-phase synthesis of peptidic ligands

The synthesis of the ligands was carried out on TCP-resin[148] following standard Fmoc strategy.[135,150,176] The first amino acid was attached to the TCP resin according to general procedure I. Amino acid couplings were carried out according to general procedures II and III to form amide bonds. Final cleavage from the resin and deprotection was accomplished according to general procedures II and VII.

Sequence	no.	Mass		R_t (min)	HPLC purity (%)
		calcd	obsd [M+H]$^+$		
EYHSWEYC	3	1115.40	1116.6	18.7[b]	100
EYHSWEY(Aha)C	4	1228.49	1229.6	17.5[a]	97
AcEYHSWEYC	5	1157.41	1158.6	20.3[b]	99
AYHSWEYC	6	1057.40	1058.4	15.8[a]	95
EAHSWEYC	7	1023.38	1024.4	16.6[b]	97
EYASWEYC	8	1049.38	1050.4	17.4[a]	95
EYHAWEYC	9	1099.41	1100.3	16.2[a]	97
EYHSAEYC	10	1000.36	1001.3	9.5[a]	95
EYHSWAYC	11	1057.40	1085.5	15.7[a]	95
EYHSWEAC	12	1023.38	1024.4	13.7[a]	95
EYHSWEYA	13	1083.43	1084.4	15.4[a]	99
eYHSWEYC	14	1115.40	1116.3	18.9[b]	97
EyHSWEYC	15	1115.40	1116.4	18.1[b]	98
EYhSWEYC	16	1115.40	1116.4	18.5[b]	98
EYHsWEYC	17	1115.40	1116.4	18.6[b]	98
EYHSwEYC	18	1115.40	1116.5	17.9[b]	98
EYHSWeYC	19	1115.40	1116.4	17.6[b]	96

Sequence	no.	Mass		R_t (min)	HPLC purity (%)
		calcd	obsd [M+H]$^+$		
EYHSWEyC	20	1115.40	1116.4	18.1[b]	98
EYHSWEYc	21	1115.40	1116.4	19.0[b]	97
Scrambled[c]	39	1115.40	1116.6	16.2[a]	99
QYHSWEYC	22	1114.42	1115.6	17.3[a]	100
DYHSWEYC	23	1101.39	1102.6	17.4[a]	100
VYHSWEYC	24	1085.43	1086.6	16.3[a]	98
EY(OMe)HSWEYC	25	1129.42	1130.4	19.7[a]	100
EFHSWEYC	26	1099.41	1100.5	18.9[a]	99
EYKSWEYC	27	1106.44	1107.5	16.0[a]	97
EY4-pySWEYC	28	1126.41	1127.5	16.6[a]	99
EYFSWEYC	29	1125.41	1126.5	21.4[a]	99
EYHTWEYC	30	1129.42	1130.6	18.9[a]	100
EYHVWEYC	31	1127.44	1128.4	19.9[a]	100
EYHSFEYC	32	1076.39	1077.6	18.7[b]	98
EYHS1-NalEYC	33	1126.41	1127.6	20.6[a]	95
EYHSWQYC	34	1114.42	1115.6	18.0[b]	100
EYHSWDYC	35	1101.39	1102.6	18.3[b]	99
EYHSWEY(OMe)C	36	1129.42	1130.4	20.6[a]	99
EYHSWEFC	37	1099.41	1100.4	21.3[b]	100
EYHSWEY	38	1012.39	1241.1	17.6[b]	100
YHSWEYC	40	986,36	987,3	18.6[b]	96
YFSWEYC	41	996,4	997,4	22.3[a]	96
HSWEYC	42	823,30	824,5	17.6[b]	99
YCSWEY	43	849.3	850.3	18.0[a]	100
YCSWDY	44	1099.41	1100.3	16.2[a]	97
YCS[1]NalEY	45	1000.36	1001.3	9.5[a]	95
YCAWEY	46	1057.40	1085.5	15.7[a]	95
YCTWEY	47	1023.38	1024.4	13.7[a]	95
YCVWEY	48	1083.43	1084.4	15.4[a]	99
YCAWDY	49	1115.40	1116.3	18.9[b]	97

Sequence	no.	Mass		R_t (min)	HPLC purity (%)
		calcd	obsd [M+H]$^+$		
YCTWDY	50	1115.40	1116.4	18.1[b]	98
YCVWDY	51	1115.40	1116.4	18.5[b]	98
yewacy	52	1115.40	1116.4	18.6[b]	98
yewvcy	53	1115.40	1116.5	17.9[b]	98
ydwacy	54	1115.40	1116.4	17.6[b]	96
ydwvcy	55	1115.40	1116.4	19.0[b]	97
SWEYC	56	686.24	687.2	18.4[b]	97
WEYC	57	600.3	600.3	15.6[a]	100
WEFC	58	583.2	584.2	21.0[a]	98
WDYC	59	585.2	586.1	17.2[a]	99
AcWDYC	60	627.2	628.2	21.5[a]	99
AcWEYC	61	641.2	642.1	21.9[a]	98
(3-IBA)EYC	62	598.2	599.2	26.2[a]	99
(3-IPA)EYC	63	584.2	585.1	24.1[a]	100
(3-IAA)EYC	64	570.2	571.1	21.9[a]	98
(3-IBA)DYC	65	584.2	585.1	17.0[a]	99
(3-IPA)DYC	66	570.2	571.4	26.3[a]	99
(3-IAA)DYC	67	556.2	557.0	21.5[a]	96

[a] *Gradient 10 → 50%;* [b] *Gradient 5 → 50%;* [c] *Sequence: ECYYEHWS;* [1]*Nal: 1-Naphthyl alanine.*

4.3.2   Solid-phase synthesis of peptidomimetic ligands

Solid-phase synthesis of peptidomimetic ligands was carried out on TCP-resin[148] following standard Fmoc strategy.[135,150,176] The first amino acid was attached to the TCP resin according to general procedure I. Amino acid couplings were carried out according to general procedures II and III to form amide bonds. Reductive alkylation on solid phase was carried out according to general procedures II, IV and V. Final cleavage from the resin and deprotection was accomplished according to general procedures II and VII.

Sequence	no.	Mass		R_t (min)	HPLC purity (%)
		calcd	obsd [M+H]$^+$		
(3-IAA)Ψ[CH$_2$NH]EYC	68	556.2	557.4	19.5[a]	98
(3-IAA)EΨ[CH$_2$NH]YC	69	556.2	557.3	18.8[a]	100
(3-IAA)EYΨ[CH$_2$NH]C	70	556.2	557.3	18.4[a]	98

[a] *Gradient 10 → 50%;* [b] *Gradient 5 → 50%;* [c] *Sequence: ECYYEHWS*

4.3.3 Immobilization of ligands to Toyopearl AF-Epoxy-650M resin.

2.5 mg of the respective peptidic or peptidomimetic ligand were dissolved in 0.25 mL of immobilization buffer (0.2 M sodium bicarbonate, pH 10.3) and 36.0 mg of Toyopearl AF-Epoxy-650M resin (corresponding to 0.125 mL of swollen resin; Tosoh Bioscience, Stuttgart, Germany) were added, followed by incubation of the mixture with gentle rotation for 48 hours. Then, the resin was washed once with immobilization buffer, once with 1 M NaCl and then 3 times with binding buffer (0.01 M HEPES, 0.1 M NaCl, 5 mM CaCl$_2$, 0.01% Tween-80; pH=7.4). The achieved ligand loading was determined by measuring the UV adsorption (280 nm) of the source solution before and after the immobilization. Immobilization data are summarized in the Supplementary Data 4 (page 246).

4.3.4 Solution synthesis of (3-IAA)EΨ[CH$_2$NH]YC (69)

Methyl (1-*tert*-butyloxycarbonyl-indol-3-yl)acetate (72).

A solution of indol-3-yl acetic acid (71) (10.2 g, 58.0 mmol, 1.0 equiv) in dry MeOH (500 mL) was cooled to 0°C and SOCl$_2$ (21.0 mL, 290 mmol, 5.0 equiv) was added slowly. After stirring for 4 h at room temperature, the mixture was concentrated under reduced pressure, the residue taken up in EtOAc (500 mL) and washed with saturated aqueous NH$_4$Cl (300 mL), saturated aqueous NaHCO$_3$
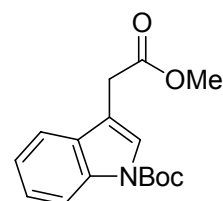
(300 mL) and brine (150 mL). After drying over MgSO$_4$, the mixture was concentrated to dryness to give the pure methyl ester as brown oil (10.8 g, 98%). Spectroscopic data (see below) agree with the literature.[631]

The methyl ester (10.6 g, 56.0 mmol, 1.0 equiv) was dissolved in acetonitrile (45 mL) and di-*tert*-butyl dicarbonate (37.4 g, 171 mmol, 3.0 equiv) and DMAP (1.34 g, 11.0 mmol, 0.2 equiv) were added.[186] The mixture was stirred for 2 h after which the solvent was removed under reduced pressure. The residue was dissolved in EtOAc (500 mL) and subsequently washed with saturated aqueous NH$_4$Cl (300 mL), saturated aqueous NaHCO$_3$ (300 mL) and brine (150 mL). After drying over MgSO$_4$, the solvent was removed in *vacuo* and the crude product purified by flash chromatography on silica gel (EtOAc/hexane; gradient 1:10 → 1:2) to obtain 72 (14.0 g, 86 %; 2 steps) as a colorless solid. Spectroscopic data agree with the literature.[632]

Methyl (indol-3-yl)acetate

R_f = 0.3 (EtOAc/hexane 1:2)

^{1}H NMR (360 MHz, CDCl$_3$): δ = 8.17 (s, 1H, H$_{arom}$), 7.65 (d, J = 7.7 Hz, 1H, NH), 7.29 (d, J = 7.8 Hz, 1H, H$_{arom}$), 7.26-7.14 (m, 2H, H$_{arom}$), 7.02 (s, 1H, H$_{arom}$), 3.82 (s, 2H, CH$_2$), 3.74 (s, 3H, CH$_3$).

^{13}C NMR (91 MHz, CDCl$_3$): δ = 172.7, 136.0, 127.1, 123.2, 122.0, 119.5, 118.6, 111.2, 108.0, 51.9, 31.0.

HRMS (EI) calcd for C$_{11}$H$_{11}$NO$_2$ 189.07898; found 189.07883.

Methyl (1-*tert*-butyloxycarbonyl-indol-3-yl)acetate (72).

RP-HPLC (10 → 100%) R_t = 27.4; 96% purity.
R_f = 0.5 (EtOAc/hexane 1:2)
mp 53°C

^{1}H NMR (500 MHz, CDCl$_3$): δ = 8.15 (d, J = 6.4 Hz, 1H, H$_{arom}$), 7.57 (s, 1H, H$_{arom}$), 7.52 (m, J = 7.8 Hz, 1H, H$_{arom}$), 7.32 (dd, J = 7.6, 7.6 Hz, 1H, H$_{arom}$), 7.24 (dd, J = 7.5, 7.5 Hz, 1H, H$_{arom}$), 3.71 (s, 2H, CH$_2$), 3.71 (s, 3H, CH$_3$), 1.66 (s, 9H, C(CH$_3$)$_3$).

^{13}C NMR (91 MHz, CDCl$_3$): δ = 171.5, 149.6, 135.5, 130.1, 124.6, 124.5, 122.7, 119.0, 115.3, 113.1, 83.6, 52.1, 30.9, 28.2.

HRMS (EI) calcd for C$_{16}$H$_{19}$NO$_4$ 289.13141; found 289.13145.

(1-***tert*-Butyloxycarbonyl-indol-3-yl)acetic acid (73).**

A solution of lithium hydroxide (LiOH*H$_2$O, 6.00 g, 143 mmol, 3 equiv) in H$_2$O (250 mL) was added to a solution of 72 (13.8 g, 47.7 mmol, 1.0 equiv) in THF (350 mL) and MeOH (150 mL). After stirring for 18 h, the mixture was concentrated in *vacuo* and a 10% aqueous solution of citric acid (300 mL) was added. The aqueous layer was extracted with EtOAc (3×200 mL) and the combined organic layers were washed with water (200 mL) and brine (200 mL) and dried over MgSO$_4$. The solvent was removed under reduced pressure and the residue purified by flash chromatography on silica gel (EtOAc/hexane gradient 1:10 → 1:1, 1% AcOH) to yield 73 (10.9 g, 83%) as a colorless solid. Spectroscopic data agree with literature.[633]
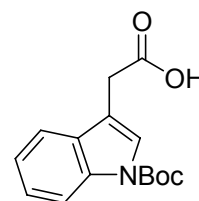
RP-HPLC (10 → 90%) R_t = 24.5; 98% purity.
R_f = 0.6 (MeOH/CHCl$_3$ 1:9, 1% AcOH)
mp 117-120°C

^{1}H NMR (500 MHz, CDCl$_3$): δ = 8.15 (s, 1H, H$_{arom}$), 7.59 (s, 1H, H$_{arom}$), 7.53 (dd, J = 7.8, 0.6 Hz, 1H, H$_{arom}$), 7.34 (dd, J = 8.2, 7.3 Hz, 1H, H$_{arom}$), 7.30-7.23 (m, 2H, H$_{arom}$), 3.76 (s, 2H, CH$_2$), 1.67 (s, 9H, C(CH$_3$)$_3$).

^{13}C NMR (125 MHz, CDCl$_3$): δ = 176.2, 149.5, 129.8, 124.8, 124.6, 122.6, 118.9, 115.3, 112.3, 83.7, 30.6, 28.1.

HRMS (EI) calcd for C$_{15}$H$_{17}$NO$_4$ 275.11576; found 275.11531.

(*S*)-*tert*-Butyl 4-(2-(1-*tert*-butyloxycarbonyl-indol-3-yl)-5-hydroxypentanoate (76).

Fmoc-Glutamol(O*t*-Bu) (74) (1.83 g, 4.45 mmol) was dissolved in piperidine/DMF (20/80, v/v; 100 mL) and after stirring for 1 h the mixture was evaporated to dryness. The resulting crude amine 75 was taken up in DMF (250 mL) and 73 (1.23 g, 4.45 mmol, 1.0 equiv), HOBt (681 mg, 4.45 mmol, 1.0 equiv) and TBTU (1.43 g, 4.45 mmol, 1.0 equiv) were added. Then, the mixture was cooled to 0°C and DIPEA (2.25 mL, 13.2 mmol, 3.0 equiv) was added. After stirring for 18 h at room temperature, the solvent was removed in *vacuo* and the residue taken up in EtOAc (300 mL). The mixture was washed with saturated aqueous NH_4Cl (2×150 mL), saturated aqueous $NaHCO_3$ (2×150 mL) and brine (150 mL). After drying over Na_2SO_4, the solvent was removed under reduced pressure and the crude product purified by flash chromatography on silica gel (MeOH/CHCl$_3$; gradient 1:50 → 1:20) to obtain 76 (1.88 g, 95%) as a hygroscopic colorless oil.
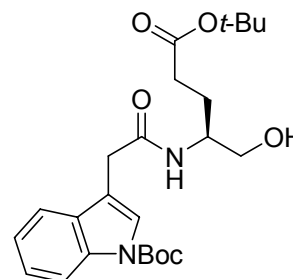
RP-HPLC (30 → 100%) R_t = 20.3; 96% purity.
R_f = 0.1 (MeOH/CHCl$_3$ 1:30), R_f = 0.3 (EtOAc/hexane 2:1)
$[\alpha]_D^{23}$ -13.2 (c 7.0, MeOH)

^{1}H NMR (500 MHz, CDCl$_3$): δ = 8.14 (s, 1H, H$_{arom}$), 7.55 (s, 1H, H$_{arom}$), 7.49 (d, J = 7.8 Hz, 1H, H$_{arom}$), 7.32 (dd, J = 7.3, 7.3 Hz, 1H, H$_{arom}$), 7.23 (dd, J = 7.5, 7.5 Hz, 1H, H$_{arom}$), 6.36 (d, J = 8.1 Hz, 1H, NH), 5.38 (s, 1H, br, OH), 3.96-3.87 (m, 1H, NHC$\underline{H}$), 3.67 (s, 2H, ArC$\underline{H}_2$CO), 3.56 (dd, J = 11.5, 3.7 Hz, 1H, CHC$\underline{H}$HOH), 3.49 (dd, J = 11.4, 5.0 Hz, 1H, CHCH$\underline{H}$OH), 2.19 (t, J = 6.9, 2H, CHCH$_2$C$\underline{H}_2$CO), 1.75 (dt, J = 14.0, 7.3 Hz, 1H, CHC$\underline{H}$HCH$_2$CO), 1.66 (s, 9H, C(CH$_3$)$_3$), 1.65-1.59 (m, 1H, CHCH$\underline{H}$CH$_2$CO), 1.40 (s, 9H, C(CH$_3$)$_3$).

^{13}C NMR (63 MHz, CDCl$_3$): δ = 173.1, 170.9, 149.4, 135.5, 129.7, 124.8, 122.8, 118.8, 115.3, 113.6, 83.8, 80.8, 64.5, 51.6, 33.3, 31.7, 28.1, 27.9, 25.4.

HRMS (EI) calcd for $C_{24}H_{34}N_2O_6$ 446.24169; found 446.24164.

(*S*)-*tert*-Butyl 4-(2-(1-*tert*-butyloxycarbonyl-indol-3-yl)acetylamino)-4-formyl-butanoate (77).

To a solution of **76** (1.2 g, 2.68 mmol, 1.0 equiv) in dry DCM (30 mL) was added Dess-Martin periodinane (3.41 g, 8.04 mmol, 3.0 equiv) in three portions over 1.5 h. The mixture was allowed to stir for another 1 h after which the suspension was diluted with DCM (30 mL) and subsequently washed with a mixture of 10% aqueous $Na_2S_2O_3$ and saturated aqueous $NaHCO_3$ (1:1, v/v; 2×30 mL), water (30 mL) and brine (30 mL). Drying over Na_2SO_4 and evaporation gave the crude aldehyde **77** (1.18 g) as a pale yellow solid which was directly used without further purification.
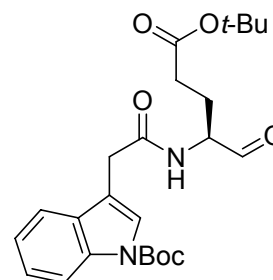
R_f = 0.2 (MeOH/CHCl$_3$ 1:30), R_f = 0.5 (EtOAc/hexane 2:1)

^{1}H NMR (360 MHz, CDCl$_3$): δ = 9.44 (s, 1H, CHO), 8.11 (d, *J* = 7.9 Hz, 1H, H$_{arom}$), 7.55 (s, 1H, H$_{arom}$), 7.48 (d, *J* = 7.7 Hz, 1H, H$_{arom}$), 7.30 (dd, *J* = 7.9, 7.9, 1H, H$_{arom}$), 7.24-7.17 (m, 1H, H$_{arom}$), 6.49 (d, *J* = 6.8 Hz, 1H, NH), 4.42 (m, 1H, NHC<u>H</u>), 3.67 (s, 2H, ArC<u>H</u>$_2$CO), 2.24-2.04 (m, 3H, CHC<u>H</u>$_2$C<u>H</u>HCO), 1.76 (m, 1H, CHCH$_2$CH<u>H</u>CO), 1.63 (s, 9H, C(CH$_3$)$_3$), 1.34 (s, 9H, C(CH$_3$)$_3$).

^{13}C NMR (91 MHz, CDCl$_3$): δ = 198.5, 172.1, 170.6, 149.4, 135.5, 129.6, 124.8, 122.8, 118.8, 115.3, 113.3, 83.8, 80.9, 58.2, 33.0, 30.8, 28.1, 27.9, 23.6.

HRMS (EI) calcd for C$_{24}$H$_{32}$N$_2$O$_6$ 444.22604; found 444.22634.

(*S*)-*tert*-Butyl 5-[(*S*)-1-methoxycarbonyl-2-(4-*tert*-butoxyphenyl)ethylamino]-4-(2-(1-*tert*-butyloxycarbonyl-indol-3-yl)acetylamino)-pentanoate (78).

The crude aldehyde **77** (1.18 g) was dissolved in dry DCM (60 mL) and Tyr(OtBu)OMe * HCl (925 mg, 3.21 mmol, 1.2 equiv) and MgSO$_4$ (1.61 g, 13.4 mmol, 5.0 equiv) were added. After reacting for 30 min, NaB(OAc)$_3$H (3.18 g, 15.0 mmol, 5.6 equiv) was added and stirring continued for additional 18 h. Then, the mixture was diluted
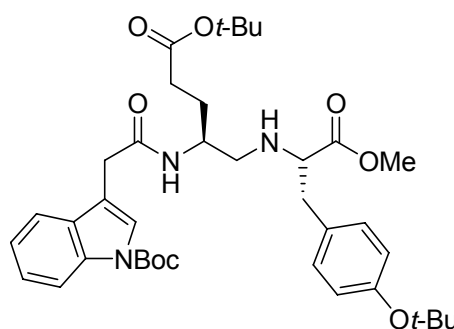
with saturated aqueous NaHCO$_3$ (50 mL) and after 30 min extracted with DCM (2×60 mL). The combined organic layers were dried over Na$_2$SO$_4$, the solvent was removed under reduced pressure and the crude product purified by flash chromatography on silica gel (EtOAc/hexane gradient 1:2 → 2:1) to give 78 (1.37 g, 75% based on 76) as a pale yellow oil.

RP-HPLC (30 → 100%) R_t = 22.5; 95% purity.

R_f = 0.5 (MeOH/CHCl$_3$ 1:30), R_f = 0.6 (EtOAc/hexane 2:1)

$[\alpha]_D^{23}$ +4.2 (c 0.3, MeOH)

^{1}H NMR (500 MHz, MeOH-d$_4$): δ = 8.12 (d, J = 8.1 Hz, 1H, H$_{arom}$(indolyl)), 7.65-7.58 (m, 2H, H$_{arom}$(indolyl)), 7.32 (dd, J = 8.2, 8.2 Hz, 1H, H$_{arom}$(indolyl)), 7.25 (dd, J = 7.5, 7.5 Hz, 1H, H$_{arom}$(indolyl)), 7.11-7.06 (m, 2H, H$_{arom}$(phenyl)), 6.95-6.90 (m, 2H, H$_{arom}$(phenyl)), 4.15-4.00 (m, 2H, NHC$\underline{H}$, H$_\alpha$(Tyr)), 3.71-3.62 (m, 5H, OCH$_3$, ArC$\underline{H}_2$CO), 3.16-2.86 (m, 4H, CHC$\underline{H}_2$NH, H$_\beta$(Tyr)), 2.23-2.16 (m, 2H, CHC$\underline{H}_2$CHHCO), 1.86-1.76 (m, 1H, CHCH$_2$C$\underline{H}$HCO), 1.67 (s, 9H, C(CH$_3$)$_3$), 1.64-1.58 (m, 1H, CHCH$_2$CH$\underline{H}$CO), 1.39 (s, 9H, C(CH$_3$)$_3$), 1.31 (s, 9H, C(CH$_3$)$_3$).

^{13}C NMR (91 MHz, CDCl$_3$): δ = 174.5, 172.5, 169.9, 153.9, 149.3, 135.4, 131.9, 129.7, 129.4, 129.3, 124.7, 124.6, 124.0, 123.9, 123.8, 122.6, 118.9, 115.2, 113.8, 83.6, 80.1, 78.0, 63.1, 51.4, 50.5, 49.0, 38.7, 33.3, 31.8, 28.6, 28.0, 27.9, 27.2.

HRMS (EI) calcd for C$_{38}$H$_{53}$N$_3$O$_8$ 679.38324; found 679.38327.

(S)-*tert*-Butyl 5-[(S)-1-((S)-1-butoxycarbonyl-2-tritylsulfanyl-ethylcarbamoyl)-2-(4-butoxyphenyl)ethylamino]-4-(2-(1-*tert*-butyloxycarbonyl-indol-3-yl)acetylamino)-pentanoate (79).

A solution of LiOH*H$_2$O (196 mg, 4.68 µmol, 3.5 equiv) in H$_2$O (5.3 mL) was added to a solution of 78 (1.06 g, 1.56 mmol, 1.0 equiv) in THF (5.3 mL) and dioxane (15.9 mL). After stirring for 1.5 h, the mixture was acidified by addition of a 10% aqueous solution of citric acid (100 mL)
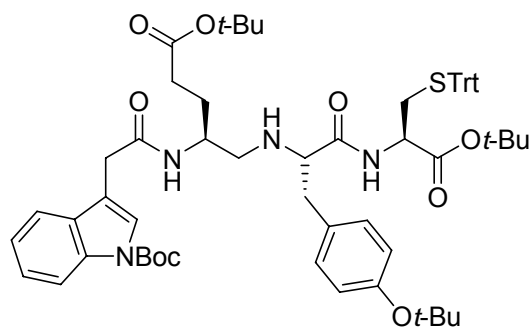
and the aqueous layer was extracted with EtOAc (3×100 mL). The combined organic layers were washed with water (100 mL) and brine (50 mL), dried (Na$_2$SO$_4$) and evaporated to give the crude acid (986 mg; 93% purity; RP-HPLC (20 → 100%) R_t = 23.0) as a pale yellow solid which was redissolved in DMF (55 mL). Then, Cys(Trt)OtBu*HCl[196] (1.06 g, 2.34 mmol, 1.5 equiv), HOBt (232 mg, 1.72 mmol, 1.1 equiv) and TBTU (552 mg, 1.72 mmol, 1.1 equiv) were added and the mixture was cooled to 10°C. 2,4,6-Collidine (1.03 mL, 7.80 mmol, 5.0 equiv) was added and the solution was stirred for 18 h at room temperature. After the solvent was evaporated, the residue was taken up in EtOAc (200 mL) and subsequently washed with saturated aqueous NH$_4$Cl (2×150 mL), saturated aqueous NaHCO$_3$ (2×150 mL) and brine (150 mL). After drying over Na$_2$SO$_4$, the solvent was removed under reduced pressure and the crude product purified by flash chromatography on silica gel (EtOAc/hexane; gradient 1:4 → 2:1) to give 79 (1.38 g, 83%) as a hygroscopic, pale yellow oil.

RP-HPLC (20 → 100%) R_t = 31.2; 97% purity.

R_f = 0.6 (EtOAc/hexane 2:1)

$[\alpha]_D^{23}$ +3.6 (c 0.6, ACN)

^{1}H NMR (500 MHz, MeOH-d$_4$): δ = 8.12 (d, J = 8.1 Hz, 1H, H$_{arom}$(indolyl)), 7.65-7.58 (m, 2H, H$_{arom}$(indolyl)), 7.32 (dd, J = 8.2, 8.2 Hz, 1H, H$_{arom}$(indolyl)), 7.25 (dd, J = 7.5, 7.5 Hz, 1H, H$_{arom}$(indolyl)), 7.11-7.06 (m, 2H, H$_{arom}$(phenyl)), 6.95-6.90 (m, 2H, H$_{arom}$(phenyl)), 4.15-4.00 (m, 2H, NHC$\underline{H}$, H$_\alpha$(Tyr)), 3.71-3.62 (m, 5H, OCH$_3$, ArC$\underline{H}_2$CO), 3.16-2.86 (m, 4H, CHC$\underline{H}_2$NH, H$_\beta$(Tyr)), 2.23-2.16 (m, 2H, CHC$\underline{H}_2$CHHCO), 1.86-1.76 (m, 1H, CHCH$_2$C$\underline{H}$HCO), 1.67 (s, 9H, C(CH$_3$)$_3$), 1.64-1.58 (m, 1H, CHCH$_2$CH$\underline{H}$CO), 1.39 (s, 9H, C(CH$_3$)$_3$), 1.31 (s, 9H, C(CH$_3$)$_3$)

^{1}H NMR (500 MHz, DMSO-d$_6$): δ = 8.95 (d, J = 7.7 Hz, 1H, NH), 8.09 (d, J = 8.0 Hz, 1H, NH), 8.05 (d, J = 8.2 Hz, 1H, NH), 7.60 (d, J = 7.8 Hz, 1H, H$_{arom}$(indolyl)), 7.57 (s, 1H, H$_{arom}$(indolyl)), 7.38-7.27 (m, 14H, H$_{arom}$(Trt) , H$_{arom}$(indolyl)), 7.27-7.20 (m, 4H, H$_{arom}$(Trt), H$_{arom}$(indolyl)), 7.10 (d, J = 8.3 Hz, 2H, H$_{arom}$(Tyr$_{phenyl}$)), 6.83 (d, J = 8.3 Hz, 2H, H$_{arom}$(Tyr)), 4.08-4.02 (m, 1H, NHC$\underline{H}$), 4.00-3.92 (m, 1H, NHC$\underline{H}$), 3.91-3.85 (m, 1H, NHC$\underline{H}$), 3.59 (d, J = 15.5 Hz, 1H, ArC$\underline{H}$HCO), 3.49 (d, J = 15.4 Hz, 21H, ArCH$\underline{H}$CO), 3.09-3.01 (m, 2H, CHC$\underline{H}_2$NH), 2.93-2.86 (m, 1H, H$_\beta$(Tyr)), 2.84-2.80

(m, 1H, H$_\beta$(Tyr)), 2.57-2.52 (m, 1H, H$_\beta$(Cys)), 2.39 (dd, J = 12.6, 5.2 Hz, 1H, H$_\beta$(Cys)), 2.14-1.98 (m, 2H, CHC$\underline{H}_2$CHHCO), 1.62 (s, 10H, C(CH$_3$)$_3$, CHCH$_2$C$\underline{H}$HCO), 1.50-1.44 (m, 1H, CHCH$_2$CH$\underline{H}$CO), 1.32 (s, 9H, C(CH$_3$)$_3$), 1.29 (s, 9H, C(CH$_3$)$_3$), 1.25 (s, 9H, C(CH$_3$)$_3$).

^{13}C NMR (125 MHz, DMSO-d$_6$): δ = 171.3, 170.4, 168.1, 166.7, 154.1, 148.9, 143.8, 134.5, 130.0, 129.8, 128.9, 128.6, 128.0, 126.7, 124.3, 124.0, 123.4, 122.3, 119.4, 114.8, 114.5, 83.4, 81.5, 79.5, 77.6, 66.4, 60.8, 52.5, 49.7, 45.7, 34.9, 32.7, 31.9, 30.6, 28.4, 27.6, 27.5, 27.3.

MS (ESI) calcd for C$_{63}$H$_{78}$N$_4$O$_9$S 1066.55; found 1067.6 [M+H]$^+$, 1089.3 [M+Na]$^+$.

5-[1-(1-Carboxy-2-mercapto-ethylcarbamoyl)-2-(4-hydroxy-phenyl)-ethylamino]-4-(2-1H-indol-3-yl-acetylamino)-pentanoic acid (69).

To a vigorously stirred mixture of 79 (500 mg, 0.47 mmol) in triisopropylethylsilane (250 µL; 2.5%) and water (250 µL; 2.5%) was added trifluoroacetic acid (9.50 mL; 95%) slowly over 8h. The mixture was stirred for additional 30 min, after which the solvent was removed in *vacuo*. The residue was dissolved in a minimum volume of acetic acid and precipitated in ice cold ether/pentane (2×20 mL) to give pure 69 (242 mg, 93%).
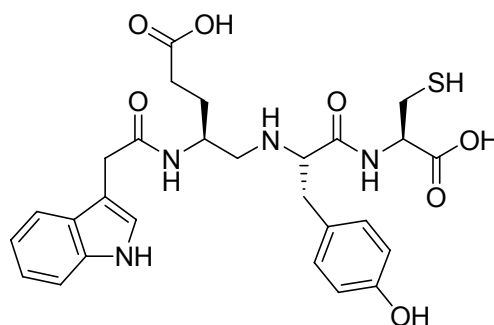
96% purity; RP-HPLC (10 → 50%) R_t = 14.4

[α]$_D^{23}$ –0.4 (c 0.2, MeOH/H$_2$O 2:1)

mp 135°C

Two conformers (ca. 4:1 ratio)

^{1}H NMR (500 MHz, MeOH-d$_4$): δ = 7.58 (d, J = 7.9 Hz, 1H, 20%, H$_{indolyl}$), 7.56 (d, J = 8.0 Hz, 1H, 80%, H$_{indolyl}$), 7.38-7.35 (m, 1H, H$_{indolyl}$), 7.22 (s, 1H, 20%, H$_{indolyl}$), 7.20 (s, 1H, 80%, H$_{indolyl}$), 7.15-7.09 (m, 1H, H$_{indolyl}$), 7.07 (d, J = 8.5 Hz, 2H,H$_{phenyl}$),

7.05-7.02 (m, 1H, H$_{indolyl}$), 6.75 (d, J = 8.46 Hz, 2H, H$_{phenyl}$), 4.54-4.46 (m, 1H, H$_\alpha$(Cys)), 4.20-4.14 (m, 1H, 20%, H$_\alpha$(Tyr)), 4.12 (t, J = 7.0, 1H, 20%, CH(CH$_2$)$_2$), 4.05 (m, 1H, 80%, H$_\alpha$(Tyr)), 3.98 (t, J = 6.9, 1H, 80%, CH(CH$_2$)$_2$), 3.77-3.63 (m, 2H, CH$_2$Ar), 3.11-3.03 (m, 2H, H$_\beta$(Cys)), 3.03-2.96 (m, 2H, H$_\beta$(Tyr)), 2.94-2.81 (m, 2H, CH$_2$NH), 2.33-2.20 (m, 2H, CHCH$_2$CH$_2$), 1.87-1.76 (m, 1H, CHCHHCH$_2$), 1.72-1.60 (m, 1H, CHCHHCH$_2$).

^{13}C NMR (125 MHz, MeOH-d$_4$): δ = 176.4, 176.3, 172.5, 170.4, 158.1, 138.2, 131.5, 131.5, 125.2, 125.1, 122.6, 120.0, 119.2, 116.8, 112.4, 109.0, 64.1 (80%), 63.2 (20%), 56.5 (20%), 56.3 (80%), 52.9 (80%), 52.5 (20%), 48.1, 37.5, 34.0 (20%), 33.9 (80%), 31.0 (80%), 30.9 (20%), 28.3 (20%), 28.0 (80%), 26.8.

HRMS (ESI) calcd for C$_{27}$H$_{33}$N$_4$O$_7$S 557.20700 [M+H]$^+$; found 557.20590 [M+H]$^+$, 1089.3 [M+Na]$^+$.

4.4 Synthesis of condensed and aromatic ring-substituted tyrosine derivatives

4.4.1 Synthesis of aromatic ring-substituted tyrosine derivatives

(S)-N^α-*tert*-Butyloxycarbonyl-*m*-iodotyrosine (109).

To a solution of *m*-iodo-L-tyrosine (108) (2.16 g, 7.02 mmol, 1.0 equiv) and NEt$_3$ (1.46 mL, 10.5 mmol, 1.5 equiv) in 100 mL of dioxan/H$_2$O (1:1) at 0°C was added di-*tert*-butyldicarbonate (1.69 g, 7.73 mmol, 1.1 equiv) in small portions and the mixture was stirred for 45 min at 0°C and additional 18 h at room temperature. After the dioxane was removed on a Rotary Evaporator, the solution was acidified by addition of a 10% aqueous solution of citric acid (200 mL) and the aqueous layer was extracted with EtOAc (3×100 mL). The combined organic layers were dried over Na$_2$SO$_4$ and the solvent removed under reduced pressure to yield 109 (2.74 g, 96%) as a colorless oil which was used without further purification. A small sample was purified by flash chromatography for characterization yielding a colorless solid.
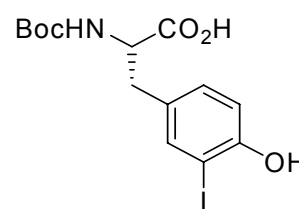
R_f = 0.15 (EtOAc/hexane 1:4, 1% AcOH)

$[\alpha]_D^{23}$ +2.4 (c 0.1, CHCl$_3$)

mp 83-85°C (lit.[634] mp 84-85°C)

^{1}H NMR (360 MHz, MeOH-d$_4$): δ = 7.53 (d, J = 1.3 Hz, 1H, H$_{arom}$), 7.03 (dd, J = 8.2, 2.1 Hz, 1H, H$_{arom}$), 6.73 (d, J = 8.2 Hz, 1H, H$_{arom}$), 4.25 (dd, J = 8.6, 5.0 Hz, 1H, H$_\alpha$), 3.02 (dd, J = 13.9, 4.9 Hz, 1H, H$_\beta$), 2.76 (dd, J = 13.8, 8.9 Hz, 1H, H$_\beta$), 1.38 (s, 9H, C(CH$_3$)$_3$).

^{13}C-NMR (90 MHz, MeOH-d$_4$): δ = 175.2, 157.7, 156.8, 141.0, 140.9, 131.4131.4, 115.6, 84.4, 80.6, 56.3, 37.3, 28.7.

MS (ESI) calcd for $C_{14}H_{18}INO_5$ 407.02; m/z 408.1 [M+H-Boc]$^+$, 852.9 [2M+K]$^+$, 1243.8 [3M+Na]$^+$, 1259.7 [3M+K]$^+$.

(S)-N^α-*tert*-Butyloxycarbonyl-*O*-benzyl-*m*-iodotyrosine benzyl ester (110).

To a solution of **109** (2.74 g, 6.73 mmol, 1.0 equiv) in acetone (20 mL), K_2CO_3 (2.90 g, 21.0 mmol, 3.0 equiv) and benzyl bromide (1.38 mL, 14.4 mmol, 2.2 equiv) were added and the mixture heated under reflux for 5 h. After the solvent was evaporated, the residue was taken up in $CHCl_3$ (240 mL), washed with saturated aqueous $NaHCO_3$ (3×80 mL) and dried over Na_2SO_4 and evaporated. Flash chromatography on silica gel (EtOAc/hexane 1:4) yielded **110** (3.30 g, 83%) as a colorless solid.
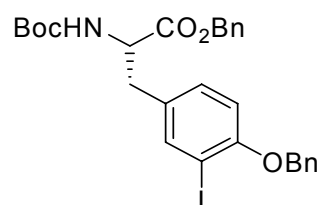
R_f = 0.20 (EtOAc/hexane, 1:4)

$[\alpha]_D^{23}$ +2.4 (c 6.1, $CHCl_3$)

mp 68-70°C

^{1}H NMR (360 MHz, $CDCl_3$): δ = 7.55 (d, J = 1.1 Hz, 1H, H_{arom}), 7.51 (m, 2H, H_{arom}), 7.36 (m, 8H, H_{arom}), 6.94 (d, J = 7.9 Hz, 1H, H_{arom}), 6.69 (d, J = 8.4 Hz, 1H, H_{arom}), 5.17 (d, J = 12.2 Hz, 1H, C$\underline{H}_2$Ph), 5.11 (d, J = 12.2 Hz, 1H, C$\underline{H}_2$Ph), 5.10 (s, 2H, C$\underline{H}_2$Ph), 5.02 (d, J = 7.6 Hz, 1H, NH), 4.57 (m, 1H, H_α), 3.08-2.88 (m, 2H, H_β), 1.44 (s, 9H, C(CH$_3$)$_3$).

^{13}C NMR (90 MHz, $CDCl_3$): δ = 171.4, 156.3, 154.9, 140.2, 136.5, 135.1, 130.5, 130.2, 128.6, 128.52, 128.49, 128.47, 127.9, 126.9, 112.5, 86.8, 80.0, 70.9, 67.2, 54.5, 36.9, 28.3.

HRMS (EI) calcd for $C_{28}H_{30}INO_5$ 587.11687; found 587.11707.

(*S*)-*N*$^\alpha$-*tert*-Butyloxycarbonyl-*O*-benzyl-*m*-phenyltyrosine benzyl ester (111).

To a solution of **110** (3.30 g, 5.62 mmol, 1.0 equiv) in degassed DME/H$_2$O (6:1; 40 mL) was added the appropriate phenyl boronic acid (1.03 g, 8.43 mmol, 1.5 equiv) and Na$_2$CO$_3$ (1.20 g, 11.2 mmol, 2.0 equiv). After five vacuum/argon cycles Pd(OAc)$_2$ (63 mg, 281 µmol, 5 mol%) and P(*o*-tolyl)$_3$ (171 mg, 562 µmol, 10 mol%) were added and the mixture heated to 80°C until completed conversion (3-8 h). After the reaction mixture was cooled to room temperature, it was passed through a short column with a bottom layer of silica gel (40-63 µm) and a top layer of NaHCO$_3$ using EtOAc as eluent. The solvent was re moved under reduce pressure and the crude product purified by flash chromatography (EtOAc/hexane 1:4) to achieve **111** (2.75 g, 91%) as a pale yellow solid.
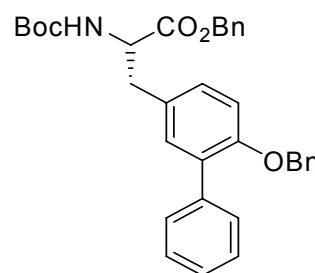
R_f = 0.25 (EtOAc/hexane, 1:4)

$[\alpha]_D^{23}$ +2.6 (c 0.6, CHCl$_3$)

mp 111-113°C

^{1}H NMR (360 MHz, CDCl$_3$): δ = 7.54 (d, *J* = 7.5 Hz, 2H, H$_{arom}$), 7.40 (dd, *J* = 7.4, 7.4 Hz, 2H, H$_{arom}$), 7.38-7.26 (m, 11H, H$_{arom}$), 7.09 (s, 1H, H$_{arom}$), 6.94 (d, *J* = 7.4 Hz, 1H, H$_{arom}$), 6.87 (d, *J* = 8.1 Hz, 1H, H$_{arom}$), 5.15 (d, *J* = 12.3, 1H, C$\underline{H}_2$Ph), 5.10 (d, *J* = 12.3, 1H, C$\underline{H}_2$Ph), 5.06-5.00 (m, 3H, C$\underline{H}_2$Ph, NH), 4.67-4.61 (m, 1H, H$_\alpha$), 3.13-3.02 (m, 2H, H$_\beta$), 1.41 (s, 9H, C(CH$_3$)$_3$).

^{13}C NMR (63 MHz, CDCl$_3$): δ = 171.7, 155.1, 154.6, 138.1, 137.1, 135.0, 132.0, 131.2, 130.3, 129.5, 129.2, 128.5, 128.43, 128.40, 128.37, 127.8, 127.5, 126.9, 126.7, 113.4, 80.0, 70.4, 67.1, 54.5, 37.3, 28.2.

HRMS (EI) calcd for C$_{34}$H$_{35}$NO$_5$ 537.25153; found 537.25207.

General procedure for synthesis of 3-aryl-substituted tyrosine analogues 112-120.

To a solution of 110 (1.0 equiv) in degassed DME/H_2O (6:1; 7 mL/mmol) was added the appropriate aryl boronic acid (1.5 equiv) and Na_2CO_3 (2.0 equiv). After five vacuum/argon cycles Pd(OAc)$_2$ (5 mol%) and P(o-tolyl)$_3$ (10 mol%) were added and the mixture heated to 80°C until completed conversion (3-8 h). After the reaction mixture was cooled to room temperature, it was passed through a short column with a bottom layer of silica gel (40-63 µm) and a top layer of NaHCO$_3$ using EtOAc as eluent. The solvent was removed under reduced pressure and the crude product purified by flash chromatography using an appropriate mixture of EtOAc and hexane as eluent.

(*S*)-*N*$^\alpha$-tert-Butyloxycarbonyl-*O*-benzyl-*m*-(*p*-tolyl)tyrosine benzyl ester (112).

Pale yellow solid; Yield 93%.

R_f = 0.25 (EtOAc/hexane, 1:4)

$[\alpha]_D^{23}$ +3.0 (c 1.3, CHCl$_3$)

mp 97-101°C

^{1}H-NMR (250 MHz, CDCl$_3$): δ = 7.45-7.38 (m, 2H, H$_{arom}$), 7.34-7.16 (m, 12H, H$_{arom}$), 7.06 (d, *J* = 1.3 Hz, 1H, H$_{arom}$), 6.89 (d, *J* = 8.5 Hz, 1H, H$_{arom}$), 6.82 (d, *J* = 8.4 Hz, 1H, H$_{arom}$), 5.12 (d, *J* = 12.3 Hz, 1H, C$\underline{H}_2$Ph), 5.06 (d, *J* = 12.4 Hz, 1H, C$\underline{H}_2$Ph), 5.05-4.95 (m, 3H, C$\underline{H}_2$Ph, NH), 4.60 (m, 1H, H$_\alpha$), 3.13-2.90 (m, 2H, H$_\beta$), 2.36 (s, 3H, CH$_3$), 1.39 (s, 9H, C(CH$_3$)$_3$).

^{13}C NMR (63 MHz, CDCl$_3$): δ = 171.8, 155.0, 154.7, 137.2, 136.6, 135.2, 135.1, 131.9, 131.1, 129.4, 128.9, 128.6, 128.5, 128.42, 128.37, 127.5, 126.8, 113.4, 79.9, 70.4, 67.1, 54.51, 37.4, 28.3, 21.2.

HRMS (EI) calcd for C$_{35}$H$_{37}$NO$_5$ 551.26715; found 551.26702.
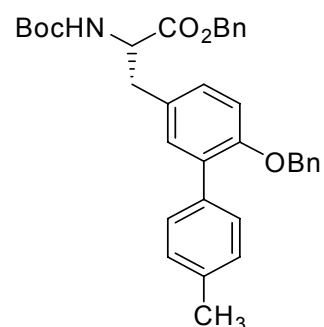
(*S*)-*N*^α-tert-Butyloxycarbonyl-*O*-benzyl-*m*-(*m*-tolyl)tyrosine benzyl ester (113).

Pale yellow solid; Yield 79%.

R_f = 0.25 (EtOAc/hexane, 1:4)

$[\alpha]_D^{23}$ +2.9 (c 2.8, CHCl$_3$)

mp 78-82°C

^{1}H-NMR (250 MHz, CDCl$_3$): δ = 7.36-7.21 (m, 13H, H$_{arom}$), 7.14-7.04 (m, 2H, H$_{arom}$), 6.92 (d, J = 8.7 Hz, 1H, H$_{arom}$), 6.85 (d, J = 8.3 Hz, 1H, H$_{arom}$), 5.13 (d, J = 12.2 Hz, 1H, CH$_2$Ph), 5.07 (d, J = 12.6 Hz, 1H, CH$_2$Ph), 5.05-4.99 (m, 3H, CH$_2$Ph, NH), 4.61 (m, 1H, H$_\alpha$), 3.12-2.98 (m, 2H, H$_\beta$), 2.36 (s, 3H, CH$_3$), 1.39 (s, 9H, C(CH$_3$)$_3$).

^{13}C NMR (63 MHz, CDCl$_3$): δ = 171.8, 155.1, 154.7, 138.0, 137.3, 137.2, 135.1, 132.0, 131.4, 130.3, 129.1, 128.53, 128.45, 128.37, 127.8, 127.7, 127.5, 126.8, 126.7, 113.4, 80.0, 70.5, 67.1, 54.6, 37.4, 28.3, 28.1, 21.5.

HRMS (EI) calcd for C$_{35}$H$_{37}$NO$_5$ 551.26715; found 551.26682.
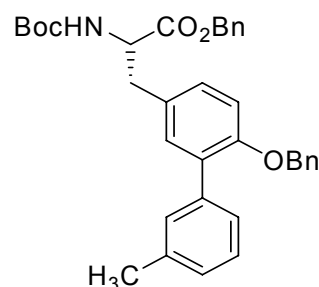
(*S*)-*N*^α-tert-Butyloxycarbonyl-*O*-benzyl-*m*-(*o*-tolyl)tyrosine benzyl ester (114).

Pale yellow oil; Yield 70%.

R_f = 0.25 (EtOAc/hexane, 1:4)

$[\alpha]_D^{23}$ +2.6 (c 1.9, CHCl$_3$)

^{1}H NMR (250 MHz, CDCl$_3$): δ = 7.30-7.20 (m, 10H, H$_{arom}$), 7.20-7.17 (m, 2H, H$_{arom}$), 7.17-7.12 (m, 2H, H$_{arom}$), 6.93 (d, J = 8.5 Hz, 1H, H$_{arom}$), 6.90-6.81 (m, 2H, H$_{arom}$), 5.14 (d, J = 12.2 Hz, 1H, CH$_2$Ph), 5.08 (d, J = 12.4 Hz, 1H, CH$_2$Ph) 5.03-4.95 (m, 3H, CH$_2$Ph, NH), 4.60 (m, 1H, H$_\alpha$), 3.13-2.92 (m, 2H, H$_\beta$), 1.39 (s, 9H, C(CH$_3$)$_3$).

^{13}C NMR (63 MHz, CDCl$_3$): δ = 171.7, 155.0, 154.8, 138.3, 137.3, 136.6, 135.1, 132.2, 131.7, 130.0, 129.5, 129.2, 128.5, 128.4, 128.3, 128.1, 127.4, 127.3, 126.5, 125.3, 113.2, 79.9, 70.3, 67.1, 54.5, 37.4, 28.3, 20.1.
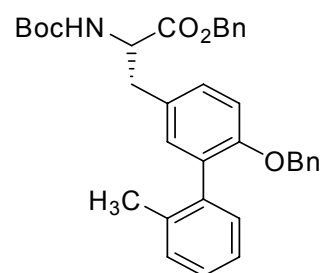
HRMS (EI) calcd for $C_{35}H_{37}NO_5$ 551.26715; found 551.26764.

(S)-N^{α}-tert-Butyloxycarbonyl-O-benzyl-m-(3-hydroxyphenyl)tyrosine benzyl ester (115).

Pale yellow solid; Two rotamers (ca. 4:1 ratio); Yield 80%.

R_f = 0.21 (EtOAc/hexane, 1:4)
$[\alpha]_D^{23}$ +3.8 (c 0.9, CHCl$_3$)
mp 65-68°C
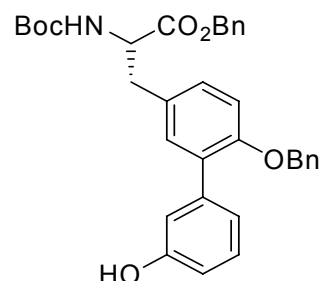
^{1}H NMR (250 MHz, CDCl$_3$): δ = 7.33-7.15 (m, 11H, H$_{arom}$), 7.11-6.95 (m, 3H, H$_{arom}$), 6.89 (dd, J = 8.3, 1.7 Hz, 1H, H$_{arom}$), 6.82 (s, 1H, H$_{arom}$), 6.78 (m, 1H, H$_{arom}$), 5.53 (s, 1H, OH), 5.15-5.00 (m, 3H, C$\underline{H}_2$Ph, NH), 4.98 (s, 2H, C$\underline{H}_2$Ph), 4.60 (m, 1H (80%), H$_\alpha$), 4.60 (m, 1H (20%), H$_\alpha$), 3.11-2.90 (m, 2H, H$_\beta$), 1.38 (s, 9H (80%), C(CH$_3$)$_3$), 1.29 (s, 9H (20%), C(CH$_3$)$_3$).

^{13}C NMR (63 MHz, CDCl$_3$): δ = 171.8, 155.4, 155.2, 154.6, 139.6, 137.1, 135.0, 131.8, 130.9, 129.2, 128.9, 128.5, 128.3, 127.5, 126.7, 121.8, 116.5, 113.9, 113.5, 80.1, 70.5, 67.1, 54.5, 37.3, 28.2.

HRMS (EI) calcd for $C_{34}H_{35}NO_6$ 553.24644; found 553.24703.

(S)-N^{α}-tert-Butyloxycarbonyl-O-benzyl-m-(3-chlorophenyl)tyrosine benzyl ester (116).

Pale yellow oil; Yield 39%.

R_f = 0.38 (EtOAc/hexane, 1:4)
$[\alpha]_D^{23}$ +3.0 (c 0.5, CHCl$_3$)

^{1}H NMR (250 MHz, CDCl$_3$): δ = 7.55 (m, 1H, H$_{arom}$), 7.42-7.22 (m, 13H, H$_{arom}$), 7.05 (d, J = 1.7 Hz, 1H, H$_{arom}$), 6.98 (d, J = 8.3 Hz, 1H, H$_{arom}$), 6.88 (d, J = 8.3 Hz, 1H, H$_{arom}$), 5.17 (d, J = 12.3 Hz, 1H, C$\underline{H}_2$Ph), 5.10 (d, J = 12.5 Hz, 1H, C$\underline{H}_2$Ph), 5.04-4.97 (m, 3H, C$\underline{H}_2$Ph, NH), 4.64 (m, 1H, H$_\alpha$), 3.20-2.92 (m, 2H, H$_\beta$), 1.42 (s, 9H, C(CH$_3$)$_3$).
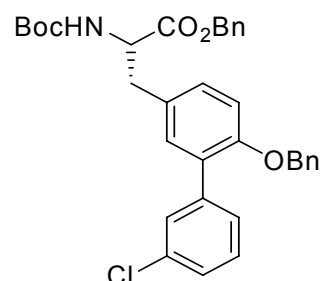
^{13}C NMR (63 MHz, CDCl$_3$): δ = 171.7, 155.0, 154.5, 139.9, 136.9, 135.1, 133.7, 131.8, 129.9, 129.7, 129.1, 128.6, 128.54, 128.46, 128.4, 127.73, 127.68, 127.0, 126.8, 113.3, 80.0, 70.5, 67.1, 54.5, 37.4, 28.3.

HRMS (EI) calcd for C$_{34}$H$_{34}$ClNO$_5$ 571.21255; found 571.21109.

(S)-N$^\alpha$-tert-Butyloxycarbonyl-O-benzyl-m-(4-fluorophenyl)tyrosine benzyl ester (117).

Pale yellow solid; Yield 94%.

R_f = 0.25 (EtOAc/hexane, 1:4)

$[\alpha]_D^{23}$ +1.3 (c 1.7, CHCl$_3$)

mp 108-110°C

^{1}H NMR (250 MHz, CDCl$_3$): δ = 7.54-7.45 (m, 2H, H$_{arom}$), 7.36-7.25 (m, 10H, H$_{arom}$), 7.12-7.03 (m, 3H, H$_{arom}$), 6.96 (d, J = 8.4Hz, 1H, H$_{arom}$), 6.88 (d, J = 8.4 Hz, 1H, H$_{arom}$), 5.17 (d, J = 12.2 Hz, 1H, CH$_2$Ph), 5.10 (d, J = 12.4 Hz, 1H, CH$_2$Ph), 5.04 (m, 3H, CH$_2$Ph, NH), 4.64 (m, 1H, H$_\alpha$), 3.20-2.95 (m, 2H, H$_\beta$), 1.42 (s, 9H, C(CH$_3$)$_3$).

^{13}C NMR (63 MHz, CDCl$_3$): δ = 171.7, 163.9, 160.0, 155.0, 154.6, 137.0, 135.1, 134.11, 134.06, 131.9, 131.2, 131.1, 130.2, 129.4, 128.5, 128.43, 128.37, 127.7, 126.8, 114.9, 114.6, 113.3, 79.9, 70.5, 67.1, 54.5, 37.4, 28.3.

HRMS (EI) calcd for C$_{34}$H$_{34}$FNO$_5$ 555.24210; found 555.24184.

(S)-N$^\alpha$-tert-Butyloxycarbonyl-O-benzyl-m-(4-carboxyphenyl)tyrosine benzyl ester (118).

Pale yellow solid; Two rotamers (ca. 7:3 ratio); Yield 92%.

R_f = 0.35 (EtOAc/hexane 1:4, 1% AcOH)

$[\alpha]_D^{23}$ -10.5 (c 0.02, CHCl$_3$)
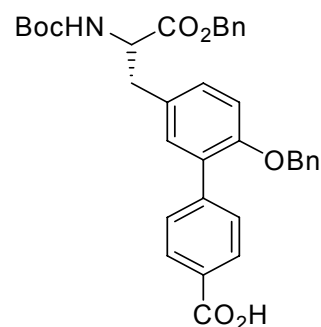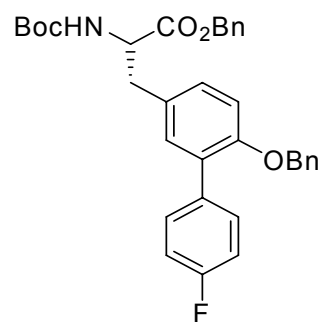
^{1}H NMR (250 MHz, CDCl$_3$): δ = 9.53 (s, 1 H, CO$_2$H), 8.12 (d, J = 7.9 Hz, 2H, H$_{arom}$), 7.63 (d, J = 8.0 Hz, 2H, H$_{arom}$), 7.39-7.22 (m, 10H, H$_{arom}$), 7.11 (s, 1H, H$_{arom}$), 6.99 (d, J = 8.4 Hz, 1H, H$_{arom}$), 6.90 (d, J = 8.2 Hz, 1H, H$_{arom}$), 5.20-5.08 (m, 2H, C$\underline{H}_2$Ph), 5.08-5.04 (m, 3H, C$\underline{H}_2$Ph, NH), 4.66 (m, 1H (70%), H$_\alpha$), 4.38 (m, 1H (30%), H$_\alpha$), 3.20-3.01 (m, 2H, H$_\beta$), 1.42 (s, 9H (70%), C(CH$_3$)$_3$), 1.32 (s, 9H (30%), C(CH$_3$)$_3$).

^{13}C NMR (125 MHz, CDCl$_3$): δ = 171.8, 171.3, 155.1, 154.7, 143.9, 136.8, 135.1, 132.0, 131.9, 129.93, 129.88, 129.7, 129.6, 128.7, 128.6, 128.5, 127.8, 127.7, 126.9, 126.8, 113.3, 80.1, 70.6, 67.2, 54.5, 37.5, 28.3.

MS (ESI) m/z 604.4 [M+Na]$^+$, 1185.1 [2M+Na]$^+$.

(**S**)-**N$^\alpha$**-tert-Butyloxycarbonyl-**O**-benzyl-**m**-(2-furanyl)tyrosine benzyl ester (119).
Pale yellow solid; Yield 99%.

R_f = 0.38 (EtOAc/hexane, 1:4)
[α]$_D^{23}$ +7.1 (c 0.3, CHCl$_3$)
mp 97-100°C
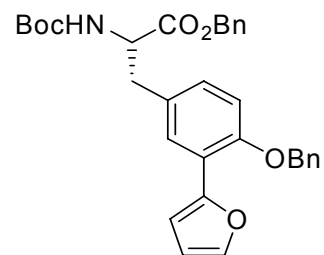
^{1}H NMR (250 MHz, CDCl$_3$): δ = 7.67 (d, J = 0.4 Hz, 1H, H$_{arom}$), 7.52-7.36 (m, 6H, H$_{arom}$), 7.35-7.30 (m, 5H, H$_{arom}$), 6.93-6.86 (m, 3H, H$_{arom}$), 6.44 (dd, J = 3.4, 1.8 Hz, 1H, H$_{arom}$), 5.17-5.12 (m, 4 H, C$\underline{H}_2$Ph), 5.05 (d, J = 7.0 Hz, 1H, NH), 4.64 (m, 1H, H$_\alpha$), 3.17-3.01 (m, 2H, H$_\beta$), 1.44 (s, 9H, C(CH$_3$)$_3$).

^{13}C NMR (63 MHz, CDCl$_3$): δ = 171.7, 155.0, 153.5, 149.9, 141.0, 136.7, 135.2, 128.61, 128.57, 128.49, 128.43, 128.3, 128.2, 128.1, 127.6, 126.9, 120.1, 112.3, 111.8, 110.3, 79.9, 70.5, 67.1, 54.6, 54.6, 37.5, 28.3.

HRMS (EI) calcd for C$_{32}$H$_{33}$NO$_6$ 527.23079; found 527.23086.

(*S*)-*N*^α-tert-Butyloxycarbonyl-*O*-benzyl-*m*-(3-thienyl)tyrosine benzyl ester (120).

Pale yellow solid; Yield 45%.

R_f = 0.37 (EtOAc/hexane, 1:4)

$[\alpha]_D^{23}$ 0.0 (c 1.2, CHCl$_3$)

mp 115-117°C
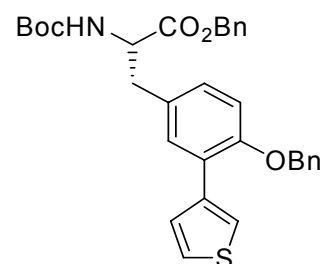
^{1}H NMR (250 MHz, CDCl$_3$): δ = 7.57 (dd, *J* = 3.0, 1.3 Hz, 1H, H$_{arom}$), 7.41 (dd, *J* = 5.1, 1.3 Hz, 1H, H$_{arom}$), 7.39-7.34 (m, 4H, H$_{arom}$), 7.34-7.23 (m, 8H, H$_{arom}$), 6.95-6.84 (m, 2H, H$_{arom}$), 5.15 (d, *J* = 12.2 Hz, 1H, C$\underline{H}_2$Ph), 5.09 (d, *J* = 12.3 Hz, 1H, C$\underline{H}_2$Ph), 5.07 (s, 2H, C$\underline{H}_2$Ph), 5.02 (m, 1H, NH), 4.63 (m, 1H, H$_\alpha$), 3.17-2.96 (m, 2H, H$_\beta$), 1.41 (s, 9H, C(CH$_3$)$_3$).

^{13}C NMR (63 MHz, CDCl$_3$): δ = 171.7, 155.0, 154.7, 137.9, 136.9, 135.1, 130.8, 128.9, 128.52, 128.49, 128.45, 128.37, 127.8, 127.1, 125.5, 124.3, 123.4, 113.2, 79.9, 70.6, 67.1, 54.5, 37.4, 28.3.

HRMS (EI) calcd for C$_{32}$H$_{33}$NO$_5$S 543.20794; found 543.20752.

(*S*)-*N*^α-*tert*-Butyloxycarbonyl-*O*-benzyl-*m*-phenyltyrosine (121).

A solution of lithium hydroxide (1.8 mg, 74 μmol, 1.0 equiv) in H$_2$O (0.11 mL) was added to a solution of **111** (40 mg, 74 μmol, 1.0 equiv) in 2 mL of THF at 0°C. After stirring for 18 h, a 10% aqueous solution of citric acid (50 mL) was added and the aqueous layer was extracted with EtOAc (3×30 mL). The combined organic layers were dried (Na$_2$SO$_4$), the solvent removed under reduced pressure and the residue purified by flash chromatography on silica gel (EtOAc/hexane 1:1, 1% AcOH) yielding **121** (28.6 mg, 86%) as a colorless solid.
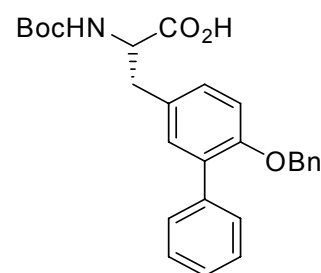
R_f = 0.30 (EtOAc/hexane 1:1, 1% AcOH)

$[\alpha]_D^{23}$ +11.3 (c 1.7, MeOH)

mp 108-110°C

^{1}H NMR (250 MHz, MeOH-d$_4$): δ = 7.53 (d, J = 7.0 Hz, 2H, H$_{arom}$), 7.35 (dd, J = 7.2, 7.2 Hz, 2H, H$_{arom}$), 7.31-7.22 (m, 6H, H$_{arom}$), 7.22-7.10 (m, 2H, H$_{arom}$), 7.02 (d, J = 8.3 Hz, 1H, H$_{arom}$), 5.02 (s, 2H, CH$_2$Ph), 4.36 (dd, J = 8.2, 5.1 Hz, 1H, H$_\alpha$), 3.15 (dd, J = 13.9, 4.8 Hz, 1H, H$_\beta$), 2.91 (dd, J = 13.8, 8.7 Hz, 1H, H$_\beta$), 1.36 (s, 9H, C(CH$_3$)$_3$).

^{13}C NMR (90 MHz, MeOH-d$_4$): δ = 175.4, 157.7, 155.9, 140.0, 138.8, 132.9, 132.5, 131.3, 130.7, 130.4, 129.3, 128.8, 128.6, 128.2, 127.8, 114.8, 80.5, 71.7, 56.3, 37.9, 28.7.

HRMS (EI) calcd for C$_{27}$H$_{29}$NO$_5$ 447.20456; found 447.20400.

(S)-N$^\alpha$-tert-Butyloxycarbonyl-O-benzyl-m-(o-tolyl)tyrosine (122).

A solution of lithium hydroxide (4.7 mg, 112 µmol, 1.0 equiv) in H$_2$O (0.17 mL) was added to a solution of 114 (62 mg, 112 µmol, 1.0 equiv) in 2 mL of THF at 0°C. After stirring for 18 h, a 10% aqueous solution of citric acid (50 mL) was added and the aqueous layer was extracted with EtOAc (3×30 mL). The combined organic layers were dried (Na$_2$SO$_4$), the solvent removed under reduced pressure and the residue purified by flash chromatography on silica gel (EtOAc/hexane 1:1, 1% AcOH) yielding 122 (43 mg, 83%) as a colorless solid.
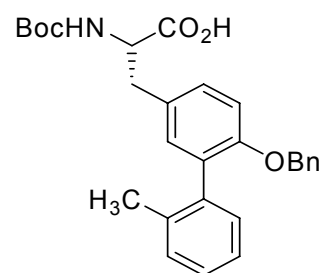
R_f = 0.30 (EtOAc/hexane 1:1, 1% AcOH)
$[\alpha]_D^{23}$ +24.1 (c 0.9, CHCl$_3$)
mp 68-72°C

^{1}H NMR (360 MHz, CDCl$_3$): δ = 7.32-7.16 (m, 9H, H$_{arom}$), 7.11 (dd, J = 8.4, 1.8 Hz, 1H, H$_{arom}$), 7.00 (s, 1H, H$_{arom}$), 6.94 (d, J = 8.4 Hz, 1H, H$_{arom}$), 5.01 (s, 2H, H$_{arom}$), 4.96 (m, 1H, NH), 4.60 (m, 1H, H$_\alpha$), 3.16 (dd, J = 14.2, 3.9 Hz, 1H, H$_\beta$), 3.04 (dd, J = 14.0, 5.6 Hz, 1H, H$_\beta$), 2.18 (s, 3H, CH$_3$), 1.42 (s, 9H, C(CH$_3$)$_3$).

^{13}C NMR (90 MHz, CDCl$_3$): δ = 176.1, 155.0, 138.3, 137.3, 136.7, 132.2, 131.9, 130.0, 129.6, 129.2, 128.3, 127.5, 127.3, 126.6, 125.3, 113.4, 80.3, 70.4, 54.4, 36.9, 28.3, 20.1.

HRMS (EI) calcd for C$_{28}$H$_{31}$NO$_5$ 461.22022; found 461.22022.

(S)-N$^{\alpha}$-tert-Butyloxycarbonyl-m-phenyltyrosine (123).

Palladium on charcoal (5% Pd/C, 0.23 g, 10mol% Pd) was added to a degassed solution of **111** (0.60 g, 1.11 mmol) in *N,N*-dimethylacetamide/MeOH (1:1, 30 mL). Hydrogenation was carried out at 1 bar hydrogen pressure for 6 h. The catalyst was removed by filtration, the solvent removed under reduced pressure and the residue purified by flash chromatography on silica gel (EtOAc/hexane 1:2, 1% AcOH) yielding **123** (373 mg, 95%) as a colorless solid.
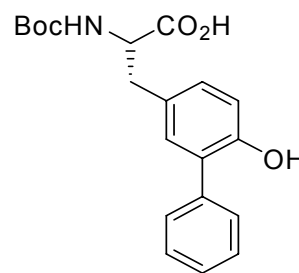
R_f = 0.26 (EtOAc/hexane 1:1, 1% AcOH)
$[\alpha]_D^{23}$ +17.9 (c 10.5, MeOH)
mp 80-82°C

^{1}H NMR (360 MHz, MeOH-d$_4$): δ = 7.61 (dd, J = 8.1, 1.0 Hz, 2H, H$_{arom}$), 7.39 (dd, J = 7.5, 7.5 Hz, 2H, H$_{arom}$), 7.29 (dd, J = 7.4, 7.4 Hz, 1H, H$_{arom}$), 7.22 (d, J = 1.6 Hz, 1H, H$_{arom}$), 7.09 (dd, J = 8.1, 1.7 Hz, 1H, H$_{arom}$), 6.92 (d, J = 8.2 Hz, 1H, H$_{arom}$), 4.43 (m, 1H, H$_\alpha$), 3.17 (dd, J = 14.0, 4.8 Hz, 1H, H$_\beta$), 2.99 (dd, J = 13.8, 8.4 Hz, 1H, H$_\beta$), 1.36 (s, 9H, C(CH$_3$)$_3$).

^{13}C NMR (90 MHz, MeOH-d$_4$): δ = 174.5, 157.1, 154.7, 140.7, 133.5, 131.1, 130.5, 129.9, 129.8, 129.7, 128.4, 117.8, 80.2, 56.6, 38.3, 21.4.

HRMS (EI) calcd for C$_{20}$H$_{23}$NO$_5$ 357,15762; found 357.15622.

(*S*)-*N*$^\alpha$-*tert*-Butyloxycarbonyl-*m*-(*o*-tolyl)tyrosine (124).

Palladium on charcoal (5% Pd/C, 0.11 g, 10mol% Pd) was added to a degassed solution of **114** (0.30 g, 0.56 mmol) in *N,N*-dimethylacetamide/MeOH (1:1, 15 mL). Hydrogenation was carried out at 1 bar hydrogen pressure for 6 h. The catalyst was removed by filtration, the solvent removed under reduced pressure and the residue purified by flash chromatography on silica gel (EtOAc/hexane 1:2, 1% AcOH) yielding **124** (179 mg, 87%) as a colorless solid.
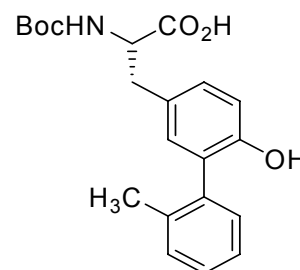
R_f=0.27 (EtOAc/hexane 1:1, 1% AcOH)

$[\alpha]_D^{23}$ +21.9 (c 0.6, MeOH)

mp 82-85°C

^{1}H NMR (360 MHz, MeOH-d$_4$): δ = 7.26-7.20 (m, 2H, H$_{arom}$), 7.20-7.14 (m, 2H, H$_{arom}$), 7.11 (dd, *J*=8.3, 1.7 Hz, 1H, H$_{arom}$), 6.97 (d, *J*=1.7 Hz, 1H, H$_{arom}$), 6.90 (d, *J*=8.2 Hz, 1H, H$_{arom}$), 4.42 (m, 1H, H$_\alpha$), 3.15 (dd, *J*=13.9, 5.0 Hz, 1H, H$_\beta$), 2.97 (dd, *J*=13.7, 8.2 Hz, 1H, H$_\beta$), 2.18 (s, 3H), 1.36 (s, 9H, C(CH$_3$)$_3$).

^{13}C NMR (90 MHz, MeOH-d$_4$): δ = 174.5, 157.0, 154.7, 140.5, 138.6, 133.7, 132.0, 131.4, 131.1, 130.4, 129.9, 128.9, 127.1, 117.2, 80.2, 56.6, 38.3, 21.2.

HRMS (EI) calcd for C$_{21}$H$_{25}$NO$_5$ 371,17327; found 371.17221.

4.4.2   Synthesis of condensed tyrosine derivatives

4-(*tert*-Butyldimethylsilyloxy)naphthalene-1-carbaldehyde (133).

A solution of 4-hydroxynaphthalene-1-carbaldehyde (**129**) (1.13 g, 6.56 mmol, 1.0 equiv) in dry THF (30 mL) was cooled to 0°C and sequentially imidazole (0.86 g, 12.6 mmol, 1.9 equiv) and *tert*-butyldimethylsilyl chloride (TBSCl) (1.72 g, 11.4 mmol, 1.7 equiv) were added. After stirring at room temperature for 18 h the reaction mixture was filtered and the solvent evaporated. The residue was taken up in EtOAc (100 mL) and washed with saturated aqueous NH$_4$Cl (40 mL), water (40 mL)
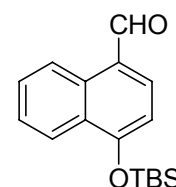
and brine (40 mL) and dried over Na_2SO_4. The solvent was removed under reduced pressure and the residue purified by flash chromatography on silica gel (EtOAc/hexane 1:20) yielding 133 (1.69 g, 88%) as a pale yellow solid.

R_f = 0.26 (EtOAc/hexane, 1:10)

mp 87-91°C

^{1}H NMR (500 MHz, CDCl$_3$): δ = 10.23 (s, 1H, CHO), 9.31 (d, J = 8.5 Hz, 1H, H$_{arom}$), 8.28 (d, J = 8.4 Hz, 1H, H$_{arom}$), 7.87 (d, J = 7.9 Hz, 1H, H$_{arom}$), 7.69 (dd, J = 7.4, 7.4 Hz, 1H, H$_{arom}$), 7.58 (dd, J = 7.6, 7.6 Hz, 1H, H$_{arom}$), 6.95 (d, J = 7.9 Hz, 1H, H$_{arom}$), 1.11 (s, 9H, C(CH$_3$)$_3$), 0.37 (s, 6H, Si(CH$_3$)$_2$).

^{13}C NMR (63 MHz, CDCl$_3$): δ = 192.1, 158.0, 139.0, 132.5, 129.4, 127.7, 126.2, 125.2, 124.9, 122.9, 111.3, 25.7, 18.4, –4.2.

HRMS (EI) calcd for $C_{17}H_{22}O_2Si$ 286.13892; found 286.13885.

(Z)-Methyl 2-(*tert*-butyloxycarbonyl)amino-3-(1-(*tert*-butyldimethylsilyloxy) naphthalene-4-yl) acrylate (134).

To a solution of $(CH_3O)_2P(O)CH(NHBoc)CO_2CH_3$ (1.47 g, 4.95 mmol, 1.5 equiv) in dry CH_2Cl_2 (3 mL) DBU (583 µL, 3.9 mmol, 1.3 equiv) was added and the mixture was stirred for 10 min at 0°C. A solution of 133 (945 mg, 3.30 mmol, 1.0 equiv) in dry CH_2Cl_2 (3 mL) was added slowly *via* syringe and the reaction mixture was warmed to
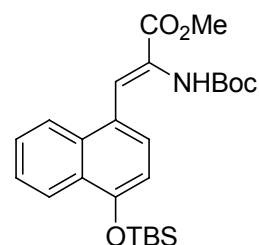
room temperature over 18 h. After the solvent was removed under reduced pressure, the residue was dissolved in EtOAc (50 mL), quickly washed with a saturated aqueous NH_4Cl (2×20 mL) and brine (20 mL) and dried over Na_2SO_4. The solvent was evaporated and the crude product purified by flash chromatography on silica gel (EtOAc/hexane 1:4, 1% NEt$_3$) yielding 134 (Z/E>90/10, 1.37 g, 91%) as a pale yellow solid. Pure (Z)-isomer was separated under the same conditions as a pale yellow solid (75% yield).

R_f = 0.43 (EtOAc/hexane, 1:2)

mp 116-120°C

^{1}H NMR (360 MHz, CDCl$_3$): δ = 8.24 (dd, J = 7.3, 2.3 Hz, 1H, H$_{arom}$), 7.95 (dd, J = 7.3, 1.9 Hz, 1H, H$_{arom}$), 7.69 (s, 1H, H$_{arom}$), 7.59 (d, J = 8.0 Hz, 1H, H$_{arom}$), 7.56-7.46 (m, 2H, H$_{arom}$), 6.86 (d, J = 8.0 Hz, 1H, CH=C), 6.08 (s, 1H, NH), 3.90 (s, 3H, CH$_3$), 1.31 (s, 9H, C(CH$_3$)$_3$), 1.10 (s, 9H, SiC(CH$_3$)$_3$), 0.31 (s, 6H, Si(CH$_3$)$_2$).

^{13}C NMR (63 MHz, CDCl$_3$): δ = 165.9, 152.7, 132.9, 127.8, 127.1, 126.9, 126.1, 125.8, 125.3, 124.0, 123.7, 123.1, 112.0, 80.7, 52.4, 27.9, 25.8, 18.4, –4.2.

HRMS (EI) calcd for C$_{25}$H$_{35}$NO$_5$Si 457.22845; found 457.22828.

(*S*)-*N*$^\alpha$-*tert*-Butyloxycarbonyl-1-(4-*tert*-butyldimethylsilyloxy)naphthylalanines methyl ester (135).

[(*S*,*S*)-(COD)-Et-DuPHOS-Rh(I)] OTf (0.38 mg, 0.52 µmol) was added to a solution of 134 (120 mg, 262 µmol, 1.0 equiv) in degassed DCM (3 mL). Hydrogenation was carried out at 40 bar hydrogen pressure for 4 h. The catalyst was removed by flash chromatography on silica gel (EtOAc/hexane 1:10) yielding 135 (114 mg, 95%) as a colorless oil.
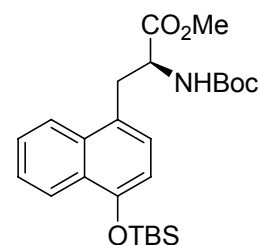
Two rotamers (ca. 4:1 ratio)
R_f = 0.31 (EtOAc/hexane, 1:4)
[α]$_D^{23}$ +20.5 (c 3.7, CHCl$_3$)

^{1}H NMR (360 MHz, CDCl$_3$): δ = 8.24 (d, J = 8.1 Hz, 1H, H$_{arom}$), 8.01 (d, J = 8.2 Hz, 1H, H$_{arom}$), 7.54 (ddd, J = 7.0, 6.8, 1.3 Hz, 1H, H$_{arom}$), 7.48 (ddd, J = 7.3, 7.0, 0.8 Hz, 1H, H$_{arom}$), 7.12 (d, J = 7.7 Hz, 1H, H$_{arom}$), 6.78 (d, J = 7.7 Hz, 1H, H$_{arom}$), 5.06 (d, J = 7.3 Hz, 1H (80%), NH), 4.86 (s, 1H (20%), NH), 4.68 (d, J = 6.9 Hz, 1H (80%), H$_\alpha$), 4.57 (s, 1H (20%), H$_\alpha$), 3.66 (s, 3H (20%), CH$_3$), 3.61 (s, 3H (80%), CH$_3$), 3.50 (dd, J = 14.0, 6.3 Hz, 1H, H$_\beta$), 3.39 (dd, J = 13.7, 6.6 Hz, 1H, H$_\beta$), 1.41 (s, 9H (80%), C(CH$_3$)$_3$), 1.17 (s, 9H (20%), C(CH$_3$)$_3$), 1.10 (s, 9H, SiC(CH$_3$)$_3$), 0.29 (s, 6H, Si(CH$_3$)$_2$).

^{13}C NMR (90 MHz, CDCl$_3$): δ = 172.7, 154.9, 151.2, 133.4, 128.2, 127.3, 126.4, 124.9, 124.8, 123.4, 123.2, 111.8, 79.7, 54.4, 52.0, 35.3, 28.2, 25.8, 18.4, –4.2.

HRMS (EI) calcd for C$_{25}$H$_{37}$NO$_5$Si 459.24411; found 459.24438.

(*S*)-*N*$^\alpha$-*tert*-Butyloxycarbonyl-1-(4-hydroxy)naphthylalanine (136).

To a solution of 135 (50.0 mg, 109 μmol, 1.0 equiv) in dry THF at 0°C was added tetrabutylammonium fluoride (36.1 mg, 114 μmol, 1.05 equiv). After stirring for 15 min, a solution of lithium hydroxide (5.04 mg, 120 μmol, 1.1 equiv) in water (182 μL) was added and the mixture was stirred for additional 3 h at room temperature. The solution was acidified by addition of a 10% aqueous solution of citric acid (20 mL), extracted with EtOAc (2×50 mL) and the combined organic layers were dried over Na_2SO_4. After the solvent was removed under reduced pressure, the crude product was purified by flash chromatography on silica gel (MeOH/CHCl$_3$ 1:9, 1% AcOH) yielding 136 (32 mg, 89%) as a colorless solid.
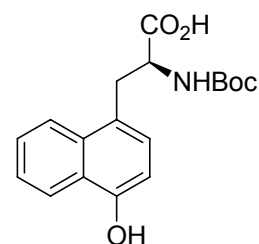
Two rotamers (ca. 5:2 ratio)

R_f = 0.18 (MeOH/CHCl$_3$ 1:9, 1% AcOH)

$[\alpha]_D^{23}$ –25.9 (c 1.6, MeOH); mp 88-92°C

^{1}H NMR (500 MHz, MeOH-d$_4$): δ = 8.24 (d, *J* = 8.4 Hz, 1H, H$_{arom}$), 8.05 (d, *J* = 8.5 Hz, 1H, H$_{arom}$), 7.51 (dd, *J* = 7.5, 7.5 Hz, 1H, H$_{arom}$), 7.42 (dd, *J* = 7.4, 7.4 Hz, 1H, H$_{arom}$), 7.17 (d, *J* = 7.7 Hz, 1H, H$_{arom}$), 6.73 (d, *J* = 7.7 Hz, 1H, H$_{arom}$), 4.44 (dd, *J* = 8.8, 5.1 Hz, 1H, H$_\alpha$), 3.68 (dd, *J* = 12.2, 2.9 Hz, 1H (30%), H$_\beta$), 3.59 (dd, *J* = 14.3, 4.9 Hz, 1H (70%), H$_\beta$), 3.17 (dd, *J* = 14.2, 9.1 Hz, 1H (70%), H$_\beta$), 2.99 (dd, *J* = 12.0, 12.0 Hz, 1H (30%), H$_\beta$), 1.34 (s, 9H (70%), C(CH$_3$)$_3$), 0.98 (s, 9H (30%), C(CH$_3$)$_3$).

^{13}C NMR (125 MHz, MeOH-d$_4$): δ = 175.9, 157.8, 154.0, 134.4, 129.4, 129.0, 127.4, 126.9, 125.26, 125.20, 124.4, 124.23, 124.19, 124.0, 108.3, 80.5, 56.8, 56.1, 37.4, 35.8, 28.7, 28.1.

HRMS (EI) calcd for C$_{18}$H$_{21}$NO$_5$ 331.14197; found 331.14097.

(**Z**)-Methyl 2-(benzyloxycarbonyl)amino-3-(1-(**tert**-butyldimethylsilyloxy) naphthalene-4-yl) acrylate (139).

$(MeO)_2P(O)CH(NHCbz)CO_2Me$ (1.10 g, 3.33 mmol, 1.5 equiv) was dissolved in dry CH_2Cl_2 (3 mL) and DBU (432 µL, 2.89 mmol, 1.3 equiv) was added. The mixture was stirred for 10 min at 0°C. Then, a solution of 133 (635 mg, 2.22 mmol, 1.0 equiv) in dry CH_2Cl_2 (3 mL) was added slowly *via* syringe and the reaction mixture was warmed to room temperature over 18 h. After the solvent was removed under reduced pressure, the residue was dissolved in EtOAc (50 mL), quickly washed with saturated aqueous NH_4Cl (2×20 mL) and brine (20 mL) and dried over Na_2SO_4. The solvent was evaporated and the crude product purified by flash chromatography on silica gel (EtOAc/hexane 1:4, 1% NEt_3) yielding 139 (948 mg, 87%) as a pale yellow oil.
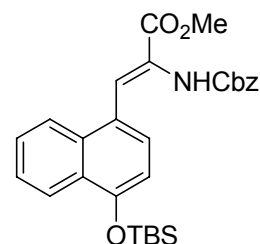
R_f = 0.33 (EtOAc/hexane, 1:2)

^1H NMR (360 MHz, $CDCl_3$): δ = 8.28-8.20 (m, 1H, H_{arom}), 7.95-7.88 (m, 1H, H_{arom}), 7.81 (s, 1H, H_{arom}), 7.56-7.47 (m, 3H, H_{arom}), 7.34-7.27 (m, 3H, H_{arom}), 7.27-7.20 (m, 2H, H_{arom}), 6.81 (d, J = 8.0 Hz, 1H, CH=C), 6.25 (s, 1H, NH), 5.06 (s, 2H, CH_2Ph), 3.86 (s, 3H, CH_3), 1.11 (s, 9H, $C(CH_3)_3$), 0.32 (s, 6H, $Si(CH_2)_2$).

^{13}C NMR (90 MHz, $CDCl_3$): δ = 165.6, 153.9, 153.0, 135.85, 133.0, 128.4, 128.1, 128.1, 128.1, 127.9, 127.3, 127.0, 125.5, 125.4, 123.9, 123.2, 123.2, 111.9, 67.3, 52.6, 25.8, 18.4, –4.2.

HRMS (EI) calcd for $C_{28}H_{33}NO_5Si$ 491.21280; found 491.21264.

(**R/S**)-**N**$^\alpha$-Acetyl-1-(4-**tert**-butyldimethylsilyloxy)naphthylalanine methyl ester (140).

To a solution of 139 (0.28 g, 0.57 mmol, 1 equiv) in degassed MeOH (30 mL) was added palladium on charcoal (5% Pd/C, 0.12 g, 10mol% Pd). Hydrogenation was carried out at 1 bar hydrogen pressure for 2 h. After the catalyst was removed by filtration, the solvent was removed under re-

duced pressure and the residue dissolved in dry DCM (10 mL). Ac_2O (60 μL, 0.68 mmol, 1.2 equiv) and NEt_3 (0.12 mL, 0.85 mmol, 1.5 equiv) were added and the mixture stirred for additional 18 h. The solvent was removed under reduced pressure, the residue taken up with EtOAc (50 mL) and subsequently washed with saturated aqueous $NaHCO_3$ (2×50 mL) and brine (50 mL) and dried over Na_2SO_4. After the solvent was removed under reduced pressure, the crude product was purified by flash chromatography on silica gel (EtOAc/hexane 1:1, 1% NEt_3) yielding 140 (194 mg, 76%) as a colorless solid.
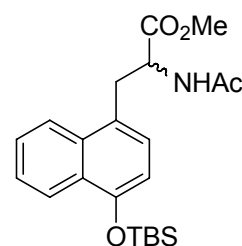
R_f = 0.16 (EtOAc/hexane 1:1, 1% NEt_3)
mp 50-55°C

^{1}H NMR (250 MHz, $CDCl_3$): δ = 8.24 (d, J = 7.9 Hz, 1H, H_{arom}), 8.01 (d, J = 7.8 Hz, 1H, H_{arom}), 7.57-7.43 (m, 2H, H_{arom}), 7.08 (d, J = 7.8 Hz, 1H, H_{arom}), 6.77 (d, J = 7.7 Hz, 1H, H_{arom}), 5.99 (d, J = 7.7 Hz, 1H, NH), 4.97 (m, 1H, H_α), 3.61 (s, 3H, OCH_3), 3.45 (dd, J = 13.9, 6.8 Hz, 1H, H_β), 3.45 (dd, J = 14.4, 6.1 Hz, 1H, H_β), 1.93 (s, 3H, $COCH_3$), 1.09 (s, 9H, $C(CH_3)_3$), 0.28 (s, 6H, $Si(CH_3)_2$).

^{13}C NMR (63 MHz, $CDCl_3$): δ = 172.4, 169.6, 151.2, 133.4, 128.1, 127.2, 126.4, 124.9, 124.7, 123.4, 123.2, 111.8, 53.2, 52.1, 34.6, 25.8, 23.0, 18.4, –4.2.

HRMS (EI) calcd for $C_{20}H_{23}NO_5$ 357.15762; found 357.15622.

(*R*)-*N*$^\alpha$-Acetyl-1-(4-hydroxy)naphthylalanines (143) and (*S*)-1-(4-hydroxy)-naphthylalanine methyl ester (142).

To a solution of 140 (100 mg, 249 μmol, 1.0 equiv) in dry THF (7 mL) at 0°C was added tetrabutylammonium fluoride (82.5 mg, 261 μmol, 1.05 equiv). After stirring for 15 min, a solution of lithium hydroxide (41.8 mg, 996 μmol, 4 equiv) in water (1.5 mL) was added and stirring was continued for additional 2 h at room temperature until complete conversion (TLC control). Thereafter, the solvent was removed under reduced pressure and the residue dissolved in water (10 mL) and adjusted to pH 7-8 by addition of 1N HCl. Acylase I (50 mg) was added and the mixture was stirred at 37°C until no further conversion was observed (2-3 h, HPLC monitoring). Additional acylase I (50 mg) was added and stirring continued for 1 h. The mixture

was diluted with water (20 mL), acidified to pH 1 by addition of 1N HCl and extracted with EtOAc (5×20 mL).

The organic phase was dried over Na$_2$SO$_4$, the solvent removed under reduced pressure and the residue further purified by a short column of silica (MeOH/CHCl$_3$ 1:3, 1% AcOH) to give 143 (31 mg, 46%) as a colorless solid.

The aqueous phase was concentrated under reduced pressure and dried. The residue was suspended in dry MeOH (30 mL) and SOCl$_2$ (1 mL) was added drop wise at 0°C. After stirring for 24 h at room temperature the mixture was concentrated under reduced pressure, diluted with 1N NaOH (30 mL) and extracted with EtOAc (5×20 mL). The organic phase was dried over Na$_2$SO$_4$, the solvent removed under reduced pressure and the residue further purified by a short column of silica (MeOH/CHCl$_3$ 1:9, 1% NEt$_3$) to obtain a pale yellow oil which was dissolved in Et$_2$O and a minimum volume of dioxane. Addition of a 1M solution of HCl in ether (2 mL) gave 142 as a colorless solid which was filtered of and dried in *vacuo*.

(*S*)-1-(4-Hydroxy)naphthylalanine methyl ester (142)

R_f = 0.50 (MeOH/CHCl$_3$ 1:9, 1% NEt$_3$)

$[\alpha]_D^{23}$ +5.2 (c 0.6, MeOH)

mp (22*HCl) >240°C

^{1}H NMR (250 MHz, CDCl$_3$): δ = 8.30 (d, J = 8.3 Hz, 1H, H$_{arom}$), 7.94 (d, J = 8.3 Hz, 1H, H$_{arom}$), 7.59 (dd, J = 7.5, 7.5 Hz, 1H, H$_{arom}$), 7.48 (dd, J = 7.4, 7.4 Hz, 1H, H$_{arom}$), 7.21 (d, J = 7.6 Hz, 1H, H$_{arom}$), 6.80 (d, J = 7.6 Hz, 1H, H$_{arom}$), 4.31 (dd, J = 7.4, 7.4 Hz, 1H, H$_\alpha$), 3.80-3.63 (m, 4H, H$_\beta$, OCH$_3$), 3.41 (dd, J = 14.5, 8.5 Hz, 1H, H$_\beta$).
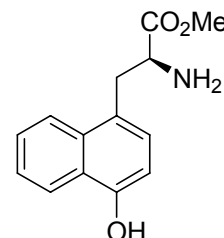
^{13}C NMR (226 MHz, CDCl$_3$): δ = 175.8, 154.4, 134.3, 129.2, 127.5, 125.5, 124.2, 108.3, 56.1, 52.6, 38.3.

HRMS (EI) calcd for C$_{14}$H$_{15}$NO$_3$ 245.10519; found 245.10519.

(*R*)-*N*$^\alpha$-Acetyl-1-(4-hydroxy)naphthylalanine (143)

R_f = 0.31 (MeOH/CHCl$_3$ 1:1, 0.1% TFA)

$[\alpha]_D^{23}$ –1.7 (c 0.5, MeOH); mp 130-134 °C
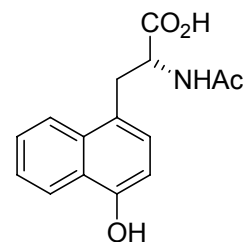
^{1}H NMR (500 MHz, MeOH-d$_4$): δ = 8.23 (d, *J* = 8.3 Hz, 1H, H$_{arom}$), 8.05 (d, *J* = 8.5 Hz, 1H, H$_{arom}$), 7.51 (dd, *J* = 7.6, 7.6 Hz, 1H, H$_{arom}$), 7.42 (dd, *J* = 7.5, 7.5 Hz, 1H, H$_{arom}$), 7.17 (d, *J* = 7.7 Hz, 1H, H$_{arom}$), 6.73 (d, *J* = 7.7 Hz, 1H, H$_{arom}$), 4.74 (dd, *J* = 8.9, 5.2 Hz, 1H, H$_\alpha$), 3.63 (dd, *J* = 14.3, 5.1 Hz, 1H, H$_\beta$), 3.21 (dd, *J* = 14.3, 9.0 Hz, 1H, H$_\beta$), 1.85 (s, 3H, CH$_3$).

^{13}C NMR (125 MHz, MeOH-d$_4$): δ = 175.4, 173.1, 154.0, 134.4, 128.8, 127.3, 126.8, 125.2, 125.1, 124.3, 124.0, 108.2, 55.0, 35.5, 22.3.

HRMS (EI) calcd for C$_{15}$H$_{15}$NO$_4$ 273.10010; found 273.10083.

General procedure for the synthesis of dipeptides 125-128, 137 and 138.

Fmoc-Val-OH (21 mg, 0.06 mmol) was attached to the TCP resin (50 mg) with DIPEA (25 µL) in anhydrous DCM (1.5 mL) at room temperature for 1 h, followed by addition of MeOH (0.1 mL) for 15 minutes for quenching, yielding 62 mg of Fmoc-Val-TCP resin (substitution level 0.71 mmol/g resin). For Fmoc-deprotection, the resin was treated with 20% piperidine in NMP (v/v) and washed with NMP (5×1 min). The coupling of side chain unprotected tyrosine analogues was achieved using 1.8 equiv (64 µmol) of the corresponding amino acid, 1.8 equiv TBTU (21 mg, 64 µmol), 1.8 equiv HOBt (8.6 mg, 64 µmol) and 10 equiv collidine (47 µL, 0.35 mmol) in NMP (1 mL) for 30 min at room temperature after which the resin was washed with NMP (5×1 min) and DCM (3×1 min). The dipeptides were deprotected and cleaved from resin by treatment with TFA/DCM/H$_2$O (50:40:10; v/v) for 1 h. The solvents were evaporated to dryness to give the pure dipeptides as colorless solids.

H-*m*-(phenyl)Tyr-Val-OH (125).

RP-HPLC (10 → 50%) R_t = 18.5; 98% purity

^{1}H NMR (500 MHz, MeOH-d$_4$): δ = 7.54 (d, J = 7.5 Hz, 2H, H$_{arom}$), 7.35 (dd, J = 7.6, 7.6 Hz, 2H, H$_{arom}$), 7.26 (dd, J = 7.4, 7.4 Hz, 1H, H$_{arom}$), 7.23 (d, J = 2.0 Hz, 1H, H$_{arom}$), 7.10 (dd, J = 8.5, 2.1 Hz, 1H, H$_{arom}$), 6.87 (d, J = 8.2 Hz, 1H, H$_{arom}$), 4.37 (d, J = 5.2 Hz, 1H, H$_\alpha$–Val), 4.16 (dd, J = 8.6, 5.0 Hz, 1H, H$_2$N-C$\underline{H}$), 3.24 (dd, J = 14.6, 4.9 Hz, 1H, H$_\beta$), 2.96 (dd, J = 14.5, 8.7 Hz, 1H, H$_\beta$), 2.21 (m, 1H, C$\underline{H}$CH$_3$), 0.98 (d, J = 6.7 Hz, 3H, CH$_3$), 0.97 (d, J = 6.7 Hz, 3H, CH$_3$).
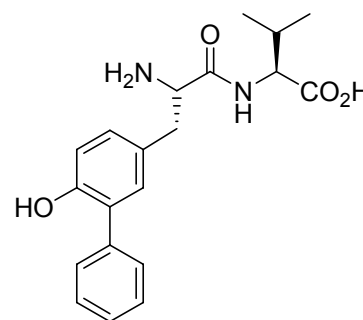
^{13}C NMR (125 MHz, MeOH-d$_4$): δ = 174.2, 170.1, 155.3, 139.9, 132.9, 130.59, 130.56, 130.5, 129.0, 127.9, 126.4, 117.6, 59.355.8, 37.9, 31.8, 19.6, 18.2.

MS (ESI) m/z 357.2 [M+H]$^+$, 713.1 [2M+Na]$^+$.

H-*m*-(*o*-tolyl)Tyr-Val-OH (126).

RP-HPLC (10 → 50%) R_t = 19.8; 98% purity.

^{1}H NMR (500 MHz, MeOH-d$_4$): δ = 7.21-7.17 (m, 2H, H$_{arom}$), 7.17-7.11 (m, 3H, H$_{arom}$) 7.01 (d, J = 2.2 Hz, 1H, H$_{arom}$), 6.85 (d, J = 8.3 Hz, 1H, H$_{arom}$), 4.36 (d, J = 5.2 Hz, 1H, H$_\alpha$–Val), 4.15 (dd, J = 8.6, 5.1 Hz, 1H, H$_2$N-C$\underline{H}$), 3.22 (dd, J = 14.5, 5.0 Hz, 1H, H$_\beta$), 2.94 (dd, J = 14.5, 8.6 Hz, 1H, H$_\beta$), 2.20 (m, 1H, C$\underline{H}$CH$_3$), 2.14 (s, 3H, CH$_3$), 0.97 (d, J = 6.7 Hz, 3H, CHC$\underline{H}_3$), 0.96 (d, J = 6.8 Hz, 3H, CHC$\underline{H}_3$).
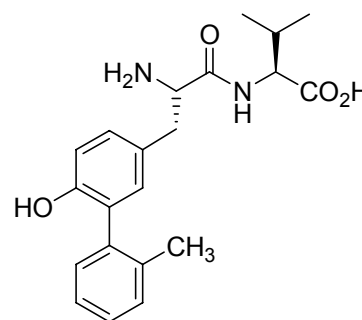
^{13}C NMR (125 MHz, MeOH-d$_4$): δ = 174.0, 170.0, 155.2, 139.7, 138.1, 133.2, 131.2, 131.1, 130.6, 130.5, 128.4, 126.5, 126.0, 59.2, 55.7, 37.8, 31.7, 20.2, 19.5, 18.2.

MS (ESI) m/z 371.2 [M+H]$^+$, 741.1 [2M+Na]$^+$.

H-*m*-(phenyl)Tyr-D-Val-OH (127).

RP-HPLC (10 → 50%) R_t = 21.9: 95% purity.

^{1}H NMR (500 MHz, MeOH-d$_4$): δ = 7.25-7.17 (m, 3H, H$_{arom}$), 7.16-7.11 (m, 2H, H$_{arom}$), 7.01 (d, J = 2.2 Hz, 1H, H$_{arom}$), 6.88 (d, J = 8.2 Hz, 1H, H$_{arom}$), 4.29 (d, J = 5.2 Hz, 1H, H$_\alpha$–Val), 4.19 (dd, J = 7.4, 7.4 Hz, 1H, H$_2$N-C$\underline{H}$), 3.14 (dd, J = 14.0, 7.2 Hz, 1H, H$_\beta$), 3.02 (dd, J = 14.0, 7.6 Hz, 1H, H$_\beta$), 2.11 (m, 1H, C$\underline{H}$CH$_3$), 0.86 (d, J = 6.9 Hz, 3H, CHC$\underline{H}_3$), 0.83 (d, J = 6.9 Hz, 3H, CHC$\underline{H}_3$).
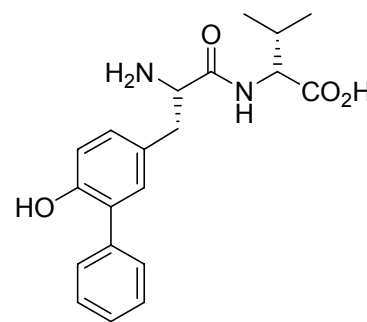
^{13}C NMR (125 MHz, MeOH-d$_4$): δ = 174.7, 169.9, 155.3, 139.6, 138.0, 133.1, 131.2, 131.1, 130.7, 130.5, 128.4, 126.5, 126.1, 117.1, 59.4, 55.8, 38.0, 31.6, 20.2, 19.5, 18.3.

MS (ESI) m/z 357.2 [M+H]$^+$, 713.2 [2M+Na]$^+$.

H-*m*-(*o*-tolyl)Tyr-D Val-OH (128).

RP-HPLC (10 → 50%) R_t = 23.1; 97% purity.

^{1}H NMR (500 MHz, MeOH-d$_4$): δ = 7.57-7.54 (m, 2H, H$_{arom}$), 7.40-7.36 (m, 2H, H$_{arom}$), 7.29 (dd, J = 7.4, 7.4 Hz, 1H, H$_{arom}$), 7.20 (d, J = 2.2 Hz, 1H, H$_{arom}$), 7.10 (dd, J = 8.3, 2.3 Hz, 1H, H$_{arom}$), 6.90 (d, J = 8.3 Hz, 1H, H$_{arom}$), 4.26 (d, J = 5.2 Hz, 1H, H$_\alpha$–Val), 4.18 (dd, J = 7.6, 7.6 Hz, 1H, H$_2$N-C$\underline{H}$), 3.13 (dd, J = 13.9, 7.6 Hz, 1H, H$_\beta$), 3.04 (dd, J = 13.9, 7.5 Hz, 1H, H$_\beta$), 2.08 (m, 1H, C$\underline{H}$CH$_3$), 0.82 (d, J = 6.9 Hz, 3H, CHC$\underline{H}_3$), 0.79 (d, J = 6.9 Hz, 3H, CHC$\underline{H}_3$).
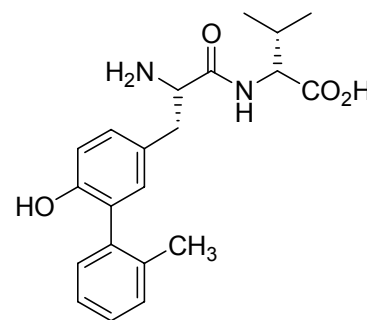
^{13}C NMR (125 MHz, MeOH-d$_4$): δ = 174.9, 169.9, 155.2, 139.8, 132.8, 130.6, 130.5, 130.4, 129.0, 127.9, 126.5, 117.6, 59.5, 55.9, 38.1, 31.6, 19.5, 18.2.

MS (ESI) m/z 371.2 [M+H]$^+$, 741.2 [2M+Na]$^+$.

H-1-(4-hydroxy)Nal-Val-OH (137).

RP-HPLC (10 → 80%) R_t = 14.7; 98% purity.

^{1}H NMR (500 MHz, MeOH-d$_4$): δ = 8.29 (d, J = 8.4 Hz, 1H, H$_{arom}$), 8.11 (d, J = 8.5 Hz, 1H, H$_{arom}$), 7.57 (dd, J = 7.6, 7.6 Hz, 1H, H$_{arom}$), 7.47 (dd, J = 7.6, 7.6 Hz, 1H, H$_{arom}$), 7.26 (d, J = 7.7 Hz, 1H, H$_{arom}$), 6.80 (d, J = 7.70 Hz, 1H, H$_{arom}$), 4.32 (d, J = 5.6 Hz, 1H, H$_\alpha$–Val), 4.28 (dd, J = 8.2, 6.6 Hz, 1H, H$_2$N-C$\underline{H}$), 3.64 (dd, J = 14.6, 6.5 Hz, 1H, H$_\beta$), 3.37 (dd, J = 14.6, 8.3 Hz, 1H, H$_\beta$), 2.17 (m, 1H, C$\underline{H}$CH$_3$), 0.98 (d, J = 6.9 Hz, 6H, CH(C$\underline{H}_3$)$_2$).
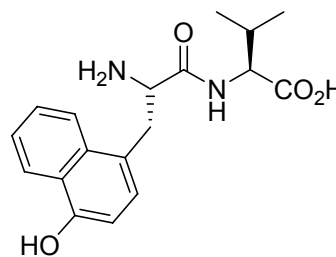
^{13}C NMR (125 MHz, MeOH-d$_4$): δ = 173.8, 170.1, 155.0, 134.4, 130.1, 127.9, 127.1, 125.7, 124.3, 124.1, 121.5, 108.5, 59.5, 54.8, 35.4, 31.8, 19.4, 18.5.

MS (ESI) m/z 331.1 [M+H]$^+$.

H-(D/L)-1-(4-hydroxy)Nal-Val-OH (138).

RP-HPLC (10 → 80%) R_t = 14.6, 18.5

^{1}H NMR (500 MHz, MeOH-d$_4$): δ = 8.28 (dd, J = 8.0, 5.4 Hz, 2H, H$_{arom}$), 8.10 (d, J = 8.5 Hz, 1H, H$_{arom}$), 8.04 (d, J = 8.5 Hz, 1H, H$_{arom}$), 7.57 (dd, J = 7.7, 7.7 Hz, 2H, H$_{arom}$), 7.47 (dd, J = 7.7, 7.7 Hz, 2H, H$_{arom}$), 7.26 (d, J = 7.7 Hz, 1H, H$_{arom}$), 7.22 (d, J = 7.7 Hz, 1H, H$_{arom}$), 6.80 (d, J = 7.4 Hz, 1H, H$_{arom}$), 6.79 (d, J = 7.5 Hz, 1H, H$_{arom}$), 4.34-4.23 (m, 3H, 2×H$_\alpha$–Val, H$_2$N-C$\underline{H}$), 4.07 (d, J = 5.6 Hz, 1H, H$_2$N-C$\underline{H}$), 3.64 (dd, J = 14.6, 6.5 Hz, 1H, H$_\beta$), 3.54 (dd, J = 13.9, 9.2 Hz, 1H, H$_\beta$), 3.44 (dd, J = 13.9, 6.6 Hz, 1H, H$_\beta$), 3.37 (dd, J = 14.6, 8.3 Hz, 1H, H$_\beta$), 2.22-2.11 (m, 1H, C$\underline{H}$CH$_3$), 1.88-1.78 (m, 1H, C$\underline{H}$CH$_3$), 0.98 (d, J = 6.9 Hz, 6H, 2×CHC$\underline{H}_3$), 0.62 (d, J = 6.9 Hz, 3H, CHC$\underline{H}_3$), 0.59 (d, J = 6.9 Hz, 3H, CHC$\underline{H}_3$).
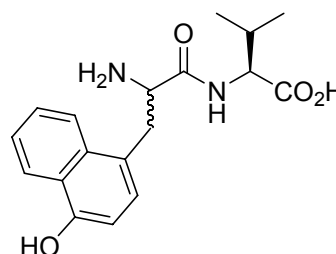
4.5 Synthesis of mono- and dimeric uPAR ligands

Peptide synthesis was carried out on TCP-resin following Fmoc-strategy according to the general procedures described above.[133-135,150]

4.5.1 Synthesis of monomeric WX360-based ligands

The linear precursor peptides were synthesized according to general procedures I-III described above. Boc-Lys(Fmoc)-OH was used for side-chain functionalization of lysine. DOTA-tris (*tert*-Bu ester)[487] was coupled according to general procedures II and IV (except: 1.5 equiv of DOTA-tris (*tert*-butyl ester), HOAt and HATU were used). Final cleavage and deprotection was accomplished according to general procedure VII. Intramolecular disulfide formation of was performed according to general procedure IX.

K(K(DOTA)-Aha-S-Aha)-WX360 (156)

R* = WX360 = -(D-Cys)-Asn-Lys-Tyr-Phe-Ser-Asn-Ile-His-Cys-Trp-OH
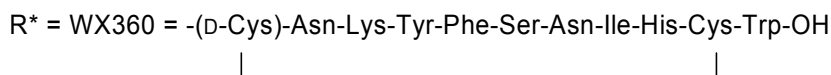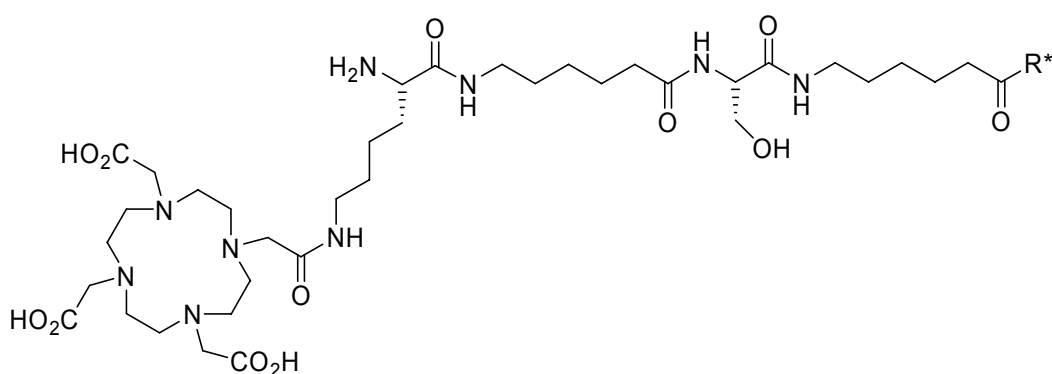
RP-HPLC (10 → 50%) R_t = 21.0

MS (ESI) calcd 2032.11; found 1116.7 [(M+2H)/2]$^+$.

K(DOTA-Aha-Ado-Aha)-WX360 (157)

R* = WX360 = -(D-Cys)-Asn-Lys-Tyr-Phe-Ser-Asn-Ile-His-Cys-Trp-OH
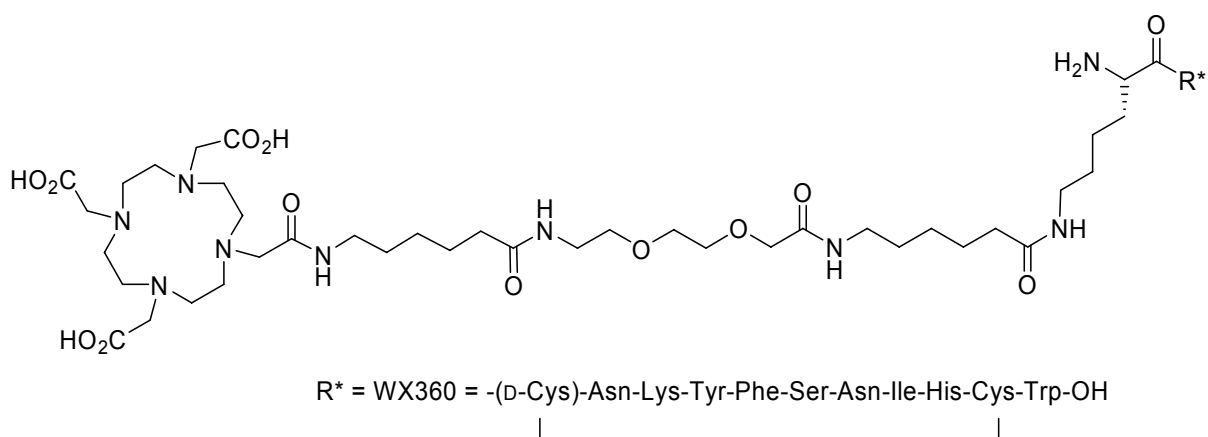
RP-HPLC (10 → 50%) R_t = 22.0

MS (ESI) calcd 2162.05; found 1081.6 [(M+2H)/2]$^+$, 721.6 [(M+3H)/3]$^+$.

4.5.2 Synthesis of monomeric AE105-based ligands

AE105-based ligands were synthesized according to general procedures I-III described above. Boc-Lys(Fmoc)-OH was used for side-chain functionalization of lysine. DOTA-tris (*tert*-butylester)[487] (Macrocyclics, Dallas, TX, USA) was coupled according to general procedures II and IV (exception: 1.5 equiv of DOTA-tris (*tert*-butyl ester), HOAt and HATU were used). Final cleavage and deprotection was accomplished according to general procedure VII.

DOTA-G-D-AE105 (158)
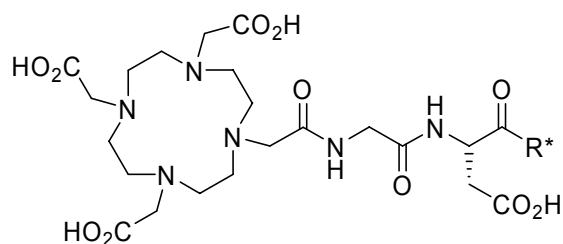
R* = AE105 = -Asp-Cha-Phe-(D-Ser)-(D-Arg)-Tyr-Leu-Trp-Ser-OH

RP-HPLC (5 → 50%) R_t = 25.9

MS (ESI) calcd 1783.84; found 1784.8 [M+H]$^+$, 893.4 [(M+2H)/2]$^+$.

DOTA-G-AE105 (159)
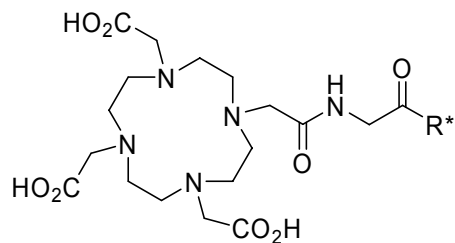
R* = AE105 = -Asp-Cha-Phe-(D-Ser)-(D-Arg)-Tyr-Leu-Trp-Ser-OH

RP-HPLC (5 → 50%) R_t = 25.8

MS (ESI) calcd 1668.81, found 1669.8 [M+H]$^+$, 835.9 [(M+2H)/2]$^+$.

DOTA-Aha-G-AE105 (160)
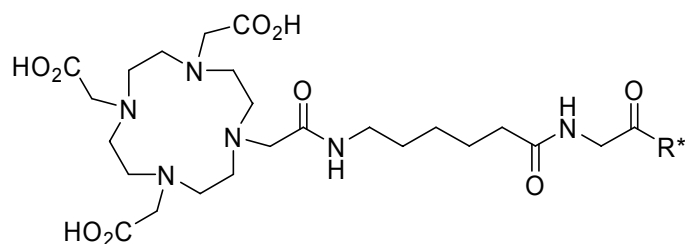
R* = AE105 = -Asp-Cha-Phe-(D-Ser)-(D-Arg)-Tyr-Leu-Trp-Ser-OH

RP-HPLC (5 → 50%) R_t = 25.7

MS (ESI) calcd 1781.90, found 1782.8 [M+H]$^+$, 892.5 [(M+2H)/2]$^+$.

DOTA-G-Aha-G-AE105 (161)
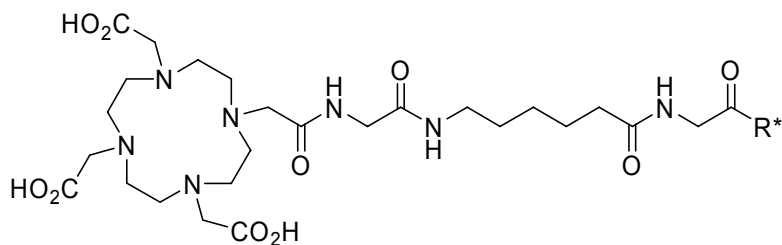
R* = AE105 = -Asp-Cha-Phe-(D-Ser)-(D-Arg)-Tyr-Leu-Trp-Ser-OH

RP-HPLC (5 → 50%) R_t = 26.1

MS (ESI) calcd 1838.92; found 1839.8 [M+H]$^+$, 921.0 [(M+2H)/2]$^+$.

DOTA-Aha-AE105 (162)
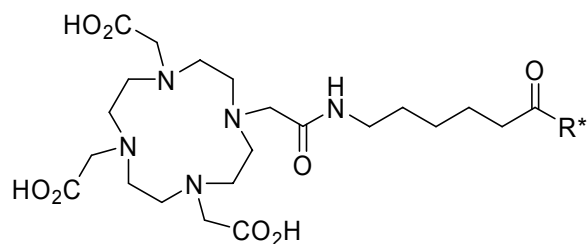
R* = AE105 = -Asp-Cha-Phe-(D-Ser)-(D-Arg)-Tyr-Leu-Trp-Ser-OH

RP-HPLC (5 → 50%) R_t = 26.5

MS (ESI) calcd 1724.88; found 1725.8 [M+H]$^+$, 863.9 [(M+2H)/2]$^+$.

DOTA-Aha-Ado-Aha-AE105 (165)
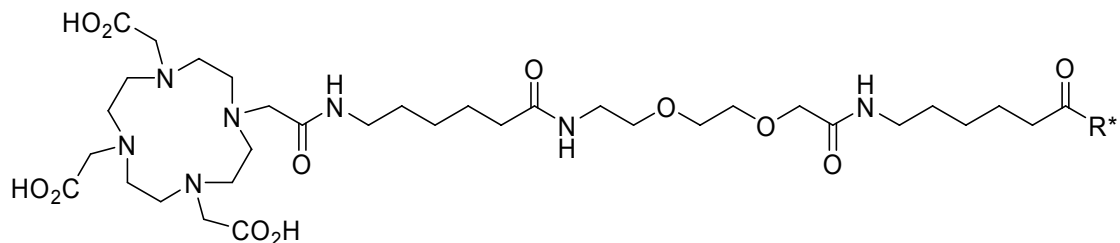
R* = AE105 = -Asp-Cha-Phe-(D-Ser)-(D-Arg)-Tyr-Leu-Trp-Ser-OH

RP-HPLC (10 → 50%) R_t = 25.4

MS (ESI) calcd 1983.00; found 1984.1 [M+H]$^+$, 993.2 [(M+2H)/2]$^+$.

K(DOTA-Aha)-S-Aha-AE105 (164)
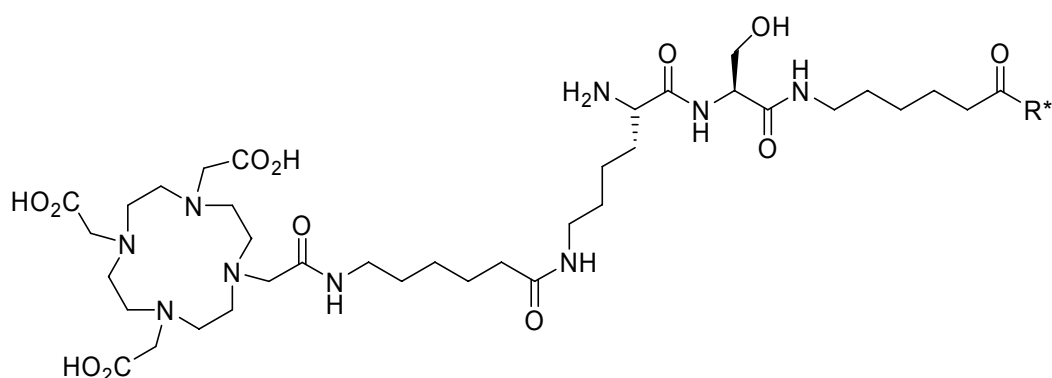
R* = AE105 = -Asp-Cha-Phe-(D-Ser)-(D-Arg)-Tyr-Leu-Trp-Ser-OH

RP-HPLC (10 → 50%) R_t = 23.7

MS (ESI) calcd 2053.09; found 1027.5 [(M+2H)/2]$^+$, 686.0 [(M+3H)/3]$^+$.

K(DOTA)-G-S-G-G-AE105 (163)
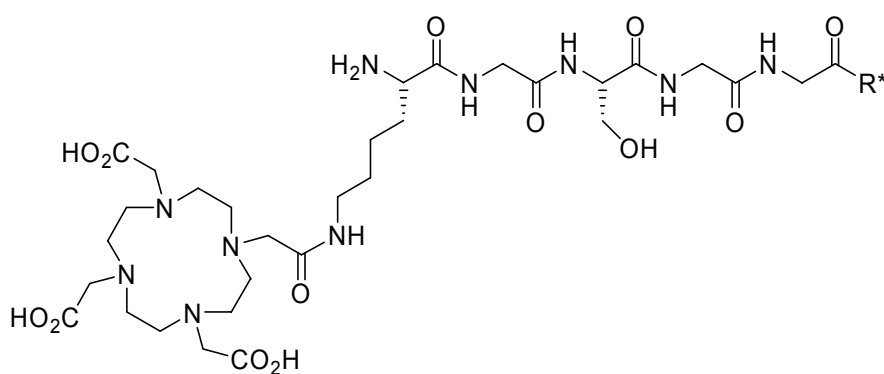
R* = AE105 = -Asp-Cha-Phe-(D-Ser)-(D-Arg)-Tyr-Leu-Trp-Ser-OH

RP-HPLC (5 → 50%) R_t = 24.8

MS (ESI) calcd 1997.98; found 1998.8 [M+H]$^+$, 1000.6 [(M+2H)/2]$^+$.

4.5.3 Synthesis of dimeric AE105-based ligands

The peptide sequence was built up by double coupling and subsequent capping according to general procedures I, II, III (2×) and V. The spacer sequence was attached by double coupling of the single building blocks and subsequent capping according to general procedures II, IV (2×) and V. Boc-Lys(Fmoc)-OH was used for side-chain functionalization of lysine. Dimerization was achieved according to general procedures II and VI and DOTA-tris (*tert*-butyl ester)[487] was attached by double coupling according to general procedures II and IV (2×). Final cleavage and deprotection was accomplished according to general procedure VII.

DOTA-(D-Glu)-[Aha-ᵋK-S-Aha-AE105]₂ (167)
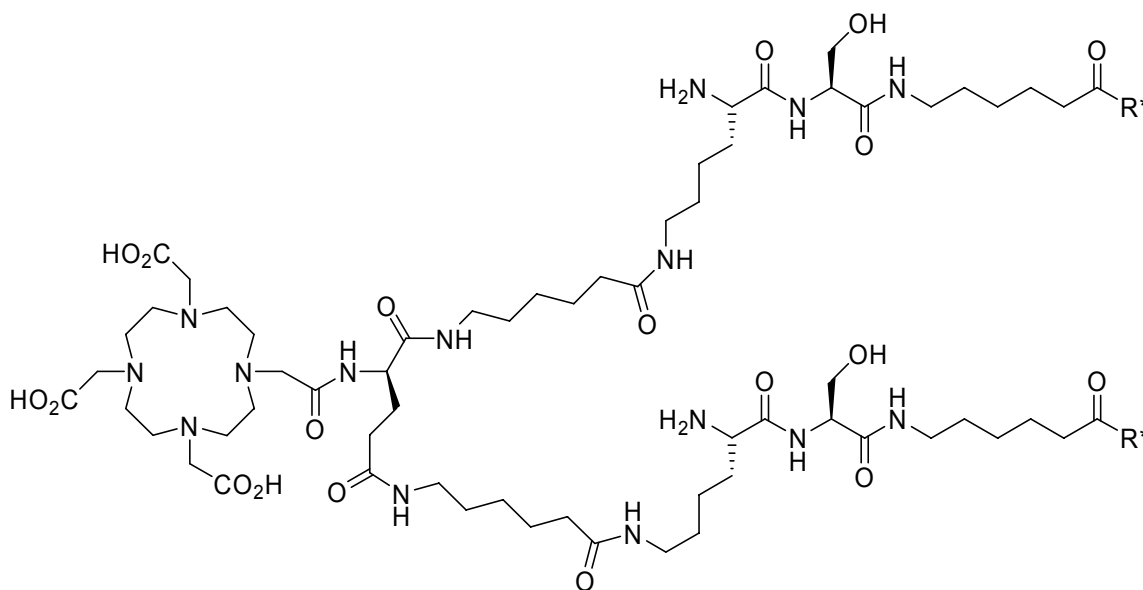
R* = AE105 = -Asp-Cha-Phe-(D-Ser)-(D-Arg)-Tyr-Leu-Trp-Se-OH

RP-HPLC (10 → 50%) R_t = 28.1

MS (ESI) calcd 3831.03; found 1917.2 $[(M+2H)/2]^+$, 1278.9 $[(M+3H)/3]^+$, 959.5 $[(M+4H)/4]^+$.

DOTA-(D-Glu)-[$^{\epsilon}$K-G-S-G-G-AE105]$_2$ (166)
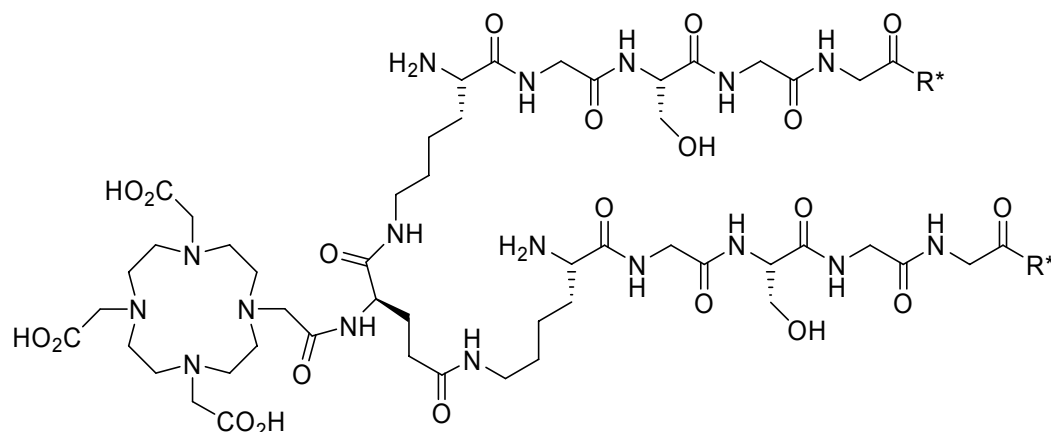
R* = AE105 = -Asp-Cha-Phe-(D-Ser)-(D-Arg)-Tyr-Leu-Trp-Ser-OH

RP-HPLC (20 → 60%) R_t = 20.8

MS (ESI) calcd 3720.82; found 1862.4 [(M+2H)/2]$^+$, 1242.1 [(M+3H)/3]$^+$, 931.9 [(M+4H)/4]$^+$.

DOTA-(D-Glu)-[Aha-Ado-Aha-AE105]$_2$ (168)
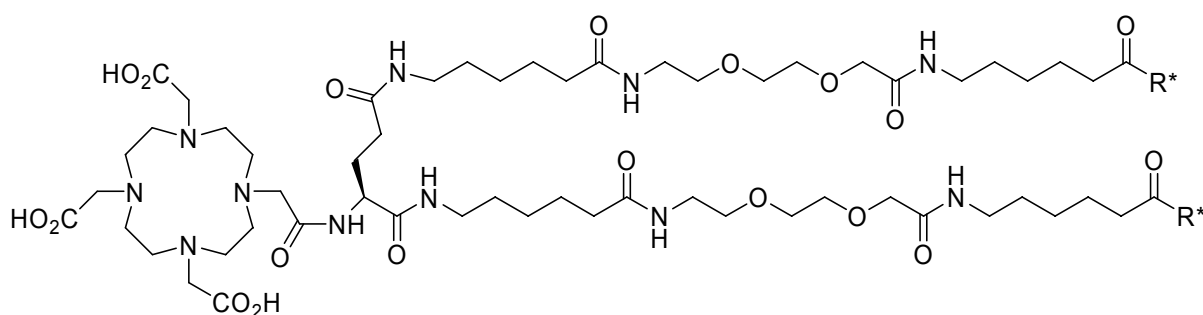
R* = AE105 = -Asp-Cha-Phe-(D-Ser)-(D-Arg)-Tyr-Leu-Trp-Ser-OH

RP-HPLC (10 → 50%) R_t = 29.6

MS (ESI) calcd 3690.92; found 1846.8 [(M+2H)/2]$^+$, 1231.3 [(M+3H)/3]$^+$.

4.6 Synthesis and application of keto- and alkynyl-functionalized DOTA derivatives

4.6.1 Synthesis of keto-functionalized DOTA derivatives

***tert*-Butyl 2-(4-acetylphenyl)acetate (178).**

To a degassed suspension of *tert*-butyl 2-bromoacetate (6.80 mL, 46.4 mmol, 1.0 equiv), Pd(OAc)$_2$ (336 mg, 1.50 mmol, 3 mol%), P(*o*-tolyl)$_3$ (1.36 g, 4.46 mmol, 10 mol%) and K$_2$CO$_3$ (34.6 g, 0.25 mol, 5.4 equiv) in THF (160 mL) under argon was added a solution of 4-acetylphenylboronic acid (176) (9.84 g, 60.0 mmol, 1.3 equiv) in THF/H$_2$O (160 mL/2.2 mL) drop wise over 1 h. After stirring for 18 h at room temperature, the mixture was filtered and the solvent removed under reduced pressure. The residue was taken up in EtOAc (250 mL) and subsequently washed with saturated aqueous NH$_4$Cl (150 mL), saturated aqueous NaHCO$_3$ (150 mL) and brine (150 mL). After drying over MgSO$_4$, the organic layer was filtered through silica gel and concentrated. Flash chromatography on silica gel (EtOAc/hexane 1:8) yielded 178 (8.30 g, 76%) as a pale yellow solid.
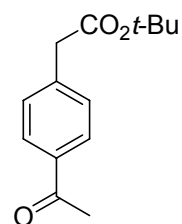
R_f = 0.27 (EtOAc/hexane, 1:4)
mp 50-52°C

^{1}H NMR (360 MHz, CDCl$_3$): δ = 7.92 (d, *J* = 8.2 Hz, 2H, H$_{arom}$), 7.37 (d, *J* = 8.1 Hz, 2H, H$_{arom}$), 3.58 (s, 2H, CH$_2$), 2.59 (s, 3H, COCH$_3$), 1.43 (s, 9H, C(CH$_3$)$_3$).

^{13}C NMR (90 MHz, CDCl$_3$): δ = 197.7, 170.0, 140.1, 135.8, 129.4 (2C), 128.5 (2C), 81.2, 42.6, 28.0, 26.5.

HRMS (EI) calcd for C$_{14}$H$_{18}$O$_3$ 234.12559; found 234.12532.

(R/S)-*tert*-Butyl 2-(4-acetylphenyl)-2-bromoacetate (180).

To a solution of 178 (2.84 g, 12.1 mmol, 1.0 equiv) in dry CCl_4 (250 mL) was added *N*-bromosuccinimide (NBS) (2.58 g, 14.5 mmol, 1.2 equiv) and Br_2 (2 drops). The mixture was heated to reflux, illuminated with a 500 W halogen lamp for 10 min and stirred for further 50 min under reflux. After cooling to room temperature, the reaction solution was filtered, the solvent concentrated and the crude product purified by flash chromatography on silica gel (EtOAc/hexane 1:10) to give 180 (3.34 g, 88%) as a pale yellow solid.
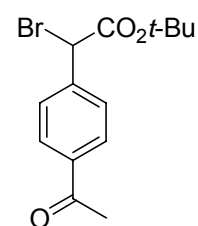
R_f = 0.27 (EtOAc/hexane, 1:4)
mp 54-56°C

^{1}H NMR (360 MHz, CDCl$_3$): δ = 7.93 (d, *J* = 8.4 Hz, 2H, H$_{arom}$), 7.62 (d, *J* = 8.3 Hz, 2H, H$_{arom}$), 5.27 (s, 1H, CH), 2.59 (s, 3H, COCH$_3$), 1.45 (s, 9H).

^{13}C NMR (90 MHz, CDCl$_3$): δ = 197.2, 166.6, 141.1, 137.3, 128.8 (2C), 128.6 (2C), 83.5, 47.1, 27.6, 26.6.

MS (EI) *m/z* (%) 314 (<1) [M(^{81}Br)]$^+$, 312 (<1) [M(^{79}Br)]$^+$, 241 (10) [M(^{81}Br)–O*t*Bu]$^+$, 239 (8) [M(^{79}Br)–O*t*Bu]$^+$.

HRMS (EI) calcd for C$_{10}$H$_8$^{81}BrO$_2$ [M(^{81}Br)–O*t*Bu] 240.96872; found 240.96833.
HRMS (EI) calcd for C$_{10}$H$_8$^{79}BrO$_2$ [M(^{79}Br)–O*t*Bu] 238.97076; found 238.97074.

(R/S)-*tert*-Butyl 2-[1-(1,4,7,10-tetraazacyclodecane)]-2-(4-acetylphenyl)acetate (182).

To a suspension of 1,4,7,10-tetraazacyclodecane (331 mg, 1.92 mmol, 1.2 equiv) and K_2CO_3 (552 mg, 3.99 mmol, 2.5 equiv) in DMF (60 mL) at room temperature was added a solution of 180 (500 mg, 1.60 mmol, 1.0 equiv) in DMF (50 mL) drop wise over 10 h. The mixture was filtered and concentrated under reduced pressure. Flash chromatography on silica gel (gradient MeOH/CHCl$_3$ 1:7 → 7:1, 1% NEt$_3$)
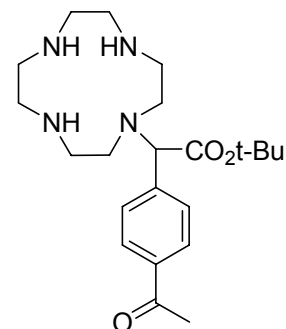
yielded 182 (488 mg, 75%) as a pale yellow solid.

R_f = 0.10 (MeOH/CHCl$_3$, 3:1, 1% NEt$_3$)

mp 33-36°C

^{1}H NMR (360 MHz, CDCl$_3$): δ = 7.91 (d, J = 8.4 Hz, 2H, H$_{arom}$), 7.43 (d, J = 8.2 Hz, 2H, H$_{arom}$), 4.62 (s, 1H, CH, H$_{arom}$), 2.90-2.67 (m, 11H, NH, NCHHCH$_2$), 2.64-2.44 (m, 10H, NH, NCHHCH$_2$, COCH$_3$), 1.47 (s, 9H, C(CH$_3$)$_3$).

^{13}C NMR (90 MHz, CDCl$_3$): δ = 197.4, 170.7, 142.3, 136.4, 129.3, 128.3, 81.9, 67.8, 49.3, 47.7, 45.9, 45.8, 28.1, 26.5.

HRMS (EI) calcd for C$_{22}$H$_{36}$N$_4$O$_3$ 404.27875; found 404.27951.

(R/S)-*tert*-Butyl 2-[1-(1,4,7,10-tetraazacyclodecane)-4,7,10-tris(*tert*-butyl-acetate)]-2-(4-acetylphenyl)acetate (173).

To a suspension of 182 (700 mg, 1.73 mmol, 1.0 equiv) and K$_2$CO$_3$ (1.08 mg, 7.79 mmol, 4.5 equiv) in DMF (50 mL) at room temperature was added a solution of *tert*-butyl 2-bromoacetate (0.84 mL, 5.71 mmol, 3.3 equiv) in DMF (20 mL) over 30 min. After stirring for 4 h, the mixture was filtrated and concentrated under reduced pressure.

Flash chromatography on silica gel (MeOH/CHCl$_3$ 1:7 → 9:1, 1% NEt$_3$) yielded 173 (930 mg, 72%) as a pale yellow solid.

RP-HPLC (10 → 100%) R_t = 22.0; 99% purity.

R_f = 0.83 (MeOH/CHCl$_3$, 3:1, 1% NEt$_3$)

mp 70-71°C

^{1}H NMR (360 MHz, CDCl$_3$): δ = 7.94 (d, J = 8.3 Hz, 2H, H$_{arom}$), 7.11 (d, J = 8.2 Hz, 2H, H$_{arom}$), 4.66 (s, 1H, CH), 3.60 (d, J = 17.3 Hz, 1H, NCHHCO$_2$), 3.45 (d, J = 17.6 Hz, 1H, NCHHCO$_2$), 3.38 (d, J = 17.5 Hz, 1H, NCHHCO$_2$), 3.22-3.05 (m, 3H, 3×NCHHCO$_2$), 2.98-2.70 (m, 6H, 6×NCHHCH$_2$), 2.61 (s, 3H, COCH$_3$), 2.61-2.48 (m, 2H, 2×NCHHCH$_2$), 2.46-2.38 (m, 1H, NCHHCH$_2$), 2.36-2.24 (m, 2H, 2×NCHHCH$_2$),
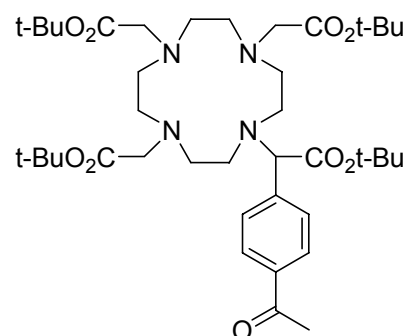
2.22-2.04 (m, 5H, 5×NC$\underline{H}$HCH$_2$), 1.49 (s, 9H, C(CH$_3$)$_3$), 1.48 (s, 9H, C(CH$_3$)$_3$), 1.46 (s, 9H, C(CH$_3$)$_3$), 1.39 (s, 9H, C(CH$_3$)$_3$).

^{13}C NMR (90 MHz, CDCl$_3$): δ = 197.6, 173.4, 173.1, 173.0, 172.9, 137.2, 136.6, 130.3 (2C), 128.1 (2C), 82.9, 82.2, 82.1, 82.0, 65.4, 56.0, 55.8, 55.5, 52.7, 52.4, 52.1, 48.5, 48.1, 48.0, 47.9, 44.5, 27.9 (3C), 27.8 (6C), 27.7 (3C), 26.6.

MS (EI) m/z (%) 746.0 (9) [M]$^+$, 645.1 (47) [M–CO$_2$$t$Bu]$^+$.
HRMS (EI) calcd for C$_{35}$H$_{57}$N$_4$O$_7$ [M–CO$_2$$t$Bu] 645.42273; found 645.42257.

Methyl 2-(4-acetylphenyl)acetate (177).

To a suspension of methyl 2-bromoacetate (3.55 mL, 37.5 mmol, 1.0 equiv), Pd(OAc)$_2$ (252 mg, 1.13 mmol, 3 mol%), P(o-tolyl)$_3$ (1.02 g, 3.35 mmol, 9 mol%) and K$_2$CO$_3$ (26.0 g, 0.19 mol, 5.0 equiv) in THF (120 mL) under argon was added a solution of 4-acetylphenylboronic acid (176) (7.38 g, 45.0 mmol, 1.2 equiv) in THF/H$_2$O (120 mL/1.7 mL) drop wise over 1 h. After stirring for 18 h at room temperature, the mixture was filtered and the solvent removed under reduced pressure. The residue was taken up in EtOAc (250 mL) and subsequently washed with saturated aqueous NH$_4$Cl (150 mL), saturated aqueous NaHCO$_3$ (150 mL) and brine. After drying over MgSO$_4$, the organic layer was filtered through a short column of silica gel and concentrated. Flash chromatography on silica gel (EtOAc/hexane 1:8) yielded 177 (4.73 g, 66%) as a pale yellow solid.
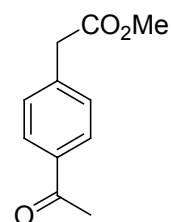
Rf = 0.13 (EtOAc/hexane, 1:4)

mp 44-44°C

^{1}H NMR (360 MHz, CDCl$_3$): δ = 7.91 (d, J = 8.3 Hz, 2H, H$_{arom}$), 7.36 (d, J = 8.3 Hz, 2H, H$_{arom}$), 3.69 (s, 3H, OCH$_3$), 3.68 (s, 2H, CH$_2$), 2.57 (s, 3H, COCH$_3$).

^{13}C NMR (90 MHz, CDCl$_3$): δ = 197.5, 171.1, 139.2, 136.0, 129.4 (2C), 128.5 (2C), 52.1, 40.9, 26.5.

HRMS (EI) calcd for C$_{11}$H$_{12}$O$_3$ 192.07864; found 192.07863.

(*R/S*)-Methyl 2-(4-acetylphenyl)-2-bromoacetate (179).

To a solution of 177 (3.00 g, 15.6 mmol, 1.0 equiv) in dry CCl_4 (300 mL) was added *N*-bromosuccinimide (3.36 g, 18.9 mmol, 1.2 equiv) and Br_2 (2 drops). The mixture was heated to reflux, illuminated with a 500 W halogen lamp for 10 min and stirred for further 50 min under reflux. After cooling to room temperature, the reaction solution was filtered, the solvent concentrated and the crude product purified by flash chromatography on silica gel (EtOAc/hexane 1:4) to give 179 (3.75 g, 89%) as a pale yellow oil.
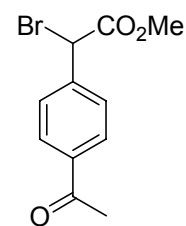
R_f = 0.18 (EtOAc/hexane, 1:4)

^{1}H NMR (360 MHz, $CDCl_3$): δ = 7.94 (d, J = 8.4 Hz, 2H, H_{arom}), 7.63 (d, J = 8.4 Hz, 2H, H_{arom}), 5.38 (s, 1H, CH), 3.79 (s, 3H, OCH_3), 2.59 (s, 3H, $COCH_3$).

^{13}C NMR (90 MHz, $CDCl_3$): δ = 197.1, 168.2, 140.4, 137.5, 128.9, 128.6, 53.5, 45.3, 26.6.

HRMS (EI) calcd for $C_{11}H_{11}{}^{81}BrO_3$ 271.98712; found 271.98716.
HRMS (EI) calcd for $C_{11}H_{11}{}^{79}BrO_3$ 269.98917; found 269.98863.

(*R/S*)-Methyl 2-[1-(1,4,7,10-tetraazacyclodecane)]-2-(4-acetylphenyl)acetate (181).

To a suspension of 1,4,7,10-tetraazacyclodecane (762 mg, 4.43 mmol, 1.2 equiv) and K_2CO_3 (1.27 g, 9.22 mmol, 2.5 equiv) in DMF (100 mL) at room temperature was added a solution of 179 (1.00 g, 3.69 mmol, 1.0 equiv) in DMF (60 mL) drop wise over 10 h. The mixture was filtrated and concentrated under reduced pressure. Flash chromatography on silica gel (gradient MeOH/$CHCl_3$ 1:7 → 7:1, 1% NEt_3) yielded 181 (829 mg, 62%) as a pale yellow solid.
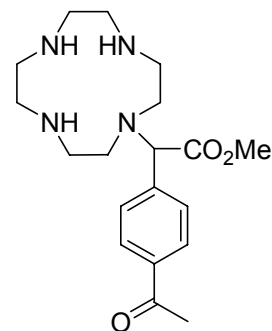
R_f = 0.10 (MeOH/$CHCl_3$, 3:1, 1% NEt_3)
mp 32-35°C

^{1}H NMR (500 MHz, MeOH-d$_4$): δ = 8.04 (d, J = 8.2 Hz, 2H, H$_{arom}$), 7.45 (d, J = 8.2 Hz, 2H, H$_{arom}$), 5.02 (s, 1H, CH), 3.77 (s, 3H, OCH$_3$), 3.37-3.30 (m, 2H, 2×NC$\underline{H}$HCH$_2$), 3.24-3.10 (m, 4H, 4×NC$\underline{H}$HCH$_2$), 3.09-3.01 (m, 4H, 4×NC$\underline{H}$HCH$_2$), 3.00-2.94 (m, 4H, 4×NC$\underline{H}$HCH$_2$), 2.63 (m, 5H, 2×NC$\underline{H}$HCH$_2$, COCH$_3$).

^{13}C NMR (125 MHz, MeOH-d$_4$): δ = 199.8, 174.1, 139.6, 138.4, 131.2 (2 C), 129.8 (2 C), 66.5, 53.2, 48.0 (2 C), 46.3 (2 C), 43.8 (2 C), 43.8 (2 C), 26.8.

MS (ESI) calcd for C$_{19}$H$_{30}$N$_4$O$_3$ 362.2; found 363.2 [M+H]$^+$.

(*R/S*)-Methyl 2-[1-(1,4,7,10-tetraazacyclodecane)-4,7,10-tris(*tert*-butyl-acetate)]-2-(4-acetyl-phenyl) acetate (183).

To a suspension of 181 (723 mg, 1.99 mmol, 1.0 equiv) and K$_2$CO$_3$ (1.24 g, 8.98 mmol, 4.5 equiv) in DMF (50 mL) at room temperature was added a solution of *tert*-butyl 2-bromoacetate (0.97 mL, 6.58 mmol, 3.3 equiv) in DMF (50 mL) over 30 min. After stirring for 4 h, the mixture was filtrated and concentrated under reduced pressure. Flash chromatography on silica gel (MeOH/CHCl$_3$ 1:10 → 7:1, 1% NEt$_3$) yielded 183 (830 mg, 83%) as a pale yellow solid.
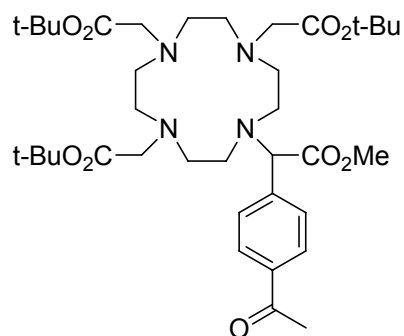
RP-HPLC (10 → 80%) R_t = 17.4; 99% purity.
R_f = 0.83 (MeOH/CHCl$_3$, 3:1, 1% NEt$_3$)
mp 73-75°C

^{1}H NMR (360 MHz, CDCl$_3$): δ = 7.95 (d, J = 8.3 Hz, 2H, H$_{arom}$), 7.16 (d, J = 8.1 Hz, 2H, H$_{arom}$), 4.75 (s, 1H, CH), 3.69 (s, 3H, OCH$_3$), 3.59 (d, J = 17.4 Hz, 1H, NC$\underline{H}$HCO$_2$), 3.42 (d, J = 17.5 Hz, 1H, NC$\underline{H}$HCO$_2$), 3.39 (d, J = 17.4 Hz, 1H, NC$\underline{H}$HCO$_2$), 3.24-3.05 (m, 3H, 3×NC$\underline{H}$HCO$_2$), 3.02-2.68 (m, 6H, 6×NC$\underline{H}$HCH$_2$), 2.59 (s, 3H, COCH$_3$), 2.57-2.42 (m, 4H, 4×NC$\underline{H}$HCH$_2$), 2.35-2.25 (m, 2H, 2×NC$\underline{H}$HCH$_2$), 2.25-2.15 (m, 2H, 2×NC$\underline{H}$HCH$_2$), 2.14-2.05 (m, 2H, 2×NC$\underline{H}$HCH$_2$), 1.48 (s, 9H, C(CH$_3$)$_3$), 1.45 (s, 18H, 2×C(CH$_3$)$_3$).

^{13}C NMR (90 MHz, CDCl$_3$): δ = 197.4, 174.5, 173.6, 173.1, 172.9, 136.9, 136.7, 130.2 (2C), 128.3 (2C), 82.5, 82.2, 82.1, 77.2, 64.8, 55.9, 55.7, 55.5, 52.7, 52.4, 52.3, 48.5, 48.0, 47.9, 47.8, 44.6, 27.9 (3C), 27.8 (3C), 27.7 (3C), 26.6.

HRMS (EI) calcd for C$_{22}$H$_{36}$N$_4$O$_3$ 404.27875; found 404.27951.

(*R/S*)-2-[1-(1,4,7,10-Tetraazacyclodecane)-4,7,10-tris(*tert*-butylacetate)]-2-(4-acetyl-phenyl)-acetic acid×½AcOH (174).

To a solution of **183** (26.0 mg, 31.7 µmol, 1.0 equiv) in THF (5 mL) at room temperature was added a solution of LiOH (1.75 mg, 72.9 µmol, 2.3 equiv) in water (150 µL) and the mixture was stirred for 18 h. After concentration under reduced pressure, the crude product was purified by preparative RP-HPLC (20 → 60%, 30 min) and lyophilized out of acetic acid to yield **2** (9.0 mg, 38%, 66% related to recovered **183**) as a colorless solid.
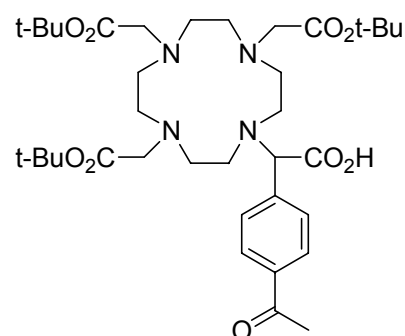
RP-HPLC (10 → 60%) R_t = 25.7; 94% purity.
mp 68-72 °C

^{1}H NMR (500 MHz, MeOH-d$_4$): δ = 8.06 (d, *J* = 8.2 Hz, 2H, H$_{arom}$), 7.63 (d, *J* = 8.1 Hz, 2H, H$_{arom}$), 5.12 (s, 1H, CH), 4.04-3.34 (m, 8H, 6×NC$\underline{H}$HCO$_2$, 2×NC$\underline{H}$HCH$_2$), 3.34-3.18 (m, 4H, 4×NC$\underline{H}$HCH$_2$), 3.15-2.66 (m, 10H, 10×NC$\underline{H}$HCH$_2$), 2.63 (s, 3H, COCH$_3$), 1.99 (s, ½×3H (AcOH)), 1.53 (s, 9H, C(CH$_3$)$_3$), 1.52 (s, 18H, 2×C(CH$_3$)$_3$).

^{13}C NMR (125 MHz, MeOH-d$_4$): δ = 199.7, 175.2, 172.7, 170.4 (br, 3C), 138.8 (2C), 132.7 (2C), 129.8 (2C), 84.1 (br, 3C), 69.9, 56.5, 52.9-51.0 (br, 8C), 29.5 (9C), 26.8, 20.8.

MS (ESI) calcd for C$_{36}$H$_{58}$N$_4$O$_9$ 690.4; found 691.4 [M+H]$^+$, 713.4 [M+Na]$^+$, 729.3 [M+K]$^+$.

4.6.2 Synthesis of alkynyl-functionalized DOTA derivatives

Methyl (4-iodophenyl)acetate (185).

To a solution of (4-iodophenyl)acetic acid (184) (15.0 g, 57.0 mmol) in dry methanol (50 mL) was added $SOCl_2$ (20.7 mL, 285 mmol, 5.0 equiv) drop wise at 0°C. After stirring for 1 h at room temperature, the solvent was removed under reduced pressure and the residue dissolved in Et_2O (400 mL). The organic phase was subsequently washed with saturated aqueous $NaHCO_3$ (400 mL), saturated aqueous NH_4Cl (400 mL) and brine (400 mL) and dried over $MgSO_4$. Concentration under reduced pressure yielded 185 (14.7 g, 93%).
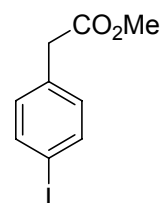
R_f = 0.57 (EtOAc/hexane, 1:4)

^{1}H NMR (360 MHz, $CDCl_3$): δ = 7.65 (d, J = 8.3 Hz, 2H, H_{arom}), 7.03 (d, J = 8.3 Hz, 2H, H_{arom}), 3.69 (s, 3H, OCH_3), 3.56 (s, 2H, CH_2).

^{13}C NMR (90 MHz, $CDCl_3$): δ = 171.3, 137.6, 133.5, 131.2, 92.5, 52.0, 40.5.

Methyl 2-(4-(2-(trimethylsilyl)ethynyl)phenyl)acetate (186).

To a solution of methyl (4-iodophenyl)acetate (185) (12.8 g, 45 mmol, 1.0 equiv), trimethylsilyl-acetylene (9.30 mL. 67.5 mmol, 1.5 equiv) and triethylamine (14.9 mL, 108 mmol, 2.4 equiv) in dry CH_3CN (120 mL) at 0°C under Argon was added $Pd(PPh_3)_4$ (3.6 g, 3.15 mmol, 0.07 equiv) and CuI (6.00 g, 31.5 mmol, 0.7 equiv). After stirring for 30 min at 0°C and 3 h at room temperature, the mixture was filtered through a short column of silica using EtOAc/hexane (1:1) as eluent. The solvent was removed under reduced pressure and the residue purified by flash chromatography on silica gel (gradient EtOAc/hexane 1:80 → 1:20) to yield 186 (10.3 g, 93%) as pale yellow crystals.
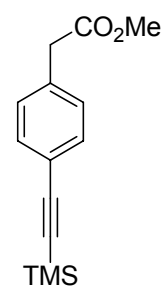
R_f = 0.27 (EtOAc/hexane, 1:10)
mp 55-58°C

^{1}H NMR (360 MHz, CDCl$_3$): δ = 7.42 (d, J = 8.4 Hz, 2H, H$_{arom}$), 7.21 (d, J = 8.5 Hz, 2H, H$_{arom}$), 3.68 (s, 3H, OCH$_3$), 3.61 (s, 2H, CH$_2$), 0.25 (s, 9H, Si(CH$_3$)$_3$).

^{13}C NMR (90 MHz, CDCl$_3$): δ = 171.4, 134.3, 132.0 (2C), 129.1 (2C), 122.0, 104.7, 94.2, 52.0, 41.0, 0.0 (3C).

HRMS (EI) calcd for C$_{14}$H$_{18}$O$_2$Si 246.10761; found 246.10744.

(*R/S*)-Methyl 2-bromo-2-(4-(2-(trimethylsilyl)ethynyl)phenyl)acetate (187).

To a solution of 186 (2.07 g, 8.40 mmol, 1.0 equiv) in dry THF (20 mL) at –78 °C was added lithium diisopropyl amide (2M solution in THF/n-heptane/ethylbenzene, 5.04 mL, 10.1 mmol, 1.2 equiv) and the solution stirred for 1 h. After this time, a suspension of *N*-bromosuccinimide (NBS) (1.79 g, 10.1 mmol, 1.2 equiv) in dry THF (20 mL) was added and the mixture warmed to room temperature over 18 h. The solvent was removed under reduced pressure, the residue suspended in CCl$_4$ (30 mL), filtered and evaporated. Purification by flash chromatography on silica gel (gradient EtOAc/hexane 1:80 $\rightarrow$ 1:20, 1% NEt$_3$) gave 187 (1.28 g, 47%; 92% related to recovered 186 (1.01 g, 49%)).
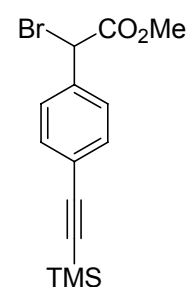
R_{f} = 0.42 (EtOAc/hexane, 1:10)
mp 82-84 °C

^{1}H NMR (360 MHz, CDCl$_3$): δ = 7.47 (d, J = 8.7 Hz, 2H, H$_{arom}$), 7.44 (d, J = 8.7 Hz, 2H, H$_{arom}$), 5.32 (s, 1H, CH), 3.77 (s, 3H, OCH$_3$), 0.25 (s, 9H, Si(CH$_3$)$_3$).

^{13}C NMR (90 MHz, CDCl$_3$): δ = 168.3, 135.7, 132.2 (2C), 128.5 (2C), 124.2, 104.1, 95.8, 53.3, 45.8, 45.8, –0.1 (3C).

HRMS (EI) calcd for C$_{14}$H$_{17}$^{81}BrO$_2$Si 326.01608; found 326.01622.

(*R/S*)-Methyl 2-[1-(1,4,7,10-tetraazacyclodecane)]-2-(4-(2-(trimethylsilyl)-ethynyl)phenyl)acetate (188).

To a suspension of 1,4,7,10-tetraazacyclodecane (cyclen) (548 mg, 3.18 mmol, 1.2 equiv) and K_2CO_3 (439 mg, 3.18 mmol, 1.2 equiv) in DMF (60 mL) at room temperature was added a solution of 187 (862 mg, 2.65 mmol, 1.0 equiv) in DMF (50 mL) drop wise over 10 h. The mixture was filtered and concentrated under reduced pressure. Flash chromatography on silica gel (gradient MeOH/CHCl$_3$ 1:9 → 9:1, 1% NEt$_3$) yielded 188 (590 mg, 53%) as a pale yellow solid.
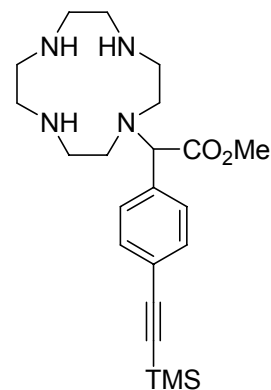
R_f = 0.10 (MeOH/CHCl$_3$, 3:1, 1% NEt$_3$)
mp 70-75°C

^{1}H NMR (500 MHz, MeOH-d$_4$): δ = 7.49 (d, J = 8.2 Hz, 2H, H$_{arom}$), 7.30 (d, J = 8.3 Hz, 2H, H$_{arom}$), 4.90 (s, 1H, CH), 3.78 (s, 3H, OCH$_3$), 3.21-3.01 (m, 6H, 6×NCHHCH$_2$), 3.01-2.82 (m, 8H, 8×NCHHCH$_2$), 2.71-2.62 (m, 2H, 2×NCHHCH$_2$), 0.23 (s, 9H, Si(CH$_3$)$_3$).

^{13}C NMR (125 MHz, MeOH-d$_4$): δ = 174.2, 135.6, 133.2 (2C), 130.8 (2C), 124.9, 105.4, 95.9, 67.2, 53.0, 48.4 (2C), 47.0 (2C), 44.9 (2C), 44.4 (2C), 0.0 (3C).

MS (ESI) calcd for $C_{22}H_{36}N_4O_2Si$ 416.3; found 417.4 [(M+H)]$^+$, 439.4 [(M+Na)]$^+$.

(*R/S*)-Methyl 2-[1-(1,4,7,10-tetraazacyclodecane)-4,7,10-tris(*tert*-butyl-acetate)]-2-(4-ethynyl)phenyl)acetate (175).

To a suspension of 188 (530 mg, 1.27 mmol, 1.0 equiv) and K_2CO_3 (634 mg, 4.57 mmol, 3.6 equiv) in DMF (50 mL) at room temperature was added a solution of *tert*-butyl 2-bromoacetate (615 µL, 4.19 mmol, 3.3 equiv) in DMF (20 mL) over 30 min. After stirring for 4 h, the mixture was filtered, concentrated under reduced pressure and the residue dissolved in THF (20 mL). Then, tetrabutylammonium fluoride (TBAF) (481 mg,
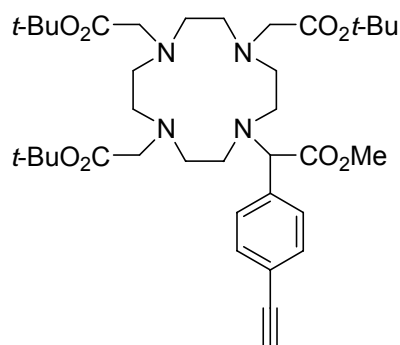
1.52 mmol, 1.2 equiv) was added and after stirring for 15 min, the solvent was removed and the crude product purified by flash chromatography on silica gel (MeOH/CHCl$_3$ 1:10, 1% NEt$_3$) to yield 175 (508 mg, 85%) as a pale yellow solid.

RP-HPLC (10 → 100%) R_t = 20.0; 99% purity.
R_f = 0.28 (MeOH/CHCl$_3$, 1:9, 1% NEt$_3$)
mp 63-68°C

^{1}H NMR (500 MHz, MeOH-d$_4$): δ = 7.48 (d, J = 8.2 Hz, 2H, H$_{arom}$), 7.20 (d, J = 8.0 Hz, 2H, H$_{arom}$), 4.83 (s, 1H, CH), 3.75 (d, J = 17.2 Hz, 1H, NCHHCO$_2$), 3.74 (s, 3H, OCH$_3$), 3.55 (s, 1H, C≡CH), 3.54 (d, J = 17.5 Hz, 1H, NCHHCO$_2$), 3.51 (d, J = 17.6 Hz, 1H, NCHHCO$_2$), 3.26-3.21 (m, 1H, NCHHCO$_2$), 3.18-3.05 (m, 4H, 2×NCHHCO$_2$, 2×NCHHCH$_2$), 2.99-2.92 (m, 3H, 3×NCHHCH$_2$), 2.89 (d, J = 17.6 Hz, 1H, NCHHCH$_2$), 2.87 (d, J = 17.6 Hz, 1H, NCHHCH$_2$), 2.74-2.63 (m, 2H, 2×NCHHCH$_2$), 2.33 (d, J = 11.5 Hz, 1H, NCHHCH$_2$), 2.28-2.12 (m, 4H, 4×NCHHCH$_2$), 2.12-2.05 (m, 2H, 2×NCHHCH$_2$), 1.54 (s, 9H, C(CH$_3$)$_3$), 1.52 (s, 18H, 2×C(CH$_3$)$_3$).

^{13}C NMR (125 MHz, MeOH-d$_4$): δ = 176.3, 175.4, 175.1, 174.7, 134.1, 132.8, 131.7, 123.8, 83.8, 83.5, 83.1, 79.7, 66.4, 59.61, 59.59, 59.57, 57.1, 56.8, 56.7, 54.2, 53.9, 53.7, 53.2, 45.9, 28.5, 28.4, 28.3, 24.8.

HRMS (EI) calcd for C$_{37}$H$_{58}$N$_4$O$_8$ 686.42546; found 686.42532.

4.6.3 Synthesis of aminooxy- and azido functionalized Tyr³-octreotate derivatives for chemoselective conjugation with keto- and alkynyl-functionalized DOTA derivatives

4.6.3.1 Synthesis of azido-functionalized linker (194)

1-Azido-3-aminopropane (193).

The literature procedure[635] was slightly modified: A solution of 1-bromo-3-aminopropane hydrobromide (5.47 g, 25.0 mmol, 1.0 equiv) and sodium azide (3.25 g, 50.0 mmol, 2.0 equiv) in 20 mL water was heated at 80°C for 24 h. The reaction mixture was cooled in an ice bath followed by addition of diethyl ether (30 mL). The pH was adjusted to 14 by addition of KOH pellets keeping the temperature below 10°C. After separation of the organic phase the aqueous layer was further extracted with diethyl ether. The combined organic layers were dried over MgSO$_4$ and carefully concentrated in *vacuo*. The remaining oil contained **193** (21.0 mmol; 84%) and about equimolar amounts of diethyl ether (based on integration of proton NMR) and was used without further purification. Spectroscopic data were identical to literature.[635]
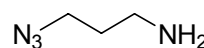
3-(3-Azidopropylcarbamoyl)propanoic acid (194).

To a solution of **193** (501 mg, 5.00 mmol, 1.1 equiv) and NEt$_3$ (693 µL, 5.00 mmol, 1.1 equiv) in 10 mL acetone was added a solution of succinic anhydride (460 mg, 4.55 mmol, 1.0 equiv) in 5 mL acetone over a period of 15 min at room temperature. The reaction mixture was stirred for 15 h at room temperature. After concentration in *vacuo* the residue was partitioned between diluted aqueous HCl (20 mL) and ethyl acetate (20mL), separated and the aqueous layer was further extracted with ethyl acetate (2×10 mL). After concentration of the combined organic layers **194** (653 mg, 3.27 mmol, 71 %) was obtained as a white solid.

228
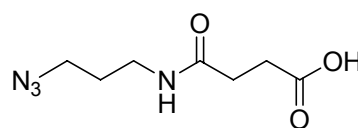
^{1}H NMR (360 MHz, MeOH-d$_4$): δ = 3.40-3.20 (m, 4H, N$_3$C$\underline{H}_2$CH$_2$C$\underline{H}_2$NH), 2.59 (dt, J = 6.5 Hz, 1.1 Hz, 2H, NHCOCH$_2$C$\underline{H}_2$CO$_2$H), 2.44 (dt, J = 6.7 Hz, 1.3 Hz, 2H, NHCO-C$\underline{H}_2$CH$_2$CO$_2$H), 1.74 (q, J = 6.8 Hz, 2H, CH$_2$C$\underline{H}_2$CH$_2$).

^{13}C NMR (90 MHz, MeOH-d$_4$): δ = 176.2, 174.7, 50.0, 37.7, 31.5, 30.2, 29.7.

MS (ESI) calcd for C$_{11}$H$_{12}$O$_3$ 200.1; found 201.1 (M+H$^+$).

4.6.3.2 Synthesis of Tyr^3-octreotate derivatives (190) and (196) and sample peptide (198).

Peptide synthesis was carried out on TCP-resin following Fmoc-strategy according to the general procedures described above.[133-135,150]

cyclo[2,7]-AoxAc-(D-Phe)-Cys-Tyr-(D-Trp)-Lys-Thr-Cys-Thr-OH (190) and **cyclo**[2,7]-3-(3-azidopropylcarbamoyl)propanoyl-(D-Phe)-Cys-Tyr-(D-Trp)-Lys-Thr-Cys-Thr-OH (196).

The linear peptide sequence H-(D-Phe)-Cys-Tyr-(D-Trp)-Lys-Thr-Cys-Thr-OH was synthesized on solid phase according to the general procedures I-III. Double-couplings were performed in every step. A sample was cleaved from the resin following procedure VII and the peptide sequence was confirmed by MALDI-TOF peptide sequence analysis. For the further procedure the resin was parted into two portions.

MS (MALDI) calcd for C$_{49}$H$_{66}$N$_{10}$O$_{12}$S$_2$ 1050.43; found 1051.40 [M+H]$^+$.

229

cyclo[2,7]-AoxAc-(D-Phe)-Cys-Tyr-(D-Trp)-Lys-Thr-Cys-Thr-OH (190):
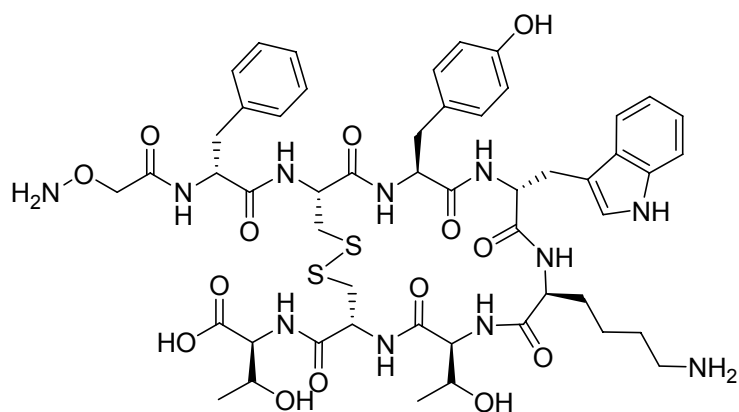
(Boc-aminoxy)acetic acid was coupled to one portion of above resin bound peptide in a similar manner to the general procedures I-III and the linear peptide was cleaved from resin following procedure VII. The disulfide cyclization was accomplished according to general procedure VIII. Great care must be taken to the quality of all solvents used in steps VII and VIII (HPLC quality). A small batch of the crude product was purified to obtain the aminooxy-functionalized Tyr[3]-octreotate 190 as a colorless solid in 58% yield after purification by semipreparative RP-HPLC (20 → 50%, 30 min).

RP-HPLC (10 → 60%) R_t = 17.3; 97% purity.

MS (ESI) calcd for $C_{51}H_{67}N_{11}O_{14}S_2$ 1121.4; found 1122.5 $[M+H]^+$, 562.1 $[(2M+2H)/2]^{2+}$.

cyclo[2,7]-3-(3-azidopropylcarbamoyl)propanoyl-(D-Phe)-Cys-Tyr-(D-Trp)-Lys-Thr-Cys-Thr-OH (196):
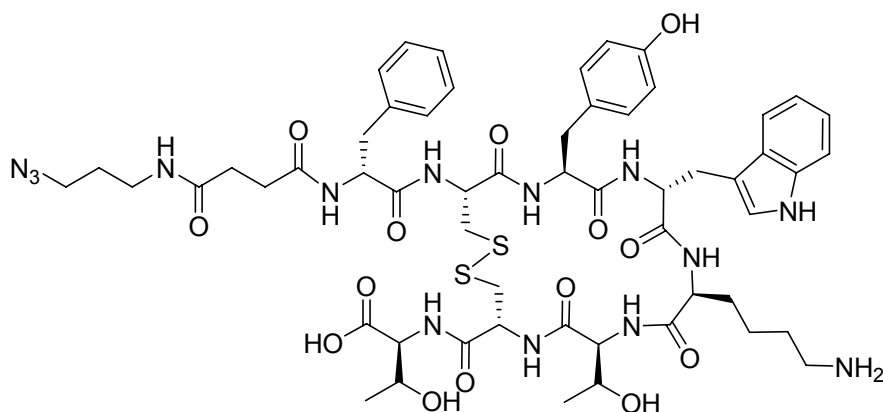
194 was coupled to one portion of above resin bound peptide in a similar manner to the general procedures I-III and the linear peptide was cleaved from resin following procedure VII. The disulfide cyclization was accomplished according to general procedure VIII. 196 was obtained as a colorless solid in 54% yield after purification by semipreparative RP-HPLC (20 → 60%, 30 min).

RP-HPLC (10 → 50%) R_t = 25.0; 96% purity.

MS (ESI) calcd for $C_{56}H_{74}N_{14}O_{14}S_2$ 1230.5; found 1231.6 [M+H]$^+$, 1253.6 [M+Na]$^+$, 1269.3 [M+K]$^+$.

Synthesis of 3-(3-azidopropylcarbamoyl)propanoyl-Tyr-Glu-Trp-Lys (198).
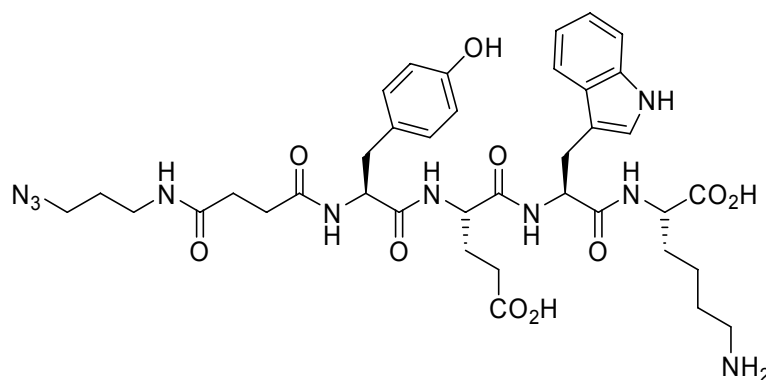
The linear peptide was synthesized on solid phase in a similar manner to the general procedures I-III and cleaved from resin following procedure VII. Peptide 198 was obtained as a colorless solid in 78% yield after purification by semipreparative RP-HPLC (20 → 50%, 30 min).

RP-HPLC (10 → 60%, 30 min) R_t = 16.8; 97% purity.

MS (ESI) calcd for $C_{38}H_{50}N_{10}O_{10}$ 806.37; found 807.6 [M+H]$^+$, 829.5 [M+Na]$^+$.

4.6.4 Chemoselective conjugation with unprotected biomolecules

Synthesis of DOTA-Tyr^3-octreotate derivative (191) *via* chemoselective oxime ligation.
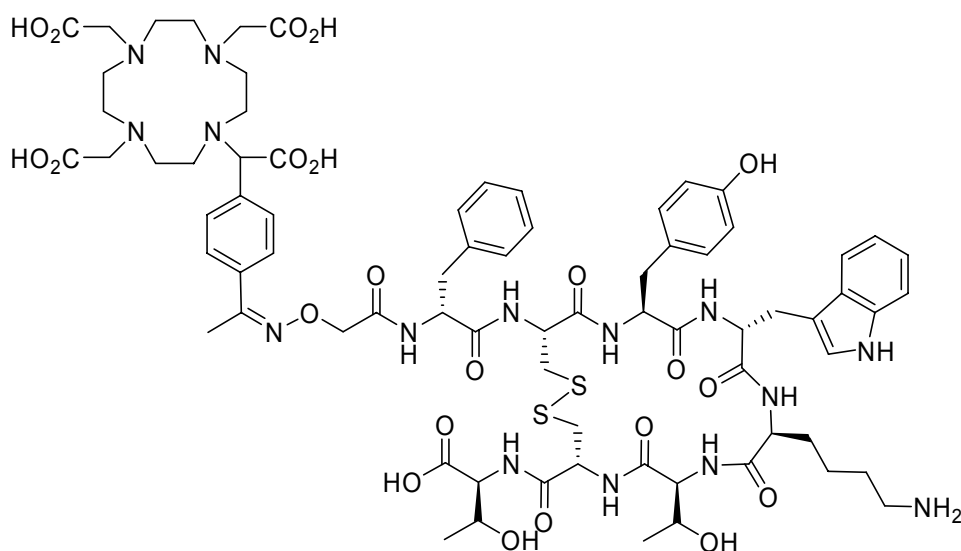
173 (3.3 mg, 4.5 µmol, 1.0 equiv) was deprotected in 10N aqueous HCl in dioxane (50/50, v/v; 2 mL) for 18 h after which the solvent was removed under reduced pressure. The residue was dissolved in CH_3CN/H_2O (1:1, v/v; 0.2 mL, HPLC grade) at pH 4 (TFA, HPLC grade) and 190 (6.1 mg, 4.5 µmol, 1.0 equiv) was added. After stirring for 18 h, the solvent was concentrated and the crude product was directly purified by semipreparative RP-HPLC (20 → 50%, 30 min) to yield 191 (6.1 mg, 73%) as a colorless powder after lyophilization.

RP-HPLC (10 → 60%) R_t = 18.1; 97% purity.

MS (ESI) calcd for $C_{75}H_{99}N_{15}O_{22}S_2$ 1625.7; found 1626.6 [M+H]$^+$, 1664.6 [M+K]$^+$.

Synthesis of DOTA-Tyr^3-octreotate derivative (197) *via* Cu(I)-catalyzed azide-alkyne cycloaddition.

To a solution of **175** (3.1 mg, 4.1 µmol, 1.0 equiv) in THF (0.2 mL) at room temperature was added a solution of LiOH (0.33 mg, 14 µmol, 3.4 equiv) in H$_2$O (30 µL) and the mixture stirred for 18 h. Subsequently, H$_2$O (0.2 mL), peptide **196** (5.5 mg, 4.1 µmol, 1.0 equiv), 0.1M aqueous CuSO$_4$ (49 µL, 4.9 µmol, 1.2 equiv) and copper powder (10 mg) were added and the mixture stirred for 18 h. After this time, the copper powder was filtered off, the solvent removed under reduced pressure and the *tert*-butyl esters were cleaved by treating with a mixture of TFA/triisopropyl silane/H$_2$O (95:5:5, v/v; 1 mL) for 2 h. The solvent was again removed and the residue was taken up THF/H$_2$O (1:1, v/v, 1 mL) to precipitate the copper salts by addition of Na$_2$S (Na$_2$S * 9H$_2$O; 12 mg, 49 µmol, 12.0 equiv). The mixture was filtrated and the crude product directly purified by semipreparative RP-HPLC (20 → 50%, 30 min) to yield linear **197** (3.0 mg, 37%) as a colorless powder after lyophilization. The linear peptide was recyclized in quantitative yield by stirring in CH$_3$CN/H$_2$O/DMSO (1:1:0.1, 4 mL) for 48h. After evaporation and lyophilization from CH$_3$CN/H$_2$O (1:2, v/v, 10 mL, pH 1-3 (TFA)), **197** (3.0 mg, 37% from **196**) was isolated as a white powder.

RP-HPLC (10 → 60%) R_t = 16.1; 97% purity.

MS (ESI) calcd for C$_{80}$H$_{106}$N$_{18}$O$_{22}$S$_2$ 1734.7; found 868.8 [(M+2H)/2]$^+$, 1735.5 [M+H]$^+$.

Synthesis of DOTA-Tyr-Glu-Trp-Lys derivative (199) *via* Cu(I)-catalyzed azide-alkyne cycloaddition.
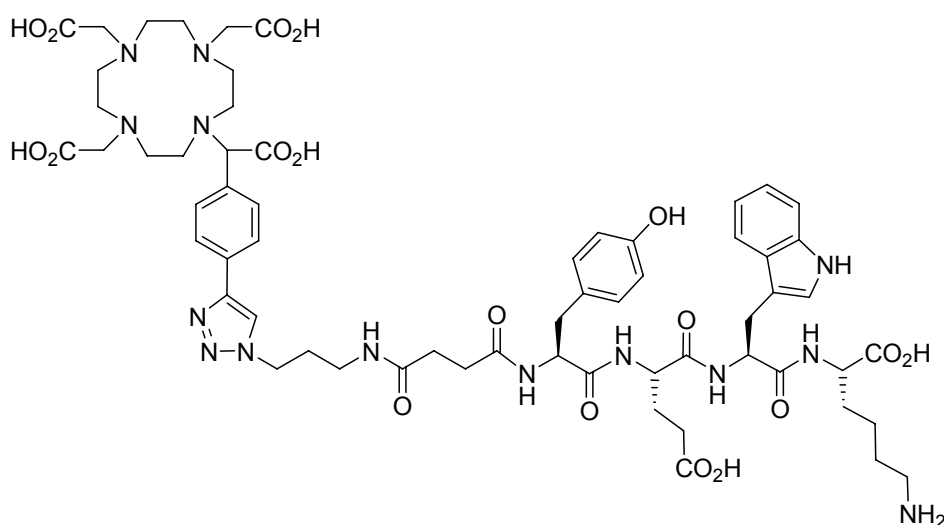
To a solution of 175 (3.1 mg, 4.1 µmol, 1.0 equiv) in THF (0.2 mL) at room temperature was added a solution of LiOH (0.3 mg, 14 µmol, 3.4 equiv) in water (30 µL) and the mixture was stirred for 18 h. Then, water (0.2 mL), peptide 198 (3.8 mg, 4.1 µmol, 1.0 equiv), 0.1 M aqueous CuSO$_4$ (49 µL, 4.9 µmol, 1.2 equiv) and copper powder (10 mg) were added subsequently and the mixture stirred for 18 h. After this time, the copper powder was filtered off and dissolved copper salts were precipitated by addition of Na$_2$S (Na$_2$S * 9H$_2$O; 12 mg, 49 µmol, 12.0 equiv). The mixture was filtrated and the solvent removed under reduced pressure. The *tert*-butyl esters were cleaved by treating with a TFA/TIPS/H$_2$O mixture (95:5:5, v/v/v; 1 mL) for 2 h. Thereafter, the solution was concentrated under reduced pressure and the crude product was directly purified by semipreparative RP-HPLC (20 → 50%, 30 min) to yield **199** (3.22 mg, 51%) as a colorless powder after lyophilization.

RP-HPLC (10 → 60%) R_t = 12.6; 95% purity.

MS (ESI) calcd for C$_{62}$H$_{82}$N$_{14}$O$_{18}$ 1310.59; found 656.9 [(M+2H)/2]$^+$, 667.9 [(M+H+Na)/2]$^+$, 1311.8 [M+H]$^+$, 1333.6 [M+Na]$^+$, 1349.5 [M+K]$^+$.

4.7   Preparation of cross-linked polymer sticks

General procedure

Cross-linked polymer sticks were prepared in glass tubes. The tubes were carefully dried and treated with a 1:1 mixture of chlorotrimethylsilane and dichlorodimethylsilane for 18 hours to ensure apolar surfaces. After washing with dichloromethane (5 times) the tubes were dried at 50°C and one end was sealed by melting. The monomer and the cross-linking agent were filtered through basic aluminum oxide (pH 10) and distilled under reduced pressure. Immediately before polymerization the monomers were degassed for 15 minutes by ultrasound in *vacuo* and ventilated in an argon atmosphere. After carefully mixing monomer, cross-linking agent and 2,2'-azobis(2-methylpropionitrile) (AIBN) to desired concentrations the mixture was filled into the prepared glass tubes and their tops sealed. Polymerization was performed for 5 days at 45°C and 2 days at 60°C.

Poly(styrene-co-divinylbenzene) sticks (P1)

The sticks were prepared from styrene and *p*-divinylbenzene (0.05, 0.10, 0.20, 0.50, 0.75, 1.00, 1.50, 2.00, 3.00, 5.00%; v/v) according to the general procedure described above. AIBN was added in the concentrations 0.005, 0.010, 0.025, 0.050, 0.075, 0.100 and 0.500% (w/v). Polymerization was carried out in glass tubes with inner diameters of 1.6, 2.4, 3.4 and 4.0 mm.
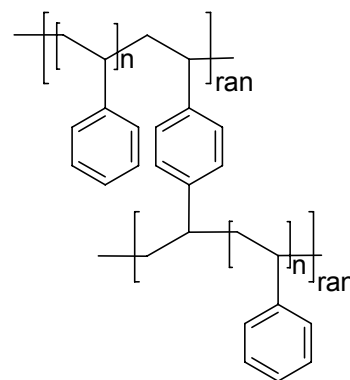
Poly(styrene-d₈-co-divinylbenzene) sticks (P2)

The sticks were prepared according to the general procedure described above except that styrene-d$_8$ was purified *via* condensation instead of distillation. Styrene-d$_8$ was mixed with variable amounts of *p*-divinylbenzene (0.2, 0.5 and 1.0%; v/v) and 0.1% (w/v) AIBN was added. Polymerization was carried out in glass tubes with inner diameter of 3.4 mm.
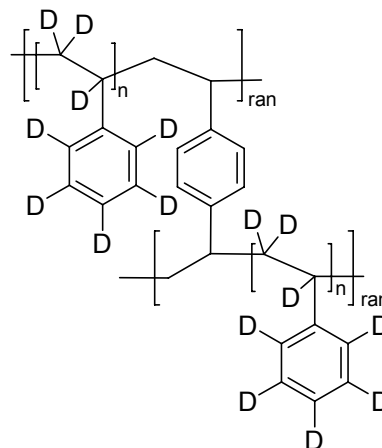
Poly(methyl methacrylate-co-ethylenglycol dimethacrylate) sticks (P3)

The sticks were prepared from methyl methacrylate and ethylenglycol dimethacrylate (0.05, 0.10, 0.20, 0.50, 0.75, 1.00, 1.50, 2.00, 3.00 and 5.00%; v/v) according to the general procedure described above. AIBN was added in the concentrations of 0.025, 0.050, 0.075, 0.100, 0.500% (w/v). Polymerization was carried out in glass tubes with inner diameters of 1.6, 2.4, 3.4 and 4.0 mm.
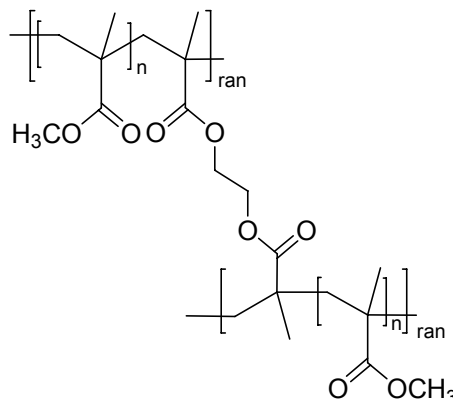
Poly(vinyl acetate-co-adipic acid divinylester) sticks (P4)

The sticks were prepared from vinyl acetate and adipic acid divinylester (0.05, 0.10, 0.20, 0.50, 0.75, 1.00, 1.50, 2.00, 3.00 and 5.00%; v/v) according to the general procedure described above. AIBN was added in the concentrations 0.10 and 0.50% (w/v). Polymerization was carried out in glass tubes with inner diameters of 1.6, 2.4, 3.4 and 4.0 mm.
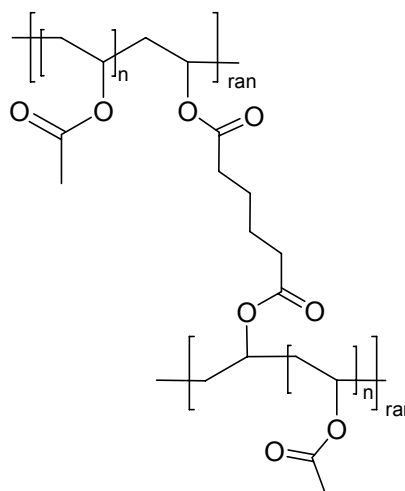
(*S*)-1-Benzyloxycarbonylethyl acrylate (213)

(*S*)-2-Hydroxypropionic acid benzylester (3.60 g, 20.0 mmol, 1.0 equiv) and DMAP (0.22 g, 2.00 mmol, 0.1 equiv) were dissolved in dry DCM (100 mL). After cooling to –78 °C, DIPEA (10.6 mL, 62.0 mmol, 3.1 equiv) and acryloyl chloride (211) (2.20 mL, 25.0 mmol, 1.3 equiv) were added subsequently and the mixture was stirred for 3 h. Thereafter, DCM (100 mL) and saturated aqueous NaCl (100 mL) were added and the aqueous layer was extracted with DCM (2×50 mL). The combined organic layers were dried over MgSO$_4$ and the solvent was removed in *vacuo*. Purification by flash chromatography on silica gel (EtOAc/hexane 1:10) yielded 213 (4.2 g, 58%) as a colorless oil.
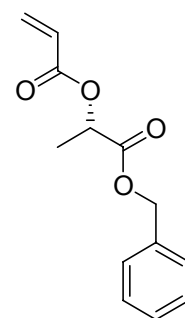
^{1}H NMR (250 MHz, CDCl$_3$): δ = 7.44-7.24 (m, 5H, H$_{arom}$), 6.30 (dd, *J* = 17.5, 1.6 Hz, 1H, C$\underline{H}_{cis}$HCH), 6.28-6.08 (m, 1H, CH$_2$C$\underline{H}$), 5.87 (dd, *J* = 10.0, 1.6 Hz, 1H, C$\underline{H}_{trans}$HCH), 5.30-5.10 (m, 3H, C$\underline{H}_2$Ph, C$\underline{H}$CH$_3$), 1.5 (d, *J* = 2.7 Hz, 3H, CHC$\underline{H}_3$).

Poly((*S*)-1-benzyloxycarbonylethyl acrylate-co-ethylenglycol dimethacrylate) sticks (P5)

The sticks were prepared from (*S*)-1-benzyloxycarbonyl ethyl acrylate (213), ethylenglycol dimethacrylate (204) (0.50 and 1.00%; v/v) and 0.10% (w/v) AIBN according to the general procedure described above. Polymerization was carried out in glass tubes with an inner diameter of 4.0 mm.

237
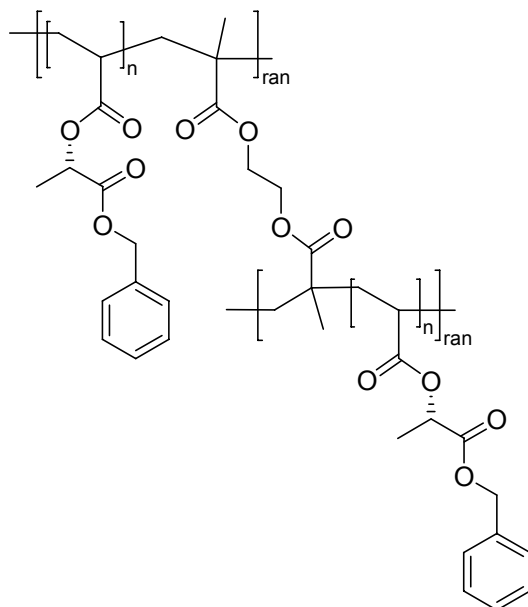
(*S*)-1-Carbamoylethyl acrylate (212)

(*S*)-2-Hydroxypropanamide (207) (4.00 g, 45.0 mmol, 1.0 equiv) and DMAP (0.50 g, 4.50 mmol, 0.1 equiv) were dissolved in dry DCM (100 mL). After cooling to –78°C, DIPEA (24.0 mL, 140 mmol, 3.1 equiv) and acryloyl chloride (211) (5.00 mL, 56.0 mmol, 1.3 equiv) were added subsequently and the mixture was stirred for 3 h. Thereafter, DCM (100 mL) and saturated aqueous NaCl (100 mL) were added and the aqueous layer was extracted with DCM (2×50 mL). The combined organic layers were dried over MgSO$_4$ and the solvent was removed in *vacuo*. Purification by flash chromatography on silica gel (EtOAc/hexane 1:1) yielded 212 (3.67 g, 59%) as a colorless oil.
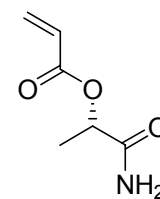
^{1}H NMR (250 MHz, CDCl$_3$): δ = 6.50 (dd, *J* = 17.5, 1.4 Hz, 1H, C<u>H</u>$_{cis}$HCH), 6.18 (dd, *J* = 17.2, 10.4 Hz, 1H, CH$_2$C<u>H</u>), 5.93 (dd, *J* = 12.5, 1.4 Hz, 1H, C<u>H</u>$_{trans}$HCH), 5.30 (q, *J* = 6.9 Hz, 1H, C<u>H</u>CH$_3$), 1.53 (d, *J* = 6.9 Hz, 3H, CHC<u>H</u>$_3$).

Poly(methyl acrylate-co-(*S*)-1-benzyloxycarbonylethyl acrylate-co-ethylenglycol dimethacrylate) sticks (P7)

Methyl acrylate (216) was mixed with (*S*)-1-benzyloxycarbonyl ethyl acrylate (212) (1:3; v/v), 1.00% (v/v) ethylenglycol dimethacrylate (204) and 0.10% (w/v) AIBN. Polymerization was carried out according to the general procedure described above in glass tubes with an inner diameter of 4.0 mm.
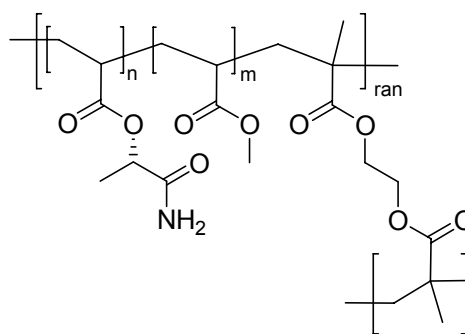
(*R*)-(5-Ethylquinuclidin-2-yl)(6-methoxyquinolin-3-yl)methyl acrylate (215)

Dihydroquinine (210) (13.0 g, 40.0 mmol, 1.0 equiv) and DMAP (0.40 g, 4.00 mmol, 0.1 equiv) were dissolved in dry DCM (100 mL). After cooling to –78°C, DIPEA (20.8 mL, 124 mmol, 3.1 equiv) and acryloyl chloride (211) (4.00 mL, 50.0 mmol, 1.3 equiv) were added subsequently and the mixture was stirred for 3 h.
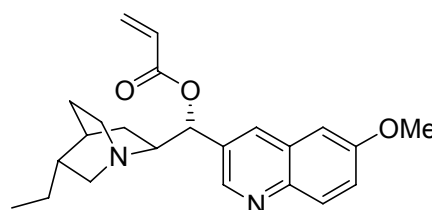
238

Thereafter, DCM (100 mL) and saturated aqueous NaCl (100 mL) were added and the aqueous layer was extracted with DCM (2×50 mL). The combined organic layers were dried over $MgSO_4$ and the solvent was removed in *vacuo*. Purification by flash chromatography on silica gel (MeOH/DCM 1:100, 1% NEt_3) yielded 215 (8.50 g, 56%) as a yellow oil.

^{1}H NMR (250 MHz, CDCl$_3$): δ = 8.68 (d, J = 4.7 Hz, 1H, H$_{arom}$), 7.95 (d, J = 9.2 Hz, 1H, H$_{arom}$), 7.52-7.38 (m, 1H, H$_{arom}$), 7.37-7.24 (m, 2H, H$_{arom}$), 6.61-6.41 (m, 2H, C$\underline{H}_{cis}$HC$\underline{H}$), 6.23-6.03 (m, 1H, C$\underline{H}_{trans}$HCH), 5.83 (d, J = 10.7 Hz, 1H, OC$\underline{H}$CH), 4.01-3.81 (m, 3H, OCH$_3$), 3.44-3.24 (m, 1H, OCHC$\underline{H}$), 3.10-2.90 (m, 2H, NC$\underline{H}_2$), 2.64-2.44 (m, 2H, NC$\underline{H}_2$), 1.44-1.24 (m, 6H, C$\underline{H}_2$C$\underline{H}$(C$\underline{H}_2$)C$\underline{H}$), 1.08-0.88 (m, 2H, C$\underline{H}_2$CH$_3$), 0.90-0.70 (m, 3H, CH$_2$C$\underline{H}_3$).

Poly(methyl acrylate-co-(*R*)-(5-ethylquinuclidin-2-yl)(6-methoxyquinolin-3-yl)methyl acrylate-co-ethylenglycol dimethacrylate) sticks (P9)

Methyl acrylate (216) was mixed with (*R*)-(5-ethylquinuclidin-2-yl) (6-methoxyquinolin-3-yl) methyl acrylate (215) in the ratios: 4:1, 6:1, 8:1, 12:1, and 16:1 (v/v). 0.50% (v/v) ethyleneglycol dime-thacrylate (204) and 0.10% (w/v)
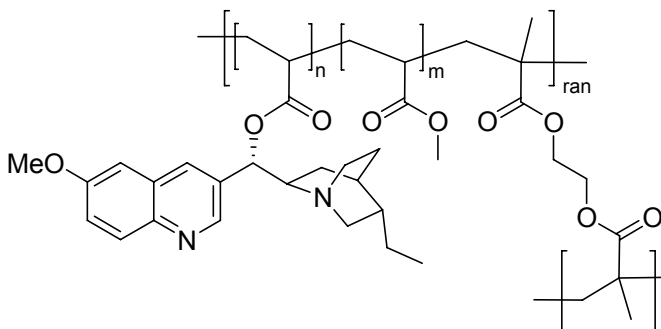
AIBN were added and polymerization was carried out according to the general procedure described above in glass tubes with an inner diameter of 4.0 mm.

(*S*)-1-((Benzyloxy)carbonyl)-2-phenylethyl acrylate (214)

(*S*)-benzyl 2-hydroxy-3-phenylpropanoate (209) (5.00 g, 19.5 mmol, 1.0 equiv) and DMAP (0.20 g, 1.95 mmol, 0.1 equiv) were dissolved in dry DCM (100 mL). After cooling to –78 °C, DIPEA (10.4 mL, 60.5 mmol, 3.1 equiv) and acryloyl chloride (211) (2.00 mL, 24.4 mmol, 1.3 equiv) were added subsequently and the mixture was stirred for 3 h. Then, DCM (100 mL) and saturated aqueous NaCl (100 mL) were added and the aqueous layer was extracted with DCM (2×50 mL). The combined organic layers were dried over MgSO$_4$ and the solvent was removed in *vacuo*. Purification by flash chromatography on silica gel (EtOAc/hexane 1:10) yielded 214 (4.33 g, 72%) as a colorless oil.
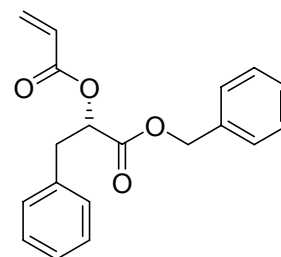
^{1}H NMR (250 MHz, CDCl$_3$): δ = 7.41-7.24 (m, 10H, H$_{arom}$), 6.48 (dd, *J* = 17.5, 1.4 Hz, 1H, C$\underline{H}_{cis}$HCH), 6.25-6.14 (m, 1H, CH$_2$C$\underline{H}$), 5.90 (dd, *J* = 10.0, 1.4 Hz, 1H, C$\underline{H}_{trans}$HCH), 5.21 (s, 2H, OC$\underline{H}_2$Ph), 5.52-5.32 (m, 1H, C$\underline{H}$CH$_2$Ph) 3.30-3.20 (m, 2H, CHC$\underline{H}_2$Ph).

Poly(methyl acrylate-co-(*S*)-1-((benzyloxy)carbonyl)-2-phenylethyl acrylate-co-ethylen-glycol dimethacrylate) sticks (P8)

Methyl acrylate (216) was mixed with (*S*)-1-((benzyloxy)carbonyl)-2-phenylethyl acrylate (214) (1:1; v/v), 1.00% (v/v) ethylenglycol dimethacrylate (204) and 0.10% (w/v) AIBN. Polymerization was carried out according to the general procedure described above in glass tubes with an inner diameter of 4.0 mm.
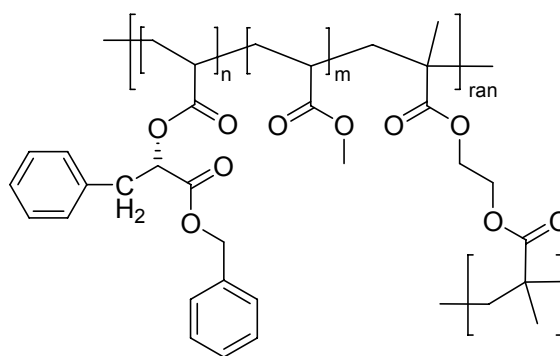
Poly((*S*)-1-((benzyloxy)carbonyl)-2-phe-nylethyl acrylate-co-ethylen-glycol dimethacrylate) sticks (P6)

The sticks were prepared from (*S*)-1-((benzyloxy)carbonyl)-2-phenylethyl acrylate (214), ethylenglycol di-methacrylate (204) (0.50 and 1.00%; v/v) and 0.10% (w/v) AIBN according to the general procedure described above. Polymerization was carried out in glass tubes with an inner diameter of 4.0 mm.
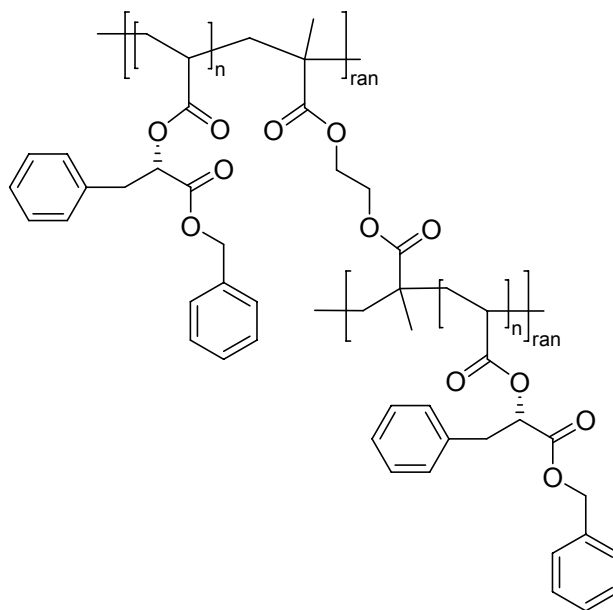
5 Appendix

Supplementary Data 1. Summary of clotting factors and characteristics

Factor	Trivial Name(s)	Pathway	Characteristic
Prekallikrein (PK)	Fletcher factor	Intrinsic	Functions with HMWK and FXII
High molecular weight kininogen (HMWK)	contact activation cofactor; Fitzgerald, Flaujeac Williams factor	Intrinsic	Cofactor in kallikrein and factor XII activation, necessary in FXIIa activation of FXI,
I	Fibrinogen	Both	-
II	Prothrombin	Both	Contains N-term. *gla* segment
III	Tissue Factor (TF)	Extrinsic	subendothelial cell-surface receptor of and cofactor for FVII -
IV	Calcium	Both	-
V	Proaccelerin	Both	
VI (same as Va)	Accelerin	Both	Protein cofactor
VII	Proconvertin	Extrinsic	Endopeptidase with *gla* residues
VIII	Antihemophiliac factor A,	Intrinsic	Protein cofactor
IX	Christmas Factor, antihemophilic factor B	Intrinsic	Endopeptidase with *gla* residues
X	Stuart-Prower Factor	Both	Endopeptidase with *gla* residues
XI	Plasma thromboplastin antecedent (PTA)	Intrinsic	Endopeptidase
XII	Hageman Factor	Intrinsic	Endopeptidase
XIII	fibrin stabilizing factor (FSF), fibrinoligase	Both	Transpeptidase

Supplementary Data 2. Regulatory and other proteins involving clot formation.

Protein	Function
von Willebrand factor (vWF)	Associated with subendothelial connective tissue; serves as a bridge between platelet glycoprotein GPIb/IX and collagen
Protein C (PC)	Activated to protein Ca (APC) by thrombin bound to thrombomodulin; then degrades factors VIIIa and Va
Protein S (PS)	Acts as a cofactor of protein C; both proteins contain *gla* residues
Thrombomodulin	Protein on the surface of endothelial cells; binds thrombin, which then activates protein C
Antithrombin III	Most important coagulation inhibitor, controls activities of thrombin and factors IXa, Xa, XIa and XIIa

Supplementary Data 3. Kinetic analysis of ligand immobilization

Immobilization kinetics of ligand 3 (EYHSWEYC) binding to Toyopearl AF-Epoxy-650M resin at different concentrations expressed as % of free peptides in solution.

Immobilization kinetics of EYHSWEYC (**1**)
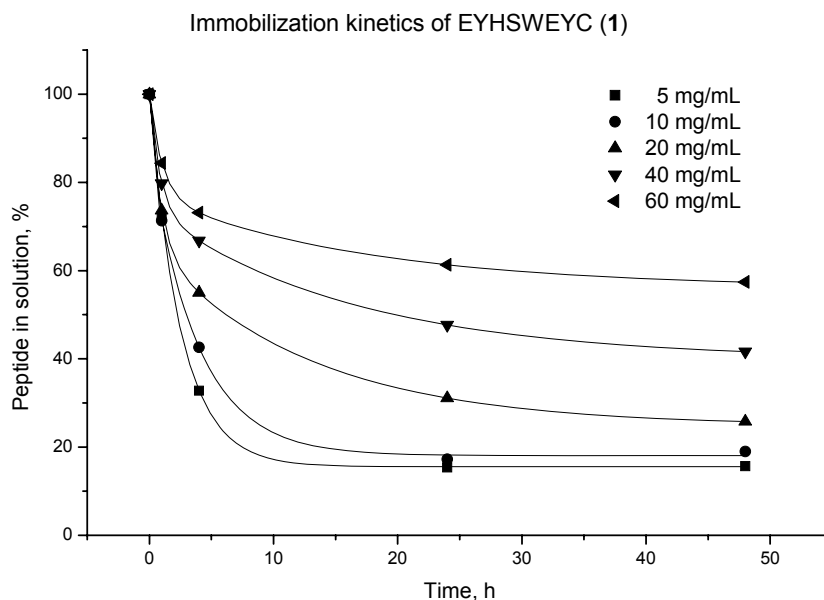
Immobilization kinetics of ligand 43 (YCSWEY) binding to Toyopearl AF-Epoxy-650M resin at different concentrations expressed as % of free peptides in solution.
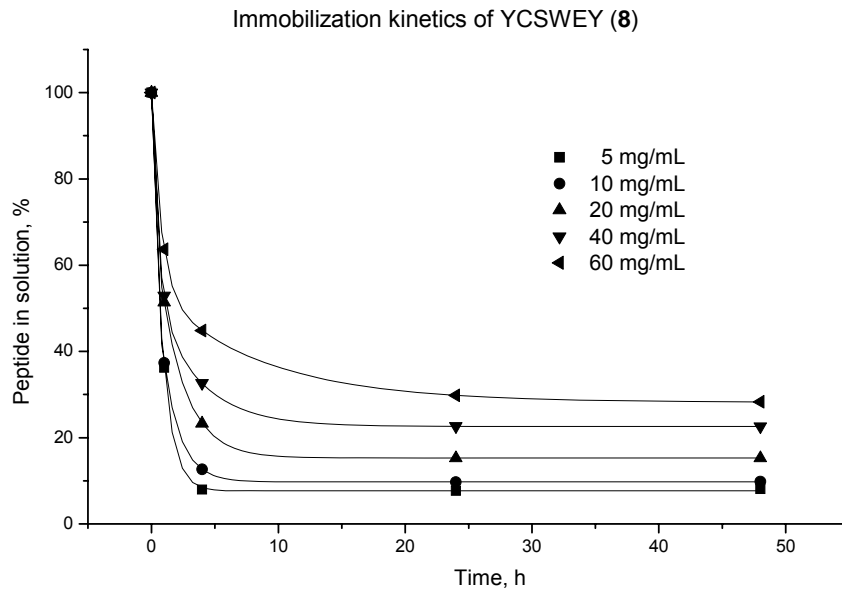
Immobilization kinetics of ligand 57 (WEYC) binding to Toyopearl AF-Epoxy-650M resin at different concentrations expressed as % of free peptides in solution.
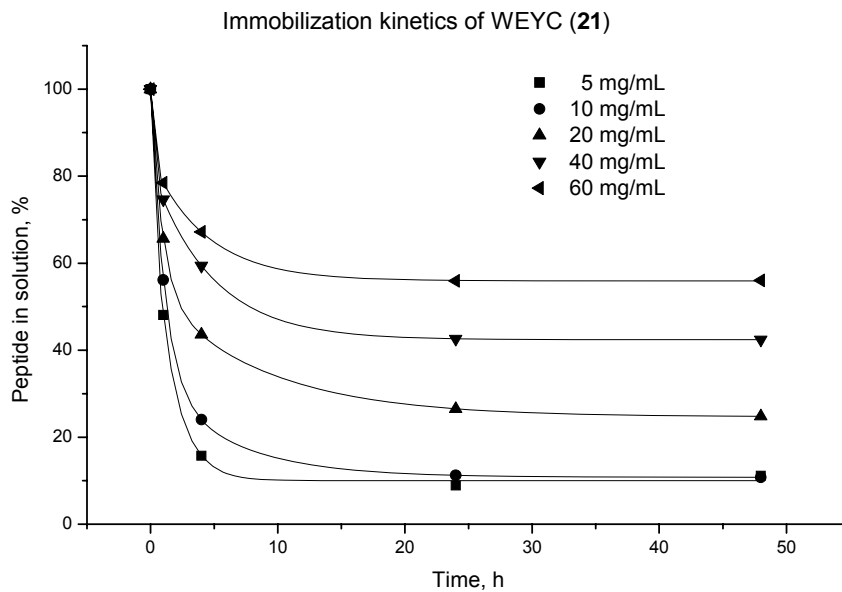
Supplementary Data 4. Immobilization- and pdFVIII binding data of FVIII ligands

Table 1. Immobilization- and pdFVIII binding data of Ala- and D-peptide mutants as well as single amino acid replacement derivatives of EYHSWEYC (3). Bold letters mark substitutions in EYHSWEYC; lower case letters denote D-amino acids.

Sequence	no.	Immobilization (%)	Ligand loading (µmol/mL)	^{125}I-pdFVIII binding, (%)[a]	Relative FVIII affinity to 3[b]
EYHSWEYC	3	69.1 ± 2.9	10.3 ± 0.4	50.2 ± 1.6	1.00 ± 0.03
EYHSWEY(Aha)C	4	65.7 ± 3.3	9.02 ± 0.5	38.8 ± 7.5	0.91 ± 0.12
AcEYHSWEYC	5	77.3 ± 1.0	12.15 ± 0.15	49.3 ± 0.9	0.86 ± 0.02
AYHSWEYC	6	81.6 ± 0.2	12.7 ± 0.1	51.6 ± 5.6	0.87 ± 0.09
EAHSWEYC	7	71.7 ± 3.6	11.5 ± 0.6	37.7 ± 9.6	0.69 ± 0.17
EYASWEYC	8	46.7 ± 4.3	8.0 ± 0.7	53.1 ± 5.8	1.50 ± 0.16
EYHAWEYC	9	50.0 ± 1.6	7.5 ± 0.2	48.8 ± 4.4	1.54 ± 0.14
EYHSAEYC	10	44.7 ± 0.8	7.3 ± 0.1	7.1 ± 0.1	0.24 ± 0.00
EYHSWAYC	11	42.9 ± 2.2	6.7 ± 0.3	11.7 ± 1.4	0.47 ± 0.06
EYHSWEAC	12	59.4 ± 2.5	9.5 ± 0.4	21.3 ± 0.6	0.47 ± 0.01
EYHSWEYA	13	5.1 ± 1.0	0.8 ± 0.2	2.0 ± 0.1	0.04 ± 0.00
eYHSWEYC	14	69.1 ± 0.7	10.3 ± 0.1	40.9 ± 1.7	0.82 ± 0.04
EyHSWEYC	15	68.6 ± 4.4	10.2 ± 0.7	33.9 ± 17.0	0.89 ± 0.10
EYhSWEYC	16	77.4 ± 4.1	11.5 ± 0.6	56.8 ± 1.0	1.03 ± 0.02
EYHsWEYC	17	74.6 ± 3.6	11.1 ± 0.5	43.7 ± 0.8	0.82 ± 0.01
EYHSwEYC	18	80.4 ± 3.8	12.0 ± 0.6	47.9 ± 2.8	0.84 ± 0.05
EYHSWeYC	19	62.3 ± 3.1	9.3 ± 0.5	42.5 ± 5.0	0.97 ± 0.11
EYHSWEyC	20	73.3 ± 2.5	10.9 ± 0.4	41.5 ± 6.8	0.79 ± 0.13
EYHSWEYc	21	63.8 ± 2.0	9.5 ± 0.3	43.0 ± 3.5	0.95 ± 0.08
scrambled[c]	39	69.5 ± 3.5	10.3 ± 0.4	6.5 ± 0.5	0.13 ± 0.01
QYHSWEYC	22	81.7 ± 4.1	12.2 ± 0.6	46.1 ± 2.6	1.00 ± 0.03
DYHSWEYC	23	62.8 ± 3.1	9.5 ± 0.5	41.7 ± 1.6	0.87 ± 0.09
VYHSWEYC	24	83.7 ± 4.2	12.7 ± 0.6	15.6 ± 12.9	0.69 ± 0.17
EY(OMe)HSWEYC	25	68.5 ± 3.4	10.1 ± 0.5	36.2 ± 13.1	1.50 ± 0.16
EFHSWEYC	26	68.4 ± 3.4	10.3 ± 0.5	41.3 ± 3.6	1.54 ± 0.14
EYKSWEYC	27	56.4 ± 2.8	8.5 ± 0.4	29.1 ± 1.7	0.24 ± 0.00
EY4-pySWEYC	28	74.5 ± 3.7	11.0 ± 0.6	23.0 ± 4.2	0.47 ± 0.06
EYFSWEYC	29	67.5 ± 14.3	10.9 ± 2.3	72.1 ± 2.9	0.47 ± 0.01
EYHTWEYC	30	69.7 ± 3.5	10.3 ± 0.5	48.2 ± 11.1	0.04 ± 0.00
EYHVWEYC	31	66.5 ± 3.3	9.8 ± 0.5	64.3 ± 0.9	0.82 ± 0.04
EYHSFEYC	32	69.7 ± 3.5	10.7 ± 0.5	14.4 ± 5.1	0.89 ± 0.10

Sequence	no.	Immobilization (%)	Ligand loading (µmol/mL)	^{125}I-pdFVIII binding, (%)	Relative FVIII affinity to 3[a]
EYHS^{1}NalEYC	33	76.1 ± 4.7	11.2 ± 0.7	27.1 ± 0.9	1.03 ± 0.02
EYHSWQYC	34	74.0 ± 3.7	11.0 ± 0.6	13.9 ± 0.1	0.82 ± 0.01
EYHSWDYC	35	68.9 ± 5.5	10.4 ± 0.8	53.8 ± 3.3	0.84 ± 0.05
EYHSWEY(OMe)C	36	73.8 ± 3.7	10.9 ± 0.5	40.6 ± 1.1	0.97 ± 0.11
EYHSWEFC	37	80.8 ± 4.0	12.2 ± 0.6	44.5 ± 7.7	0.79 ± 0.13
EYHSWEY	38	9.4 ± 3.6	9.4 ± 0.5	3.6 ± 0.3	0.95 ± 0.08

[a] *pdFVIII binding is given as % of total bindable material;* [b] *The data are based on the corresponding peptide 3 binding property at an equal peptide density;* [c] *Sequence: ECYYEHWS.* ^{1}*Nal: 1-Naphthyl alanine; Aha: 6-aminohexanoic acid.*

Table 2. Analytical data and binding properties of minimized hepta- and hexapeptidic mutants of EYHSWEYC (1).

Sequence	no.	Immobilization (%)	Ligand loading (µmol/mL)	^{125}I-pdFVIII binding (%)[a]	Relative FVIII affinity
YHSWEYC	40	85.2 ± 4.3	14.0 ± 0.7	61.3 ± 3.2	0.98 ± 0.05[b]
YFSWEYC	41	84.3 ± 6.1	15.2 ± 1.1	66.8 ± 7.2	1.03 ± 0.11[b]
HSWEYC	42	83.6 ± 4.2	12.7 ± 0.6	39.8 ± 16.8	0.67 ± 0.30[b]
YCSWEY	43	82.0 ± 2.4	17.0 ± 0.5	62.0 ± 0.4	0.92 ± 0.04[b]
YCSWDY	44	79.2 ± 0.5	16.7 ± 1.0	69.8 ± 12.2	1.14 ± 0.20[c]
YCS^{1}NalEY	45	62.0 ± 3.1	12.7 ± 0.6	35.3 ± 3.0	0.76 ± 0.06[c]
YCAWEY	46	58.0 ± 2.9	12.2 ± 0.6	72.1 ± 7.2	1.63 ± 0.16[c]
YCTWEY	47	72.9 ± 3.6	14.9 ± 0.7	70.7 ± 2.4	1.27 ± 0.04[c]
YCVWEY	48	63.2 ± 3.2	12.9 ± 0.6	94.1 ± 4.7	1.97 ± 0.10[c]
YCAWDY	49	90.0 ± 4.5	19.3 ± 1.0	72.0 ± 15.5	1.07 ± 0.23[c]
YCTWDY	50	84.7 ± 0.1	17.6 ± 0.0	73.6 ± 0.7	1.16 ± 0.01[c]
YCVWDY	51	79.3 ± 4.0	16.5 ± 0.8	72.0 ± 1.2	1.18 ± 0.02[c]
yewacy	52	60.9 ± 3.0	12.8 ± 0.6	53.6 ± 2.5	1.14 ± 0.05[c]
yewvcy	53	68.6 ± 3.4	14.1 ± 0.7	77.0 ± 4.2	1.47 ± 0.08[c]
ydwacy	54	84.0 ± 4.2	18.0 ± 0.9	75.1 ± 0.6	1.16 ± 0.01[c]
ydwvcy	55	88.9 ± 4.4	18.5 ± 0.9	73.4 ± 5.6	1.12 ± 0.08[c]

[a] *pdFVIII binding is given as % of total bindable material,* [b] *The data are based on the corresponding peptide 3 binding property at an equal peptide;* [c] *The data are based on the corresponding peptide 43 binding property at an equal peptide density.* ^{1}*Nal: 1-Naphthyl alanine.*

Table 3. Analytical data and binding properties of minimized penta- and tetrapeptidic and peptido-mimetic mutants of EYHSWEYC (1).

Sequence	no.	Immobilization (%)	Ligand loading (µmol/mL)	^{125}I-pdFVIII binding (%)[a]	Relative FVIII affinity to 3[b]
SWEYC	56	81.0 ± 1.7	22.7 ± 0.5	46.4 ± 1.7	0.65 ± 0.02
WEYC	57	79.9 ± 0.3	19.9 ± 0.1	45.4 ± 0.4	0.65 ± 0.02
WEFC	58	46.5 ± 2.3	13.3 ± 0.7	24.0 ± 0.1	0.40 ± 0.00
WDYC	59	71.6 ± 3.6	20.5 ± 1.0	62.8 ± 6.9	0.89 ± 0.10
AcWDYC	60	56.0 ± 2.8	17.8 ± 0.9	47.4 ± 1.7	0.69 ± 0.03
AcWEYC	61	78.0 ± 3.9	24.3 ± 1.2	56.9 ± 1.9	0.79 ± 0.03
(3-IBA)EYC	62	79.2 ± 4.0	26.4 ± 1.3	62.7 ± 3.9	0.87 ± 0.05
(3-IPA)EYC	63	93.5 ± 4.7	32.0 ± 1.6	53.2 ± 4.9	0.73 ± 0.07
(3-IAA)EYC	64	66.8 ± 3.3	23.4 ± 1.2	76.7 ± 1.6	1.07 ± 0.02
(3-IBA)DYC	65	74.0 ± 3.7	25.3 ± 1.3	57.2 ± 7.2	0.79 ± 0.10
(3-IPA)DYC	66	78.9 ± 3.9	27.7 ± 1.4	60.7 ± 4.1	0.84 ± 0.06
(3-IAA)DYC	67	67.6 ± 1.8	24.3 ± 0.7	67.7 ± 2.8	0.94 ± 0.04
(3-IAA)Ψ[CH$_2$NH]EYC	68	61.8 ± 3.1	18.4 ± 0.9	53.7 ± 1.9	0.78 ± 0.03
(3-IAA)EΨ[CH$_2$NH]YC	69	69.6 ± 3.5	20.8 ± 1.0	65.3 ± 3.0	0.93 ± 0.04
(3-IAA)EYΨ[CH$_2$NH]C	70	53.6 ± 2.7	16.0 ± 0.8	43.4 ± 2.3	0.66 ± 0.03

[a] pdFVIII binding is given as % of total bindable material; [b] The data are based on the corresponding peptide *3* binding property at an equal peptide density.

Supplementary Data 5. Additional ligands not discussed in the main text.

Table 1. pdFVIII binding data of various peptide-coated resins.

Sequence	Ligand loading (µmol/mL)	^{125}I-pdFVIII binding (%)[a]	Relative FVIII affinity to 3[b]
AEYHSWEYC	10.5 ± 4	32.0 ± 2.6	0.6 ± 0.1
Ac-AEYHSWEYC	07.9 ± 4	30.8 ± 1.4	0.9 ± 0.1
KEYHSWEYC	03.3 ± 3	01.8 ± 0.6	0.5 ± 0.1
Ac-KEYHSWEYC	07.3 ± 1	25.9 ± 0.5	0.9 ± 0.1
K(Ac)EYHSWEYC	06.9 ± 4	39.3 ± 1.6	1.5 ± 0.1
Ac-EYHSWEYC	11.8 ± 4	57.5 ± 3.7	1.0 ± 0.1
EYHSWEBpaC	11.7 ± 3	41.5 ± 2.5	0.9 ± 0.1
EYHSWEPhgC	08.8 ± 1	50.8 ± 2.6	1.2 ± 0.1

Sequence	Ligand loading (μmol/mL)	^{125}I-pdFVIII binding (%)[a]	Relative FVIII affinity to 3[b]
EYHSWEhFC	11.5 ± 0.4	41.2 ± 4.6	0.8 ± 0.1
EYHAbuWEYC	09.0 ± 0.3	50.6 ± 2.4	1.2 ± 0.1
EYGSWEYC	09.0 ± 0.1	42.8 ± 3.0	1.0 ± 0.1
EYPhgSWEYC	10.2 ± 0.4	57.9 ± 4.9	1.2 ± 0.1
EY(hF)SWEYC	10.4 ± 0.3	56.1 ± 2.1	1.1 ± 0.1
EYWSWEYC	12.9 ± 0.6	70.4 ± 3.5	1.2 ± 0.1
E(1-Nal)HSWEYC	10.3 ± 0.3	44.1 ± 1.6	0.9 ± 0.1
E(2-Nal)HSWEYC	09.5 ± 0.1	39.7 ± 1.6	0.9 ± 0.1
EPhgHSWEYC	09.5 ± 0.4	19.1 ± 2.2	0.4 ± 0.1
EhFHSWEYC	11.7 ± 0.3	41.2 ± 1.9	0.7 ± 0.1
E4-pyHSWEYC	10.8 ± 0.1	18.6 ± 1.2	0.4 ± 0.1
Ac-AYHSWEYC	08.1 ± 0.4	41.7 ± 3.1	1.2 ± 0.1
EY3-pySWEYC	06.4 ± 0.3	25.6 ± 4.0	1.1 ± 0.1
EY4-pySWEYC	11.0 ± 0.1	23.0 ± 1.9	0.4 ± 0.1
EY(2-Nal)SWEYC	11.2 ± 0.4	39.3 ± 0.8	0.7 ± 0.1

[a] pdFVIII binding is given as % of total bindable material; [b] The data are based on the corresponding peptide 3 binding property at an equal peptide density.

Table 2. pdFVIII binding data of various octapeptide-coated resins. The ligand loading of the corresponding coated resins has not been determined.

Sequence	^{125}I-pdFVIII binding (%)[a]	Sequence	^{125}I-pd-FVIII binding (%)[a]
AcEYFAbuWEYC	63 ± 4	EYHSWEBpaC	62 ± 5
EYHSWEPhgC	53 ± 4	EYHSBpaEYC	57 ± 4
AcEYFSWEYC	46 ± 3	EYHAbuWEYC	51 ± 2
EYHTWDBpaC	33 ± 1	EY*homo*FSWEYC	56 ± 2
AcEYHAbuWEYC	49 ± 3	AcEYHTWEYC	33 ± 1
EYH*homo*SWEYC	56 ± 4	AcEYHSWDYC	53 ± 3
AcDYHSWEAC	38 ± 3	EYHSWDBpaC	49 ± 3
DYHSWEYC	42 ± 3	AYHSWEBpaC	42 ± 3
AcEYHSBpaEYC	20 ± 2	AYHSWEBpaC	46 ± 3
AsEYHSWEBpaC	42 ± 1	EYfSWEYC	48 ± 2
AcEYHSWEPhgC	10 ± 1	EYHS^{2}NalEYC	38 ± 4
AcEYHSBpaEPhgC	07 ± 1	AYHSBpaEYC	36 ± 3

Sequence	^{125}I-pdFVIII binding (%)[a]	equence	^{125}I-pd-FVIII binding (%)[a]
EYHSBpaE(D/L-Phg)C	30 ± 1	AYHSBpaEPhgC	39 ± 2
EYHSBpaE(D/L-Phg)C	46 ± 3	AcEYHVWEYC	29 ± 2
AcEYHS(2,4-Cl$_2$-F)EYC	32 ± 2	EYHSWEYGC	34 ± 1
AcAYHSWEYC	39 ± 3	AcEYhSWEYC	36 ± 1
EYWSWEYC	35 ± 1	EYYSWEYC	39 ± 2
EBpaHSWEYC	34 ± 6	EWKSWEYC	34 ± 2
CAYHSWEY	08 ± 1	EYHSWYEC	18 ± 4

[a] *pdFVIII binding is given as % of total bindable material. Bpa: p-Benzoylphenyl alanine; Abu: α-aminobutyric acid; Phg: phenyl glycine; homoS: homo-serine; homoF: homo-phenylalanine; Bta: Benzothienyl alanine; 2-Nal: 2-naphthyl alanine; Bip: p-binphenyl alanine; (2,4-Cl$_2$-F): 2,4-di-chlorophenyl alanine.*

Table 3. pdFVIII binding data of various heptapeptide-coated resins. The ligand loading of the corresponding coated resins has not been determined.

Sequence	^{125}I-pdFVIII binding (%)[a]	Sequence	^{125}I-pd-FVIII binding (%)[a]
YHS(2,4-Cl$_2$-F)EYC	34 ± 3	YHSWDYC	52 ± 3
AcYHSWEYC	42 ± 1	AcYhSWEYC	41 ± 1
YFAbuWEFC	13 ± 1	YHSBpaEBpaC	32 ± 4
YHSWEBipC	51 ± 3	YHSWEBpaC	54 ± 3
YHSWE^{2}NalC	51 ± 3	YHTWDYC	47 ± 3
YHSEBpaEPhgC	28 ± 1	YFAbuWEYC	63 ± 4
YHSBpaEYC	37 ± 1	YHSWEPhgC	35 ± 1
YFAbuWDYC	46 ± 1	YHVWEYC	26 ± 1
YHS^{2}NalEYC	60 ± 2	YHS2-NalEYC	25 ± 1
YHSBtaEYC	06 ± 1		

[a] *pdFVIII binding is given as % of total bindable material. Bpa: p-Benzoylphenyl alanine; Abu: α-aminobutyric acid; Phg: phenyl glycine; homoC: homo-cysteine; Bta: Benzothienyl alanine; ^{2}Nal: 2-naphthyl alanine; Bip: p-binphenyl alanine; 2,4-Cl$_2$-F: 2,4-dichlorophenyl alanine.*

Table 4. pdFVIII binding data of various hexapeptide-coated resins. The ligand loading of the corresponding coated resins has not been determined.

Sequence	^{125}I-pdFVIII binding (%)[a]	Sequence	^{125}I-pd-FVIII binding (%)[a]
ESWEYC	38 ± 2	AcESWEYC	40 ± 3
Ac-YCSWEY	55 ± 3	YCSWEPhg	38 ± 3
YCSWEY-NH$_2$	56 ± 1	YSWEYC	50 ± 1
FSWEYC	40 ± 1		

[a] *pdFVIII binding is given as % of total bindable material. Phg: Phenyl glycine.*

Table 5. pdFVIII binding data of various pentapeptide-coated resins. The ligand loading of the corresponding coated resins has not been determined.

Sequence	^{125}I-pdFVIII binding (%)[a]	Sequence	^{125}I-pd-FVIII binding (%)[a]
TWEYC	37 ± 2	SEWPhgC	38 ± 2
YWEYC	48 ± 1	SWEY*homo*C	33 ± 2
CSWEY	48 ± 3	AbuWEYC	35 ± 2
SBpaEBpaC	11 ± 3	SWDYC	48 ± 3

[a] *pdFVIII binding is given as % of total bindable material. Bpa: p-Benzoylphenyl alanine; Abu: α-aminobutyric acid; Phg: phenyl glycine; homoC: homo-cysteine.*

Supplementary Data 6. Conditions for FVIII affinity purification using peptido-mimetic 69-coated resin.

Affinity purification of pdFVIII using (69)-coated resin.

69-coated resin (1 mL) (prepared from 69 (25 mg) and Toyopearl resin (360 mg) as described above) was packed into a glass column (GE Healthcare, Piscataway, NJ) and purification was performed employing a Waters 650E Advanced Protein Purification System at a flow-rate of 0.5 mL min^{-1} using purification buffer (0.01 M Hepes, 5 mM CaCl$_2$, 0.01% Tween-80) containing 0.1 M (buffer-1) or 1.0 M NaCl (buffer-2). Elution was monitored by a flow-through UV detector at 280 nm.

pdFVIII (0.5 mg), purified as described above, was mixed with cell-conditioned fetal bovine serum (FBS)-containing Delbucco's Modified Eagles Medium (DMEM),

which was diluted with 0.01 M Hepes, 5 mM $CaCl_2$, 0.01% Tween-80 to a final salt concentration of 0.1 M NaCl. The mixture was applied onto the column, followed by subsequent washing with buffer-1 until OD280 had returned to background and with a mixture of buffer-1 and buffer-2 (85:15, v/v). FVIII was eluted using a mixture of buffer-1 and buffer-2 (4:6, v/v). The control experiment without added media was performed in an analogous manner except that FVIII was eluted directly after wash with buffer-1 using a mixture of 20% buffer-1 and 80% buffer-2. Elution fractions were analyzed by determining OD280 and by SDS-PAGE and Western blot analysis and FVIII activity was confirmed by APTT assay (described below).

Supplementary Data 7. Preparation and FVIII binding data of cyclic FVIII ligands.

The linear peptides were synthesized on TCP-resin (100-200 mg) according to the general procedures I (loading), II (Fmoc-deprotection), III (Coupling) and X (cleavage). First amino acid was cysteine in every case. The linear, side-chain protected peptides were cyclized according to general procedures XI and deprotected (VII). The crude peptides were purified by preparative RP-HPLC.

Table 1. Synthesis and FVIII binding ability of cyclic ligands relative to their respective linear precursors. Lower case letters denote D-amino acid residues.

Ligand	no.	pdFVIII binding (%)	Ligand	no.	pdFVIII binding (%)
c(FSWEYC)	81	29 ± 1	c(YCSWEY)	93	33 ± 2
c(FSWEYc)	82	59 ± 2	c(YcSWEY)	94	47 ± 4
c(FSWEyC)	83	37 ± 3	c(YCSWEY)	95	29 ± 1
c(FSWEyc)	84	44 ± 3	c(YcSWEY)	96	46 ± 4
c(FSWeYC)	85	22 ± 3	c(YCSWEY)	97	32 ± 3
c(FSWeEYc)	86	23 ± 2	c(YcSWEY)	98	32 ± 2
c(FSwEYC)	87	47 ± 1	c(YCSWEY)	99	50 ± 1
c(FSwEYc)	88	18 ± 2	c(YcSWEY)	100	45 ± 1
c(FsWEYC)	89	56 ± 3	c(YCSWEY)	101	49 ± 1
c(FsWEYc)	90	49 ± 3	c(YcSWEY)	102	24 ± 1
c(fSWEYC)	91	47 ± 1	c(YCSWEY)	103	45 ± 1
c(fSWEYc)	92	44 ± 5	c(YcSWEY)	104	26 ± 3

Supplementary Data 8. FVIII affinity purification using tetrapeptide 57-coated resin.

Purification of pdFVIII from different media using tetrapeptide 57-coated resin. 0.5 mg pdFVIII was applied to 1 mL of resin. The samples from elution fractions were analyzed by 10% SDS-PAGE followed by silver staining and Western blotting using monoclonal anti-mouse antibodies (mAb C5 and mAb 413) against FVIII. (a) Purification profile, SDS-PAGE and Western Blot from the adsorption and elution of pure pdFVIII using ligand 2-coated resin. SDS-PAGE: Lane 1: source solution with pure FVIII for the column; Lane 2: flow-through; Lane 3: wash solution; Lane 4: elution fraction with 1 M NaCl; Western Blot: Lane 5: source solution with pure FVIII for the column; Lane 6: flow-through; Lane 7: elution fraction with 1 M NaCl. (b) Purification profile, SDS-PAGE and Western Blot from the purification from cell-conditioned FBS-containing media spiked with FVIII using ligand 2-coated resin. SDS-PAGE: Lane 1: media; Lane 2: media with FVIII for the column; Lane 3: flow-through; Lane 4: elution fraction with 1 M NaCl; Western Blot: Lane 5: source solution with pure FVIII for the column; Lane 6: flow-through; Lane 7: elution fraction with 1 M NaCl.
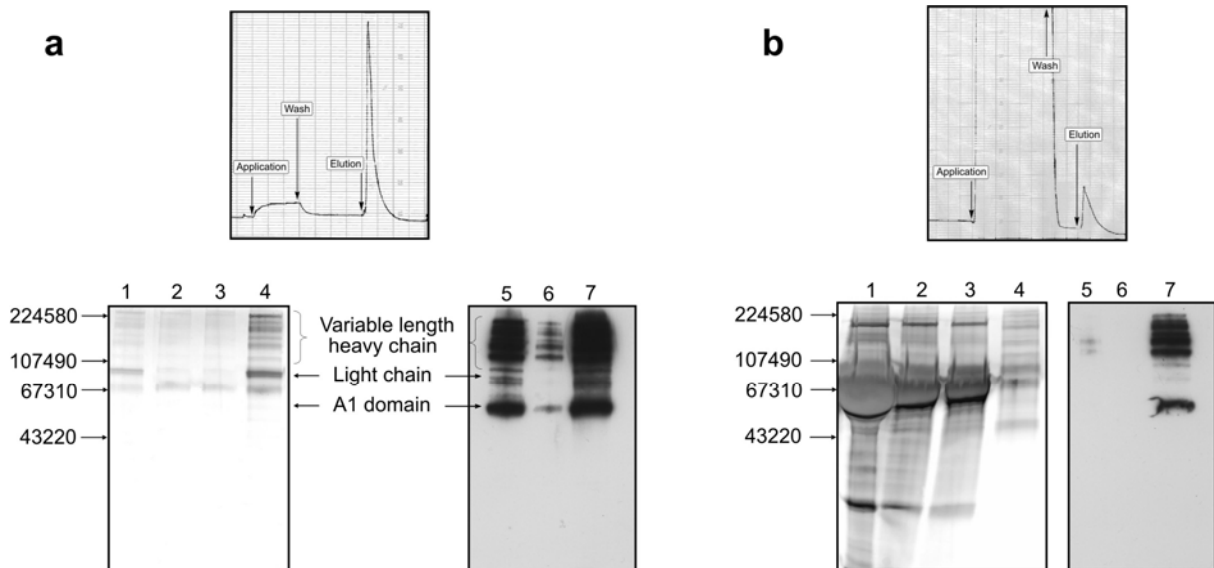
Supplementary Data 9. Verification of the enantiomeric purity of the 3-aryl-substituted tyrosine analogues Boc-*m*-(phenyl)Tyr (123) and Boc-*m*-(*o*-tolyl)Tyr (124). Both amino acids were coupled to L-valine and D-valine and the corresponding crude dipeptides Boc-*m*-(phenyl)Tyr—L-Val (125) and Boc-*m*-(phenyl)Tyr—D-Val (127) as well as Boc-*m*-(*o*-tolyl)Tyr—L-Val (126) and Boc-*m*-(*o*-tolyl)Tyr—D-Val (128) were analyzed by NMR and HPLC. The spectra are shown below.

HPLC spectrum (10 → 50%) of H-*m*-(phenyl)Tyr—L-Val (125).
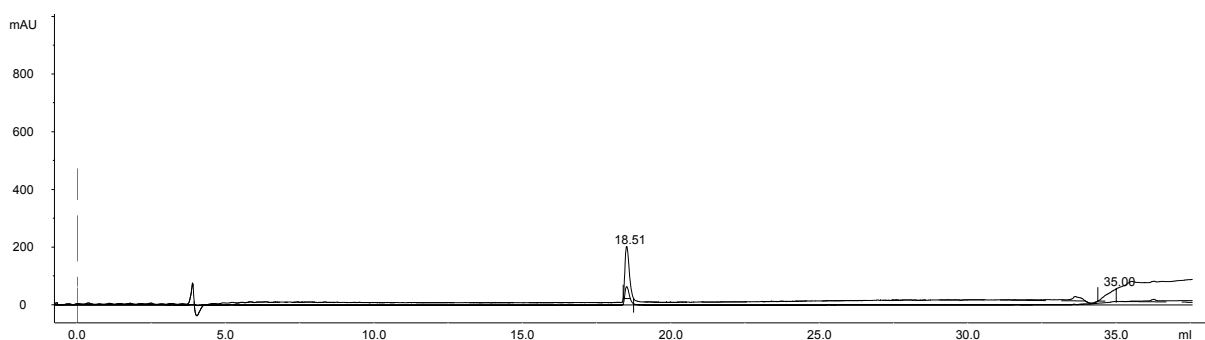
HPLC spectrum (10 → 50%) of H-*m*-(phenyl)Tyr—D-Val-OH (127).

^{1}H-NMR spectrum of H-*m*-(phenyl)Tyr—L-Val (125).

500 Mhz, MeOH-d$_4$

^{1}H-NMR spectrum of H-*m*-(phenyl)Tyr—D-Val-OH (127).

500 Mhz, MeOH-d$_4$

^{1}H-NMR spectrum of H-*m*-(*o*-tolyl)Tyr—Val-OH (126).

500 Mhz, MeOH-d$_4$
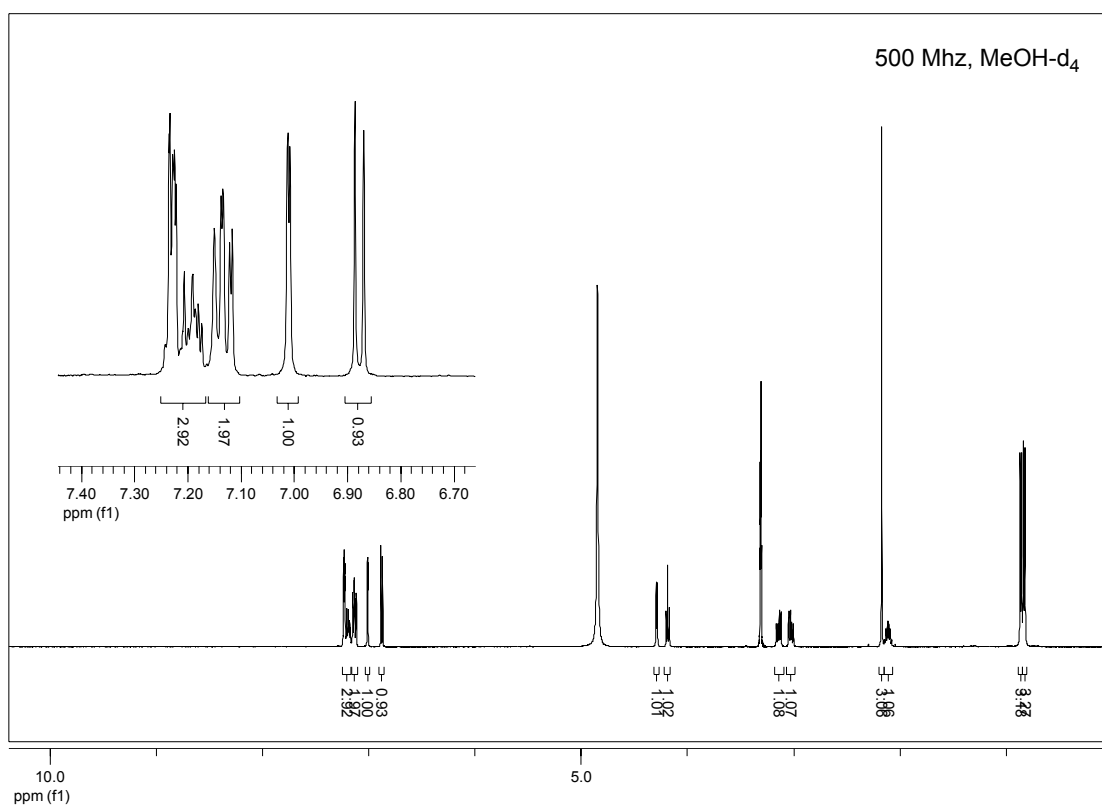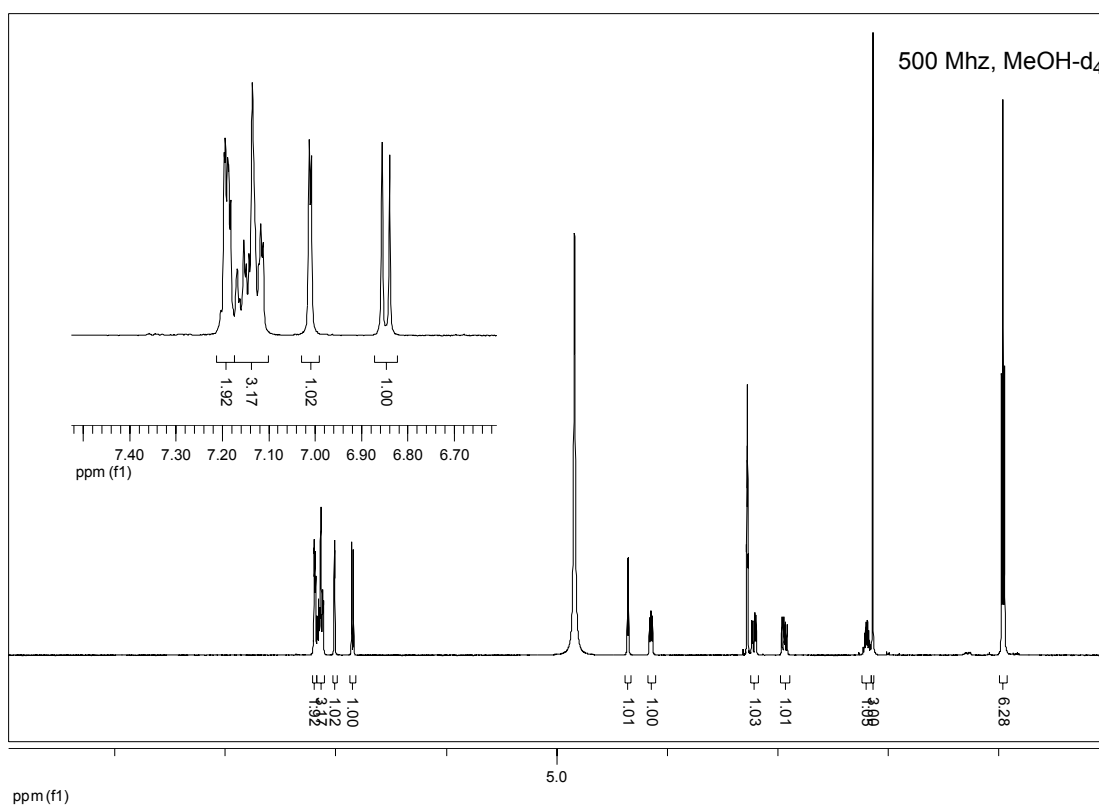
^{1}H-NMR spectrum of H-*m*-(*o*-tolyl)Tyr—D-Val-OH (128).

500 Mhz, MeOH-d$_4$

256
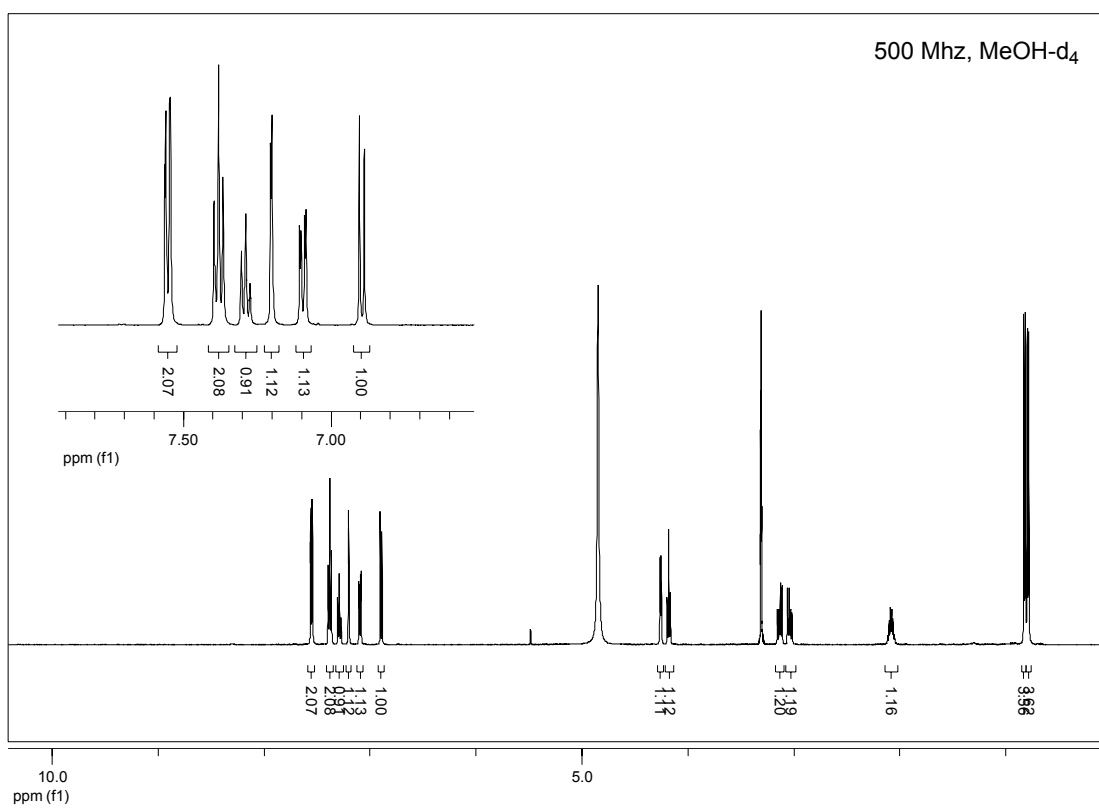
HPLC spectrum (10 → 50%) of H-*m*-(*o*-tolyl)Tyr—Val-OH (126).
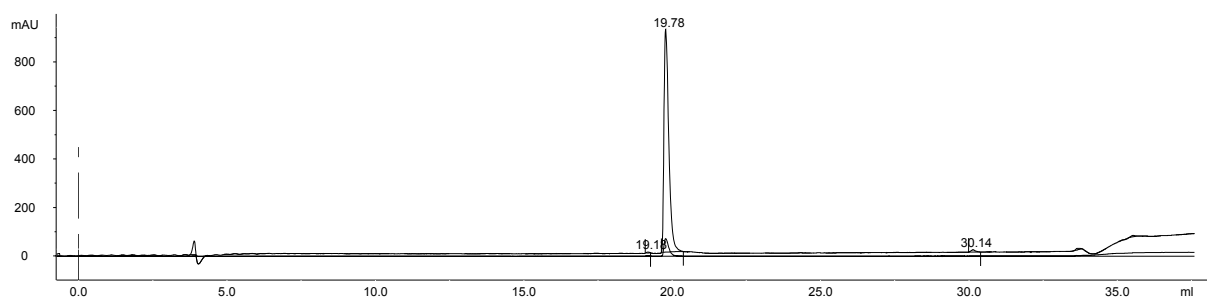
HPLC spectrum (10 → 50%) of H-*m*-(*o*-tolyl)Tyr—D-Val-OH (128).
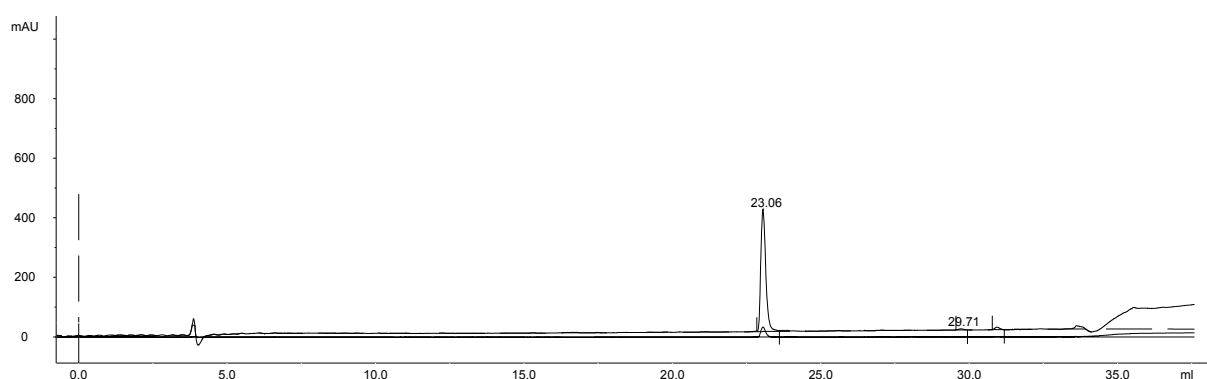
Supplementary Data 10. Verification of the enantiomeric purity of (S)-Boc-4-hydroxy-naphthyl alanine (136) obtained by asymmetric hydrogenation. (S)-136 was coupled to L-valine to yield the (S,S)-dipeptide 137. Racemic 136 was coupled in a similar manner to achieve the analogous diastereomeric mixture (S/R, S)-138. Both dipeptides were analyzed by NMR and HPLC. The spectra are shown below.

HPLC spectrum (10 → 50%) of H-(*S*)-(4-hydroxy)Nal-Val-OH (136).
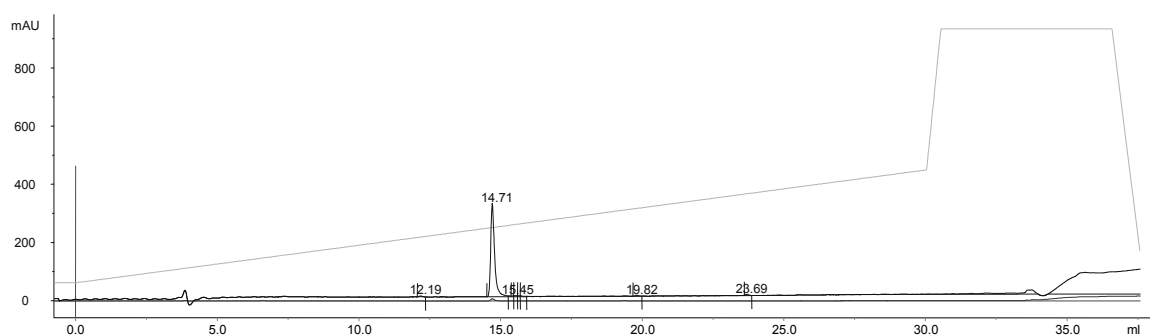
HPLC spectrum (10 → 50%) of H-(*S/R*)-(4-hydroxy)Nal-Val-OH (138).
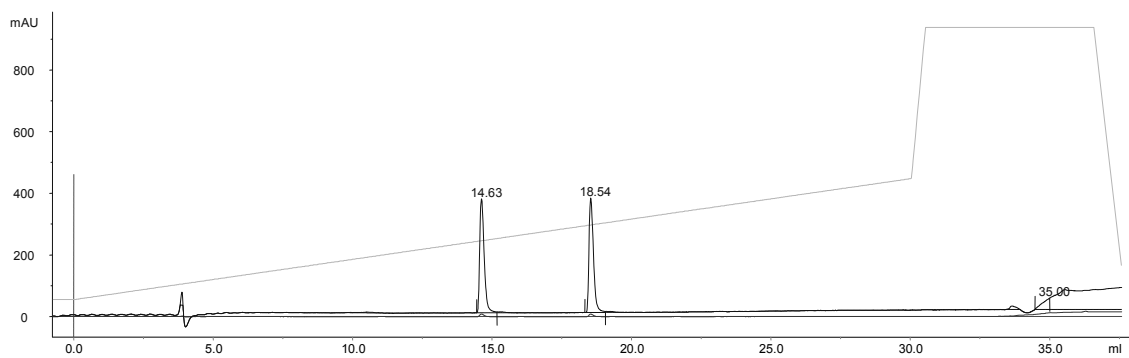
^{1}H-NMR spectrum of H-(*S*)-(4-hydroxy)Nal-Val-OH (136).
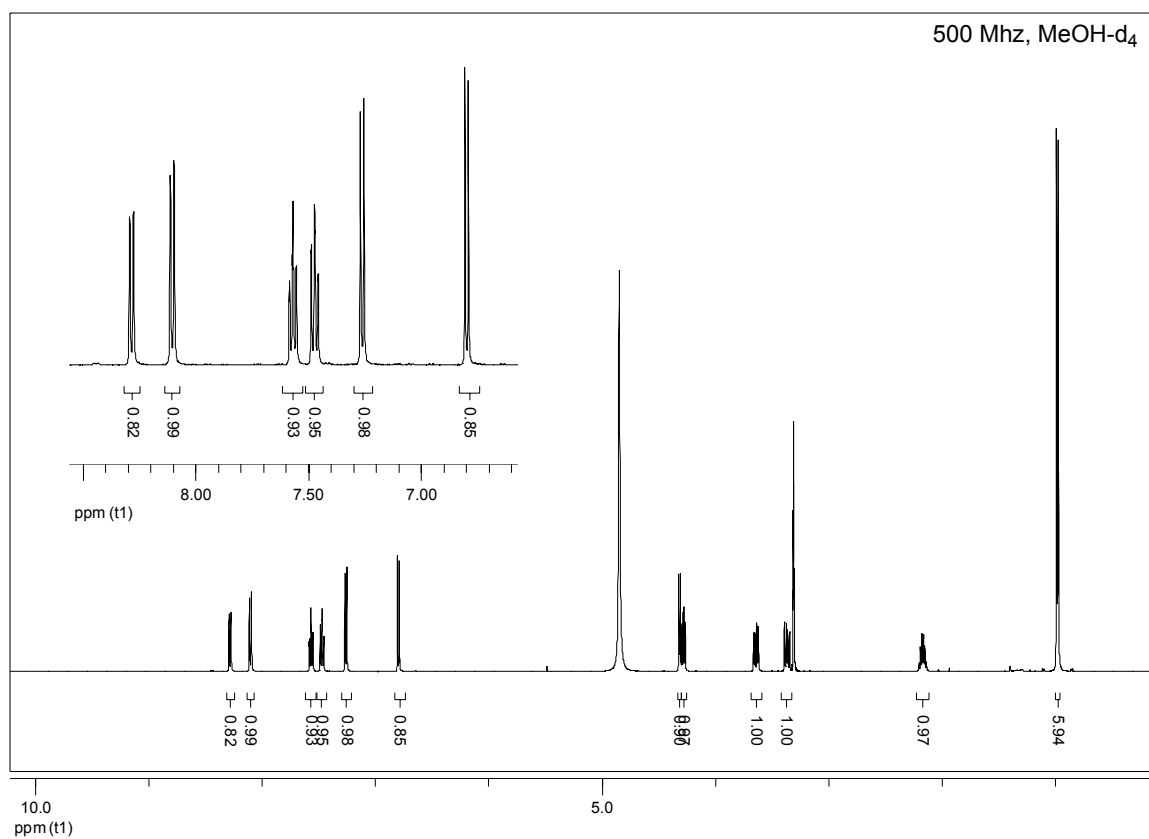
^{1}H-NMR spectrum of H-(*S/R*)-(4-hydroxy)Nal-Val-OH (138).
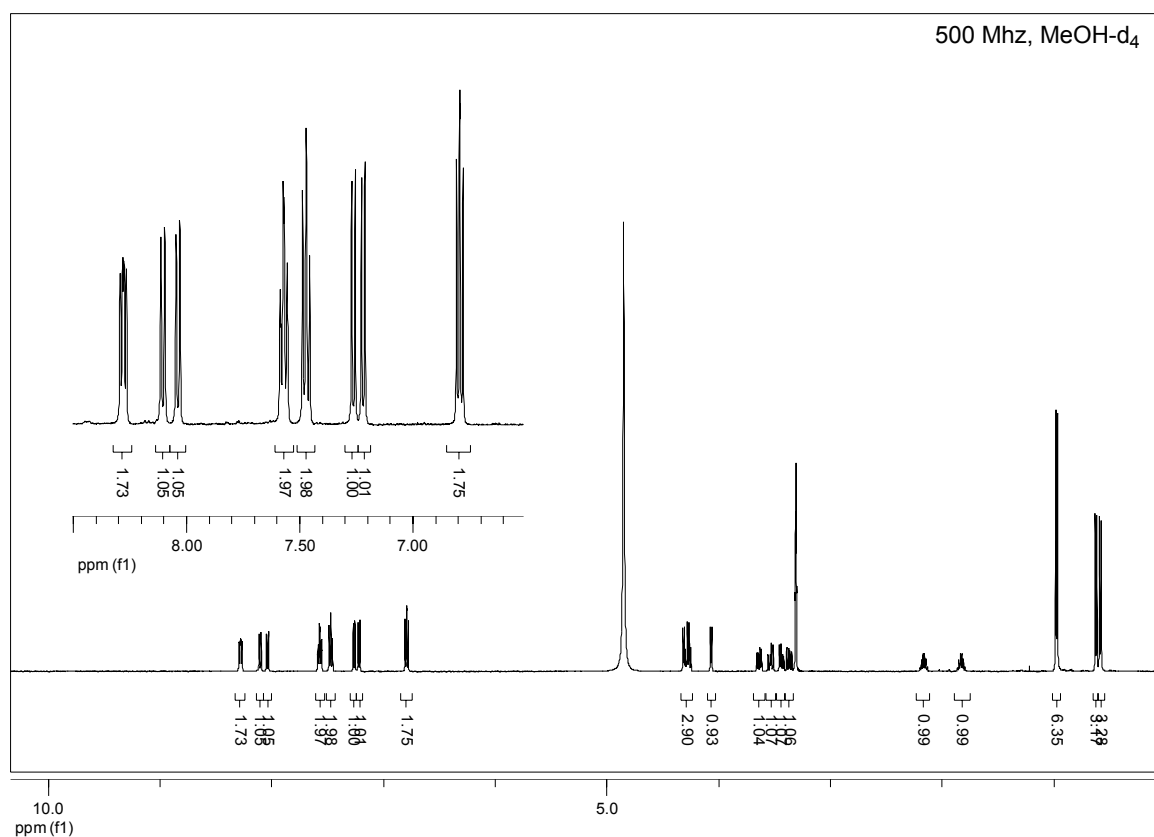
Supplementary Data 11. HPLC spectrum (10 → 50%) of crude DOTA conjugate 199 obtained by Cu(I)-catalyzed azide-alkyne cycloaddition of alkyny-functionalized DOTA derivative 175 and azido-functionalized sample peptide 198.
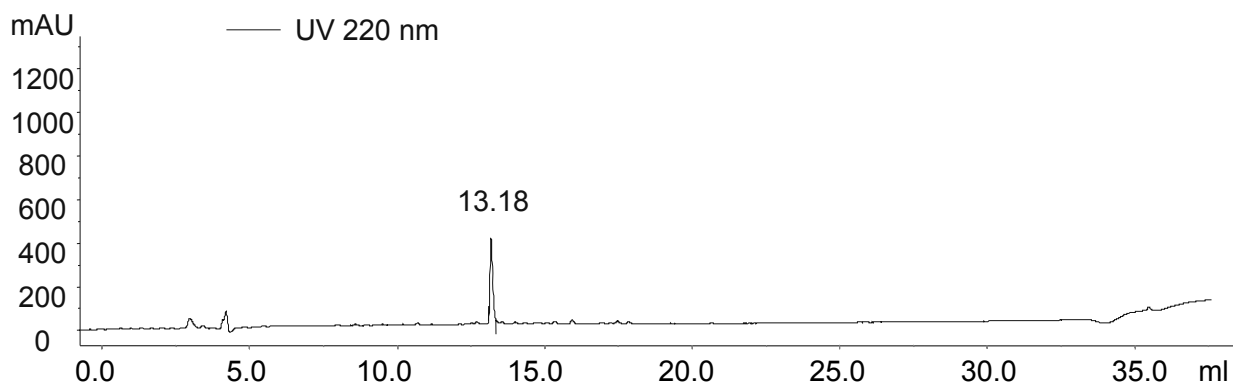
Supplementary Data 12. Binding of [213]Bi-labeled monomeric and dimeric peptides to U937 cells following removal of uPAR-bound uPA via acid wash.

[213]Bi-labeled peptide	Binding to cells [%]	Binding to cells after preincubation with (pro)-uPA (12 μg) [%]	Binding to cells after preincubation with suPAR (1.6 μg) [%]	Binding to cells after preincubation with suPAR (4.8 μg) [%]
163	13.6 ± 5.6	02.2 ± 1.4	11.1 ± 2.1	–
166	46.3 ± 7.2	11.4 ± 3.3	21.7 ± 2.0	13.1 ± 3.8
164	07.1 ± 0.1	02.2 ± 1.4	04.8 ± 1.2	–
167	36.9 ± 1.1	17.2 ± 3.3	19.1 ± 3.5	15.1 ± 3.4

6 Abbreviations and Symbols

α_1-AT	α_1-antitrypsin
α_2-AP	α_2-antiplasmin
α_2MR	α_2-macroglobulin receptor
δ	chemical shift in NMR spectroscopy
λ	wavelength
1D, 2D, 3D	one-, two-, three dimensional
4-py	4-pyridylalanine
a	activated
Ac	acetyl
Ado	8-amino-3,6-dioxaoctanoic acid
AE105	Asp–Cha-Phe–(D-Ser)–(D-Arg)–Tyr–Leu–Trp-Ser
Aha	6-aminohexanoic acid
AIBN	2,2'-azobisisobutyronitrile
APC	activated protein C
aq.	aqueous
Ar, arom	aromatic
ATF	amino-terminal fragment
ATIII	antithrombin III
BDD-rFVIII	B domain deleted recombinant FVIII
BFCA	bifunctional chelating agent

biFVa	bovine FVa
Bn	benzyl
Boc	*tert*-butyloxycarbonyl
br	broad singulet
c	concentration
c	cyclic
calcd	calculated
CCK	cholecystokinin
Cha	cyclohexyl alanine
CK	casein kinase
CT	computed tomography
d	doublet/day
DBP	dibenzoylperoxide
DBU	1,8-diazabicyclo[5.4.0]undec-7-ene
DCC	dicyclohexylcarbodiimide
DCE	dichloroethane
DCM	dichloromethane
dd	doublet of doublets
de	diastereomeric excess
DIPEA	diisopropylethyl amine
DMAP	4-dimethylamino pyridine
DME	dimethoxyethane
DMEM	Dulbecco's Modified Eagle Medium
DMF	*N,N*-dimethylformamide
DMSO	dimethyl sulfoxide

DOTA	1,4,7,10-tetraazacyclodecane-1,4,7,10-tetracetic acid
DOTATATE	DOTA-Tyr^3-octreotate
DOTATOC	DOTA-Tyr^3-octreotide
dt	doublet of triplets
DTPA	diethylene triamine pentaacetic acid
DVB	divinylbenzene
ECM	extracellular matrix
ee	enantiomeric excess
EGF	epidermal growth factor
EI	electron ionization
EM	electron microscopy
EPI	extrinsic pathway inhibitor
equiv	equivalents
ERK	extracellular-signal-regulated kinase
ESI	electrospray ionization
Fab	fragment antigen binding
FAK	focal adhesion kinase
FBS	fetal bovine serum
FDA	Food and Drug Administration
FDG	2-fluorodeoxyglucose
FITC	fluorescein isothiocyanate
FL-rFVIII	full-length recombinant FVIII
Fmoc	9-fluorenylmethoxycarbonyl
FMT	fluorescence-mediated molecular tomography

FPRL	formyl peptide receptor-like
FSF	fibrinoligase
FTIR	Fourier transform infrared spectroscopy
g	gram
G protein	guanine nucleotide-binding protein
GABA	γ-amino-butyric acid
GAG	glycosaminoglycan
GC	gas chromatography
GEP	gastroenteropancreatic
GFD	growth factor-like domain
gla	γ-carboxyglutamate
GLP	glucagon like peptide
GPCR	G protein coupled receptor
GPI	glycosyl-phosphatidylinositol
GRB	growth factor receptor-bound
GRP	gastrin releasing peptide
HATU	*O*-(7-azabenzotriazol-1-yl)-*N,N,N',N'*-tetramethyluronium hexafluorophosphate
HC	heavy chain
Hck	haematopoietic cell kinase
hCp	human plasma copper-binding protein ceruloplasmin
HEPES	(4-(2-hydroxyethyl)-1-piperazineethanesulfonic acid
HIV	human immunodeficiency virus
HMQC	heteronuclear multiple quantum coherence

HMW	high molecular weight
HMWK	high-molecular-weight kininogen
HOAt	1-hydroxy-7-azabenzotriazole
HOBt	1-hydroxybenzotriazol
HPLC	high performance liquid chromatography
hr(s)	hour(s)
HRMS	high resolution mass spectrometry
Hz	Hertz
i.p.	intraperitoneal
i.v.	intravenal
IAA	indolylacetic acid
IBA	indolylbutyric acid
IC_{50}	median inhibition concentration (concentration that reduces the effect by 50%)
ID	injected dose
IPA	indolylpropionic acid
J	coupling constant in NMR spectroscopy
JAK	Janus kinase
K	Kelvin
LACI	lipoprotein-associated coagulation inhibitor
LC	light chain
Lck	lymphocyte protein tyrosine kinase
LDA	lithium diisopropyl amide
LDL	low-density lipoprotein
LET	linear energy transfer
LHRH	luteinising hormone releasing hormone

LMW	low molecular weight
LXA4R	lipoxin A4 receptor
m	multiplet
M	molar
m/*z*	mass-charge relation
mAb	monoclonal antibody
MAPK	mitogen-activated protein kinase
MEK	MAPK/ERK kinase
MHz	Megahertz
min	minute
mL	milliliter
mmol	millimole
MMP	matrix metalloproteinase
mp	melting point
MRI	magnetic resonance imaging
MS	mass spectrometry
MTT	3-(4,5-dimethylthiazol-2-yl)-2,5-diphenyltetrazolium bromide
MW	molecular weight
N	normal
Nal	naphthyl alanine
NBS	*N*-bromosuccinimide
NGF	nerve growth factor
NHL	non-Hodgkin's lymphomas
NK	neurokinin
NMP	*N*-methyl-2-pyrrolidon

NMR	nuclear magnetic resonance
NOESY	Nuclear Overhauser effect spectroscopy
NOTA	1,4,7-triazacyclononane-1,4,7-triyltriacetic acid
OTf	trifluoromethane sulfonate
p.i.	*post* injection
PAI	plasminogen activator inhibitor
Pbf	2,2,4,6,7-pentamethyldihydrobenzofuran-5-sulfonyl
PBLG	poly-γ-benzyl-L-glutamate
PBS	phosphate-buffered saline
PC	protein C
PCBP	4-*n*-pentyl-4'-cyanobiphenyl
pdFVIII	plasma-derived human FVIII
PDMS	polydimethylsiloxane
PELG	poly-γ-ethyl-L-glutamate
PET	positron emission tomography
PI3K	phosphatidylinositol 3-kinase
PI-PLC/PI-PLD	phosphatidylinositol-specific phospholipase C/D
PK	prekallikrein
PKA	protein kinase A
PKC	protein kinase C
PL	phospholipid
PMMA	poly(methyl methacrylate)
ppm	parts per million
PROK	Proteinase K

PS	protein S, polystyrene
PVA	poly(vinyl acetate)
q	quartet
quant.	quantitative
ran	random
RDC	residual dipolar coupling
rf	reflux
R_f	retention factor
rFVIII	recombinant FVIII
RP	reverse phase
rpm	rotations per minute
rt	room temperature
R_t	retention time
s	singulet
SAG	strain induced alignment in a gel
SAR	structure-activity relationships
SEM	standard error of mean
SPECT	single photon emission computed tomography
SPPS	solid-phase peptide synthesis
sst	somatostatin
STAT	ignal transducer and activator of transcription
suPAR	soluble urokinase-type plasminogen activator receptor
t	triplet
TAFI	thrombin-activatable fibrinolysis inhibitor
TAT	thrombin–antithrombin III complex

TBAF	tetrabutyl ammonium fluoride
TBS	tert-butyldimethyl silyl
TBTU	O-(benzotriazol-1-yl)-N,N,N',N'-tetramethyluronium tetrafluoroborate
t-Bu	tertiary butyl
TCP	trityl chloride polystyrene (
TF	tissue factor
TFA	trifluoroacetic acid
TFPI	tissue factor pathway inhibitor
TGF	transforming growth factor
THF	tetrahydrofurane
TIPS	triisopropyl silane
TLC	thin layer chromatography
TMOF	trimethylorthoformate
TMS	trimethylsilyl
TOF	time of flight
tPA	Tissue plasminogen activator
Trt	trityl
uPA	urokinase-type plasminogen activator
uPAR	urokinase-type plasminogen activator receptor
UV/Vis	ultraviolett/visible
v/v	volume by volume
vWF	von Willebrand factor
w/v	weight by volume
WX360	($cyclo$[21,29][D-Cys^{21}Cys^{29}]-uPA$_{21-30}$)

269

The nomenclature used in this work is based on the guidelines recommended by Chemical Abstracts (Chemical Abstracts, 'Index Guide', 77, 210) and the IUPAC-IUB commissions (IUPAC, Eur. J. Biochem. 1971, 21, 455-477; IUPAC, Pure Appl. Chem. 1996, 68, 1919; IUPAC Commission on Nomenclature of Organic Chemistry (CNOC) and IUPAC-IUB Joint Commission on Biochemical Nomenclature (JCBN), Biochemistry 1974, 10, 3983; IUPAC-IUB (JCBN), Eur. J. Biochem. 1984, 138, 9-37). Expressions derived from the latin language are written in italic.

7 Bibliography

[1]   D. Voet, J. G. Voet, *Biochemie*, 1st ed., VHC, Weinheim, New York, Basel, Tokyo, 1994.

[2]   E. W. Davie, O. D. Ratnoff, *Science* 1964, *145*, 1310-1312.

[3]   E. W. Davie, *J Biol Chem* 2003, *278*(51), 50819-50832.

[4]   S. Butenas, K. G. Mann, *Biochemistry (Mosc)* 2002, *67*(1), 3-12.

[5]   T. E. Adams, J. A. Huntington, *Arterioscler. Thromb. Vasc. Biol.* 2006, *26*(8), 1738-1745.

[6]   P. Bishop, J. Lawson, *Nat. Rev. Drug. Discov.* 2004, *3*(8), 684-694.

[7]   R. Zhuo, C. A. Siedlecki, E. A. Vogler, *Biomaterials* 2006, *27*(24), 4325-4332.

[8]   D. L. Tankersley, J. S. Finlayson, *Biochemistry* 1984, *23*(2), 273-279.

[9]   M. Silverberg, J. T. Dunn, L. Garen, A. P. Kaplan, *J. Biol. Chem.* 1980, *255*(15), 7281-7286.

[10]   P. H. Bolton-Maggs, K. J. Pasi, *Lancet* 2003, *361*, 1801-1809.

[11]   J. A. Huntington, T. P. Baglin, *Trends Pharmacol. Sci.* 2003, *24*(11), 589-595.

[12]   P. J. Lenting, J. A. van Mourik, K. Mertens, *Blood* 1998, *92*(11), 3983-3996.

[13]   M. A. Panteleev, M. V. Ovanesov, D. A. Kireev, A. M. Shibeko, E. I. Sinauridze, N. M. Ananyeva, A. A. Butylin, E. L. Saenko, F. I. Ataullakhanov, *Biophys. J.* 2006, *90*(5), 1489-1500.

[14]   T. Bombeli, D. R. Spahn, *Br. J. Anaesth.* 2004, *93*(2), 275-287.

[15]   K. G. Mann, K. Brummel, S. Butenas, *J. Thromb. Haemost.* 2003, *1*(7), 1504-1514.

[16]   R. Radcliffe, Y. Nemerson, *J. Biol. Chem.* 1975, *250*(2), 388-395.

[17] M. Kjalke, A. Silveira, A. Hamsten, U. Hedner, M. Ezban, *Arterioscler. Thromb. Vasc. Biol.* 2000, *20*(7), 1835-1841.

[18] P. F. Neuenschwander, M. M. Fiore, J. H. Morrissey, *J. Biol. Chem.* 1993, *268*(29), 21489-21492.

[19] L. V. Rao, T. Williams, S. I. Rapaport, *Blood* 1996, *87*(9), 3738-3748.

[20] S. Butenas, K. G. Mann, *Biochemistry* 1996, *35*(6), 1904-1910.

[21] M. Yamamoto, T. Nakagaki, W. Kisiel, *J. Biol. Chem.* 1992, *267*(27), 19089-19094.

[22] P. Wildgoose, W. Kisiel, *Blood* 1989, *73*(7), 1888-1895.

[23] J. H. Lawson, M. Kalafatis, S. Stram, K. G. Mann, *J. Biol. Chem.* 1994, *269*(37), 23357-23366.

[24] B. Osterud, S. I. Rapaport, *Proc. Natl. Acad. Sci. USA* 1977, *74*(12), 5260-5264.

[25] V. J. Bom, R. M. Bertina, *Biochem. J.* 1990, *265*(2), 327-336.

[26] C. H. Gemmell, G. J. Broze, Jr., V. T. Turitto, Y. Nemerson, *Blood* 1990, *76*(11), 2266-2271.

[27] K. W. Watt, T. Takagi, R. F. Doolittle, *Proc. Natl. Acad. Sci. USA* 1978, *75*(4), 1731-1735.

[28] C. Fuss, J. C. Palmaz, E. A. Sprague, *J. Vasc. Interv. Radiol.* 2001, *12*(6), 677-682.

[29] G. Cesarman-Maus, K. A. Hajjar, *Br. J. Haematol.* 2005, *129*(3), 307-321.

[30] P. F. Bodary, K. J. Wickenheiser, D. T. Eitzman, *Expert Rev. Mol. Med.* 2002, *2002*, 1-10.

[31] A. Rimon, Y. Shamash, B. Shapiro, *J. Biol. Chem.* 1966, *241*(21), 5102-5107.

[32] M. Moroi, N. Aoki, *J. Biol. Chem.* 1976, *251*(19), 5956-5965.

[33] N. Aoki, M. Moroi, M. Matsuda, K. Tachiya, *J. Clin. Invest.* 1977, *60*(2), 361-369.

[34] E. W. Brown, S. Ravindran, P. A. Patston, *Blood Coagul. Fibrin.* 2002, *13*(8), 711-714.

[35] J. Graw, H. H. Brackmann, J. Oldenburg, R. Schneppenheim, M. Spannagl, R. Schwaab, *Nat. Rev. Genet.* 2005, *6*(6), 488-501.

[36]   M. Jacquemin, M. De Maeyer, R. D'Oiron, R. Lavend'Homme, K. Peerlinck, J. M. Saint-Remy, *J. Thromb. Haemost.* 2003, *1*(3), 456-463.

[37]   J. Oldenburg, N. M. Ananyeva, E. L. Saenko, *Haemophilia* 2004, *10*(Suppl 4), 133-139.

[38]   J. Klinge, N. M. Ananyeva, C. A. Hauser, E. L. Saenko, *Semin. Thromb. Hemost.* 2002, *28*(3), 309-322.

[39]   E. L. Saenko, N. Ananyeva, D. Kouiavskaia, H. Schwinn, D. Josic, M. Shima, C. A. E. Hauser, S. Pipe, *Vox Sang.* 2002, *83*(2), 89-96.

[40]   P. M. Mannucci, *J. Thromb. Haemost.* 2003, *1*(7), 1349-1355.

[41]   W. K. Hoots, *Haemophilia* 2001, *7*(Suppl 1), 4-9.

[42]   United Kingdom Haemophilia Centre Doctors' Organisation (UKHCDO), *Haemophilia* 2003, *9*(1), 1-23.

[43]   A. Ishiwata, J. Mimuro, Y. Kashiwakura, M. Niimura, K. Takano, T. Ohmori, S. Madoiwa, H. Mizukami, T. Okada, H. Naka, A. Yoshioka, K. Ozawa, Y. Sakata, *Thromb Res* 2006, *118*(5), 627-635.

[44]   M. A. Kay, K. High, *Proc. Natl. Acad. Sci. USA* 1999, *96*(18), 9973-9975.

[45]   S. Connelly, J. Mount, A. Mauser, J. M. Gardner, M. Kaleko, A. McClelland, C. D. Lothrop, Jr., *Blood* 1996, *88*(10), 3846-3853.

[46]   S. Connelly, J. L. Andrews, A. M. Gallo, D. B. Kayda, J. Qian, L. Hoyer, M. J. Kadan, M. I. Gorziglia, B. C. Trapnell, A. McClelland, M. Kaleko, *Blood* 1998, *91*(9), 3273-3281.

[47]   C. Balague, J. Zhou, Y. Dai, R. Alemany, S. F. Josephs, G. Andreason, M. Hariharan, E. Sethi, E. Prokopenko, H. Y. Jan, Y. C. Lou, D. Hubert-Leslie, L. Ruiz, W. W. Zhang, *Blood* 2000, *95*(3), 820-828.

[48]   J. A. Bristol, A. Gallo-Penn, J. Andrews, N. Idamakanti, M. Kaleko, S. Connelly, *Hum. Gene Ther.* 2001, *12*(13), 1651-1661.

[49]   F. Park, K. Ohashi, M. A. Kay, *Blood* 2000, *96*(3), 1173-1176.

[50]   Y. Yang, F. A. Nunes, K. Berencsi, E. E. Furth, E. Gonczol, J. M. Wilson, *Proc. Natl. Acad. Sci. USA* 1994, *91*(10), 4407-4411.

[51]   V. R. Arruda, *J. Thromb. Haemost.* 2006, *4*(6), 1215-1217.

[52] W. M. McCormack, Jr., M. P. Seiler, T. K. Bertin, K. Ubhayakar, D. J. Palmer, P. Ng, T. C. Nichols, B. Lee, *J. Thromb. Haemost.* 2006, *4*(6), 1218-1225.

[53] K. P. Ponder, *Curr. Opin. Hematol.* 2006, *13*(5), 301-307.

[54] A. Farrugia, *Haemophilia* 2004, *10*(4), 327-333.

[55] P. M. Mannucci, *J. Thromb. Haemost.* 2003, *1*(2), 216-217.

[56] W. K. Hoots, *Transfus Med. Rev.* 2001, *15*(2), 11-19.

[57] W. K. Hoots, *Transfus Med. Rev.* 2001, *15*(2 Suppl 1), 3-10.

[58] J. Gitschier, W. I. Wood, T. M. Goralka, K. L. Wion, E. Y. Chen, D. H. Eaton, G. A. Vehar, D. J. Capon, R. M. Lawn, *Nature* 1984, *312*(5992), 326-330.

[59] W. I. Wood, D. J. Capon, C. C. Simonsen, D. L. Eaton, J. Gitschier, B. Keyt, P. H. Seeburg, D. H. Smith, P. Hollingshead, K. L. Wion, et al., *Nature* 1984, *312*(5992), 330-337.

[60] J. J. Toole, J. L. Knopf, J. M. Wozney, L. A. Sultzman, J. L. Buecker, D. D. Pittman, R. J. Kaufman, E. Brown, C. Shoemaker, E. C. Orr, et al., *Nature* 1984, *312*(5992), 342-347.

[61] R. J. Kaufman, S. W. Pipe, *Haemophilia* 1998, *4*(4), 370-379.

[62] E. L. Saenko, N. M. Ananyeva, M. Shima, C. A. Hauser, S. W. Pipe, *J. Thromb. Haemost.* 2003, *1*(5), 922-930.

[63] C. Lee, *Thromb. Haemost.* 1999, *82*(2), 516-524.

[64] S. W. Pipe, J. M. Saint-Remy, C. E. Walsh, *Haemophilia* 2004, *10*(Suppl 4), 55-63.

[65] J. P. Betts, *BMJ* 1998, *316*(7141), 1385.

[66] A. Azzi, R. De Santis, M. Morfini, K. Zakrzewska, R. Musso, E. Santagostino, G. Castaman, *Blood* 2001, *98*(8), 2571-2573.

[67] R. K. Eriksson, C. Fenge, E. Lindner-Olson, C. Ljungqvist, J. Rosenquist, A. L. Smeds, A. Ostlin, T. Charlebois, M. Leonard, B. D. Kelley, A. Ljungqvist, *Semin. Hematol.* 2001, *38*(2 (Suppl. 4)), 24-31.

[68] N. Ananyeva, A. Khrenov, F. Darr, R. Summers, A. Sarafanov, E. Saenko, *Expert Opin. Pharmacother.* 2004, *5*(5), 1061-1070.

[69] J. Barbara, P. Flanagan, *BMJ* 1998, *316*(7133), 717-718.

[70]   Medical and Scientific Advisory Council (MASAC) of the National Hemophilia Foundation. MASAC recommencations concerning the treatment of Hemophilia and other bleeeding disorders, *MASAC Document #151* 2003, http://www.hemophilia.org/NHFWeb/Resource/StaticPages/menu0/menu5/menu57/masac151.pdf.

[71]   A. Bird, P. Isarangkura, D. Almagro, A. Gonzaga, A. Srivastava, *Haemophilia* 1998, *4*(4), 481-485.

[72]   G. A. Vehar, B. Keyt, D. Eaton, H. Rodriguez, D. P. O'Brien, F. Rotblat, H. Oppermann, R. Keck, W. I. Wood, R. N. Harkins, et al., *Nature* 1984, *312*(5992), 337-342.

[73]   W. Wang, Y. J. Wang, D. N. Kelner, *Int. J. Pharm.* 2003, *259*(1-2), 1-15.

[74]   M. L. Koschinsky, W. D. Funk, B. A. van Oost, R. T. MacGillivray, *Proc. Natl. Acad. Sci. USA* 1986, *83*(14), 5086-5090.

[75]   W. H. Kane, E. W. Davie, *Proc. Natl. Acad. Sci. USA* 1986, *83*(18), 6800-6804.

[76]   J. J. Toole, D. D. Pittman, E. C. Orr, P. Murtha, L. C. Wasley, R. J. Kaufman, *Proc. Natl. Acad. Sci. USA* 1986, *83*(16), 5939-5942.

[77]   A. V. Khrenov, N. M. Ananyeva, E. L. Saenko, *Blood Coagul. Fibrin.* 2006, *17*(5), 379-388.

[78]   P. J. Fay, M. T. Anderson, S. I. Chavin, V. J. Marder, *Biochim. Biophys. Acta* 1986, *871*(3), 268-278.

[79]   P. J. Fay, *Blood Rev.* 2004, *18*(1), 1-15.

[80]   S. S. Stoylova, P. J. Lenting, G. Kemball-Cook, A. Holzenburg, *J. Biol. Chem.* 1999, *274*(51), 36573-36578.

[81]   H. J. Weiss, I. I. Sussman, L. W. Hoyer, *J. Clin. Invest.* 1977, *60*(2), 390-404.

[82]   E. G. D. Tuddenham, L. W. Hoyer, *Thromb. Haemost.* 1977, *38*(1), 9-9.

[83]   E. L. Saenko, D. Scandella, *J. Biol. Chem.* 1997, *272*(29), 18007-18014.

[84]   M. Jacquemin, A. Benhida, K. Peerlinck, B. Desqueper, L. V. Elst, R. Lavend'homme, R. d'Oiron, R. Schwaab, M. Bakkus, K. Thielemans, J. G. Gilles, J. Vermylen, J. M. Saint-Remy, *Blood* 2000, *95*(1), 156-163.

[85] R. J. Wise, A. J. Dorner, M. Krane, D. D. Pittman, R. J. Kaufman, *J. Biol. Chem.* 1991, *266*(32), 21948-21955.

[86] R. J. Kaufman, S. W. Pipe, *Thromb. Haemost.* 1999, *82*(2), 201-208.

[87] J. Over, J. J. Sixma, M. H. Bruine, M. C. Trieschnigg, R. A. Vlooswijk, N. H. Beeser-Visser, B. N. Bouma, *J. Clin. Invest.* 1978, *62*(2), 223-234.

[88] K. Nogami, M. Shima, K. Hosokawa, M. Nagata, T. Koide, E. L. Saenko, I. Tanaka, M. Shibata, A. Yoshioka, *J. Biol. Chem.* 2000, *275*(33), 25774-25780.

[89] L. M. Regan, P. J. Fay, *J. Biol. Chem.* 1995, *270*(15), 8546-8552.

[90] R. T. Barrow, J. F. Healey, M. G. Jacquemin, J. M. Saint-Remy, P. Lollar, *Blood* 2001, *97*(1), 169-174.

[91] E. L. Saenko, D. Scandella, A. V. Yakhyaev, N. J. Greco, *J. Biol. Chem.* 1998, *273*(43), 27918-27926.

[92] P. A. Foster, C. A. Fulcher, R. A. Houghten, T. S. Zimmerman, *Blood* 1990, *75*(10), 1999-2004.

[93] K. P. Pratt, B. W. Shen, K. Takeshima, E. W. Davie, K. Fujikawa, B. L. Stoddard, *Nature* 1999, *402*(6760), 439-442.

[94] P. J. Fay, K. Koshibu, *J. Biol. Chem.* 1998, *273*(30), 19049-19054.

[95] P. J. Fay, M. Mastri, M. E. Koszelak, H. Wakabayashi, *J. Biol. Chem.* 2001, *276*(15), 12434-12439.

[96] P. J. Lenting, J. W. van de Loo, M. J. Donath, J. A. van Mourik, K. Mertens, *J. Biol. Chem.* 1996, *271*(4), 1935-1940.

[97] G. E. Gilbert, R. J. Kaufman, A. A. Arena, H. Miao, S. W. Pipe, *J. Biol. Chem.* 2002, *277*(8), 6374-6381.

[98] P. J. Fay, D. Scandella, *J. Biol. Chem.* 1999, *274*(42), 29826-29830.

[99] P. J. Fay, T. Beattie, C. F. Huggins, L. M. Regan, *J. Biol. Chem.* 1994, *269*(32), 20522-20527.

[100] K. Nogami, M. Shima, K. Hosokawa, T. Suzuki, T. Koide, E. L. Saenko, D. Scandella, M. Shibata, S. Kamisue, I. Tanaka, A. Yoshioka, *J. Biol. Chem.* 1999, *274*(43), 31000-31007.

[101] I. Zaitseva, V. Zaitsev, G. Card, K. Moshkov, B. Bax, A. Ralph, P. Lindley, *J. Biol. Inorg. Chem.* 1996, *1*(1), 15-23.

[102] S. Pemberton, P. Lindley, V. Zaitsev, G. Card, E. G. Tuddenham, G. Kemball-Cook, *Blood* 1997, *89*(7), 2413-2421.

[103] A. J. Gale, J. L. Pellequer, *J. Thromb. Haemost.* 2003, *1*(9), 1966-1971.

[104] W. H. Hakeos, H. Miao, N. Sirachainan, G. Kemball-Cook, E. L. Saenko, R. J. Kaufman, S. W. Pipe, *Thromb. Haemost.* 2002, *88*(5), 781-787.

[105] T. E. Adams, M. F. Hockin, K. G. Mann, S. J. Everse, *Proc. Natl. Acad. Sci. USA* 2004, *101*(24), 8918-8923.

[106] S. Stoilova-McPhie, B. O. Villoutreix, K. Mertens, G. Kemball-Cook, A. Holzenburg, *Blood* 2002, *99*(4), 1215-1223.

[107] V. S. Purohit, K. Ramani, R. S. Kashi, M. J. Durrani, T. J. Kreiger, S. V. Balasubramanian, *Biochim Biophys Acta* 2003, *1617*(1-2), 31-38.

[108] L. Autin, M. A. Miteva, W. H. Lee, K. Mertens, K. P. Radtke, B. O. Villoutreix, *J. Thromb. Haemost.* 2005, *3*(9), 2044-2056.

[109] K. Takeshima, C. Smith, J. Tait, K. Fujikawa, *Thromb. Haemost.* 2003, *89*(5), 788-794.

[110] H. Brandstetter, M. Bauer, R. Huber, P. Lollar, W. Bode, *Proc. Natl. Acad. Sci. USA* 1995, *92*(21), 9796-9800.

[111] P. J. Fay, P. V. Jenkins, *Blood Rev.* 2005, *19*(1), 15-27.

[112] K. Mertens, P. H. Celie, J. A. Kolkman, P. J. Lenting, *Thromb. Haemost.* 1999, *82*(2), 209-217.

[113] Cuatreca.P, M. Wilchek, C. B. Anfinsen, *Proc. Natl. Acad. Sci. USA* 1968, *61*(2), 636-643.

[114] O. Mejan, V. Fert, M. Delezay, M. Delaage, R. Cheballah, A. Bourgois, *Thromb. Haemost.* 1988, *59*(3), 364-371.

[115] D. N. Fass, G. J. Knutson, J. A. Katzmann, *Blood* 1982, *59*(3), 594-600.

[116] J. E. Addiego, E. Gomperts, S. L. Liu, P. Bailey, S. G. Courter, M. L. Lee, G. G. Neslund, H. S. Kingdon, M. J. Griffith, *Thromb. Haemost.* 1992, *67*(1), 19-27.

[117] B. G. Boedeker, *Transfus Med. Rev.* 1992, *6*(4), 256-260.

[118] E. Gomperts, R. Lundblad, R. Adamson, *Transfus Med. Rev.* 1992, *6*(4), 247-251.

[119] J. J. Jakubik, S. M. Vicik, M. M. Tannatt, B. D. Kelley, *Haemophilia* 2004, *10*(1), 69-74.

[120] R. Jiang, T. Monroe, R. McRogers, P. J. Larson, *Haemophilia* 2002, *8*(Suppl. 2), 1-5.

[121] G. W. Jack, D. J. Beer, *Methods Mol. Biol.* 1996, *59*, 187-196.

[122] R. K. Scopes, *Protein purification: Principles and Practice*, 3rd ed., Springer, New York, 1994.

[123] A. C. Roque, C. R. Lowe, M. A. Taipa, *Biotechnol. Prog.* 2004, *20*(3), 639-654.

[124] N. E. Labrou, *J. Chromatogr. B Analyt. Technol. Biomed. Life Sci.* 2003, *790*(1-2), 67-78.

[125] C. R. Lowe, A. R. Lowe, G. Gupta, *J. Biochem. Biophys. Methods* 2001, *49*(1-3), 561-574.

[126] Y. D. Clonis, *J. Chromatogr. A* 2006, *1101*(1-2), 1-24.

[127] E. L. Saenko, J.-M. Saint-Remy.

[128] C. R. Lowe, *Curr. Opin. Chem. Biol.* 2001, *5*(3), 248-256.

[129] B. D. Kelley, M. Tannatt, R. Magnusson, S. Hagelberg, J. Booth, *Biotechnol. Bioeng.* 2004, *87*(3), 400-412.

[130] B. D. Kelley, J. Booth, M. Tannatt, Q. L. Wub, R. Ladner, J. Yuc, D. Potter, A. Ley, *J. Chromatogr. A* 2004, *1038*(1-2), 121-130.

[131] K. Amatschek, R. Necina, R. Hahn, E. Schallaun, H. Schwinn, D. Josic, A. Jungbauer, *J. High Resolut. Chromatogr.* 2000, *23*(1), 47-58.

[132] K. Pflegerl, R. Hahn, E. Berger, A. Jungbauer, *J. Pept. Sci.* 2002, *59*(4), 174-182.

[133] R. B. Merrifield, *J. Am. Chem. Soc.* 1963, *85*, 2149-2154.

[134] B. Merrifield, *Angew. Chem. Int. Edit.* 1985, *24*(10), 799-810.

[135] L. A. Carpino, G. Y. Han, *J. Org. Chem.* 1972, *37*(22), 3404-3409.

[136] L. A. Carpino, B. J. Cohen, K. E. Stephens, S. Y. Sadataalaee, J. H. Tien, D. C. Langridge, *J. Org. Chem.* 1986, *51*(19), 3732-3734.

[137] G. B. Fields, R. L. Noble, *Int. J. Pept. Protein Res.* 1990, *35*(3), 161-214.

[138] T. Curtius, *J. Prakt. Chem.* 1881, *24*, 239-240.

[139] E. Fischer, *Chem. Ber.* 1902, *35*, 1095 - 1106.

[140] F.Hofmeister, *Ergeb. Physiol. Biol. Chem. Exp. Pharmacol* 1902, *1*, 759.

[141] E. Fischer, *Chem. Ber.* 1906, *39*, 530-537.

[142] J. A. McLaren, *Aust. J. Chem.* 1958, *11*, 360-365.

[143] M. Bergmann, L. Zervas, *Chem. Ber.* 1932, *65*, 1192-1201.

[144] G. Barany, R. B. Merrifield, *J. Am. Chem. Soc.* 1977, *99*(22), 7363-7365.

[145] R. Schwyzer, H. Kappeler, *Helvetica Chimica Acta* 1963, *46*(5), 1550-1572.

[146] M. Bodanszky, V. Du Vigneaud, *Nature* 1959, *183*(4671), 1324-1325.

[147] C. Chan, D. White, *Fmoc solid phase peptide synthesis: a practical approach*, Oxford University Press, Oxford, 2000.

[148] K. Barlos, D. Gatos, J. Kallitsis, G. Papaphotiu, P. Sotiriu, W. Q. Yao, W. Schafer, *Tetrahedron Lett.* 1989, *30*(30), 3943-3946.

[149] P. Sieber, *Tetrahedron Lett.* 1987, *28*(19), 2107-2110.

[150] L. A. Carpino, D. Sadat-Aalaee, H. G. Chao, R. H. DeSelm, *J. Am. Chem. Soc.* 1990, *112*(26), 9651-9652.

[151] H. Chantrenne, *Nature* 1947, *160*(4070), 603-604.

[152] J. Kovacs, Kisfalud.L, M. Q. Ceprini, *J. Am. Chem. Soc.* 1967, *89*(1), 183-&.

[153] J. C. Sheehan, G. P. Hess, *J. Am. Chem. Soc.* 1955, *77*(4), 1067-1068.

[154] M. Bodanszky, *Principles of peptide synthesis*, Springer Verlag, Berlin, 1984.

[155] F. Albericio, J. M. Bofill, A. El-Faham, S. A. Kates, *J. Org. Chem.* 1998, *63*(26), 9678-9683.

[156] R. Knorr, A. Trzeciak, W. Bannwarth, D. Gillessen, *Tetrahedron Lett.* 1989, *30*(15), 1927-1930.

[157] V. Dourtoglou, J. C. Ziegler, B. Gross, *Tetrahedron Lett.* 1978(15), 1269-1272.

[158] B. Castro, J. R. Dormoy, G. Evin, C. Selve, *Tetrahedron Lett.* 1975(14), 1219-1222.

[159] J. Coste, D. Lenguyen, B. Castro, *Tetrahedron Lett.* 1990, *31*(2), 205-208.

[160] J. M. Humphrey, A. R. Chamberlin, *Chem. Rev.* 1997, *97*(6), 2243-2266.

[161] H. P. Koch, M. P. Kavanaugh, C. S. Esslinger, N. Zerangue, J. M. Humphrey, S. G. Amara, A. R. Chamberlin, R. J. Bridges, *Mol. Pharmacol.* 1999, *56*(6), 1095-1104.

[162] V. Dourtoglou, B. Gross, V. Lambropoulou, C. Zioudrou, *Synthesis-Stuttgart* 1984(7), 572-574.

[163] W. König, R. Geiger, *Chem. Ber.-Recl.* 1970, *103*(7), 2024-2033.

[164] W. König, R. Geiger, *Chem. Ber.-Recl.* 1970, *103*(7), 2034-2040.

[165] W. König, R. Geiger, *Chem. Ber.-Recl.* 1970, *103*(3), 788-798.

[166] L. A. Carpino, *J. Am. Chem. Soc.* 1993, *115*(10), 4397-4398.

[167] L. A. Carpino, A. Elfaham, *J. Org. Chem.* 1994, *59*(4), 695-698.

[168] Y. X. Han, F. Albericio, G. Barany, *J. Org. Chem.* 1997, *62*(13), 4307-4312.

[169] S. Knör, A. Khrenov, B. Laufer, E. L. Saenko, C. A. E. Hauser, H. Kessler., *J. Med. Chem.* 2007, submitted.

[170] H. Gerlach, V. Prelog, Owtschin.Ja, *Helv. Chim. Acta* 1964, *47*(8), 2294-&.

[171] V. Prelog, H. Gerlach, *Helv. Chim. Acta* 1964, *47*(8), 2288-&.

[172] M. M. Shemyakin, Y. A. Ovchinnikov, V. T. Ivanov, *Angew. Chem. Int. Edit.* 1969, *8*(7), 492-499.

[173] M. Chorev, M. Goodman, *Accounts Chem. Res.* 1993, *26*(5), 266-273.

[174] M. Goodman, M. Chorev, *Accounts Chem. Res.* 1979, *12*(1), 1-7.

[175] J. Wermuth, S. L. Goodman, A. Jonczyk, H. Kessler, *J. Am. Chem. Soc.* 1997, *119*(6), 1328-1335.

[176] A. Paquet, *Can. J. Chemistry* 1981, *60*, 976-980.

[177] V. Krchnak, A. S. Weichsel, D. Cabel, Z. Flegelova, M. Lebl, *Mol. Divers.* 1996, *1*(3), 149-164.

[178] H. Nagase, in *Handbook of Proteolytic Enzymes, Vol. 2* (Eds.: A. J. Barrett, N. D. Rawlings, J. F. Woessner), Elsevier, London, 2004, pp. 512-523.

[179] N. Sewald, H.-D. Jakubke, *Peptides: Chemistry and Biology*, WILEY-VCH Verlag GmbH, Weinheim, 2002.

[180] L. Zervas, I. Photaki, *J. Am. Chem. Soc.* 1962, *84*(20), 3887-3897.

[181] F. Siedler, E. Weyher, L. Moroder, *J. Pept. Sci.* 1996, *2*(4), 271-275.

[182] M. Goodman, L. Levine, *J. Am. Chem. Soc.* 1964, *86*(14), 2918-2922.

[183] B. Henkel, L. S. Zhang, E. Bayer, *Liebigs Ann.-Recl.* 1997(10), 2161-2168.

[184] W. Steglich, G. Hofle, *Angew. Chem. Int. Edit.* 1969, *8*(12), 981.

[185] H. M. L. Davies, R. J. Townsend, *J. Org. Chem.* 2001, *66*(20), 6595-6603.

[186] P. Micuch, D. Seebach, *Helv. Chim. Acta* 2002, *85*(6), 1567-1577.

[187] S. T. Hilton, T. C. T. Ho, G. Pljevaljcic, K. Jones, *Org. Lett.* 2000, *2*(17), 2639-2641.

[188] T. T. Tidwell, *Synthesis-Stuttgart* 1990(10), 857-870.

[189] A. J. Mancuso, S. L. Huang, D. Swern, *J. Org. Chem.* 1978, *43*(12), 2480-2482.

[190] J. N. Denis, A. Correa, A. E. Greene, *J. Org. Chem.* 1991, *56*(24), 6939-6942.

[191] M. A. Blaskovich, G. A. Lajoie, *J. Am. Chem. Soc.* 1993, *115*(12), 5021-5030.

[192] R. Grigg, W. S. MacLachlan, D. T. MacPherson, V. Sridharan, S. Suganthan, M. Thornton-Pett, J. Zhang, *Tetrahedron* 2000, *56*(35), 6585-6594.

[193] D. Gryko, J. Chalko, J. Jurczak, *Chirality* 2003, *15*(6), 514-541.

[194] D. B. Dess, J. C. Martin, *J. Org. Chem.* 1983, *48*(22), 4155-4156.

[195] D. B. Dess, J. C. Martin, *J. Am. Chem. Soc.* 1991, *113*(19), 7277-7287.

[196] E. Masiukiewicz, B. Rzeszotarska, *Org. Prep. Proced. Int.* 1999, *31*(5), 571-572.

[197] D. A. Pearson, M. Blanchette, M. L. Baker, C. A. Guindon, *Tetrahedron Lett.* 1989, *30*(21), 2739-2742.

[198] S. Knör, A. Khrenov, B. Laufer, A. Benhida, R. Schwaab, J. Oldenburg, N. Beaufort, V. Magdolen, J.-M. Saint-Remy, E. L. Saenko, C. A. E. Hauser, H. Kessler, *J. Thromb. Haemost.* 2007, submitted.

[199] S. Monroc, E. Badosa, L. Feliu, M. Planas, E. Montesinos, E. Bardaji, *Peptides* 2006, *27*(11), 2567-2574.

[200] P. Y. Huang, G. A. Baumbach, C. A. Dadd, J. A. Buettner, B. L. Masecar, M. Hentsch, D. J. Hammond, R. G. Carbonell, *Bioorgan. Med. Chem.* 1996, *4*(5), 699-708.

[201] M. A. Jankowski, H. Patel, J. C. Rouse, L. A. Marzilli, S. B. Weston, P. J. Sharpe, *Haemophilia* 2007, *13*(1), 30-37.

[202] W. F. Schilow, E. Schoemer-Burkhardt, R. Seitz, *Thromb. Haemost.* 2004, *92*(2), 427-428.

[203] S. Raut, S. Villard, S. Grailly, J. G. G. Gilles, C. Granier, J. M. R. Saint-Remy, T. W. Barrowcliffe, *Thromb. Haemost.* 2003, *90*(3), 385-397.

[204] P. C. Spiegel, M. Jacquemin, J. M. R. Saint-Remy, B. L. Stoddard, K. P. Pratt, *Blood* 2001, *98*(1), 13-19.

[205] K. Fischer, V. Lutz, O. Wilhelm, M. Schmitt, H. Graeff, P. Heiss, T. Nishiguchi, N. Harbeck, H. Kessler, T. Luther, V. Magdolen, U. Reuning, *FEBS Lett.* 1998, *438*(1-2), 101-105.

[206] U. Reuning, M. Schmitt, B. Luber, V. Beck, V. Magdolen, *Methods Mol. Med.* 2006, *120*, 427-440.

[207] R. Haubner, D. Finsinger, H. Kessler, *Angew. Chem. Int. Edit.* 1997, *36*(13-14), 1375-1389.

[208] H. Kessler, in *Trends in Drug Research, Vol. 13* (Ed.: V. Claassen), Elsevier, 1990, pp. 73-84.

[209] H. Kessler, *Angew. Chem. Int. Edit.* 1982, *21*, 512-523.

[210] D. Heckmann, *Dissertation* 2007, Technische Universität München.

[211] A. Y. Jeng, P. Savage, M. E. Beil, C. W. Bruseo, D. Hoyer, C. A. Fink, A. J. Trapani, *Clin. Sci.* 2002, *103*, 98S-101S.

[212] M. Goodman, H. Shao, *Pure Appl. Chem.* 1996, *68*(6), 1303-1308.

[213] M. A. Dechantsreiter, E. Planker, B. Mathä, E. Lohof, G. Hölzemann, A. Jonczyk, S. L. Goodman, H. Kessler, *J. Med. Chem.* 1999, *42*(16), 3033-3040.

[214] S. Knör, B. Laufer, H. Kessler, *J. Org. Chem.* 2006, *71*(15), 5625-5630.

[215] W. Wang, J. Y. Zhang, C. Y. Xiong, V. J. Hruby, *Tetrahedron Lett.* 2002, *43*(12), 2137-2140.

[216] M. J. Burk, J. R. Lee, J. P. Martinez, *J. Am. Chem. Soc.* 1994, *116*(23), 10847-10848.

[217] M. J. Burk, M. F. Gross, T. G. P. Harper, C. S. Kalberg, J. R. Lee, J. P. Martinez, *Pure Appl. Chem.* 1996, *68*(1), 37-44.

[218] W. Wang, C. Y. Xiong, J. Y. Zhang, V. J. Hruby, *Tetrahedron* 2002, *58*(15), 3101-3110.

[219] W. Wang, M. Y. Cai, C. Y. Xiong, J. Y. Zhang, D. Trivedi, V. J. Hruby, *Tetrahedron* 2002, *58*(36), 7365-7374.

[220] S. Kotha, K. Lahin, *Biopolymers* 2003, *69*(4), 517-528.

[221] S. M. Birnbaum, L. Levintow, R. B. Kingsley, J. P. Greenstein, *J. Biol. Chem.* 1952, *194*(1), 455-470.

[222] M. A. Vela, F. R. Fronczek, G. W. Horn, M. L. Mclaughlin, *J. Org. Chem.* 1990, *55*(9), 2913-2918.

[223] U. Schmidt, A. Lieberknecht, J. Wild, *Synthesis-Stuttgart* 1984(1), 53-60.

[224] U. Schmidt, H. Griesser, V. Leitenberger, A. Lieberknecht, R. Mangold, R. Meyer, B. Riedl, *Synthesis-Stuttgart* 1992(5), 487-490.

[225] M. J. Burk, *J. Am. Chem. Soc.* 1991, *113*(22), 8518-8519.

[226] M. J. Burk, J. E. Feaster, W. A. Nugent, R. L. Harlow, *J. Am. Chem. Soc.* 1993, *115*(22), 10125-10138.

[227] M. J. Burk, M. F. Gross, J. P. Martinez, *J. Am. Chem. Soc.* 1995, *117*(36), 9375-9376.

[228] M. J. Burk, J. G. Allen, W. F. Kiesman, *J. Am. Chem. Soc.* 1998, *120*(4), 657-663.

[229] H. Kessler, M. Molter, *Angew. Chem. Int. Edit.* 1973, *12*(12), 1011-1012.

[230] D. Hanahan, R. A. Weinberg, *Cell* 2000, *100*(1), 57-70.

[231] E. Ruoslahti, *Sci Am* 1996, *275*(3), 72-77.

[232] W. J. Guo, F. G. Giancotti, *Nat. Rev. Mol. Cell Biol.* 2004, *5*(10), 816-826.

[233] F. Zhang, C. C. Tom, M. C. Kugler, T. T. Ching, J. A. Kreidberg, Y. Wei, H. A. Chapman, *J. Cell Biol.* 2003, *163*(1), 177-188.

[234] K. Danø, P. A. Andreasen, J. Grondahl-Hansen, P. Kristensen, L. S. Nielsen, L. Skriver, *Adv. Cancer Res.* 1985, *44*, 139-266.

[235] O. Wilhelm, U. Reuning, F. Jänicke, M. Schmitt, H. Graeff, *Onkologie* 1994, *17*(4), 358-366.

[236] S. Cook, http://www.steve.gb.com/science/extracellular_matrix.html.

[237] A. M. Mercurio, *Trends Cell Biol.* 1995, *5*(11), 419-423.

[238] D. R. Critchley, *Curr. Opin. Cell Biol.* 2000, *12*(1), 133-139.

[239] E. Ruoslahti, *Adv. Cancer Res.* 1999, *76*, 1-20.

[240] M. Lee, R. Fridman, S. Mobashery, *Chem. Soc. Rev.* 2004, *33*(7), 401-409.

[241] M. Schmitt, H. Graeff, F. Jänicke, T. Genz, B. Lampe, *Prospects in Diagnosis and Treatment of Breast Cancer: Proceedings of the Joint International Symposium, Munich, Germany, 10-11 November 1993*, Elsevier Science, Amsterdam, 1994.

[242] D. R. Edwards, G. Murphy, *Nature* 1998, *394*(6693), 527-528.

[243] M. Johnsen, L. R. Lund, J. Romer, K. Almholt, K. Danø, *Curr. Opin. Cell Biol.* 1998, *10*(5), 667-671.

[244] M. Egeblad, Z. Werb, *Nat. Rev. Cancer* 2002, *2*(3), 161-174.

[245] N. Johansson, M. Ahonen, V. M. Kahari, *Cell. Mol. Life Sci.* 2000, *57*(1), 5-15.

[246] J. E. Koblinski, M. Ahram, B. F. Sloane, *Clinica Chimica Acta* 2000, *291*(2), 113-135.

[247] S. Nozaki, Y. Endo, H. Nakahara, K. Yoshizawa, T. Ohara, E. Yamamoto, *Anti-Cancer Drugs* 2006, *17*(10), 1109-1117.

[248] M. Schmitt, O. G. Wilhelm, U. Reuning, A. Krüger, N. Harbeck, E. Lengyel, H. Graeff, B. Gänsbacher, H. Kessler, M. Bürgle, J. Stürzebecher, S. Sperl, V. Magdolen, *Fibrinolysis & Proteolysis* 2000, *14*(2-3), 114-132.

[249] P. A. Andreasen, R. Egelund, H. H. Petersen, *Cell. Mol. Life Sci.* 2000, *57*(1), 25-40.

[250] M. Schmitt, F. Jänicke, H. Graeff, *Fibrinolysis* 1992, *6*, 3-26.

[251] F. J. Castellino, V. A. Ploplis, *Thromb. Haemost.* 2005, *93*(4), 647-654.

[252] J. S. Rao, *Nat. Rev. Cancer* 2003, *3*(7), 489-501.

[253] K. Uhland, *Cell. Mol. Life Sci.* 2006, *63*(24), 2968-2978.

[254] W. G. Stetler-Stevenson, L. A. Liotta, D. E. Kleiner, Jr., *FASEB J* 1993, *7*(15), 1434-1441.

[255] P. Basset, J. P. Bellocq, C. Wolf, I. Stoll, P. Hutin, J. M. Limacher, O. L. Podhajcer, M. P. Chenard, M. C. Rio, P. Chambon, *Nature* 1990, *348*(6303), 699-704.

[256] M. M. Mohamed, B. F. Sloane, *Nat. Rev. Cancer* 2006, *6*(10), 764-775.

[257] B. F. Sloane, *Semin. Cancer Biol.* 1990, *1*(2), 137-152.

[258] H. Rochefort, *Breast Cancer Res. Treat.* 1990, *16*(1), 3-13.

[259] K. Danø, N. Behrendt, G. Høyer-Hansen, M. Johnsen, L. R. Lund, M. Ploug, J. Romer, *Thromb. Haemost.* 2005, *93*(4), 676-681.

[260] S. W. Hall, J. E. Humphries, S. L. Gonias, *J. Biol. Chem.* 1991, *266*(19), 12329-12336.

[261] A. Meissauer, M. D. Kramer, V. Schirrmacher, G. Brunner, *Exp. Cell Res.* 1992, *199*(2), 179-190.

[262] G. E. Stillfried, D. N. Saunders, M. Ranson, *Breast Cancer Res.* 2007, *9*(1), R14.

[263] V. Ellis, N. Behrendt, K. Danø, *J. Biol. Chem.* 1991, *266*(19), 12752-12758.

[264] A. Gils, P. J. Declerck, *Thromb. Haemost.* 1998, *80*(4), 531-541.

[265] R. W. Carrell, P. E. Stein, *Biol. Chem. Hoppe Seyler* 1996, *377*(1), 1-17.

[266] D. Olson, J. Pollanen, G. Høyer-Hansen, E. Rønne, K. Sakaguchi, T. C. Wun, E. Appella, K. Danø, F. Blasi, *J. Biol. Chem.* 1992, *267*(13), 9129-9133.

[267] F. Al-Ejeh, D. Croucher, M. Ranson, *Exp. Cell. Res.* 2004, *297*(1), 259-271.

[268] M. V. Cubellis, T. C. Wun, F. Blasi, *EMBO J.* 1990, *9*(4), 1079-1085.

[269] D. Croucher, D. N. Saunders, M. Ranson, *J. Biol. Chem.* 2006, *281*(15), 10206-10213.

[270] R. P. Czekay, T. A. Kuemmel, R. A. Orlando, M. G. Farquhar, *Mol. Biol. Cell* 2001, *12*(5), 1467-1479.

[271] A. Nykjaer, M. Conese, E. I. Christensen, D. Olson, O. Cremona, J. Gliemann, F. Blasi, *EMBO J.* 1997, *16*(10), 2610-2620.

[272] M. Conese, A. Nykjaer, C. M. Petersen, O. Cremona, R. Pardi, P. A. Andreasen, J. Gliemann, E. I. Christensen, F. Blasi, *J. Cell. Biol.* 1995, *131*(6 Pt 1), 1609-1622.

[273] S. Mayor, H. Riezman, *Nat. Rev. Mol. Cell Biol.* 2004, *5*(2), 110-120.

[274] M. Conese, F. Blasi, *Biol. Chem. Hoppe Seyler* 1995, *376*(3), 143-155.

[275] L. H. Engelholm, B. S. Nielsen, K. Danø, N. Behrendt, *Trends Cardiovas. Med.* 2001, *11*(1), 7-13.

[276] H. Jin, Y. M. P. Song, G. Boel, J. Kochar, V. Pancholi, *J. Mol. Biol.* 2005, *350*(1), 27-41.

[277] J. Sturge, D. Wienke, L. East, G. E. Jones, C. M. Isacke, *J. Cell. Biol.* 2003, *162*(5), 789-794.

[278] T. C. Wun, L. Ossowski, E. Reich, *J. Biol. Chem.* 1982, *257*(12), 7262-7268.

[279] Y. Nagamine, R. L. Medcalf, P. Munoz-Canoves, *Thromb. Haemost.* 2005, *93*(4), 661-675.

[280] A. P. Hansen, A. M. Petros, R. P. Meadows, D. G. Nettesheim, A. P. Mazar, E. T. Olejniczak, R. X. Xu, T. M. Pederson, J. Henkin, S. W. Fesik, *Biochemistry* 1994, *33*(16), 4847-4864.

[281] W. A. Günzler, G. J. Steffens, F. Otting, G. Buse, L. Flohe, *Hoppe Seylers Z. Physiol. Chem.* 1982, *363*(2), 133-141.

[282] G. J. Steffens, W. A. Günzler, F. Otting, E. Frankus, L. Flohe, *Hoppe Seylers Z. Physiol. Chem.* 1982, *363*(9), 1043-1058.

[283] P. H. Quax, J. M. Grimbergen, M. Lansink, A. H. Bakker, M. C. Blatter, D. Belin, V. W. van Hinsbergh, J. H. Verheijen, *Arterioscler. Thromb. Vasc. Biol.* 1998, *18*(5), 693-701.

[284] R. W. Stephens, A. M. Bokman, H. T. Myohanen, T. Reisberg, H. Tapiovaara, N. Pedersen, J. Grondahl-Hansen, M. Llinas, A. Vaheri, *Biochemistry* 1992, *31*(33), 7572-7579.

[285] W. Strassburger, A. Wollmer, J. E. Pitts, I. D. Glover, I. J. Tickle, T. L. Blundell, G. J. Steffens, W. A. Günzler, F. Otting, L. Flohe, *FEBS Lett.* 1983, *157*(2), 219-223.

[286] S. Sperl, U. Jacob, N. Arroyo de Prada, J. Stürzebecher, O. G. Wilhelm, W. Bode, V. Magdolen, R. Huber, L. Moroder, *Proc. Natl. Acad. Sci. USA* 2000, *97*(10), 5113-5118.

[287] G. Spraggon, C. Phillips, U. K. Nowak, C. P. Ponting, D. Saunders, C. M. Dobson, D. I. Stuart, E. Y. Jones, *Structure* 1995, *3*(7), 681-691.

[288] N. Schmiedeberg, *Dissertation* 2002, Technische Universität München.

[289] H. Kobayashi, M. Schmitt, L. Goretzki, N. Chucholowski, J. Calvete, M. Kramer, W. A. Günzler, F. Jänicke, H. Graeff, *J. Biol. Chem.* 1991, *266*(8), 5147-5152.

[290] E. Koivunen, M. L. Huhtala, U. H. Stenman, *J. Biol. Chem.* 1989, *264*(24), 14095-14099.

[291] B. B. Wolf, J. Vasudevan, J. Henkin, S. L. Gonias, *J. Biol. Chem.* 1993, *268*(22), 16327-16331.

[292] L. Goretzki, M. Schmitt, K. Mann, J. Calvete, N. Chucholowski, M. Kramer, W. A. Günzler, F. Jänicke, H. Graeff, *FEBS Lett.* 1992, *297*(1-2), 112-118.

[293] M. Schmitt, L. Goretzki, F. Jänicke, J. Calvete, M. Eulitz, H. Kobayashi, N. Chucholowski, H. Graeff, *Biomed. Biochim. Acta* 1991, *50*(4-6), 731-741.

[294] J. D. Vassalli, D. Baccino, D. Belin, *J. Cell. Biol.* 1985, *100*(1), 86-92.

[295] N. Behrendt, E. Rønne, K. Danø, *Biol. Chem. Hoppe Seyler* 1995, *376*(5), 269-279.

[296] N. Behrendt, M. Ploug, L. Patthy, G. Houen, F. Blasi, K. Danø, *J. Biol. Chem.* 1991, *266*(12), 7842-7847.

[297] J. D. Vassalli, *Fibrinolysis* 1994, *8*, 172-181.

[298] M. Ploug, N. Behrendt, D. Løber, K. Danø, *Semin. Thromb. Hemost.* 1991, *17*(3), 183-193.

[299] F. Blasi, N. Behrendt, M. V. Cubellis, V. Ellis, L. R. Lund, M. T. Masucci, L. B. Møller, D. P. Olson, N. Pedersen, M. Ploug, et al., *Cell. Differ. Dev.* 1990, *32*(3), 247-253.

[300] M. V. Cubellis, M. L. Nolli, G. Cassani, F. Blasi, *J. Biol. Chem.* 1986, *261*(34), 15819-15822.

[301] E. Appella, E. A. Robinson, S. J. Ullrich, M. P. Stoppelli, A. Corti, G. Cassani, F. Blasi, *J. Biol. Chem.* 1987, *262*(10), 4437-4440.

[302] M. P. Stoppelli, A. Corti, A. Soffientini, G. Cassani, F. Blasi, R. K. Assoian, *Proc. Natl. Acad. Sci. USA* 1985, *82*(15), 4939-4943.

[303] S. Temerinac, S. Klippel, E. Strunck, S. Roder, M. Lubbert, W. Lange, M. Azemar, G. Meinhardt, H. E. Schaefer, H. L. Pahl, *Blood* 2000, *95*(8), 2569-2576.

[304] L. B. Møller, M. Ploug, F. Blasi, *Eur. J. Biochem.* 1992, *208*(2), 493-500.

[305] L. B. Møller, J. Pollanen, E. Rønne, N. Pedersen, F. Blasi, *J. Biol. Chem.* 1993, *268*(15), 11152-11159.

[306] N. Behrendt, E. Rønne, M. Ploug, T. Petri, D. Løber, L. S. Nielsen, W. D. Schleuning, F. Blasi, E. Appella, K. Danø, *J. Biol. Chem.* 1990, *265*(11), 6453-6460.

[307] A. L. Roldan, M. V. Cubellis, M. T. Masucci, N. Behrendt, L. R. Lund, K. Danø, E. Appella, F. Blasi, *EMBO J.* 1990, *9*(2), 467-474.

[308] M. Ploug, H. Rahbek-Nielsen, P. F. Nielsen, P. Roepstorff, K. Danø, *J. Biol. Chem.* 1998, *273*(22), 13933-13943.

[309] Q. Huai, A. P. Mazar, A. Kuo, G. C. Parry, D. E. Shaw, J. Callahan, Y. D. Li, C. Yuan, C. B. Bian, L. Q. Chen, B. Furie, B. C. Furie, D. B. Cines, M. D. Huang, *Science* 2006, *311*(5761), 656-659.

[310] P. Llinas, M. H. Le Du, H. Gårdsvoll, K. Danø, M. Ploug, B. Gilquin, E. A. Stura, A. Menez, *EMBO J.* 2005, *24*(9), 1655-1663.

[311] Y. Wang, J. Dang, L. K. Johnson, J. J. Selhamer, W. F. Doe, *Eur. J. Biochem.* 1995, *227*(1-2), 116-122.

[312] I. P. Witz, *J. Cell. Biochem.* 2000, *77*(S34), 61-66.

[313] M. Ploug, V. Ellis, *FEBS Lett.* 1994, *349*(2), 163-168.

[314] N. Ohkura, S. Inoue, K. Ikeda, K. Hayashi, *Biochem. Biophys. Res. Commun.* 1994, *204*(3), 1212-1218.

[315] J. Petranka, J. Zhao, J. Norris, N. B. Tweedy, R. E. Ware, P. J. Sims, W. F. Rosse, *Blood Cells Mol. Dis.* 1996, *22*(3), 281-296.

[316] C. M. Fletcher, R. A. Harrison, P. J. Lachmann, D. Neuhaus, *Structure* 1994, *2*(3), 185-199.

[317] R. Eshel, A. Zanin, O. Sagi-Assif, T. Meshel, N. I. Smorodinsky, O. Dwir, R. Alon, R. Brakenhoff, G. van Dongen, I. P. Witz, *J. Biol. Chem.* 2000, *275*(17), 12833-12840.

[318] T. P. Gumley, I. F. McKenzie, M. S. Sandrin, *Immunol. Cell. Biol.* 1995, *73*(4), 277-296.

[319] M. Bürgle, *Dissertation* 1998, Technische Universität München.

[320] O. G. Wilhelm, S. Wilhelm, G. M. Escott, V. Lutz, V. Magdolen, M. Schmitt, D. B. Rifkin, E. L. Wilson, H. Graeff, G. Brunner, *J. Cell. Physiol.* 1999, *180*(2), 225-235.

[321] G. Brunner, C. N. Metz, H. Nguyen, J. Gabrilove, S. R. Patel, M. A. Davitz, D. B. Rifkin, E. L. Wilson, *Blood* 1994, *83*(8), 2115-2125.

[322] H. Gårdsvoll, K. Danø, M. Ploug, *J. Biol. Chem.* 1999, *274*(53), 37995-38003.

[323] M. Ploug, H. Rahbek-Nielsen, V. Ellis, P. Roepstorff, K. Danø, *Biochemistry* 1995, *34*(39), 12524-12534.

[324] M. Ploug, S. Østergaard, L. B. Hansen, A. Holm, K. Danø, *Biochemistry* 1998, *37*(11), 3612-3622.

[325] M. Ploug, S. Østergaard, A. Holm, C. Holst-Hansen, R. W. Stephens, K. Danø, *PCT Int. Appl.* 2000, WO 00/01802, 1-75.

[326] K. Bdeir, A. Kuo, A. Mazar, B. S. Sachais, W. Xiao, S. Gawlak, S. Harris, A. A. Higazi, D. B. Cines, *J. Biol. Chem.* 2000, *275*(37), 28532-28538.

[327] K. K. Wary, A. Mariotti, C. Zurzolo, F. G. Giancotti, *Cell* 1998, *94*(5), 625-634.

[328] H. A. Chapman, Y. Wei, D. I. Simon, D. A. Waltz, *Thromb. Haemost.* 1999, *82*(2), 291-297.

[329] S. Monier, R. G. Parton, F. Vogel, J. Behlke, A. Henske, T. V. Kurzchalia, *Mol. Biol. Cell* 1995, *6*(7), 911-927.

[330] M. Resnati, I. Pallavicini, J. M. Wang, J. Oppenheim, C. N. Serhan, M. Romano, F. Blasi, *Proc. Natl. Acad. Sci. USA* 2002, *99*(3), 1359-1364.

[331] L. Ossowski, J. A. Aguirre-Ghiso, *Curr. Opin. Cell Biol.* 2000, *12*(5), 613-620.

[332] F. Blasi, P. Carmeliet, *Nat. Rev. Mol. Cell Biol.* 2002, *3*(12), 932-943.

[333] N. Sidenius, F. Blasi, *Cancer Metastasis Rev.* 2003, *22*(2-3), 205-222.

[334] H. A. Chapman, *Curr. Opin. Cell. Biol.* 1997, *9*(5), 714-724.

[335] W. Xue, I. Mizukami, R. F. Todd, 3rd, H. R. Petty, *Cancer Res* 1997, *57*(9), 1682-1689.

[336] W. Xue, A. L. Kindzelskii, R. F. Todd, 3rd, H. R. Petty, *J Immunol* 1994, *152*(9), 4630-4640.

[337] M. Yebra, G. C. Parry, S. Stromblad, N. Mackman, S. Rosenberg, B. M. Mueller, D. A. Cheresh, *J Biol Chem* 1996, *271*(46), 29393-29399.

[338] D. I. Simon, Y. Wei, L. Zhang, N. K. Rao, H. Xu, Z. Chen, Q. Liu, S. Rosenberg, H. A. Chapman, *J Biol Chem* 2000, *275*(14), 10228-10234.

[339] H. R. Petty, R. F. Todd, 3rd, *Immunol Today* 1996, *17*(5), 209-212.

[340] J. Bohuslav, V. Horejsi, C. Hansmann, J. Stockl, U. H. Weidle, O. Majdic, I. Bartke, W. Knapp, H. Stockinger, *J Exp Med* 1995, *181*(4), 1381-1390.

[341] A. L. Kindzelskii, M. M. Eszes, R. F. Todd, 3rd, H. R. Petty, *Biophys J* 1997, *73*(4), 1777-1784.

[342] P. Franco, I. Vocca, M. V. Carriero, D. Alfano, L. Cito, I. Longanesi-Cattani, P. Grieco, L. Ossowski, M. P. Stoppelli, *J Cell Sci* 2006, *119*(Pt 16), 3424-3434.

[343] P. Chaurasia, J. A. Aguirre-Ghiso, O. D. Liang, H. Gårdsvoll, M. Ploug, L. Ossowski, *J Biol Chem* 2006, *281*(21), 14852-14863.

[344] J. A. Aguirre Ghiso, K. Kovalski, L. Ossowski, *J. Cell. Biol.* 1999, *147*(1), 89-104.

[345] T. Tarui, A. P. Mazar, D. B. Cines, Y. Takada, *J. Biol. Chem.* 2001, *276*(6), 3983-3990.

[346] J. A. Aguirre-Ghiso, D. Liu, A. Mignatti, K. Kovalski, L. Ossowski, *Mol. Biol. Cell* 2001, *12*(4), 863-879.

[347] D. H. Nguyen, A. D. Catling, D. J. Webb, M. Sankovic, L. A. Walker, A. V. Somlyo, M. J. Weber, S. L. Gonias, *J. Cell. Biol.* 1999, *146*(1), 149-164.

[348] Y. Koshelnick, M. Ehart, P. Hufnagl, P. C. Heinrich, B. R. Binder, *J. Biol. Chem.* 1997, *272*(45), 28563-28567.

[349] I. Dumler, A. Weis, O. A. Mayboroda, C. Maasch, U. Jerke, H. Haller, D. C. Gulba, *J. Biol. Chem.* 1998, *273*(1), 315-321.

[350] I. Dumler, A. Kopmann, A. Weis, O. A. Mayboroda, K. Wagner, D. C. Gulba, H. Haller, *Arterioscler. Thromb. Vasc. Biol.* 1999, *19*(2), 290-297.

[351] N. Sidenius, A. Andolfo, R. Fesce, F. Blasi, *J. Biol. Chem.* 2002, *277*(31), 27982-27990.

[352] O. D. Liang, K. Bdeir, R. L. Matz, T. Chavakis, K. T. Preissner, *J. Biochem. (Tokyo)* 2003, *134*(5), 661-666.

[353] G. Deng, S. A. Curriden, G. Hu, R. P. Czekay, D. J. Loskutoff, *J. Cell. Physiol.* 2001, *189*(1), 23-33.

[354] S. Stefansson, D. A. Lawrence, *Nature* 1996, *383*(6599), 441-443.

[355] Y. Okumura, Y. Kamikubo, S. A. Curriden, J. Wang, T. Kiwada, S. Futaki, K. Kitagawa, D. J. Loskutoff, *J. Biol. Chem.* 2002, *277*(11), 9395-9404.

[356] N. Sidenius, F. Blasi, *FEBS Lett.* 2000, *470*(1), 40-46.

[357] O. D. Liang, T. Chavakis, S. M. Kanse, K. T. Preissner, *J. Biol. Chem.* 2001, *276*(31), 28946-28953.

[358] G. Høyer-Hansen, N. Behrendt, M. Ploug, K. Danø, K. T. Preissner, *FEBS Lett.* 1997, *420*(1), 79-85.

[359] K. T. Preissner, D. Seiffert, *Thromb. Res.* 1998, *89*(1), 1-21.

[360] B. R. Binder, J. Mihaly, G. W. Prager, *Thromb. Haemost.* 2007, *97*(3), 336-342.

[361] D. H. Nguyen, D. J. Webb, A. D. Catling, Q. Song, A. Dhakephalkar, M. J. Weber, K. S. Ravichandran, S. L. Gonias, *J. Biol. Chem.* 2000, *275*(25), 19382-19388.

[362] B. Degryse, M. Resnati, S. A. Rabbani, A. Villa, F. Fazioli, F. Blasi, *Blood* 1999, *94*(2), 649-662.

[363] F. Fazioli, M. Resnati, N. Sidenius, Y. Higashimoto, E. Appella, F. Blasi, *EMBO J.* 1997, *16*(24), 7279-7286.

[364] V. S. Misheneva, *Ukr. Biokhim. Zh.* 1963, *35*, 566-572.

[365] J. F. Davidson, G. P. McNicol, G. L. Frank, T. J. Anderson, A. S. Douglas, *Br. Med. J.* 1969, *1*(5636), 88-91.

[366] B. Astedt, E. Lundgren, G. Roos, G. Abu Sinna, *Thromb. Res.* 1978, *13*(6), 1031-1037.

[367] B. Astedt, L. Holmberg, *Nature* 1976, *261*(5561), 595-597.

[368] K. Mengele, N. Harbeck, U. Reuning, V. Magdolen, M. Schmitt, *Hamostaseologie* 2005, *25*(3), 301-310.

[369] C. Dellas, D. J. Loskutoff, *Thromb. Haemost.* 2005, *93*(4), 631-640.

[370] R. D. Balsara, F. J. Castellino, V. A. Ploplis, *J. Biol. Chem.* 2006, *281*(32), 22527-22536.

[371] U. Reuning, V. Magdolen, O. Wilhelm, K. Fischer, V. Lutz, H. Graeff, M. Schmitt, *Int. J. Oncol.* 1998, *13*(5), 893-906.

[372] Y. B. Chen, R. J. Kelm, R. C. Budd, B. E. Sobel, D. J. Schneider, *Journal of Cellular Biochemistry* 2004, *92*(1), 178-188.

[373] G. Deng, S. A. Curriden, S. J. Wang, S. Rosenberg, D. J. Loskutoff, *Journal of Cell Biology* 1996, *134*(6), 1563-1571.

[374] N. Harbeck, R. E. Kates, K. Gauger, A. Willems, M. Kiechle, V. Magdolen, M. Schmitt, *Thromb. Haemost.* 2004, *91*(3), 450-456.

[375] F. Jänicke, M. Schmitt, H. Graeff, *Semin Thromb Hemost* 1991, *17*(3), 303-312.

[376] F. Jänicke, M. Schmitt, L. Pache, K. Ulm, N. Harbeck, H. Höfler, H. Graeff, *Breast Cancer Res Treat* 1993, *24*(3), 195-208.

[377] H. C. Kwaan, J. Wang, K. Svoboda, P. J. Declerck, *Br J Cancer* 2000, *82*(10), 1702-1708.

[378] P. Rossignol, B. Ho-Tin-Noe, R. Vranckx, M. C. Bouton, O. Meilhac, H. R. Lijnen, M. C. Guillin, J. B. Michel, E. Angles-Cano, *J Biol Chem* 2004, *279*(11), 10346-10356.

[379] M. Schmitt, N. Harbeck, C. Thomssen, O. Wilhelm, V. Magdolen, U. Reuning, K. Ulm, H. Höfler, F. Jänicke, H. Graeff, *Thromb Haemost* 1997, *78*(1), 285-296.

[380] N. Harbeck, C. Thomssen, *Zentralbl. Gynakol.* 2003, *125*(9), 362-367.

[381] M. J. Duffy, P. O'Grady, D. Devaney, L. O'Siorain, J. J. Fennelly, H. J. Lijnen, *Cancer* 1988, *62*(3), 531-533.

[382] F. Jänicke, M. Schmitt, K. Ulm, W. Gossner, H. Graeff, *Lancet* 1989, *2*(8670), 1049.

[383] C. E. de Bock, Y. Wang, *Med. Res. Rev.* 2004, *24*(1), 13-39.

[384] M. J. Duffy, *Curr. Pharm. Des.* 2004, *10*(1), 39-49.

[385] J. A. Foekens, F. Buessecker, H. A. Peters, U. Krainick, W. L. van Putten, M. P. Look, J. G. Klijn, M. D. Kramer, *Cancer Res.* 1995, *55*(7), 1423-1427.

[386] J. A. Foekens, H. A. Peters, M. P. Look, H. Portengen, M. Schmitt, M. D. Kramer, N. Brunner, F. Jänicke, M. E. Meijer-van Gelder, S. C. Henzen-Logmans, W. L. van Putten, J. G. Klijn, *Cancer Res.* 2000, *60*(3), 636-643.

[387] V. Pillay, C. R. Dass, P. F. Choong, *Trends Biotechnol.* 2007, *25*(1), 33-39.

[388] J. Romer, B. S. Nielsen, M. Ploug, *Curr. Pharm. Des.* 2004, *10*(19), 2359-2376.

[389] R. Mazzieri, F. Furlan, S. D'Alessio, M. Chiaravalli, F. Blasi, *Thromb. Haemost.* 2005, *93*(4), A11-A11.

[390] R. Mazzieri, F. Furlan, S. D'Alessio, E. Zonari, F. Talotta, P. Verde, F. Blasi, *Oncogene* 2007, *26*(5), 725-732.

[391] R. Mazzieri, F. Blasi, *Thromb. Haemost.* 2005, *93*(4), 641-646.

[392] R. Mazzieri, S. D'Alessio, R. K. Kenmore, L. Ossowski, F. Blasi, *Thromb. Haemost.* 2005, *93*(4), A18-A18.

[393] S. Sperl, M. M. Mueller, O. G. Wilhelm, M. Schmitt, V. Magdolen, L. Moroder, *Drug News Perspect.* 2001, *14*(7), 401-411.

[394] D. E. Milenic, E. D. Brady, M. W. Brechbiel, *Nat. Rev. Drug Discov.* 2004, *3*(6), 488-499.

[395] D. M. Goldenberg, R. M. Sharkey, *Q. J. Nucl. Med. Mol. Imaging* 2006, *50*(4), 248-264.

[396] J. C. Reubi, H. R. Mäcke, E. P. Krenning, *J. Nucl. Med.* 2005, *46 Suppl 1*, 67S-75S.

[397] M. Ginj, H. Zhang, B. Waser, R. Cescato, D. Wild, X. Wang, J. Erchegyi, J. Rivier, H. R. Mäcke, J. C. Reubi, *Proc. Natl. Acad. Sci. USA* 2006, *103*(44), 16436-16441.

[398] D. Artemov, *J. Cell. Biochem.* 2003, *90*(3), 518-524.

[399] M. V. Knopp, H. von Tengg-Kobligk, P. L. Choyke, *Mol. Cancer Ther.* 2003, *2*(4), 419-426.

[400] V. Ntziachristos, C. H. Tung, C. Bremer, R. Weissleder, *Nat. Med.* 2002, *8*, 757-760.

[401] M. Rudin, R. Weissleder, *Nat. Rev. Drug Discov.* 2003, *2*(2), 123-131.

[402] W. A. Weber, N. Avril, M. Schwaiger, *Strahlenther. Onkol.* 1999, *175*(8), 356-373.

[403] Z. Keidar, O. Israel, Y. Krausz, *Semin. Nucl. Med.* 2003, *33*(3), 205-218.

[404] M. Glaser, S. K. Luthra, F. Brady, *Int. J. Oncol.* 2003, *22*(2), 253-267.

[405] L. Varagnolo, M. P. Stokkel, U. Mazzi, E. K. Pauwels, *Nucl. Med. Biol.* 2000, *27*(2), 103-112.

[406] H. Anderson, P. Price, *Eur. J. Cancer* 2000, *36*(16), 2028-2035.

[407] P. Rigo, P. Paulus, B. J. Kaschten, R. Hustinx, T. Bury, G. Jerusalem, T. Benoit, J. Foidart-Willems, *Eur J Nucl Med* 1996, *23*(12), 1641-1674.

[408] H. Lundqvist, V. Tolmachev, *Biopolymers* 2002, *66*(6), 381-392.

[409] E. P. Krenning, D. J. Kwekkeboom, W. H. Bakker, W. A. Breeman, P. P. Kooij, H. Y. Oei, M. van Hagen, P. T. Postema, M. de Jong, J. C. Reubi, et al., *Eur J Nucl Med* 1993, *20*(8), 716-731.

[410] M. Gotthardt, M. Fischer, I. Naeher, J. B. Holz, H. Jungclas, H. W. Fritsch, M. Behe, B. Goke, K. Joseph, T. M. Behr, *Eur J Nucl Med Mol Imaging* 2002, *29*(5), 597-606.

[411] T. M. Behr, M. P. Behe, *Semin Nucl Med* 2002, *32*(2), 97-109.

[412] E. Garcia-Garayoa, P. Blauenstein, M. Bruehlmeier, A. Blanc, K. Iterbeke, P. Conrath, D. Tourwe, P. A. Schubiger, *J Nucl Med* 2002, *43*(3), 374-383.

[413] D. E. Milenic, E. D. Brady, M. W. Brechbiel, *Nat. Rev. Drug. Discov.* 2004, *3*(6), 488-499.

[414] O. H. Aina, T. C. Sroka, M. L. Chen, K. S. Lam, *Biopolymers* 2002, *66*(3), 184-199.

[415] J. A. Katzenellenbogen, *J. Nucl. Med.* 1995, *36*(6), S8-S13.

[416] J. Fichna, A. Janecka, *Bioconjugate Chem.* 2003, *14*(1), 3-17.

[417] R. E. Weiner, M. L. Thakur, *Appl. Radiat. Isotopes* 2002, *57*(5), 749-763.

[418] A. Heppeler, S. Froidevaux, A. N. Eberle, H. R. Maecke, *Curr. Med. Chem.* 2000, *7*(9), 971-994.

[419] S. Kneifel, D. Cordier, S. Good, M. C. S. Ionescu, A. Ghaffari, S. Hofer, M. Kretzschmar, M. Tolnay, C. Apostolidis, B. Waser, M. Arnold, J. Mueller-Brand, H. R. Maecke, J. C. Reubi, A. Merlo, *Clin. Cancer Res.* 2006, *12*(12), 3843-3850.

[420] J. P. Norenberg, B. J. Krenning, I. R. Konings, D. F. Kusewitt, T. K. Nayak, T. L. Anderson, M. de Jong, K. Garmestani, M. W. Brechbiel, L. K. Kvols, *Clin. Cancer Res.* 2006, *12*(3 Pt 1), 897-903.

[421] M. Behe, G. Kluge, W. Becker, M. Gotthardt, T. M. Behr, *J. Nucl. Med.* 2005, *46*(6), 1012-1015.

[422] S. Panigone, A. D. Nunn, *Q. J. Nucl. Med. Mol. Imaging* 2006, *50*(4), 310-321.

[423] D. Wild, M. Behe, A. Wicki, D. Storch, B. Waser, M. Gotthardt, B. Keil, G. Christofori, J. C. Reubi, H. R. Mäcke, *J. Nucl. Med.* 2006, *47*(12), 2025-2033.

[424] M. de Jong, W. A. Breeman, R. Valkema, B. F. Bernard, E. P. Krenning, *J. Nucl. Med.* 2005, *46 Suppl 1*, 13S-17S.

[425] M. de Jong, W. A. Breeman, B. F. Bernard, W. H. Bakker, M. Schaar, A. van Gameren, J. E. Bugaj, J. Erion, M. Schmidt, A. Srinivasan, E. P. Krenning, *Int J Cancer* 2001, *92*(5), 628-633.

[426] O. Ugur, P. J. Kothari, R. D. Finn, P. Zanzonico, S. Ruan, I. Guenther, H. R. Maecke, S. M. Larson, *Nucl Med Biol* 2002, *29*(2), 147-157.

[427] J. Carlsson, E. Forssell Aronsson, S. O. Hietala, T. Stigbrand, J. Tennvall, *Radiother Oncol* 2003, *66*(2), 107-117.

[428] D. J. Kwekkeboom, J. Mueller-Brand, G. Paganelli, L. B. Anthony, S. Pauwels, L. K. Kvols, M. O'Dorisio T, R. Valkema, L. Bodei, M. Chinol, H. R. Maecke, E. P. Krenning, *J. Nucl. Med.* 2005, *46 Suppl 1*, 62S-66S.

[429] O. Couturier, S. Supiot, M. Degraef-Mougin, A. Faivre-Chauvet, T. Carlier, J. F. Chatal, F. Davodeau, M. Cherel, *Eur. J. Nucl. Med. Mol. Imaging* 2005, *32*(5), 601-614.

[430] C. Seidl, H. Schrock, S. Seidenschwang, R. Beck, E. Schmid, M. Abend, K. F. Becker, C. Apostolidis, T. Nikula, E. Kremmer, M. Schwaiger, R. Senekowitsch-Schmidtke, *Eur. J. Nucl. Med. Mol. Imaging* 2005, *32*(3), 274-285.

[431] M. R. Zalutsky, O. R. Pozzi, *Q. J. Nucl. Med. Mol. Imaging* 2004, *48*(4), 289-296.

[432] J. Elgqvist, H. Andersson, T. Back, I. Claesson, R. Hultborn, H. Jensen, B. R. Johansson, S. Lindegren, M. Olsson, S. Palm, E. Warnhammar, L. Jacobsson, *J. Nucl. Med.* 2006, *47*(8), 1342-1350.

[433] R. Huber, C. Seidl, E. Schmid, S. Seidenschwang, K. F. Becker, C. Schuhmacher, C. Apostolidis, T. Nikula, E. Kremmer, M. Schwaiger, R. Senekowitsch-Schmidtke, *Clin. Cancer Res.* 2003, *9*(10), 3922s-3928s.

[434] R. Senekowitsch-Schmidtke, C. Schuhmacher, K. F. Becker, T. K. Nikula, C. Seidl, I. Becker, M. Miederer, C. Apostolidis, C. Adam, R. Huber, E. Kremmer, K. Fischer, M. Schwaiger, *Cancer Res.* 2001, *61*(7), 2804-2808.

[435] T. Nayak, J. Norenberg, T. Anderson, R. Atcher, *Cancer Biother. Radio.* 2005, *20*(1), 52-57.

[436] S. J. Mather, *Mol. Biosyst.* 2007, *3*(1), 30-35.

[437] B. M. Tashtoush, A. A. Traboulsi, L. Dittert, A. A. Hussain, *Anal. Biochem.* 2001, *288*(1), 16-21.

[438] P. J. Fraker, J. C. Speck, *Biochemical and Biophysical Research Communications* 1978, *80*(4), 849-857.

[439] A. A. Wilson, R. F. Dannals, H. T. Ravert, J. J. Frost, H. N. Wagner Jr., *J. Med. Chem.* 1989, *32*(5), 1057-1062.

[440] G. Vaidyanathan, D. J. Affleck, J. Li, P. Welsh, M. R. Zalutsky, *Bioconjugate Chem.* 2001, *12*(3), 428-438.

[441] G. Espuna, G. Arsequell, G. Valencia, J. Barluenga, J. M. Alvarez-Gutierrez, A. Ballesteros, J. M. Gonzalez, *Angewandte Chemie-International Edition* 2004, *43*(3), 325-329.

[442] G. Espuna, D. Andreu, J. Barluenga, X. Perez, A. Planas, G. Arsequell, G. Valencia, *Biochemistry* 2006, *45*(19), 5957-5963.

[443] S. M. Ametamey, V. Treyer, J. Streffer, M. T. Wyss, M. Schmidt, M. Blagoev, S. Hintermann, Y. Auberson, F. Gasparini, U. C. Fischer, A. Buck, *J. Nucl. Med.* 2007, *48*(2), 247-252.

[444] S. M. Ametamey, L. J. Kessler, M. Honer, M. T. Wyss, A. Buck, S. Hintermann, Y. P. Auberson, F. Gasparini, P. A. Schubiger, *J. Nucl. Med.* 2006, *47*(4), 698-705.

[445] I. Madar, B. Bencherif, J. Lever, R. F. Heitmiller, S. C. Yang, M. Brock, J. Brahmer, H. Ravert, R. Dannals, J. J. Frost, *J. Nucl. Med.* 2007, *48*(2), 207-213.

[446] W. B. Mathews, J. A. Monn, H. T. Ravert, D. P. Holt, D. D. Schoepp, R. F. Dannals, *J. Labelled Compd. Rad.* 2006, *49*(9), 829-834.

[447] J. Liu, V. Kepe, A. Zabjek, A. Petric, H. C. Padgett, N. Satyamurthy, J. R. Barrio, *Mol. Imaging Biol.* 2007, *9*(1), 6-16.

[448] M. Ogawa, K. Hatano, S. Oishi, Y. Kawasumi, N. Fujii, M. Kawaguchi, R. Doi, M. Imamura, M. Yamamoto, K. Ajito, T. Mukai, H. Saji, K. Ito, *Nucl. Med. Biol.* 2003, *30*(1), 1-9.

[449] R. Haubner, H.-J. Wester, W. A. Weber, C. Mang, S. I. Ziegler, S. L. Goodman, R. Senekowitsch-Schmidtke, H. Kessler, M. Schwaiger, *Cancer Res.* 2001, *61*(5), 1781-1785.

[450] D. S. Wilbur, *Bioconjugate Chem.* 1992, *3*(6), 433-470.

[451] T. Poethko, M. Schottelius, G. Thumshirn, U. Hersel, M. Herz, G. Henriksen, H. Kessler, M. Schwaiger, H. J. Wester, *J Nucl Med* 2004, *45*(5), 892-902.

[452] M. W. Brechbiel, O. A. Gansow, *Bioconjug Chem* 1991, *2*(3), 187-194.

[453] Y. H. Jang, M. Blanco, S. Dasgupta, D. A. Keire, J. E. Shively, W. A. Goddard, *Journal of the American Chemical Society* 1999, *121*(26), 6142-6151.

[454] M. Li, C. F. Meares, *Bioconjug Chem* 1993, *4*(4), 275-283.

[455] B. Sadeghi, C. Arvieux, O. Glehen, A. C. Beaujard, M. Rivoire, J. Baulieux, E. Fontaumard, A. Brachet, J. L. Caillot, J. L. Faure, J. Porcheron, J. L. Peix, Y. Francois, J. Vignal, F. N. Gilly, *Cancer* 2000, *88*(2), 358-363.

[456] D. M. Parkin, F. Bray, J. Ferlay, P. Pisani, *CA-Cancer J. Clin.* 2005, *55*(2), 74-108.

[457] G. Bolis, A. Villa, P. Guarnerio, C. Ferraris, N. Gavoni, G. Giardina, M. Melpignano, G. Scarfone, F. Zanaboni, F. Parazzini, *Cancer* 1996, *77*(1), 128-131.

[458] J. S. Rao, C. Gondi, C. Chetty, S. Chittivelu, P. A. Joseph, S. S. Lakka, *Mol. Cancer Ther.* 2005, *4*(9), 1399-1408.

[459] B. Setyono-Han, J. Stürzebecher, W. A. Schmalix, B. Muehlenweg, A. M. Sieuwerts, M. Timmermans, V. Magdolen, M. Schmitt, J. G. Klijn, J. A. Foekens, *Thromb. Haemost.* 2005, *93*(4), 779-786.

[460] U. Reuning, S. Sperl, C. Kopitz, H. Kessler, A. Krüger, M. Schmitt, V. Magdolen, *Curr. Pharm. Des.* 2003, *9*(19), 1529-1543.

[461] T. K. Stutchbury, F. Al-Ejeh, G. E. Stillfried, D. R. Croucher, J. Andrews, D. Irving, M. Links, M. Ranson, *Mol. Cancer Ther.* 2007, *6*(1), 203-212.

[462] C. F. Qu, E. Y. Song, Y. Li, S. M. Rizvi, C. Raja, R. Smith, A. Morgenstern, C. Apostolidis, B. J. Allen, *Clin. Exp. Metastasis* 2005, *22*(7), 575-586.

[463] Y. J. Song, C. F. Qu, S. M. Rizvi, Y. Li, G. Robertson, C. Raja, A. Morgenstern, C. Apostolidis, A. C. Perkins, B. J. Allen, *Cancer Lett.* 2006, *234*(2), 176-183.

[464] S. M. A. Rizvi, Y. Li, E. Y. J. Song, C. F. Qu, C. Raja, A. Morgenstern, C. Apostollidis, B. J. Allen, *Cancer Biol. Ther.* 2006, *5*(4), 386-393.

[465] N. Schmiedeberg, M. Schmitt, C. Rol, V. Truffault, M. Sukopp, M. Bürgle, O. G. Wilhelm, W. Schmalix, V. Magdolen, H. Kessler, *J. Med. Chem.* 2002, *45*(23), 4984-4994.

[466] M. Ploug, S. Østergaard, H. Gårdsvoll, K. Kovalski, C. Holst-Hansen, A. Holm, L. Ossowski, K. Danø, *Biochemistry-US* 2001, *40*(40), 12157-12168.

[467] V. Magdolen, M. Bürgle, N. A. de Prada, N. Schmiedeberg, C. Riemer, F. Schroeck, J. Kellermann, K. Degitz, O. G. Wilhelm, M. Schmitt, H. Kessler, *Biol. Chem.* 2001, *382*(8), 1197-1205.

[468] M. Bürgle, M. Koppitz, C. Riemer, H. Kessler, B. König, U. H. Weidle, J. Kellermann, F. Lottspeich, H. Graeff, M. Schmitt, L. Goretzki, U. Reuning, O. Wilhelm, V. Magdolen, *Biol. Chem.* 1997, *378*(3-4), 231-237.

[469] E. Appella, E. A. Robinson, S. J. Ullrich, M. P. Stoppelli, A. Corti, G. Cassani, F. Blasi, *J. Biol. Chem.* 1987, *262*(10), 4437-4440.

[470] V. Magdolen, P. Rettenberger, M. Koppitz, L. Goretzki, H. Kessler, U. H. Weidle, B. König, H. Graeff, M. Schmitt, O. Wilhelm, *Eur. J. Biochem.* 1996, *237*(3), 743-751.

[471] R. J. Goodson, M. V. Doyle, S. E. Kaufman, S. Rosenberg, *Proc. Natl. Acad. Sci. USA* 1994, *91*(15), 7129-7133.

[472] R. J. Tressler, P. A. Pitot, J. R. Stratton, L. D. Forrest, S. Q. Zhuo, R. J. Drummond, S. Fong, M. V. Doyle, L. V. Doyle, H. Y. Min, S. Rosenberg, *APMIS* 1999, *107*(1), 168-173.

[473] M. Ploug, *Biochemistry* 1998, *37*(47), 16494-16505.

[474] M. Ploug, S. Østergaard, L. B. L. Hansen, A. Holm, K. Danø, *Biochemistry* 1998, *37*(11), 3612-3622.

[475] K. S. Lam, M. Lebl, V. Krchnak, *Chem. Rev.* 1997, *97*(2), 411-448.

[476] B. Jacobsen, H. Gårdsvoll, G. Juhl Funch, S. Østergaard, V. Barkholt, M. Ploug, *Protein Expr. Purif.* 2007, *52*(2), 286-296.

[477] L. H. Engelholm, N. Behrendt, *Biol. Chem.* 2001, *382*(3), 435-442.

[478] M. Ploug, H. Gårdsvoll, T. J. D. Jørgensen, L. L. Hansen, K. Danø, *Biochem. Soc. T.* 2002, *30*, 177-183.

[479] H. Gårdsvoll, B. Gilquin, M. H. Le Du, A. Menez, T. J. D. Jørgensen, M. Ploug, *J. Biol. Chem.* 2006, *281*(28), 19260-19272.

[480] C. Barinka, G. Parry, J. Callahan, D. E. Shaw, A. Kuo, K. Bdeir, D. B. Cines, A. Mazar, J. Lubkowski, *J. Mol. Biol.* 2006, *363*(2), 482-495.

[481] S. Knör, S. Sato, T. Huber, A. Morgenstern, F. Bruchertseifer, M. Schmitt, H. Kessler, R. Senekowitsch-Schmidtke, V. Magdolen, C. Seidl, *Eur. J. Nucl. Med. Mol. Imaging* 2007, submitted.

[482] M. Sukopp, *Dissertation* 2003, Technische Universität München.

[483] G. Thumshirn, U. Hersel, S. L. Goodman, H. Kessler, *Chem.-Eur. J.* 2003, *9*(12), 2717-2725.

[484] H. J. Wester, H. Kessler, *J. Nucl. Med.* 2005, *46*(12), 1940-1945.

[485] M. Mammen, S. K. Choi, G. M. Whitesides, *Angew. Chem. Int. Edit.* 1998, *37*(20), 2755-2794.

[486] R. M. Owen, C. B. Carlson, J. W. Xu, P. Mowery, E. Fasella, L. L. Kiessling, *Chembiochem* 2007, *8*(1), 68-82.

[487] A. Heppeler, S. Froidevaux, H. R. Mäcke, E. Jermann, M. Behe, P. Powell, M. Hennig, *Chem. Eur. J.* 1999, *5*(7), 1974-1981.

[488] C. Will, O. Wilhelm, S. Hohl, V. Möbus, U. Weidle, R. Kreienberg, F. Jänicke, M. Schmitt, H. Graeff, *Int. J. Oncol.* 1994, *5*(4), 753-761.

[489] E. Vegt, J. F. Wetzels, F. G. Russel, R. Masereeuw, O. C. Boerman, J. E. van Eerd, F. H. Corstens, W. J. Oyen, *J. Nucl. Med.* 2006, *47*(3), 432-436.

[490] J. E. van Eerd, E. Vegt, J. F. Wetzels, F. G. Russel, R. Masereeuw, F. H. Corstens, W. J. Oyen, O. C. Boerman, *J. Nucl. Med.* 2006, *47*(3), 528-533.

[491] J. C. Reubi, *Endocr. Rev.* 2003, *24*(4), 389-427.

[492] B. Lambert, M. Cybulla, S. M. Weiner, C. Van De Wiele, H. Ham, R. A. Dierckx, A. Otte, *Radiat. Res.* 2004, *161*(5), 607-611.

[493] E. J. Rolleman, R. Valkema, M. de Jong, P. P. Kooij, E. P. Krenning, *Eur. J. Nucl. Med. Mol. Imaging* 2003, *30*(1), 9-15.

[494] L. Bodei, M. Cremonesi, S. Zoboli, C. Grana, M. Bartolomei, P. Rocca, M. Caracciolo, H. R. Mäcke, M. Chinol, G. Paganelli, *Eur. J. Nucl. Med. Mol. Imaging* 2003, *30*(2), 207-216.

[495] J. S. Jaggi, S. V. Seshan, M. R. McDevitt, G. Sgouros, E. Hyjek, D. A. Scheinberg, *Int. J. Radiat. Oncol. Biol. Phys.* 2006, *64*(5), 1503-1512.

[496] T. Kakizaki, Y. Yokoyama, M. Natsuhori, N. Yamada, M. Hashimoto, K. Sato, N. Ito, G. B. Daniel, *J. Vet. Pharmacol. Ther.* 2005, *28*(6), 559-564.

[497] M. Schottelius, M. Schwaiger, H.-J. Wester, *Tetrahedron Lett.* 2003, *44*(11), 2393-2396.

[498] K. P. Eisenwiener, P. Powell, H. R. Mäcke, *Bioorg. Med. Chem. Lett.* 2000, *10*(18), 2133-2135.

[499] P. L. Anelli, L. Lattuada, M. Gabellini, P. Recanati, *Bioconjugate Chem.* 2001, *12*(6), 1081-1084.

[500] L. Camera, S. Kinuya, K. Garmestani, C. Wu, M. W. Brechbiel, L. H. Pai, T. J. McMurry, O. A. Gansow, I. Pastan, C. H. Paik, J. A. Carasquillo, *J. Nucl. Med.* 1994, *35*(5), 882-889.

[501] T. J. McMurry, M. Brechbiel, K. Kumar, O. A. Gansow, *Bioconjugate Chem.* 1992, *3*(2), 108-117.

[502] L. M. De Leon-Rodriguez, Z. Kovacs, G. R. Dieckmann, A. D. Sherry, *Chem. Eur. J.* 2004, *10*(5), 1149-1155.

[503] M. Oliver, M. R. Jorgensen, A. D. Miller, *Synlett* 2004(3), 453-456.

[504] J. J. Peterson, R. H. Pak, C. F. Meares, *Bioconjugate Chem.* 1999, *10*(2), 316-320.

[505] G. Thumshirn, U. Hersel, H. Kessler, *Chem. Eur. J.* 2003, *9*, 2717-2725.

[506] T. Poethko, M. Schottelius, G. Thumshirn, U. Hersel, M. Herz, G. Henriksen, H. Kessler, M. Schwaiger, H. J. Wester, *J. Nucl. Med.* 2004, *45*(5), 892-902.

[507] P. C. Lin, S. H. Ueng, M. C. Tseng, K. J.L., K. T. Huang, S. C. Yu, A. K. Adak, Y. J. Chen, C. C. Lin, *Angew. Chem. Int. Edit.* 2006, *45*(26), 4286-4290.

[508] J. Hovinen, *Chem. Biodivers.* 2006, *3*(3), 296-303.

[509] H. C. Kolb, M. G. Finn, K. B. Sharpless, *Angew. Chem. Int. Edit.* 2001, *40*(11), 2004-2021.

[510] K. Rose, *J. Am. Chem. Soc.* 1994, *116*(1), 30-33.

[511] J. Shao, J. P. Tam, *J. Am. Chem. Soc.* 1995, *117*(14), 3893-3899.

[512] C. W. Tornoe, C. Christensen, M. Meldal, *J. Org. Chem.* 2002, *67*(9), 3057-3064.

[513] D. D. Diaz, K. Rajagopal, E. Strable, J. Schneider, M. G. Finn, *J. Am. Chem. Soc.* 2006, *128*(18), 6056-6057.

[514] P. Marceau, C. Bure, A. F. Delmas, *Bioorg. Med. Chem. Lett.* 2005, *15*(24), 5442-5445.

[515] T. Poethko, M. Schottelius, G. Thumshirn, M. Herz, R. Haubner, G. Henriksen, H. Kessler, M. Schwaiger, H.-J. Wester, *Radiochim. Acta* 2004, *92*(4-6), 317-327.

[516] G. Tuchscherer, D. Grell, M. Mathieu, M. Mutter, *J. Pept. Res.* 1999, *54*(3), 185-194.

[517] D. Boturyn, J. L. Coll, E. Garanger, M. C. Favrot, P. Dumy, *J. Am. Chem. Soc.* 2004, *126*(18), 5730-5739.

[518] M. Kurth, A. Pelegrin, K. Rose, R. E. Offord, S. Pochon, J. P. Mach, F. Buchegger, *J. Med. Chem.* 1993, *36*(9), 1255-1261.

[519] F. Wahl, M. Mutter, *Tetrahedron Lett.* 1996, *37*(38), 6861-6864.

[520] L. E. Canne, A. R. Ferré-D'Amaré, S. K. Burley, S. B. H. Kent, *J. Am. Chem. Soc.* 1995, *117*(11), 2998-3007.

[521] L. S. Zhang, T. R. Torgerson, X. Y. Liu, S. Timmons, A. D. Colosia, J. Hawiger, J. P. Tam, *Proc. Natl. Acad. Sci. USA* 1998, *95*(16), 9184-9189.

[522] R. Huisgen, *Angew. Chem. Int. Edit.* 1963, *75*(13), 604-637.

[523] R. Huisgen, *Angew. Chem. Int. Edit.* 1963, *75*(16-7), 742-754.

[524] R. Huisgen, *Pure Appl. Chem.* 1989, *61*(4), 613-628.

[525] R. Huisgen, R. Knorr, L. Mobius, G. Szeimies, *Chem. Ber.-Recl.* 1965, *98*(12), 4014-4021.

[526] A. Krasinski, Z. Radic, R. Manetsch, J. Raushel, P. Taylor, K. B. Sharpless, H. C. Kolb, *J. Am. Chem. Soc.* 2005, *127*(18), 6686-6692.

[527] P. Wu, A. K. Feldman, A. K. Nugent, C. J. Hawker, A. Scheel, B. Voit, J. Pyun, J. M. Frechet, K. B. Sharpless, V. V. Fokin, *Angew. Chem. Int. Edit.* 2004, *43*(30), 3928-3932.

[528] B. Khanetskyy, D. Dallinger, C. O. Kappe, *J. Comb. Chem.* 2004, *6*(6), 884-892.

[529] Q. Wang, T. R. Chan, R. Hilgraf, V. V. Fokin, K. B. Sharpless, M. G. Finn, *J. Am. Chem. Soc.* 2003, *125*(11), 3192-3193.

[530] S. Sen Gupta, K. S. Raja, E. Kaltgrad, E. Strable, M. G. Finn, *Chem. Commun.* 2005(34), 4315-4317.

[531] S. Punna, E. Kaltgrad, M. G. Finn, *Bioconjugate Chem.* 2005, *16*(6), 1536-1541.

[532] S. Knör, A. Modlinger, T. Poethko, M. Schottelius, H. J. Wester, H. Kessler, *Chem. Eur. J.* 2007, in press.

[533] A. Modlinger, *Dissertation Technische Universität München*, Verlag Dr. Hut, München, 2005.

[534] S. Froidevaux, A. N. Eberle, M. Christe, L. Sumanovski, A. Heppeler, J. S. Schmitt, K. Eisenwiener, C. Beglinger, H. R. Mäcke, *Int. J. Cancer* 2002, *98*(6), 930-937.

[535] S. Froidevaux, A. N. Eberle, *Biopolymers* 2002, *66*(3), 161-183.

[536] M. de Jong, W. A. P. Breeman, W. H. Bakker, P. P. M. Kooij, B. F. Bernard, L. J. Hofland, T. J. Visser, A. Srinivasan, M. A. Schmidt, J. L. Erion, J. E. Bugaj, H. R. Mäcke, E. P. Krenning, *Cancer Res.* 1998, *58*(3), 437-441.

[537] C. H. Van Eijck, *Brit. J. Surg.* 2005, 92(11), 1333-1334.

[538] G. Weckbecker, I. Lewis, R. Albert, H. A. Schmid, D. Hoyer, C. Bruns, *Nat. Rev. Drug. Discov.* 2003, *2*(12), 999-1017.

[539] H. J. Wester, M. Schottelius, T. Poethko, K. Bruus-Jensen, M. Schwaiger, *Cancer Biother. Radio.* 2004, *19*(2), 231-244.

[540] L. J. Gooßen, *Chem. Commun.* 2001, 669-670.

[541] P. Magnus, T. Gallagher, *J. Chem. Soc. Chem. Comm.* 1984(6), 389-390.

[542] R. F. Borch, L. D. Weber, Grudzins.Cv, D. A. Peterson, *J. Org. Chem.* 1972, *37*(8), 1141-&.

[543] M. B. Soellner, K. A. Dickson, B. L. Nilsson, R. T. Raines, *J. Am. Chem. Soc.* 2003, *125*(39), 11790-11791.

[544] J. T. Lundquist, J. C. Pelletier, *Org. Lett.* 2001, *3*(5), 781-783.

[545] P. B. Alper, S. C. Hung, C. H. Wong, *Tetrahedron Lett.* 1996, *37*(34), 6029-6032.

[546] D. T. S. Rijkers, H. H. R. van Vugt, H. J. F. Jacobs, R. M. J. Liskamp, *Tetrahedron Lett.* 2002, *43*(20), 3657-3660.

[547] K. Sonogashira, Y. Tohda, N. Hagihara, *Tetrahedron Lett.* 1975(50), 4467-4470.

[548] S. R. Nagarajan, B. Devadas, M. E. Zupec, S. K. Freeman, D. L. Brown, H. F. Lu, P. P. Mehta, N. S. Kishore, C. A. McWherter, D. P. Getman, J. I. Gordon, J. A. Sikorski, *J. Med. Chem.* 1997, *40*(10), 1422-1438.

[549] D. A. Evans, T. C. Britton, J. A. Ellman, R. L. Dorow, *J. Am. Chem. Soc.* 1990, *112*(10), 4011-4030.

[550] S. Chandrasekaran, A. F. Kluge, J. A. Edwards, *J. Org. Chem.* 1977, *42*(24), 3972-3974.

[551] V. D. Bock, H. Hiemstra, J. H. van Maarseveen, *Eur. J. Org. Chem.* 2006(1), 51-68.

[552] D. E. Prasuhn, Jr., R. M. Yeh, A. Obenaus, M. Manchester, M. G. Finn, *Chem. Commun.* 2007, *12*, 1269-1271.

[553] B. Luy, H. Kessler, in *Handbook of Modern NMR-Methods* (Ed.: D. Craik), 2007, p. in press.

[554] F. Kramer, M. V. Deshmukh, H. Kessler, S. J. Glaser, *Concept. Magn. Reson. A* 2004, *21A*(1), 10-21.

[555] A. Bax, *Protein Sci.* 2003, *12*(1), 1-16.

[556] C. R. Sanders, B. J. Hare, K. P. Howard, J. H. Prestegard, *Prog. Nucl. Mag. Res. Sp.* 1994, *26*, 421-444.

[557] B. Simon, M. Sattler, *Angew. Chem. Int. Edit.* 2002, *41*(3), 437-440.

[558] N. Tjandra, A. Bax, *Science* 1997, *278*(5340), 1111-1114.

[559] J. R. Tolman, J. M. Flanagan, M. A. Kennedy, J. H. Prestegard, *P. Natl. Acad. Sci. USA* 1995, *92*(20), 9279-9283.

[560] J. H. Prestegard, *Nat. Struct. Mol. Biol.* 1998, *5*, 517-522.

[561] R. Tycko, F. J. Blanco, Y. Ishii, *J. Am. Chem. Soc.* 2000, *122*(38), 9340-9341.

[562] H. J. Sass, G. Musco, S. J. Stahl, P. T. Wingfield, S. Grzesiek, *J. Biomol. NMR* 2000, *18*(4), 303-309.

[563] Y. Ishii, M. A. Markus, R. Tycko, *J. Biomol. NMR* 2001, *21*(2), 141-151.

[564] J. J. Chou, S. Gaemers, B. Howder, J. M. Louis, A. Bax, *J. Biomol. NMR* 2001, *21*(4), 377-382.

[565] M. R. Hansen, L. Mueller, A. Pardi, *Nat. Struct. Mol. Biol.* 1998, *5*(12), 1065-1074.

[566] M. Rückert, G. Otting, *J. Am. Chem. Soc.* 2000, *122*(32), 7793-7797.

[567] K. Fleming, D. Gray, S. Prasannan, S. Matthews, *J. Am. Chem. Soc.* 2000, *122*(21), 5224-5225.

[568] M. Martin-Pastor, C. A. Bush, *J. Biomol. NMR* 2001, *19*(2), 125-139.

[569] D. I. Freedberg, *J. Am. Chem. Soc.* 2002, *124*(10), 2358-2362.

[570] H. Neubauer, J. Meiler, W. Peti, C. Griesinger, *Helvetica Chimica Acta* 2001, *84*(1), 243-258.

[571] H. F. Azurmendi, C. A. Bush, *Carbohydrate Res.* 2002, *337*(10), 905-915.

[572] C. M. Thiele, *J. Org. Chem.* 2004, *69*(22), 7403-7413.

[573] C. M. Thiele, S. Berger, *Org. Lett.* 2003, *5*(5), 705-708.

[574] L. Verdier, P. Sakhaii, M. Zweckstetter, C. Griesinger, *J. Magn. Reson.* 2003, *163*(2), 353-359.

[575] A. Mangoni, V. Esposito, A. Randazzo, *Chem. Commun.* 2003(1), 154-155.

[576] C. Aroulanda, V. Boucard, F. Guibe, J. Courtieu, D. Merlet, *Chem. Eur. J.* 2003, *9*(18), 4536-4539.

[577] J. L. Yan, F. Delaglio, A. Kaerner, A. D. Kline, H. P. Mo, M. J. Shapiro, T. A. Smitka, G. A. Stephenson, E. R. Zartler, *J. Am. Chem. Soc.* 2004, *126*(15), 5008-5017.

[578] J. L. Yan, T. Corpora, P. Pradhan, J. H. Bushweller, *J. Biomol. NMR* 2002, *22*(1), 9-20.

[579] B. Luy, K. Kobzar, H. Kessler, *Angew. Chem. Int. Edit.* 2004, *43*(9), 1092-1094.

[580] J. C. Freudenberger, P. Spiteller, R. Bauer, H. Kessler, B. Luy, *J. Am. Chem. Soc.* 2004, *126*(45), 14690-14691.

[581] P. Lesot, D. Merlet, A. Loewenstein, J. Courtieu, *Tetrahedron-Asymmetr.* 1998, *9*(11), 1871-1881.

[582] C. Canlet, D. Merlet, P. Lesot, A. Meddour, A. Loewenstein, J. Courtieu, *Tetrahedron-Asymmetr.* 2000, *11*(9), 1911-1918.

[583] M. Panar, W. D. Phillips, *J. Am. Chem. Soc.* 1968, *90*(14), 3880-&.

[584] A. Meddour, I. Canet, A. Loewenstein, J. M. Pechine, J. Courtieu, *J. Am. Chem. Soc.* 1994, *116*(21), 9652-9656.

[585] B. Bendiak, T. T. Fang, D. N. M. Jones, *Can. J. Chem.* 2002, *80*(8), 1032-1050.

[586] B. Deloche, E. T. Samulski, *Macromolecules* 1981, *14*(3), 575-581.

[587] P. Sentosa, F. Fujara, H. Sillescu, *Makromol. Chem.* 1992, *193*(9), 2421-2431.

[588] L. C. ter Beek, F. M. Linseisen, *Macromolecules* 1998, *31*(15), 4986-4989.

[589] R. J. Cormier, M. L. Kilfoil, P. T. Callaghan, *Phys. Rev. E* 2001, *6405*(5), -.

[590] E. T. Samulski, *Polymer* 1985, *26*(2), 177-189.

[591] P. Haberz, J. Farjon, C. Griesinger, *Angew. Chem. Int. Edit.* 2005, *44*(3), 427-429.

[592] S. Meier, D. Haussinger, S. Grzesiek, *J. Biomol. NMR* 2002, *24*(4), 351-356.

[593] B. Luy, K. Kobzar, S. Knör, J. Furrer, D. Heckmann, H. Kessler, *J. Am. Chem. Soc.* 2005, *127*(17), 6459-6465.

[594] J. C. Freudenberger, S. Knör, K. Kobzar, D. Heckmann, T. Paululat, H. Kessler, B. Luy, *Angew. Chem. Int. Edit.* 2005, *44*(3), 423-426.

[595] B. Luy, A. Frank, H. Kessler, in *Drug Properties: Measurement and computation* (Ed.: R. Mannhold), Wiley-VCH, Weinheim, 2007, p. in press.

[596] A. D. Jenkins, P. Kratochvil, R. F. T. Stepto, U. W. Suter, *Pure Appl. Chem.* 1996, *68*(12), 2287-2311.

[597] G. Odian, *Principles of polymerization*, 4th ed., Wiley, Hoboken, NJ, 2004.

[598] J. M. G. Cowie, *Chemie und Physik der synthetischen Polymeren.*, 2nd ed., Vieweg, Braunschweig/Wiesbaden, 1997.

[599] T. Cierpicki, J. H. Bushweller, *J. Am. Chem. Soc.* 2004, *126*(49), 16259-16266.

[600] P. W. Kuchel, B. E. Chapman, N. Muller, W. A. Bubb, D. J. Philp, A. M. Torres, *J. Magn. Reson.* 2006, *180*(2), 256-265.

[601] T. Alfrey, G. Goldfinger, *J. Chem. Phys.* 1944, *12*(6), 205-209.

[602] F. R. Mayo, F. M. Lewis, *J. Am. Chem. Soc.* 1944, *66*, 1594-1601.

[603] F. T. Wall, *J. Am. Chem. Soc.* 1944, *66*, 2050-2057.

[604] J. Brandrup, *Polymer handbook*, Wiley, Hoboken, N. J., 1999.

[605] H. Jacobelli, M. Bartholin, A. Guyot, *J. App. Polym. Sci.* 1979, *23*(3), 927-939.

[606] E. VivaldoLima, P. E. Wood, A. E. Hamielec, A. Penlidis, *Ind. Eng. Chem. Res.* 1997, *36*(4), 939-965.

[607] O. Fuchs, in *Polymer Handbook* (Eds.: J. Brandrup, E. H. Immergut), Wiley, New York, 1989, pp. 379-407.

[608] B. Luy, K. Kobzar, S. Knör, J. Furrer, D. Heckmann, H. Kessler, *J. Am. Chem. Soc.* 2005, *127*(17), 6459-6465.

[609] T. J. Wenzel, J. D. Wilcox, *Chirality* 2003, *15*(3), 256-270.

[610] D. Parker, *Chem. Rev.* 1991, *91*, 1441-1457.

[611] E. Sackmann, S. Meiboom, L. C. Snyder, A. E. Meixner, R. E. Dietz, *J. Am. Chem. Soc.* 1968, *90*(13), 3567-3569.

[612] M. Sarfati, P. Lesot, D. Merlet, J. Courtieu, *Chem. Commun.* 2000(21), 2069-2081.

[613] M. Sarfati, J. Courtieu, P. Lesot, *Chem. Commun.* 2000(13), 1113-1114.

[614] C. Aroulanda, D. Merlet, J. Courtieu, P. Lesot, *J. Am. Chem. Soc.* 2001, *123*(48), 12059-12066.

[615] D. Merlet, J. W. Emsley, P. Lesot, J. Courtieu, *J. Chem. Phys.* 1999, *111*(15), 6890-6896.

[616] A. S. Tracey, P. Diehl, *FEBS Lett.* 1975, *59*(1), 131-132.

[617] K. Baczko, C. Larpent, P. Lesot, *Tetrahedron-Asymmetry* 2004, *15*(6), 971-982.

[618] A. S. Tracey, *Mol. Phys.* 1977, *33*(2), 339-350.

[619] E. Lafontaine, J. P. Bayle, J. Courtieu, *J. Am. Chem. Soc.* 1989, *111*(21), 8294-8296.

[620] C. Aroulanda, M. Sarfati, J. Courtieu, P. Lesot, *Enantiomer* 2001, *6*(5), 281-287.

[621] B. E. Weiss-Lopez, M. Azocar, R. Montecinos, B. K. Cassels, R. Araya-Maturana, *Langmuir* 2001, *17*(22), 6910-6914.

[622] I. Canet, J. Courtieu, A. Loewenstein, A. Meddour, J. M. Pechine, *J. Am. Chem. Soc.* 1995, *117*(24), 6520-6526.

[623] E. Lafontaine, J. M. Pechine, J. Courtieu, C. L. Mayne, *Liq. Cryst.* 1990, *7*(2), 293-298.

[624] J. M. Pechine, A. Meddour, J. Courtieu, *Chem. Commun.* 2002(16), 1734-1735.

[625] K. Kobzar, H. Kessler, B. Luy, *Angew. Chem. Int. Edit.* 2005, *44*(20), 3145-3147.

[626] M. M. Green, J. W. Park, T. Sato, A. Teramoto, S. Lifson, R. L. B. Selinger, J. V. Selinger, *Angew. Chem. Int. Edit.* 1999, *38*(21), 3139-3154.

[627] M. M. Green, M. P. Reidy, R. J. Johnson, G. Darling, D. J. Oleary, G. Willson, *J. Am. Chem. Soc.* 1989, *111*(16), 6452-6454.

[628] N. A. Lakomek, T. Carlomagno, S. Becker, C. Griesinger, J. Meiler, *J. Biomol. NMR* 2006, *34*(2), 101-115.

[629] M. D. Mukrasch, P. Markwick, J. Biernat, M. Bergen, P. Bernado, C. Griesinger, E. Mandelkow, M. Zweckstetter, M. Blackledge, *J. Am. Chem. Soc.* 2007, *129*(16), 5235-5243.

[630] J. Gante, H. Kessler, C. Gibson, in *Houben-Weyl: Methods of Organic Chemistry, Vol. E 22c* (Eds.: A. F. M. Goodmann, L. Moroder, C. Toniolo), Thieme Verlag, Stuttgart, New York, 2003, p. 311.

[631] T. Fukuyama, X. Q. Chen, G. Peng, *J. Am. Chem. Soc.* 1994, *116*(7), 3127-3128.

[632] H. M. Davies, R. J. Townsend, *J. Org. Chem.* 2001, *66*(20), 6595-6603.

[633] V. J. Jasys, P. R. Kelbaugh, D. M. Nason, D. Phillips, K. J. Rosnack, N. A. Saccomano, J. G. Stroh, R. A. Volkmann, *J. Am. Chem. Soc.* 1990, *112*(18), 6696-6704.

[634] W. H. Walker, S. E. Rokita, *J. Org. Chem.* 2002, *68*(4), 1563-1566.

[635] B. Carboni, A. Benalil, M. Vaultier, *J. Org. Chem.* 1993, *58*(14), 3736-3741.

Curriculum vitae

Personal

	Sebastian Knör, Dipl.-Chem. Univ.
Address	Fürstenrieder Straße 10, 80687 München (Germany)
Nationality	German
Sex	male
E-mail	sebastian.knoer@arcor.de
Date and place of birth	22.03.1977, Burghausen (Germany)
Marital status	married

Professional Experiences

Since Oct. 2002	Research associate, Technische Universität, München
	Department Chemistry, Institute of Organic Chemistry, Prof. Dr. H. Kessler

University & Education

Since Oct. 2002	PhD thesis, Technische Universität, München
	Department Chemistry, Institute of Organic Chemistry, Prof. Dr. H. Kessler
	„Design and synthesis of FVIII- and uPAR-selective Ligands and cross-linked polymers as media for NMR-spectroscopy"
	Date of doctoral degree ceremony: 3rd quarter 2007
10.1996 – 03.2002	Studies in Chemistry, Ludwig-Maximilians-Universität, München (10.1996 – 09.1998 TU München)
	Main courses: Organic Chemistry, Macromolecular Chemistry
	Diploma thesis, Prof. Dr. W. Steglich, Institute of Organic Chemistry: *"Studies towards the total synthesis of the mushroom metabolite (+)-Calopin"*, Grade 1.0 (very good)
	25th March, 2002; Diploma in Chemistry, Grade 1.0 (very good)

1987 – 1996	High school: Tassilo-Gymnasium Simbach am Inn
	General certificate (Abitur), Grade 1.5 (very good) Main courses: Physics and Chemistry

Awards

2001	Book Award of the Department of Chemistry (LMU München) for excellence in oral diploma exams
1996	Book Award of the Tassilo-Gymnasium Simbach am Inn for excellence in A-level (Abitur) exams

Oral Presentations

S. Knör. Development and solution phase synthesis of a novel peptide-mimetic factor VIII affinity ligand. *3rd Summer School Medicinal Chemistry,* Regensburg, 25. – 27. Sept., 2006.

Continuing education

Sept. 2006	Workshop Presentation, College Team, Job Center München
Sept. 2006	Third Summer School Medicinal Chemistry, Research Training Group Regensburg
Mai 2006 – July 2006	English for technical purposes II, University Language Center, Technische Universität München
Since April 2006	French, Language School München Aktiv, München
Feb. 2006	50th Annual Conference of the Society of Thrombosis and Haemostasis Research e. V., Basel (Schweiz)
June 2005	Workshop Medicinal Chemistry, Lilly Deutschland GmbH, München
July 2004	Users Seminar, Linear ion trap and Fourier transform ion cyclotron resonance mass spectroscopy, Thermo Electron Corp., München
Oct. 2003	Project Management, Dr. Nestel (German Chemical Society e. V.), München
Sept. 2003	Workshop Bioprocessing, Merck KGaA, München
Oct. 2002 – April 2003	Modern Greek, Language School Lingua-Nova, München